Ecology and Variation of Cretaceous and Recent Cephalopods

Dissertation

zur

Erlangung der naturwissenschaftlichen Doktorwürde
(Dr. sc. nat.)

vorgelegt der

Mathematisch-naturwissenschaftlichen Fakultät

der

Universität Zürich

von

Amane Tajika

aus

Japan

Promotionskommission

Prof. Dr. Christian Klug (Leitung der Dissertation)
Prof. Dr. Hugo Bucher
Prof. Dr. Marcelo Sánchez

Zürich, 2017

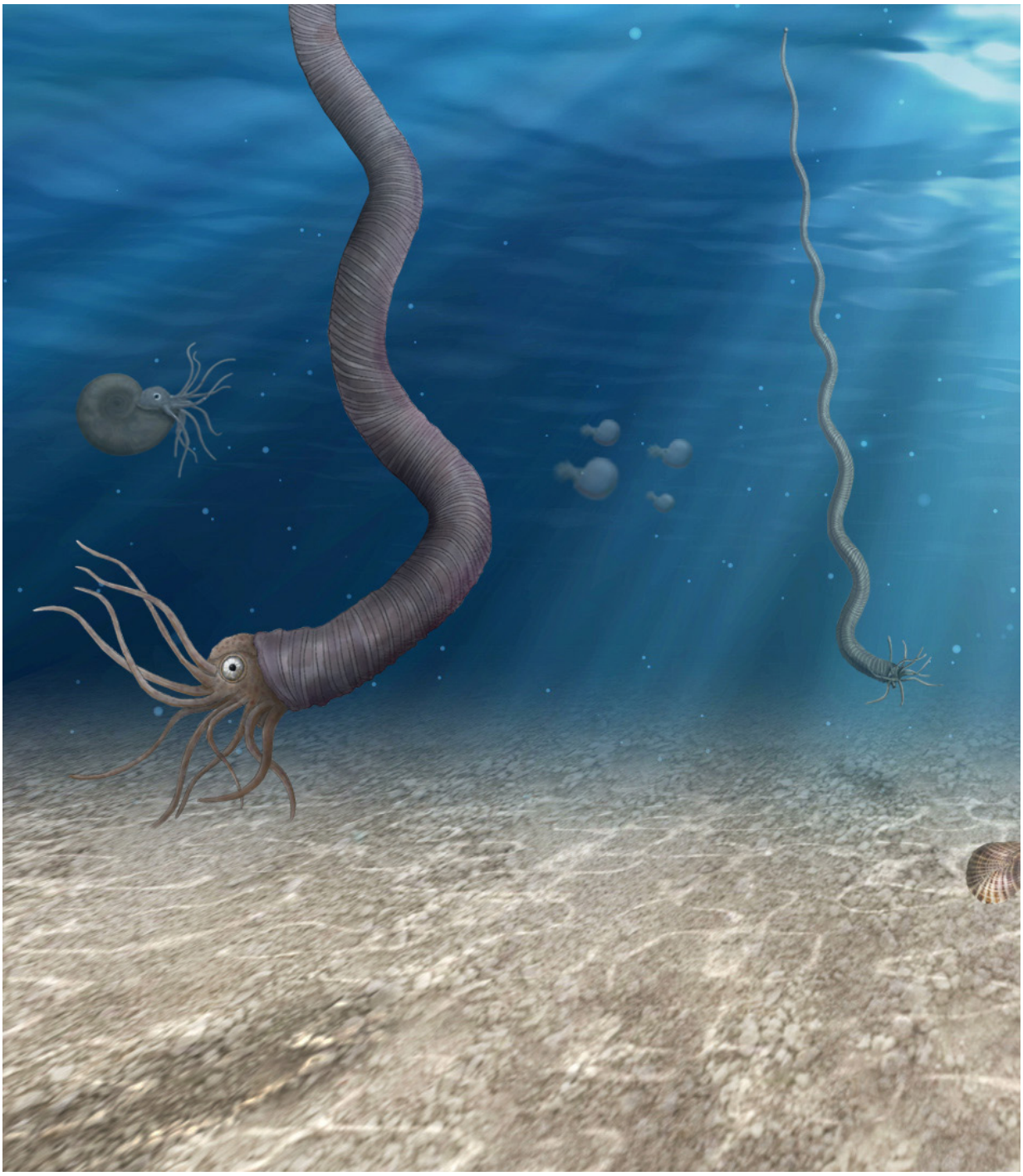

This PhD thesis is dedicated to my late grandmother Ryoko Tajika.

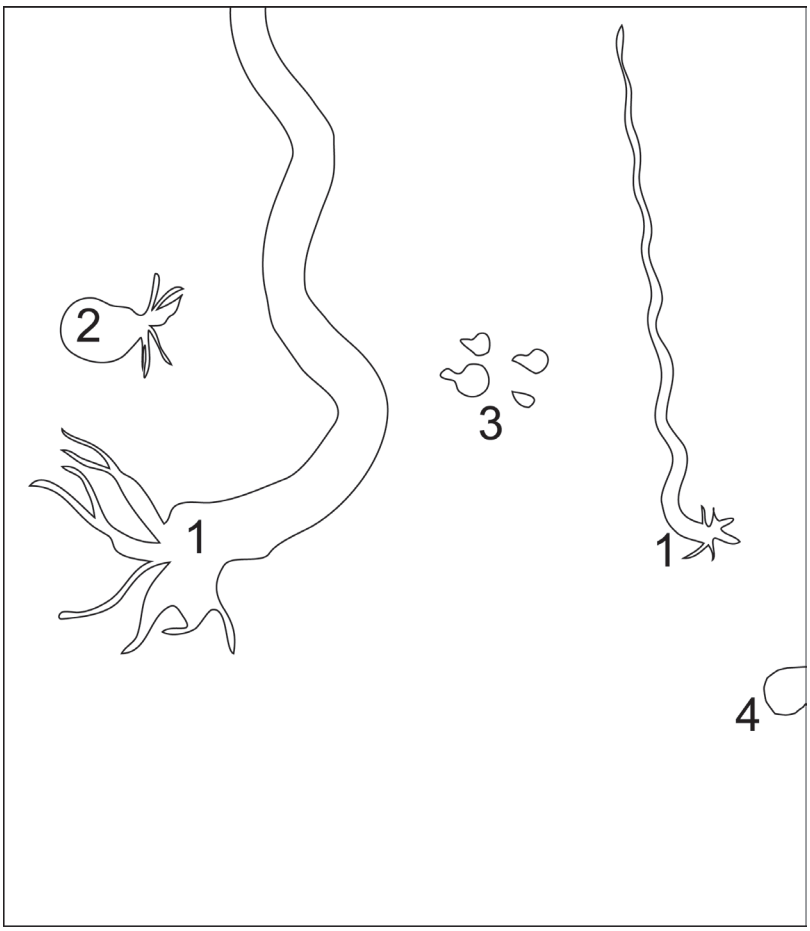

Cover illustration. Life reconstrcution of some Cretaceous ammonites. 1, *Eubostrychoceras valdelaxum*. 2, *Gaudryceras tenuiliratum*. 3, *Tetragonites* sp. 4, *Platyceramus japonicus*. This drawing was prepared for the temporary exhibition (summer, 2017) of the Mikasa City Museum (Hokkaido, Japan).

Contents

Abstract

Palaeodiversity, palaeoecology and organismic evolution are essential disciplines in palaeontology. Although major trends and changes in biodiversity through the Phanerozoic are more or less well known, much more work is needed to understand ecological details as well as all the involved biases linked with biodiversity analyses. As far as evolution is concerned, variation produces the raw material for selection, and thus is of great importance. Within this work, questions of evolutionary processes, morphological intraspecific variation and palaeoecology of cephalopods have been addressed because cephalopods are excellent model organisms to study such fields due to their abundance and morphological diversity.

The first part of this (Chapter I and II) thesis documents cephalopod associations and their ecology from the Alpstein massif in Switzerland. It is based on remains of over 1000 macrofossil taxa. Although this region has been sedimentologically and geologically studied in great detail, the fossil associations are much less well-known. To fill this gap, all available cephalopod fossils from the Alpstein were examined comprehensively. In total, at least 100 ammonite taxa, 6 nautilid taxa and 4 coleoid taxa occurred in the Alpstein region. Macrofossil associations of various ages from the Alpstein were also examined in order to assess palaeoecological and environmental changes through the Cretaceous. To quantify these changes, two diversity indices of taxonomic richness and ecological disparity were employed. Results show that taxonomic richness and ecological disparity are decoupled, i.e., taxonomic richness did not show a strong fluctuation with around 20 families through time, whereas ecological disparity fluctuated strongly. These results imply that, when environmental changes occur, ecological disparity is more susceptible than taxonomic richness at family level.

In the second part (Chapter III and IV), phenotypic intraspecific variation of cephalopods and its ontogenetic trajectories were investigated. Knowledge of intraspecific variability is a prerequisite to study diversity, palaeobiogeography and chronobiostratigraphy because these can be only carried out correctly with accurate taxonomic assignments. Ammonoids are extinct externally shelled cephalopods (ectocochleates), which had high evolutionary rates and occur worldwide in great numbers. If complete, ammonoid conchs record their entire ontogeny because of their accretionary growth and thus are, like many other mollusks, ideal to study ontogeny. However, ammonoid intraspecific variation is often underestimated or ignored when a new taxon is introduced, which resulted in oversplitting in many cases. To understand intraspecific variation in ammonoids, Recent *Nautilus* was used as a reference since fossil materials introduce a set of additional biases (e.g., taphonomy, time averaging). A quantitative approach using 3D morphometry was employed to analyze the phenotypic intraspecific variation of three conch parameters of three geographically separated *Nautilus* populations through ontogeny. Results illustrate that there are commonalities in the pattern of ontogenetic change of intraspecific variation between the three populations: In early ontogenetic stages, variation is higher and decreases until it shows an increase again before maturity. This pattern was compared with that of some ammonoids and belemnites, which revealed that this ontogenetic pattern of intraspecific variation is common among some groups of cephalopods.

The second part of this thesis (Chapter III and IV) also included applications of (destructive and non-destructive) tomography technique to fossil cephalopods. As in the above mentioned study on intraspecific variation of *Nautilus*, 3D morphometry was carried out to examine several ammonoid species in order to understand ontogenetic patterns of phragmocone chamber volume increase and its intraspecific variation. When the results of ammonoids and *Nautilus* are compared, the ammonoids show a much stronger ontogenetic variation of chamber volumes than nautilids. The driving factors behind this variation will be part of my postdoctoral study.

In the last part of this thesis (Chapter V), the roles of ammonoids in the marine food web and their incumbent replacement after their extinction at the end of the Cretaceous are discussed. Globally, Cretaceous ammonites occur in great numbers. This stresses the importance for the question for the post-Cretaceous re-occupation of this ecospace. First, reproductive rates of large Cretaceous ammonoids were reconstructed, which yielded numbers of up to 100 million eggs (hatchling size 0.5 to 1 mm) for an adult female ammonite with two meters conch diameter. Combining that large ammonites with a diameter exceeding half a meter are abundant globally, this implies a key role of ammonite (and also belemnite) hatchlings in the plankton of Mesozoic seas. With the end-Cretaceous mass-extinction, this ecospace became available. Remarkably, holoplanktonic gastropods resembling ammonite and belemnite hatchlings in form, size and habitat originated early in the Palaeogene and subsequently provided the ecological prerequisites for the evolution of large filter feeders such as mantas, whale sharks and baleen whales.

Zusammenfassung

Paläobiodiversität, Paläoökologie und die Evolution von Organismen sind essentielle Disziplinen innerhalb der Paläontologie. Obwohl die wichtigsten Trends und Veränderungen der Biodiversität im Verlauf des Phanerozoikums mehr oder weniger gut belegt sind, besteht noch einiges an Forschungsbedarf hinsichtlich des Verständnisses ökologischer Details sowie der inhärenten Fehler von Biodiversitäts-Analysen. Was die Evolution betrifft, so liefert die Variation das Rohmaterial für die Selektion und ist daher von grosser Bedeutung. Aufgrund der Häufigkeit ihrer fossilen Überreste und ihrer morphologischen Vielfalt eignen sich Kopffüsser hervorragend als Modell-Organismen zur Untersuchung dieser Fragestellungen. Im Rahmen der vorliegenden Dissertation wurden deshalb Fragen untersucht, die evolutionäre Prozesse, morphologische innerartliche Variation und Paläoökologie der Kopffüsser betreffen.

Im ersten Teil der Dissertation werden Cephalopoden-Vergesellschaftungen vom Alpstein-Massiv (Schweiz) dokumentiert und deren Ökologie untersucht. Diese Studie umfasst über 1000 Taxa von Makrofossilien. Obwohl dieses Gebiet sedimentologisch und geologisch bereits sehr detailliert untersucht wurde, sind die regionalen Fossil-Vorkommen weitaus weniger gut bekannt. Um diese Lücke zu füllen, habe ich alle mir zugänglichen fossilen Cephalopoden des Alpsteins umfassend untersucht. Insgesamt wurden über 100 Ammoniten-Taxa, 6 Nautiliden-Taxa und 4 Coleoideen-Taxa für den Alpstein belegt. Um die Änderungen der Paläoökologie und der Paläo-Umwelt nachzuvollziehen, wurden ausserdem Assoziationen von Wirbellosen begutachtet. Um diese Änderungen zu quantifizieren, habe ich zwei Indizes taxonomischer Vielfalt und ökologischer Disparität verwendet. Diese Analysen ergaben, dass taxonomische Vielfalt und ökologische Disparität entkoppelt sind, das bedeutet, Dass die taxonomische Vielfalt keine starken Veränderungen zeigt mit etwa 20 Familien pro Zeiteinheit, während die ökologische Disparität deutlicher fluktuiert. Dies impliziert, dass die ökologische Disparität empfindlicher oder stärker auf Umwelt-Veränderungen reagiert als die taxonomische Vielfalt.

Der zweite Teil widmet sich der innerartlichen Variation von Kopffüssern und deren ontogenetischen Trajektorien. Die Kenntnis der innerartlichen Variation ist eine Voraussetzung für die Untersuchung von Diversität, Paläobiogeographie und Chronobiostratigraphie, weil für diese Felder genaue taxonomische Bestimmungen benötigt werden. Die Ammonoideen sind ausgestorbene Kopffüsser mit äusserem Gehäuse (ectocochleat). Sie hatten hohe Evolutionsraten und ihre Fossilien sind weltweit häufig. Vollständige Ammonoideen-Gehäuse enthalten Informationen aus der ganzen Ontogenese wegen des akkretionären Wachstums. Wie viele andere Mollusken sind Ammonoideen deswegen ideale Objekte um Ontogenese zu untersuchen. Trotzdem wird die innerartliche Variation oft unterschätzt oder ignoriert, wenn neue Taxa beschrieben werden, was in vielen Fällen zu übermässiger Aufspaltung von Arten führte. Um die innerartliche Variation von Ammonoideen besser zu verstehen, wurde der heute lebende *Nautilus* (Perlboot) als Vergleich verwendet, weil fossile Materialien eine Reihe von Fehlern (z.B.: Taphonomie, time averaging) einführen. Für die Analyse phänotypischer innerartlicher Variation wurde auf einen quantitativen Ansatz zurückgegriffen, Bei den Gehäusen von *Nautilus* drei verschiedener Populationen wurden 3D-morphometrisch Veränderungen dreier Parameter durch die Ontogenie gemessen. Die Ergebnisse belegen, dass es Gemeinsamkeiten in den Mustern ontogenetischer Änderung von Variation in den drei Populationen gibt: In frühen ontogenetischen Stadien ist die Variation erhöht, nimmt dann in der Jugend ab, um gegen Ende in Richtung der Reife wieder zuzunehmen. Dieses Muster wurde des Weiteren mit demjenigen mancher Ammonoideen und Belemniten verglichen, wobei sich herausstellte, dass dasselbe Muster bei verschiedenen Gruppen von Cephalopoden anzutreffen ist.

Im zweiten Teil dieser Arbeit wurden verschiedene tomographische Techniken (destruktiv und nicht-destruktiv) auf fossile Kopffüsser angewandt. Wie in der oben erwähnten Studie über die innerartliche Variation bei *Nautilus*, wurde 3D-Morphometrie verwendet um ontogenetische Muster in der Veränderung der Phragmokon-Kammer-Volumina und deren innerartliche Variation bei mehreren Ammonoideen-Arten zu untersuchen. Im Vergleich zeigen die Ammonoideen eine viel stärkere innerartliche Variation in den ontogenetischen Änderungen der Phragmokon-Kammer-Volumina als Nautiliden. Der Frage nach der Ursache für diese Unterschiede soll nach Abschluss der Dissertation nachgegangen werden.

Im letzten Teil dieser Dissertation diskutiere ich die die Rolle der Ammonoideen in marinen Nahrungsnetzen und deren ökologischen Austausch nach deren Aussterben am Ende der Kreide. Kreide-Ammoniten kommen weltweit in grosser Zahl vor. Dies zeigt, dass die Frage nach der Wieder-Besetzung des freigewordenen ökologischen Potentials nach der Kreide durchaus von Interesse ist. Zunächst

wurden Reproduktions-Raten grosser Kreide-Ammoniten rekosntruiert; dies ergab, dass Weibchen mit zwei Metern Gehäusedurchmesser bis zu hundert Millionen Eier (Schlüpfling-Grösse 0,5 bis 1 mm) legen konnten. Zusammen mit der Tatsache, dass Ammoniten mit einem Gehäusedurchmesser von über einem halben Meter global nicht selten sind, wird klar, dass Schlüpflinge von Ammoniten (und auch Belemniten) eine wichtige Rolle als Plankton in den mesozoischen Meeren gespielt haben. Mit dem Ende der Kreide wurde der von den Schlüpflingen besetzte ökologische Raum verfügbar. Bemerkenswerterweise entstanden im Paläogen verschiedene Gruppen holoplanktonischer Gastropoden, die in Form, Grösse und Lebensraum Ammoniten und Belemniten stark ähneln. Damit schufen die Gastropoden auch die ökologische Grundlage für die Evolution riesiger Filtrierer wie Mantas, Walhaie und Bartenwale.

Introduction

Palaeontology is an important division contributing important data for evolutionary biology. Knowledge of palaeobiodiversity, palaeoecology and about changing palaeoenvironments is relevant for the understanding of contemporary environmental and ecological problems that we face today. Accordingly, I collected data to quantitatively assess palaeoenvironmental changes and their effects (Chapters I and II) and furthermore, I studied the variation, palaeocology and mode of life of externally shelled cephalopods (Chapters III to V).

In the first part (Chapters I and II), I focus on a region of Switzerland with a Cretaceous sequence to document fossil assemblages in a monograph. I incorporated these raw data in a palaeoecological analysis where links to various environmental changes are evaluated. The second part (Chapters III to IV) includes two studies on the variation of chamber growth through ontogeny in ammonites and nautilids, both fossil and recent. Morphologic (phenotypic) variation is important because it is relevant to separate taxa and it reflects a mix of genotypic variation and environmental influences. Recent *Nautilus*, a so-called living fossil, was studied because of its morphological similarities to ammonite conchs. Correspondingly, *Nautilus* has often been used for comparisons with fossil externally shelled cephalopods and morphometry is expected to yield information useful to improve our understanding of fossil cephalopods.

Although the ammonoids thrived with a great abundance, they went extinct at the end of the Cretaceous, which raises a question about their ecological roles in the marine realm: What organisms filled the ecospace previously occupied by ammonoids? Thus, in the last part (Chapter V), I addressed the role of ammonoids and its ontogenetic changes in the marine food webs and the replacement by other organisms after the Cretaceous. In the following, I will present the background of each topic included in this thesis.

Cretaceous

The Mesozoic is one of the times in Earth history, which receives a lot of public attention because it was the age of highly popular organisms such as dinosaurs and ammonites. Similarly, the Cretaceous is probably one of the better studied geologic times, partially because of the large outcrop area due to sea-level highstands (Haq 2014) and partially because the above-mentioned famous groups became extinct at the end of this period around 65 Ma (e.g., Landman et al. 2014; Brusatte et al. 2015; Landman et al. 2015). This extinction is known to be one of the 'Big Five', where 40 % of all marine genera (estimated 76 % of species) were lost (Barnosky et al. 2011; McGhee et al. 2013), which was most likely caused by an asteroid impact on Yucatan (Mexico) and/ or the Deccan volcanism (e.g., Archibald et al. 2010; Schulte et al. 2010; Font et al. 2016).

Today, global warming is one of the major human-induced environmental problems. In this context, increasing attention of scientists is paid to the Cretaceous, which is not only known for its much warmer climate but also for a global sea-level that was up to 250 meters higher than today (Haq 2014). Cretaceous climate can be reconstructed by using information like occurrences of tillites (glaciation), coals or evaporates (aridity). Geochemical analytical methods dramatically improved our possibilities to reconstruct past climates. As shown in Fig. 1A, the sea level was generally high through the Cretaceous (75-250 m higher than today; Haq 2014), with a rapidly increasing trend from the late Early to the early Late Cretaceous (from near the end of the Albian or the beginning of the Cenomanian). Similarly, temperature and humidity were rising from the Barremian to the Cenomanian, i.e. from around 35 million years (Fig. 1A). Also, large-scale tectonic movements together with sea level changes created vast epicontinal seas (Fig. 1B), which must have greatly influenced the biogeographic distribution of organisms in the Cretaceous. Such climatic conditions as well as tectonic activities likely drove speciation or accelerated dispersal of organisms, which likely contributed to an increase of global biodiversity in the Cretaceous (Fig. 2). For instance, extinct taxa of ectocochleate (externally shelled) cephalopods, namely ammonoids, showed the greatest morphological diversification in their evolution with the emergence of some of the most bizarre forms (heteromorphs) such as *Didymoceras, Polyptychoceras* and *Nipponites* (Fig. 3). In Chapter I and II, palaeoecological changes linked to regional environmental changes from the Barremian to the Cenomanian, i.e. for exactly the same time span of rising global temperatures (Fig. 1A), is discussed. Previously, there were only few studies that address palaeoecology changes in response to the massive environmental changes (e.g., Hofmann et al. 2013a,b; Frey et al. 2014).

Palaeobiodiversity studies and their biases

Changes in biodiversity of both animals and plants

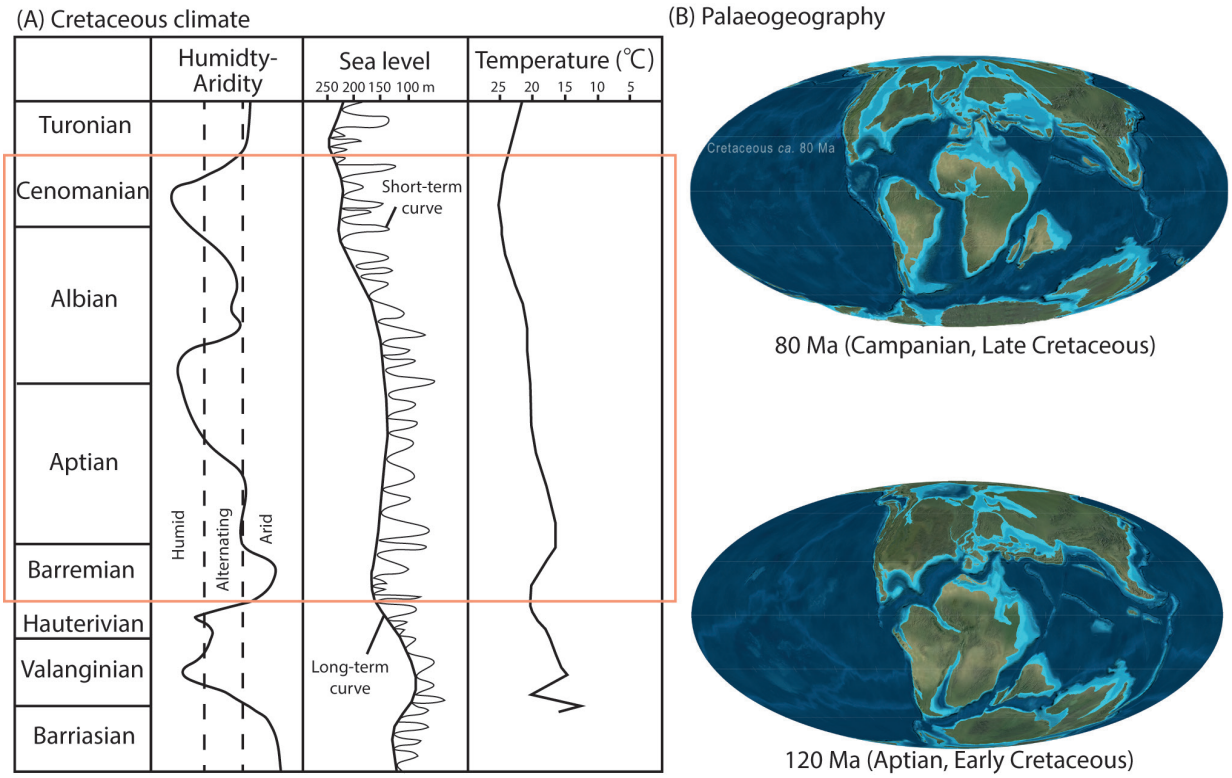

Fig. 1. Cretaceous climate and palaeogeography. A. Humidity, sea level and temperature changes in the Cretaceous, Integrated from various sources (Hallam et al. 1991; Pucéat et al. 2003; Haq 2014). B. Palaeogeographical changes from the Aptian (Early Cretaceous) to the Campanian (Late Cretaceous). Maps are from Deep Time Maps (Blakey, 2016; https://deeptimemaps.com/)

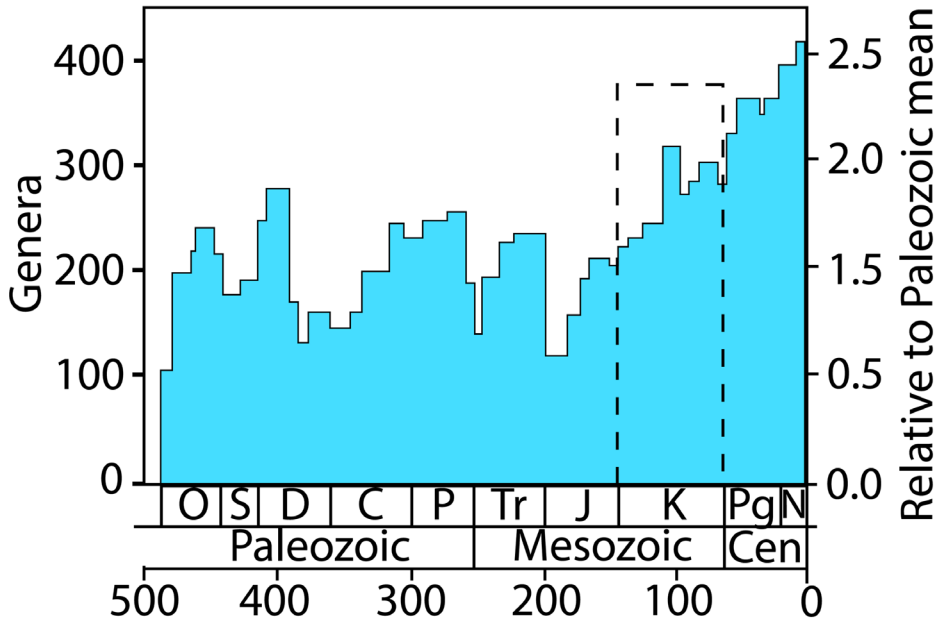

Fig. 2. Phanerozoic diversification of marine organisms. Modified from Bush and Bambach (2015).

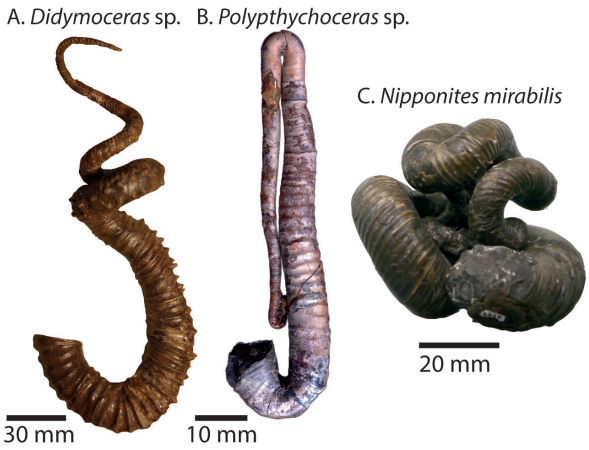

Fig. 3. Heteromorphic ammonites in the Cretaceous. A. *Didymoceras* sp. B. *Polyptychoceras* sp. Image courtesy of Kenji Ikuno (Yokohama). C. N*ipponites mirabilis*.

have been frequently studied particularly in the context of taxonomic richness at a either global or local scale over the past decades (e.g., Sanders 1968; Raup 1972; 1975; Sepkoski et al. 1981; Niklas et al. 1983; Sepkoski 1984; 1988; Bush and Bambach 2004; Alroy et al. 2008; Hofmann et al. 2013a,b; Cleal and Cascales-Miñana 2014; Frey et al. 2014; Bush and Bambach 2015). Thanks to various methodological advancements in conducting such studies, we more or less agree that the global diversity of marine animals increased substantially from the Phanerozoic to the Cenozoic (e.g., Bush and Bambach 2015; Fig. 2). However, global-scale studies, especially those using data compiled from databases such as the PBDB (Palaeobiology Database), can be strongly biased. These include sampling biases (e.g, Sanders 1968; Raup 1977; Bernard et al. 2010), taphonomic biases (e.g., Raup 1972; Kidwell 2002; Powell and Kowalewski 2002; Bush and Bambach 2004; Kidwell 2005), latitudinal biases (e.g., Crame 2002; Bush and Bambach 2004) and taxonomic biases (e.g., Lane and Benton 2003; Forey et al. 2004). Despite the fact that some of these biases can be corrected using certain statistical methods such as rarefaction (Sanders 1968), some biases need special attention depending on the field under consideration. For instance, the Ammonoidea, which is a highly diverse extinct group that occurs sometimes in great abundance, is a well-known example of such taxonomic uncertainty (e.g., De Baets et al. 2015a). This roots in the underestimation or incomplete knowledge of the intraspecific variability of ammonoids. Thus, improving our understanding of ammonoid intraspecific variability is fundamental to more accurately identify ammonoids and thus to correctly quantify their biodiversity. In this context, I attempted to improve the understanding of cephalopods in general, which can be also an important reference to ammonoids in Chapter III and IV. Furthermore, large-scale biodiversity studies tend to conceal details of the complex connections and interactions between diversity, palaeoecolgy and palaeoenvironments. Therefore, primary data of how organisms responded to environmental changes are needed and regional studies can provide those, which is addressed in Chapter I and II.

Ammonoids and nautiloids

What are ammonoids and nautiloids?

Ammonoids are an extinct group of externally shelled cephalopods (ectocochleates). They originated in the Devonian (e.g., De Baets et al. 2013a; Klug et al. 2015), underwent a number of adaptive radiations (Kennedy 1977), suffered from the great mass extinctions and went extinct at the end of the Cretaceous (e.g., House 1989; Ward 1996; Landman et al. 2014;). Nautiloids are also a group of externally shelled cephalopods with the extant representatives *Nautilus* and *Allonautilus*. Recent *Nautilus* has often been studied in order to understand palaeoecology of extinct ammonoids because of similarities in conch morphology (e.g., Ward 1987; Saunders and Landman 2009), although it is widely accepted that ammonoids are phylogenetically closer to coleoids (octopus, squids and cuttlefish) than to nautiloids (Fig. 4; Jacobs and Landman 1993; Kröger et al. 2011).

Ammonoids in the marine food web

The role of ammonoids in marine food webs has been superficially assessed based on the scarce fossil record of buccal organs (radula and mandibles), traces of sublethal injuries (prey) and stomach contents as well as actualistic comparisons. Morphology and function of the buccal organs became better

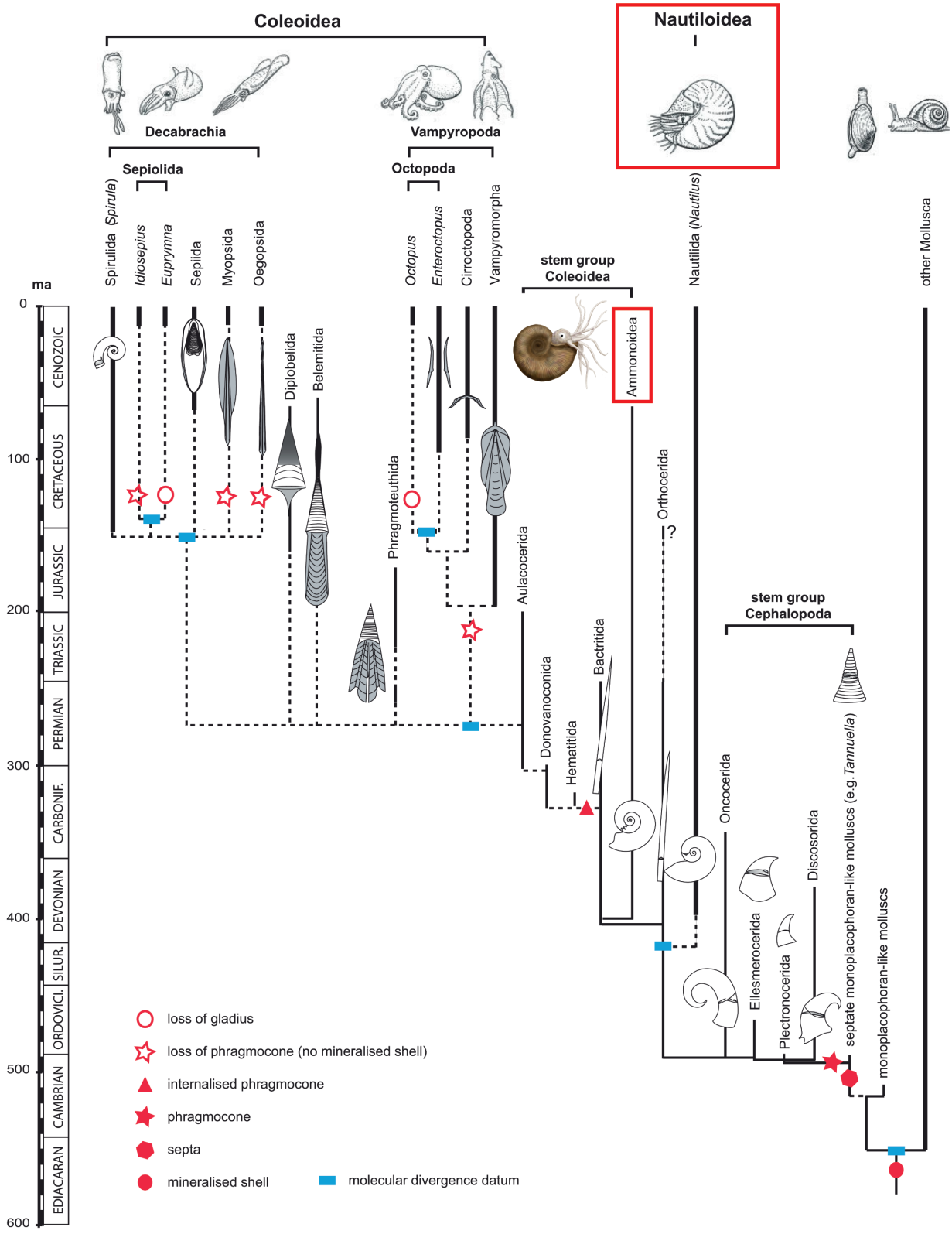

Fig. 4. Cephalopod phylogeny. Modified from Kröger et al. (2011).

known when Kruta et al. (2011) published reconstructions of jaws and radula of the Cretaceous heteromorphic ammonite Baculites using phase-contrast synchrotron X-ray tomography. They argue that jaws of Baculites and other aptychophoran ammonites (Engeser and Keupp 2002) are adapted to capture small planktonic organisms in the water column (crustaceans and gastropod larva), which were preserved in their examined specimens with the mouthparts. They also suggest that this feeding strategy might have driven the evolution of new groups of plankton. It is also known that ammonites fed on juvenile ammonites considering that the size of hatchlings is considerably small (around 1 mm; e.g., Tajika and Wani 2011; De Baets et al. 2012; Klug and Lehmann 2015). In fact, ammonoid hatchlings and jeveniles are sometimes reported as ammonite stomach contents (Lehmann 1971; Jäger and Fraaye 1997; Keupp 2000; Keupp 2012). Predation on more or less mature ammonites also occurred (e.g., Ward 1981; Klug 2007; Zatoń 2010; Keupp 2012). These studies suggest possible predators such as marine vertebrates (fish and sharks), coleoids and nautiloids, although the direct evidence is still poor.

Ammonite hatchlings were extremely small (around 1 mm) and their mode of life is thought to be different from that of older ammonites, i.e., juveniles were still planktonic and not yet active nektonic swimmers (e.g., Chamberlain 1976; Mapes and Nützel 2009; Naglik et al. 2015b). As mentioned above, hatchlings and juveniles are sometimes reported as ammonite stomach contents (Lehmann 1971; Jäger and Fraaye 1997; Keupp 2000; Keupp 2012), which suggests that ammonites preyed on juveniles. Taking their small size into consideration, it is likely that other organisms also preyed on juvenile ammonites. In addition, ammonoids are often referred to as K-strategists due to their small embryo size (De Baets et al. 2015b), which have a high fecundity and invest little energy in the individuals of their countless progeny. This implies that ammonoid hatchlings and juveniles played an important role as a food source of bigger predators in the marine food web.

Conchs and their usefulness in palaeontological research

One of the important morphological features of ammonoids and nautiloids is their external conch. The conch consists of two main parts (Fig. 5). One of them contains many chambers separated by walls dubbed septa; this part is called phragmocone, which is used as a buoyancy device (Ward 1987). The other is the body chamber, which houses and protects the soft tissues of the animal. The phragmocone chambers are usually gas-filled, and thus allow for buoyancy regulation in the sea (e.g., Ward 1987; Hoffmann et al. 2015). The conch is also of great importance because it preserves a record of growth thanks to the accretionary growth as in other mollusks. Thus, ammonoids, which occur in high abundance, can easily be used to study ontogeny and intraspecific variability (Bucher et al. 1996; De Baets et al. 2012, 2013b, 2015a).

Although ammonoid conchs are often used to reveal their mysterious palaeoecology, they are also used to study other important aspects of palaeontology. For example, ammonoid fossils occur worldwide from a wide range of geologic times and they had high evolutionary rates. Unsurprisingly, they produced a considerable morphological diversity, which makes them optimal organisms for biostratigraphy. Furthermore, they are also an essential model to examine macroevolutionary patterns or to test biogeographic hypotheses (Kennedy 1977; Korn et al. 2012; Korn and De Baets 2015; Lehmann et al. 2015; Yacobucci 2015). Unfortunately, we know little about their soft tissues (e.g., Klug and Lehmann 2015), which would provide useful information on their physiology such as metabolism, locomotory capability and reproductive mode. But since ammonoid soft tissue is hardly fossilized with some exceptions, it is necessary to extract more information from the conch to infer their palaeoecology.

Evolution, ecology, and taxonomy of nautiloids

Compared to the abundant and morphologically diverse ammonoids, nautilids were overshadowed by ammonoids in these terms until the Cretaceous, although their origination dates back to the Silurian, i.e. before the ammonoids (Fig. 4; Kröger et al. 2011). Interestingly, since the end-Cretaceous extinction event, nautiloids have shown no remarkable diversification and on the contrary, most genera went extinct by the end of the Miocene (Ward et al. 2016), which may suggest their ecological requirements differed from those of ammonoids. In modern seas, only two genera, namely *Nautilus* and *Allonautilus*, are recognized with three to six species. These include the undoubted species N. pompilius, N. macromphalus, and A. scrobiculatus plus some controversial morphospecies (Vandepas et al. 2016; Ward et al. 2016). Recently, some biologists and palaeontologists argue that they are on the

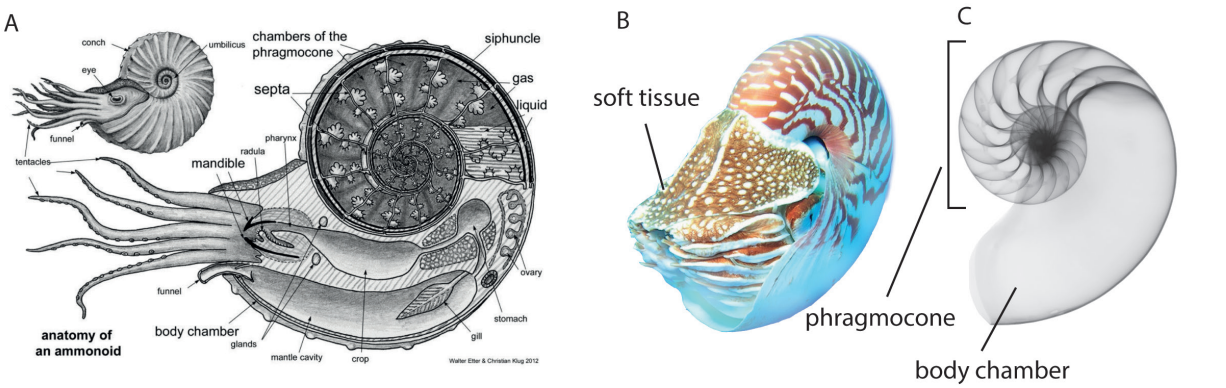

Fig. 5. Conch morphology and anatomy of ammonoids and Recent *Nautilus*. A. Ammonoid anatomy (modified from Klug and Etter 2012), B. Picture of *Nautilus pompilius* from American Samoa (Ward et al. 2016), C. CT-scan of *Nautilus pompilius*.

brink of extinction due of overfishing by humans (del Norte-Campos 2005; Dunstan et al. 2010; De Angelis 2012; Barord 2015; Ward et al. 2016) and consequently are now listed in the CITES. As mentioned previously, modern nautiloid morphology and ecology were intensively studied by palaeontologists for comparative purposes and dramatically improved our understandings of modern nautiloids (Ward 1987; Saunders and Landman 2009). However, we still have not unveiled their ecology entirely. Several questions concern their habitat and behavior. Dunstan et al. (2011) tracked Australian *Nautilus* using ultrasonic telemetry, which revealed that different geographically separated populations of *Nautilus* may have different patterns of migration. Also, *Nautilus* morphology was intensively studied in the 1980's (Tanabe et al. 1983, 1985; Swan and Saunders 1987; Tanabe and Tsukahara 1987). Their ontogenetic changes of shell morphology and their variability within geographically separated populations, species and genera are still poorly known, although such information is needed to better understand extinct ectocochleate cephalopods. In recent years, the genetics of modern nautiloids have been revealed in detail (Wray et al. 1995; Bonnaud et al. 2004; Sinclair et al. 2007; Williams et al. 2015; Ward et al. 2016). It is also of great importance to fill the gap of knowledge of morphology and genetics because such knowledge can reveal how the genotype is reflected in the phenotype, particularly conch morphology. As far as fossil nautiloids are concerned, their taxonomy needs comprehensive revision (e.g., Ward et al. 2016), which largely roots in the fact that traditionally, intraspecific variation was not taken into consideration when a new species was introduced. Naturally, this holds true for the majority of ammonoid taxa. In order to correctly conduct taxonomic work, knowledge of intraspecific variability is required (De Baets et al. 2015a). In Chapter III and IV, phenotypic intraspecific variation of Recent *Nautilus* is discussed in detail.

Virtual palaeontology

Methods for 3D reconstructions used in palaeontology

External and internal structures of conchs retain information on palaeoecology of fossil ectocochleate cephalopods. Palaeontologists have obtained morphological information mostly from the outside of the conch or from single 2D-sections. The internal conch structure, however, is difficult to examine three dimensionally. Thus, studies, which require 3D-information on the internal structure, employed indirect methods such as theoretical modeling (Heptonstall 1970; Saunders and Shapiro 1986; Jacobs and Chamberlain 1996). But there is some uncertainty about the correctness of such methods because coiling and shell thickness vary through ontogeny. Therefore, a new technique, which allows the examination of such complex three dimensional parameters, was overdue. Although tomography has been frequently used in vertebrate palaeontology, its application to invertebrate fossils started only recently.

Tomography can be divided into (1) non-destructive and (2) destructive methods (Fig. 6). The former includes neutron tomography (NT), magnetic resonance imaging (MRI), optical tomography and X-ray computed tomography (CT; Sutton et al. 2014). These techniques use different kinds of penetrative radiation, which is absorbed differently by a sample. Neutrons are absorbed more strongly by organic materials than rocks. Therefore, NT is the method which is more appropriate for organic preservation (Sutton 2008). MRI is commonly

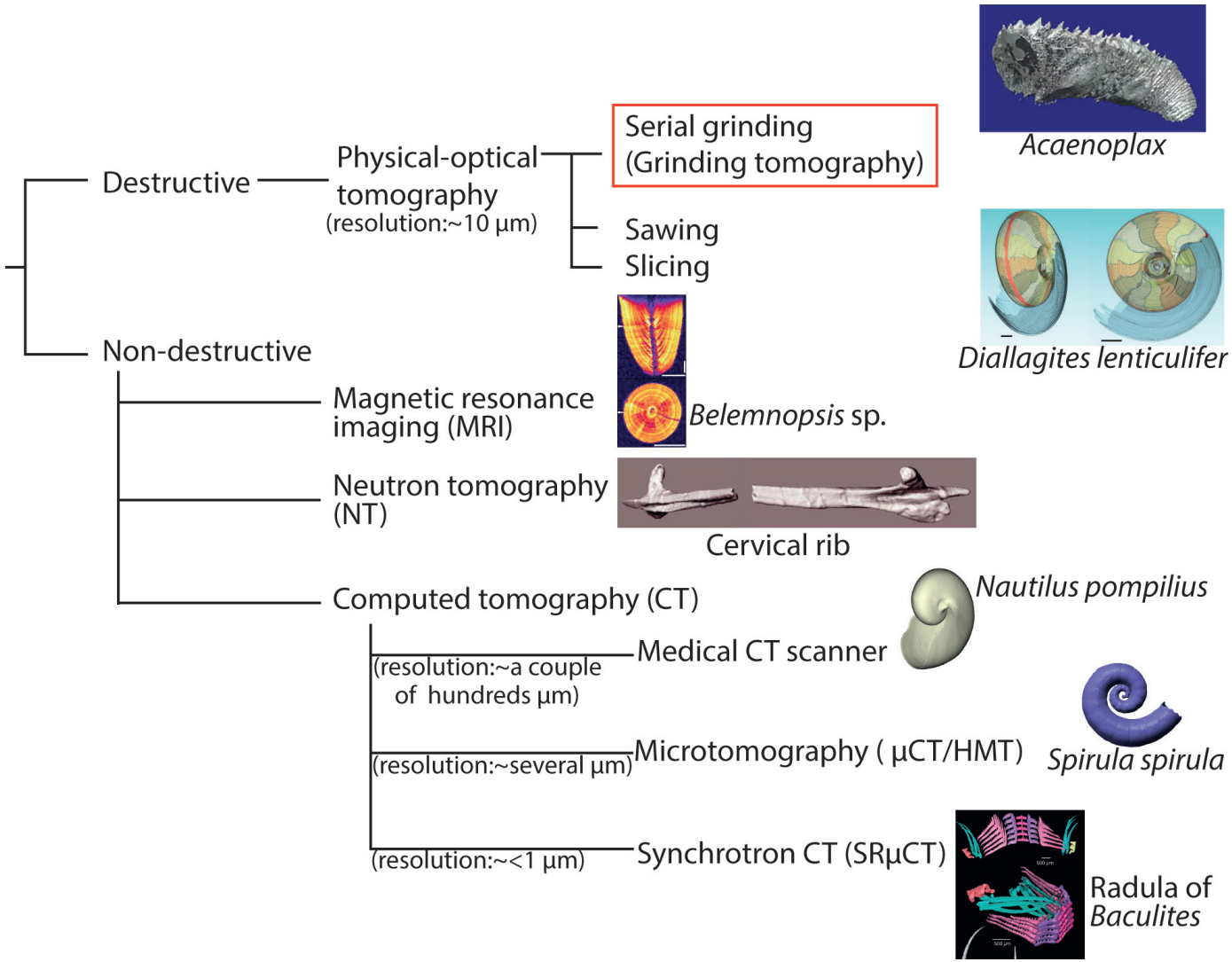

Fig. 6. Tomography techniques used in Palaeontology (Summarized from Sutton et al. 2008; Hoffmann et al. 2014). Images from Sutton et al. (2001; *Acaenoplax*), Mietchen et al. (2008; *Belemnopsis* sp.), Naglik et al. (2015; *Diallagites Ienticulifer*), Schwarz et al. (2005; cervical rib), *Nautilus pompilius* (my own scan), Hoffmann et al. (2014; *Spirula spirula*) and Kruta et al. (2011; *Baculites*)

used in medicine. It maps properties relating to the chemical environment of certain elements, especially hydrogen (Sutton 2008). As such, this method is not suitable for fossilized cephalopods, which usually lack these elements. X-ray computed tomography, which maps X-ray attenuation, is by far the most frequently tested method to analyze fossil or living cephalopods. The most easily accessible device is medical CT scanners, which are optimal to analyze relatively large samples such as Recent *Nautilus* shells (Hoffmann and Zachow 2011; Hoffmann et al. 2014). However, small samples cannot be examined successfully because a high resolution cannot be achieved with this method (> a couple of hundreds of micrometers), which also produces partial volume effect. This effect is caused by materials with the same density and different thickness, which thus do not provide the same contrast. Microtomography (μCT) recently became an important tool in palaeontological studies (plants, vertebrates and invertebrates) with relatively easy availability and reduced costs. Normally, this method allows for a reasonably high resolution (up to several micrometers) and is suitable for small objects. But the beam is often not strong enough to penetrate some dense specimens or does not provide sufficient contrast between materials of similar X-ray density (Sutton 2008). This was exemplified by some recent studies on fossilized cephalopods (Kruta et al. 2011; Hoffmann et al. 2014; Naglik et al. 2015a). Tomography based on synchrotron beam lines has been recently employed to acquire both exceptionally high contrast and resolution with high-resolution detectors (Chaimanee et al. 2003; Hagadorn et al. 2006; Friis et al. 2007; Kruta et al. 2011; Takeda et al. 2016). This method allows to examine samples with low attenuation contrast (Sutton 2008) but also produces a huge amount of data per sample (Hoffmann et al. 2014), which makes the post-scanning procedure considerably time-consuming.

Destructive tomography is an alternative to computed tomography and is actually a rather classical methodology (Sollas 1904; Sollas and Sollas 1914; Muir-Wood 1934; Ager 1965; Kermack 1970; Kielan-Jaworowska et al. 1986), including serial grinding, sawing, slicing, methods summarized as physical-optical tomography in Sutton et al. (2014). Although X-ray computed tomography is sufficient to reconstruct materials with high attenuation, it does not yield images with sufficient contrast for materials with low attenuation. Instead, the destructive method underwent some technological revolution with the introduction of digital photography, which enables convenient visualization (Sutton 2008). Thus, although it is destructive, this method is still often applied and high-quality reconstructions have been achieved recently (Sutton et al. 2001, 2012, 2014; Sutton 2008; Garwood et al. 2010; Naglik et al. 2015a, 2016). Another advantage of this method is that color information is retained, which is useful in segmentation of complex elements of a sample. Yet, the post-scanning segmentation process is still very time-consuming. Reconstructed 3D models started to be used to analyze essential parameters of internal conch structures such as volumes (Naglik et al. 2015a, 2016). Depending on the purpose, material, required resolution and contrast, a suitable method may be selected (Fig. 6).

Applications of 3D-analyses in palaeontology beyond visualization

Applications of tomography techniques to palaeontological objects help to better understand morphology, function and ecology of extinct organisms. Methods, which are necessary to carry out such analyses, were developed in the field of vertebrate palaeontology, likely because X-ray computed tomography can be more easily applied to materials with high attenuation such as bone. First, some researchers applied three-dimensional morphometry to vertebrate skulls (e.g., Goswami et al. 2011). Also, mammal teeth were sometimes analyzed with tomography data (3D micro wear texture analysis; e.g., Ungar et al. 2010). Other techniques include finite-element analysis (testing of stress and strain in skulls; e.g., Rayfield et al. 2001) and body size estimation of dinosaurs (e.g., Hutchinson et al. 2007). As far as fossil and modern cephalopods are concerned, there is only a limited number of researchers, who applied CT data to the above mentioned fields. Naglik et al. (2015a) employed physical-optical tomography with serial grinding (grinding tomography) to reconstruct Palaeozoic ammonoids and calculated volumes of phragmocone chamber volumes. Naglik et al. (2016) tested buoyancy and shell orientation of the reconstructed Palaeozoic ammonoids. Lemanis et al. (2015; 2016a, b) applied high resolution computed tomography to ammonoid and modern cephalopod shells for buoyancy reconstruction, examination of curvature and finite element analysis. However, quantitative analyses of cephalopod conchs have not been carried out previously. In Chapter III and IV, I applied destructive and non-destructive tomography techniques to fossil and modern cephalopod quantitatively.

Chapter I

Cephalopod associations and palaeoecology of the Cretaceous (Barremian-Cenomanian) succession of the Alpstein, northeastern Switzerland

Tajika, A. Kürsteiner, P. Pictet, A. Lehmann, J. Tschanz, K. Jattiot, R. Klug, C.

Published in
Cretaceous Research
70: 15-54

Cretaceous Research 70 (2017) 15–54

Contents lists available at ScienceDirect

Cretaceous Research

journal homepage: www.elsevier.com/locate/CretRes

Cephalopod associations and palaeoecology of the Cretaceous (Barremian–Cenomanian) succession of the Alpstein, northeastern Switzerland

Amane Tajika [a, *], Peter Kürsteiner [b], Antoine Pictet [c], Jens Lehmann [d], Karl Tschanz [e], Romain Jattiot [a], Christian Klug [a]

[a] Paläontologisches Institut und Museum, Universität Zürich, Karl Schmid-Strasse 4, CH-8006 Zürich, Switzerland
[b] Naturmuseum St. Gallen, Rorschacherstrasse 263, CH-9016 St. Gallen, Switzerland
[c] Institute of Earth Sciences, Bâtiment Géopolis, CH-1015 Lausanne, Switzerland
[d] Fachbereich Geowissenschaften, Universität Bremen, Klagenfurter Strasse, 28359 Bremen, Germany
[e] Schneeglöggliweg 37, CH-8048 Zürich, Switzerland

ARTICLE INFO

Article history:
Received 10 June 2016
Received in revised form
19 September 2016
Accepted in revised form 25 September 2016
Available online 28 September 2016

Keywords:
Ammonoids
Nautilids
Palaeoecology
Taxonomy
Alpstein
Switzerland

ABSTRACT

The Alpstein (cantons of Appenzell Ausserrhoden, Appenzell Innerrhoden and St. Gallen, northeastern Switzerland) has been of great interest for geologists over the last decades because of its excellent outcrops. However, there was no comprehensive overview over its Cretaceous fossil content. Here, we describe the cephalopod associations, which are moderately to highly diverse in some strata of the Alpstein. Furthermore, we document the regional palaeoecological changes that occurred during the radiation of heteromorph ammonites (ancyloceratids, scaphitids, turrilitids). To examine the palaeoecological changes, we quantitatively determined the macrofossil content of 11 associations of Barremian to early Cenomanian age. Here, we document 6 species (3 genera) of nautilids and 77 species (45 genera) of ammonoids (29 of the species are recorded from Switzerland for the first time). Our palaeoecological analyses revealed the disappearance of nektoplanktonic forms after the late Barremian to the middle early Aptian in the course of the development of a shallow carbonate platform. The upper lower Aptian to middle Albian strata were eroded due to successive emersion phases and condensation processes. In the late Albian, the number of nektoplanktonic species surged again with some benthos, followed by the Cenomanian fauna, which is dominated by nektoplanktonic elements including ammonites, belemnites and nautilids with only very little benthos. These results correlate well with the regional sea level fluctuations.

1. Introduction

The Ammonoidea is a well-known and highly diverse invertebrate group. Because of their high evolutionary rates, ammonoids are widely used as index fossils for about two centuries. Especially during the Jurassic and Cretaceous periods, ammonoids evolved a high diversity and morphological disparity (Page, 1996) combined with a commonly high intraspecific variability (e.g., De Baets et al., 2015; Tajika et al., 2015a). Remarkably, several taxa of three-dimensionally coiled ammonites evolved (heteromorphs; e.g., Cecca, 1997; Guex, 2006).

The Early Cretaceous was a time when large-scale plate tectonic movements and sea level changes (Haq, 2014) affected many ammonite habitats and their dispersal (Lehmann et al., 2015). Although a lot of research has been carried out on global sea-level changes (e.g., Mörner, 1981; Haq, 2014), which strongly influenced the dispersal of ammonoids, the number of regional datasets on alpha diversity and palaeoecology are low. Such studies are important because they contribute primary data to better understand the larger scale palaeoecological changes. In turn, this improved knowledge will increase our understanding of ammonoid autecology including aspects such as habitat and dispersal (e.g., Lukeneder, 2015).

* Corresponding author.
E-mail address: amane.tajika@pim.uzh.ch (A. Tajika).

http://dx.doi.org/10.1016/j.cretres.2016.09.010
0195-6671/

Recently, Bush et al. (2007) introduced a novel approach using a three dimensional ecospace model. Comparison of palaeoecology between geological units both through geologic time and between regions or localities using this ecospace approach provides profound information on palaeoenvironmental changes through time and space.

In the Alpstein (cantons of Appenzell Innerrhoden and Ausserrhoden as well as St. Gallen, Switzerland), a large amount of work has been dedicated to sedimentology and structural geology for the past decades due to its excellently exposed Cretaceous deposits (Funk, 1969; Trümpy, 1980; Föllmi and Ouwehand, 1987; Ouwehand, 1987; Bodin et al., 2006; Sala et al., 2014; Bonvallet, 2015; Wohlwend et al., 2015). The overview of lithofacies of the Alpstein is more or less summarized in Eugster et al. (1982). Although the mostly carbonatic deposits of the Cretaceous sequence (mainly Hauterivian to Cenomanian) contain a large number of macro- and microfossils, the regional biofacies have been studied only sporadically (for the Barremian see, e.g., Bodin et al., 2006). To fill this gap in knowledge, we have sampled eleven highly fossiliferous layers throughout the section in order to obtain semiquantitative data for alpha-diversity and other palaeoecological analyses.

In this study, we (1) document the available cephalopod taxa from the Alpstein (Barremian to Cenomanian), (2) semi-quantitatively analyse palaeoecolgical changes from the Barremian to Cenomanian using macrofossils with a focus on ecospace utilisation through time and (3) discuss palaeoenvironmental factors and their changes.

2. Locality and geological setting

The Helvetic nappes, which belong to the northern Tethyan margin, extend from northeastern to southwestern Switzerland (Fig. 1; Bodin et al., 2006). The Alpstein massif (Fig. 2A) is located in northeastern Switzerland close to the border to Austria. In this region, the mountains Altmann (2436 m), Säntis (2502 m), and Wildhuser Schafberg (2373 m) are situated. Being part of the Alpstein massif, they mainly consist of Cretaceous deposits of the "Säntis-Decke" (Säntis nappe), which is detached from the Jurassic succession by the Säntis Thrust (Sala et al., 2014). The investigated sedimentary sequence is as follows:

Tierwis Formation (uppermost Hauterivian to upper Barremian; Funk, 1969; Fig. 2B): The Tierwis Formation consists of two subunits, the Altmann Member and the Drusberg Member. The Altmann Member is composed of glauconite-rich marls and sandy limestones with abundant trace fossils that are occasionally pyritized. More condensed and phosphatic layers contain ammonites in a moderate to high abundance. The Drusberg Member lies above the Altmann Member, which is characterized by alternating marl and marly limestones. The latter also contains macrofauna, mostly benthos such as sea-urchins, bivalves and brachiopods, and rarely, necton such as ammonites.

Schrattenkalk Formation (upper Barremian to middle lower Aptian; Bollinger, 1988): The Schrattenkalk Formation is characterized by massive light grey limestones, which often contain many bioclasts. The sediments are from a shallow marine setting with abundant corals, sponges, algae, rudist bivalves and thick-shelled gastropods. The Schrattenkalk Formation is separated into two thick limestone layers (Lower and Upper Schrattenkalk Members) which are separated by the Rawil Member (Schenk, 1992; Föllmi et al., 2007). The Rawil Member, also formerly referred to as Lower Orbitolina Beds, starts with marly to sandy limestone beds which contain a rich benthic fauna of echinoids (*Heteraster oblongus*, *Leptosalenia prestensis*) and gastropods (*Harpagodes pelagi*) occasionally accompanied by wood remains. The Rawil Member lies in the middle of the Schrattenkalk Formation, starting with marly beds containing some wood remains. The marly Orbitolina Bed at the top of the Rawil Member marks the boundary between the Barremian and the lowermost Aptian (Bonvallet, 2015). These layers are rich in the foram *Orbitolina* as well as abundant sea-urchins (*Heteraster olbongus*, *Leptosalenia prestensis*). The boundary between the Upper Schrattenkalk Member and the Garschella Formation is marked by a layer with phosphorites that also contains fossils (e.g., belemnoid rostra; Föllmi, 1986, 1989a; Ouwehand, 1987).

Garschella Formation (upper lower Aptian to lowermost Cenomanian; Föllmi and Ouwehand, 1987; Fig. 2D): In the Säntis area, a large part of the Aptian (Grünten, Brisi Members and lower part of the Selun Member) is missing due to erosion, non-deposition and condensation processes, resulting in a 13 m.y. hiatus. The Garschella Formation commences with dark greenish marls and marly limestones at the base (Sellamatt Beds; Föllmi and Ouwehand, 1987), containing several fossiliferous, phosphatic conglomerates (Durschlägi and Wannenalp Beds; Föllmi and Ouwehand, 1987). These are overlain by glauconitic limestones with greyish limestone nodules in various sizes and amounts (Aubrig Beds; Föllmi and Ouwehand, 1987). This upper part of the Garschella Formation contains some indications for condensation such as fragmented ammonoids, phosphoritic internal moulds of fossils, and the fact that several ammonite zones are comprised in this thin sedimentary sequence. At the top of the Garschella Formation, glauconitic sandstones and nodular limestones are deposited, namely a condensation horizon called Kamm Bed that yields abundant and highly diverse ammonoid faunas.

Seewen Formation (lower Cenomanian–lower Santonian: Bolli, 1944; Föllmi, 1986; Fig. 2E): The Seewen Formation is characterized by light greyish pelagic limestone successions. At the base of the Seewen Formation, a bed with abundant ammonoids including large puzosiids (Fig. 2F), rare large turrilitids and normal-sized belemnoids can be found (exposed between Tierwis and the summit of Säntis).

3. Material and methods

All the examined fossils are from the Alpstein, Switzerland (Figs. 1, 2). Most of them were collected by Peter Kürsteiner (St. Gallen) and Karl Tschanz (Zürich). Further specimens were kindly put at our disposal by Urs Oberli (St. Gallen) and Thomas Bolliger (Aathal). Our own fieldwork yielded further specimens. Most of these specimens will be deposited in the Naturmuseum St.Gallen with the numbers NMSG (Coll. followed by initials of the collector and a number). Abbreviations of the collector names are PK (Peter Kürsteiner), KT (Karl Tschanz), UO (Urs Oberli), TB (Thomas Bolliger) and AT (Amane Tajika). Further specimens were examined in the collections of the Federal institute of technology, Zurich (ETH ZH). These are stored in the ETH collections with the abbreviation ETHZ. Exact localities for collections of the ETH ZH and the Naturmuseum St.Gallen are often uncertain. Localities from which most of our specimens were collected are indicated in Fig. 1B.

For palaeoecological analyses, we sampled distinct fossiliferous layers between Tierwis and pillar 2 (second pillar of the cable car Schwägalp-Säntis "Stütze 2", below the summit of Säntis). Wherever possible, we tried to achieve a minimum sample size of 100 determinable specimens in order to obtain statistically representative data.

To quantitatively analyse the palaeoecological changes through geologic time, the method to compare ecospace utilization introduced by Bush et al. (2007) was employed. Accordingly, all fossils

were classified based on the ecological parameters tiering, motility and feeding mechanism and were subsequently plotted into the three-dimensional ecospace. The assignment to an ecological guild was carried out following Table 1 in Bush et al. (2007). Moreover, we added some taxa missing in Bush et al. (2007) in accordance with our fossils. The revised classification is summarized in Table 1. It should be noted that studies on ammonoid palaeoecology suggest different modes of life in ammonoids (planktonic or nektonic). Their mode of life probably changed throughout ontogeny (Ritterbush et al., 2014; Lukeneder, 2015; Moriya, 2015). Nevertheless, ammonoid habitat and mode of life is still not completely unravelled. In fact, many of the aspects cannot be fully tested. Thus, we considered ammonoids including heteromorphs to be part of the pelagic habitat with free and fast motility on the basis of the recent buoyancy reconstruction of ammonoids (Hoffman et al., 2015; Naglik et al., 2015; Tajika et al., 2015b). However, the ecological differences between various ammonoids would not affect the results of our palaeoecological study. Fossils are often poorly preserved and thus difficult or impossible to determine at the species level. Nevertheless, identifications allow assigning them to an ecospace unit sensu Bush et al. (2007).

To investigate changes of palaeoecology from the Barremian to Cenomanian, macrofossils were counted in the field. We started counting fossils with a layer of the condensed phosphatic limestones of the Altmann Member (lower Barremian; mixing of *N. pulchella* and *K. compressissima* Zones). A total of 156 fossils were counted and assigned to modes of life. Due to the lack of fossiliferous layers in the upper part of the Tierwis Formation (Drusberg Member), only fossils from above the mentioned layer have been counted for the palaeoecological analysis.

The Schrattenkalk Formation contains mostly bioclastic shallow water limestones in its upper part. We counted fossils from eight different bedding planes (S1–S8; for their stratigraphic position see Fig. 3). Fossils were counted within 4.0 m^2 (S1), 0.50 m^2 (S2), 0.040 m^2 (S3), 0.048 m^2 (S4), 22.50 m^2 (S5), 22.50 m^2 (S6), 4.0 m^2 (S7) and 0.024 m^2 (S8). The numbers of determined fossils that could be assigned to a mode of life are 88 (S1), 207 (S2), 210 (S3), 322 (S4), 96 (S5), 92 (S6), 45 (S7) and 80 (S8).

The Garschella Formation contains some phosphatic and condensed layers, which are represented in the Twariberg Niederi, Sellamatt, Wannenalp, Aubrig, and Kamm Bed. We focused on two marly limestone layers (Wannenalp Bed), which contain the late Albian *Hysteroceras binum*, *H. crassicostatum*, *H. orbignyi*, *H. varicosum*, and *Mortoniceras inflatum*. It should be noted that the fauna from the examined marly limestone layers may not represent a single environment in time, considering that the above-mentioned ammonoids sometimes co-occur due to condensation and reworking (e.g., Kidwell and Bosence, 1991). Nevertheless, the faunal mixing (time averaging) is low enough to demonstrate a distinct change in palaeoenvironment from shallow water organisms (dominated by rudists, corals, sponges and algae) to deeper water (dominated by ammonoids, belemnoids and nautilids). Due to the 13 m.y. hiatus at the top of the Urgonian platform and faunal mixing, fine ecological details of the ecological transition from a very shallow, photic zone carbonate platform environment to a deeper, pelagic environment dominated by nektoplanktonic forms cannot be extracted. However, the major change could be documented from the differences in faunal assemblages from the early Aptian to late Albian, because we did not find the shallow water indicators such as corals, sponges and photosynthetic organisms being mixed into the younger fauna. A total of 251 fossils from the Garschella Formation was plotted into ecospace (Wannenalp and Aubrig Beds). The Kamm Bed also shows condensation documented in the co-occurrence of the latest Albian *Stoliczkaiella* with the early Cenomanian *Mantelliceras saxbii*. A total of 240 specimens from the Kamm Bed were plotted into the ecospace graph. At the base of the Seewen Formation (lower Cenomanian), 98 specimens were counted on a widely exposed bedding plane.

The morphologic terms for the description of cephalopods were adopted from Arkell (1957) and Korn (2010). Further details are given in Klug et al. (2015). Abbreviations of the measurements of conchs are dm (conch diameter), ww (whorl width), wh (whorl height) and uw (umbilical width).

4. Results

4.1. Cretaceous cephalopod associations of the Alpstein

From all stratigraphic levels, a total of 6 species (3 genera) of nautilids and 77 species (45 genera) of ammonoids were documented (see the systematic palaeontology section). The Tierwis Formation (upper Hauterivian to upper Barremian) yielded 3 species (2 genera) of nautilids and 16 species (12 genera) of ammonoids; we counted 4 species (2 genera) of nautilids and 27 species (17 genera) from the Garschella Formation (except the Kamm Bed); the Kamm Bed alone yielded 3 species (1 genus) of nautilids and 42 species (25 genera) of ammonoids. The Barremian ammonite associations of the Alpstein are dominated by weakly ornamented forms such as *Barremites*, followed by strongly ornamented Holcodiscidae and heteromorphic forms. The late Albian ammonite associations are dominated by heteromorphic forms, while the early Cenomanian ammonoid fauna contains many large puzosiids with smooth conchs and moderately sized, strongly ornamented acanthoceratids.

Here, we document 29 species, which we report from Switzerland for the first time: *Cymatoceras subradiatum* (d'Orbigny, 1850), *Eutrephoceras sublaevigatum* (d'Orbigny, 1850), *Torcapella davydovi* (Trautschold, 1886), *T. falcata* Busnardo, 1970, *Puzosia lata* Seitz, 1931, *Hysteroceras binum* (Sowerby, 1815), *H. crassicostatum* (Jayet, 1929), *H. varicosum* (Sowerby, 1824), *Mortoniceras* cf. *inflatum* (Sowerby, 1818), *Dipoloceras* cf. *pseudaon* Spath 1931, *Stoliczkaiella* (*Lamnayella*) *juigneti* Wright and Kennedy, 1978, *S. (L.) crotaloides* (Stoliczka, 1864), *Astieridiscus morleti* (Kilian, 1889), *Parasaynoceras tzankovi* (Avram, 1995), *Tetragonites timotheanus timotheanus* Pictet, 1847, *Kossmatella muhlenbecki* (Fallot, 1885), *Douvilleiceras* sp., *Hamulinites* sp., *Sciponoceras roto* Cieśliński, 1959, *Hamites simplex* d'Orbigny, 1842, *Ham.* cf. *maximus* Sowerby, 1814, *Ham.* cf. *similis* Casey, 1961, *Ostlingoceras costulatum* (Pervinquiére, 1910), *Hypoturrilites* cf. *sharpei* Wright and Kennedy, 1996, *Hyp. gravesianus* (d'Orbigny, 1842), *Neostlingoceras carcitanense* (Matheron, 1842), *Eoscaphites subcircularis* (Spath, 1937), *Hyphoplites curvatus curvatus* Mantell, 1822, *Gorethophylloceras subalpinum* (d'Orbigny, 1841).

4.2. Palaeoecological changes from the Barremian to Cenomanian

Fossil abundances and ecological classification based on Bush et al. (2007) are summarized in Fig. 4 and Table 2. The results illustrate distinct faunal turnovers from the Barremian through to the early Cenomanian. Nektoplanktonic organisms dominate the faunules of the Barremian, late Albian and early Cenomanian, while faunules exclusively with benthos are from the late Barremian throughout to the early Aptian.

5. Systematic palaeontology

Order Nautilida Grey, 1821
Family Cymatoceratidae Spath, 1927

Genus *Cymatoceras* Hyatt, 1884

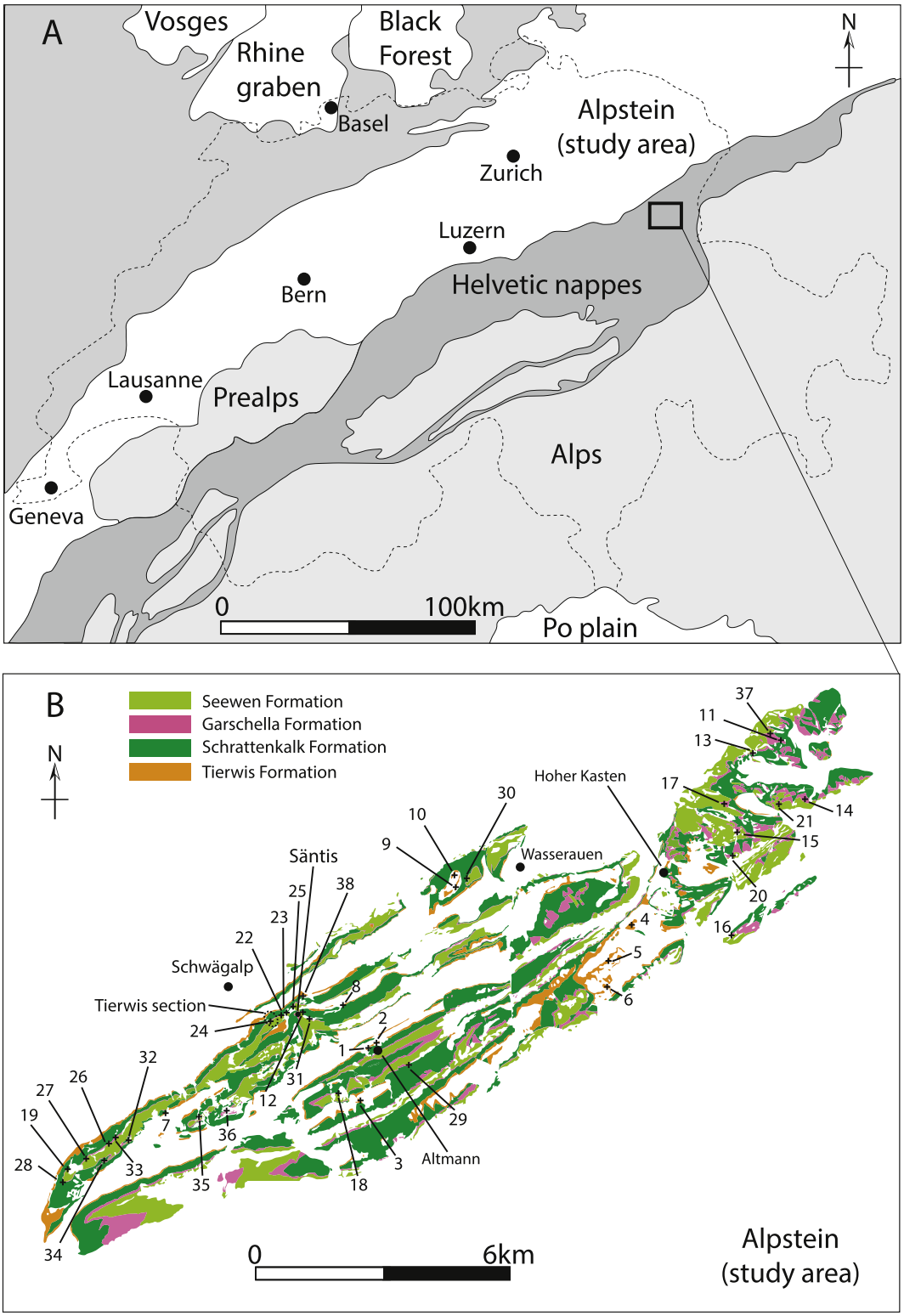
A
Vosges
Rhine graben
Black Forest
Basel
Zurich
Alpstein (study area)
Luzern
Bern
Helvetic nappes
Lausanne
Prealps
Alps
Geneva
0
100km
Po plain
N
B
Seewen Formation
Garschella Formation
Schrattenkalk Formation
Tierwis Formation
N
Hoher Kasten
Wasserauen
Säntis
Schwägalp
Tierwis section
Altmann
0
6km
Alpstein (study area)

Fig. 2. Field images from the Alpstein near Tierwis. A, Tierwis area seen from Stütze 2. B, Tierwis Formation and Schrattenkalk Formation. C, Schrattenkalk Formation. D, Garschella Formation and Kamm Bed. E, cross sections of acanthoceratid ammonites at the base of the Seewen Formation. F, cross section of a big puzosiid ammonite at the base of the Seewen Formation.

Cymatoceras* cf. *neocomiense (d'Orbigny, 1840)
Fig. 5E, F

Synonymy. See Delanoy et al. (2012).
Lectotype. *Nautilus neocomiensis* d'Orbigny, 1840; p. 74, 5, 91, 95, 97, pl.11, fig 1–3.

Material. 1 deformed and eroded phragmocone fragment (NMSG Coll. PK. 7.B.06.01). A slightly compressed phragmocone with one completely eroded side (NMSG Coll. PK. 5A.13.05).
Locality and horizon. Oberrieter Chienberg, Garschella Formation, Albian (NMSG Coll. PK. 7.B.06.01); Wis (SW Alp Rohr); Altmann

Fig. 1. Location & geological map of the Alpstein. A. Location of the Alpstein. Simplified from Bodin et al. (2006). B, Localities in which fossils are collected (simplified from Eugster et al., 1982). 1, Altmann-Sattel, Südwest-Seite I. 2, Altmann-Sattel Nordost-Seite I. 3, Litten, Chreialp. 4, Wis (SW Alp Rohr). 5, Vorderalp, Frümsner Alp. 6, Chobel, Frümsner Berg. 7, Obertal (W Lütispitz). 8, Lochtem-Wagenlücke. 9, Chobel, Gartenalp. 10, Gartenwald, N Chobel. 11, Oberrieter Chienberg. 12, Säntis, Gasthaus-Galerie and surrounding. 13, Oberrieter Strüssler SE. 14, Schlatt (above Rüthi SG). 15, In Ränken, Plona. 16, Bergli, Sennwald. 17, Stofel, Lenziwis. 18, Wildhuser Schafboden gegen Pt. 2171. 19, Tal W II (NE Neuenalpspitz). 20, Chelen-Geren (SW Plona). 21, Unter-Hard, Rüthi SG. 22, Tierwis-Stütze 2 Säntisbahn I. 23, Stütze 2 Säntisbahn S. 24, Tierwis NE II. 25, Stütze 2 – Girenspitz/Säntis, Weg. 26, Hornwald (Hinter Gräppelen). 27, Tal-Wänneli (NE Neuenalpspitz). 28, Neuenalp-Kamm. 29, Zwinglipass Nordost. 30, Ebenalp, Übergang gegen Gartenalp. 31, Säntis, Gasthaus-Hang. 32, Hinterwinden (Hinter Gräppelen). 33, Hinterwinden-Hornwald (Hinter Gräppelen). 34, Hinderhorn (Hinter Gräppelen). 35, Mutteli. 36, Troosen. 37, Oberrieter Chienberg West. 38, Blauschnee-Girenspitz.

Table 1
Ecologic categories for tiering, motility level and feeding mechanism (modified from Bush et al., 2007).

Ecologic category	Examples
Tiering	
1. Pelagic	ammonoids, belemnoids, fish, nautilids
2. Erect	crinoids, corals, sponges
3. Surficial	echinoids, brachiopods, gastropods
4. Semi-infaunal	"normal" bivalves, rudist bivalves, scaphopods
5. Shallow infaunal	many clams
6. Deep infaunal	the clam *Panope*
Motility level	
1. Freely, fast	ammonoids, belemnoids, fish, some arthropods
2. Freely, slow	gastropods, echinoids, nautilids
3. Facultative, unattached	many clams, polychaetes: Sedentaria
4. Facultative, attached	corals, mussels
5. Non-motile, unattached	reclining brachiopods, scaphopods
6. Non-motile, attached	boring bivalves, rudist bivalves, pedunculated brachiopods, sponges
Feeding mechanism	
1. Suspension	boring bivalves, brachiopods, bryozoans, corals, rudists, scaphopods, sponges
2. Surface deposit	tellinid bivalves, polychaetes
3. Mining	nuculid bivalves
4. Grazing	echinoids, gastropods
5. Predatory	ammonoids, belemnoids, nautilids, fish
6. Other	

Member, uppermost Hauterivian–upper lower Barremian (NMSG Coll. PK. 5A.13.05).
Description. NMSG (Coll. PK. 7.B.06.01) is deformed with a maximum conch diameter of 170 mm. The conch shape is involute (uw/dm = 0.11) and pachyconic (ww/dm = 0.30). The whorl section is much higher than wide (ww/wh = 0.61). Conspicuous falcate ribs are present without bifurcation. The number of ribs per half a whorl is 35.
Discussion. This species is one of the most compressed species of *Cymatoceras*. *C. bifurcatum* is similarly compressed, but it differs in having bifurcating ribs. According to Pictet (1847), *C. neckerianum* is similar to this species but less compressed.
Occurrence. Lower Cretaceous (Hauterivian–Albian); Spain, France, Germany, Switzerland, Austria, Hungary, Romania, Bulgaria, Ukraine, Turkey, Iran, Turkmenistan, Algeria, Japan.

Cymatoceras subradiatum (d'Orbigny, 1850)
Fig. 5G, H

1840 *Nautilus laevigatus*, d'Orbigny. d'Orbigny, p.84–86, 94, 95, 96, 97, pl.17, figs.1–4.
1960 *Eutrephoceras sublaevigatum* (d'Orbigny) 1850. Wiedmann, p.165, pl.19, fig.O, pl.20, fig.A, pl.23, fig.L.
1979 *Eutrephoceras sublaevigatum* (d'Orbigny). Wiedmann and Schneider, p.652, pl.2, figs.2, 3, text-fig.4A.
2006 *Eutrephoceras sublaevigatum* d'Orbigny, 1840. Gauthier, p.20, pl.2, figs. 5a, b, 6.

Holotype. *Nautilus radiatus*, Sowerby, 1822; p. 78, pl.356.
Material. An internal mould of a phragmocone and a partial body chamber with remains of the ventral ornamentation (NMSG Coll. PK. 5A.06.02, NMSG Coll. PK. 5A.05.02. A well preserved internal mould with some shell remains (ETHZ 10435).
Locality and horizon. Altmann-Sattel Nordost-Seite I (NMSG Coll. PK. 5A.06.02), Altmann-Sattel, Südwest-Seite I (NMSG Coll. PK. 5A.05.02), Altmann Member, late lower Barremian; Toggenburg, ? Altmann Member, uppermost Hauterivian–upper lower Barremian (ETHZ 10435).
Description. ETHZ 10435 has a maximum diameter of 104 mm. The conch is thickly discoidal (ww/dm = 0.57) and involute (uw/dm = 0.12). The whorl section is slightly wider than high (ww/wh = 1.07). There are 4–5 ribs between two septa on the ventral part. The septa are almost straight or slightly curved, projecting adperturally.
Discussion. This species is close to *C. neckerianum*. Kummel (1956) illustrated whorl sections of *Cymatoceras* in which *C. subradiatum* has a slightly larger umbilicus than *C. neckerianum* and *C. neocomiense* is more compressed.
Occurrence. Lower–Upper Cretaceous (Cenomanian); Spain, England, France, Ukraine, Georgia.

Genus *Eucymatoceras* Spath, 1927

Eucymatoceras plicatum (Fitton, 1835)
Fig. 5A, B, M, N

Synonymy. See Delanoy et al. (2012).
Holotype. *Nautilus plicatus* Fitton, 1835; p. 129, text-fig.
Material. Three large internal moulds of phragmocones with shell remains (NMSG Coll. PK. 5.B.03.19, ETHZ 10434, NMSG Coll. AT. 1).
Locality and horizon. Chobel, Gartenalp, Drusberg Member, Barremian (NMSG Coll. PK. 5.B.03.19); Kohlbett below the Seealpsee, Säntis, ?Barremian (ETHZ 10434); Lochtem-Wagenlücke (NMSG Coll. Tajika 1), Altmann Member, uppermost Hauterivian–upper lower Barremian.
Description. NMSG (Coll. PK. 5.B.03.19) with a maximum diameter of 149 mm. The conch is thinly globular (ww/dm = 0.89) with rounded whorl section and the umbilicus is almost closed (uw/dm = 0.07). The whorl section is wider than high (ww/wh = 2.0). Approximately 30 conspicuous zig zag ribs, which are characteristic for this genus, can be counted per half whorl.
Discussion. The above mentioned characters (the globose conch shape, the zig-zag ribs and the angular part of the zig-zag ribs lying on the venter) corresponds to the illustration (pl. 10, *Nautilus Requienianum*) in d'Orbigny (1840) which is a synonym of *C. plicatum*.
Occurrence. Lower Cretaceous (Albian); England, Spain, France, Germany, Switzerland, Austria, Romania, Bulgaria, Ukraine, Georgia.

Genus *Eutrephoceras* Hyatt, 1894

Eutrephoceras montmollini (Pictet and Campiche, 1859)
Fig. 6A–D

Synonymy. No report with comprehensive description has been published since the original description of Pictet and Campiche (1859).
Syntypes. *Nautilus montmollini* Pictet and Campiche, 1859; p. 147, pl. 18, figs. 4–6.
Material. Internal moulds of phragmocones with some erosion (NMSG Coll. PK. 7.C.02.11, NMSG Coll. PK. 7.C.13.23, NMSG Coll. PK. 7.C.02.19, NMSG Coll. PK. 7.C.02.40, NMSG Coll. PK. 7.B.25.36).
Locality and horizon. Stütze 2 Säntisbahn S (NMSG Coll. PK. 7.C.02.11, 7.C.02.19, 7.C.02.40), Säntis, Gasthaus-Hang (NMSG Coll. PK. 7.C.13.23), Kamm Bed, uppermost Albian–lowermost Cenomanian; Bergli, Sennwald, Garschella Formation, Albian (NMSG Coll. PK. 7.B.25.36).
Description. The specimen NMSG (Coll. PK. 7.C.02.11; dm = 38 mm), is involute (uw/dm = 0.03) and thinly pachyconic (ww/dm = 0.68) with weakly depressed and semi-circular whorl cross section. The whorl section is slightly higher than wide (ww/wh = 1.13; wh/dm = 0.64). The whorls overlap strongly. There are 8 suture lines within half a whorl with broadly rounded median and dorsal saddles.

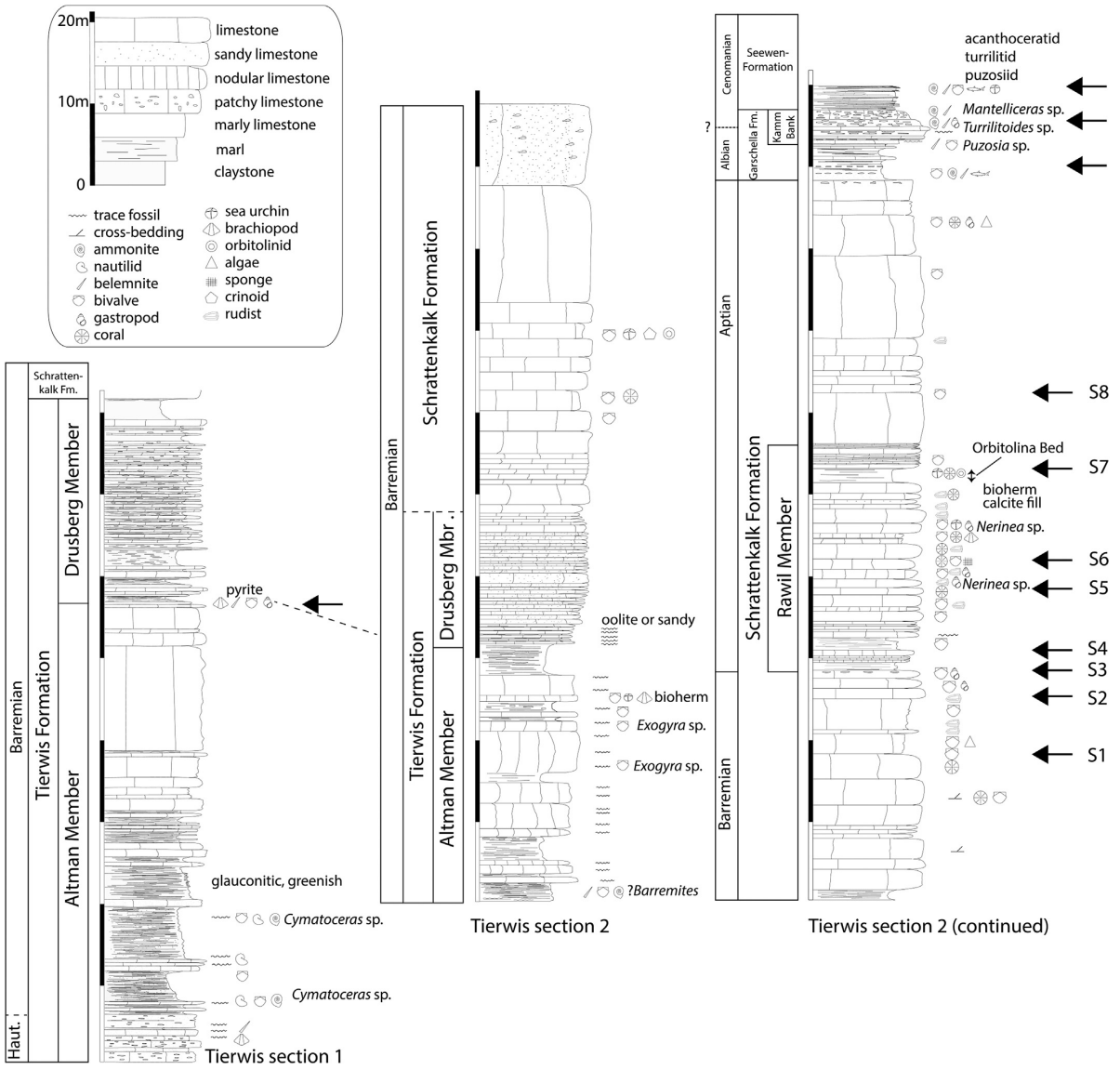

Fig. 3. Stratigraphic sections of the Cretaceous at Tierwis of the Alpstein. Tierwis section 1, Tierwis Formation (Barremian)–Schrattenkalk Formation (Aptian). Tierwis section 2, Tierwis Formation (Barremian)–Seewen Formation (Cenomanian). Arrows indicate bedding planes or horizons in which palaeoecological study was carried out.

Discussion. This species has a very small umbilicus. The specimens have dimensions similar to those of the syntypes measured in Pictet and Campiche (1859). Over the last decades, taxonomic and systematic studies on Cretaceous nautilids have been conducted much less frequently than on Cretaceous ammonoids. A comprehensive revision is required to solve the current taxonomic confusion.
Occurrence. Lower Cretaceous (Barremian–Albian); Germany, Switzerland, Russia.

Eutrephoceras perlatum (Morton, 1834)
Figs. 5I, J, 6G, H

1834 *Nautilus perlatus* Morton, p.33, pl.13, fig.4.
1852 *Nautilus Dekayi*. Giebel, pp.150/1.
1960 *Eutrephoceras dekayi* (Morton). Wiedmann, p.151, 155/6, pl.17, figs.A–C, pl.23, fig.B.
1962 *Eutrephoceras dekayi* (Morton). Miller and Garner, pp. 102–111, pl.65, figs.1–6, pl.66, figs.1,2, pl.67, figs.1–9.

Holotype. *Nautilus perlatus* Morton 1834; p. 33, pl.13, fig.4.
Material. Internal moulds of phragmocones (ETHZ 10430, NMSG Coll. KT. HW-A-0038, NMSG Coll. PK. 7.C.12.07, 7.B.37.08, 7.C.15.08, 7.C.15.30), internal moulds of phragmocones with partial body chamber (NMSG Coll. PK. 7.B.09.02, 7.C.18.01, 7.C.15.08) and a deformed specimen (NMSG Coll. PK.7.B.25.09).

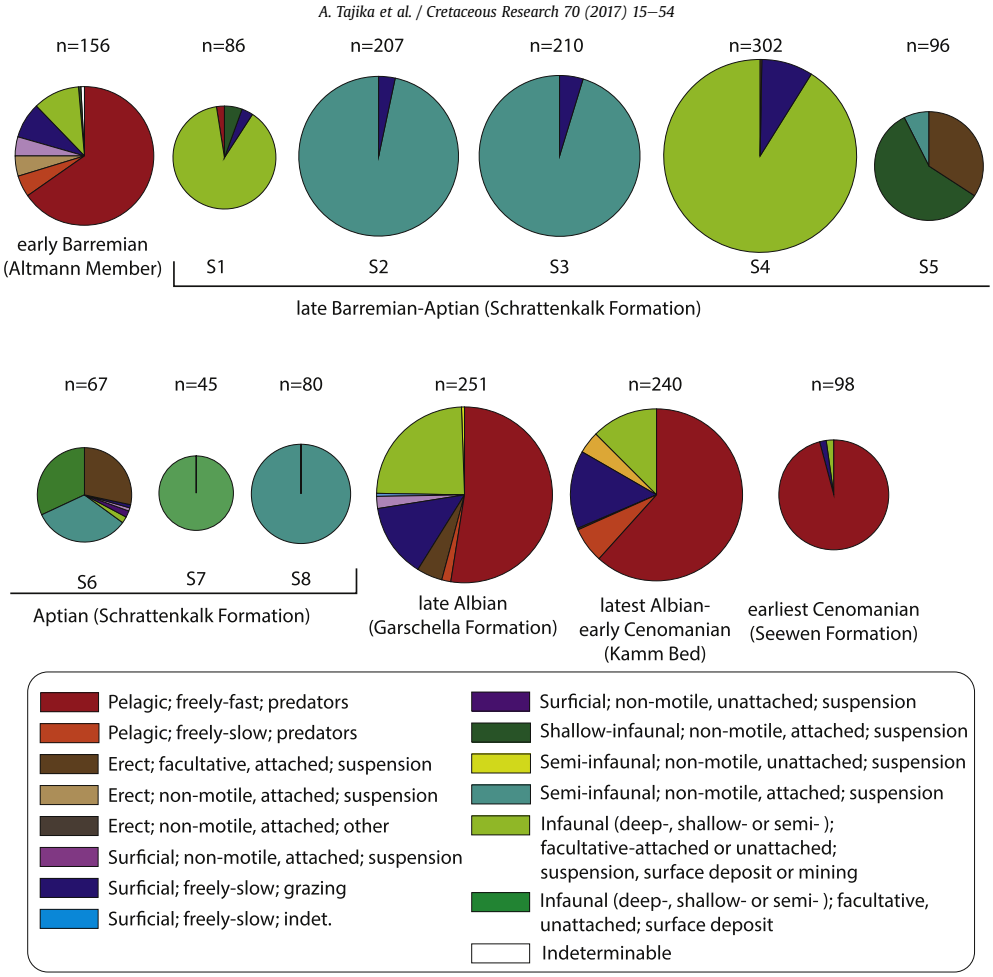

Fig. 4. Changes of ecospace use from the early Barremian (Altmann Member) to the early Cenomanian (Seewen Formation). Relative abundances of ecospace use are plotted. Size of the pie charts represents the sampling size.

Table 2
Fossil abundances from the early Barremian (Altmann Member) to the early Cenomanian (base of the Seewen Formation).

	Lower Barremian (Altmann Mb.)	Upper Barremian–lower Aptian (Schrattenkalk Formation)								Uppermost Albian (Garschella Fm.)	Uppermost Alb.–lowermost Cnm. (Kamm Bank)	Lowermost Cnm. (Seewen Fm.)
		S1	S2	S3	S4	S5	S6	S7	S8			
Ammonites	96									129	143	54
Belemnites	6										2	37
Fish										3	3	3
Nautilids	8									4	16	
Bivalves	17	76			275		2			61	30	2
Boring bivalves		2				7	29					
Bivalves (rudists)			200	200		56	30		80			
Bivlaves (oysters)							2					
Gastropods	1	3	7	10	26		1			31	23	
Corals					1	33				12	1	
Algaes		5					2					
Brachiopods	13						1			6	12	
Echinoids	6							45		4		1
Sponges	7											
Polychaete	1											
Decapod										1		
Scaphopoda										1		
Total	156	86	207	210	302	96	67	45	80	251	240	98

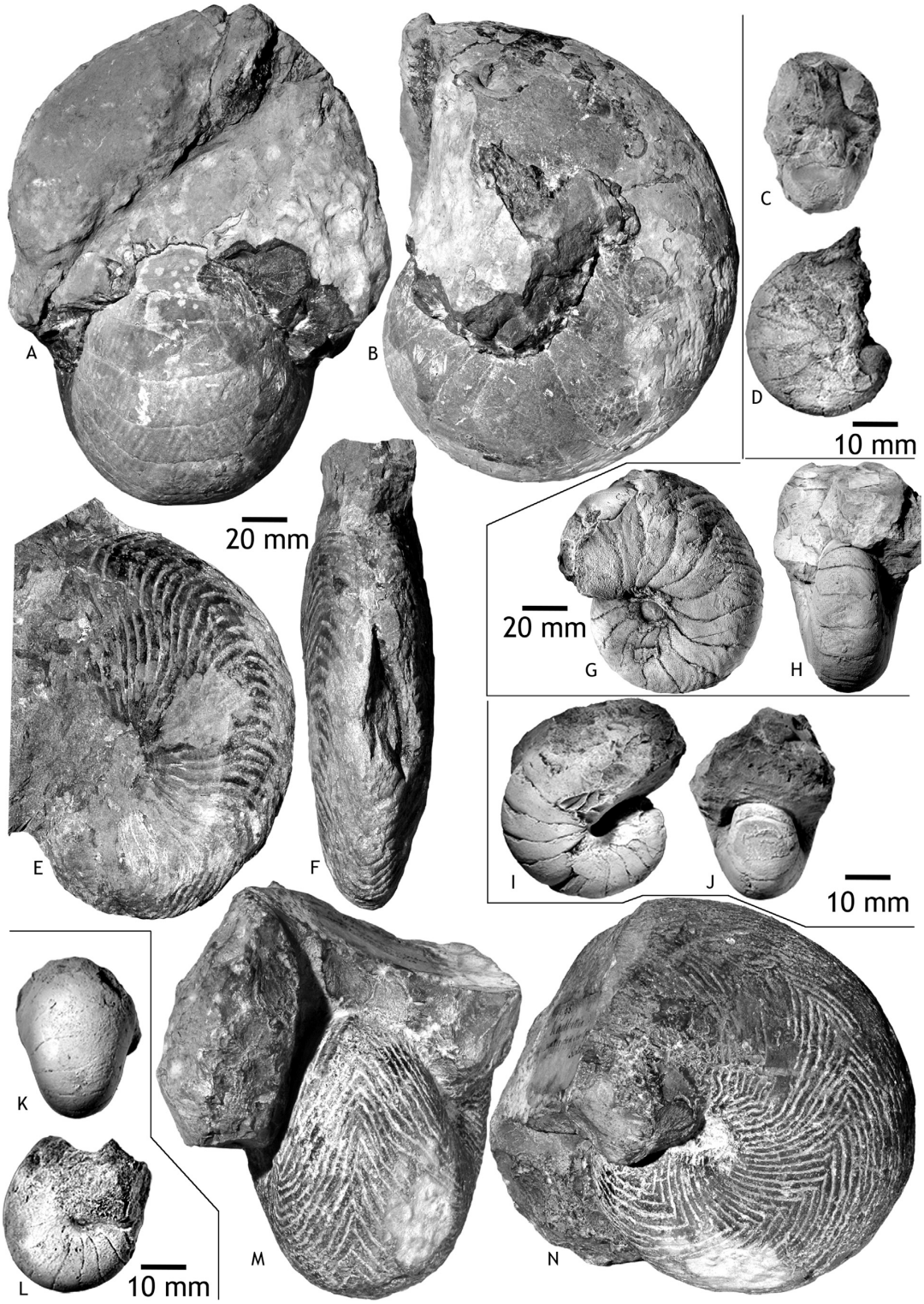

Fig. 5. Nautilids from the Alpstein. A, B, M, N. *Eucymatoceras plicatum* (Fitton, 1835); A, B – NMSG (Coll. AT. 1), Lochtem-Wagenlücke; M, N–ETHZ 10434, Kohlbett below the Seealpsees. C, D, K, L, *Eutrephoceras sublaevigatum* (d'Orbigny, 1850); C, D – NMSG (Coll. KT. HW-A-0039-1), Hinterwinden-Hornwald (Hinter Gräppelen). K, L–NMSG (Coll. PK. 7.B.25.33), Bergli, Sennwald. E, F, *Cymatoceras* cf. *neocomiense* (d'Orbigny), 1840; NMSG (Coll. PK. 7.B.06.01), Oberrieter Chienberg. G, H, *Cymatoceras subradiatum* (d'Orbigny, 1850); ETHZ 10435, Toggenburg. I, J, *Eutrephoceras perlatum* (Morton, 1834); NMSG (Coll. PK. 7.C.18.01), Mutteli.

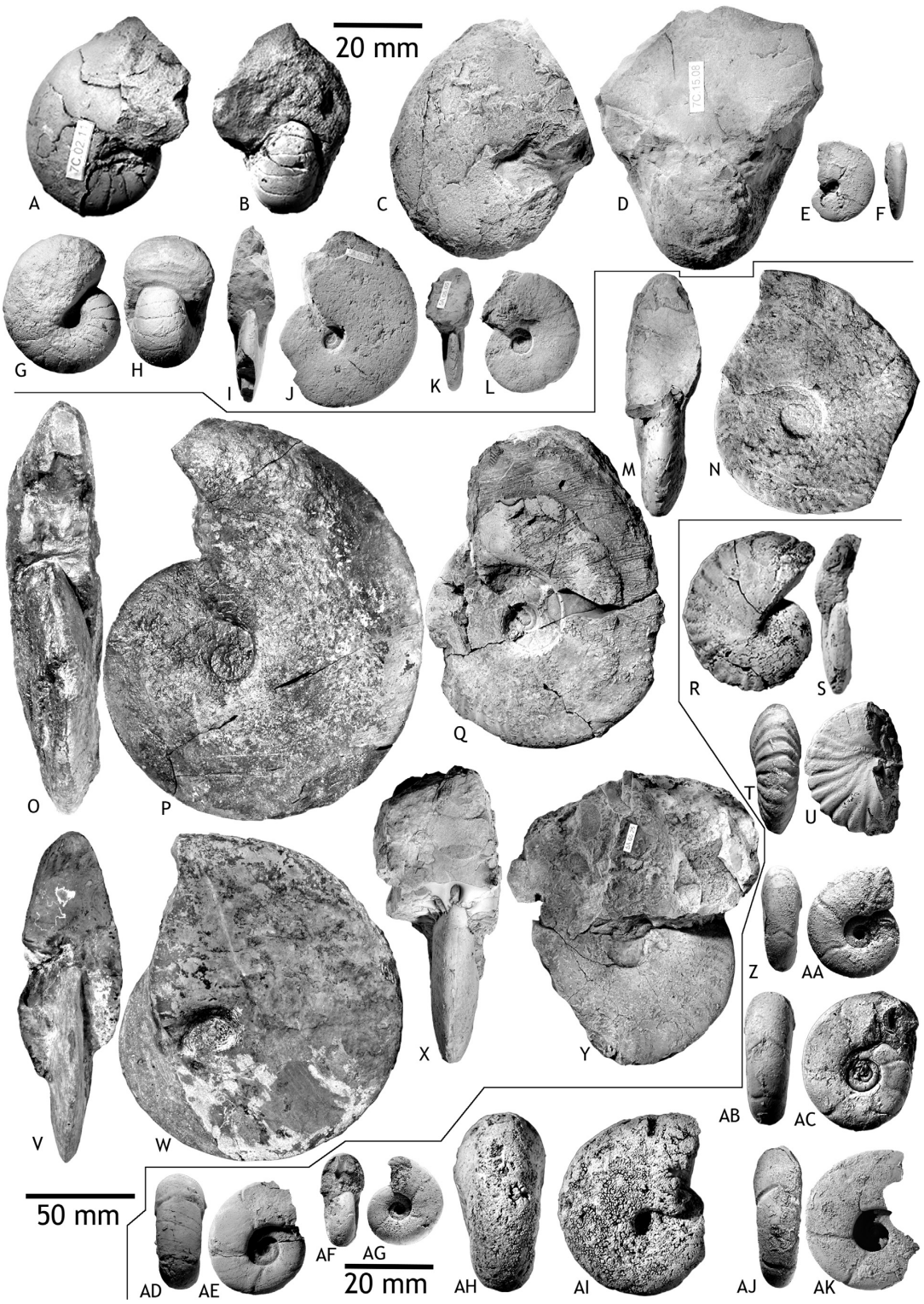
20 mm
A
B
C
D
E
F
G
H
I
J
K
L
M
N
O
P
Q
R
S
T
U
V
W
X
Y
Z
AA
AB
AC
50 mm
AD
AE
AF
AG
20 mm
AH
AI
AJ
AK

Locality and horizon. ?St. Fähnern, Appenzell (ETHZ 10430), ? Albian; Hinterwinden-Hornwald (Hinter Gräppelen) (NMSG Coll. KT. HW-A-0038), Ebenalp, Übergang gegen Gartenalp (NMSG Coll. PK. 7.C.12.07), Mutteli (NMSG Coll. PK.7.C.18.01), Hinterwinden-Hornwald (Hinter Gräppelen; NMSG Coll. PK. 7.C.15.08, 7.C.15.30), Kamm Bed, uppermost Albian–lowermost Cenomanian; Chelen-Geren (SW Plona; NMSG Coll. PK. 7.B.37.08), Säntis, Gasthaus-Galerie and surrounding (NMSG Coll. PK. 7.B.09.02), Bergli, Sennwald (NMSG Coll. PK.7.B.25.09), Garschella Formation, Albian.
Description. NMSG (Coll. PK.7.C.18.01) is 31 mm in maximum diameter. The conch is involute (uw/dm = 0.10) and pachyconic (ww/dm = 0.73) with widely rounded whorl section. The whorl section is higher than wide (ww/wh = 1.39; wh/dm = 0.53). The whorls overlap strongly. The suture line is slightly curved. There are 9 suture lines within half a whorl with very broad median and dorsal saddles.
Discussion. The specimens have conch parameters similar to those of the specimens illustrated on Plates 65–67 in Miller and Garner (1962). Our specimens also show similarities to the holotype in Morton (1834; pl. 13, fig. 4) in coiling and the falcoid suture lines.
Occurrence. Lower–Upper Cretaceous; Germany, Poland, Sweden, Canada, USA (New Jersey, Texas).

Eutrephoceras sublaevigatum (d'Orbigny, 1850)
Fig. 5C, D, K, L

Synonymy. See the revision by Gauthier (2006).
Syntypes. *Nautilus laevigatus* d'Orbigny, 1850; p. 84–86, 94,–97, pl. 17, figs. 1–4.
Material. Internal moulds of phragmocones (NMSG Coll. KT. HW-A-0039-1, NMSG Coll. PK. 7.C.02.41, 7.C.09.02, 7.B.25.33). Internal mould of a phragmocone with a partial body chamber (NMSG Coll. PK. 7.C.12.02).
Locality and horizon. Hinterwinden-Hornwald (Hinter Gräppelen) (NMSG Coll. KT. HW-A-0039-1), Stütze 2 Säntisbahn S (NMSG Coll. PK. 7.C.02.41), Zwinglipass Nordost (NMSG Coll. PK. 7.C.09.02), Ebenalp, Übergang gegen Gartenalp (NMSG Coll. PK. 7.C.12.02), Kamm Bed, uppermost Albian–lowermost Cenomanian; Bergli, Sennwald, Garschella Formation, Albian (NMSG Coll. PK. 7.B.25.33).
Description. NMSG (Coll. PK. 7.B.25.09) measures 33 mm diameter. The conch is involute (uw/dm = 0.06) and thickly pachyconic (ww/dm = 0.78; wh/dm = 0.64) with rounded whorl section. The suture line is slightly curved. The whorls overlap moderately to strongly. There are 9 suture lines with broadly rounded median and dorsal saddle.
Remarks. This species has a small umbilicus and a rounded aperture. The specimens have parameters similar to those of the syntype illustrated on Plate 17 in d'Orbigny (1840).
Occurrence. Lower–Upper Cretaceous (Albian–Santonian); England, Germany, Italy, Czech Republic, Poland, Bulgaria, Libya, India.

Order Ammonoidea Zittel, 1884
Family Barremitidae Breskovski, 1977

Genus *Barremites* Killian, 1913

Barremites* cf. *difficilis (d'Orbigny, 1841)
Fig. 6E, F, I–L, O, P, V, W

Synonymy. See Klein and Vašíček (2011); the species was also referred to by Lukeneder (2012; without description).
Lectotype. *Ammonites difficilis* d'Orbigny, 1841; 9. 135, pl. 41, fig. 3, 4.
Material. 33 internal moulds (NMSG Coll. PK. 5.A.05.05, 5.A.05.25, 5.A.05.46, 5.A.05.48, 5.A.05.65 to 5.A.05.80, 5.A.10.03, 5.A.06.01, 5.A.10.02, 5.A.10.03, 5.A.13.04, 5.A.17.03, 5.A.17.04, NMSG Coll. KT. AS-W-0001, AS-W-0005, AS-W-0022, AS-W-0024, AS-W-0025, NMSG Coll. UO. 001).
Locality and horizon. Altmann-Sattel, Südwest-Seite I (NMSG Coll. PK. 5.A.05.05, 5.A.05.25, 5.A.05.46, 5.A.05.48, 5.A.05.65 to 5.A.05.80, NMSG COLL. KT. AS-W-0001, AS-W-0005, AS-W-0025), Altmann-Sattel Nordost-Seite I (NMSG Coll. PK. 5.A.06.01), Litten, Chreialp (NMSG Coll. PK. 5.A.10.02, 5.A.10.03), Wis (SW Alp Rohr; NMSG Coll. PK. 5.A.13.04), Chobel, Frümsner Berg (NMSG Coll. PK. 5.A.17.03, 5.A.17.04), Spitzbergli (NMSG Coll. UO. 001), Altmann Member, uppermost Hauterivian–upper lower Barremian.
Description. NMSG (Coll. PK. 5.A.05.73) is an internal mould with some shell remains, measuring 41 mm in diameter. The conch is extremely discoidal (ww/dm = 0.20) and involute (uw/dm = 0.15). The whorl section is much higher than wide (ww/wh = 0.38) with a moderately flattened ventral part. Ribs appear to be intercalated by weak lirae. The largest specimens are NMSG (Coll. PK. 5.A.06.01) and NMSG (Coll. PK. 5.A.10.02), measuring 220 mm and 111 mm in conch diameter, respectively. The other specimens range from 35 mm to 76 mm. All the specimens with nearly complete conchs are extremely discoidal (ww/wh = 0.19–0.29) and, in most specimens, involute (uw/dm = 0.10–0.15) while others are subinvolute (uw/dm = 0.16–0.25; NMSG (Coll. KT. AS-W-0005, AS-W-0022), NMSG (Coll. PK. 5.A.06.01, 5.A.05.67, 5.A.13.04). The whorl section is oval to triangular and much higher than wide (ww/wh = 0.38–0.54) with the maximum width in the mid flank. Ribs and constrictions are hardly discernible in all specimens except NMSG (Coll. PK. 5.A.05.75), in which 5 ribs are present per half whorl.
Discussion. Although all the specimens show similar characteristics (very compressed and narrow umbilicus), the ornamentation is poorly preserved, hampering the species-level determination.
Occurrence. Lower Cretaceous (Barremian); France, Switzerland, Italy, Austria, Czech Republic, Romania, Bulgaria, Russia, Egypt, Japan.

Genus *Torcapella* Busnardo, 1970

Torcapella davydovi (Trautschold, 1886)
Fig. 7A, B

Synonymy. See Klein and Vašíček (2011).
Type. *Ammonites davydovi* Trautschold, 1886; p. 141.
Material. 1 eroded conch (NMSG Coll. PK. 5.A.17.01).

Fig. 6. Nautilids and ammonoids from the Alpstein. A–D, *Eutrephoceras montmollini* (Pictet and Campiche), 1859; A, B–NMSG (Coll. PK. 7.C.02.11); C, D–NMSG (Coll. PK. 7.C.02.19), Stütze 2 Säntisbahn S. E, F, I–L, O, P, V, W, *Barremites* cf. *difficilis* (d'Orbigny, 1841); E, F–NMSG (Coll. PK. 5.A.05.74); I, J–NMSG (Coll. PK. 5.A.05.25); K, L–NMSG (Coll. PK. 5.A.05.75), Altmann-Sattel, Südwest-Seite I; O, P–NMSG (Coll. PK. 5.A.06.01), Altmann-Sattel Nordost-Seite; V, W–NMSG (Coll. UO. 001), Spitzbergli. G, H, *Eutrephoceras perlatum* (Morton, 1834); NMSG (Coll. PK. 7.B.09.02) Säntis, Gasthaus-Galerie and surrounding. M, N, *Torcapella* cf. *fabrei* (Torcapel, 1884); NMSG (Coll. PK. 5.A.05.30), Altmann-Sattel, Südwest-Seite I. Q, *Torcapella* sp.; NMSG (Coll. PK. 5.A.05.29), Altmann-Sattel, Südwest-Seite I. R, S, *Kotetishvilia compressissima* (d'Orbigny, 1841); NMSG (Coll. PK. 5.A.05.26), Altmann-Sattel, Südwest-Seite I. T, U, *Nicklesia pulchella* (d'Orbigny, 1841); NMSG (Coll. KT. AS-W-0026), Altmann-Sattel, Südwest-Seite I. X, Y, *Torcapella falcata* Busnardo, 1970; NMSG (Coll. PK. 5.A.05.87), Altmann-Sattel, Südwest-Seite I. Z–AC, *Puzosia* (*Puzosia*) *quenstedti quenstedti* (Parona and Bonarelli, 1897); Z, AA – NMSG (Coll. PK. 7.B.23.34), In Ränken, Plona; AB, AC – NMSG (Coll. PK. 7.C.02.38), Stütze 2 Säntisbahn S. AD, AE, *Puzosia* (*Puzosia*) *provincialis* (Parona and Bonarelli, 1897); NMSG (Coll. PK. 7.B.20.73), Schlatt (above Rüthi SG). AF, AG, *Puzosia* (*Puzosia*) *lata* Seitz, 1931; NMSG (Coll. PK. 7.B.20.74), Schlatt (above Rüthi SG). AH, AI, *Desmoceras* (*Desmoceras*) *latidorsatum* (Michelin, 1838); NMSG (Coll. PK. 7.B.32.04), Wildhuser Schafboden gegen Pt. 2171. AJ, AK, *Puzosia* (*Puzosia*) *mayoriana* (d'Orbigny, 1841); NMSG (Coll. PK. 7.B.23.05), In Ränken, Plona.

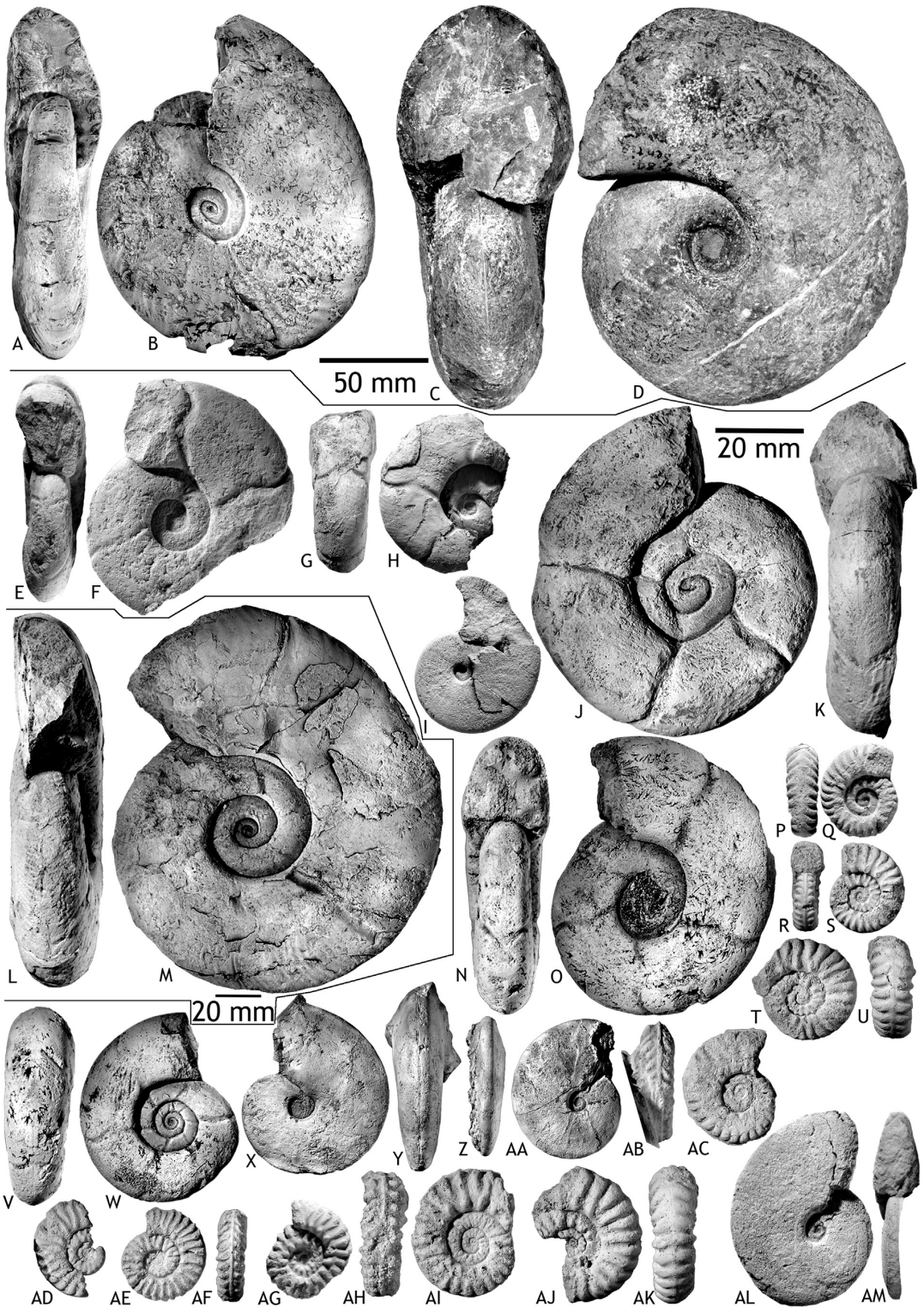
A
B
50 mm
C
D
E
F
G
H
20 mm
J
K
I
L
M
N
O
P
Q
R
S
T
U
20 mm
V
W
X
Y
Z
AA
AB
AC
AD
AE
AF
AG
AH
AI
AJ
AK
AL
AM

Locality and horizon. Chobel, Frümsner Berg, Altmann Member, uppermost Hauterivian–upper lower Barremian.
Description. NMSG (Coll. PK. 5.A.17.01) is a slightly deformed specimen, measuring 132 mm in diameter. The conch is extremely discoidal (ww/dm = 0.30) and subinvolute (uw/dm = 0.22). The whorl section is oval and compressed (ww/wh = 0.72) with maximum whorl width in the mid flank. There are 18 ribs per quarter whorl with falcoid shape.
Discussion. See Busnardo (1970).
Occurrence. Lower Cretaceous (lower Barremian, *Kotetishvilia compressissima* Zone); England, France, Austria, Poland, Bulgaria, Madagascar.

Torcapella falcata Busnardo, 1970
Fig. 6X, Y

Synonymy. See Klein and Vašíček (2011).
Holotype. *Torcapella falcata* Busnardo, 1970; p. 112, pl. 2, fig. 2, textfigs. 34, 35.
Material. 1 eroded conch (NMSG Coll. PK. 5.A.05.87).
Locality and horizon. Altmann-Sattel, Südwest-Seite I, Altmann Member, uppermost Hauterivian–upper lower Barremian.
Description. NMSG (Coll. PK. 5.A.05.87) is a slightly weathered specimen, measuring 147 mm in diameter. The conch is extremely thinly discoidal (ww/dm = 0.28) and involute (uw/dm = 0.15). The whorl section is triangular and very compressed (ww/wh = 0.57) with the maximum whorl width in the mid flank. There are 18 falcoid ribs per quarter whorl.
Discussions. See Busnardo (1970).
Occurrence. Lower Cretaceous (lower Barremian; *K. compressissima* Zone); England, France, Austria, Poland, Bulgaria, Madagascar.

Torcapella* cf. *fabrei (Torcapel, 1884)
Fig. 6M, N

Synonymy. See Klein and Vašíček (2011).
?*Topotype*. *Ammonites fabrei* Torcapel, 1884; p. 1. pl. V.
Material. 1 conch (NMSG Coll. PK. 5.A.05.30).
Locality. Altmann-Sattel, Südwest-Seite I, the Altmann Member, uppermost Hauterivian–upper lower Barremian.
Description. NMSG (Coll. PK. 5.A.05.30) is a weathered specimen, measuring 112 mm in maximum diameter. The conch is extremely discoidal (ww/dm = 0.29) and subinvolute (uw/dm = 0.33). The whorl section is oval and compressed (ww/wh = 0.64) with maximum whorl width on the mid flank. The straight to slightly falcoid ribs, which are apparently not bifurcating, are poorly visible.
Discussion. See Busnardo (1970).
Occurrence. Lower Cretaceous (lower Barremian, *N. pulchella* to *C. darsi* Zone); England, France, Austria, Poland, Bulgaria, Madagascar.

Torcapella sp.
Fig. 6Q

Material. 1 heavily eroded conch (NMSG Coll. PK. 5.A.05.29) and 2 conch fragments (NMSG Coll. KT. AS-W-0003, AS-W-0027).
Locality and horizon. Altmann-Sattel, Südwest-Seite I (NMSG Coll. PK. 5.A.05.29, NMSG Coll. KT. AS-W-0003, AS-W-0027), Altmann Member, uppermost Hauterivian–upper lower Barremian.
Description. NMSG (Coll. PK. 5.A.05.29) measures 112 mm in diameter. The conch is extremely discoidal (ww/dm = 0.26) and subinvolute (uw/dm = 0.21). The whorl section is oval and very compressed (ww/wh = 0.58). Ribs are present, most of which are hardly visible.
Discussion. Most ribs, which are one of the most important diagnostic characters, are not well preserved, thus hampering species assignment.
Occurrence. Lower Cretaceous (lower Barremian, *K. compressissima* Zone; for the genus).

Family Desmoceratidae Zittel, 1895
Subfamily Puzosiinae Spath, 1922

Genus *Puzosia* (*Puzosia*) Bayle, 1878

Puzosia (Puzosia) lata Seitz, 1931
Figs. 6AF, AG, 7J, K

Synonymy. See Klein and Vašíček (2011).
Holotype. *Ammonites planulatus* Quenstedt, 1847; p. 403, pl. 17, figs. 13a, b.
Material. 4 fragments (NMSG Coll. PK. 7.B.20.35, 7.B.20.74, 7.C.15.13, 7.C.23.20).
Locality and horizon. In Ränken, Plona (NMSG Coll. PK. 7.C.23.20), Schlatt (above Rüthi SG; NMSG Coll. PK. 7.B.20.35, 7.B.20.74), Garschella Formation, Albian; Hinterwinden-Hornwald (Hinter Gräppelen; NMSG Coll. PK. 7.C.15.13), Kamm Bed, latest Albian–Cenomanian.
Description. NMSG (Coll. PK. 7.C.15.13) is a slightly deformed specimen, measuring 72 mm in diameter. The conch is subevolute (uw/dm = 0.36) and thinly discoidal (ww/dm = 0.36). The whorl width exceeds whorl height (ww/wh = 1.08). There are four nearly straight to slightly sinuous constrictions per whorl. NMSG (Coll. PK. 7.B.20.74) measures 19 mm in diameter. Its conch is subevolute (uw/dm = 0.33) and thinly discoidal (ww/dm = 0.47). The whorl width exceeds whorl height (ww/wh = 1.13). There are five very slightly sigmoidally bent constrictions per whorl.
Discussion. This species is mainly characterized by its depressed and rounded whorl section with the maximum thickness at the mid-flank.
Occurrence. Lower Cretaceous (middle–upper Albian); France, Italy (Sardinia), Austria, Madagascar, Venezuela.

Puzosia (Puzosia) mayoriana (d'Orbigny, 1841)
Fig. 7E–H, L–O

Synonymy. See Kennedy and Klinger (2014).
Lectotype. *Ammonites planulatus* Sowerby 1827; p. 597, pl. 570, fig. 5.
Material. 13 fragments of phragmocones (NMSG Coll. PK. 7.B.20.19, 7.B.20.46, 7.B.23.05, 7.B.23.13, 7.B.23.14, 7.B.26.19, 7.B.37.09, 7.B.38.02, 7.C.07.01, 7.C.07.04, 7.C.13.12, 7.C.13.40, 7.C.15.22).

Fig. 7. Ammonoids from the Alpstein. A, B, *Torcapella davydovi* (Trautschold, 1886); NMSG (Coll. PK. 5.A.17.01), Chobel, Frümsner Berg. C, D, Puzosiinae indet.; ETHZ 10437, locality, unknown. E–H, L–O, *Puzosia* (*Puzosia*) *mayoriana* (d'Orbigny, 1841); E, F – NMSG (Coll. PK. 7.C.13.12), Säntis, Gasthaus-Hang; G, H – NMSG (Coll. PK. 7.B.23.13), In Ränken, Plona; L, M–NMSG (Coll. PK. 7.C.07.04), Tal-Wänneli (NE Neuenalpspitz); N, O – NMSG (Coll. PK. 7.C.13.40), Säntis, Gasthaus-Hang. I, X–AA, AL, AM, *Beudanticeras* cf. *beudanti* (Brongniart, 1822); I – NMSG (Coll. PK. 7.B.17.01), Oberrieter Strüssler SE; X, Y – NMSG (Coll. PK. 7.B.20.14); Z, AA – NMSG (Coll. PK. 7.B.20.41), Schlatt (above Rüthi SG), AL, AM–NMSG (Coll. PK. 7.B.25.10), Bergli, Sennwald. J, K, *Puzosia (Puzosia) lata* Seitz 1931; NMSG (Coll. PK. 7.C.15.13), Hinterwinden-Hornwald (Hinter Gräppelen). P–S, AD, *Hysteroceras orbignyi* Spath, 1922; P, Q – NMSG (Coll. PK. 7.B.25.02), AD – NMSG (Coll. PK. 7.B.25.35) Bergli, Sennwald; R, S, NMSG (Coll. PK. 7.B.26.06), Stofel, Lenziwis. T, U, *Hysteroceras crassicostatum* (Jayet, 1929); NMSG (Coll. PK. 7.B.26.16), Stofel, Lenziwis. V, W, *Puzosia* (*Puzosia*) cf. *provincialis* (Parona and Bonarelli, 1897); NMSG (Coll. PK. 7.B.26.01), Stofel, Lenziwis. AB, AC, *Hysteroceras binum* (Sowerby, 1815); NMSG (Coll. PK. 7.B.20.36), Schlatt (above Rüthi). AE–AI, *Cantabrigites* sp.; AE, AF – NMSG (Coll. PK. 7.C.15.31), AH, AI – NMSG (Coll. PK. 7.C.15.21), Hinterwinden-Hornwald (Hinter Gräppelen); AG – NMSG (Coll. PK. 7.B.35.01), Tal W II (NE Neuenalpspitz). AJ, AK, *Hysteroceras varicosum* (Sowerby, 1824); NMSG (Coll. PK. 7.B.23.21), In Ränken, Plona.

Locality and horizon. Chelen-Geren (SW Plona; NMSG Coll. PK. 7.B.37.09), In Ränken, Plona (NMSG Coll. PK. 7.B.23.05, 7.B.23.13, 7.B.23.14), Schlatt (above Rüthi SG; NMSG Coll. PK. 7.B.20.46, 7.B.20.19), Unter-Hard, Rüthi SG (NMSG Coll. PK. 7.B.38.02, Stofel, Lenziwis (NMSG Coll. PK. 7.B.26.19, Garschella Formation, Albian; Säntis, Gasthaus-Hang (NMSG Coll. PK. 7.C.13.40), Tal-Wänneli (NE Neuenalpspitz; NMSG Coll. PK. 7.C.07.01), Säntis, Gasthaus-Hang (NMSG Coll. PK. 7.C.13.12), Hinterwinden-Hornwald (Hinter Gräppelen; NMSG Coll. PK. 7.C.15.13, 7.C.15.22), Kamm Bed, uppermost Albian–lowermost Cenomanian.
Description. NMSG (Coll. PK. 7.B.23.14) measures 28 mm in maximum diameter. The conch is sub-involute (um/dm = 0.26) and extremely discoidal (ww/dm = 0.34). The whorl section is much higher than wide (ww/wh = 0.80). There are four constrictions per whorl. NMSG (Coll. PK. 7.C.13.12) has a maximum diameter of 50 mm. The conch is subinvolute (um/dm = 0.27) and extremely discoidal (ww/dm = 0.30). The whorl section is much higher than wide (ww/wh = 0.71). In our specimens, five constrictions were counted per whorl. NMSG (Coll. PK. 7.B.20.46) is a slightly deformed specimen with a diameter of 33 mm. The conch is subevolute (uw/dm = 0.33) and extremely discoidal (ww/dm = 0.33). The whorl section is slightly higher than wide (ww/wh = 0.85). This specimen displays five sinuous constrictions per whorl.
Discussion. See Wright and Kennedy (1984) as well as Cooper and Kennedy (1987).
Occurrence. Lower–Upper Cretaceous (upper Albian–late Cenomanian); western Europe–Iran, India, South Africa (KwaZulu-Natal), USA (off Florida), Japan.

Puzosia (Puzosia)* cf. *provincialis (Parona and Bonarelli, 1897)
Figs. 6AD, AE, 7V, W

Synonymy. See Kennedy and Klinger (2014).
Holotype. *Desmoceras provincialis* Parona and Bonarelli, 1897; p. 81, pl. XI (II), figs. 4a.
Material. 8 fragments of phragmocones (NMSG Coll. PK. 7.B.20.02, 7.B.20.30, 7.B.20.73, 7.B.25.29, 7.B.26.01, 7.B.26.20, 7.B.37.33, 7.B.38.04).
Locality and horizon. Stofel, Lenziwis (NMSG Coll. PK. 7.B.26.01, 7.B.26.20), Chelen-Geren (SW Plona; NMSG Coll. PK. 7.B.37.33), Unter-Hard, Rüthi SG (NMSG Coll. PK. 7.B.38.04), Bergli, Sennwald (NMSG Coll. PK. 7.B.25.29), Schlatt (above Rüthi SG; NMSG Coll. PK. 7.B.20.30, 7.B.20.73), Garschella Formation, Albian.
Description. NMSG (Coll. PK. 7.B.20.73) is a small specimen with a diameter of 24 mm. The conch is subinvolute (uw/dm = 0.26) and thinly discoidal (ww/dm = 0.44). The width and height of the whorl section is almost equal (ww/wh = 0.94). There are 5 or more nearly straight constrictions per whorl. NMSG (Coll. PK. 7.B.26.01) is a well preserved internal mould with a maximum diameter of 42 mm. The conch is sub-evolute (uw/dm = 0.36) and thinly discoidal (ww/dm = 0.36). Width and height of the whorl section are almost equal (ww/wh = 1.00). There are six sinuous constrictions per whorl.
Discussion. The holotype of *Puzosia (Puzosia)* cf. *provincialis* measures 22.5 mm with a subevolute (uw/dm = 0.40) and thinly discoidal conch (ww/dm = 0.44). The whorl section is as high as wide (ww/wh = 1.00). Our specimens agree more or less with the conch parameters of this rather than with those of other species. For details, see Kennedy and Klinger (2014).
Occurrence. Lower–Upper Cretaceous (middle–upper Albian); Spain (Mallorca), Italy (Sadinia), Switzerland, Romania, Bulgaria, Angola, possibly Egypt, Madagascar, Venezuela, Japan.

Puzosia (Puzosia) quenstedti quenstedti (Parona and Bonarelli, 1897)
Fig. 6Z–AC

Synonymy. See Kennedy and Fatmi (2014).
Holotype. *Desmoceras Quenstedti* Parona and Bonarelli, 1897; p. 81, pl. XI (II), figs. 3a, b.
Material. 9 fragments of phragmocones (NMSG Coll. PK. 7.B.20.42, 7.B.23.34, 7.B.23.22, 7.B.26.14, 7.B.25.19, 7.B.25.25, 7B.37.27, 7.C.02.38, 7.C.07.10).
Locality and horizon. Chelen-Geren (SW Plona; NMSG Coll. PK. 7B.37.27), Bergli, Sennwald (NMSG Coll. PK. 7.B.25.19, 7.B.25.25), Schlatt (above Rüthi SG; NMSG Coll. PK. 7.B.20.42), In Ränken, Plona (NMSG Coll. PK. 7.B.23.34, 7.B.23.22), Garschella Formation, Albian; Tal-Wänneli (NE Neuenalpspitz; NMSG Coll. PK. 7.C.07.10), Kamm Bed, latest Albian–Cenomanian; unknown (Stütze 2 Säntisbahn S).
Description. NMSG (Coll. PK. 7.B.23.14) measures 36 mm in diameter. The conch is subinvolute (uw/dm = 0.29) and thinly discoidal (ww/dm = 0.35). The whorl section is higher than wide (ww/wh = 0.79). There are five slightly sinuous constrictions per whorl.
Discussion. According to Marcinowski and Wiedmann (1990), who divided the species into five subspecies, *Puzosia quenstedti quenstedti* is characterized by its whorl section (slightly higher than wide) and a more pronounced ribbing of the external whorls. However, as Kennedy and Klinger (2014) mentioned, there have been various interpretations of this species. Thus, further studies on this group are necessary.
Occurrence. Lower–Upper Cretaceous (upper Aptian–lower Cenomanian); France, Italy (Sardinia), Austria, Pakistan, Madagascar, South Africa (KwaZulu-Natal), Venezuela.

Puzosiinae indet.
Fig. 7C, D

Material. 1 conch (ETHZ 10437).
Locality and horizon. Locality, unknown, Altmann Member, uppermost Hauterivian–upper lower Barremian.
Description. ETHZ 10437 is an internal mould with a diameter of 174 mm. The conch is sub-involute (uw/dm = 0.33) and moderately discoidal (ww/dm = 0.43). Width and height of the whorl section is almost equal (ww/wh = 0.95). Ribs are not preserved.
Discussion. The specimen has an umbilical width index (uw/dm = 0.33) similar to those of the two specimens of *Melchiorites lechicus* (0.29 and 0.34, respectively) figured in plate XV of Uhlig (1883). But our specimen shows much more rounded flanks and lacks constrictions, which are a diagnostic character of *Melchiorites*.
Subfamily Beudanticeratinae Breistroffer, 1953

Genus *Beudanticeras* (*Beudanticeras*) Hitzel, 1902

Beudanticeras* cf. *beudanti (Brongniart, 1822)
Fig. 7I, X–AA, AL, AM

Synonymy. See Klein and Vašíček (2011).
Lectotype. *Ammonites Beudanti* Brongniart, 1822, p. 394, pl. VII, figs. 2A, B.
Material. 7 conchs (NMSG Coll. PK. 7.B.17.01, 7.B.20.03, 7.B.20.04, 7.B.20.14, 7.B.20.41, 7.B.25.10, 7.B.26.03), 1 shell fragment (NMSG Coll. PK. 7.B.20.39).
Locality and horizon. Schlatt (above Rüthi SG; NMSG Coll. PK. 7.B.20.14, 7.B.20.41, 7.B.20.39, 7.B.20.04, 7.B.20.03), Stofel, Lenziwis (NMSG Coll. PK. 7.B.26.03), Oberrieter Strüssler SE (NMSG Coll. PK. 7.B.17.01), Bergli, Sennwald (NMSG Coll. PK. 7.B.25.10), Garschella Formation, Albian.
Description. NMSG (Coll. PK. 7.B.20.14) measures 73 mm in diameter. The conch is extremely discoidal (ww/dm = 0.30) and involute (uw/dm = 0.13). The whorl section is oval and very compressed (ww/wh = 0.56) with flat to broadly arched venter. Ribs are faint but present. It appears that they are more conspicuous on the outer flank than on the inner flank. There are about 8 blunt ribs per

whorl. NMSG (Coll. PK. 7.B.20.41) measures 61 mm in diameter. The conch is extremely discoidal (ww/dm = 0.27) and sub-involute (uw/dm = 0.16). The whorl section is oval and very compressed (ww/wh = 0.55) with flat to broadly arched venter. Slightly sigmoidal ribs are visible on the outer whorl but only faintly developed on the inner whorl.
Discussion. The umbilical width index of the type specimen (Plate VII, Fig 2, Brongniart, 1822; uw/dm = 0.18) is similar to those of our specimens. Weak ornamentation, compressed whorl cross section, flattened flanks and steep umbilical shoulder characterize the species.
Occurrence. Lower Cretaceous (lower part of upper Albian to the early uppermost Albian); England, France, Italy (Sardinia), Switzerland, Austria, Hungary, Caucasus, Iran, Angola, Morocco.

Subfamily Desmoceratinae Zittel, 1895

Genus Desmoceras (Desmoceras) Zittel, 1885

Desmoceras (Desmoceras) latidorsatum (Michelin, 1838)
Figs. 6AH, AI, 8U, V, 9E, F

Synonymy. See Kennedy and Fatmi (2014).
Holotype. *Ammonites latidorsatus* Michelin, 1838, p. 101, pl. 10, fig. 9.
Material. 1 heavily eroded conch (NMSG Coll. PK. 7.B.32.04). 2 internal moulds (NMSG Coll. PK. 7.B.37.10, 7.C.15.15).
Locality and horizon. Chelen-Geren (SW Plona; NMSG Coll. PK. 7.B.37.10), Wildhuser Schafboden gegen Pt. 2171 (NMSG Coll. PK. 7.B.32.04), Garschella Formation, Albian; Hinterwinden-Hornwald (Hinter Gräppelen; NMSG Coll. PK. 7.C.15.15), Kamm Bed, uppermost Albian–lowermost Cenomanian.
Description. NMSG (Coll. PK. 7.B.32.04) measures 41 mm in diameter. The conch is thickly discoidal (ww/dm = 0.49) and involute (uw/dm = 0.13). Its whorl section is compressed (ww/wh = 0.88) with broadly rounded flanks and venter. There is only one constriction preserved. NMSG (Coll. PK. 7.B.37.10) measures 21 mm in diameter. Its conch is thinly pachyconic (ww/dm = 0.61) and subinvolute (uw/dm = 0.24). The whorl cross section is rectangular and much wider than high (ww/wh = 1.34). Six straight to faintly curved constrictions are present per whorl.
Discussion. See Wiedmann and Dienni (1968) and Kennedy and Fatmi (2014).
Occurrence. Lower–Upper Cretaceous (middle Albian–late Cenomanian); England, Spain, France, Germany, Italy (Sardinia), Switzerland, Austria, Hungary, Poland, Serbia, Ukraine, Pakistan, India, Angola, Egypt, Madagascar, Mozambique, South Africa (KwaZulu-Natal), Tunisia,.USA (off Florida), Cuba, Venezuela, Japan.

Superfamily Pulchelliaceae Douvillè, 1890
Family Pulchellidae Douvillè, 1890

Genus *Kotetishvilia* Vermeulen, 1997

Kotetishvilia compressissima (d'Orbigny, 1841)
Fig. 6R, S

Synonymy. See Vermeulen (2002). The species was also referred to by Vermeulen et al. (2014).
Holotype. *Ammonites compressissimus* d'Orbigny, 1841; p. 210, pl. 61, fig. 4, 5.
Material. 3 conchs (NMSG Coll. PK. 5.A.05.81, 5.A.05.26, 5.A.05.82).
Locality and horizon. Altmann-Sattel, Südwest-Seite I, Altmann Member, uppermost Hauterivian–upper lower Barremian.
Description. NMSG (Coll. PK. 5.A.05.26) measures 40 mm in diameter. The conch is involute (uw/dm = 0.04). There are 14 ribs per half whorl, which are stronger on the dorsal part of the flank than ventrally. The venter is flat while the flank is convex with its maximum width on the midflank.
Discussion. See Vermeulen (2002).
Occurrence. Lower Cretaceous (lower Barremian, *K. compressissima* Zone); Spain, France, Italy, Switzerland, Austria, Czech Republic, Slovakia, Hungary, Romania, Bulgaria, Russia, Morocco, USA (California), Colombia.

Genus *Nicklesia* Hyatt, 1903

Nicklesia pulchella (d'Orbigny, 1841)

Fig. 6T, U

Synonymy. See Vermeulen (2002). The species was also referred to by Vermeulen et al. (2014).
Lectotype. *Ammonites pulchellus* d'Orbigny, 1841, p. 133, pl. 40, fig. 1, 2.
Material. 1 conch (NMSG Coll. KT. AS-W-0026).
Locality and horizon. Altmann-Sattel, Südwest-Seite I, Altmann Member, uppermost Hauterivian–upper lower Barremian.
Description. NMSG (Coll. KT. AS-W-0026) measures 31 mm in diameter. The conch is thinly discoidal (ww/dm = 0.39) and involute (uw/dm = 0.10). The whorl section is oval and much higher than wide (ww/wh = 0.71). The venter is slightly rounded. Ribs are stronger on the ventral part of the flank than dorsally. 13 ribs present in half a whorl.
Discussion. See Vermeulen (2002).
Occurrence. Lower Cretaceous (lower Barremian; *Nicklesia pulchella* Zone); Spain, France, Italy, Switzerland, Austria, Hungary, Romania, Crimea, Georgia, Algeria, Tunisia, Morocco, Colombia.

Superfamily Perisphinctaceae Steinmann, 1890
Family Holcodiscidae Spath, 1923

Genus *Astieridiscus* Kilian, 1910

Astieridiscus morleti (Kilan, 1889)
Fig. 8AC, AD

Synonymy. See Klein (2005).
Type. *Holcodiscus Morleti*, Kilian 1889; p. 676. Pl. XVII, figs. 4a, b.
Material. 1 conch (NMSG Coll. PK. 5A.13.06).
Locality and horizon. Wis (SW Alp Rohr), Altmann Member, uppermost Hauterivian–upper lower Barremian.
Description. NMSG (Coll. PK. 5A.13.06) measures 30 mm in diameter. Its conch is extremely thinly to thinly discoidal (ww/dm = 0.29) and subinvolute (uw/dm = 0.28). The whorl section is slightly higher than wide (ww/wh = 0.90) with flattened flanks. Fine ribs are single or bifurcate on the midflank.
Discussion. The specimen is similar to the holotype in having fine and bifurcated ribs, a similar whorl section and umbilical width index.
Occurrence. Lower Cretaceous (lower Barremian, *N. pulchella* Zone); France, Bulgaria, Crimea, Georgea, Caribbean.

Genus *Holcodiscus* Uhlig, 1882

Holcodiscus caillaudianus (d'Orbigny, 1850)
Fig. 9M, N, U, V

Synonymy. See Klein (2005).
Type. *Holcodiscus tzankovi* Avram, p. 17, pl. 3, fig. 10.
Material. 8 conchs (NMSG Coll. PK. 5.A.05.03, 5.A.05.22, 5.A.05.23, 5.A.05.27, 5.A.05.83 to 5.A.05.85, 5.A.17.02).
Locality and horizon. Altmann-Sattel, Südwest-Seite I (NMSG Coll. PK. 5.A.05.03, 5.A.05.22, 5.A.05.23, 5.A.05.27, 5.A.05.83 to 5.A.05.85), Chobel, Frümsner Berg (NMSG Coll. PK. 5.A.17.02), Altmann Member, latest Hauterivian–late Barremian.
Description. NMSG (Coll. PK. 5.A.05.85) measures 33 mm in diameter. The conch is thinly to moderately discoidal (ww/dm = 0.47) and subinvolute (uw/dm = 0.24). Height and width of the whorl section is more or less equal (ww/wh = 0.98) with a slightly flattened venter. Fine and straight to flexuose ribs are truncated by

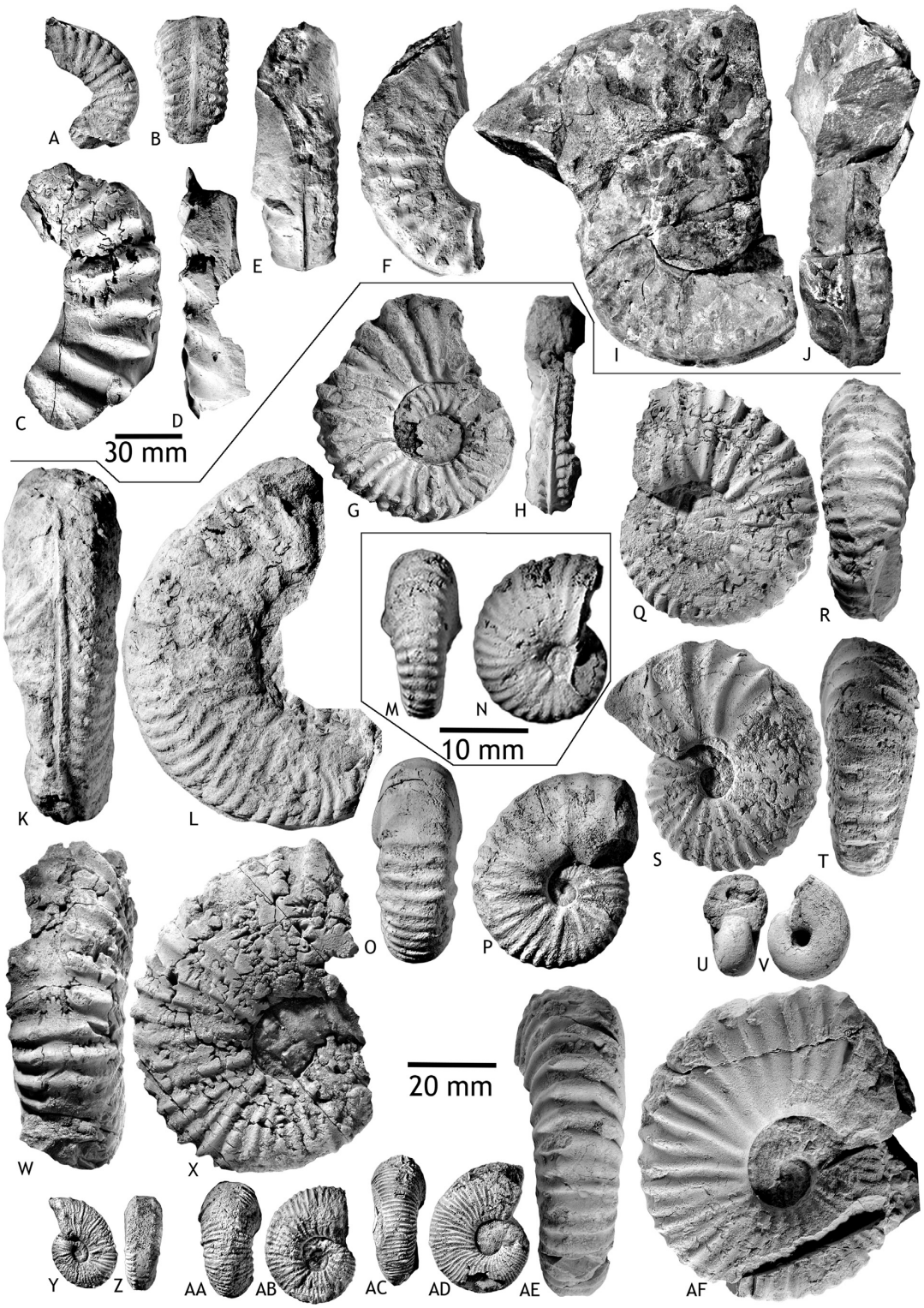
A
B
E
F
I
J
C
D
30 mm
G
H
Q
R
M
N
10 mm
K
L
S
T
O
P
U
V
20 mm
W
X
Y
Z
AA
AB
AC
AD
AE
AF

thickened ribs on which ventral tubercles are present. 3 to 6 fine ribs are visible between the thickened ribs. NMSG (Coll. PK. 5.A.05.86) measures 36 mm in diameter. Its conch is discoidal (ww/dm = 0.48) and subinvolute (uw/dm = 0.26). The whorl section is wider than high (ww/wh = 1.16) with a slightly flattened ventral side. Fine and more or less straight ribs are truncated by thickened ribs. Ventral and lateral tubercles are well developed on the thickened ribs. The thickened ribs are often bifurcated by the lateral tubercles. 5 to 6 fine ribs are developed between the thickened ribs.
Discussion. See Avram (1995).
Occurrence. Lower Cretaceous (lower Barremian, *K. compressissima* Zone); France, Hungary, Czech Republic, ?Poland (Silesia), Bulgaria, Romania, Caucasus, Crimea, Switzerland.

Holcodiscus sp.
Fig. 8AA, AB

Material. 2 conchs (NMSG Coll. PK. 5.A.05.42, 5.A.16.01).
Locality and horizon. Altmann-Sattel, Südwest-Seite I (NMSG Coll. PK. 5.A.05.42), Vorderalp, Frümsner Alp (NMSG Coll. PK. 5.A.16.01), Altmann Member, uppermost Hauterivian–upper lower Barremian.
Description. NMSG (Coll. PK. 5.A.05.42) measures 27 mm in diameter. Its conch is thickly discoidal (ww/dm = 0.51) and subinvolute (uw/dm = 0.27). The whorl section is rounded and wider than high (ww/wh = 1.10). Ribs are moderately coarse and occasionally bifurcating from lateral tubercles. No tubercles are developed on the rounded venter. NMSG (Coll. PK. 5.A.16.01) measures 28 mm in diameter. Its conch is thinly discoidal (ww/dm = 0.38) and subinvolute (uw/dm = 0.24). The whorl section is higher than wide (ww/wh = 0.84) with a flattened venter. Ribs are bifurcating on the flank. There are two rows of ventral tubercles between which the ribs are hardly visible.
Discussion. The constant ribs of NMSG (Coll. PK. 5.A.05.42) without tuberculation resemble *H. uhligi* but our specimen shows a much wider whorl section and bears coarser ribs. The ribs of *A. morleti* are also similar but our specimen has a much wider whorl section. Our specimen may be a depressed variant of *H. uhligi* or *A. morleti* which are actually very similar to each other. The whorl section of NMSG (Coll. PK. 5.A.16.01) is like *Holcodiscus diversecostatus* but our specimen bears primary and secondary ribs, which differ from *H. diversecostatus*.
Occurrence. Lower Cretaceous (lower Barremian, *N. pulchella–K. compressissima* Zones; for the genus).

Genus *Parasaynoceras* Breistroffer, 1947

Parasaynoceras tzankovi (Avram, 1995)
Fig. 9W, X

Types. *Holcodiscus caillaudianus* Uhlig, p. 243–244, pl. 19, figs 2–4, 6, 7, 13, 14.
Material. 1 chonch (NMSG Coll. PK. 5.A.05.86).
Locality. Altmann-Sattel, Südwest-Seite I, (NMSG Coll. PK. 5.A.05.86), Altmann Member, uppermost Hauterivian–upper lower Barremian.
Description. NMSG (Coll. PK. 5.A.05.86) measures 36 mm in diameter. Its conch is discoidal (ww/dm = 0.48) and subinvolute (uw/dm = 0.26). The whorl section is wider than high (ww/wh = 1.16) with a slightly flattened ventral side. Fine and more or less straight ribs are truncated by thickened ribs. Ventral and lateral tubercles are well developed on the thickened ribs. The thickened ribs are often bifurcated by the lateral tubercles. 5 to 6 fine ribs are developed between the thickened ribs.
Discussion. According to Avram (1995), this species is similar to *H. caillaudianus* and *H. perezianus* but differs in having subcircular a whorl section, a high whorl expansion rate and strong lateral tubercles.
Occurrence. Lower Cretaceous (lower Barremian); France, Romania, Bulgaria, Crimea, Georgia.

Superfamily Hoplitaceae Douvillé, 1890
Family Hoplitidae Douvillé, 1890
Subfamily Hoplitinae Douvillé, 1890

Genus *Callihoplites* Spath, 1925a

Callihoplites tetragonus (Seeley, 1865)
Fig. 9Q. R

Synonymy. See Kennedy et al. (2008).
Holotype. *Ammonites raulinianus* var. *tetragonus* Seeley, 1865; p. 243.
Material. 1 conch (NMSG Coll. UO. 017).
Locality and horizon. Säntis, Kamm Bed, uppermost Albian–lowermost Cenomanian.
Description. NMSG (Coll. UO. 017) measures 48 mm in diameter. The conch is discoidal (ww/dm = 0.50) and subinvolute (uw/dm = 0.29). The whorl section is wider than high (ww/wh = 1.14) with rounded venter. The maximum thickness is at the umbilical edge. Umbilical tubercles give rise to one or two pairs of looped ribs, which bear ventrolateral tubercles. The numbers of umbilical and ventrolateral tubercles per whorl are 10 and about 16, respectively.
Discussion. See Kennedy et al. (2008).
Occurrence. Lower Cretaceous (upper Albian, *M. fallax* Zone); England, France, Belgium, Switzerland, Tibet.

Genus *Hyphoplites* Spath 1922

Hyphoplites curvatus curvatus Mantell, 1822
Fig. 9AC, AD

Synonymy. See Kennedy (1994). The species was also mentioned by Gauthier (2006).
Holotype. *Hyphoplites curvatus curvatus* Mantell, 1822; p. 118, pl. 21, fig.18.
Material. 1 conch fragment (NMSG Coll. TB. STWG_CE34)
Locality and horizon. Blauschnee-Girenspitz, Kamm Bed, uppermost Albian–lowermost Cenomanian.
Description. NMSG (Coll. TB. STWG_CE34) measures 41 mm in diameter. Its whorl height and width are nearly the same (ww/uw = 0.97). The flanks are flattened with fine ribs. Umbilical bullae give rise to 3 to 4 prosiradiate ribs. There are inner- and outer well-developed ventrolateral tubercles interrupting some of the ribs. A siphonal groove is present.
Discussion. See Wright and Kennedy (1984).

Fig. 8. Ammonoids from the Alpstein. A, B, *Mortoniceras perinflatum* (Sowerby, 1817); NMSG (Coll. KT. HW-A-0030), Hinterwinden-Hornwald (Hinter Gräppelen). C, D, *Mortoniceras* sp.; NMSG (Coll. PK. 7.B.20.20), Schlatt (above Rüthi SG). E–J, *Mortoniceras* cf. *inflatum* (Sowerby, 1818); E, F – NMSG (Coll. PK. 7.B.20.44); I, J – NMSG (Coll. KT. Rü-S-0021), Schlatt (above Rüthi SG). G, H, *Mortoniceras rostratum* (Sowerby, 1817); NMSG (Coll. PK. 7.B.20.57), Schlatt (above Rüthi SG). K, L, *Dipoloceras* cf. *pseudaon* Spath, 1931; NMSG (Coll. PK. 7.B.20.23), Schlatt (above Rüthi SG). M, N, *Stoliczkaiella* (*Stoliczkaiella*) *notha* (Seeley, 1865); NMSG (Coll. PK. 7.C.12.03), Ebenalp, Übergang gegen Gartenalp. O, P, *Stoliczkaiella* (*Stoliczkaiella*) *clavigera* (Neumayr, 1875); NMSG (Coll. PK. 7.C.12.04), Ebenalp, Übergang gegen Gartenalp. Q, R, W, X, AE, AF, *Mantelliceras saxbii* (Sharpe, 1857); Q, R–NMSG F 5672, locality unknown; W, X – NMSG (Coll. KT. TW-G-0001), Stütze 2 Säntisbahn S; AE, AF – NMSG (Coll. UO. 003), Säntis. S, T, *Stoliczkaiella (Lamnayella) crotaloides* (Stoliczka, 1864); NMSG (Coll. PK. 7.C.12.01), Ebenalp, Übergang gegen Gartenalp. U, V, *Desmoceras* (*Desmoceras*) *latidorsatum* (Michelin, 1838); NMSG (Coll. PK. 7.C.15.15), Hinterwinden-Hornwald (Hinter Gräppelen). Y, Z, AA, AB, *Holcodiscus* sp.; Y, Z–NMSG (Coll. PK. 5.A.16.01), Vorderalp, Frümsner Alp; AA, AB–NMSG (Coll. PK. 5.A.05.42), Altmann-Sattel, Südwest-Seite I. AC, AD, *Astieridiscus morleti* (Kilian, 1889); NMSG (Coll. PK. 5.A.13.06), Wis (SW Alp Rohr).

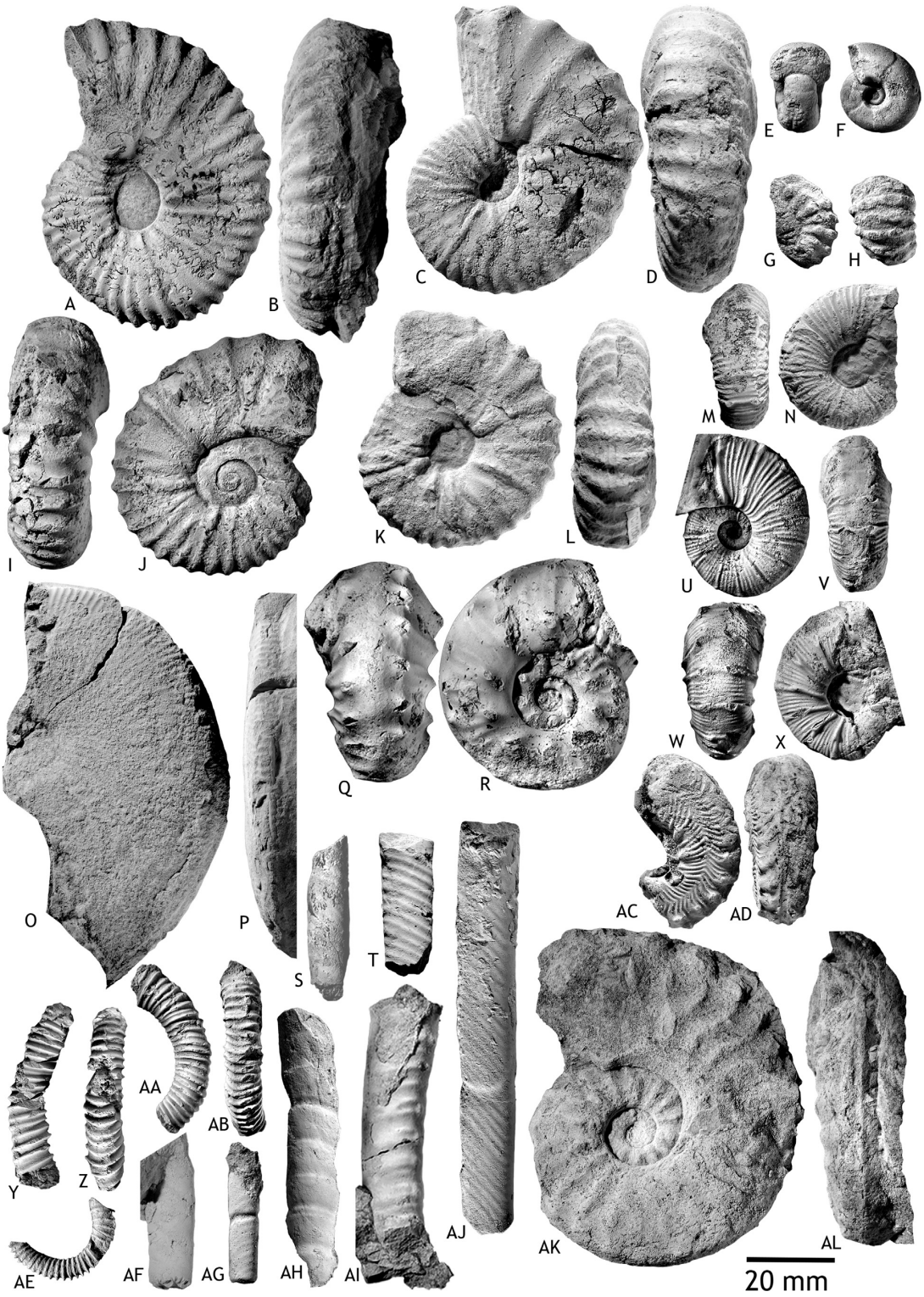
A
B
C
D
E
F
G
H
I
J
K
L
M
N
U
V
O
P
Q
R
W
X
S
T
AC
AD
AA
AB
Y
Z
AE
AF
AG
AH
AI
AJ
AK
AL
20 mm

Occurrence. Upper Cretaceous (lower Cenomanian); England, France, Germany, Romania, Crimea, Iran, Turkmenistan.

Superfamily Acanthocerataceae Grossouvre, 1894
Family Brancoceratidae Spath, 1934
Subfamily Brancoceratinae Spath, 1934

Genus *Hysteroceras* Hyatt, 1900

Hysteroceras binum (Sowerby, 1815)
Fig. 7AB, AC

Synonymy. See Lehmann et al. (2007).
Holotype. *Ammonites binus* Sowerby, 1815; p. 208, pl. 92, fig.3.
Material. 1 conch (NMSG Coll. PK. 7.B.20.36).
Locality and horizon. Schlatt (above Rüthi SG), Garschella Formation, Albian.
Description. NMSG (Coll. PK. 7.B.20.36) measures 27 mm. The conch is involute (uw/dm = 0.32) and extremely discoidal (ww/dm = 0.29). The whorl section is compressed (ww/wh = 0.74). There are 15 ventrolateral bullae per half whorl. Ribs are faint on the midflank. The keel is distinct.
Discussion. According to Spath (1934), this species is very compressed with flattened flanks. The inner bullae are prominent.
Occurrence. upper Albian; England, Spain, Italy (Sadinia), Hungary, Bulgaria, Dagestan, Turkmenistan, Angola, Madagascar, Nigeria, Mexico.

Hysteroceras crassicostatum (Jayet, 1929)
Fig. 7T, U

Synonymy. See Föllmi (1989b).
Type. *Schloenbachia (Pervinquieria) varicosa* var. *crassicostata* Jayet, 1929; p. 4, 5, fig. 7, no. 2.
Material. 1 shell fragment (NMSG Coll. PK. 7.B.26.16).
Locality and horizon. Stofel, Lenziwis, Garschella Formation, Albian.
Description. NMSG (Coll. PK. 7.B.26.16) is a partially weathered specimen, measuring 23 mm in diameter. The conch is thinly discoidal (ww/dm = 0.46) and sub-evolute (uw/dm = 0.40). The whorl section is rectangular and much wider than high (ww/wh = 1.32). The ribs are more or less straight, which number 23 per whorl. Some of them are bifurcated. Blunt umbilical bullae give rise to one or two ribs. The weak keel separates the ribs.
Discussion. According to Föllmi (1989b), the species has a depressed whorl section with widely spaced ribs. Ribs are simple or bifurcated. *H. orbignyi* is similar to this species but differs in having denser ribbing. *H. varicosum* is also similar but differs in having simple ribs.
Occurrence. Lower Cretaceous (upper Albian, *Mortoniceras Inflatum* Zone); England, France, Austria, Madagascar.

Hysteroceras orbignyi Spath, 1922
Fig. 7P–S, AD

Synonymy. See Föllmi (1989b).
Type. *Ammonites varicosus* Sowerby, determined in d'Orbigny, 1841; p. 294, pl. 87, fig. 3.
Material. 6 shell fragments (NMSG Coll. PK. 7.B.25.02, 7.B.25.34, 7.B.26.06, 7.B.25.35, 7.B.26.15, 7.B.26.22).
Locality and horizon. Bergli, Sennwald (NMSG Coll. PK. 7.B.25.02, 7.B.25.34, 7.B.25.35), Stofel, Lenziwis (NMSG Coll. PK. 7.B.26.06, 7.B.26.22, 7.B.26.22), Garschella Formation, Albian.
Description. NMSG (Coll. PK. 7.B.25.02) is a well preserved specimen measuring 22 mm in diameter. The conch is extremely discoidal (ww/dm = 0.32) and subevolute (uw/dm = 0.40). The whorl section is rounded and slightly higher than wide (ww/wh = 0.90). The ribs are weakly curved, there are about 16 per half whorl. Some of them are bifurcated.
Discussion. According to Spath (1934), the species has a subquadrate whorl cross section, which varies from slightly compressed to slightly depressed. Traces of a blunt keel are present in early ontogenetic stages. Ribs are bifurcating or long and short in alternation. Renz (1982) stated that the majority of ribs on the outer whorl are bifurcating from umbilical bullae but occasionally are single.
Occurrence. Lower Cretaceous (upper Albian, *Mortoniceras inflatum* Zone, *H. orbignyi* Subzone); Spain, France, Switzerland, Poland, Romania, Slovakia, Ukraine, Georgia, Angola, Madagascar, Mozambique, South Africa (KwaZulu-Natal), USA (Texas), Venezuela.

Hysteroceras varicosum (Sowerby, 1824)
Fig. 7AJ, AK

Synonymy. See Marcinowski and Wiedmann (1990).
Type. *Ammonites varicosus* Sowerby 1824; p.74, pl. 451, fig.5.
Material. 1 shell fragment (half of the conch missing; NMSG Coll. PK. 7.B.23.21) and 1 weathered conch (NMSG Coll. KT. Dü-St-0003).
Locality and horizon. In Ränken, Plona (NMSG Coll. PK. 7.B.23.21), Garschella Formation, Albian; Stofel, Lenziwis (NMSG Coll. KT. Dü-St-0003), the Wannenalp Bank, Albian.
Description. NMSG (Coll. PK. 7.B.23.21) is 31 mm in maximum measurable diameter. The conch is thinly discoidal (ww/dm = 0.35) and subevolute (uw/dm = 0.40). The whorl height and width are nearly equal (ww/wh = 1.02). The ribs are coarse, more or less straight and broad, about 15 per whorl. Umbilical bullae give rise to ribs with occasional intercalated ribs in between. There is a blunt keel on the venter.
Discussion. According to Marcinowski and Wiedmann (1990), the species has a rectangular whorl section (ww/wh = 1.0) and a strong ventrolateral tuberculation. Spath (1934) mentioned that ribs are rarely bifurcating but mostly, there are alternating long and short ribs. Our specimen is similar to Sowerby's holotype figured in Spath (1934).
Occurrence. Lower Cretaceous (upper Albian; *Hysteroceras varicosum* Subzone; Casey, 1966); England, France, Germany, Poland, Romania, Serbia, Ukraine, Crimea, Angola, Madagascar, USA (Texas), Mexico, Venezuela, Suriname.

Fig. 9. Ammonoids from the Alpstein. A, B, *Mantelliceras saxbii* (Sharpe, 1857); A, B – NMSG (Coll. PK. 7.C.13.28), Säntis, Gasthaus-Hang. C, D, *Stoliczkaiella* (*Stoliczkaiella*) *clavigera* (Neumayr, 1875); NMSG (Coll. PK. 7.C.12.05), Ebenalp, Übergang gegen Gartenalp. E, F, *Desmoceras (Desmoceras) latidorsatum* (Michelin, 1838); NMSG (Coll. PK. 7.B.37.10), Chelen-Geren (SW Plona). G, H, *Douvilleiceras* sp.; NMSG (Coll. PK. 7.B.42.14), Bergli Nord, Sennwald. I–L, *Stoliczkaiella (Lamnayella) juigneti* Wright and Kennedy, 1978; I, J – NMSG (Coll. PK. 7.C.05.04), Hornwald (Hinter Gräppelen); K, L – NMSG (Coll. PK. 7.C.11.09), Säntis, Gasthaus-Galerie and surrounding. M, N, U, V, *Holcodiscus caillaudianus* (d'Orbigny, 1850); M, N – NMSG (Coll. PK. 5.A.05.27); U, V – NMSG (Coll. PK. 5.A.05.85), Altmann-Sattel, Südwest-Seite I. W, X – *Parasaynoceras tzankovi* (Avram, 1995); NMSG (Coll. PK. 5.A.05.86), Altmann-Sattel, Südwest-Seite I. O, P, *Forbesiceras largilliertianum* (d'Orbigny, 1841); NMSG (Coll. PK. 7.C.13.35), Säntis, Gasthaus-Hang. Q, R, *Callihoplites tetragonus* (Seeley, 1865); NMSG (Coll. UO. 017), Säntis. S, T, AF, *Lechites gaudini* (Pictet and Campiche, 1861); S – NMSG (Coll. PK. 7.C.14.03), Hinterwinden (Hinter Gräppelen); T – NMSG (Coll. PK. 7.B.20.06), Schlatt (above Rüthi SG); AF–NMSG (Coll. PK. 7.C.13.42), Lochtem-Grüenböhl. Y, Z, *Hamulinites* sp.; NMSG (Coll. KT. ASW_0048), Altmann-Sattel, Südwest-Seite I. AA, AB, AE, *Leptoceratoides* cf. *heeri* Ooster, 1860; AA, AB – NMSG (Coll. PK. 5.A.05.24); AE – NMSG (Coll. KT. AS-W-0043), Altmann-Sattel Südwest-Seite. I. AC, AD, *Hyphoplites curvatus curvatus* Mantell, 1822; NMSG (Coll. TB. STWG_CE34), Blauschnee-Girenspitz. AG, *Sciponoceras baculoides* (Mantell, 1822); NMSG (Coll. PK. 7.C.13.06), Säntis, Gasthaus-Hang. AH, Bochianitinae indet.; NMSG (Coll. KT. ASW_0045) Altmann-Sattel, Südwest-Seite I. AI, *Anisoceras armatum* (Sowerby, 1817); NMSG (Coll. KT. NA-K-0001), Neuenalp-Kamm, Kamm Bed. AJ, *Sciponoceras roto* Cieśliński, 1959; NMSG (Coll. UO. 008), Säntis. AK, AL, *Schloenbachia varians* (Sowerby, 1817); NMSG (Coll. UO. 018), Säntis.

Subfamily Mortoniceratinae Douvillé, 1912

Genus *Cantabrigites* Spath, 1933

Cantabrigites sp.
Fig. 7AE–AI.

Material. 5 conchs (NMSG Coll. PK. 7.B.35.01, 7.C.13.14, 7.C.15.10, 7.C.15.21, 7.C.15.31).
Locality and horizon. Hinterwinden-Hornwald (Hinter Gräppelen; NMSG Coll. PK. 7.C.15.10, 7.C.15.21, 7.C.15.31), Säntis, Gasthaus-Hang (NMSG Coll. PK. 7.C.13.14), Kamm Bed, uppermost Albian–lowermost Cenomanian; Tal W II (NE Neuenalpspitz; NMSG Coll. PK. 7.B.35.01), Garschella Formation, Albian.
Description. NMSG (Coll. PK. 7.C.15.31) is 21 mm in maximum diameter. The conch is extremely discoidal (ww/dm = 0.34) and subevolute (uw/dm = 0.42). The whorl section is rectangular and only slightly higher than wide (ww/wh = 0.91). There are 17 ribs per whorl. Umbilical bullae give rise to coarse ribs with intercalated ribs. The moderately distinct keel separates the ribs on the venter. NMSG (Coll. PK. 7.C.15.21) measures 29 mm in diameter. The conch is extremely discoidal (ww/dm = 0.32) and subevolute (uw/dm = 0.40). The whorl section is rectangular and slightly higher than wide (ww/wh = 0.93). The ribs are very coarse and carry two to three bullae. There are 15 ribs per half whorl. The keel is conspicuous. NMSG (Coll. PK. 7.C.13.14) reaches 30 mm in diameter. Its conch is extremely discoidal (ww/dm = 0.30) and subevolute (uw/dm = 0.42). The whorl section is rectangular and slightly higher than wide (ww/wh = 0.91). Its ribs are coarse and carry inner and outer ventrolateral tubercles. There are 29 ribs per whorl.
Discussion. *Cantabrigites* was documented as a genus with very small conchs with simple ribs, relatively strong ventrolateral tubercles and distinct keels, but sometimes these characters are developed very similarly to *Hysteroceras*. *Mortoniceras* also shows similar characters, perhaps because it may be the macroconch counterpart of *Cantabrigites* and *Hysteroceras*. Thus, these three genera often are confused and thus wrongly determined. A quantitative analysis of conch morphology based on well-preserved materials is needed to revise the taxonomy of these genera.
Occurrence. Lower Cretaceous (upper Albian; for the genus); England, France, Switzerland.

Genus *Mortoniceras* (*Mortoniceras*) Meek, 1876

Mortoniceras perinflatum (Sowerby, 1817)
Fig. 8A, B

Synonymy. See Kennedy and Latil (2007).
Holotype. *Ammonites inflatus* Pictet and Campiche 1860, p. 178, pl. 21, figs. 5; pl. 22, fig. 3.
Material. 1 shell fragment (NMSG Coll. KT. HW-A-0030).
Locality and horizon. Hinterwinden-Hornwald (Hinter Gräppelen), Kamm Bed, Albian.
Description. NMSG (Coll. KT. HW-A-0030) is 58 mm long. The conch is pachyconic (ww/dm = 0.61) with depressed and rectangular whorl section (ww/wh = 1.35). Ribs are dense with angles of around 18° between two succeeding ribs. There are 4 tubercles on each rib.
Discussion. According to Kennedy and Latil (2007), *M. perinflatum* is similar to *M. rostratum* but differs in having a more depressed whorl section.
Occurrence. Lower Cretaceous (upper Albian, *M. perinflatum* Zone); England, France, Switzerland, Hungary, Romania, Crimea, Caucasus, Iran, Angola, South Africa (KwaZulu-Natal), USA (Texas).

Mortoniceras rostratum (Sowerby, 1817)
Fig. 8G, H

Synonymy. See Kennedy and Latil 2007.
Holotype. *Ammonites rostratus* Sowerby 1817, p. 163, pl. 173.
Material. 1 conch (NMSG Coll. PK. 7.B.20.57) from Garschella-Formation, Alpstein.
Locality and horizon. Schlatt (above Rüthi SG), Garschella Formation, Albian.
Description. NMSG (Coll. PK. 7.B.20.57) is an eroded specimen, measuring 50 mm in conch diameter. The conch is sub-evolute (uw/dm = 0.36). The whorl section is rectangular and higher than wide (ww/wh = 0.67). There are 18 multituberculated ribs per half whorl. The number of tubercles on a rib is approximately 5.
Discussion. See discussion for *M. inflatum* above.
Occurrence. Lower Cretaceous (upper Albian, *M. rostratum* Zone); England, Spain, France, Germany, Hungary, Romania, Caucasus, Iran, Turkmenistan, USA (Texas), Japan.

Mortoniceras* cf. *inflatum (Sowerby, 1818)
Fig. 8E, F, I, J

Synonymy. See Amédro et al. (2003)
Holotype. *Ammonites inflatus* Sowerby, 1818; p. 170, pl. 178.
Material. 4 shell fragments (NMSG Coll. PK. 7.B.20.24, 7.B.20.25, 7.B.20.44, NMSG Coll. KT. Rü-S-0021)
Locality and horizon. Schlatt (above Rüthi SG), Garschella Formation, Albian.
Description. NMSG (Coll. KT. Rü-S-0021) measures 163 mm in diameter. The conch is extremely discoidal (ww/dm = 0.34) and subevolute (uw/dm = 0.36). The whorl section is slightly compressed (ww/wh = 0.92) with flattened flank. There are primary ribs, originating from umbilical tubercles, intercalated by secondary ribs. On the phragmocone, the ribs are more closely spaced (angle between two ribs is approximately 20°) than on the body chamber (more or less 40°). There are 3 tubercles present on the phragmocone, which are stronger than on the body chamber.
Discussion. *M. inflatum* has 3 tubercles, one of which can become a bulla during late ontogeny on the primary ribs. *M. pricei*, *M. fallax* and *M. rostratum* have two, three and four tubercles, respectively. Our specimens carry 3 tubercles on a rib but the ornamentation is very weak, which hampers the clear separation from *M. fallax*. For a revision of *Mortoniceras*, see Amédro et al. (2003).
Occurrence. Lower Cretaceous (upper Albian, *Mortoniceras inflatum* Zone); France, Germany, Poland, Russia, Crimea, Georgia, Angola, Morocco, Tunisia, Japan.

Mortoniceras sp.
Fig. 8C, D

Material. 1 shell fragment (NMSG Coll. PK. 7.B.20.20).
Locality and horizon. Schlatt (above Rüthi SG), Garschella Formation, Albian.
Description. NMSG (Coll. PK. 7.B.20.20) is a conch fragment, measuring 113 mm in diameter. Its whorl section appears to be as high as wide or slightly higher than wide. There are 2 tubercles on each rib. The interspace is wide.
Discussion. According to Amédro et al. (2003), *M. pricei* has developed two tubercles on a rib, which corresponds to our specimen. But the holotype of Spath (1930) shows more closely spaced septa.
Occurrence. Lower Cretaceous (upper Albian; for the genus).

Subfamily Mojsisovicziinae Hyatt, 1903

Genus *Dipoloceras* Hyatt, 1900

Dipoloceras* cf. *pseudaon Spath, 1931.
Fig. 8K, L

1931 *Dipoloceras pseudaon* Spath, p.373. pl. XXXII, Fig. 11; pl. XXXIV, figs. 1–3.
2011 *Dipoloceras boucharidianum*, Gale et al., fig. 20B. no description.

Holotype. *Dipoloceras pseudaon* Spath, 1931; p. 373, pl. 14, figs. 1–3.
Material. 1 phragmocone fragment (NMSG Coll. PK. 7.B.20.23).
Locality and horizon. Schlatt (above Rüthi SG; NMSG Coll. PK. 7.B.20.23), Garschella Formation, Albian.
Description. NMSG (Coll. PK. 7.B.20.23) is a weathered specimen, measuring 79 mm in diameter. The whorl section is nearly rectangular and compressed (ww/wh = 0.78) with a sulcate venter and a keel. Weakly sigmoidal ribs are bifurcating between the midflank and umbilical shoulder. Approximately 30 ribs are present per half whorl.
Discussion. The species is similar to *D. elegans* in having a compressed and oval whorl section and sigmoidal ribs, but *D. elegans* has more strongly developed ventrolateral tubercles. Our specimen is also similar to *D. pseudaon* var. *moniliformis* in Spath (1931; pl. XXXII, fig. 10) in its fine ribbing and relatively flattened flank but the holotype of *D. pseudaon* is somewhat less compressed than our specimen.
Occurrence. Lower Cretaceous (upper Albian); England, France, Colombia, Japan.

Family Acanthoceratidae de Grossouvre, 1894
Subfamily Mantelliceratinae Hyatt, 1903

Genus *Mantelliceras* Hyatt, 1903

Mantelliceras saxbii (Sharpe, 1857)
Fig. 8Q, R, W, X, AE, AF

Synonymy. See Kennedy et al., 2015.
Lectotype. *Ammonites Saxbii* Sharpe, 1857; p. 45, pl. 20, fig. 3.
Material. 8 conchs (NMSG Coll. PK. 7.C.02.03, 7.C.03.03, 7.C.11.02, 7.C.13.27, 7.C.13.28, NMSG Coll. UO. 002, 003, NMSG Coll. KT. TW-G-0001).
Locality and horizon. Stütze 2 Säntisbahn S. (NMSG Coll. KT. TW-G-0001), Tierwis NE II (NMSG Coll. PK. 7.C.03.03), Säntis, Gasthaus-Hang (NMSG Coll. PK., 7.C.13.27, 7.C.13.28), Stütze 2 Säntisbahn S (NMSG Coll. PK. 7.C.02.03), Säntis, Gasthaus-Galerie and surrounding (NMSG Coll. PK. 7.C.11.02), Säntis (NMSG F 5672, NMSG Coll. UO. 002, 003), Kamm Bed, uppermost Albian–lowermost Cenomanian.
Description. NMSG (Coll. UO. 002) measures 70 mm in diameter. The conch is extremely thinly discoidal (ww/dm = 0.34) and subinvolute (uw/dm = 0.27). The flank is more or less flat with the maximum width in the middle. There are 20 ribs on the last demi-whorl. The ribs, which are finer and denser on the inner whorl than on the outer, are nearly straight to feebly concave toward the aperture. Ventrolateral tubercles and umbilical bullae are relatively prominent but there are no conspicuous lateral tubercles.
Discussion. According to Wright and Kennedy (1984), *M. picteti* and *M. saxbii* are the species with compressed whorl section and flat flank. *M. picteti* develops strong ribs with quadrituberculation, which distinguishes the two species.
Occurrence. Upper Cretaceous (lower Cenomanian, *M. mantelli* Zone, common in *M. saxbii* Subzone); England, Spain, France, Germany, Switzerland, Poland, Romania, Bulgaria, Kazakhstan, Iran, Angola, Madagascar, South Africa (KwaZulu-Natal), Tunisia, Japan.

Family Lyelliceratidae, Spath 1921
Subfamily Stoliczkaiellinae, Cooper 2012

Genus *Stoliczkaiella* Cooper, 2012
Subgenus *Stoliczkaiella* Cooper, 2012

Stoliczkaiella* (*Stoliczkaiella*) *clavigera (Neumayr, 1875)
Fig. 8O, P. 9C, D

Synonymy. See Kennedy and Klinger (2013).
Holotype. *Ammmonites dispar* Stoliczka, 1864; p. 85, pl. 45, fig. 1.
Material. 4 conchs (NMSG Coll. PK. 7C.12.04, 7.C.12.05, 7.C.13.04, NMSG Coll. UO. 003).
Locality and horizon. Säntis, (NMSG Coll. UO. 003), Ebenalp, Übergang gegen Gartenalp (NMSG Coll. PK. 7C.12.04, 7.C.12.05), Säntis, Gasthaus-Hang (NMSG Coll. PK. 7.C.13.04), Kamm Bed, uppermost Albian–lowermost Cenomanian.
Description. NMSG (Coll. PK. 7C.12.04) measures 47 mm in diameter. Its conch is thinly discoidal (ww/dm = 0.40) and subinvolute (uw/dm = 0.23). The whorl section is slightly compressed (ww/wh = 0.90) with flattened flanks and broadly rounded venter. There are 32 ribs per whorl. The ribs, which are finer and denser on the inner whorl than on the outer, are nearly straight and originate from small umbilical bullae. Primary ribs are intercalated between secondary ribs or bifurcating.
Discussion. See Wright and Kennedy (1994) as well as Kennedy and Klinger (2013).
Occurrence. Lower Cretaceous (upper Albian *M. rostratum* and *Arrhaphoceras briacensis* Zone); England, France, Switzerland, Romania, Turkmenistan, India, Japan.

Stoliczkaiella* (*Stoliczkaiella*) *notha (Seeley, 1865)
Fig. 8M, N

Synonymy. See Wright and Kennedy (1994).
Lectotype. *Ammonites navicularis* Mantell var. *nothus* Seeley 1865; p. 232.
Material. 1 conch (NMSG Coll. PK.7.C.12.03).
Locality and horizon. Ebenalp, Übergang gegen Gartenalp, Kamm Bed, uppermost Albian–lowermost Cenomanian.
Description. NMSG (Coll. PK.7.C.12.03) measures 47 mm in diameter. The conch is thinly discoidal (ww/dm = 0.40) and involute (uw/dm = 0.12). The whorl section is compressed (ww/wh = 0.74) with flattened flanks and broadly rounded venter. There are 32 ribs per whorl. The ribs, which are generated from small umbilical bullae, are nearly straight and mostly bifurcating. There are constant ventrolateral tubercles.
Discussion. See Wright and Kennedy (1994).
Occurrence. Lower Cretaceous (latest Albian, *M. rostratum* Zone); England, France, Switzerland, Serbia, Romania, Turkmenistan, Crimea, India, Algeria, Angola, Madagascar, USA (California), Japan.

Subgenus *Lamnayella* Wright and Kennedy, 1978

Stoliczkaiella (Lamnayella) crotaloides (Stoliczka, 1864)
Fig. 8S, T

Synonymy. See Kennedy and Klinger (2013).
Holotype. *Ammonites crotaloides* Stoliczka 1864; p. 88, pl. 46, fig. 3.
Material. 1 conch (NMSG Coll. PK. 7.C.12.01).
Locality and horizon. Ebenalp, Übergang gegen Gartenalp, Kamm Bed, uppermost Albian–lowermost Cenomanian.
Description. NMSG (Coll. PK. 7.C.12.01) is slightly deformed, measuring 53 mm in diameter. The conch is thinly discoidal (ww/dm = 0.41) and subinvolute (uw/dm = 0.26). The whorl width and height is nearly equal (ww/wh = 0.96) with flattened flanks and rounded venter. There are 17 straight ribs per whorl. Ribs on the body chamber are distant and blunt while those on the phragmocone are rather sharp and less distantly spaced. Ventrolateral bullae are faint.
Discussion. See Kennedy and Klinger (2013).
Occurrence. Lower Cretaceous (upper Albian, *M. perinflatum* Zone); England, India, Angola, South Africa (KwaZulu-Natal), USA (Texas).

Stoliczkaiella (Lamnayella) juigneti Wright and Kennedy, 1978

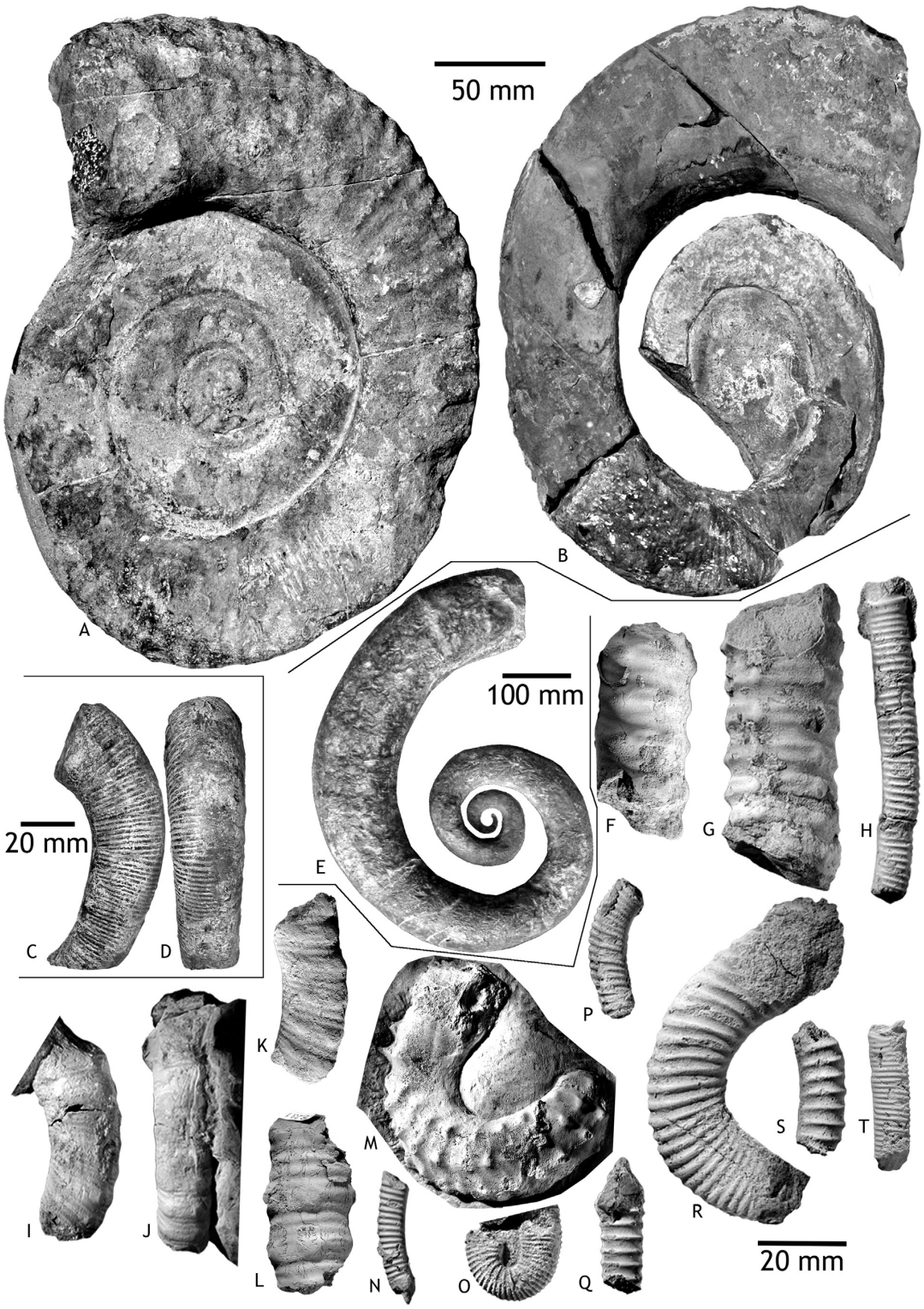
50 mm
A
B
100 mm
E
F
G
H
20 mm
C
D
K
P
I
J
M
L
N
O
Q
R
S
T
20 mm

Fig. 9I–L

Synonymy. Wright and Kennedy (1984).
Holotype. *Stoliczkaia* sp. Wright and Kennedy 1971; p. 398, pl. 37, figs. 1–4.
Material. 7 conchs (NMSG Coll. PK. 7.C.01.11, 7.C.05.04, 7.C.11.04, 7.C.11.08, 7.C.11.09, 7.C.15.28, NMSG Coll. KT. HW-A-0024).
Locality and horizon. Hinterwinden-Hornwald (Hinter Gräppelen; NMSG Coll. KT. HW-A-0024, NMSG Coll. PK. 7.C.15.28), Säntis, Gasthaus-Galerie and surrounding (NMSG Coll. PK. 7.C.11.04, 7.C.11.08, 7.C.11.09), Hornwald (Hinter Gräppelen; NMSG Coll. PK. 7.C.05.04), Tierwis-Stütze 2 Säntisbahn I (NMSG Coll. PK. 7.C.01.11), Kamm Bed, uppermost Albian–lowermost Cenomanian.
Description. NMSG (Coll. PK. 7.C.05.04) measures 61 mm in diameter. Its conch is thinly discoidal (ww/dm = 0.39) and subevolute (uw/dm = 0.34). The whorl cross section is slightly higher than wide (ww/wh = 0.92) with flattened flanks and rounded venter. There are 15 straight ribs per half whorl. Primary ribs, on which small bullae are present, are intercalated by shorter and non-bullate ribs.
Discussion. See Wright and Kennedy (1984).
Occurrence. Upper Cretaceous (lower Cenomanian, *M. mantelli* zone); England, France, Egypt.

Family Forbesiceratidae Wright, 1952

Genus *Forbesiceras* Kossmat, 1897

Forbesiceras largilliertianum (d'Orbigny, 1841)
Fig. 9O, P

Synonymy. See Kennedy et al. (2013).
Lectotype. *Ammonite largilliertianus* d'Orbigny 1841, p. 320, pl. 95.
Material. 1 shell fragment (NMSG Coll. PK. 7.C.13.35).
Locality and horizon. Säntis, Gasthaus-Hang, Kamm Bed, uppermost Albian–lowermost Cenomanian.
Description. NMSG (Coll. PK. 7.C.13.35) is an eroded conch fragment, measuring 92 mm in diameter. Its conch is involute (uw/dm = 0.06) and appears very compressed although one side of the flank is not preserved. The venter is very narrow and flat. Ribs are not well preserved but fine.
Discussion. See Delamette and Kennedy (1991) as well as Kennedy et al. (2013).
Occurrence. Upper Cretaceous (lower–middle Cenomanian); England, Spain, France, Germany, Switzerland, Romania, Iran, India, Algeria, Madagascar, South Africa (KwaZulu-Natal), Tunisia, Japan.

Suborder Ancyloceratina Wiedmann, 1966
Superfamily Ancyloceratoceae Gill, 1871
Family Bochianitidae Spath, 1922
Subfamily Bochianitinae Spath, 1922

Bochianitinae indet.
Fig. 9AH

Material. 1 shell fragment (NMSG Coll. KT. ASW_0045).
Locality and horizon. Altmann-Sattel, Südwest-Seite I, Altmann Member, uppermost Hauterivian–upper lower Barremian.
Description. NMSG (Coll. KT. ASW_0045) is a straight form, measuring 75 mm in diameter. Its whorl section is slightly rounded (wh/ww = 0.84). There are 6 distinct prorsiradiate constrictions.
Discussion. The above-mentioned characters are similar to those of *Bochianites* and *Kabylites*. According to Wright (1996), the main differences between the two genera lie in the suture line course. Our specimen does not show sutures.
Occurrence. Lower Cretaceous (lower Barremian, *N. pulchella*–*K. compressissima* Zones).

Family Ancyloceratidae Gill, 1871
Subfamily Crioceratitinae Gill, 1871

Genus *Crioceratites* Léveillé, 1837

Crioceratitites sp.
Fig. 10C, D

Material. 1 conch fragment (ETHZ 10438).
Locality and horizon. Altmann, the Altmann Member, uppermost Hauterivian–upper lower Barremian.
Description. ETHZ 10438, whose surface has been evidently carved, measures 157 mm in diameter. The specimen is loosely coiled (crioconic) with regular and dense ribs with sporadic tubercles. The whorl width and height is more or less equal (ww/wh = 0.95).
Discussion. Regularly spaced strong and rectiradiate ribs, which are typical for the genus, are not yet developed. The regular, straight ribs are sometimes hardly distinguishable from the artificially carved ribs. The characters mentioned above agree with of the definition of *Crioceratites*.
Occurrence. Lower Cretaceous (uppermost Valanginian to lower Barremian; for the genus).

Genus *Emericiceras* Sarkar, 1954

Emericiceras sp.
Fig. 10B, E

Material. 5 conchs (NMSG Coll. PK. 5A.02.14, 5A.02.15, NMSG Coll. UO. 006, NMSG Coll. KT. AS-W-0018, NMSG F 13599).
Locality and horizon. Altmann-Sattel, Südwest-Seite I (NMSG Coll. KT. AS-W-0018), Hüenerberg, (NMSG Coll. UO. 006), Tierwis NE II (NMSG Coll. PK. 5.A.02.14, 5A.02.15), Seealp (NMSG F 13599), Altmann Member, uppermost Hauterivian–upper lower Barremian.
Description. NMSG (Coll. PK. 5A.02.15) is an eroded specimen with a diameter of 274 mm. It is loosely coiled (crioconic) and planispiral. Its whorl section is higher than wide but at earlier ontogenetic stages, it is more rounded than in later stages. The main ribs are intercalated by a few minor ribs. Two to three lateral tubercles and ventrolateral spines are present but not well preserved. One side of the flank is deeply eroded and shows no diagnostic features.
Discussion. The conch of this genus is planispirally coiled with a whorl section that is higher than wide. There are periodical main ribs with intercalated finer ribs. According to Wright (1996), this genus differs from *Crioceratites* in having more frequent and more pronounced periodic ribs with stronger spines. The surface of our specimen is eroded, showing no further details. *Honnoratia* also shows very similar characters, which could be synonymized.

Fig. 10. Ammonoids from the Alpstein. A. *Pseudothurmannia* sp.; ETHZ 10436, Weesen. B, E, *Emericiceras* sp.; B – NMSG (Coll. PK. 5.A.02.15), Tierwis NE II; E– NMSG F 13599, Seealp. C, D, Crioceratitinae ind.; ETHZ 10438, Altmann. F, K, L, *Anisoceras armatum* (Sowerby, 1817); NMSG (Coll. PK. 7.C.07.05), Tal-Wänneli (NE Neuenalpspitz); K – NMSG (Coll. PK. 7.B.25.23), Bergli, Sennwald; L, NMSG (Coll. PK. 7.B.23.15), In Ränken, Plona. G, *Anisoceras perarmatum* Pictet and Campiche, 1861; NMSG (Coll. PK. 7.C.06.03), Tal W (NE Neuenalpspitz). H, *Hamites* cf. *maximus* Sowerby, 1814; NMSG (Coll. KT. HW-A-0013), Hinterwinden-Hornwald (Hinter Gräppelen). I, J, *Anisoceras pseudoelegans* (Pictet and Campiche, 1861); I, J – NMSG (Coll. PK. 7.C.15.11), Hinterwinden-Hornwald (Hinter Gräppelen). M, *Prohelicoceras moutonianum* (d'Orbigny, 1850); NMSG (Coll. PK. 7.B.26.04), Stofel, Lenziwis. N, *Hamites simplex* d'Orbigny, 1842; NMSG (Coll. PK. 7.C.13.05), Säntis, Gasthaus-Hang. O, *Hamites* cf. *similis* Casey, 1961; NMSG (Coll. PK. 7.B.23.28), In Ränken, Plona. P, *Hamites subvirgulatus* Spath, 1941; NMSG (Coll. PK. 7.C.02.07), Stütze 2 Säntisbahn S. Q, *Hamites* sp.; NMSG (Coll. KT. CH-O-0001), Oberrieter Chienberg. R, *Hamites compressus* Sowerby, 1814; NMSG (Coll. PK. 7.C.11.01), Säntis, Gasthaus-Galerie and surrounding. S, *Hamites virgulatus* Brongniart, 1822; NMSG (Coll. PK. 7.B.26.13), Stofel, Lenziwis. T, *Hamites duplicatus* Pictet and Campiche, 1861; NMSG (Coll. PK. 7.C.19.04), Lochtem-Grüenböhl.

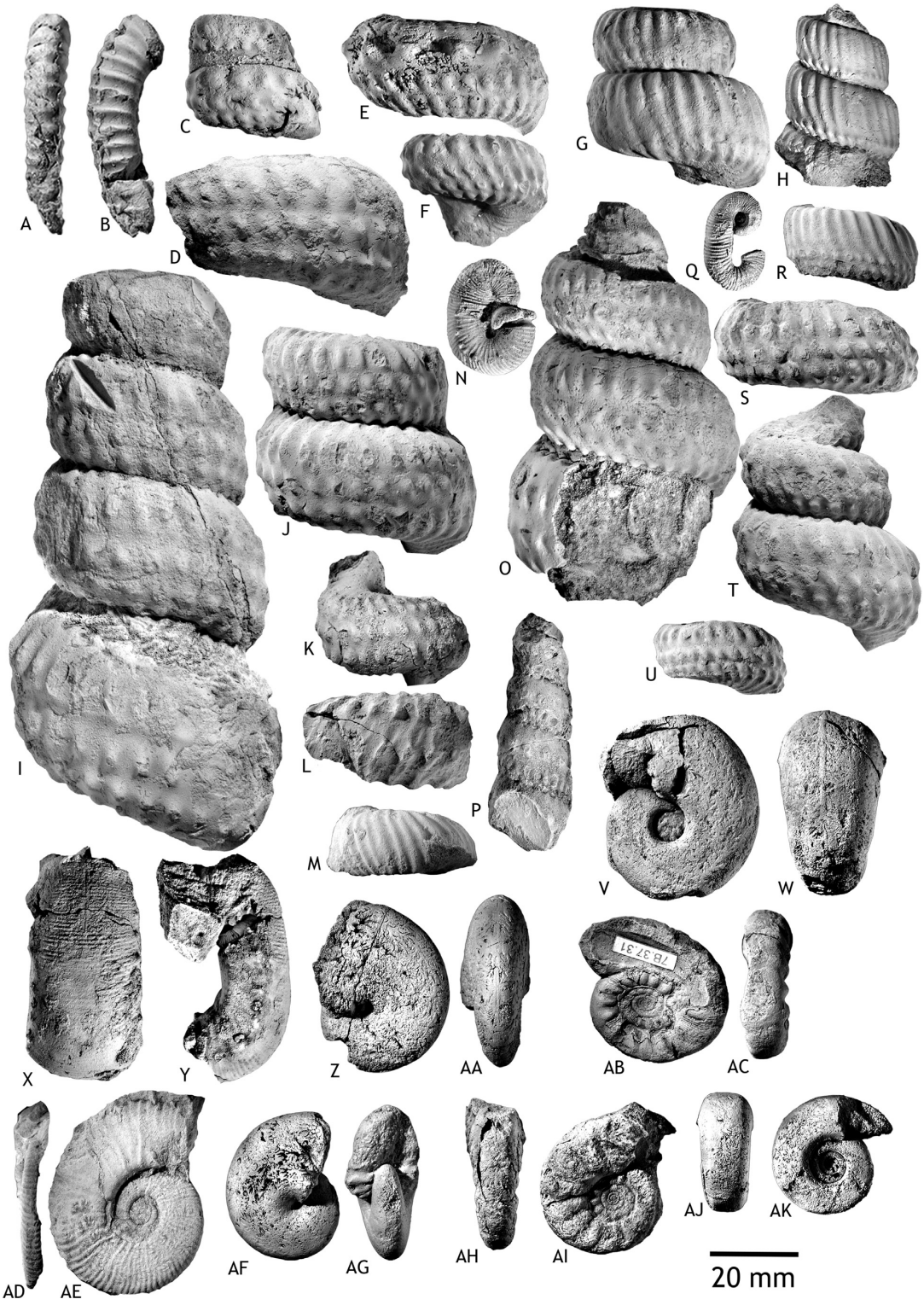
A
B
C
D
E
F
G
H
I
J
K
L
M
N
O
P
Q
R
S
T
U
V
W
X
Y
Z
AA
AB
AC
AD
AE
AF
AG
AH
AI
AJ
AK
20 mm

Occurrence. Lower Cretaceous (late Hauterivian–lower Barremian; for the genus).

Genus *Pseudothurmannia* Spath, 1923

Pseudothurmannia mortilleti (Pictet and De Loriol, 1858)
Fig. 11AD, AE

Synonymy. See Hoedemaeker (2013).
Lectotype. *Ammonites Mortilleti* Pictet and De Loriol, 1958; p. 21, pl. 4, fig. 2a-d.
Material. 1 conch (NMSG 5627).
Locality and horizon. Locality, unknown, Altmann Member, uppermost Hauterivian–upper lower Barremian.
Description. NMSG 5627 measures 48 mm in diameter. Its conch is subevolute (uw/ww = 0.34). The whorl section appears very compressed with flattened flanks, although one side is missing. Umbilical bullae give rise to densely spaced ribs (45 ribs per half whorl), which are straight to slightly falcoid, and bear occasional bifurcations on the middle of the flank. The venter is nearly straight.
Discussion. See Hoedemaeker (2013).
Occurrence. Lower Cretaceous (latest Hauterivian, Highest *Balearites balearis* and *P. ohmi* Zones; Spain, France, Switzerland, Austria, Slovakia, Crimea, Georgia.

Subfamily Douvilleiceratinae Parona and Bonarelli, 1897

Genus *Douvilleiceras* Grossouvre, 1894

Douvilleiceras sp.
Fig. 9G, H

Material. 3 fragments (NMSG Coll. PK. 7.B.42.12, 7.B.42.13, 7.B.42.14).
Locality and horizon. Bergli Nord, Sennwald, Garschella Formation, Albian.
Description. NMSG (Coll. PK. 7.B.42.14) measures 20 mm in maximum measurable conch diameter. Its whorl section is much wider than high. There are thick ribs on which 4 simple tubercles are situated. NMSG (Coll. PK. 7.B.42.13) has a diameter of 29 mm. Its whorl section is wider than high (ww/wh = 1.35). Only 3 ribs are preserved, which carry strong ventrolateral tubercles with 2 grooves each.
Discussion. *Douvilleiceras* changes its ornamentation throughout ontogeny. At an early ontogenetic stage, some species have a quite similar ornamentation, which is not distinguishable. See Casey (1962) for details.
Occurrence. Lower Cretaceous (lower Albian–middle Albian; for the genus).

Subfamily Leptoceratoidae Thieuloy, 1966

Genus *Leptoceratoides* Thieuloy, 1966

Leptoceratoides* cf. *heeri (Ooster, 1860)
Fig. 9AA, AB, AE

Synonymy. See *Karsteniceras*? *heeri* in Vašíček and Wiedmann (1994).
Type. *Ancyloceras Heeri* Ooster, 1860; p. 32, pl. 38, figs. 1–3, 5.
Material. 3 fragments (NMSG Coll. PK. 5.A.05.24, NMSG Coll. KT. AS-W-0007, AS-W-0043).
Locality and horizon. Altmann-Sattel, Südwest-Seite I, the Altmann Member, uppermost Hauterivian–upper lower Barremian.
Description. NMSG (Coll. PK. 5.A.05.24) is a 40 mm long fragment of a crioconic conch. The whorl section is circular (ww/wh = 0.96). Its simple ribs are rectiradiate or slightly rursiradiate, fine, and uniform without bifurcation. The number of ribs per quarter whorl is 21.
Discussion. All specimens resemble the original drawing by Ooster (1860) in the number and shape of ribs.
Occurrences. Lower Cretaceous (Barremian); Switzerland.

Genus *Hamulinites* Thieuloy, 1966

Hamulinites sp.
Fig. 9Y, Z

Material. 1 shell fragment (NMSG Coll. KT. ASW_0048).
Locality and horizon. Altmann-Sattel, Südwest-Seite I, Altmann Member, uppermost Hauterivian–upper lower Barremian.
Description. NMSG (Coll. KT. ASW_0048) measures 44 mm in diameter. Its conch is ancyloceraticonic and slightly curved. There are 16 ribs on the fragment. The whorl cross section is slightly higher than wide (ww/wh = 0.89).
Discussion. Its ancyloceraticonic conch morphology distinguishes this genus from *Leptoceratoides* and *Orbignyceras*.
Occurrence. Lower Cretaceous (Barremian; for the genus).

Superfamily Turrilitaceae Gill, 1871
Family Anisoceratidae Hyatt, 1900

Genus *Anisoceras* Pictet, 1854

Anisoceras armatum (Sowerby, 1817)
Figs. 9AI, 10F, K, L

Synonymy: See Kennedy and Latil (2007).
Holotype. *Hamites armatus* Sowerby, 1817; p. 153, pl. 168.
Material. 6 shell fragments (NMSG Coll. PK. 7.C.07.05, 7.C.07.11, 7.C.13.25, 7.C.15.14, NMSG Coll. KT. HW-A-0010, NA-K-0001).
Locality and horizon. Hinterwinden-Hornwald (Hinter Gräppelen) (NMSG Coll. PK. 7.C.15.14, NMSG Coll. KT. HW-A-0010), Neuenalp-Kamm (NMSG Coll. KT. NA-K-0001), Tal-Wänneli (NE Neuenalpspitz; NMSG Coll. PK. 7.C.07.05, 7.C.07.11), Säntis, Gasthaus-Hang (NMSG Coll. PK. 7C.13.25), Kamm Bed, uppermost Albian–lowermost Cenomanian.
Description. NMSG (Coll. PK. 7.C.07.11) is a straight shaft with a length of 56 mm. The whorl section is rounded (ww/wh = 0.96) with a whorl height of 24 mm. Its ornament consists of looped and

Fig. 11. Ammonoids from the Alpstein. A, B, *Idiohamites* cf. *dorsetensis* Spath, 1926; NMSG (Coll. PK. 7.C.02.23), Stütze 2 Säntisbahn S. C, *Hypoturrilites* cf. *collignoni* Wright and Kennedy, 1996; NMSG (Coll. PK. 7.C.01.14), Tierwis-Stütze 2 Säntisbahn I. D, I, K, *Mariella bergeri* (Brongniart, 1822); D – NMSG (Coll. PK. 7.C.13.01), Säntis, Gasthaus-Hang. I – NMSG (Coll. UO. 010), Säntis; K – NMSG (Coll. PK. 7.C.08.06), Neuenalp-Kamm. E, *Hypoturrilites gravesianus* (d'Orbigny, 1842); NMSG (Coll. PK. 7.C.15.19), Hinterwinden-Hornwald (Hinter Gräppelen). F, *Hypoturrilites* cf. *sharpei* Wright and Kennedy, 1996; NMSG (Coll. PK. 7.C.15.34), Hinterwinden-Hornwald (Hinter Gräppelen). G, *Ostlingoceras costulatum* (Pervinquiére, 1910); NMSG (Coll. PK. 7.C.06.02), Tal W (NE Neuenalpspitz). H, R, *Ostlingoceras puzosianum* (d'Orbigny, 1842); H – NMSG (Coll. UO. 015), Säntis; R – NMSG (Coll. Kürsteiner 7.C.15.32), Hinterwinden-Hornwald. J, O, S–U, *Mariella miliaris* (Pictet and Campiche, 1861); J – NMSG (Coll. PK. 7.C.19.09), Lochtem-Grüenböhl; O – NMSG (Coll. UO. 014), Säntis; S – NMSG (Coll. PK. 7.C.19.10), Lochtem-Grüenböhl; T – NMSG (Coll. PK. 7.C.15.33), Hinterwinden-Hornwald; U – NMSG (Coll. UO. 013); Säntis. L, *Mariella gresslyi* (Pictet and Campiche, 1861); NMSG (Coll. PK. 7.B.37.20), Chelen-Geren (SW Plona). M, *Turrilitoides intermedius* (Pictet and Campiche, 1861); NMSG (Coll. KT. SG-AG-0002) Säntis, Gasthaus-Hang. N, *Scaphites hugardianus* d'Orbigny 1842; NMSG (Coll. UO. 016), Säntis. P, *Neostlingoceras carcitanense* (Matheron, 1842); ETHZ_10424, Gartenalp. Q, *Eoscaphites subcircularis* (Spath, 1937); NMSG (Coll. PK. 7.B.26.02), Stofel, Lenziwis. V, W, *Tetragonites jurinianus jurinianus* (Pictet, 1847); NMSG (Coll. PK. 7.C.11.03), Säntis, Gasthaus-Galerie and surrounding. X, Y, *Scaphites* cf. *simplex* (Jukes-Browne), 1875; NMSG (Coll. KT. Sä-GS-0020), Säntis, Gasthaus Hang, Wannenalp-Schicht. Z, AA, *Phylloceras* (*Hypophylloceras*) *velledae velledae* (Michelin, 1834); NMSG (Coll. PK. 7.C.02.04), Stütze 2 Säntisbahn S. AB, AC, *Kossmatella muhlenbecki* (Fallot, 1885); NMSG (Coll. PK. 7.B.37.31), Chelen-Geren (SW Plona). AD, AE, *Pseudothurmannia mortilleti* (Pictet and De Loriol, 1858); NMSG 5627, locality unknown. AF, AG, *Gorethophylloceras subalpinum* (d'Orbigny, 1841); NMSG (Coll. PK. 7.B.20.21), Schlatt (above Rüthi SG). AH, AI, *Kossmatella agassiziana* (Pictet, 1847); NMSG (Coll. PK. 7.C.14.02), Hinterwinden. AJ, AK, *Tetragonites timotheanus timotheanus* (Pictet, 1847); NMSG (Coll. PK. 7.B.23.03), In Ränken, Plona.

rursiradiate ribs. Thick, strong and tuberculated ribs are intercalated by two or three fine, non-tuberculated and blunt ribs.
Discussion. See Kennedy and Latil (2007).
Occurrence. Lower–Upper Cretaceous (upper Albian–lower Cenomanian); England, Spain, France, Belgium, Germany, Switzerland, Hungary, Romania, Serbia, India, Angola, Mozambique, South Africa (KwaZulu-Natal), USA (Texas).

Anisoceras perarmatum Pictet and Campiche, 1861
Fig. 10G

Synonymy. See Kennedy and Latil (2007).
Lectotype. *Anisoceras perarmatum* Pictet and Campiche, 1861; p. 65, pl. 49, fig. 1.
Material. 2 shell fragments (NMSG Coll. PK. 7.C.06.03, NMSG Coll. KT. EB-Ch-0002).
Locality and horizon. Ebenalp, Übergang gegen Gartenalp (NMSG Coll. KT. EB-Ch-0002), Tal W (NE Neuenalpspitz; NMSG Coll. PK. 7.C.06.03), Kamm Bed, uppermost Albian–lowermost Cenomanian.
Description. NMSG (Coll. PK. 7.C.06.03) is a straight shaft with a length of 73 mm. Its whorl section is oval (ww/wh = 0.85) with a whorl height of 27 mm. Pairs of ribs are connected in the lateral tubercles and fade out dorsally. Intercalated ribs are absent.
Discussion. According to Kennedy et al. (1998), this species differs from *A. armatum* in having no (or few intercalated) ribs.
Occurrence. Lower Cretaceous (upper Albian–lowermost Cenomanian); England, Spain, France, Germany, Switzerland, Hungary, Romania, Ukraine, Crimea, Caucasus, India, Angola, Mozambique, Nigeria, South Africa (Kwazulu-Natal), USA (Texas).

Anisoceras pseudoelegans (Pictet and Campiche, 1861)
Fig. 10I, J

Synonymy. See Marcinowski and Wiedmann (1990).
Type. *Hamites Saussureanus* Pictet, 1847; p. 118, pl. 13.
Material. 7 shell fragments (NMSG Coll. PK. 7.C.02.25, 7.C.15.11, 7.B.23.15, 7.B.23.32, 7.B.25.23, 7.B.26.18, NMSG Coll. UO. 009).
Locality and horizon. Hinterwinden-Hornwald (Hinter Gräppelen; NMSG Coll. PK. 7.C.15.11); Stütze 2 Säntisbahn S (NMSG Coll. PK. 7.C.02.25), Säntis (NMSG Coll. UO. 009), Kamm Bed, uppermost Albian–lowermost Cenomanian; Bergli, Sennwald (NMSG Coll. PK. 7.B.25.23), Stofel, Lenziwis (NMSG Coll. PK. 7.B.26.18), In Ränken, Plona (NMSG Coll. PK. 7.B.23.15, 7.B.23.32), Garschella Formation, Albian.
Description. NMSG (Coll. PK. 7.B.25.23) is a slightly curved shaft with a length of 41 mm. The whorl section is oval (ww/wh = 0.89) with a whorl height of 17 mm. Its ornament consists of looped and rursiradiate ribs. Tuberculated ribs are intercalated by two or three, very fine ribs. Fine ribs are also present on the dorsum while tuberculated ribs do not occur there.
Discussion. This species is similar to *A. armatum*, but it has finer ribs.
Occurrence. Lower Cretaceous (upper Albian); England, France, Italy (Sardinia), Switzerland, Hungary, South Africa (KwaZulu-Natal), Japan.

Genus *Prohelicoceras* Spath, 1925a

Prohelicoceras moutonianum (d'Orbigny, 1850)
Fig. 10M

Synonymy. See Marcinowski and Wiedmann (1990).
Type. *Helicoceras Moutonianum* d'Orbigny, 1850; p. 127, n° 106.
Material. 1 shell fragment (NMSG Coll. PK. 7.B.26.04).
Locality and horizon. Stofel, Lenziwis, Garschella Formation, Albian.
Description. NMSG (Coll. PK. 7.B.26.04) is a helicoidal shell fragment with a maximum whorl height of 20 mm. The whorl section is circular (ww/wh = 1.0). Its ornament consists of looped and rursiradiate ribs. Tuberculated ribs are intercalated by two or three, very fine ribs. Fine ribs are present on the dorsum while tuberculated ribs are missing.
Discussion. See Marcinowski and Wiedmann (1990).
Occurrence. Lower Cretaceous (upper Albian); England, France, Switzerland, Poland.

Family Hamitidae Gill, 1871

Genus *Hamites* Parkinson, 1811

Hamites compressus Sowerby, 1814
Fig. 10R

Synonymy. See Klein (2015).
Holotype. *Hamites compressus* Sowerby, 1814; p. 138, pl. 61, figs. 7, 8.
Material. 1 shell fragment (NMSG Coll. PK. 7.C.11.01).
Locality and horizon. Säntis, Gasthaus-Galerie and surrounding, Kamm Bed, uppermost Albian–lowermost Cenomanian.
Description. NMSG (Coll. PK. 7.C.11.01) is a hook-shaped conch fragment with a length of 50 mm and a whorl height of 22 mm. Its flanks are flattened, while both dorsum and venter are rounded. Its ribs are sharp and more or less straight. There are 6 ribs on a whorl segment equal to whorl height.
Discussion. This species has a very compressed whorl section. The number of ribs on a whorl segment equal to whorl height is 5 according to Sowerby (1814) and Föllmi (1989b) and 6 to 7 according to Spath (1941).
Occurrence. Lower Cretaceous (upper Albian, lower part of *M. inflatum* Zone); England, France, Switzerland, Poland, Angola.

Hamites duplicatus Pictet and Campiche, 1861
Fig. 10T

Synonymy. See Klein (2015).
Lectotype. *Hamites duplicatus* Pictet and Campiche 1861; p. 391, pl. 14 fig. 7, 9.
Material. 1 shell fragment (NMSG Coll. PK. 7.C.19.04).
Locality and horizon. Lochtem-Grüenböhl, Kamm Bed, uppermost Albian–lowermost Cenomanian.
Description. NMSG (Coll. PK. 7.C.19.04) is a straight conch fragment with a length of 31 mm. The whorl section is slightly oval (ww/wh = 0.91) with a whorl height of 82 mm. Ribs with a number of 7 in a diameter equal to the whorl height are sharp, very fine, feebly prorsiradiate and attenuated on the dorsum.
Discussion. The number of ribs on a length equal to the whorl height is 7–10 (Spath, 1941; Gale et al., 1996). For details, see Gale et al. (1996).
Occurrence. Lower–Upper Cretaceous (upper Albian–upper Cenomanian); England, France, Germany, Switzerland, Hungary, Poland, Georgia, Iran, Kazakhstan, Angola, Japan.

Hamites simplex d'Orbigny, 1842
Fig. 10N

Synonymy. See Klein (2015).
Lectotype. *Hamites simplex* d'Orbigny 1842; p. 550, pl. 134, figs. 12–14.
Material. 1 fragment (NMSG Coll. PK. 7.C.13.05).
Locality and horizon. Säntis, Gasthaus-Hang, Kamm Bed, uppermost Albian–lowermost Cenomanian.
Description. NMSG (Coll. PK. 7.C.13.05) is a slightly flexuose shaft with a length of 28 mm. The whorl section is oval (ww/wh = 0.84) with a whorl height of 8 mm. Ribs are fine, prorsiradiate and weak on the dorsum. The number of ribs in a diameter equal to its whorl height is 6.
Discussion. See Cecca (2001).

Occurrence. Upper Cretaceous (lower–middle Cenomanian); England, France, Germany, Poland, Daghestan, USA (Western Interior), Australia.

Hamites subvirgulatus (Spath, 1941)
Fig. 10P

Synonymy. See Klein (2015).
Holotype. *Hamites* (*Stomohamites*) *subvirgulatus* Spath, 1941; p. 645, text-fig. 234a–h.
Material. 1 fragment (NMSG Coll. PK. 7.C.02.07).
Locality and horizon. Stütze 2 Säntisbahn S, Kamm Bed, uppermost Albian–lowermost Cenomanian.
Description. NMSG (Coll. PK. 7.C.02.07) is a gryconic fragment with a length of 35 mm. The whorl section is more or less circular (ww/wh = 0.95) with a whorl height of 9 mm. Five sharp, fine prorsiradiate ibs are visible on a diameter equal to its whorl heightand are absent on the dorsum.
Discussion. See Gale et al. (1996).
Occurrence. Lower Cretaceous (upper Albian–middle Cenomanian); England, possibly Germany, Switzerland, Italy (Sardinia), Poland, Romania, Angola, Madagascar.

Hamites virgulatus Brongniart, 1822
Fig. 10S

Synonymy. See Föllmi (1989b).
Type. *Hamites virgulatus* Brongniart, 1822; pl. 10, fig. 6.
Material. 3 fragments (NMSG Coll. PK. 7.B.26.13, 7.B.37.13, 7.B.38.01).
Locality and horizon. Chelen-Geren (SW Plona; NMSG Coll. PK. 7.B.37.13), Unter-Hard, Rüthi SG (NMSG Coll. PK. 7.B.38.01), Stofel, Lenziwis (NMSG Coll. PK. 7.B.26.13), Garschella Formation, Albian.
Description. NMSG (Coll. PK. 7.B.26.13) is weakly bent with a length of 30 mm. The whorl section is oval (ww/wh = 0.86) with a height of 12 mm. Ribs are sharp, straight to faintly rursiradiate; there are 4 ribs on a segment equal to its whorl height.
Discussion. Our specimens are similar to the one described in Pictet (1847) in rib spacing and whorl cross section.
Occurrence. Lower–Upper Cretaceous (upper Albian–lower Cenomanian); England, Spain, France, Switzerland, Poland, Italy, Madagascar, Mozambique, USA, Mexico.

Hamites* cf. *maximus Sowerby, 1814
Fig. 10H

Synonymy. See Föllmi (1989b).
Type. *Hamites maximus* Sowerby, 1814; p. 138, pl. 62, fig. 1.
Material. 3 fragments (NMSG Coll. PK. 7.B.25.32, NMSG Coll. KT. HW-A-0013).
Locality and horizon. Bergli, Sennwald (NMSG Coll. PK. 7.B.25.32), Hinterwinden-Hornwald (Hinter Gräppelen; NMSG Coll. KT. HW-A-0013), Garschella Formation, Albian.
Description. NMSG (Coll. KT. HW-A-0013) is a straight shaft, measuring 70 mm. The whorl section is slightly compressed (ww/wh = 0.88) with a whorl height of 93 mm. Its ribs are relatively blunt and straight. There are 5 ribs on a whorl length equalling whorl height.
Discussion. This species has a more or less circular whorl section. Its ribs are blunt. The number of ribs in a length equal to whorl height is 6 according to Sowerby (1814) and 4 to 6 according to Spath (1941).
Occurrence. Lower Cretaceous (middle–lower upper Albian); England, France, Austria.

Hamites* cf. *similis (Casey, 1961)
Fig. 10O

Synonymy. See Klein (2015).
Type. *Lytohamites similis* Casey, 1961; p. 92.
Material. 2 fragments (NMSG Coll. PK. 7.B.23.28, NMSG Coll. KT. Rä-IR-0009).
Locality and horizon. In Ränken, Plona, Garschella Formation, Albian.
Description. NMSG (Coll. PK. 7.B.23.28) is a hook-shaped conch fragment with a length of 24 mm. The whorl section is slightly oval (ww/wh = 0.93) with a whorl height of 10 mm. Its ribs are dense, sharp, very fine, and prorsiradiate. There are 9 ribs in a diameter equal to the whorl height.
Discussion. The number of ribs of Spath's (1941) specimen (*Hamites* (*Stomohamites?*) *multicostatus*; Text-fig. 219i, f) is 9 or 10 in a whorl segment equal to whorl height. Some specimens figured in Föllmi (1989b) appear to have the same number of ribs in a length equal to whorl height. But as Wright and Kennedy (1995) pointed out, following Spath (1941), a separation of the species belonging to the genus *Hamites* in the Late Albian is doubtful. The difference lies merely in the sharpness and distance of the ribs of small specimens.
Occurrence. Lower Cretaceous (upper Albian); England, Angola.

Hamites sp.
Fig. 10Q

Material. 1 fragment (NMSG Coll. KT. CH-O-0001).
Locality and horizon. Oberrieter Chienberg West (NMSG Coll. KT. CH-O-0001), Kamm Bed, uppermost Albian–lowermost Cenomanian.
Description. NMSG (Coll. KT. CH-O-0001) is a straight shaft with a length of 25 mm. The whorl section is slightly oval (ww/wh = 0.91) with a whorl height of 25 mm. Ribs are blunt, widely spaced, and straight. There are 4 ribs on a whorl segment equal to the corresponding whorl height.
Discussion. Spath (1941) mentioned that the ribs of *Hamites maximus* are blunt and become widely spaced late in ontogeny. Our specimen has a wide whorl interspace and blunt ribs; in these respectes, it is similar to a specimen illustrated by Gauthier (2006: plate 44, fig10). The ribs of our specimens are slightly too widely spaced for the size.
Occurrence. Lower–Upper Cretaceous (for the genus).

Genus *Idiohamites* Spath, 1925b

Idiohamites* cf. *dorsetensis Spath, 1926
Fig. 11A, B

Synonymy. See Klein (2015).
Holotype. *Anisoceras alternatus* Mantell, Pictet and Campiche, 1861; p. 71, pl. 51, figs. 2, 3.
Material. 1 fragment (NMSG Coll. PK. 7.C.02.23).
Locality and horizon. Stütze 2 Säntisbahn S, Kamm Bed, Alpstein.
Description. NMSG (Coll. PK. 7.C.02.23) is a more or less gyroconic conch fragment with a length of 52 mm. The whorl section is compressed and oval (ww/wh = 0.75). Coarse and widely spaced ribs are present on the flank, weakening on the dorsum. Two small ventrolateral bullae are present on each rib. There are 4 ribs on a whorl segment equal to the whorl height.
Discussion. The specimen is similar to that figured by Spath (1941). His specimen has some ventrolateral tubercles. Our specimen displays ventrolateral bullae on most of the ribs, but they are not conspicuous. Wright and Kennedy (1995) stated that *H. alternatus* is very similar to *H. dorsetensis*. They argue that Spath (1941) did not provide a clear explanation on how to differentiate between the two species. *H. dorsetensis*, in this respect, may be a synonym of *H. alternatus*.
Occurrence. Lower Cretaceous (upper Albian, *M. perinflatum* Zone); England, France, Switzerland, Kazakhstan.

Family Turrilitidae Gill, 1871

Genus *Mariella* Nowak, 1916

Mariella bergeri (Brongniart, 1822)
Fig. 11D, I, K

Synonymy. See Klein (2015).
Holotype. *Turrilites bergeri* Brongniart, 1822; p. 399, pl. 7, fig. 3.
Material. 14 fragments (NMSG Coll. PK. 7.C.01.04, 7.C.01.12, 7.C.01.13, 7.C.02.15, 7.C.04.01, 7.C.08.06, 7.C.11.06, 7.C.13.01, 7.C.13.02, 7.C.19.02, NMSG Coll. KT. GS-BS-0008, NMSG Coll. UO. 010, 011, 012).
Locality and horizon. Blauschnee-Girenspitz (NMSG Coll. KT. GS-BS-0008), Lochtem-Grüenböhl (NMSG Coll. PK. 7.C.19.02), Neuenalp-Kamm (NMSG Coll. PK. 7.C.08.06), Tierwis-Stütze 2 Säntisbahn I ((NMSG Coll. PK. 7.C.02.15), Stütze 2 Säntisbahn S (NMSG Coll. PK. 7.C.01.04, 7.C.01.12, 7.C.01.13), Säntis, Gasthaus-Galerie and surrounding (NMSG Coll. PK. 7.C.11.06), Stütze 2 – Girenspitz/Säntis, Weg (NMSG Coll. PK. 7.C.04.01), Säntis, Gasthaus-Hang (NMSG Coll. PK. 7.C.13.01, 7.C.13.02), Säntis (NMSG Coll. UO. 12, 13, 17), Kamm Bed, uppermost Albian–lowermost Cenomanian.
Description. NMSG (Coll. UO. 12) has 4 whorls and measures 147 mm in maximum measureable diameter. The whorl height of the last whorl is 39 mm. Four obliquely aligned rows of tubercles are present on the flank. They are elongated in the first row from dorsal and more or less rounded in the other rows. The fourth row carries the smallest tubercles. The widest space between rows is between the first and second one and the narrowest is between the third and fourth row. The number of tubercles is 14 per half whorl of each row.
Discussion. This is one of the most common heteromorphs of the Alpstein. For a discussion of the species, see Klinger and Kennedy (1978).
Occurrence. Lower Cretaceous (upper Albian); England, Spain, France, Germany, Switzerland, Italy (Sardinia), Hungary, Romania, Iran, Algeria, Madagascar, Morocco, USA (California), Venezuela.

Mariella gresslyi (Pictet and Campiche, 1861)
Fig. 11L

Synonymy. See Klein (2015).
Syntype. *Turrilites gresslyi*, Pictet and Campiche, 1861; p. 132, pl. LVII, figs. 11–13.
Material. 1 fragment (NMSG Coll. PK. 7.B.37.20).
Locality and horizon. Chelen-Geren (SW Plona), Garschella Formation, Albian.
Description. NMSG (Coll. PK. 7.B.37.20) measures 39 mm in diameter with a whorl height of 23 mm. There are four rows of obliquely aligned tubercles, all of which are connected by looped ribs. The lowest row of tubercles is normally covered by the next whorl. There are 7 tubercles per quarter whorl per row.
Discussion. Our specimen resembles the figured specimens in Pictet and Campiche (1861) in having three or four rows of obliquely aligned tubercles, which are connected by ribs.
Occurrence. Lower Cretaceous (upper Albian); England, Switzerland, Hungary, USSR, Angola, Madagascar.

Mariella miliaris (Pictet and Campiche, 1861)
Fig. 11J, O, S–U

Synonymy. See Klein (2015).
Type. Holotype, *Turrilites Bergeri* Brongniart, var. *miliaris* Pictet and Campiche, 1861; p. 136, pl. 58, fig. 5.
Material. 9 fragments (NMSG Coll. PK. 7.C.06.04, 7.C.13.19, 7.C.15.12, 7.C.15.33, 7.C.19.01, 7.C.19.09, 7.C.19.10, NMSG Coll. UO. 013, 014).
Locality and horizon. Hinterwinden-Hornwald (Hinter Gräppelen; NMSG Coll. PK. 7.C.15.12, 7.C.15.33), Säntis, Gasthaus-Hang (NMSG Coll. PK. 7.C.13.19), Lochtem-Grüenböhl (NMSG Coll. PK. 7.C.19.01, 7.C.19.09, 7.C.19.10), Tal W (NE Neuenalpspitz; NMSG Coll. PK. 7.C.06.04), Säntis (NMSG Coll. UO. 013, 014), Kamm Bed, uppermost Albian–lowermost Cenomanian.
Description. NMSG (Coll. UO. 014) has nearly 3 whorls and measures 90 mm in maximum measurable height. The whorl height of the last whorl is 29 mm. The apical angle is 24°. Four obliquely aligned rows of tubercles are present on the flank. Tubercles of the first row are slightly oval, while the others are subcircular. The tubercles of the 4th row are smaller than the others in size and closer to the adjacent row.
Discussion. The specimen shows similar characteristics to *M. bergeri* described above. The tubercles are finer and denser than *M. bergeri*: the number of tubercles is 17 for each row per half whorl. For details see Wright and Kennedy (1996).
Occurrence. Lower–Upper Cretaceous (upper Albian–lower Cenomanian, *M. mantelli* Zone); England, France, Switzerland, Italy (Sardinia), Hungary, Romania, Turkmenistan, Madagascar, South Africa (KwaZulu-Natal).

Genus *Ostlingoceras* Hyatt, 1900

Ostlingoceras costulatum (Pervinquiére, 1910)
Fig. 11G

Synonymy. See Wright and Kennedy (1996).
Lectotype. *Turrilites costatus* var. *costulata* Pervinquiére, 1910; p. 50, pl. 14 (5), figs. 6, 7.
Material. 1 fragment (NMSG Coll. PK. 7.C.06.02).
Locality and horizon. Tal W (NE Neuenalpspitz), Kamm Bed, uppermost Albian–lowermost Cenomanian.
Description. NMSG (Coll. PK. 7.C.06.02) has 3 whorls and measures 49 mm in total height. The whorl height of the last whorl is 24 mm. The apical angle is approximately 26° (the specimen is somewhat deformed). The whorl section is nearly rectangular with a flat to slightly concave flank. Straight to faintly oblique ribs, which cover the upper and middle flank, are coarse; there are about 26 ribs per whorl carrying two (or three; the second and third rows are almost fused) rows of tubercles on the lower flank. 10 tubercles per quarter whorl are present from which a rib originates.
Discussion. See Wright and Kennedy (1996).
Occurrence. Upper Cretaceous (lower Cenomanian); England, probably Italy, Madagascar, South Africa, Tunisia.

Ostlingoceras puzosianum (d'Orbigny, 1842)
Fig. 11H, R

Synonymy. See Klein (2015).
Syntypes. *Turrilites puzosianus* d'Orbigny, 1842; p. 587, pl. 143, figs. 1, 2.
Material. 7 fragments (NMSG Coll. PK. 7.C.07.03, 7.C.08.01, 7.C.15.18, 7.C.15.32, NMSG Coll. KT. EB-Ch-0001, HW-A-0053, NMSG Coll. UO. 015).
Locality and horizon. Hinterwinden-Hornwald (Hinter Gräppelen; NMSG Coll. PK. 7.C.15.18, 7.C.15.32, NMSG Coll. KT. HW-A-0053), Ebenalp, Übergang gegen Gartenalp (NMSG Coll. KT. EB-Ch-0001), Tal-Wänneli (NE Neuenalpspitz; NMSG Coll. PK. 7.C.07.03), Neuenalp-Kamm (NMSG Coll. PK. 7.C.08.01), Säntis (NMSG Coll. UO. 015), Kamm Bed, uppermost Albian–lowermost Cenomanian.
Description. NMSG (Coll. UO. 015) has 2 whorls with a maximum whorl height of 29 mm. Its apical angle measures 17°. The whorl section is rectangular with a flattened flank on which conspicuous obliquely aligned ribs are present. Each rib covers the upper and middle flank. One or two tubercles at the lower flank give rise to a rib. At the lower edge of the imprint zone, two rows of tubercles are present but a part of the lower tubercle row is covered by the next whorl. The number of ribs and tubercles per row in one whorl is 26 and 34.

Discussion. See Marcinowski and Wiedmann (1990) and Kennedy and Latil (2007).
Occurrence. Lower Cretaceous (upper Albian, *M. rostratum* and *M. perinflatum* Zone); England, Spain, France, Switzerland, Austria, Italy (Sardinia), Hungary, Poland, Romania, Crimea, Caucasus, Georgia, Iran, Turkmenistan, Madagascar.

Genus *Hypoturrilites* Dubourdieu, 1953

Hypoturrilites gravesianus (d'Orbigny, 1842)
Fig. 11E

Synonymy. See Klein (2015).
Type. *Turrilites Gravesianus* d'Orbigny, 1842; p. 596, pl. 144, figs. 3, 4, 5.
Material. 1 fragment (NMSG Coll. PK. 7.C.15.19).
Locality and horizon. Hinterwinden-Hornwald (Hinter Gräppelen), Kamm Bed, uppermost Albian–lowermost Cenomanian.
Description. NMSG (Coll. PK. 7.C.15.19) has a whorl with a maximum whorl height of 27 mm. The whorl cross section is broadly rounded. The tubercles of the first row are the largest and sharp, occupying half of the flank. The other tubercles, two of which are almost fused, are conical and rounded on the top. There are 7 tubercles per half whorl in the first row, while in the lower rows, there are 16 per half whorl.
Discussion. See Wright and Kennedy (1996).
Occurrence. Upper Cretaceous (lower Cenomanian, *M. mantelli* Zone); England, France, Germany, Kazakhstan, Turkmenistan, South Africa (KwaZulu-Natal), USA (Gulf coast), Argentina, Japan, Australia.

Hypoturrilites* cf. *collignoni Wright and Kennedy, 1996.
Fig. 11C

Synonymy. See Wright and Kennedy (1996).
Holotype. *Hypoturrilites collignoni* Wright and Kennedy, 1996; p. 376, pl. 99, fig. 33.
Material. 2 fragments (NMSG Coll. PK. 7.C.01.14, 7.C.13.41).
Locality and horizon. Tierwis-Stütze 2 Säntisbahn I (NMSG Coll. PK. 7.C.01.14), Säntis, Gasthaus-Hang (NMSG Coll. PK. 7.C.13.41), Kamm Bed, uppermost Albian–lowermost Cenomanian.
Description. NMSG (Coll. PK. 7.C.01.14) has 2 whorls and measures 40 mm in total height. The whorl height of the last whorl is 11 mm. The apical angle is 25°. Its whorl section is almost rectangular. There are four obliquely aligned rows of tubercles, three of which are subequidistant while the fourth one is situated closer to the third one. The tubercles of the first row are slightly elongate while the others are conical to subspherical. All tubercles have a flat top. The number of tubercles in the first row is lower (8 per half whorl) than in the other rows (10 per half whorl). NMSG (Coll. PK. 7.C.13.41) has 2 whorls with a maximum height of 42 mm. The apical angle is 19°. The whorl cross section is nearly rectangular with a flat to slightly concave flank. There are four obliquely aligned rows of tubercles. The third and fourth tubercles are situated closer to each other and are slightly smaller than those of the other two rows. The tubercles in the first row are elongated while the other ones are rounded. The number of tubercles in the first row is lower (6 per half whorl) than in the other rows (8 per half whorl).
Discussion. See Wright and Kennedy (1996).
Occurrence. Upper Cretaceous (lower Cenomanian, *M. mantelli* Zone, *Neostlingoceras carcitanense* Subzone); England, France, Switzerland, Madagascar.

Genus *Pseudhypoturrilites* Cooper, 1999

Pseudhypoturrilites* cf. *sharpei (Wright and Kennedy, 1996)
Fig. 11F

Synonymy. See Wright and Kennedy (1996).
Holotype. *Hypoturrilites sharpei* Wright and Kennedy 1996; p. 378, pl. 100, fig. 15.
Material. 1 fragment (NMSG Coll. PK. 7.C.15.34).
Locality and horizon. Hinterwinden-Hornwald (Hinter Gräppelen), Kamm Bed, uppermost Albian–lowermost Cenomanian.
Description. NMSG (Coll. PK. 7.C.15.34) has a maximum whorl height of 16 mm. The whorl section is rectangular. Four obliquely aligned and somewhat pointed tubercles are present, between which weak ribs are developed. The first and second rows of tubercles are larger than the others, occupying two thirds of the flank. There are 11 tubercles per half whorl in the first row, while in the lower rows, there are 13.
Discussion. See Wright and Kennedy (1996).
Occurrence. Upper Cretaceous (lower Cenomanian, *M. mantelli* Zone, *Neostlingoceras carcitanense* Subzone); England.

Genus *Neostlingoceras* Klinger and Kennedy, 1978

Neostlingoceras carcitanense (Matheron, 1842)
Fig. 11P

Synonymy. See Klein (2015).
Holotype. *Turrilites tuberculatus* Matheron 1842; p. 267, pl. 41, fig. 4.
Material. 2 conchs (ETHZ 10424, NMSG Coll. PK. 7.C.13.34).
Locality and horizon. Gartenalp (ETHZ 10424), ?uppermost Albian–lowermost Cenomanian; Säntis, Gasthaus-Hang (NMSG Coll. PK. 7.C.13.34), Kamm Bed, uppermost Albian–lowermost Cenomanian.
Description. ETHZ 10424 has a maximum whorl height of 14 mm with a rectangular whorl section. Two rows of tubercles are present, the upper of which with conical tubercles. These tubercles are located just above the middle flank while the lower row carries slightly elongated tubercles just above the whorl suture. The numbers of tubercles in the upper and lower rows are 7 and 12 per half whorl, respectively. NMSG (Coll. PK. 7.C.13.34) measures 63 mm in maximum diameter. Its whorl section is rectangular with flattened flanks. Two rows of tubercles are present on the middle and lowest part of the flank. The numbers of tubercles in the upper and lower rows are 7 and 13 per half whorl, respectively.
Discussion. See Wright and Kennedy (1996).
Occurrence. Upper Cretaceous (lower Cenomanian); England, France, Germany, Poland, Kazakstan, Iran, India, Madagascar, South Africa (KwaZulu-Natal), USA (Gulf coast), Japan.

Genus *Turrilitoides* Gill, 1871

Turrilitoides intermedius (Pictet and Campiche, 1861)
Fig. 11M

Synonymy. See Klein (2015).
Lectotype. *Turrilites intermedius* Pictet and Campiche, 1861; p. 127, pl. 57, fig. 12.
Material. 1 fragment (NMSG Coll. KT. SG-AG-0002).
Locality and horizon. Säntis, Gasthaus-Hang, Kamm Bed, uppermost Albian–lowermost Cenomanian.
Description. NMSG (Coll. KT. SG-AG-0002) has a maximum whorl height of 16 mm. Its whorl section is rounded and higher than wide. 15 non-tuberculate ribs per demi whorl are present.
Discussion. See Marcinowski and Wiedmann (1990).
Occurrence. Lower Cretaceous (upper Albian); England, France, Hungary, Poland, Switzerland, South Africa (KwaZulu-Natal).

Family Baculitidae Meek, 1876

Genus *Lechites* Nowak, 1908

Lechites gaudini (Pictet and Campiche, 1861)

Fig. 9S, T, AF

Synonymy. See Kennedy and Latil (2007).
Type. *Baculites gaudini* Pictet and Campiche, 1861, p. 112, pl. 55, figs. 5–7.
Material. 5 fragments (NMSG Coll. PK. 7.B.20.06, 7.C.02.09, 7.C.13.07, 7.C.14.03, NMSG Coll. UO. 007).
Locality and horizon. Lochtem-Grüenböhl (NMSG Coll. PK. 7.C.13.07), Stütze 2 Säntisbahn S (NMSG Coll. PK. 7.C.02.09), Hinterwinden (Hinter Gräppelen; NMSG Coll. PK. 7.C.14.03), Säntis, (NMSG Coll. UO. 007), Kamm Bed, uppermost Albian–lowermost Cenomanian; Schlatt (above Rüthi SG; NMSG Coll. PK. 7.B.20.06), Garschella Formation, Albian.
Description. NMSG (Coll. PK. 7.C.14.03) has a straight shaft, which has a diameter of 38 mm with a slightly compressed whorl section (ww/wh = 0.93). Its ornament is composed of prorsiradiate ribs, which fade out dorsally. There are 5 ribs in a diameter equal to whorl height. NMSG (Coll. PK. 7.C.13.42) is a straight shaft of 32 mm diameter with a compressed whorl section (ww/wh = 0.87). Its conch is smooth with very oblique ribs. There are two ribs in a diameter equal to whorl height.
Discussion. NMSG (Coll. PK. 7.C.13.42) is a variant with less dense ribbing, previously referred to as *L. raricostatus*. See Cooper and Kennedy (1977).
Occurrence. Lower–Upper Cretaceous (upper Albian, *M. pricei* Zone–Lower Cenomanian); England, France, Germany, Switzerland, Italy (Sardinia), Hungary, Romania, India, Algeria, Madagascar, South Africa (KwaZulu-Natal), Mexico, Japan.

Genus *Sciponoceras* Hyatt, 1894

Sciponoceras baculoides (Mantell, 1822)
Fig. 9AG

Synonymy. See Kennedy et al. (2011).
Lectotype. *Sciponoceras baculoides* Mantell; Kennedy, 1971, p. 9, pl. 1, figs. 12–18.
Material. 1 conch fragment (NMSG Coll. PK. 7.C.13.06).
Locality and horizon. Säntis, Gasthaus-Hang, Kamm Bed, uppermost Albian–lowermost Cenomanian.
Description. NMSG (Coll. PK. 7.C.13.06) is a fragment, measuring 27 mm in maximum length. The whorl section is slightly compressed (ww/wh = 0.94). Ribs are oblique and unconspicuous. There is one strong constriction with a dorsal sinus. It appears that there was a second constriction where the specimen broke. There are 6 ribs between these two constrictions.
Discussion. See Wright and Kennedy (1995).
Occurrence. Upper Cretaceous (Cenomanian); France, Belgium, Germany, Switzerland, Hungary, Poland, Romania, Russia, India, Madagascar, South Africa (KwaZulu-Natal), USA (California, Texas), Japan, New Zealand.

Sciponoceras roto Cieśliński, 1959
Fig. 9AJ

Synonymy. See Kennedy et al. (2011).
Lectotype. *Sciponoceras roto* Cieśliński, 1959; p. 39, 75, 89, text-Fig. 10(2).
Material. 1 fragment (NMSG Coll. UO. 008).
Locality and horizon. Säntis, Kamm Bed, uppermost Albian–lowermost Cenomanian).
Description. NMSG (Coll. UO. 008) is a straight shaft measuring 93 mm in length. Its conch is gradually expanding with a slightly oval whorl section (ww/wh = 0.93). There are 6 oblique (45–50°) and weak ribs on a whorl segment equal to the whorl height. There is only one oblique and blunt constriction preserved in this specimen.
Discussion. See Wright and Kennedy (1995).
Occurrence. Upper Cretaceous (Cenomanian, probably restricted to the lower Cenomanian); England, France, Germany, Poland, Kazakhstan, Tunisia.

Superfamily Scaphitaceae Gill, 1871
Family Sacphitidae Gill, 1871
Subfamily Scaphitinae Gill, 1871

Genus *Scaphites* Parkinson, 1811

Scaphites* cf. *simplex (Jukes-Browne, 1875)
Fig. 11X, Y

Synonymy. See Wiedmann (1965).
Type. *Scaphites Meriani* var. *simplex* Juke-Browne, 1875; p. 287, pl. 14, fig. 3.
Material. 3 fragment of body chamber (NMSG Coll. PK. 7.C.13.20, NMSG 5673, NMSG Coll. KT. Sä-GS-0020).
Locality and horizon. Säntis, Gasthaus-Hang (NMSG Coll. PK. 7.C.13.20), Säntis, Gasthaus Hang, Wannenalp-Schicht (NMSG Coll. KT. Sä-GS-0020), uppermost Albian–lowermost Cenomanian; Unknown (NMSG 5673).
Description. NMSG (Coll. KT. Sä-GS-0020) is a straight shaft with a weathered normally coiled part, and most of the following U-shaped hook, measuring 50 mm in length. The normally coiled part is globose. The body chamber is compressed with a broad and flat venter. The ribs on the body chamber are very fine; these ribs carry 7 pairs of tubercles.
Discussion. Spath (1937) described this species as a member of *Scaphites* with nearly involute, globose initial whorls and a depressed body chamber. Mainly the body chamber is preserved in our specimen, showing the depressed whorl section. Cooper (1990) considered that *Sc. meriani* Pictet and Campiche, 1861 and *Sc. simplex* Jukes Browne, 1865 are synonyms of *H. hugardianus* d'Orbigny, 1842, showing the characteristic morphological intraspecific variation of the species. By contrast, Wright and Kennedy (1996) considered *Sc. hugardianus* as a *nomen dubium*, stating that the main difference between the above mentioned species is the suture line course. We tentatively regard *Sc. simplex* and *Sc. hugardianus* as independent and valid species until a thorough revision has been carried out and published.
Occurrence. Lower Cretaceous (upper Albian); England, Spain, France, Germany, Switzerland, Iran, Madagascar.

Scaphites hugardianus d'Orbigny 1842
Fig. 11N

Synonymy. See Cooper (1990).
Lectotype. *Scaphites hugardianus* d'Orbigny, 1842; p. 521, 525.
Material. 1 phragmocone (NMSG Coll. PK. 7.C.07.09) and 1 conch (NMSG Coll. UO. 016).
Locality. Tal-Wänneli (NE Neuenalpspitz; NMSG Coll. PK. 7.C.07.09), Säntis (NMSG Coll. UO. 016), Kamm Bed, uppermost Albian–lowermost Cenomanian.
Description. NMSG (Coll. UO. 016) is an adult specimen with lappet at the aperture, measuring 23 mm in diameter. Its phragmocone is involute with a completely closed umbilicus. The whorl section is depressed with a very broadly rounded venter. Its flank is rounded with lateral tubercles between which 2–3 fine ribs are present on the body chamber. The ribs are very dense and cross the venter. The number of ribs in a distance equal to the whorl width is approximately 17.
Discussion. As mentioned previously, some morphological characters of this species overlap with those of *S. simplex*. The main difference (except their suture lines) appears to be in their tuberculation. *S. hugardianus* retains pericodic tubercles on the body chamber. Furthermore *S. hugardianus* reaches only a small adult size.

Occurrence. Lower Cretaceous (upper Albian–?lower Cenomanian); England, Spain, France, Switzerland, Italy (Sardinia), Hungary, Algeria, Madagascar.

Genus *Eoscaphites* Breistroffer, 1947

Eoscaphites subcircularis (Spath, 1937)
Fig. 11Q

Synonymy. See Wiedmann (1965). The species was also mentioned by Gale et al. (2011).
Type. *Scaphites subcircularis* Spath, 1937; p. 501, text-fig. 175e, pl. 57, figs. 10–12.
Material. 1 fragment (ETHZ 10425) and 1 complete conch (NMSG Coll. PK. 7.B.26.02).
Locality and horizon. Stofel, Lenziwis (NMSG Coll. PK. 7.B.26.02), ?St. Fähnern, Appenzell (ETHZ 10425), Garschella Formation, Albian.
Description. NMSG (Coll. PK. 7.B.26.02) is a complete conch, measuring 22 mm in maximum length and 10 mm in diameter of the regularly coiled part. The latter part of the conch, which is followed by the straight body chamber, is subinvolute (uw/dm = 0.29). The straight shaft of the body chamber ends with a U-shaped hook whose fine and radiate ribs cover the entire conch; these can be single or bifurcating.
Discussion. See Wiedmann (1965).
Occurrence. Lower Cretaceous (upper Albian, *M.pricei* Zone); England, France, Austria, Madagascar.

Suborder Lytoceratina Hyatt, 1889
Superfamily Tetragonitaceae Hyatt, 1900
Family Tetragonitidae Hyatt, 1900

Genus *Tetragonites* Kossmat, 1895

Tetragonites jurinianus jurinianus (Pictet, 1847)
Fig. 11V, W

Synonymy. See Klein et al. (2009).
Holotype. *Ammonite Jurinianus* Pictet, 1847; p. 297, pl. 3, figs. 3a–c.
Material. 3 conchs (NMSG Coll. PK. 7.C.01.09, 7.C.11.03, 7.C.15.15).
Locality and horizon. Säntis, Gasthaus-Galerie and surrounding (NMSG Coll. PK. 7.C.11.03), Tierwis-Stütze 2 Säntisbahn I (NMSG Coll. PK. 7.C.01.09), Hinterwinden-Hornwald (Hinter Gräppelen; NMSG Coll. PK. 7.C.15.15), Kamm Bed, uppermost Albian–lowermost Cenomanian.
Description. NMSG (Coll. PK. 7.C.11.03) measures 39 mm in diameter. Its conch is thickly discoidal (ww/dm = 0.59) and subinvolute (uw/dm = 0.22). The whorl section is rectangular and wider than high (ww/wh = 1.24). Only some parts of saddles are preserved.
Discussion. Our specimen with the above mentioned measurements fits well with specimens shown in figure 6 of Cooper and Kennedy (1979).
Occurrence. Lower–Upper Cretaceous (upper Albian–lower Cenomanian); France, Italy (Sardinia), Switzerland, Poland, India, Angola, Madagascar, Canada (British Columbia), USA (Alaska, California, Florida).

Tetragonites timotheanus timotheanus (Pictet, 1847)
Fig. 11AJ, AK

Synonymy. See Klein et al. (2009).
Lectotype. *Ammonites timotheanus* Pictet, 1847; p. 295, pl. 3, figs. 1a–c.
Material. 1 conch (NMSG Coll. PK. 7.B.23.03).
Locality and horizon. In Ränken, Plona, Garschella Formation, Albian.
Description. NMSG (Coll. PK. 7.B.23.03) measures 26 mm in diameter. The conch is discoidal (ww/dm = 0.46) and subevolute (uw/dm = 0.35). Its whorl section is rectangular and wider than high (ww/wh = 1.2). There are three constrictions per whorl.
Discussion. This species is characterized by a wide umbilicus and trapezoidal whorl sections. For a detailed description, see Wiedmann (1962).
Occurrence. Lower Cretaceous (middle Albian–lower Cenomanian); England, Spain, France, Germany, Hungary, Iran, India, Egypt, Madagascar.

Genus *Kossmatella* Jocob, 1907

Kossmatella agassiziana (Pictet, 1847)
Fig. 11AH, AI

Synonymy. See Scholz (1979).
Type. *Ammonite Agassizianus* Pictet, p. 303, pl. 4, fig. 3a–c.
Material. 2 conchs (NMSG Coll. PK. 7.C.14.02, 7.C.13.29).
Locality and horizon. Hinterwinden (Hinter Gräppelen; NMSG Coll. PK. 7.C.14.02), Säntis, Gasthaus-Hang (NMSG Coll. PK. 7.C.13.29), Kamm Bed, uppermost Albian–lowermost Cenomanian.
Description. NMSG (Coll. PK. 7.C.14.02) measures 29 mm in diameter. Its conch is thinly discoidal (ww/dm = 0.38) and subinvolute (uw/dm = 0.28). The whorl section is slightly rounded and higher than wide (ww/wh = 0.81). There are 8 bulges with very fine ribs on the flank per half a whorl.
Discussion. The ornamentation is like that of *K. muhlenbecki*. Both our specimens have a narrower umbilicus than the specimens described as *K. muhlenbecki* in Wiedmann and Dienni (1968; uw/dm = 0.40–0.42). As mentioned above, the definition of this species is not yet clear. We tentatively regard this species as involute variant of *Kossmatella*. For details see Scholz (1979).
Occurrence. Lower Cretaceous (middle–upper Albian); Spain, France, Switzerland, Italy, Hungary, Serbia, Crimea, Caucasus, Azerbaijan.

Kossmatella muhlenbecki (Fallot, 1885)
Fig. 11AB, AC

Synonymy. See Klein et al. (2009). The species was also mentioned by Gale et al. (2011).
Type. *Ammonites (Desmoceras) Muhlenbecki* Fallot, 1885; p. 233, pl. IV, fig. 1a.
Material. 1 conch (NMSG Coll. PK. 7B.37.31).
Locality and horizon. Chelen-Geren (SW Plona), Garschella Formation, Albian.
Description. NMSG (Coll. PK. 7B.37.31) measures 37 mm in diameter. Its conch is thinly discoidal (ww/dm = 0.33) and subevolute (uw/dm = 0.40). The whorl cross section is sub-rectangular (flattened venter and flanks) and slightly higher than wide (ww/wh = 0.91). There are 16 bulges with very fine ribs on the flank in the outermost whorl.
Discussion. Scholz (1979) discussed the taxonomy of *Kossmatella*. He considered that some *Kossmatella* species (*K. muhlenbecki*, *K. romana, K. schwindewolfi, K. oosteri* and *K. agassiziana*) could be synonymized. This may be reasonable because previous studies often overlooked or ignored intraspecific variability. However, our materials do not permit to solve the problem because of the low number of specimens and the moderate preservation. See also Wiedmann and Dienni (1968) for a further discussion.
Occurrence. Lower Cretaceous (middle–upper Albian); Spain, France, Italy (Sardinia), Hungary.

Family Schloenbachiidae Parona and Bonarelli, 1897

Genus *Schloenbachia* Neumayr, 1875

Schloenbachia varians (Sowerby, 1817)
Fig. 9AK, AL

Synonymy. See Wright and Kennedy (2015).

Lectotype. *Ammonites varians* Sowerby, 1817: p. 169, pl. 176, uppermost figure.
Material: 1 eroded conch (NMSG Coll. UO. 018).
Locality and horizon. Säntis, Kamm Bed, uppermost Albian–lowermost Cenomanian.
Description. NMSG (Coll. UO. 018) measures 81 mm in diameter. Its conch is sub-involute (uw/dm = 0.27). The whorl section appears compressed, although one side is not preserved. The flank is nearly flat to widely rounded with strongly developed ribs on which umbilical, lateral and ventrolateral tubercles are present. Umbilical tubercles give rise to 1 or 2 ribs. The number of ribs per half whorl is 12. A distinct keel is present.
Discussion. See Wright and Kennedy (2015).
Occurrences. Upper Cretaceous (Cenomanian); England, Germany, Switzerland, Iran, Greenland.

Suborder Phylloceratina Arkell, 1950
Superfamily Phylloceratacea Zittel, 1884
Family Phylloceratidae Zittel, 1884
Subfamily Phylloceratinae Zittel, 1884

Genus *Phylloceras* Suess, 1865
Subgenus *Hypophylloceras* Salfeld, 1924

Phylloceras* (*Hypophylloceras*) *velledae velledae (Michelin, 1834)
Fig. 11Z, AA

Synonymy. See Kennedy and Fatmi (2014).
Neotype. *Phylloceras* (*Hypophylloceras*) *velledae* Wiedmann, 1964; p. 209, pl. 11, fig. 1, pl. 13, fig. 4, pl. 21, fig.4, text-fig. 49a, b.
Material. 1 conch (NMSG Coll. PK. 7.C.02.04).
Locality and horizon. Stütze 2 Säntisbahn S, Kamm Bed, uppermost Albian–lowermost Cenomanian.
Description. NMSG (Coll. PK. 7.C.02.04) measures 38 mm in diameter. Its conch is thinly discoidal (ww/dm = 0.37) and involute (uw/dm = 0.08). The whorl section is compressed (ww/wh = 0.64) with nearly flat flanks and a rounded venter.
Discussion. See Kennedy and Klinger (1977) and Joly (2000).
Occurrence. Lower–Upper Cretaceous (middle Aptian–Cenomanian); Spain (the Baleric Islands), France, Italy, Switzerland, AustriaHungary, Romanian, Algeria, Egypt, Madagascar, Mozambique, South Africa (Kwazulu-Natal), Tunisia, Pakistan, USA (California).

Subgenus *Gorethophylloceras* Collignon, 1949

Gorethophylloceras subalpinum (d'Orbigny, 1841)
Fig. 11AF, AG

Synonymy. See Joly and Delamette (2008). The species was also mentioned by Matrion (2010).
Type. Lectotype *Ammonites alpinus* d'Orbigny, 1841; p. 283, pl. 83, figs. 1–3.
Material. 2 conchs (NMSG Coll. PK. 7.B.20.21, 7.B.20.75).
Locality and horizon. Schlatt (above Rüthi SG), Garschella Formation, Albian.
Description. NMSG (Coll. PK. 7.B.20.21) measures 32 mm in diameter. Its conch is moderately discoidal (ww/dm = 0.47) and involute (uw/dm = 0.09) with a compressed whorl section (ww/wh = 0.79) with broadly rounded flanks and a rounded venter.
Discussion. See Joly and Delamette (2008).
Occurrence. Lower Cretaceous (upper Aptian–upper Albian); France.

6. Discussion

6.1. Time-averaging

In palaeoecological studies, time-averaging is a major problem (Kidwell and Bosence, 1991). Condensation is often linked with

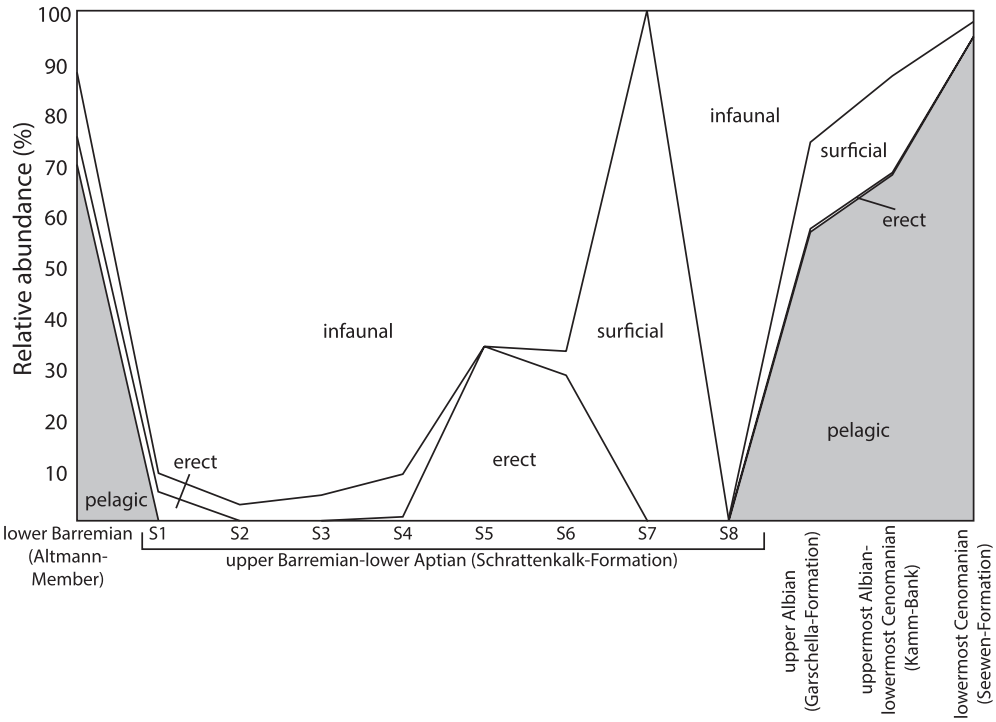

Fig. 12. Changes of tiering from the Early Barremian from the Barremian (Altmann Member) to the Early Cenomanian (Seewen Formation). Relative abundances are plotted.

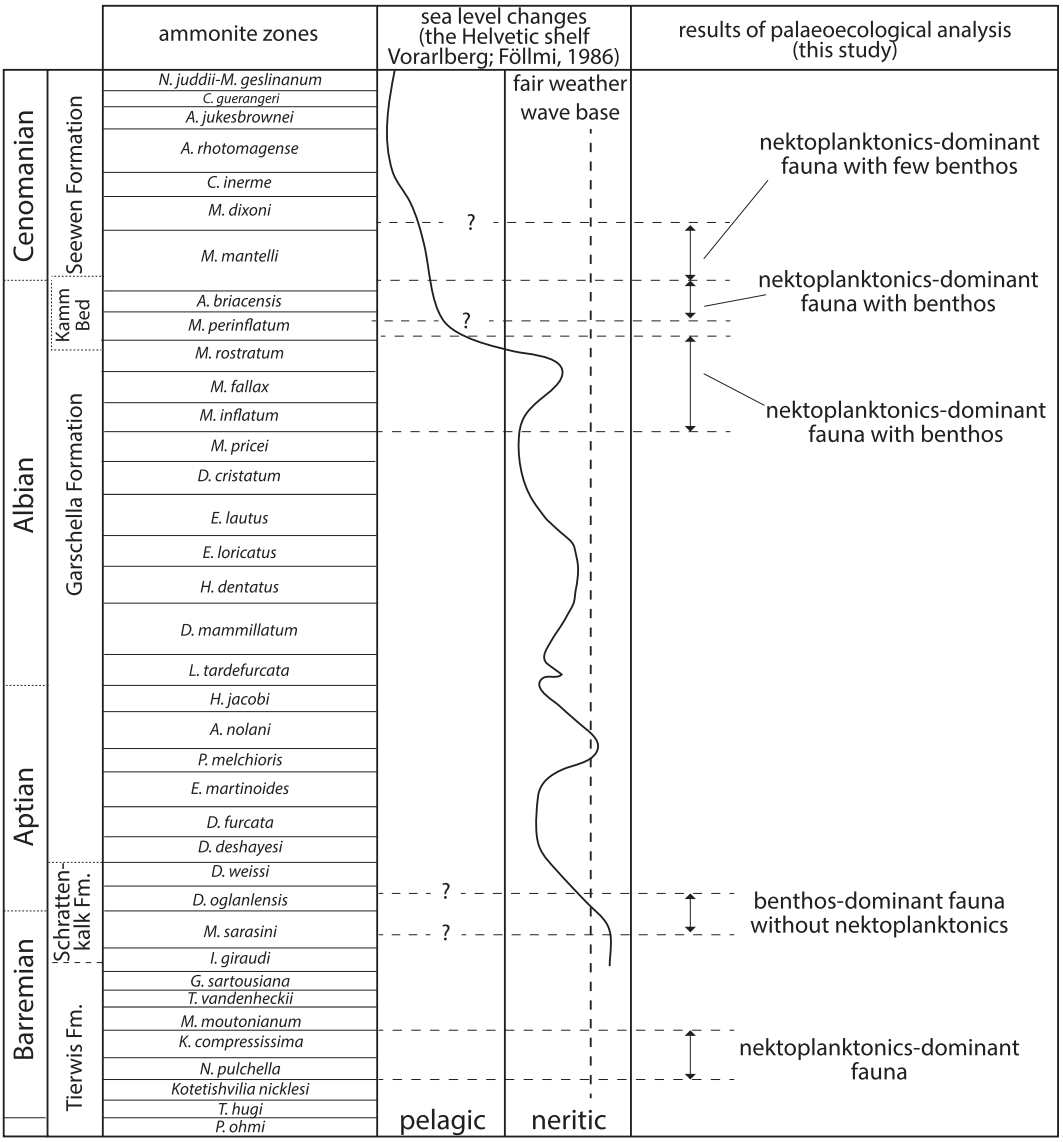

Fig. 13. Correlation between sea level changes and palaeoecology. Ammonite zones are from Reboulet et al. (2014), Wright and Kenndy (1984) and Gale et al. (2011).

environmental changes, which are too rapid to become well-documented in the sedimentary record. This is caused by the low sediment accumulation rate or currents which reduce the sedimentation (Lukeneder et al., 2012). Bearing these problems in mind, our fossil assemblages from the Altmann Member, the Garschella Formation, and particularly the Kamm Bed do not represent a single local community. This means that the faunules examined from these units may include a few successive assemblages from non-uniform environments. However, the changes in faunal composition between subsequent faunules are quite distinct and the ecological coherence within these time-averaged faunules is quite strong (e.g., no or only little mixing of typical shallow water elements (such as corals, sponges and photosynthetic organisms) with characteristic deep water elements (such as cephalopods); a strong domination of one group of modes of life within each faunule). Therefore, we suggest that the overall trends in ecospace utilization and the longterm patterns are recorded well enough to draw conclusions on the major trends in spite of likely faunal mixing; by contrast, subtle and shortterm trends are overprinted by this time-averaging and thus lost.

6.2. Palaeoecological changes and palaeoenvironmental factors

We documented ecological shifts from the Barremian to the early Cenomanian. These shifts in faunal composition through time reflect changes in environmental factors. Here, we discuss the faunal turnovers and related palaeoenvironmental factors with a focus on sea level changes.

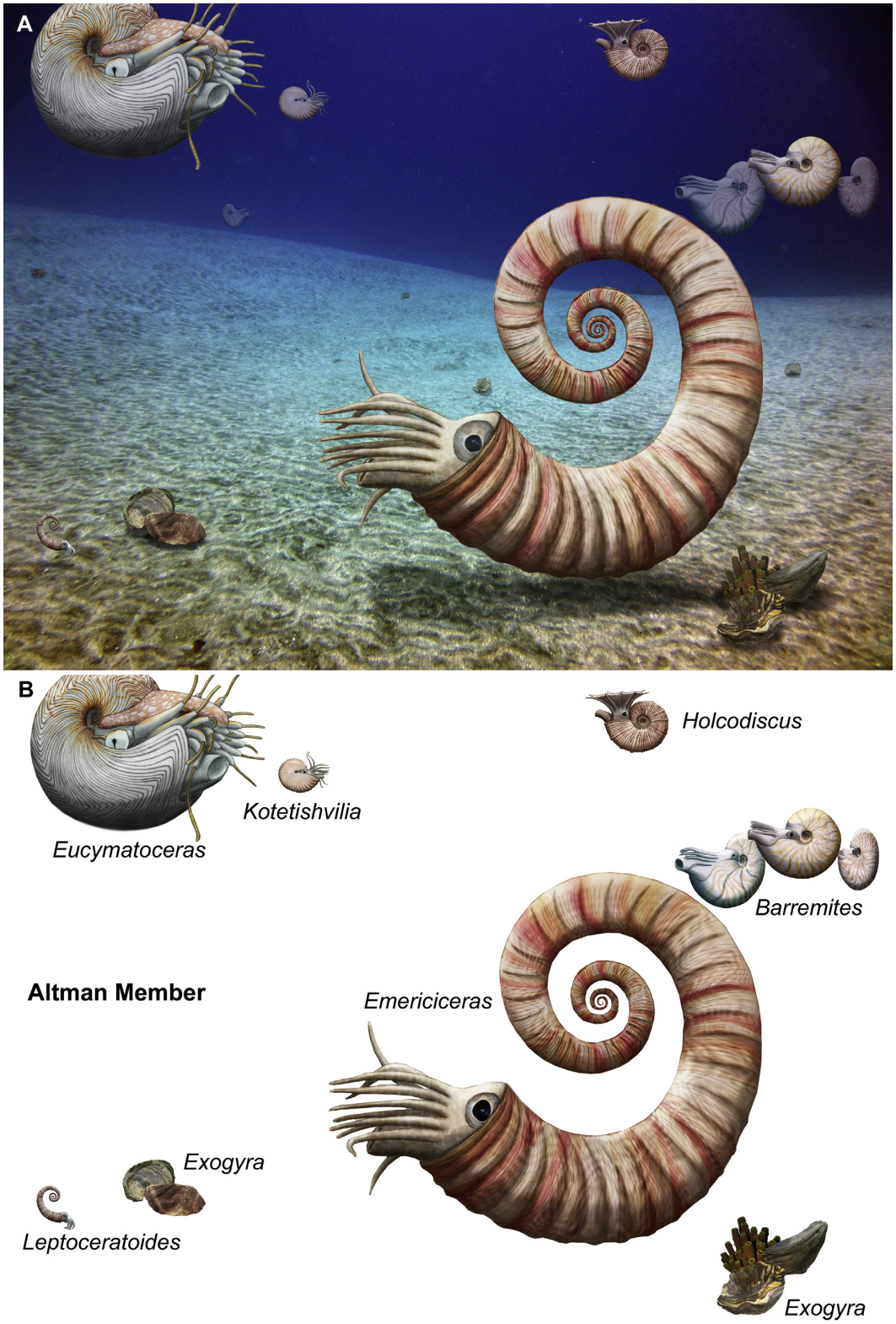

Fig. 14. Palaeoecological reconstruction of the early late Barremian. (A) Habitat of the early late Barremian. (B) Representatives of the early late Barremian macroorganism association.

6.2.1. Faunule of the Altmann Member (lower Barremian)

Six different predominant modes of life defined by Bush et al. (2007) were found in the lower Barremian (*Nicklesia pulchella* and *Kotetishvilia compressissima* Zones; Fig. 4). The fauna is dominated by nektoplanktonic forms (ammonoids). The lower Barremian strata are rich in clays and marls (Fig. 3). According to Bollinger (1988) and Föllmi et al. (2007), the Tierwis section is composed of mainly heterozoan, partially hemipelagic marl and marly carbonates. Such palaeoenvironments with moderately deep water at the time were probably much more favoured by

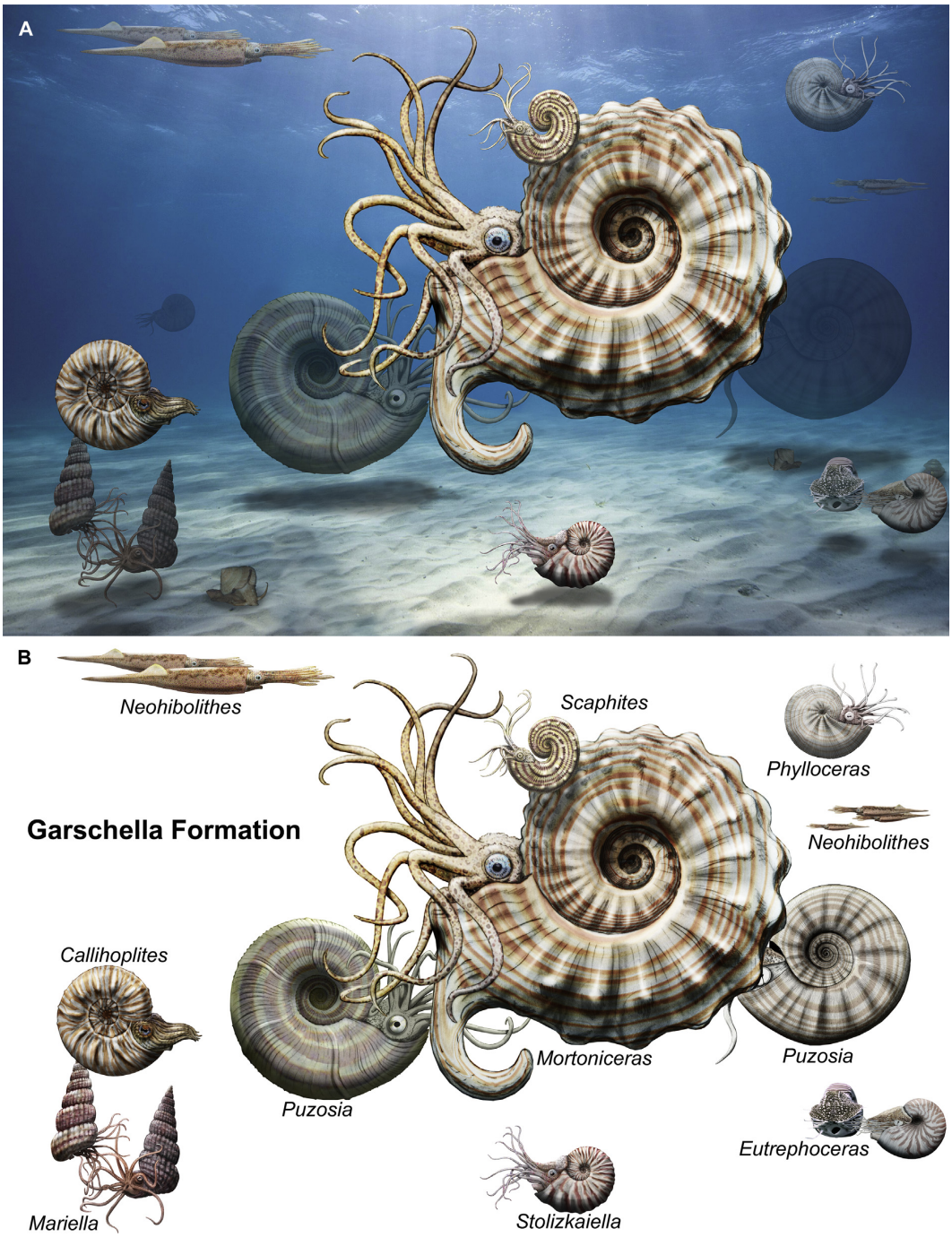

Fig. 15. Palaeoecological reconstruction of the late Albian. (A) Habitat of the late Albian. (B) Representatives of the late Albian macroorganism association.

nektoplanktonic organisms than benthos. The frequent bioturbation of the sediments of the Altmann Member indicates at least temporarily abundant benthic life, of which no body fossils are preserved. By contrast, *Exogyra* and sponges occur in varying numbers. Note that aragonitic elements are more susceptible to dissolution than calcitic elements, which would have affected the preservation potential (Bush and Bambach, 2004).

6.2.2. Faunules of the Schrattenkalk member (upper Barremian–lower Aptian)

The analysed faunules of the upper Barremian are strongly dominated by shallow marine benthos (S1-S7 in Fig. 4; Fig. 12). According to Funk et al. (1993), the upper Drusberg Member and Lower Schrattenkalk Formation are characterized by renewed growth and progradation of a healthy carbonate platform during a shallowing phase. Bonvallet (2015) also reported a shallowing upward trend in facies of the Lower Schrattenkalk Formation and lagoonal faces at its upper part. This is followed by the Rawil Member, which has been deposited during a transgression. During the deposition of the marly beds at the base of the Rawil Member, which contain wood remains, the carbonate platform was emersed occationally (Bonvallet, 2015). These shallow marine settings explain the dominance of benthos in these faunules (photozoan assemblage including, scleractinian corals, rudists, stromatoporoids and larger foraminifera; Masse, 1992; Fig. 12). The macro-faunule S8 in the lower Aptian (Fig. 4, 12) consists only of benthos (rudists). Föllmi et al. (2007) noted that the lithofacies of the Upper Schrattenkalk Formation is similar to that of the Lower Schrattenkalk. Taking this into consideration, it is not surprising that the palaeoenvironment during deposition of layer S8 was quite similar to that of S1-S7.

Föllmi (1986) investigated the palaeogeography of the eastern part of the Helvetic shelf (Vorarlberg) from the Aptian to the Santonian. He documented a transgressive trend from the late Barremian to the Cenomanian (Fig. 13). According to him, the sea level remained low until the early middle Aptian and then started to rise toward the end of Aptian. Our palaeoecological data of the layers S1-S8 most likely derive from the time when the palaeoenvironment was still too shallow for nektoplanktonic organisms (probably a few meters water depth) with dominance of reef builders.

6.2.3. Faunule of the Garschella Formation (upper Albian)

During the early late Albian, nektoplanktonic and nektonic forms (ammonoids and nautilids) regained (Fig. 4; 12). According to Föllmi (1986), the water was slightly deeper than the fair weather wave base from the early to late Albian (Fig. 13). The faunule of the upper Albian is dominated by nektoplanktonic organisms (*Mortoniceras inflatum* and*M. rostratum* Zones), reflecting a sea level, which is higher than that of S1 to S8 horizons that contain exclusively benthos (upper Barremian to lower Aptian).

6.2.4. Faunule of the Kamm Bed (top of the Garschella Formation; uppermost Albian to lowermost Cenomanian)

The faunule of the Kamm Bed shows a higher proportion of nektoplanktonic organisms (ammonoids, belemnites and nautilids) than the upper Albian deposits (Fig. 4). This may reflect the onset of a rapid sea level rise in the Aptian to Albian (Föllmi, 1986; Fig. 13). This rapid sea level rise together with reinforcement of bottom water currents was probably associated with the environmental change that caused the condensed sedimentation of the Kamm Bed (Föllmi, 1986, 1989a).

6.2.5. Faunule at the base of the Seewen Formation (lower Cenomanian)

The faunule in the layers at the base of the Seewen Formation consists largely of nektoplanktonic organisms (ammonoids and belemnites) with few benthic organisms. This correlates well with the rapid transgression of the latest Albian and a possibly rather moderate transgressive trend, which started in the early Cenomanian (Föllmi, 1986; Fig. 13). In the Tierwis area, the subsequent sedimentary succession of the Seewen Formation contains macrofossils only occasionally. This decrease in fossil content may suggest that (i) either sediment accumulation rates increased, letting the relative fossil abundance diminish, that (ii) somehow, conditions impoverished, sustaining only a lower number of animals or that (iii) the palaeoenvironment lied below the aragonite compensation depth (unlikely).

Reconstructions of habitas of the early late Barremian and late Albian are shown in Figs. 14 and 15. A more detailed investigation of the palaeoecology and alpha-diversity (i.e., richness of taxa in a single locality; Sepkoski, 1988) of the Alpstein is in preparation. Its results might shed more light on such issues.

7. Conclusions

1. We investigated the Cretaceous cephalopod associations of the Alpstein (Switzerland) and documented 6 species (3 genera) of nautilids and 77 species (45 genera) of ammonoids, 29 of which are apparently recorded for the first time from Switzerland (the result section contains a complete list).
2. In the early Barremian, the faunal association of the Alpstein region was dominated by nektoplanktonic forms (ammonoids and nautilids). Considerable changes in ecospace utilisation occurred in the late Barremian and early Aptian where nektoplanktonic elements are largely absent. Then the proportion of nektoplanktonic forms regained, especially during the late Albian (although the stratigraphic resolution is low due to condensed sedimentation in parts of the sections). This taxonomic richness is probably caused by condensation linked with the transgressive trend from the early Aptian to the early Albian. Later, nektoplanktonic forms continued to increase in alpha-diversity and became more abundant until the earliest Cenomanian with only few benthic organisms. Analyses with a finer resolution in time are needed to document details of the changes in alpha-diversity of the region.
3. The regional ecological changes from the early Barremian to the early Cenomanian were more or less strongly linked with regional sea level fluctuations. We compared the regional sea level curve for the Cretaceous of Föllmi (1986) with palaeoecological and facies data of the Alpstein. The early Barremian fauna was dominated by nektoplanktonic organism, which probably resulted from the moderately deep water, which is more favourable for nektoplanktonic organisms than a low water depth. The late Barremian and early Aptian yielded benthos-dominated faunules which correlate well with the low sea level that persisted until the early Aptian. The rising number of nektoplanktonic elements after the late Albian was supposedly related to the transgression (deeper facies) after the early Aptian. The early Cenomanian fauna dominated by nektoplanktonic organisms; this might have resulted from another rapid sea level rise at the end of the Albian.

Acknowledgements

We greatly appreciate the support by the Swiss National Science Foundation SNF (project No. 200021_149119). We thank Toni

Bürgin (St. Gallen) for providing access to the collections of the Naturmuseum St. Gallen and for being a generous host. Urs Oberli (St. Gallen) showed us his great collection of Alpstein fossils and kindly donated some important cephalopod specimens. Additionally, he prepared some of the specimens. Thomas Bolliger (Aathal) kindly put his collection at our disposal. We are also grateful to Alexander Lukeneder (Vienna) and an anonymous reviewer for their critical comments.

References

Arkell, W.J., 1957. Introduction to Mesozoic Ammonoidea. In: Moore, R.C. (Ed.), Treatise on Invertebrate Paleontology, Part L, Mollusca 4, Cephalopoda-Ammonoidea. Geological Society of America and University of Kansas Press.

Amédro, F., Matrion, B., Tomasson, R., Magniez-Jannin, F., Collete, C., 2003. L'Albien supérieur de Vallentigny dans la région stratotypique (Aube, F.): nouvelles données et révision de l'ammonite *Mortoniceras* (*M.*) *inflatum* (J. Sowerby, 1818). Bulletin de la Société géologique de Normandie et des Amis du Muséum du Havre 90 (2), 5–28.

Avram, E., 1995. Representatives of the Family Holcodiscidae Spath, 1924 (Ammonitina) in Rumania. Memorie carta Geologica d'Italia 51, 11–45.

Bayle, É., 1878. Fossiles pincipaux des terrains Explication de la Carte Géologique de la France, vol. 4 part 1 (atlas). Paris. 158 pl.

Bodin, S., Godet, A., Vermeulen, J., Linder, P., Föllmi, K.B., 2006. Biostratigraphy, sedimentology and sequence stratigraphy of the latest Hauterivian–early Barremian drowning episode of the Northern Tethyan margin (Altmann Member, Helvetic Nappes, Switzerland). Eclogae Geologicae Helvetiae 99 (2), 157–174.

Bolli, H., 1944. Zur Stratigraphie der Oberen Kreide in den höheren helvetischen Decken. Eclogae Geologicae Helvetiae 37, 216–330.

Bollinger, D., 1988. Die Entwicklung des distalen osthelvetischen Schelfs im Barremian und Früh-Aptian: Drusberg-, Mittagsspitz und Schrattenkalk-Fm. im Vorarlberg und Allgäu. Dissertation. University of Zurich.

Bonvallet, L., 2015. Evolution of the Helvetic Shelf (Switzerland) During the Barremian–Early Aptian: Paleoenvironmental, Paleogeographic and Paleooceanographic Controlling Factors. Dissertation. University of Lausanne.

Breistroffer, M., 1947. Sur les zones d'ammonites dans l'Albien de France et d'Angleterre. Travaux du Laboratoire Géologie de la Faculté des Sciences de Grenoble 26, 17–104, 1946–1947.

Breistroffer, M., 1953. Commentaires taxonomiques. In: Breistroffer, M. (Ed.), Villoutreys O de, Les ammonites albiennes de Peille (Alpes–Maritimes), Travaux du Laboratoire de Géologie de la Faculté des Science de l'Université de Grenoble, vol. 30, pp. 71–74.

Breskovski, S., 1977. Sur la classification de la famille Desmoceratidae Zittel, 1895 (Ammonoidea, Crétacé). Comptes rendus de l'Académie Bulgare des Sciences 30 (6), 891–894.

Brongniart, A., 1822. Sur quelques terrains de Crai hors du Bassin de Paris. In: Cuvier, G., Brongniart, A. (Eds.), Description géologique des environs de Paris, 8+428 p.

Busnardo, R., 1970. *Torcapella*, nouveau genre d'ammonites du Barrémien inférieur. Documents des Laboratories de Géologie Lyon 37, 85–132.

Bush, A.M., Bambach, R.K., 2004. Did alpha diversity increase during the Phanerozoic? Lifting the veils of taphonomic, latitudinal, and environmental biases. The Journal of Geology 112, 625–642.

Bush, A.M., Bambach, R.K., Daley, G.M., 2007. Changes in theoretical ecospace utilization in marine fossil assemblages between the mid-Paleozoic and late Cenozoic. Paleobiology 33 (1), 76–97. http://dx.doi.org/10.1666/06013.1.

Casey, R.A., 1961. A monograph of the Ammonoidea of the Lower Greensand. Part II. Palaeontological Society 114, 45–118.

Casey, R.A., 1962. A monograph of the Ammonoidea of the Lower Greensand, Part IV. Palaeontological Society 116, 217–288.

Casey, R.A., 1966. Palaeontology of the Gault. In: Smart, J.G.O., Bisson, G., Worssam, B.C. (Eds.), Geology of the Country around Canterbury and Folkestone. The Stationery Office Books, London, pp. 102–113.

Cecca, F., 1997. Late Jurassic and Early Cretaceous uncoiled ammonites: trophism-related evolutionary processes. C. R. Acad, Sci. Paris, Sciences de la terre et des planètes 325, 629–634.

Cecca, F., 2001. The ammonites of the Cenomanian—Turonian transition of Anse de l'Arène section (Cassis, SE France). Geobios 34 (2), 215–223.

Cieśliński, S., 1959. Alb i Cenoman północnego obrzeżenia Gór Świętokrzyskich. Instytut Geologiczny Prace 28, 1–95.

Collignon, M., 1949. Faunes néocomiennes des couches à Criocères de Belohasifaka (Cercle de Sitampiky) Madagascar. Annales géologiques du Service des Mines, Gouvernement général de Madagascar et Dépendances, Paris 15, 53–85, 6 pls.

Cooper, M.R., 1990. A revision of the Scaphitidae (Cretaceous Ammonoidea) from the Cambridge Greensand. Neues Jahrbuch für Geologie und Paläontologie, Abhandlungen 178, 285–308.

Cooper, M.R., 2012. New names for Late Jurassic-Cretaceous ammonites. Neues Jahrbuch für Geologie und Paläontologie, Abhandlungen 266, 185–186.

Cooper, M.R., Kennedy, W.J., 1977. A revision of the Baculitidae of the Cambridge Greensand. Neues Jahrbuch für Geologie und Paläontologie, Monatshefte 11, 641–658.

Cooper, M.R., Kennedy, W.J., 1979. Uppermost Albian (*Stoliczkaia dispar* Zone) ammonites from the Angolan littoral. Annals of the South African Museum 77, 175–308.

Cooper, M.R., Kennedy, W.J., 1987. A revision of the Puzosiinae (Cretaceous ammonites) of the Cambridge Greensand. Neues Jahrbuch für Geologie und Paläontologie, Abhandlungen 174, 105–121.

Cooper, M.R., 1999. Towards a phylogenetic classification of the Cretaceous ammonites. VII. Turrilitidae. Neues Jahrbuch für Geologie und Paläontologie, Abhandlungen 213, 1–18.

De Baets, K., Bert, D., Hoffmann, R., Monnet, C., Yacobucci, M.M., Klug, C., 2015. Ammonoid intraspecific variability. In: Klug, C., Korn, D., De Baets, K., Kruta, I., Mapes, R.H. (Eds.), Ammonoid paleobiology, Volume I: from anatomy to ecology, Topics in Geobiology, 43, pp. 329–389.

Delamette, M., Kennedy, W.J., 1991. Cenomanian ammonites from the condensed deposits of the Helvetic Domain (Western Alps, France and Switzerland). Journal of Paleontology 65, 435–465.

Delanoy, G., Baudouin, C., Gonnet, R., Conte, G., 2012. On the presence of genres *Heminautilus* SPATH, 1927 and *Eucymatoceras* SPATH, 1927 (Nautilida, Nautilaceae) in the Lower Barremian Gard (south-eastern France). Annales Muséum d'Histoire Naturelle de Nice 27, 155–195.

Douvillé, H., 1890. Sur la classification des Cératites de la Craie. Bulletin de la Société Géologique de France 3 (XVIII), 275–292.

Douvillé, H., 1912. Note accompagnant la présentation de l' Atlas de t. iv de l'Explication de la Carte géologique de France de E. Bayle et R. Zeiller. Bulletin de la Société Géologique de France 3 (7), 91–92.

Dubourdieu, G., 1953. Ammonites nouvelles des Monts du Mellégue. Bulletin du Service de la Carte Géologique de l'Algerie (serie 1, Paleontologie) 16, 1–76 fig. 1–20, pl. 1–4.

Eugster, H., Forrer, M., Fröhlicher, H., Kempf, T., Schlatter, L., Blaser, R., Funk, H., Langenegger, H., Spoerri, M., Habicht, K., 1982. Säntis (map sheet 1115), Geological Atlas of Switzerland 1:25.000, N. 78. Federal Office of Topography, Swisstopo.

Fallot, J.E., 1885. Étude géologique sur les étages moyens et supérieurs du Terrain Crétacé. Annales des Sciences géologiques 18 (1), 262 p. 8 pls.

Fitton, W.H., 1835. Observations on some of the Strata between the Chalk and the Oxford Oolite, in the South-east of England. Transactions of the Geological Society of London 2 (4), 103–388.

Föllmi, K.B., 1986. Die Garschella-und Seewerkalkformation (Aptian-Santonian) im Voralberger Helvetikum und Ultrahelvetikum. Mitteilungen aus dem Geologischen Institut der eidgenössischen Hochschule und der Universität Zürich, Neue Folge 262, 1–391.

Föllmi, K.B., 1989a. Evolution of the mid-Cretaceous triad: platform carbonates, phosphatic sediments, and pelagic carbonates along the northern Tethys margin. Lecture Notes in Earth Sciences 23, 153 p.

Föllmi, K.B., 1989b. Beschreibung neugefundener Ammonoidea aus der Vorarlberger Garschella Formation (Aptian-Albian). Jahrbuch der Geologischen Bundesanstalt Wien 132 (1), 105–189.

Föllmi, K.B., Ouwehand, P.J., 1987. Garschella Formation und Götzis-Schichten (Aptian-Coniacian): Neue stratigraphische Daten aus dem Helvetikum der Ostschweiz und des Vorarlbergs. Eclogae Geologicae Helvetiae 80 (1), 141–191.

Föllmi, K.B., Bodin, S., Godet, A., Linder, P., Van De Schootbrugge, B., 2007. Unlocking paleo-environmental information from Early Cretaceous shelf sediments in the Helvetic Alps: stratigraphy is the key! Swiss Journal of Geosciences 100, 349–369.

Funk, H., 1969. Typusprofile der helvetischen Kieselkalk Formation und der Altmann-Schichten. Eclogae Geologicae Helvetiae 62, 191–203.

Funk, H., Föllmi, K.B., Mohr, H., 1993. Evolution of the Tithonian-Aptian Carbonate Platform along the Northern Tethyan Margin, Eastern Helvetic Alps: Chapter 31. In: Simo, J.A.T., Scott, R.W., Masse, J.P. (Eds.), Cretaceous Carbonate Platforms, AAPG Memoir, 56, pp. 387–407.

Gale, A.S., Kennedy, W.J., Burnett, J.A., Caron, M., Kidd, B.E., 1996. The Late Albian to Early Cenomanian succession at Mont Risou near Rosans (Drôme, SE France): an integrated study (ammonites, inoceramids, planktonic foraminifera, nannofossils, oxygen and carbon isotopes). Cretaceous Research 17, 515–606.

Gale, A.S., Bown, P., Caron, M., Crampton, J.S., Crowhurst, S.J., Kennedy, W.J., Petrizzo, M.R., Wray, D.S., 2011. The uppermost Middle and Upper Albian succession at the Col de Palluel, Hautes-Alpes, France: an integrated study (ammonites, inoceramid bivalves, planktonic foraminifera, nannofossils, geochemistry, stable oxygen and carbon isotopes, cyclostratigraphy). Cretaceous Research 32, 59–130.

Gauthier, H., 2006. Révision critique de la Paléontologie Française d'Alcide d'Orbigny. In: Volume IV, Céphalopodes Crétacés. Backhuys, Leiden, pp. 1–292.

Giebel, C., 1852. Deutschlands Petrefacten: ein systematisches Verzeichniss aller in Deutschland und den angrenzenden Ländern vorkommenden Petrefacten, nebst Angabe der Synonymen und Fundorte. Verlag von Ambrosius Abel, Leipzig, 706 p.

Gill, T., 1871. Arrangement of the families of mollusks. Smithsonian Miscellaneous Collections 227 xvi + 49 p.

Gray, J.E., 1821. A natural arrangement of Mollusca, according to their internal structure. The London Medical Repository 15, 229–239.

Grossouvre, A. de, 1894. Recherches sur la Craie supérieure. Deuxiéme partie: Paléontologie. Les ammonites de la Craie supérieure. Mémoires du Sérvice de la Carte Géologique Détaillée de la France 18993, 264 p. 89, figs., 39 pls. (atlas).

Guex, J., 2006. Reinitialization of evolutionary clocks during sublethal environmental stress in some invertebrates. Earth and Planetary Science Letters 242, 240–253.

Haq, B.U., 2014. Cretaceous eustasy revisited. Global and Planetary Change 113, 44–58.

Hitzel, E., 1902. Sur les fossiles de l'étage Albien recueillis Par MA Guébhard dans la région d'Ecragnolles (A.-M.). Bulletin de la Société géologique de France 2 (serie 4), 874–880.

Hoedemaeker, P., 2013. Genus *Pseudothurmannia* Spath, 1923 and related subgenera *Crioceratites* (*Balearites*) Sarkar, 1954 and *C. (Binelliceras)* Sarkar, 1977 (Lower Cretaceous Ammonoidea). Revue de Paléobiologie 32, 1–209.

Hoffmann, R., Lemanis, R., Naglik, C., Klug, C., 2015. Ammonoid buoyancy. In: Klug, C., Korn, D., De Baets, K., Kruta, I., Mapes, R.H. (Eds.), Ammonoid Paleobiology, Volume I: From Anatomy to Ecology, Topics in Geobiology, 43, pp. 613–648.

Hyatt, A., 1884. Genera of fossil Cephalopods. Proceedings of the Boston Society of Natural History 22, 273–338.

Hyatt, A., 1894. Phylogeny of an acquired characteristic. Proceedings of the American Philosophical Society 32, 349–647.

Hyatt, A., 1889. Genesis of the Arietidae. Smithsonian Contributions to Knowledge 673, Washington, DC xi, 16.

Hyatt, A., 1900. Cephalopoda. In: Zittel, K.A.V. (Ed.), Textbook of Palaeontology. Eastman, London and New York, pp. 502–592.

Hyatt, A., 1903. Pseudoceratites of the Cretaceous. Monographs of the United States Geological Survey 44, 128–144.

Jacob, C., 1907. Études paléontologiques et stratigraphiques sur la partie moyenne des terrains Crétacés dans les Alpes Françaises et les régions voisines. Annales de l'Université de Grenoble 19 (2), 221–534, 6 pls.

Jayet, A., 1929. La variation individuelle chez les ammonites et la diagnose des espéces. Note préliminaire basée sur l'analyse d'*Inflaticeras varicosum* (SOWERBY). Mémoires de la Société Paléontologique Suisse 49, 1–115.

Joly, B., 2000. Les Juraphyllitidae, Phylloceratidae, Neophylloceratidae (Phylloceratoceae, Phylloceratina, Ammonoidea) de France au Jurassique et au Crétacé. Geobios Mémoire 23, 1–204.

Joly, B., Delamette, M., 2008. Les Phylloceratoidea (Ammonoidea) aptiens et albiens du bassin vocontien (Sud-Est de la France). Carnets de Géologie, Brest, Mémoire 4.

Jukes-Browne, A.J., 1875. On the relations of the Cambridge Gault and Greensand. Quarterly Journal of the Geological Society 31 (1–4), 256–316.

Kennedy, W.J., 1971. Cenomanian ammonites from southern England. Special Papers in Palaeontology 8, 1–133.

Kennedy, W.J., 1994. Cenomanian ammonites from Cassis, Bouches-du-Rhone, France. Palaeopelagos Special Publication 1, 209–254.

Kennedy, W.J., Klinger, H.C., 1977. Cretaceous faunas from Zululand and Natal, South Africa. The ammonite family Phylloceratidae. Bulletins of the British Museum of Natural History 27 (5), 349–380.

Kennedy, W.J., Latil, J.L., 2007. The Upper Albian ammonite succession in the Montlaux section, Hautes-Alpes, France. Acta Geologica Polonica 57 (4), 453–478.

Kennedy, W.J., Klinger, H.C., 2013. Cretaceous faunas from Zululand and Natal, South Africa. The ammonite Subfamily Stoliczkaiinae Breistroffer, 1953. African Natural History 9, 1–38.

Kennedy, W.J., Fatmi, A.N., 2014. Albian ammonites from northern Pakistan. Acta Geologica Polonica 64, 47–98.

Kennedy, W.J., Klinger, H.C., 2014. Cretaceous faunas from Zululand and Natal, South Africa. *Valdedorsella, Pseudohaploceras, Puzosia, Bhimaites, Pachydesmoceras, Parapuzosia (Austiniceras)* and *P.* (*Parapuzosia*) of the ammonite subfamily Puzosiinae Spath, 1922. African Natural History 10, 1–46.

Kennedy, W.J., Cobban, W.A., Gale, A.S., 1998. Ammonites from the Weno limestone (Albian) in northeast Texas. American Meseum Novitates 3236, 46 p.

Kennedy, W.J., Jagt, W.M., Amédro, F., Robasyznski, F., 2008. The late Late Albian (*Mortoniceras fallax* Zone) cephalopod fauna from the Bracquegnies Formation at Strépy-Thieu (Hainaut, southern Belgium). Geologica Belgica 11, 35–69.

Kennedy, W.J., Amédro, F., Robaszynski, F., Jagt, J.W., 2011. Ammonite faunas from condensed Cenomanian-Turonian sections ('Tourtias') in southern Belgium and northern France. Netherlands Journal of Geosciences 90 (2–3), 209–238.

Kennedy, W.J., Walaszczyk, I., Gale, A.S., Dembicz, K., Praszkier, T., 2013. Lower and Middle Cenomanian ammonites from the Morondava Basin, Madagascar. Acta Geologica Polonica 63 (4), 625–655.

Kennedy, W.J., Klinger, H.C., Lehmann, J., 2015. Cretaceous faunas from Zululand and Natal, South Africa. The ammonite subfamily Mantelliceratinae Hyatt, 1903. African Natural History 11, 1–42.

Kidwell, S.M., Bosence, D.W., 1991. Taphonomy and time-averaging of marine shelly faunas. In: Allison, P.A., Briggs, D.E.G. (Eds.), Taphonomy: releasing the data locked in the fossil record. Plenum, New York, pp. 115–209.

Kilian, C.C.C.W., 1889. Sur quelques fossils nouveaux ou peu connus du Crétacé inférieur de la Provence. Bulletin de la Société Géologique de France (séries 3) 16, 663–691, 1888.

Kilian, C.C.C.W., 1910. Erste Abteilung: Unterkreide (Palaeocretacicum). Lieferung 2: Das bthyale Palaeocretacicum im südostlichen Frankreich; Valendis-Stufe; Hauterive-Stufe; Barreme-Stufe; Apt-Stufe. In: Frech, F. (Ed.), Lethaea Geognostica. II. Das Mesozoicum, Band 3 (Kreide) (1907–1913). Schweizerbart, Stuttgart, pp. 169–288 pls. 1–8.

Kilian, C.C.C.W., 1913. Erste Abteilung: Unterkreide (Palaeocretacicum). Lieferung 2: Das bathyale Palaeocretacicum im südostlichen Frankreich: Apt-Stufe: Urgonfacies im südostlichen Frankreich. In: Frech, F. (Ed.), Lethaea Geognostica. II. Das Mesozoicum, Band 3 (Kreide) (1907–1913). Schweizerbart, Stuttgart, pp. 289–398.

Klein, J., 2005. Fossilium Catalogus I: Animalia pars 139. Lower Cretaceous Ammonites I: Perisphinctaceae 1, Himalayitidae, Olcostephanidae, Holcodiscidae, Neocomitidae, Oosterellidae. Backhuys Publishers, Leiden, 484 p.

Klein, J., 2015. Fossilium Catalogus I: Animalia pars 154. Lower Cretaceous Ammonites VIII – Turrilitoidea 1; Anisoceratidae, Hamitidae, Turrilitidae, including the Upper Cretaceous Representatives. Backhuys Publishers, Leiden, 484 p.

Klein, J., Vašíček, Z., 2011. Fossilium Catalogus I: Animalia pars 148. Lower Cretaceous Ammonites V: Desmoceratoidea. Margraf Publishers, Weikersheim, 316 p.

Klein, J., Hoffmann, R., Joly, B., Shigeta, Y., Vašíček, Z., 2009. Fossilium Catalogus I: Animalia pars 146. Lower Cretaceous Ammonites IV: Boreophylloceratoidea, Phylloceratoidea, Lytoceratoidea, Tetragonitoidea, Haploceratoidea including the Upper Cretaceous representatives. Backhuys Publishers, Leiden. Margraf Publishers, Weikersheim. 416 p.

Klinger, H.C., Kennedy, W.J., 1978. Turrilitidae (Cretaceous Ammonoidea) from South Africa, with a discussion of the evolution and limits of the family. Journal of Molluscan Studies 44, 1–48.

Klug, C., Korn, D., Landman, N.H., Tanabe, K., De Baets, K., Naglik, C., 2015. Describing ammonoid shells. In: Klug, C., Korn, D., De Baets, K., Kruta, I., Mapes, R.H. (Eds.), Ammonoid Paleobiology, Volume I: From Anatomy to Ecology, Topics in Geobiology 43. Springer, Dordrecht, pp. 3–24.

Korn, D., 2010. A key for the description of Palaeozoic ammonoids. Fossil Record 13 (1), 5–12.

Kossmat, F., 1895-1898. Untersuchungen über die Südindische Kreideformation. Beiträge zur Geologie und Paläontologie Österreichs. Ungarens und des Orient 9 (1895), 97–203 (1–107); 10(1897), 1–46 (108–153); 11 (1898), 89-152 (154–217).

Kummel, B., 1956. Post-triassic nautiloid genera. Bulletin of the Museum of Comparative Zoology, Harvard 114, 324–493.

Lehmann, J., Friedrich, O., Luppold, F.W., Weiss, W., Erbacher, J., 2007. Ammonites and associated macrofauna from around the Middle/Upper Albian boundary of the Hannover-Lahe core, northern Germany. Cretaceous Research 28, 719–742.

Lehmann, J., Ifrim, C., Bulot, L., Frau, C., 2015. Paleobiogeography of Early Cretaceous Ammonoids. In: Klug, C., Korn, D., De Baets, K., Kruta, I., Mapes, R.H. (Eds.), Ammonoid Paleobiology, Volume I: From Anatomy to Ecology, Topics in Geobiology 43, pp. 229–257.

Léveillé, C., 1837. Description de quelques nouvelles coquilles fossiles du département des Basses-Alpes. Memoires de la Societe Geologique de France (series 1).

Lukeneder, A., 2012. New biostratigraphic data on an Upper Hauterivian–Upper Barremian ammonite assemblage from the Dolomites (Southern Alps, Italy). Cretaceous Research 35, 1–21.

Lukeneder, A., 2015. Ammonoid habitats and life history. In: Klug, C., Korn, D., De Baets, K., Kruta, I., Mapes, R.H. (Eds.), Ammonoid Paleobiology, Volume I: From Anatomy to Ecology, Topics in Geobiology 43, pp. 689–791.

Lukeneder, A., Uchman, A., Gaillard, C., Olivero, D., 2012. The late Barremian Halimedides horizon of the Dolomites (Southern Alps, Italy). Cretaceous Research 35, 199–207.

Mantell, G.A., 1822. The Fossils of the South Downs; or Illustrations of the Geology of Sussex. Lupton Relfe, London, 327 p.

Marcinowski, R., Wiedmann, J., 1990. The Albian ammonites of Poland. Palaeontologia Polonica 50, 3–94.

Masse, J.P., 1992. The Lower Cretaceous Mesogean benthic ecosystems: palaeocologic aspects and palaeobiogeographic implications. Palaeogeography, Palaeoclimatology, Palaeoecology 91, 331–345.

Matheron, P., 1842. Catalogue méthodique et descriptive des corps organisés fossils du Département des Bouches-du-Rhône et lieux circonvoisins. Marseille, 269 p., 41 pls.

Matrion, B., 2010. Les ammonites. In: Colleté, C. (Ed.), Stratotype Albien. Muséum national d'Histoire naturelle, Paris; Biotope, Mèze; BRGM, Orléans, Paris, pp. 99–193 (314–323: references).

Meek, F.B., 1876. A report on the invertebrate Cretaceous and Tertiary fossils of the Upper Missouri Country. In: Hayden, F.V. (Ed.), Report of the United States Geological and Geographical Surveys of the Territories, vol. 9 lxiv + 629 p., 84 figs., 45 pls.

Michelin, J.L.H., 1834. Coquilles fossiles de Gérodot (Aubc). Magazine de Zoologie de Guérin-Méneville, Paris, n° 3, classe V, 35 pls.

Michelin, H., 1838. Note sur une argile dépendant du Gault. Mémoires de la Société géologique de France 3 (séries 1), 97–103.

Miller, A.K., Garner, H.F., 1962. Cretaceous nautiloids of New Jersey. In: Richards, H.G., et al. (Eds.), The Cretaceous fossils of New Jersey, Bulletin of the New Jersey Bureau of Geology and Topography, 61(2), pp. 101–111.

Moriya, K., 2015. Evolution of habitat depth in the Jurassic–Cretaceous ammonoids. Proceedings of the National Academy of Sciences 112, 15540–15541.

Morton, S.G., 1834. Synopsis of the Organic Remains of the Cretaceous Group of the United States. Appendix. Catalogue of the fossil shells of the Tertiary formation of the United States by Timothy A. Conrad, 1–88, App. pp.1–8, Philadelphia.

Mörner, N.A., 1981. Revolution in Cretaceous sea-level analysis. Geology 9, 344–346.

Naglik, C., Rikhtegar, F., Klug, C., 2015. Buoyancy of some Palaeozoic ammonoids and their hydrostatic properties based on empirical 3D-models. Lethaia 49, 3–12. http://dx.doi.org/10.1111/let.12125.

Neumayr, M., 1875. Die Ammoniten der Kreide und die Systematik der Ammonitiden. Zeitschrift der Deutschen Geologischen Gesellschaft 27, 854–942.

Nowak, J., 1908. Untersuchungen über Cephalopoden der oberen Kreide in Polen: I. Teil Genus Baculites Lamarck. Bulletin International de l'Académie des Sciences de Cracovie B 327–353.

Nowak, J., 1916. Über die bifiden Loben der oberkretazischen Ammoniten und ihre Bedeutung für die Systematik. Bulletin international de l 'Académie des Sciences de Cracovie, Classe des Sciences Mathématiques et Naturelles B 1915, 1–13.

Ooster, W.A., 1860. Catalogue des céphalopodes fossiles des Alpes suisses. IV. Partie: Céphalopodes tentaculifères, Ammonitides, G. *Scaphites. Ancyloceras, Crioceras, Toxoceras, Hamites. Ptychoceras, Baculites, Heteroceras, Turrilites, Anisoceras*. Neue Denkschriften der Allgemeinen Schweizerischen Gesellschaft der Gesamten Naturwissenschaften 18, 160 p.

d'Orbigny, A., 1840–1842. Paléontologie française. Terrains Crétacés. I: Céphalopodes. Masson, Paris, 662 p. 148pls.

d'Orbigny, A., 1850. Prodrome de Paléontologie stratigraphique universelle des animaux mollusques & rayonées faisant suite au cours élémentaire de paléontologie et géologie stratigraphique. Paris, vol. I, 394 p., vol. II, 427 p.

Ouwehand, P.J., 1987. Die Garschella-Formation ("Helvetischer Gault", Aptian-Cenomanian) der Churfirsten-Alvier Region (Ostschweiz): Sedimentologie, Phosphoritgenese, Stratigraphie. Mitteilungen des Geologischen Institutes der ETH und der Universität Zürich, Neue Folge 275, 296 p.

Page, K.N., 1996. Mesozoic ammonoids in space and time. In: Landman, N.H., Tanabe, K., Davis, R.A. (Eds.), Ammonoid Paleobiology. Plenum, New York, London, pp. 755–794.

Parkinson, J., 1811. The Fossil Starfish, Echini, Shells, Insects, Amphibia, Mammalia & c. In: The Organic Remains of a Former World, vol. 3. Sherwood, Neely, and Jones, London xvi + 479 p, 22 pls.

Parona, C.F., Bonarelli, G., 1897. Fossili Albiani d'Escragnolles, del Nizzardo e della Liguria occidentale. Palaeontologica Italiana 2, 53–112, 1896.

Pervinquière, L., 1910. Sur quelques ammonites du crètacè algèrien. Mémoires de la Société Géologique de France, Paléontologie 17, mémoir 42, 1–86.

Pictet, F.J., 1847. Déscription des mollusques fossiles qui se trouvent dans les grès verts des environs de Genève. Mémoire de la Société de Physique et d'Histoires de Genève 11, 257–412.

Pictet, F.J., 1854. Traité de Paléontologie. Tomé deuxiéme, 5e famille – Ammonitides, second ed. J.-B. Bailliére, Paris, pp. 654–716. pl. 52–56.

Pictet, F.J., Campiche, G., 1858-60. Description des fossiles du terrain Cretacé des environs de Sainte-Croix. I. Matériaux pour la Paléontologie Suisse 2 (série, 2), 29–368. Kessmann & Georg, Geneva (no. 1: feuilles 1–3, carte geologique, pls. 1–2; April 1858, no. 2: feuilles 4–7, pls. 3–8; June 1858, no. 3: feuilles 8–12, pls. 9–13; October 1858, no. 4: feuilles 13–18, pls. 14–15; March 1859, no. 5: feuilles 19–22, pls. 18–23; August 1859, no. 6: feuilles 23–26, pls. 24–29; September 1859, no. 7: feuilles 27–32, pls. 30–34; January 1860, no. 8: feuilles 33–38, pls. 34–38; March 1860, no. 9: feuilles 39–48, pls. 39–43; May 1860).

Pictet, F.J., Campiche, G., 1858-64. Matériaux pour la paléontologie Suisse. Description des fossiles du terrain Crétacé des environs de Ste. Croix. Mat. pal. Suisse 1, 1–380 (1858–60); 2, 1–752 (1861–64).

Pictet, F.J., De Loriol, P., 1858. Description des fossils contenus dans le Terrain Néocomien des Voirons; seconde partie: description des animaux invertébrés. Matériaux pour la Paléontologie Suisse, Seconde Série (1858–60) 2, 64 p., 12 pl.

Quenstedt, F.A., 1847. Petrefactenkunde Deutschlands. 1. Die Cephalopoden, p. 580, 36 pl. Tübingen.

Reboulet, S., Szives, O., Aguirre-Urreta, B., Barragán, R., Company, M., Idakieva, V., Tavera, J.M., 2014. Report on the 5th International Meeting of the IUGS Lower Cretaceous Ammonite Working Group, the Kilian Group (Ankara, Turkey, 31st August 2013). Cretaceous Research 50, 126–137.

Renz, O., 1982. The Cretaceous Ammonites of Venezuela. Birkhauser, Maravan, a subsidiary of Petroleos de Veneyuela, S.A, 132 p., 40 pls.

Ritterbush, K.A., Hoffmann, R., Lukeneder, A., De Baets, K., 2014. Pelagic palaeoecology: the importance of recent constraints on ammonoid palaeobiology and life history. Journal of Zoology 292, 229–241.

Sala, P., Pfiffner, O.A., Frehner, M., 2014. The Alpstein in three dimensions: fold-and-thrust belt visualization in the Helvetic zone, eastern Switzerland. Swiss Journal of Geosciences 10, 177–195.

Salfeld, H., 1924. Die Bedeutung der Konservativstämme für die Stammesentwicklung der Ammonoideen. Grundlinien für die Erforschung der Entwicklung der Ammonoideen der Jura- und Kreidezeit. Verlag Max Weg, Leipzig, 16 p., 16 pls.

Sarkar, S., 1954. Some new genera of uncoiled ammonites from Lower Cretaceous. Science and Culture 19, 618–620.

Schenk, K., 1992. Die Drusberg- and Schrattenkalk-Formation (Unterkreide) im Helvetikum des Berner Oberlandes. Unpublished Ph.D. thesis. Geological Institute, University of Berne, 169 p.

Scholz, G., 1979. Die Ammoniten des Vracon (Oberalb, *Dispar*-Zone) des Bakony-Gebirges (Westungarn) und eine Revision der wichtigsten Vracon-Arten der westmediterranen Faunenprovinz. Palaeontographica A 165 (1–2), 1–136.

Seeley, H.G., 1865. On Ammonites from the Cambridge Greensand. Annals and Magazine of Natural History 3 (16), 225–247.

Seitz, O., 1931. Zur Morphologie der Ammoniten aus dem Albien II. Jahrbuch der Preußischen Geologischen Landesanstalt 52, 391–415, 1931.

Sepkoski, J.J., 1988. Alpha, beta, or gamma: where does all the diversity go? Paleobiology 14, 221–234.

Sharpe, D., 1857. Description of the fossil remains of Mollusca found in the Chalk of England. Part 3: Cephalopoda. Palaeontographical Society, London, pp. 37–70 pls. 17–27 (1856).

Sowerby, J., 1812–1846. The mineral conchology of Great Britain, vols. 1–4. London, 1: pls. 1–9 (1812); pls. 10–44(1813); pls. 45–78 (1814); pls. 79–102 (1815); 2: pls. 103–114 (1815); pls. 115–50 (1816); pls. 151–186 (1817); pls. 187–203 (1818); 3: pls. 204–221 (1818); pls. 222–253 (1819); pls. 254–271 (1820), pls. 272–306 (1821); 4: pls. 307–318 (1821); pls.319–383 (1822); pls 384–407 (1823); 5: pls. 408–443 (1823), pls. 444–485 (1824); pls. 486–603 (1825); 6: pls. 504–544 (1826); pls. 545–580 (1827); pls. 581–597 (1828); pls. 598–609 (1829); 7: pls. 610–618 (1840); pls. 619–623 (1841); pls. 624–628 (1843); pls. 629–643 (1844); pls. 644–648 (1846).

Spath, L.F., 1921. On Cretaceous Cephalopoda from Zululand. Annals of the South African Museum 12, 217–321.

Spath, L.F., 1922. On Cretaceous Ammonoidea from Angola, collected by Professor J.W. Gregory, D. Sc., F.R.S. Transactions of the Royal Society of South Africa 53, 91–160.

Spath, L.F., 1923-1943. A Monograph of the Ammonoidea of the Gault. Palaeontographical Society, London (1923) I, pp. 1–72, pls. 1-4; (1925a) II, pp. 73–110, pls. 5-8 ; III, pp. 111–146, pls. 9-12;(1926) IV, pp. 147–186, pls. 13-16; (1927) V, pp. 187–206. pls. 17–20; (1930), VII. pp. 265–311, pls. 25–30; (1931) VIII, pp. 313–378. pls. 30–36; (1932) IX, pp. 779–410, pls. 37–42; (1933) X. pp. 411–442, pls. 43–48; (1934) XI, pp. 443–496, pls. 49–56; (1937) XII, pp. 497–540, pls. 57, 58; (1939) XIII, pp. 541–608, pls. 59–64 ; (1941) XIV, pp. 609–668, pls. 65–72 ; (1942) XV, pp. 669–720 : (1943) XVI, pp. 721–787 et i-x.

Spath, L.F., 1925b. On Upper Albian Ammonoidea from Portuguese East Africa, with an appendix on Upper Cretaceous ammonites from Maputoland. Annals of the Transvaal Museum 11, 179–200.

Steinmann, G., 1890. In: Steinmann, G., Döderlein, L. (Eds.), Elemente der Paläontologie. Wilhelm Engelmann, Leipzig, 848 p.

Stoliczka, F., 1863–1866. The fossil Cephalopoda of the Cretaceous rocks of southern India. Ammonitidae with revision of the Nautilidae etc. Memoirs of the Geological Survey of India. (1), Palaeontologica Indica 3 (1), 41–56 (1863); (2–5), 57–106(1864); (6–9), 107–154(1865); (10–13), 155–216(1866).

Suess, E., 1865. Über Ammoniten. In: Sitzungsberichte der Kaiserlichen Akademie der Wissenschaften in Wien, mathematisch-naturwissenschaftliche Klasse 52, Abteilung 1, pp. 71–89.

Tajika, A., Morimoto, N., Wani, R., Naglik, C., Klug, C., 2015a. Intraspecific variation of phragmocone chamber volumes throughout ontogeny in the modern nautilid *Nautilus* and the Jurassic ammonite *Normannites*. PeerJ 3, e1306.

Tajika, A., Naglik, C., Morimoto, N., Pascual-Cebrian, E., Hennhöfer, D., Klug, C., 2015b. Empirical 3D model of the conch of the Middle Jurassic ammonite microconch Normannites: its buoyancy, the physical effects of its mature modifications and speculations on their function. Historical Biology 27, 181–191.

Thieuloy, J.P., 1966. Leptocères berriasiens du massif de la Grande-Chartreuse. Travaux du Laboratoire Géologie de la Faculté des Sciences de Grenoble 42, 281–295.

Torcapel, A., 1884. Quelques fossils nouveaux de l'Urgonien du Languedoc. Bulletin de la Société d'Étude des Sciences Naturelles de Nîmes 11, 133–212.

Trautschold, H.A., 1886. Le Néocomien de Sably en Crimée. Nouveaux Mémoires de la Société impérial des Naturalistes de Moscou 15 (4), 1–25.

Trümpy, R., 1980. Geology of Switzerland, a guide-book: Schweizerische Geologische Kommission. Wepf & Co., Basel, 334p.

Uhlig, V., 1882. Die Wernsdorfer Schichten und ihre Äquivalente. Sitzungberichte der Kaiserlichen Akademie der Wissenschaften in Iwen, Mathematisch-Naturwissenshaftliche Klasse 86 (1), 86–117.

Uhlig, V., 1883. Die Cephaloopodenfauna der Werndorfer Schichten. Denkschriften der kaiserlichen Akademie der Wissenschaften, Wien, Mathematisch-Naturwissenschaftliche Classe 46, 127–290.

Vašíček, Z., Wiedmann, J., 1994. The Leptoceratoidinae: small heteromorph ammonites from the Barremian. Palaeontology 37, 203–239.

Vermeulen, J., 1997. *Kotetishvilia*, nouveau genre barrémien de la sous-famille des Psilotissotiinae (Pulchelliidae, Endemoceratceae, Ammonoidea). Géologie Alpine 1996 (72), 117–125.

Vermeulen, J., 2002. Etude stratigraphique et paléontologique de la famille des Pulchelliidae (Ammonoidea, Ammonitina, Endemoceratceae). Geologie alpine. Memoire H.S, 42, Université Joseph-Fourier-Grenoble I, 333 p.

Vermeulen, J., Lazarin, P., Lepinay, P., Leroy, L., Mascarelli, E., 2014. Ammonites du Barrémien du Sud-Est de la France (Ammonitina, Ancyloceratina, Turrilitina). Strata 50, 1–95.

Wiedmann, J., 1960. Zur Systematik jungmesozoischer Nautiloidea. Palaeontographica A 115, 144–206.

Wiedmann, J., 1962. Ammoniten aus der Vascogotischen Kreide (Nordspanien) I. Phylloceratina, Lytoceratina. Palaeontographica A 118, 119–237.

Wiedmann, J., 1964. Unterkreide-Ammoniten von Mallorca. 2. Lieferung: Phylloceratina. Akademie der Wissenschaften und der Literatur. Abhandlungen der mathematisch-naturwissenschaftliche Klasse 4(1963), pp. 151–264.

Wiedmann, J., 1965. Origin, limits, and systematic position of *Scaphites*. Palaeontology 8, 397–453.

Wiedmann, J., 1966. Stammesgeschichte und System der posttriadischen Ammonoideen. Neues Jahrbuch für Geologie und Paläontologie, Abhandlungen 127, 13–81.

Wiedmann, J., Dieni, I., 1968. Die Kreide Sardiniens und ihre Cephalopoden. Palaeontographia Italica 64, 1–171.

Wiedmann, J., Schneider, H.L., 1979. Cephalopoden und Alter der Cenoman-Transgression von Mühlheim-Broich, SW-Westfalen. In: Wiedmann, Jost (Ed.),

Aspekte der Kreide Europas, International Union of Geological Sciences, series A 6. Schweizerbart, Stuttgart, pp. 645–680.
Wright, C.,W., 1952. A classificationo of the Cretaceous ammonites. Journal of Paleontology 26, 213–222.
Wohlwend, S., Hart, M., Weissert, H., 2015. Ocean current intensification during the Cretaceous oceanic anoxic event 2—evidence from the northern Tethys. Terra Nova 27, 147–155.
Wright, C., 1996. Treatise on Invertebrate Paleontology. Part L, Mollusca 4: Cretaceous Ammonoidea. xx+ 1–362 (with contributions by Calloman J.H., and Howarth, M.K.). Geological Society of America and University of Kansas, Lawrence, Kansas and Boulder.
Wright, C.W., Kennedy, W.J., 1978. The ammonite *Stoliczkaia* from the Cenomanian of England and northern France. Palaeontology 21, 393–409.
Wright, C.W., Kennedy, W.J., 1984. The Ammonoidea of the Lower Chalk. Part 1. Palaeontographical Society Monograph, pp. 295–319.
Wright, C.W., Kennedy, W.J., 1994. Evolutionary relationships among Stoliczkaiinae (Cretaceous ammonites) with an account of some species from the English *Stoliczkaia dispar* Zone. Cretaceous Research 15, 547–582.
Wright, C.W., Kennedy, W.J., 1995. The Ammonoidea of the Lower Chalk. Part 4. Palaeontographical Society Monograph 1–126.
Wright, C.W., Kennedy, W.J., 1996. The Ammonoidea of the Lower Chalk. Part 5. Palaeontographical Society Monograph 320–403.
Wright, C.W., Kennedy, W.J., 2015. The Ammonoidea of the Lower Chalk. Part 6. Palaeontographical Society Monograph 404–460.
Zittel, K.A. v., 1881–1885. Handbuch der Palaeontologie 1. Abtheilung, Palaeozoologie. In: Mollusca und Arthropoda, II. Band. Verlag R. Oldenbourg, München und Leipzig, 893, 1109 p.
Zittel, K.A. v, 1895. Grundzüge der Palaeontologie. Oldenbourg, Münich and Leipzig, 971 p.

Chapter II

Ecological disparity precedes taxonomic richness; Palaeoecological changes induced by environmental changes during the Cretaceous in the Alpstein (northeastern Switzerland)

Tajika, A. Kürsteiner, P. Klug, C.

Submitted to
Swiss Journal of Palaeontology

Ecological disparity precedes taxonomic richness; Palaeoecological changes induced by environmental changes during the Cretaceous in the Alpstein (northeastern Switzerland)

Amane Tajika[1] • Peter Kürsteiner[2] • Christian Klug[1]

[1]Paläontologisches Institut und Museum, Universität Zürich, Karl Schmid-Strasse 4, CH-8006 Zürich, Switzerland

[2]Naturmuseum St. Gallen, Rorschacherstrasse 263, CH-9016 St. Gallen, Switzerland

Abstract

Studies of global palaeoecology through time usually ignore regional details. Such regional studies on palaeoecology are required to better understand both regional- and global- scale palaeoecolgical changes. We analyzed the palaeoecolgy of a Cretaceous sedimentary sequence in the Alpstein (cantons of Appenzell Ausserrhoden, Appenzell Innerrhoden and St. Gallen, northeastern Switzerland), which covers the Barremian to the Cenomanian. Two diversity indices of taxonomic richness and disparity (ecospace occupation) with the trophic nucleus concept were employed in order to document changes in palaeocommunity through time. Our results illustrate that taxonomic richness did not change dramatically, while distinct changes were found in ecospace occupation through time. The changes in ecospace utilization most likely root in fluctuations in water depth. In addition to these sea level changes, our results suggest that water depth was higher eastwards within the Alpstein. Ecospace occupation was moderately diverse through time, which is likely linked with the favorable conditions such as moderate water depth, which made the region habitable for a range of organisms. Only during the late Barremian, the sea was maybe too shallow, thus preventing high diversity associations. These results confirmed that regional environmental changes affected ecological disparity more strongly than taxonomic richness.

Introduction

The 'Big Five' mass extinctions (End-Ordovician, Late Devonian, End-Permian, End-Triassic and End-Cretaceous) are known to have severely affected the earth's ecosystems and ecology (e.g., Murphy et al. 2000; Sheehan 2001; Hesselbo et al. 2007; Knoll et al. 2007; Archibald et al. 2010). Recently, Barnosky et al. (2011) examined fossil and modern biodiversity data in order to assess whether current extinction rates are as disruptive as those of the previous major mass extinctions. In the article, the authors conclude that we are facing the 'sixth mass extinction'. It is thus of great importance to examine changes in palaeocommunities in relation to palaeoenvironmental changes, although it is often discussed that such palaeoecological analyses tend to suffer from biases of sampling, fossilization potential, taphonomy, taxonomic uncertainties and time averaging (e.g., Bambach 1977; Koch and Sohl 1983; Cherns and Wright 2000; Kidwell 2002; Powell and Kowalewski 2002; Lane and Benton 2003; Bush and Bambach 2004; Kowalewski et al. 2006; Alroy 2010; Bernard et al. 2010).

Palaeoecological studies on a regional and global scale have been of great interest for palaeontologists over the past decades (e.g. Bambach 1977, 1983; Sepkoski 1981; Sepkoski et al. 1981; Sepkoski and Sheehan 1983; Sepkoski 1984, 1988; Bush and Bambach 2004, 2015; Bush et al. 2007; Hofmann et al. 2013; Frey et al. 2014). However, the number of large regional data sets of palaeoecology and alpha diversity data, i.e. primary information for a higher resolved picture of the global ecology through the Phanerozoic, is still low. For that purpose, documentation of both taxonomic richness and eco-

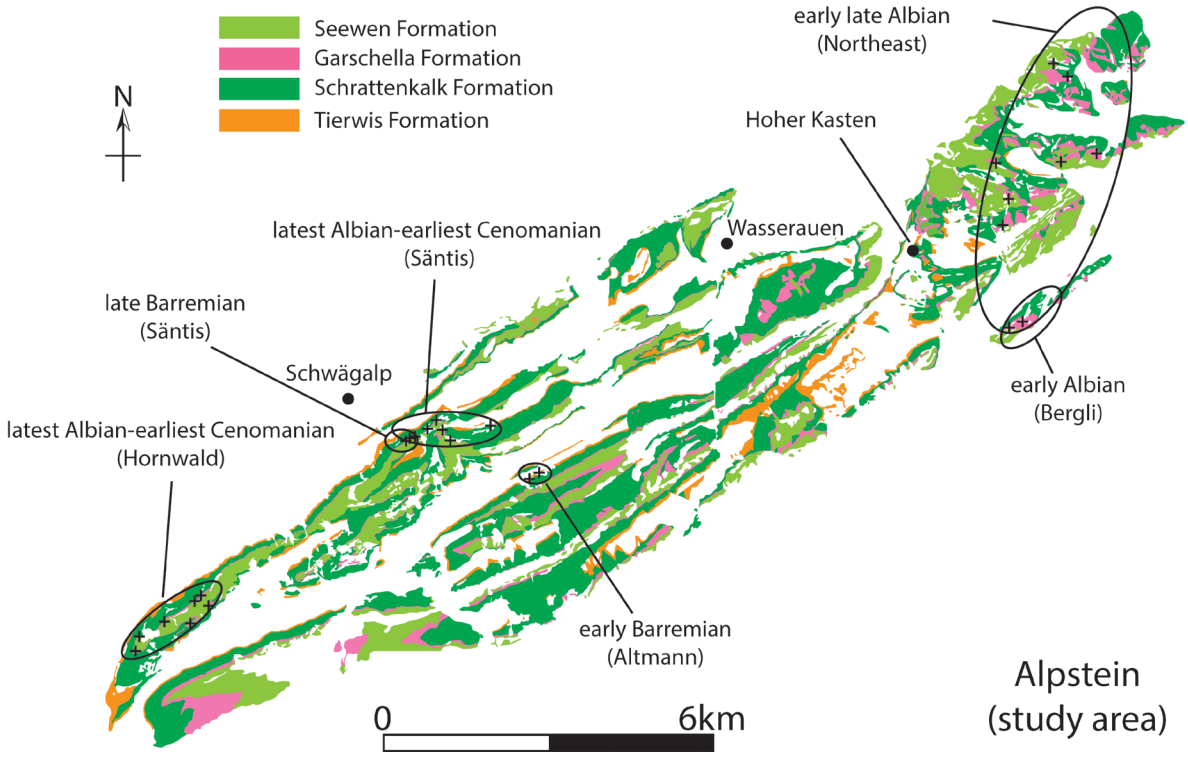

Fig. 1. Geological map of the Alpstein (reproduced from Eugster et al. 1982 and Tajika et al. 2017). Localities, from which palaeoecological samples were taken, are marked by ellipses.

logical disparity within communities is necessary. Bambach (1983) introduced the concept of ecological guilds such as body plan, food source and tiering, which permitted to analyze palaeoecological changes through time. This method was further developed by Bush et al. (2007) to theoretical ecospace use. They also included relative abundance of organisms in their analysis in order to evaluate the ecological importance of various ecologic types through time. Data resulting from such analyses are also necessary to discuss the link between the external environments and ecologic changes.

The Alpstein (cantons of Appenzell Ausserrhoden, Appenzell Innerrhoden and St. Gallen of northeastern Switzerland) is well known for excellently-exposed Cretaceous successions. Although a number of studies have been carried out to examine the geology of this region (Funk 1969; Föllmi and Ouwehand 1987; Ouwehand 1987; Bodin et al. 2006; Sala et al. 2014; Wohlwend et al. 2015), a comprehensive overviews of relatively diverse faunas, especially cephalopods, was reported only recently by Sulser et al. (2013) and Tajika et al. (2017). In the latter article, we also discussed palaeoecology of the region and its link to external environments from the Barremian to the early Cenomanian. In the same article, we documented dynamic faunal turnovers throughout time, which were most likely linked with regional sea level changes. However, taxon counts were compiled from raw samples without correction of variations in sample size and furthermore, taxonomic resolution was low (identifications were conducted only at the order level). In order to accurately document the alpha diversity and palaeoecology in all detail, we herein use a much refined database. Accordingly, we examine the palaeoecology of the Alpstein in detail in order to answer the following questions: (1) How did the alpha diversity, i.e., taxonomic richness, change from the early Barremian to the earliest Cenomanian? (2) What main ecologic categories occurred through time? (3) What caused the palaeoecological changes between successive faunas? (4) Is there any difference in changes between taxonomic richness and ecological disparity through time?

Locality and geological setting

The Alpstein massif is located in the northern part of the Helvetic nappes, which span from southwestern to northeastern Switzerland (figure 1 of Tajika et al. 2017; Fig. 1). The study area (Alpstein) includes a part of the Swiss Alps (e.g., Altmann, Hoher Kasten, Wildhuser Schafberg and Säntis), which mainly comprises Cretaceous sediments of the Säntis nappe (Pfiffner 2011). The investigated

stratigraphic sequence and localities are summarized in Fig. 1 and Table 1. Descriptions of each stratigraphic unit are provided in Tajika et al. (2017) and repeated here:

Tierwis Formation (uppermost Hauterivian to upper Barremian; Funk 1969): The Tierwis Formation consists of two subunits, the Altmann Member and the Drusberg Member. The Altmann Member is composed of glauconite-rich marls and sandy limestones with abundant trace fossils that are occasionally pyritized. More condensed and phosphatic layers contain ammonites in a moderate to high abundance. Our ecological analysis for the early Barremian was carried out at the Altmann Member of Altmann Sattel (Fig. 1). The Drusberg Member lies above the Altmann Member, which is characterized by alternating marl and marly limestones. The latter also contains macrofauna, mostly benthos such as sea-urchins, bivalves and brachiopods, and rarely, necton such as ammonites.

Schrattenkalk Formation (upper Barremian to middle lower Aptian; Bollinger 1988): The Schrattenkalk Formation is characterized by massive light grey limestones, which often contain many bioclasts. The sediments are from a shallow marine setting with abundant corals, sponges, algae, rudist bivalves and thick-shelled gastropods. The Schrattenkalk Formation is separated into two thick limestone layers (Lower and Upper Schrattenkalk Members) which are separated by the Rawil Member (Schenk 1992; Föllmi et al. 2007). The Rawil Member, also formerly referred to as Lower Orbitolina Beds, starts with marly to sandy limestone beds which contain a rich benthic fauna of echinoids (*Heteraster oblongus*, *Leptosalenia prestensis*) and gastropods (*Harpagodes pelagi*) occasionally accompanied by wood remains. Our palaeoecological analysis for the late Barremian was conducted in the middle of the Rawil Member. The marly Orbitolina Bed at the top of the Rawil Member marks the boundary between the Barremian and the lowermost Aptian (Bonvallet 2015). The boundary between the Upper Schrattenkalk Member and the Garschella Formation is marked by a layer with phosphorites that also contains fossils (e.g., belemnite rostra; Föllmi 1986; Ouwehand 1987; Föllmi 1989a, b).

Garschella Formation (upper lower Aptian to lowermost Cenomanian; Föllmi and Ouwehand 1987): In the Säntis area, a large part of the Aptian (Grünten Member, Brisi Member and lower part of the Selun Member) is missing due to erosion, non-deposition and condensation processes, resulting in a 13 m.y. hiatus. The Garschella Formation commences with dark greenish marls and marly limestones at the base (Sellamatt Beds; Föllmi and Ouwehand 1987), containing several fossiliferous, phosphatic conglomerates (Durschlägi and Wannenalp Beds; Föllmi and Ouwehand 1987). These are overlain by glauconitic limestones with greyish limestone nodules in various sizes and amounts (Aubrig Beds; Föllmi and Ouwehand 1987). This upper part of the Garschella Formation contains some indications for condensation such as fragmented ammonoids, phosphoritic internal moulds of fossils, and the fact that some ammonite zones are comprised in this thin sedimentary sequence. At the top of the Garschella Formation, glauconitic sandstones and nodular limestones are deposited, namely a condensation horizon called Kamm Bed that yields abundant and highly diverse ammonoid faunas. We carried out our palaeoecological analysis at three different stratigraphic sequences of the Garschella Formation: 1) early Albian (*Leymeriella tardefurcata* and *Douvilleiceras mammillatum* zone), 2) early late Albian (most likely Wannenalp Beds with the occurrences some species of *Mortoniceras*), 3) latest Albian-earliest Cenomanian (Kamm Bed with *Stoliczkaiella* and *Mantelliceras*).

Material and Methods

Sampling

We examined fossils from the Alpstein, Switzerland. Part of the examined fossils, which were collected by PK and documented by Tajika et al. (2017), are housed in the Naturmuseum St. Gallen with the numbers NMSG (Coll. XX).

We focused on 6 fossiliferous layers to sample macrofossils for palaeoecological analyses. The fossils were either collected or counted along the bedding planes (Table 1) for quantitative analyses. Due to the varying quality of preservation, the fossils were often determinable only to family level. As such, the taxonomic level family was used to examine taxonomic richness.

There is a certain degree of faunal mixing in the examined layers: co-occurrence of *Nicklesia pulchella* and *Kotetishvilia compressissima* (early Barremian, Altmann Member), *Leymeriella tardefurcata* and *Douvilleiceras mammillatum*, (early Albian, Garschella Formation), probably some species of *Mortoniceras* (early late Albian, Garschella Formation), latest Albian Stoliczkaiella and early Cenomanian Mantelliceras (latest Albian-earliest Cenomanian; Kamm Bed of the Garschella Formation). Such faunal mixing indicates that our analy-

Table 1. Data of abundance of fossils, stratigraphic sequences and localities, in which palaeoecological analysis was carried out. Asterisk indicates fossils counted on a bedding plane but not collected.

	N	stage	stratigraphic sequence	ammonite zone (s)	locality (Fig. 1)
Palaeoecology 1	87	early Barremian	Altmann Mb. (Tierwis Fm.)	*Nicklesia pulchella* and *Kotetishvilia compressissima* zones	Altmann Sattel
Palaeoecology 2	96	late Barremian	Lower Schrattenkalk Mb. (Schrattenkalk Fm.)	no ammonite record	Säntis
Palaeoecology 3	255	early Albian	Garschella Fm.	*Douvilleiceras mammillatum* zone	Bergli
Palaeoecology 4	208	early late Albian	Garschella Fm.	*Mortoniceras* zones	NE of Alpstein
Palaeoecology 5	132	latest Albian-earliest Cenomanian	Kamm Bed (Garschella Fm.)	probably part of *Arrhaphoceras briacensis* and *Mantelliceras mantelli*	Hornwald
Palaeoecology 6	70	latest Albian-earliest Cenomanian			Säntis

sis does not represent a single environment in time and some time-averaging occurred (Kidwell and Bosence 1991). However, all faunas do not show a mix of shallow water organisms (corals, sponges and algae) and deep water forms (cephalopods), which suggests that the degree of ecological mixing of remains of organisms from extremely different environmental conditions is low.

Alpha diversity (taxonomic richness)

To compare alpha diversities (taxonomic richness) of faunas from the different geologic units, the abundances of each family were counted per faunal association. Since some fossils were available only as cross sections and thus, not determinable to family level in the late Barremian, the taxonomic richness could not be assessed. Rarefaction analysis was carried out to estimate the effect of sample size and to standardize on a certain sample size. This test was performed with the software PAST 3.15 (Hammer et al. 2001).

Ecospace utilization

We applied the concept of ecospace utilization introduced by Bush et al. (2007). Accordingly, the fossils were classified based on their ecological parameters (tiering, motility and feeding) and plotted into a theoretical ecospace. We followed the ecological classification illustrated in table 1 of Tajika et al. (2017) with some corrections and additions (Table 2). In order to detect, which taxa and modes of life were dominant in each fauna, the 'nucleus of a biocoenosis' concept (Neyman 1967; later referred to as 'trophic nucleus' by some researchers) was applied. Accordingly, ecologies of organisms, which constitute 80% of a fauna were regarded as being ecologically prevalent.

Results

Alpha diversity (taxonomic richness)

Taxonomic richness of each fauna is shown in Table 3. Since the sample sizes of the examined faunas vary, which can lead to biased estimates of taxo-

Table 2. Ecologic categories of tiering, motility and feeding types (modified from Bush et al. 2007 and Tajika et al. 2017).

Ecologic category	Examples
Tiering	
1. Pelagic	ammonoids, belemnoids, fish, nautilids
2. Erect	crinoids, corals, sponges
3. Surficial	echinoids, brachiopods, gastropods, *Exogyra*
4. Semi-infaunal	„normal" bivalves, rudist bivalves, scaphopods
5. Shallow infaunal	many clams
6. Deep infaunal	the clam *Panope*
Motility Level	
1. Freely, fast	ammonoids, belemnoids, fish, some arthropods
2. Freely, slow	gastropods, echinoids, nautilids, scaphopods
3. Facultative, unattached	many clams, polychaetes: Sedentaria
4. Facultative, attached	corals, mussels
5. Non-motile, unattached	reclining brachiopods, boring bivalves
6. Non-motile, attached	rudist bivalves, pedunculated brachiopods, sponges
Feeding Mechanism	
1. Suspension	boring bivalves, brachiopods, bryozoans, corals, rudists, scaphopods, sponges
2. Surface deposit	tellinid bivalves, polychaetes
3. Mining	nuculid bivalves
4. Grazing	echinoids, gastropods
5. Predatory	ammonoids, belemnoids, nautilids, fish
6. Other	

nomic richness, the original data was rarefied. Raw data of taxonomic richness and rarefied data are plotted in Fig. 2A and B. The Rarefaction analysis shows that taxonomic richness of faunas with high sample size tends to be overestimated. For instance, the early Albian fauna consists of 255 specimens, which yielded the highest diversity in the raw data, which was then estimated more or less as high as that of the other times after the sample size was rarefied to 70. As a result, taxonomic richness stayed at more or less 20 except the early late Albian (Fig. 2), although data from the late Barremian are missing due to poor fossil preservation, which hampers taxonomic assignments.

Ecospace utilization

Changes in the three ecologic categories (tiering, motility and feeding) from the early Barremian to the earliest Cenomanian are shown in Fig. 3. A big change occurs at the late Barremian with the disappearance of pelagic elements (ammonites, belemnites, nautiloids and fish). Feeding modes of the late Barremian includes only suspension feeding, while several other feeding modes are prevalent in the other examined stratigraphic units. The late Barremian is also characterized by the dominance of facultative and non-motile 'attached' animals. Although in the latest Albian, the analysis was carried out in two localities of Hornwald and Säntis, results provided a more or less identical ecospace utilization (Fig. 3).

Ecologic changes in three dimensional theoretical ecospace are shown in the left column of Fig. 4. The trophic nucleus was also determined in order to illustrate the ecology of prevalent organisms in each stratigraphic unit (right column of Fig. 4). It appears that the most extensive ecospace utilisation lies in either the early Barremian, early Albian or early late Albian. But when the trophic nucleus is taken into consideration, the early Albian is probably the time, in which the organisms with the most diverse ecologies were present. By contrast, the late Barremian is the time where the lowest diversity of ecospace utilization was present; however, this partially roots in the sampling mode, because in this case, we counted specimens on a weathered bedding plane using cross sections of fossils. The results demonstrate that only a small number of groups are ecologically dominant within each fauna (right column of Fig. 4), even though sometimes, ecological occupation appears to be more or less elevated such as in the early Barremian, early late Albian and latest Albian-earliest Cenomanian of the Säntis (left column of Fig. 4).

Discussion

As shown in the result section and discussed by Tajika et al. (2017), a big shift in ecology happened in the late Barremian and the early Aptian, which was the only time period where pelagic elements were not documented. Tajika et al. (2017) correlated the absence or presence of pelagic elements with regional sea level changes, which was previously reported by Föllmi (1986; Fig. 5). The early Barremian of the Altmann Member is characterized by heterozoan, partially hemipelagic marl and marly limestones (Bollinger 1988; Föllmi et al. 2007), which implied moderately deep marine settings. The results of our palaeoecological analysis document relatively diverse modes of life at the time (Fig. 3, 4), although the fauna is dominated by pelagic and freely swimming predators such as ammonoids (right column of Fig. 4). Facies changes that occurred between the early Barremian and the early late Aptian (Bollinger 1988), which were documented by our field data as well as that of Tajika et al. (2017), suggest that the massive limestones of the Schrattenkalk Formation of late Barremian to early Aptian age was laid down under shallow marine conditions. This is further corroborated by the presence of red algae, scleractinians, rudists and other shallow marine organisms (Föllmi et al. 2007). A shallow marine environment is further supported by the abundance of remains of land plants, which occur at the base of the Rawil Member. The examined late Barremian fauna derives from the the Rawil member, when the platform was temporarily emersed (Bonvallet 2015). These shallow to non-marine environments were not inhabitable by pelagic predators (ammonoids, belemnites and nautiloids). Our results also indicate that the sea level changes affected not only the number of habitats but also the variation in motility of the animals. Correspondingly, the late Barremian environment with low sea levels fostered the dominance of (facultative and non-motile) attached animals like algae, corals, sponges and rudists (Tajika et al. 2017). The three-dimensional ecospace occupation in the late Barremian is much smaller than in the other examined stratigraphic units. Bambach (1977) examined differences in species richness and abundance among bivalves between different habitats through the Phanerozoic. He documented an increasing trend of diversity and abundance from inshore environments with adverse ecological conditions through nearshore to open marine environments. Although we lack sufficient data on taxonomic richness of the shallow marine late Barremian to early Aptian environments due to the

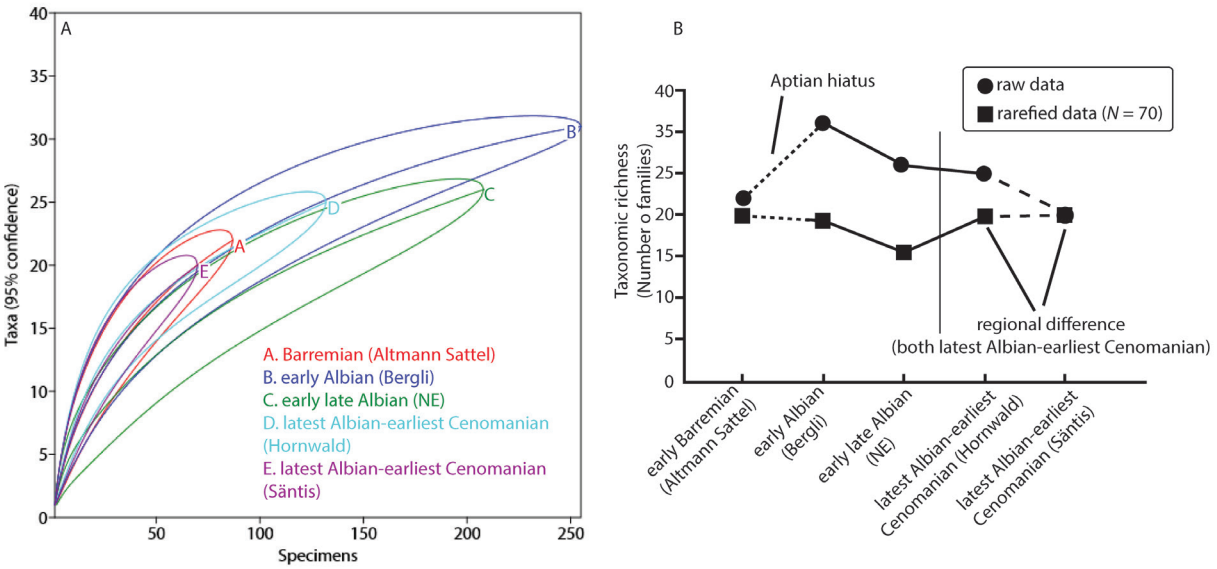

Fig. 2. Rarefaction analysis and taxonomic richness in studied geologic times. A Rarefaction analysis of raw data on taxonomic richness. B Raw and rarefied data of taxonomic richness.

Table 3. Taxonomic richness of each fauna and abundance. Groups in the trophic nucleus are indicated by asterisks.

early Barremian (Säntis)		early Albian (Bergli)		early late Albian (NE)	
family	abundance	Family	abundance	Family	abundance
Barremitidae	27*	Sellithyrididae	64*	Desmoceratidae	62*
Holcodiscidae	11*	Desmoceratidae	46*	Inoceramidae	56*
Terebrataliidae	9*	Douvilleiceratidae	20*	Brancoceratidae	34*
Ancyloceratidae	7*	Trochidae	17*	Ancyloceratidae	7*
Oxyteuthididae	4*	Inoceramidae	16*	Hamitidae	7*
Pectinoidae	4*	Anisoceratidae	11*	Cymatoceratidae	5*
Nuculidae	3*	Cymatoceratidae	10*	Phylloceratidae	5*
Pulchellidae	3*	Plicatula	9*	Pleurotomariidae	4
Gryphaeidae	2	Dentalidae	8*	Holasteridae	3
Sellithyrididae	2	Hamitidae	8*	Sellithyrididae	3
Cyclothyrididae	2	Tetragonitidae	7	Tetragonitidae	3
Toxasteridae	2	Buchiidae	4	Turrilitidae	3
Cymatoceratidae	2	Terebrataliidae	4	Ichthyodectiformes indet. 1	2
Desmoceratidae	1	Leymeriellidae	3	Sacphitidae	2
Ammonite indet. 1	1	Turbinidae	3	Baculitidae	1
Ammonite indet. 2	1	Amberleyidae	2	Buchiidae	1
Arcidae	1	Aporrhaidae	2	Cephalaspida	1
Seaurchin indet. 1	1	Cerithiidae	2	Dentaliidae	1
Holectypidae	1	Cirsotrema	2	Ficidae	1
Pleurotomariidae	1	Gadilidae	2	Haplaraeidae	1
Sponge indet. 1	1	Hoplitidae	2	Laqueidae	1
Serpulidae	1	Metacerithiidae	2	Norellidae	1
		Phylloceratidae	2	Plicatulidae	1
		Vanikoroidea	2	Ringiculidae	1
		Burrirhynchia	1	Terebrataliidae	1
		Clypeidae	1	Turbinidae	1
		Cyclothyrididae	1		
		Lytoceratidae	1		
		Pholadomyidae	1		
		Ringiculidae	1		
		Toxasteridae	1		

Table 3 (continued). Taxonomic richness of each fauna and abundance. Groups in the trophic nucleus are indicated by asterisks.

latest Albian-earliest Cenomanian (Hornwald)	
Family	abundance
Turrilitidae	27*
Inoceramidae	15*
Acanthoceratidae	14*
Lyelliceratidae	10*
Cymatoceratidae	8*
Desmoceratidae	8*
Baculitidae	7*
Sellithyrididae	7*
Hamitidae	6*
Discoididae	4*
Holasteridae	4*
Brancoceratidae	3
Pleurotomariidae	3
Scaphitidae	3
Tetragonitidae	3
Ampullinidae	1
Anisoceratidae	1
Archaeolamnidae	1
Basiliolidae	1
Forbesiceratidae	1
Glycymeridae	1
Lamniformes indet. 1	1
Mesohibolitidae	1
Phylloceratidae	1
Phylloceratidae	1

latest Albian-earliest Cenomanian (Säntis)	
Family	abundance
Turrilitidae	18*
Desmoceratidae	8*
Inoceramidae	8*
Anisoceratidae	6*
Brancoceratidae	5*
Discoididae	3*
Pleurotomariidae	3*
Tetragonitidae	3*
Baculitidae	2
Cymatoceratidae	2
Lyelliceratidae	2
Sellithyrididae	2
Ampullinidae	1
Aporrhaidae	1
Archaeolamnidae	1
Holasteridae	1
Hoplitidae	1
Mesohibolitidae	1
Scaphitidae	1
Turbinidae	1

poor fossil preservation, which impeded even family-level determination, it appears like this ecology was rather monotonous, considering ecospace for only a moderate number of species.

According to Föllmi (1986), the sea level began to rise in the early late Aptian and reached a relatively high level during the early Albian (Fig. 5). The most extensive ecospace occupation occurred in the early Albian (Fig. 4), which suggests that the habitat provided favorable ecological conditions for various organisms including pelagic predators to thrive. The transgressive trend intensified in the latest Albian. This rapid environmental change likely caused condensation and thus time averaging (Kidwell and Bosence 1991). The high diversity of the early Albian suggests subtle environmental differences such as differences in water depth between the eastern and the western Alpstein region. In contrast to the moderately rich and diverse fauna of the early Albian in the Bergli area, late Aptian to early Albian faunas are absent in the Säntis area. This phenomenon might be linked with phases of temporal subaerial exposure of the carbonate platform of the Säntis area and/ or increased current intensity, possibly in connection with short term shifts in current direction (Föllmi 1989b), which did not affect the Bergli area strongly. Moreover, the 'non-motile, attached' mode is one of the dominant ecologic modes of motility in the Bergli area, thus indicating a moderate water depth, considering the fact that shallow water late Barremian fauna is dominated by 'non-motile, attached' forms (Fig. 3). The same holds true for the feeding modes, where suspension feeding is much more common in the early Albian than in the younger stratigraphic units (Fig. 3), which may also indicate relatively shallow environments. Similarly, when the roughly contemporary ecospace occupation in the two regions Hornwald and Säntis of the latest Albian to earliest Cenomanian age are compared, there is a difference in ecology of 'prevalent organisms' (trophic nucleus): benthic forms were less common in the Säntis than in the Hornwald area (right column of Fig. 4), although the overall ecospace occupation are nearly identical in both areas (Fig. 3). This might be caused by the greater water depth of the Säntis area compared to the Hornwald region. The presence of the Kamm Bed in the Alpstein suggests an inner shelf environment when these sediments were deposited (Föllmi 1989a). Also, Föllmi (1986) found that the inner shelf lied in the western and northern part of the region with its margin running from the southwest (Feldkirch; 10 km east of the Alpstein region) via the northeast (around 1 km south of Ebnit) to the east. Taking this into consideration, it appears likely that the water depth slightly increased eastwards as well within the inner shelf. In addition, the above-mentioned sea level changes appear to also have brought in waters with a higher palaeotemperature from the Tethys reconstructed by Pucéat et al. (2003). Since temperature fluctuations can have a strong effect on sea level changes, i.e., melting of in-

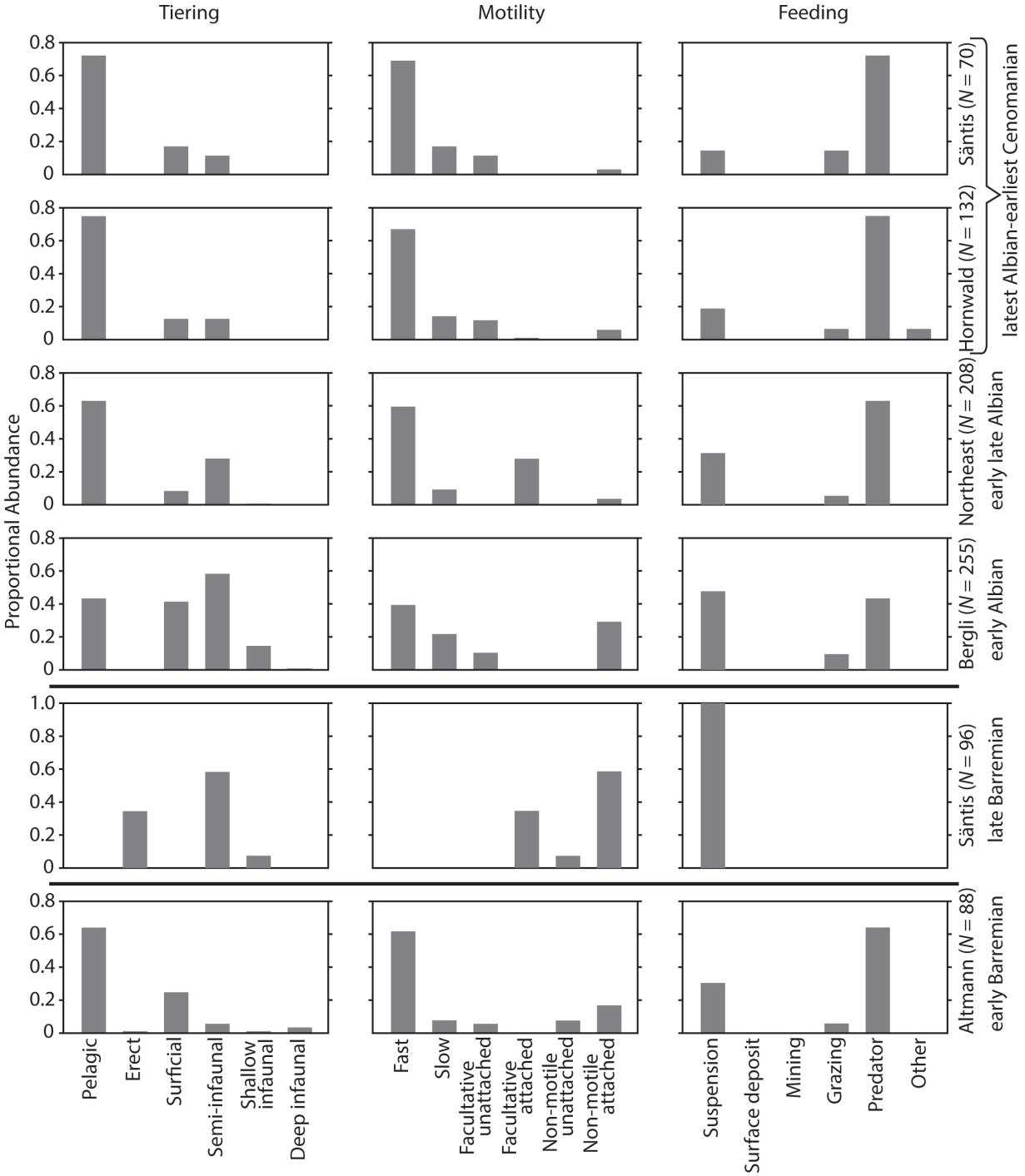

Fig. 3. Changes in relative abundances of tiering, motility and feeding from the early Barremian to the latest Albian-earliest Cenomanian.

land ice and inflation of sea water volume by heat, palaeotemperature probably indirectly caused the changes of ecology in the Alpstein.

As far as taxonomic richness is concerned, one can see a rather stable diversity from the early Barremian to the earliest Cenomanian, when samples are rarefied to 70. A relatively low taxonomic richness appears in the early late Albian, although the ecospace occupation of the fauna is relatively diverse (Fig. 4). Taking the effects of time averaging into account, this may root in unevenness of time range between compared faunas, i.e., heavily time-averaged faunas logically seem artificially more diverse. However, the overall taxonomic richness has values around 20 with a low degree of variation, thus suggesting that the above discussed sea level change might not have affected taxonomic richness as strongly as the ecospace occupation (Fig. 6). That is, changes of ecologic disparity precede those of taxonomic richness, when environmental changes occur.

Bush and Bambach (2004) discussed the preservation potential of aragonitic versus calcitic shell materials because aragonite is more susceptible to

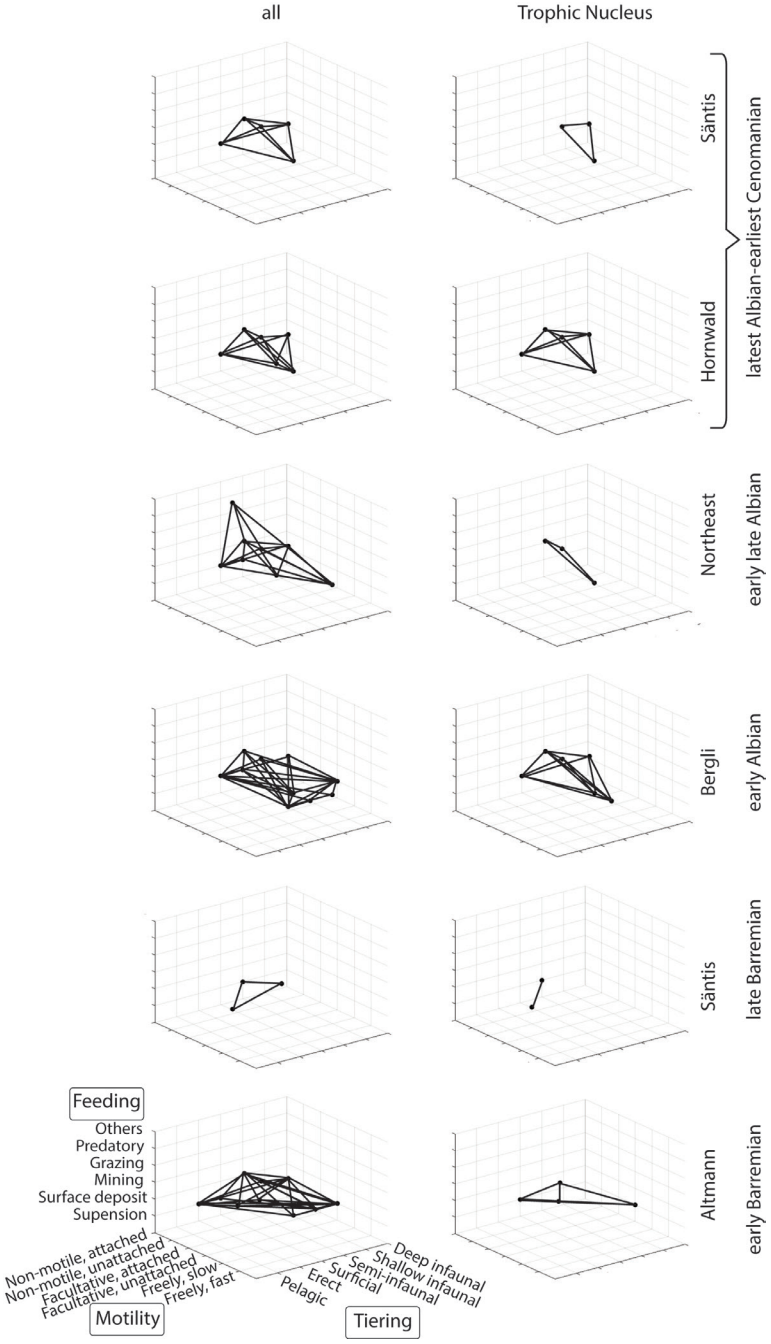

Fig. 4. Three dimensional plot of ecospace utilization through time. Left column includes all analyzed groups. Right column includes only groups of the trophic nucleus.

dissolution than calcite in sea water and thus, has a lower fossilization potential (Canfield and Raiswell 1991; Smith et al. 1992; Brachert and Dullo 2000; Morse and Arvidson 2002; Kowalewski et al. 2006). Some researchers examined this bias employing different methods (Koch and Sohl 1983; Cherns and Wright 2000). In contrast to the latter authors, Kidwell (2005) argued that these differences in preservability do not have a big impact on studies on macroevolutionary patterns and biodiversity changes in mollusks. Our study covers only a rather short period in geologic time (between ca. 129 Ma and 93 Ma), during which there were no major changes in proportion of mollusks with aragonitic, calcitic or bimineralic shells (Kidwell 2005). Also, assuming that preservation potential is nearly the same within a group with the same shell mineralogy, we consider that this bias does not strongly affect our results. Additionally, Bush and Bambach (2004) discussed the effect of latitudes on diversity measurements, since some studies documented a gradient of diversity between temperate and tropical regions (e.g., Crame 2002). However, as mentioned before, the studied time interval is too short for significant effects of changes in latitude and thus, the effects of such a biogeographical bias is likely negligible. Therefore, the results of our palaeoecological analysis likely reflect mainly environmental changes with regional and global causes.

Conclusions

We analyzed the palaeoecology of the Alpstein region from the early Barremian to the earliest Cenomanian with focuses on the taxonomic richness and ecological disparity (ecospace utilization).

Alpha diversity of the Alpstein–Our raw data show a fluctuation in taxonomic richness through time. After rarefaction of the palaeobiodiversity data, however, it turned out that taxonomic richness did not change dramatically from the early Barremian to the earliest Cenomanian.

Ecospace utilization–A distinct change in ecospace utilization occurred during the late Barremian, when the fauna was dominated by organisms with monotonous ecological requirements such as

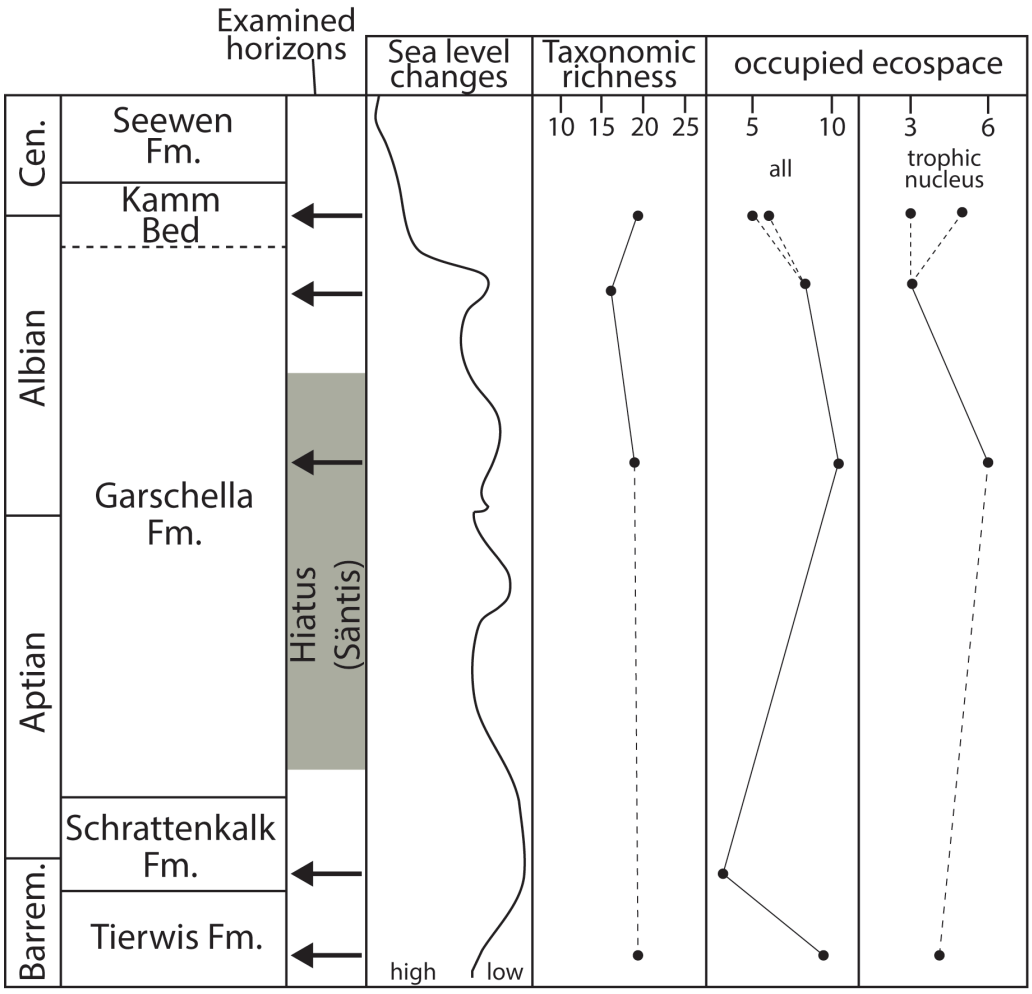

Fig. 5. Summary of the ecological analysis. The sea level curve is reproduced from Föllmi (1986).

non-pelagic, facultative or non-motile and suspension feeding groups. We documented the widest ecospace occupation for the early Albian. Ecospace utilization of prevalent groups (trophic nucleus) is reduced in the early Barremian, early late Albian and latest Albian to earliest Cenomanian in the Säntis area.

What caused the changes in palaeoecology?–Although there are some biases affecting our palaeoecological analyses, they do not significantly alter our results. In contrast, our results most likely reflect actual environmental changes. The differences in ecospace occupation were probably caused by regional and global sea-level fluctuations. The fact that the more monotonous pelagic-dominated faunas were found eastwards in the latest Albian to the earliest Cenomanian suggests that water depth slightly increased towards the east within the inner shelf.

Difference in changes between taxonomic changes and ecologic disparity–Our results show that taxonomic richness was relatively stable through time, whereas ecological disparity changed more dramatically. This confirmed that ecological disparity is more susceptible to environmental changes than taxonomic richness is.

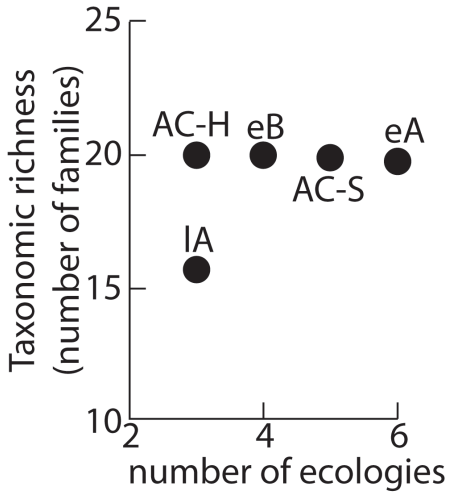

Fig. 6. Scatter plots of taxonomic richness vs. number of ecologies through time. eB = early Barremian, eA = early Albian, lA = late Albian, AC-H = latest Albian-earliest Cenomanian in Hornwald, AC-S = latest Albian-earliest Cenomanian in Säntis. Taxonomic richness is stable except the early Albian, while the number of ecologies varies through time.

Acknowledgements

This study was supported by the Swiss National Science Foundation (project numbers: 200020_169847 and 200021_149119). We would like to thank Bernhard Hostettler (Bern), René Kindlimann (Aathal), Heinz A. Kollmann (Vienna), Ursula Menkveld-Gfeller (Bern), Iwan Stössel (Schaffhausen) and Karl Tschanz (Zurich) for their help with taxonomic identifications of the fossils. We greatly appreciate the constructive reviews of XXX and XXX.

References

Alroy, J. (2010). Fair sampling of taxonomic richness and unbiased estimation of origination and extinction rates. Quantitative methods in paleobiology. Paleontological Society Papers, 16, 55-80.

Archibald, J. D., Clemens, W., Padian, K., Rowe, T., Macleod, N., Barrett, P. M., Gale, A., Holroyd, P., Sues, H.-D., & Arens, N. C. (2010). Cretaceous extinctions: multiple causes. Science, 328(5981), 973-973.

Bambach, R. K. (1977). Species richness in marine benthic habitats through the Phanerozoic. Paleobiology, 152-167.

Bambach, R. K. (1983). Ecospace utilization and guilds in marine communities through the Phanerozoic. In M. J. S. Tevesz & P. L. McCall (Eds.), Biotic interactions in recent and fossil benthic communities (pp. 719-746). New York: Springer US.

Barnosky, A. D., Matzke, N., Tomiya, S., Wogan, G. O. U., Swartz, B., Quental, T. B., Marshall, C., McGuire, J. L., Lindsey, E. L., Maguire, K. C., Mersey, B., & Ferrer, E. A. (2011). Has the Earth's sixth mass extinction already arrived? Nature, 471(7336), 51-57.

Bernard, E. L., Ruta, M., Tarver, J. E., & Benton, M. J. (2010). The fossil record of early tetrapods: Worker effort and the end-Permian mass extinction. Acta Palaeontologica Polonica, 55(2), 229-239.

Bodin, S., Godet, A., Vermeulen, J., Linder, P., & Föllmi, K. B. (2006). Biostratigraphy, sedimentology and sequence stratigraphy of the latest Hauterivian–early Barremian drowning episode of the Northern Tethyan margin (Altmann Member, Helvetic Nappes, Switzerland). Eclogae Geologicae Helvetiae, 99(2), 157-174.

Bollinger, D. (1988). Die Entwicklung des distalen osthelvetischen Schelfs im Barremian und Früh-Aptian: Drusberg-, Mittagsspitz und

Schrattenkalk-Fm. im Vorarlberg und Allgäu. Dissertation. Universität Zürich.

Bonvallet, L. (2015). Evolution of the Helvetic Shelf (Switzerland) During the Barremian–Early Aptian: Paleoenvironmental, Paleogeographic and Paleoocianographic Controlling Factors. Dissertation. University of Lausanne.

Brachert, T., & Dullo, W.-C. (2000). Shallow burial diagenesis of skeletal carbonates: selective loss of aragonite shell material (Miocene to Recent, Queensland Plateau and Queensland Trough, NE Australia) - implications for shallow cool-water carbonates. Sedimentary Geology, 136(3), 169-187.

Bush, A. M., & Bambach, R. K. (2004). Did alpha diversity increase during the Phanerozoic? Lifting the veils of taphonomic, latitudinal, and environmental biases. The Journal of geology, 112(6), 625-642.

Bush, A. M., & Bambach, R. K. (2015). Sustained Mesozoic–Cenozoic diversification of marine Metazoa: A consistent signal from the fossil record. Geology, 43(11), 979-982.

Bush, A. M., Bambach, R. K., & Daley, G. M. (2007). Changes in theoretical ecospace utilization in marine fossil assemblages between the mid-Paleozoic and late Cenozoic. Paleobiology, 33(01), 76-97.

Canfield, D., & Raiswell, R. (1991). Carbonate precipitation and dissolution: its relevance to fossil preservation. In P. Alison & D. Briggs (Eds.), Taphonomy: releasing the data locked in the fossil record (pp. 411-453). New York: Plenum.

Cherns, L., & Wright, V. P. (2000). Missing molluscs as evidence of large-scale, early skeletal aragonite dissolution in a Silurian sea. Geology, 28(9), 791-794.

Crame, J. (2002). Evolution of taxonomic diversity gradients in the marine realm: a comparison of Late Jurassic and Recent bivalve faunas. Paleobiology, 28(2), 184-207.

Eugster, H., Forrer, M., Fröhlicher, H., Kempf, T., Schlatter, L., Blaser, R., Funk, H., Langenegger, H., Spoerri, M., & Habicht, K. (1982). Säntis (map sheet 1115), Geological Atlas of Switzerland 1:25.000, N. 78. Wabern: Federal Office of Topography, Swisstopo.

Föllmi, K. (1986). Die Garschella-und Seewerkalkformation (Aptian-Santonian) im Voralberger Helvetikum und Ultrahelvetikum. Mitteilungen aus dem Geologischen Institut der Eidgenössischen Technischen Hochschule und der Universität Zürich, Neue Folge, 262, 1-391.

Föllmi, K. (1989a). Evolution of the mid-Cretaceous triad: platform carbonates, phosphatic sediments, and pelagic carbonates along the northern Tethys margin. Springer-Verlag Berlin Heidelberg.

Föllmi, K. (1989b). Mid-Cretaceous platform drowning, current-induced condensation and phosphogenesis, and pelagic sedimentation along the eastern Helvetic shelf (northern Tethys margin). Cretaceous of the Western Tethys: Stuttgart, E. Schweizerbart'sche Verlagsbuchhandlung, 585-606.

Föllmi, K., Bodin, S., Godet, A., Linder, P., & Van De Schootbrugge, B. (2007). Unlocking paleo-environmental information from Early Cretaceous shelf sediments in the Helvetic Alps: stratigraphy is the key! Swiss Journal of Geosciences, 100(3), 349-369.

Föllmi, K., & Ouwehand, P. (1987). Garschella-Formation und Götzis-Schichten (Aptian-Coniacian): Neue stratigraphische Daten aus dem Helvetikum der Ostschweiz und des Vorarlbergs. Eclogae Geologicae Helvetiae, 80(1), 141-191.

Frey, L., Naglik, C., Hofmann, R., Schemm-Gregory, M., Frýda, J., Kroeger, B., Taylor, P. D., Wilson, M. A., & Klug, C. (2014). Diversity and palaeoecology of Early Devonian invertebrate associations in the Tafilalt (Anti-Atlas, Morocco). Bulletin of Geosciences, 89(1), 75-112.

Funk, H. (1969). Typusprofile der helvetischen Kieselkalk Formation und der Altmann-Schichten. Eclogae Geologicae Helvetiae 62, 191-203.

Hammer, Ø., Harper, D., & Ryan, P. (2001). Paleontological Statistics Software: Package for Education and Data Analysis. Palaeontologia Electronica, 4(1), 9.

Hesselbo, S. P., McRoberts, C. A., & Pálfy, J. (2007). Triassic-Jurassic boundary events: problems, progress, possibilities. Palaeogeography, Palaeoclimatology, Palaeoecology, 244(1), 1-10.

Hofmann, R., Hautmann, M., Wasmer, M., & Bucher, H. (2013). Palaeoecology of the Spathian Virgin Formation (Utah, USA) and its implications for the Early Triassic recovery. Acta Palaeontologica Polonica, 58(1), 149-173.

Kidwell, S. M. (2002). Time-averaged molluscan death assemblages: palimpsests of richness, snapshots of abundance. Geology, 30(9), 803-806.

Kidwell, S. M. (2005). Shell composition has no net impact on large-scale evolutionary patterns

in mollusks. Science, 307(5711), 914-917.

Kidwell, S.M., Bosence, D.W., 1991. Taphonomy and time-averaging of marine shelly faunas. In: Allison, P.A., Briggs, D.E.G. (Eds.), Taphonomy: releasing the data locked in the fossil record. Plenum, New York, pp. 115-209.

Knoll, A. H., Bambach, R. K., Payne, J. L., Pruss, S., & Fischer, W. W. (2007). Paleophysiology and end-Permian mass extinction. Earth and Planetary Science Letters, 256(3), 295-313.

Koch, C. F., & Sohl, N. F. (1983). Preservational effects in paleoecological studies: Cretaceous mollusc examples. Paleobiology, 9(01), 26-34.

Kowalewski, M., Kiessling, W., Aberhan, M., Fürsich, F. T., Scarponi, D., Wood, S. L. B., & Hoffmeister, A. P. (2006). Ecological, taxonomic, and taphonomic components of the post-Paleozoic increase in sample-level species diversity of marine benthos. Paleobiology, 32(4), 533-561.

Lane, A., & Benton, M. J. (2003). Taxonomic level as a determinant of the shape of the Phanerozoic marine biodiversity curve. The American Naturalist, 162(3), 265-276.

Morse, J. W., & Arvidson, R. S. (2002). The dissolution kinetics of major sedimentary carbonate minerals. Earth-Science Reviews, 58(1), 51-84.

Murphy, A. E., Sageman, B. B., & Hollander, D. J. (2000). Eutrophication by decoupling of the marine biogeochemical cycles of C, N, and P: A mechanism for the Late Devonian mass extinction. Geology, 28(5), 427-430.

Neyman, A. (1967). Limits to the application of the 'trophic group' concept in benthic studies. OCEANOLOGY-Academy of Sciences of the USSR, 7(2), 149-155.

Ouwehand, P. J. (1987). Die Garschella-Formation (" Helvetischer Gault", Aptian-Cenomanian) der Churfirsten-Alvier Region (Ostschweiz). Dissertation. ETH Zürich.

Pfiffner, O. A. (2011): Structural Map of the Helvetic Zone of the Swiss Alps, including Vorarlberg (Austria) and Haute Savoie (France), 1: 100 000. Geological Special Map 128. Explanatory notes.Swisstopo, Wabern.

Powell, M. G., & Kowalewski, M. (2002). Increase in evenness and sampled alpha diversity through the Phanerozoic: comparison of early Paleozoic and Cenozoic marine fossil assemblages. Geology, 30(4), 331-334.

Pucéat, E., Lécuyer, C., Sheppard, S. M., Dromart, G., Reboulet, S., & Grandjean, P. (2003). Thermal evolution of Cretaceous Tethyan marine waters inferred from oxygen isotope composition of fish tooth enamels. Paleoceanography, 18(2), 1029.

Sala, P., Pfiffner, O. A., & Frehner, M. (2014). The Alpstein in three dimensions: fold-and-thrust belt visualization in the Helvetic zone, eastern Switzerland. Swiss journal of geosciences, 107(2-3), 177-195.

Schenk, K. (1992). Die Drusberg- and Schrattenkalk-Formation (Unterkreide) im Helvetikum des Berner Oberlandes. Ph.D. thesis. Geological Institute, University of Berne. 1-169.

Sepkoski, J. J. (1981). A factor analytic description of the Phanerozoic marine fossil record. Paleobiology, 36-53.

Sepkoski, J. J. (1984). A kinetic model of Phanerozoic taxonomic diversity. III. Post-Paleozoic families and mass extinctions. Paleobiology, 10(02), 246-267.

Sepkoski, J. J. (1988). Alpha, beta, or gamma: where does all the diversity go? Paleobiology, 14(03), 221-234.

Sepkoski, J. J., Bambach, R. K., Raup, D. M., & Valentine, J. W. (1981). Phanerozoic marine diversity and the fossil record. Nature, 293(5832), 435-437.

Sepkoski, J. J. J., & Sheehan, P. M. (1983). Diversification, faunal change, and community replacement during the Ordovician radiations. In M. J. S. Tevesz & P. L. McCall (Eds.), Biotic interactions in recent and fossil benthic communities (pp. 673-717). New York: Springer US.

Sheehan, P. M. (2001). The Late Ordovician Mass Extinction. Annual Review of Earth and Planetary Sciences, 29(1), 331-364. doi:10.1146/annurev.earth.29.1.331

Smith, A., Nelson, C., & Danaher, P. (1992). Dissolution behaviour of bryozoan sediments: taphonomic implications for nontropical shelf carbonates. Palaeogeography, palaeoclimatology, palaeoecology, 93(3), 213-226.

Sulser, H., Friebe, G., & Kürsteiner, P. (2013). Little-known brachiopods from the Cretaceous of the Helvetic realm of NE Switzerland (Alpstein) and W Austria (Vorarlberg). Swiss Journal of Geosciences, 106(2), 397-408.

Tajika, A., Kürsteiner, P., Pictet, A., Lehmann, J., Tschanz, K., Jattiot, R., & Klug, C. (2017). Cephalopod associations and palaeoecology of the Cretaceous (Barremian–Cenomanian) succession of the Alpstein, northeastern Switzerland. Cretaceous Research, 70, 15-54.

Wohlwend, S., Hart, M., & Weissert, H. (2015). Ocean current intensification during the Cretaceous oceanic anoxic event 2–evidence from the northern Tethys. Terra Nova, 27(2), 147-155.

Chapter III

Intraspecific variation of phragmocone chamber volumes throughout ontogeny in the modern nautilid *Nautilus* and the Jurassic ammonite *Normannites*

Tajika, A. Morimoto, N. Wani, R,
Naglik, C. Klug, C

Published in
Peer J

Intraspecific variation of phragmocone chamber volumes throughout ontogeny in the modern nautilid *Nautilus* and the Jurassic ammonite *Normannites*

Amane Tajika[1], Naoki Morimoto[2], Ryoji Wani[3], Carole Naglik[1] and Christian Klug[1]

[1] Paläontologisches Institut und Museum, Universität Zürich, Zürich, Switzerland
[2] Laboratory of Physical Anthropology, Graduate School of Science, Kyoto University, Kyoto, Japan
[3] Faculty of Environment and Information Sciences, Yokohama National University, Yokohama, Japan

ABSTRACT

Nautilus remains of great interest to palaeontologists after a long history of actualistic comparisons and speculations on aspects of the palaeoecology of fossil cephalopods, which are otherwise impossible to assess. Although a large amount of work has been dedicated to *Nautilus* ecology, conch geometry and volumes of shell parts and chambers have been studied less frequently. In addition, although the focus on volumetric analyses for ammonites has been increasing recently with the development of computed tomographic technology, the intraspecific variation of volumetric parameters has never been examined. To investigate the intraspecific variation of the phragmocone chamber volumes throughout ontogeny, 30 specimens of Recent *Nautilus pompilius* and two Middle Jurassic ammonites (*Normannites mitis*) were reconstructed using computed tomography and grinding tomography, respectively. Both of the ontogenetic growth trajectories from the two *Normannites* demonstrate logistic increase. However, a considerable difference in *Normannites* has been observed between their entire phragmocone volumes (cumulative chamber volumes), in spite of their similar morphology and size. Ontogenetic growth trajectories from *Nautilus* also show a high variation. Sexual dimorphism appears to contribute significantly to this variation. Finally, covariation between chamber widths and volumes was examined. The results illustrate the strategic difference in chamber construction between *Nautilus* and *Normannites*. The former genus persists to construct a certain conch shape, whereas the conch of the latter genus can change its shape flexibly under some constraints.

Subjects Developmental Biology, Evolutionary Studies, Marine Biology, Paleontology, Zoology
Keywords Ammonoidea, Nautilida, Intraspecific variability, Sexual dimorphism, Growth, 3D reconstruction, Jurassic, CT scan, Cephalopoda

INTRODUCTION

Ammonoids and nautiloids are well-known, long-lived molluscan groups, both of which faced devastation at the end of the Cretaceous, but with different responses: extinction versus survival. What these two groups have in common is the external conch, which makes

them superficially similar. Because of that, a number of palaeontologists investigated the ecology and anatomy of living *Nautilus* as an analogy for those of extinct ammonites over the last decades (e.g., *Collins, Ward & Westermann, 1980*; *Saunders & Landman, 1987*; *Ward, 1987*; *Ward, 1988*). However, it was *Jacobs & Landman (1993)* who argued that, despite its superficial morphologic similarity, *Nautilus* was an insufficient model to reconstruct ammonoid palaeoecology, given their phylogenetic positions, which are distant within the Cephalopoda. This argument is now widely accepted (e.g., *Warnke & Keupp, 2005*). Whereas palaeoecology and evolution of ammonoids need to be discussed based on their own fossil record, those of modern *Nautilus* can be satisfactorily analogized to fossil nautilids, which have borne persistent conch morphologies throughout their evolution (*Ward, 1980*).

Molluscan conchs are not only exoskeletal structures but also retain a complete record of their ontogeny because of their accretionary growth. One of the most important apomorphic structures of cephalopods, the chambered part of their conch (phragmocone), was used by most cephalopods and is still used by some cephalopods as a buoyancy device. The ammonite phragmocone has been of great interest for palaeontologists, in order to reveal otherwise-obscure aspects of ammonite palaeoecology (Geochemical analyses: *Moriya et al., 2003*; *Lukeneder et al., 2010*; *Stevens, Mutterlose & Wiedenroth, 2015*; 2 dimensional analyses of septal angles: *Kraft, Korn & Klug, 2008*; *Arai & Wani, 2012*). Buoyancy had not been examined by quantifying phragmocone volumes due to the lack of adequate methods until modern scanning technique enabled to reconstruct complete ammonite empirical volume models (*Lemanis et al., 2015*; *Naglik, Rikhtegar & Klug, 2015*; *Tajika et al., 2015*). Unfortunately, all of these contributions included only one specimen per species due to the great expenditure of time needed for segmenting the image stacks. Conclusions from such limited studies may be biased if the examined specimens represent more or less extreme variants of one species (intraspecific variation). The life mode of living *Nautilus* is known to be essentially demersal, retaining their buoyancy as either roughly neutral when active or slightly negative when at rest (*Ward & Martin, 1978*), even though they change their habitat frequently via vertical migration (*Dunstan, Ward & Marshall, 2011*). The majority of *Nautilus* ecology research has included studies on anatomy, behaviour, and habitat, whereas geometry and volume of their phragmocones, which are similar to that of fossil nautiloids, have been examined less frequently (e.g., *Ward, 1979*; *Hoffmann & Zachow, 2011*). Investigation of the relationship between *Nautilus* conchs and their ecology could become a reference to examine the relationship between fossil cephalopods and their palaeoecology.

Multiple methods have been applied to reconstruct conchs of cephalopods including both fossilized and extant animals (*Kruta et al., 2011*; *Hoffmann et al., 2014*; *Lemanis et al., 2015*; *Naglik et al., 2015*; *Tajika et al., 2015*; for general aspects of virtual palaeontology, see *Garwood, Rahman & Sutton, 2010*; *Sutton, Rahman & Garwood, 2014*). Non-destructive computed tomography (CT) superficially appears to be the best suitable method because rare fossils can be analysed without destroying them. Medical scanners are often used, but they often yield insufficient contrast between conch and internal sediment or cement because these materials may have similar densities (e.g., *Garwood, Rahman & Sutton,*

2010; *Hoffmann & Zachow, 2011*). Furthermore, the resolution obtained from medical scanners is not adequate, specifically in such cases where accurate measurements of minute structures such as ammonite protoconchs (as small as 0.5 mm in diameter; e.g., *Lemanis et al., 2015*) are required. Fossil cephalopods are thus difficult materials to examine by this non-destructive method, but conchs of living cephalopods with no sediment filling can easily be reconstructed with a good resolution. Computed microtomography (μCT) is an alternative because it has a stronger beam, resulting in high resolution and thus better reconstructions. μCT-imagery produced using high energy levels has greater penetrative power but suffers from the lack of contrast, however, making the subsequent segmentation process difficult.

By contrast, *Lemanis et al. (2015)* presented the first successful attempt to reconstruct an ammonite ammonitella in detail. They scanned a perfectly preserved hollow ammonite using phase contrast tomography. Propagation phase contrast X-ray synchrotron microtomography (PPC-SR-μCT) was employed by *Kruta et al. (2011)* who reconstructed ammonite radulae in detail. The limited availability of the facility, heavy data load, and potential contrast problems discourage application of this method for fossil cephalopods. In contrast to the non-destructive methods, destructive grinding tomography can be used to reconstruct fossilized cephalopods (*Naglik et al., 2015*; *Tajika et al., 2015*). This method, which preserves colour information of the shells (aiding in segmentation), does not require hollow preservation of fossils, thus permitting the examination of all well-preserved fossils without suffering from noise such as beam hardening or poor contrast, which commonly occur when using CT.

Volumetric analyses of intraspecific variability of phragmocone chambers throughout ontogeny have not previously been analysed in either *Nautilus* or ammonoids. Such data may contribute to the better understanding of the palaeoecology of extinct ammonoids and nautiloids. The aims of this study are to answer the following questions based on empirical 3D models reconstructed from real specimens: (1) How did chamber volumes change through ontogenetic development of ammonites and nautilids? (2) How much did the volumetric growth trajectories differ between two conspecific ammonites (exemplified using middle Jurassic *Normannites*)? (3) What was the intraspecific variation of volumetric growth trajectories of modern *Nautilus*? (4) Are the differences in chamber volumes between male and female nautilids significant? (5) Is there a difference in construction of chambers between the ammonites and modern *Nautilus*?

MATERIAL

Two ammonite specimens examined are from the Middle Jurassic and belong to the genus *Normannites* (*Normannites mitis*). One of them (Nm. 1) was reconstructed by *Tajika et al. (2015)* to test its buoyancy. Both specimens were found in the Middle Bajocian (Middle Jurassic) of Thürnen, Switzerland. The nicely preserved specimens are suitable for 3D reconstruction, even though one of the specimens (Nm. 2) has an incomplete aperture, which does not allow for buoyancy calculation. The maximum conch diameters of Nm. 1 and Nm. 2 are 50.0 mm and 49.0 mm, respectively.

An additional 30 conchs of Recent *Nautilus pompilius* (21 adults: 12 males, 9 females; 9 juveniles) were also studied. All of the conchs were collected in the Tagnan area in the Philippines (see Fig. 1 in *Wani, 2004*; Fig. 1 in *Yomogida & Wani, 2013*). Maturity of *Nautiilus* was defined as bearing black band, or septal crowding (for mature modification of *Nautilus* see *Klug, 2004*). Males and females were differentiated based on previous studies: mature males have larger shells and a broader, rounder aperture than females (*Stenzel, 1964*; *Haven, 1977*; *Saunders & Spinosa, 1978*; *Arnold, 1984*). In the juvenile stage, however, the sex is indeterminable since the morphological differences of shells are not profound. The details of the specimens are summarized in Table 1. The specimens are stored in Mikasa City Museum, Hokkaido, Japan.

METHODS

3D reconstructions of ammonites

Grinding tomography was employed to reconstruct the two Jurassic ammonite specimens. This method has been applied to previous studies for invertebrates, e.g., bivalves (*Götz, 2003*; *Götz, 2007*; *Götz & Stinnesbeck, 2003*; *Hennhöfer, Götz & Mitchell, 2012*; *Pascual-Cebrian, Hennhöfer & Götz, 2013*) and ammonoids (*Naglik et al., 2015*; *Tajika et al., 2015*). During each of the 422 grinding phases, 0.06 mm was automatically ground off of the specimens until the specimen was completely destroyed. Subsequently, each ground surface was automatically scanned with a resolution of 2,400 dpi. Due to the very high number of slices and the very time consuming segmenting process, only every fourth scan of the obtained image stack was segmented. The voxel sizes of *x*, *y* and *z* dimensions are 0.025, 0.025 and 0.24 mm, respectively. We separately segmented the external conch, all septa, and the siphuncle manually using Adobe® Illustrator (Adobe Systems). The segmented image stacks have been exported to VGstudiomax® 2.1 (Volume Graphics), which produced 3D models out of the 2D image stacks. Further technical details for the ammonite reconstructions are given in *Tajika et al. (2015)* and for the general procedure of grinding tomography in *Pascual-Cebrian, Hennhöfer & Götz (2013)*.

3D reconstructions of modern *Nautilus*

Conchs of all specimens were scanned at the Laboratory of Physical Anthropology of Kyoto University using a 16-detector-array CT device (Toshiba Alexion TSX-032A) with the following data acquisition and image reconstruction parameters: beam collimation: 1.0 mm; pitch: 0.688; image reconstruction kernel: sharp (FC30); slice increment: 0.2 mm; tube voltage and current: 120 kV 100 mA. This resulted in volume data sets with isotropic spatial resolution in the range of 0.311 and 0.440 mm. The obtained data sets were exported to Avizo® 8.1 (FEI Visualization Sciences Group) where segmentation was conducted. As mentioned in *Hoffmann et al. (2014)*, the calculated mass of a specimen based on the CT data set does not correspond exactly to the actual mass measured on the physical specimen due to noise and the partial volume effect (PVE) from the scan, which may cause significant errors during the segmentation process. *Wormanns et al. (2004)* reported that segmentation can also introduce errors between specimens. In our scans,

Table 1 Details of the studied specimens, *Normannites mitis* from the Middle Jurassic, Switzerland, and modern *Nautilus pompilius* from the Philippines.

Specimen number	Species	Maturity	Sex	Maximum diameter (mm)	Number of chambers
Nm.1	*Normannites mitis*	Mature	Male	50	60?
Nm.2	*Normannites mitis*	Mature	Male	49	59?
7	*Nautilus pompilius*	Mature	Female	189	35
8	*Nautilus pompilius*	Mature	Female	152	30
10	*Nautilus pompilius*	Mature	Female	175	32
11	*Nautilus pompilius*	Mature	Female	165	30
12	*Nautilus pompilius*	Mature	Female	168	33
15	*Nautilus pompilius*	Mature	Female	189	33
16	*Nautilus pompilius*	Mature	Male	183	33
17	*Nautilus pompilius*	Mature	Male	183	33
20	*Nautilus pompilius*	Immature	Indet.	105	26
23	*Nautilus pompilius*	Immature	Indet.	112	26
30	*Nautilus pompilius*	Immature	Indet.	147	30
31	*Nautilus pompilius*	Immature	Indet.	136	29
32	*Nautilus pompilius*	Immature	Indet.	136	32
33	*Nautilus pompilius*	Immature	Indet.	135	27
34	*Nautilus pompilius*	Immature	Indet.	144	32
35	*Nautilus pompilius*	Immature	Indet.	124	28
36	*Nautilus pompilius*	Immature	Indet.	157	37
38	*Nautilus pompilius*	Mature	Male	150	31
39	*Nautilus pompilius*	Mature	Male	147	32
40	*Nautilus pompilius*	Mature	Male	151	30
41	*Nautilus pompilius*	Mature	Male	184	34
42	*Nautilus pompilius*	Mature	Female	169	33
43	*Nautilus pompilius*	Mature	Male	155	31
44	*Nautilus pompilius*	Mature	Male	164	35
46	*Nautilus pompilius*	Mature	Male	160	31
48	*Nautilus pompilius*	Mature	Male	165	35
51	*Nautilus pompilius*	Mature	Female	179	33
53	*Nautilus pompilius*	Mature	Male	181	36
54	*Nautilus pompilius*	Mature	Male	164	29
56	*Nautilus pompilius*	Mature	Female	176	32

the resulting differences between the actual masses of the conchs and the calculated mass ranged from 50 to 63%. However, use of the same devices and methods and a combination of the same grey-scale threshold value for the outer whorls and the manual tracing for the innermost whorls reduce the noise and preserve the overall trend of variability in volumes between each specimen. Out of 45 scanned specimens, only 30 scanned specimens with nearly the same contrast were carefully chosen and analysed, while scans from other 15 specimens with different contrasts were discarded to minimize errors which may occur from differences in contrast between scans. Nevertheless, the variability is to some degree affected by the errors due to the noise and PVE. A list of the differences between calculated

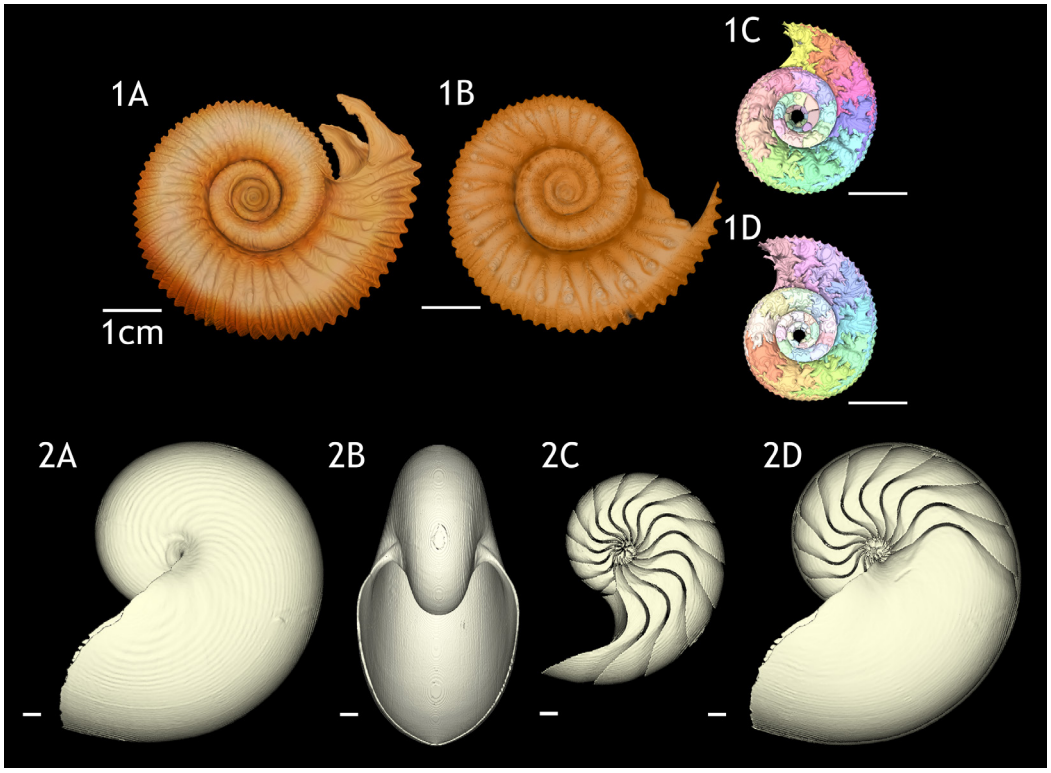

Figure 1 3D reconstructions of the two specimens of *Normannites mitis*, modern *Nautilus pompilius* (specimen 17), and their phragmocones. (1A) 3D model of *Normannites mitis* (Nm. 1); (1B) 3D model of *Normannites mitis* (Nm. 2); (1C) extracted phragmocone of Nm. 1 (1D); extracted phragmocone of Nm. 2; (2A, B) 3D models of *Nautilus pompilius* (specimen 17); (2C) extracted phragmocone of *Nautilus pompilius* (specimen 17); (2D) Backface of 3D model of *Nautilus pompilius* (specimen 17). Scale bars are 1 cm.

shell volumes and estimated actual shell volumes calculated from mass measurements is provided in Table S1 (estimated volume error: 60.8–91.3%). The segmented data sets were exported as STL files using the software Avizo® 8.1. The volumetric data from the phragmocone were extracted and calculated in Meshlab (ISTL–CNR research center) and Matlab 8.5 (Math Works), respectively. The measurements of the diameters and widths of the conchs were conducted with the program ForMATit developed by NM.

RESULTS

Difference between two *Normannites* specimens in ontogenetic volume changes

Constructed 3D models of the ammonites are shown in Fig. 1 (1A–1D). Measured chamber volumes (Table 2) were plotted against chamber numbers (Fig. 2). In the two *Normannites* specimens, the overall trends of growth trajectories of individual chamber volumes (Fig. 2A) are more or less the same, showing logistic increase throughout ontogeny until the onset of the so-called '*terminal countdown*' (*Seilacher & Gunji, 1993*) when they start showing a downward trend over the last 5 chambers (Nm. 1) and over the last 7 chambers (Nm. 2). The curve from Nm. 1 illustrates a nearly steady growth

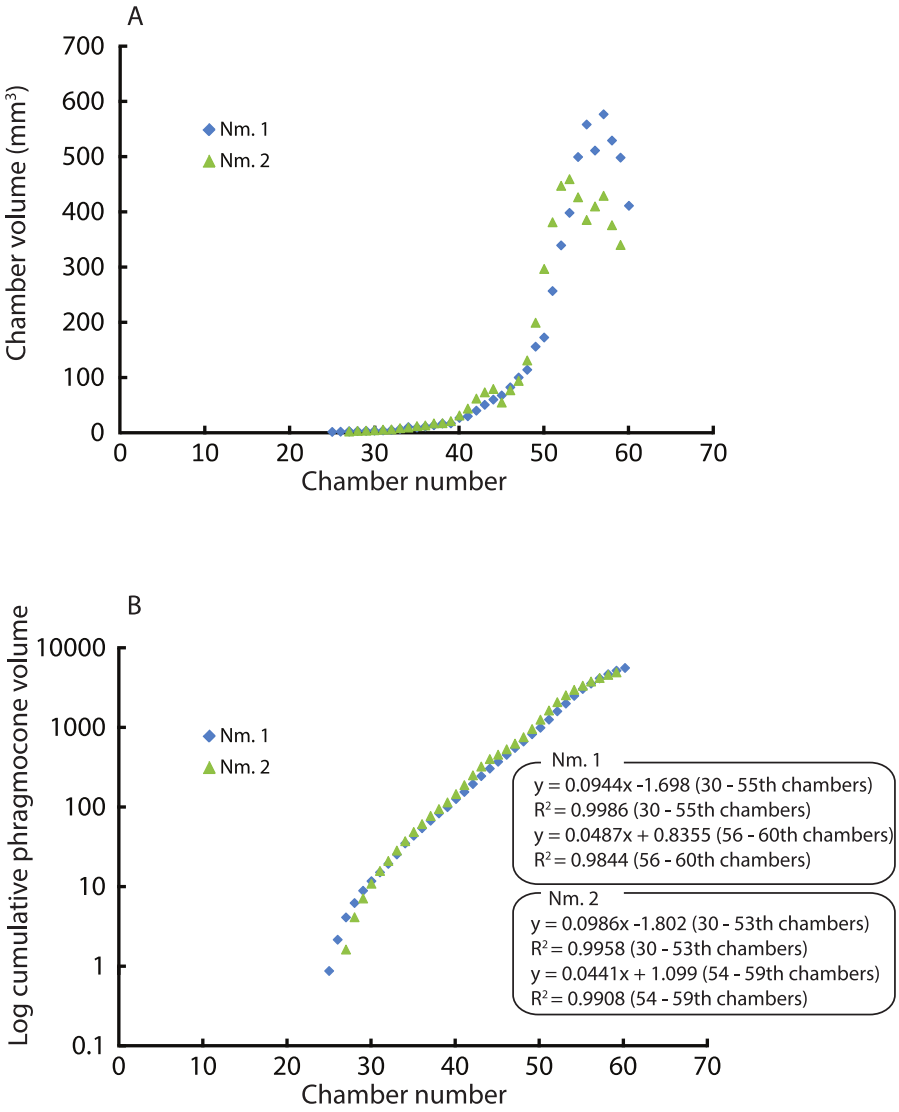

Figure 2 Volumes plotted against chamber numbers in *Normannites mitis*. The volumes prior to chamber 25 (Nm. 1) and 27 (Nm. 2) have not been measured. (A) Scatter plot of chamber numbers and individual chamber volumes; (B) Scatter plot of chamber numbers and cumulative phragmocone volumes.

rate even though a *syn vivo* epizoan worm with mineralized tube grew on the fifth whorl of the ammonite (*Tajika et al., 2015*). By contrast, Nm. 2 does not show traces of any *syn vivo* epizoans, but it displays a sudden decrease of the volume of the 45th chamber where another trend sets off, which persists to the last chamber. In addition, we plotted the cumulative volumes of the phragmocone chambers against chamber numbers (Fig. 2B). Since the curves are derivatives of those of Fig. 2, the phragmocone volumes increase with the same trend. The cumulative phragmocone volume of Nm. 1 is larger than that of Nm. 2, although the latter retained the larger phragmocone volume throughout ontogeny until the onset of the morphologic countdown.

Table 2 **Raw data of measured chamber volumes and widths in *Normannites mitis*.**

Normannites mitis				
Specimen	**Nm. 1**		**Nm. 2**	
Chamber	**Volume (mm^3)**	**Width (mm)**	**Volume (mm^3)**	**Width (mm)**
25	0.9	–	–	–
26	1.3	–	–	–
27	2.0	–	1.6	–
28	2.1	2.6	2.5	–
29	2.6	2.6	3.0	–
30	2.9	2.7	3.8	–
31	3.4	2.6	4.8	–
32	4.2	3.1	5.3	–
33	6.0	4.1	7.4	–
34	9.6	4.1	8.8	–
35	8.6	4.6	11.3	–
36	10.7	4.6	12.4	–
37	12.9	4.6	16.2	3.9
38	16.0	4.6	16.8	3.9
39	16.2	4.7	20.4	4.8
40	26.1	5.5	30.8	5.8
41	28.9	5.8	43.1	7.2
42	39.2	6.5	61.0	7.7
43	49.7	7.4	72.4	7.7
44	59.1	7.9	78.6	7.7
45	66.7	8.4	54.0	7.2
46	81.4	8.9	76.3	7.2
47	99.4	9.4	93.1	7.9
48	113.3	9.8	130.4	8.6
49	155.1	10.3	198.6	11.0
50	171.8	11.3	296.0	13.2
51	255.9	12.5	380.5	15.1
52	338.7	14.6	446.4	15.1
53	397.6	15.1	458.6	15.1
54	498.5	16.6	425.7	13.9
55	557.4	16.6	384.6	13.4
56	510.2	17.5	409.1	15.1
57	576.1	17.5	428.5	15.4
58	528.4	18.0	375.1	15.9
59	497.3	18.0	339.3	15.4
60	410.5	18.0	–	–

Intraspecific variability of modern *Nautilus* in ontogenetic volume changes

Constructed 3D models of modern *Nautilus* are shown in Fig. 1(2A–2D). As in the Jurassic ammonite, individual chamber volumes and phragmocone volumes (Table 3) were plotted against chamber numbers (Figs. 3A and 3B). Figure 3 shows that all the curves increase

Table 3 **Raw data of measured chamber volumes in *Nautilus pompilius*.**

Nautilus pompilius

	Volumes (ml)									
Chamber	**7**	**8**	**10**	**11**	**12**	**15**	**16**	**17**	**20**	**23**
1	0.0011	0.0080	0.0082	0.0118	0.0139	0.0088	0.0099	0.0101	0.0153	0.0120
2	0.0123	0.0331	0.0257	0.0416	0.0384	0.0317	0.0145	0.0307	0.0329	0.0370
3	0.0468	0.1013	0.0760	0.1056	0.1091	0.0866	0.0424	0.0882	0.0922	0.1440
4	0.1142	0.1951	0.1539	0.1980	0.1809	0.1571	0.1109	0.1584	–	0.1904
5	0.1837	0.2417	0.2028	0.2214	0.2050	0.2032	0.1859	1.9870	0.2939	0.1658
6	0.2236	0.1264	0.1397	0.1244	0.1081	0.1327	0.2182	1.2660	0.1387	–
7	0.1287	0.1987	0.1736	0.2603	0.1742	0.1711	0.1610	0.1911	0.1504	0.1875
8	0.1767	0.2520	0.2027	0.2639	0.2046	0.1654	0.2183	0.2065	0.1695	0.2451
9	0.2265	0.2800	0.2472	0.3593	0.2370	0.2352	0.2730	0.2418	0.2092	0.3563
10	0.2619	0.3126	0.2873	0.4043	0.3378	0.2344	0.3047	0.2709	0.2314	0.3615
11	0.3097	0.4201	0.3461	0.4913	0.3364	0.2671	0.3856	0.3332	0.3010	0.2962
12	0.3254	0.5510	0.4246	0.5882	0.3992	0.3542	0.4402	0.4326	0.4017	0.5029
13	0.3419	0.6398	0.4958	0.6988	0.4677	0.4407	0.5293	0.4632	0.3846	0.6454
14	0.4342	0.8348	0.6386	0.9175	0.5496	0.5297	0.6218	0.5654	0.5069	0.7712
15	0.5986	0.9723	0.7534	1.1123	0.7096	0.5844	0.7034	0.7108	0.5902	0.8968
16	0.6954	1.1514	0.9129	1.2902	0.8697	0.6870	0.8370	0.8858	0.7431	1.0808
17	0.7329	1.5420	0.9722	1.5716	0.9987	0.8377	1.1188	1.0799	0.9711	1.3026
18	0.8595	1.8436	1.2630	2.0393	1.1376	1.0711	1.3181	1.3902	1.1740	1.5484
19	1.1690	2.4328	1.6209	2.3768	1.4889	1.4076	1.6280	1.7581	1.5174	1.7800
20	1.3495	2.8077	1.6611	3.1048	1.8336	1.6886	1.8692	2.2017	1.8071	2.4023
21	1.7666	3.4284	2.2127	3.8014	2.2195	2.2858	2.3806	2.7137	2.2284	2.8600
22	2.0429	4.7002	2.4138	5.1772	2.8784	2.6827	3.0621	2.9842	2.8115	3.4343
23	2.6836	5.8684	3.6654	6.4984	3.4312	3.0022	3.8081	4.2956	3.3740	4.4262
24	3.1432	7.3975	3.9932	6.3292	4.0784	3.9945	4.8836	5.7708	4.3020	5.5624
25	3.8981	9.2433	5.9550	10.8780	4.8802	5.2016	6.4403	6.5720	5.5132	6.8422
26	4.7613	12.1851	7.2257	13.0345	6.1415	6.9912	7.7378	8.3211	6.5154	8.3682
27	6.2645	14.8837	9.1428	15.1136	7.1537	6.9741	10.2469	9.7510	–	–
28	7.6362	18.9061	11.6261	15.0097	9.3969	9.9014	11.9939	12.6750	–	–
29	8.9947	23.4334	14.3625	18.0443	11.4332	13.0762	15.4993	15.4005	–	–
30	11.6532	21.7685	18.6543	16.2038	13.7770	15.9414	18.4287	17.8146	–	–
31	14.3670	–	22.4427	–	17.3911	21.2605	21.4919	22.5759	–	–
32	18.7249	–	25.6854	–	19.8835	25.8978	26.6814	25.5356	–	–
33	22.7825	–	–	–	19.3914	23.7399	21.6118	29.6341	–	–
34	28.9011	–	–	–	–	–	–	–	–	–

Chamber	30	31	32	33	34	35	36	38	39	40
1	0.0009	0.0081	0.0015	0.0081	0.0076	0.0010	0.0216	0.0098	0.0106	0.0101
2	0.0093	0.0307	0.0112	0.0138	0.0238	0.0151	0.0566	0.0283	0.0415	0.0413
3	0.0491	0.1274	0.0372	0.0523	0.0673	0.0441	0.1162	0.0987	0.0610	0.1276
4	0.1152	0.0900	0.1024	–	–	0.1044	0.1356	0.1778	0.1955	0.2445
5	0.2002	0.1677	0.1703	0.2591	0.1836	0.1951	0.0903	0.2302	0.2274	0.2826
6	0.2263	0.2333	0.2108	0.3325	0.0731	0.1551	0.0677	0.1288	0.1437	0.1377
7	0.1298	0.1515	0.1059	0.1488	0.1445	0.1211	0.0875	0.1754	0.2137	0.1577
8	0.2507	0.1968	0.1578	0.2810	0.1506	0.2130	0.1325	0.2319	0.2327	0.2791
9	0.2457	0.2774	0.1513	0.3327	0.1912	0.2311	0.1384	0.2424	0.2748	0.3210
10	0.3184	0.3346	0.2389	0.3967	0.2178	0.3198	0.1650	0.3559	0.3628	0.3354
11	0.3811	0.4392	0.2743	0.4897	0.2891	0.3354	0.1998	0.3528	0.3506	0.4696
12	0.4743	0.4943	0.2953	0.5830	0.2969	0.4166	0.2167	0.4391	0.4582	0.5265
13	0.5728	0.5368	0.3519	0.6721	0.3613	0.4578	0.2776	0.5343	0.5336	0.6694
14	0.6597	0.5660	0.4364	0.7652	0.4548	0.4956	0.3469	0.6659	0.5510	0.7933
15	0.8527	0.6376	0.4978	0.9763	0.5328	0.6623	0.3984	0.8642	0.7349	0.9906
16	0.9906	0.9415	0.5625	1.1348	0.6799	0.8069	0.4671	1.0654	0.8903	1.1742
17	1.2034	1.2099	0.6816	1.5905	0.8066	0.9817	0.5594	1.2510	1.1273	1.4877
18	1.5362	1.4315	0.8131	1.7629	0.9474	1.2012	0.7268	1.5251	1.3187	1.8743
19	1.7694	1.7856	0.9522	2.2513	1.2071	1.3979	0.8601	1.8645	1.6630	2.3415
20	2.0389	1.9788	1.1264	3.0569	1.4379	1.8163	0.9568	2.3037	2.1185	2.8293
21	2.8880	2.6252	1.4726	3.5649	1.7398	2.2560	1.1435	3.0019	2.5387	3.4876
22	3.3829	3.0792	1.5172	4.5086	2.0732	2.7278	1.3670	3.8435	3.1226	4.1792
23	3.6387	4.1283	2.0698	5.8497	2.6354	3.5553	1.4716	5.0250	4.3051	5.2172
24	5.5978	4.8777	2.5775	7.8330	3.0635	4.2451	1.9052	5.9666	5.0770	6.9681
25	6.6551	6.6584	2.9776	10.0561	3.7968	5.6042	2.1254	7.4867	6.4071	9.1711
26	8.4330	8.2790	3.7357	12.3302	4.6313	7.0547	2.4165	9.5045	7.9895	11.4558
27	10.9828	10.7209	4.2277	16.8159	5.7833	8.7436	3.1417	12.3553	9.9455	14.8504
28	14.0144	13.7381	5.9748	–	6.7042	11.2815	3.9028	15.4332	12.1152	18.7030
29	17.9875	16.9861	6.9056	–	8.9703	–	4.0146	19.5149	16.8772	21.2875
30	22.9906	–	8.7325	–	10.3012	–	5.5218	22.3363	19.1758	20.7897
31	–	–	11.0929	–	13.7366	–	6.4224	21.7169	22.8448	–
32	–	–	13.4910	–	16.1578	–	8.3757	–	10.9346	–
33	–	–	–	–	–	–	9.7338	–	–	–
34	–	–	–	–	–	–	13.6863	–	–	–
35	–	–	–	–	–	–	15.1073	–	–	–
36	–	–	–	–	–	–	19.3678	–	–	–

(*continued on next page*)

Table 3 (*continued*)

Chamber	41	42	43	44	46	48	51	53	54	56
1	0.0100	0.0054	0.0090	0.0050	0.0265	0.0047	0.0175	0.0061	0.0100	0.0093
2	0.0292	0.0247	0.0306	0.0186	0.0771	0.0183	0.0470	0.0181	0.0342	0.0315
3	0.0905	0.0708	0.0881	0.0496	0.1503	0.0468	0.1091	0.0549	0.0913	0.0873
4	0.1417	0.1532	0.1587	0.1075	0.1971	0.0971	0.1735	0.1069	0.1690	0.1472
5	0.2076	0.2127	0.2030	0.1600	0.1691	0.1455	0.1890	0.1296	0.1763	0.2053
6	0.1124	0.1729	0.1402	0.1743	0.1699	0.1296	0.1049	0.0991	0.0946	0.2054
7	0.1508	0.1493	0.1831	0.1235	0.2227	0.0904	0.1476	0.0782	0.2062	0.1376
8	0.1697	0.2169	0.2357	0.1846	0.2459	0.1272	0.1975	0.1243	0.1836	0.1697
9	0.2163	0.2819	0.2991	0.1938	0.3018	0.1317	0.2505	0.1579	0.2436	0.2927
10	0.2786	0.3644	0.3365	0.2052	0.3498	0.1749	0.2403	0.1804	0.3114	0.3502
11	0.3207	0.4320	0.3932	0.2967	0.4234	0.1962	0.3590	0.2276	0.3474	0.3969
12	0.4028	0.5334	0.4842	0.3297	0.4885	0.2544	0.3641	0.2631	0.3622	0.4777
13	0.3789	0.6502	0.5946	0.4074	0.6444	0.2892	0.4552	0.2786	0.4824	0.5308
14	0.3697	0.8009	0.7316	0.4628	0.7167	0.3641	0.5052	0.3390	0.5973	0.7307
15	0.4970	1.1199	0.8541	0.5346	0.9162	0.4755	0.6910	0.4319	0.7167	0.9280
16	0.7079	1.3768	1.0209	0.6888	1.1237	0.5788	0.8284	0.5339	0.9275	1.0657
17	0.8187	1.6980	1.3506	0.8180	1.4206	0.7132	0.9799	0.6473	1.0603	1.3458
18	0.9482	2.1715	1.5373	0.9756	1.5012	0.7694	1.2509	0.7253	1.3217	1.4686
19	1.1905	2.5023	1.9608	1.2337	2.1029	0.9727	1.4561	1.0164	1.5396	1.8512
20	1.4391	3.1098	2.1780	1.5515	2.4645	1.2410	1.7334	1.0873	1.9675	2.3222
21	1.7595	4.1807	2.9540	1.9814	3.2696	1.4992	2.1757	1.4246	2.4795	2.8080
22	2.1740	5.2048	3.5435	2.6261	3.7837	1.9494	2.6698	1.6820	3.0712	3.4655
23	2.6913	6.7107	4.6642	2.7189	4.6898	2.2113	3.5267	1.9744	3.6531	4.4481
24	3.3197	8.3822	5.6355	4.1850	6.2850	2.6959	3.8889	2.5256	4.6271	5.2782
25	3.9711	9.8258	7.2365	4.8333	7.7151	3.3410	5.4467	3.2210	5.7637	6.6173
26	5.1796	14.0874	8.8481	6.3843	9.6012	4.1416	7.0138	3.7303	7.4533	8.4093
27	6.3708	16.9760	10.8568	7.8972	12.4969	5.2332	8.5615	4.3930	9.1647	10.4171
28	7.3239	20.3430	13.3318	10.4022	16.2270	6.3615	10.4667	4.8603	10.4041	13.1087
29	9.5327	25.8620	16.3558	13.1177	19.5241	7.5145	13.5815	6.7250	13.7364	15.5874
30	11.9083	24.6416	18.0790	17.3703	24.7367	9.4214	17.3426	8.8509	18.1738	20.3345
31	14.4140	–	20.2377	20.7735	20.2453	12.4135	20.6539	11.0477	22.7498	22.5689
32	18.5821	–	–	27.8035	–	15.0377	25.8738	14.1953	24.6066	19.6485
33	23.3349	–	–	27.8442	–	18.3685	21.4921	17.2212	15.7064	–
34	27.2882	–	–	–	–	22.6245	–	22.1384	–	–
35	–	–	–	–	–	26.4088	–	26.0839	–	–
36	–	–	–	–	–	–	–	21.8776	–	–

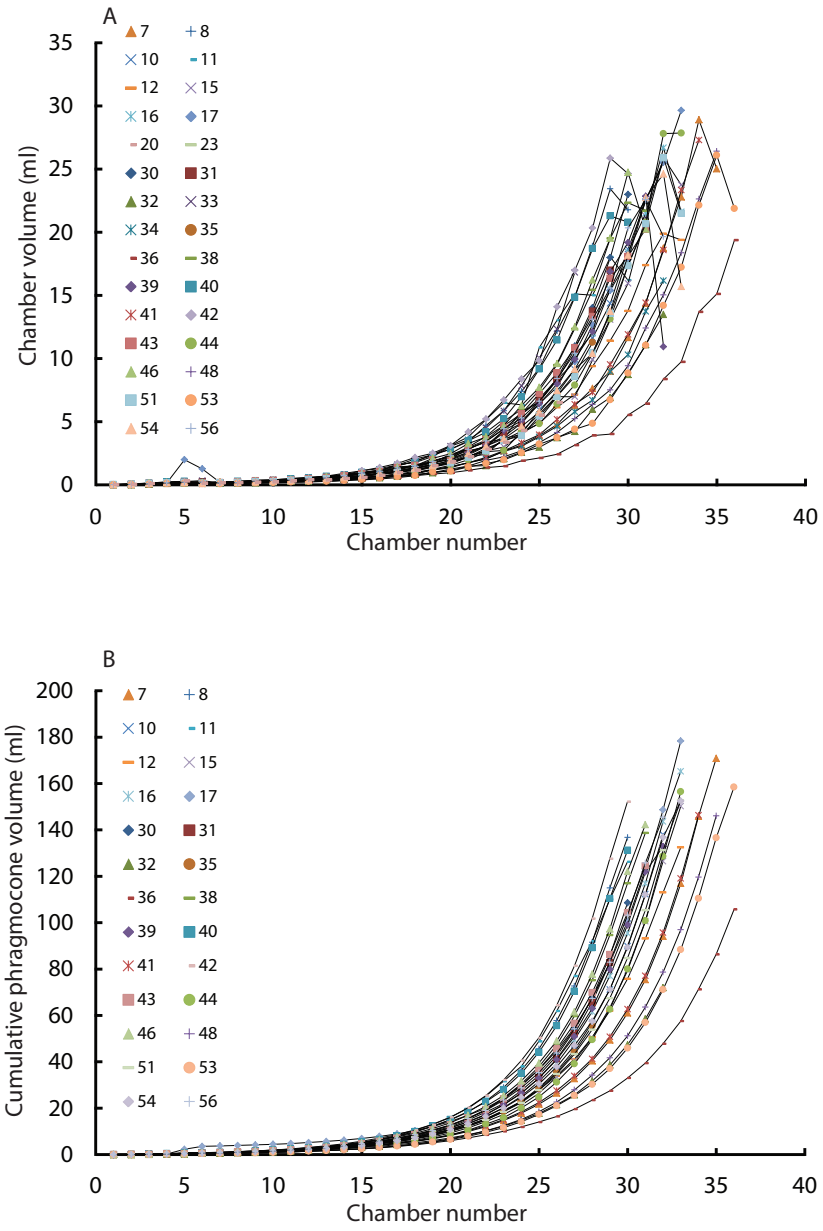

Figure 3 Chamber volumes plotted against chamber numbers in all examined *Nautilus pompilius*. (A) Scatter plot of chamber numbers and individual chamber volumes; (B) Scatter plot of chamber numbers and phragmocone volumes.

logistically, as in the ammonites, with a rather high variability. As far as the terminal countdown is concerned, only the last or no chamber of the adult specimens shows the volume decrease. By contrast, the two ammonites show this decrease over the last 5–7 chambers (even higher numbers of chambers may be included in other ammonite species: e.g., 18 in the Late Devonian *Pernoceras*, 14 in the Early Carboniferous *Ouaoufilalites*; see *Korn, Bockwinkel & Ebbighausen, 2010*; *Klug et al., 2015*) bearing the irregular growth. It has been reported that mature males of *Nautilus* from the Fiji Islands have larger shells and

a broader, rounder aperture than those of females (*Stenzel, 1964*; *Haven, 1977*; *Saunders & Spinosa, 1978*; *Arnold, 1984*) but there were no significant differences between sexes in shell form in *Nautilus* from the Philippines (*Tanabe et al., 1983*). In order to assess the differences between male and female conchs, their growth trajectories are shown in Fig. 4. Maximum diameters of the conchs versus number of chambers (Fig. 5A) and maximum diameters versus phragmocone volumes are also plotted (Fig. 5B) to assess if previously-recognized morphologic differences between males and females of *Nautilus* are detectable here. A statistical test (analysis of the residual sum of squares; ARSS) was carried out to determine whether there are differences between males and females in growth trajectories (Fig. 4B) and morphological features (maximum diameters of conchs vs. number of chambers; maximum diameters of conchs vs. phragmocone volumes; Figs. 5A and 5B). This test is used to compare linear models (*Zar, 1996*). A similar statistical test, which compares non-linear models, described by *Akamine (2004)* was also conducted for growth trajectories of males and females (Fig. 4C) to verify whether or not the results from ARSS are valid. The results of the statistical tests suggest that there are significant differences between males and females (Tables 5 and 6).

Comparison of chamber formation between ammonites and *Nautilus*

Widths (for *Normannites*: Table 2; for *Nautilus*: Table 4) and volumes of each chamber were plotted against chamber numbers for the ammonites (Fig. 6) and *Nautilus* (Fig. 7). It should be noted that the widths of each chamber for the ammonites may not be very accurate. For instance, for the widths of the 42nd to 44th chamber of Nm. 2 (Fig. 6B), we obtained the same value (7.7 mm), which presumably does not represent the actual width. This has been caused by the reduction in resolution resulting from segmenting only every 4th slice with an increment between two images 0.24 mm in voxel *z* (instead of 0.06 mm; see the method section above for details). In addition to the low resolution, the obscure limit between chambers and septa at the edges of the chambers (on the flanks) in the slices might also have resulted in some errors in segmentation. However, the overall trend of the widths through ontogeny should still be correctly depicted and thus, the errors mentioned above were negligible for our study (Fig. 6B).

DISCUSSION

Ontogenetic volumetric growth of ammonites

Due to preservation and limited resolution, the chambers in the first two whorls of the Jurassic ammonites could not be precisely measured. Therefore, the chamber numbers referred to below were estimated based on recognizable chambers and more or less constant septal spacing. There appears to be a subtle point where the slope of the curves changes at around the 28–29th chamber (Fig. 2B), corresponding to a conch diameter of about 4.5 mm. This change may represent the end of the second growth stage of ammonoids, the neanic stage, because it has been reported that the neanic stage of ammonoids lasts until a conch diameter of 3–5 mm (*Bucher et al., 1996*). This point may have been related to the change of their mode of life, i.e., from planktonic to

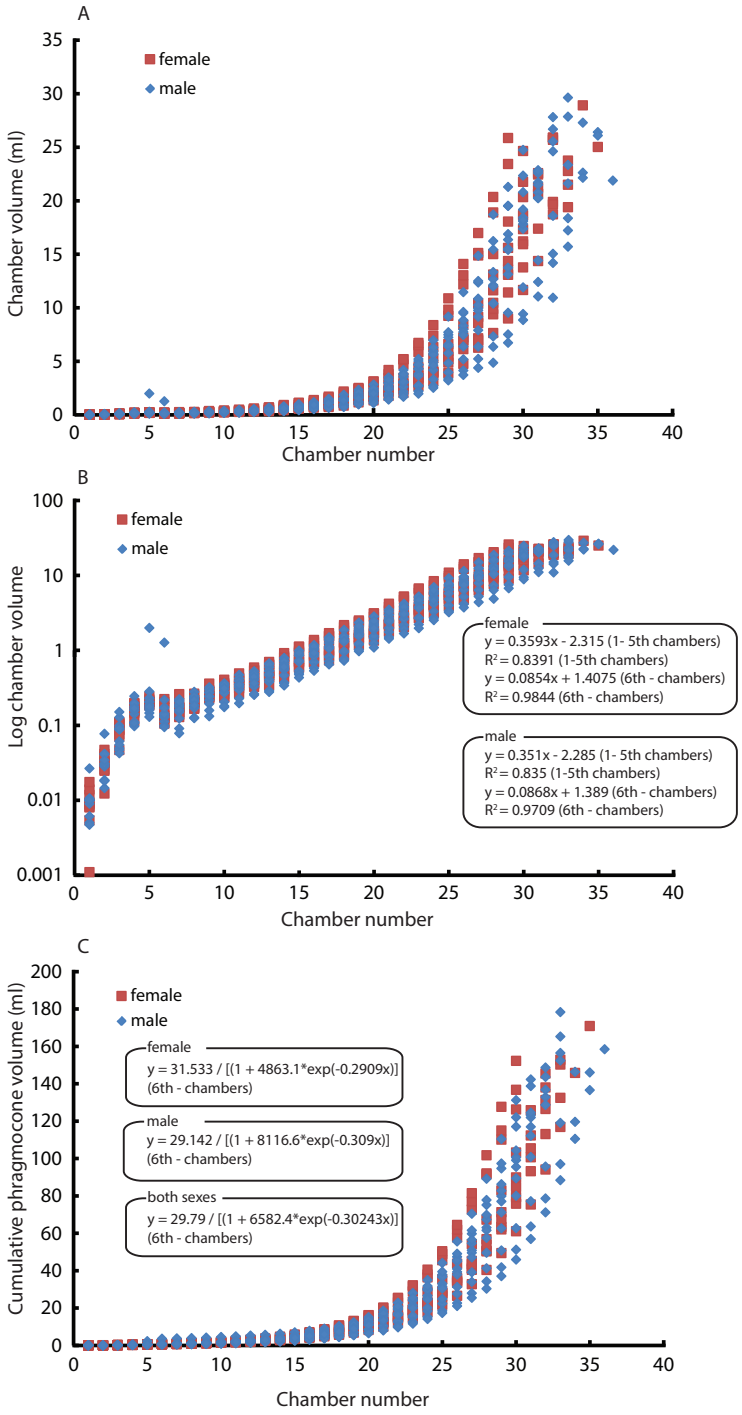

Figure 4 Comparison between males and females. Chamber volumes plotted against chamber numbers in *Nautilus pompilius*. Squares and diamonds represent the female and male, respectively. (A) Scatter plot of chamber numbers and individual volumes; (B) Semilog scatter plot of chamber numbers and individual volumes; (C) Scatter plot of chamber numbers and cumulative phragmocone volumes.

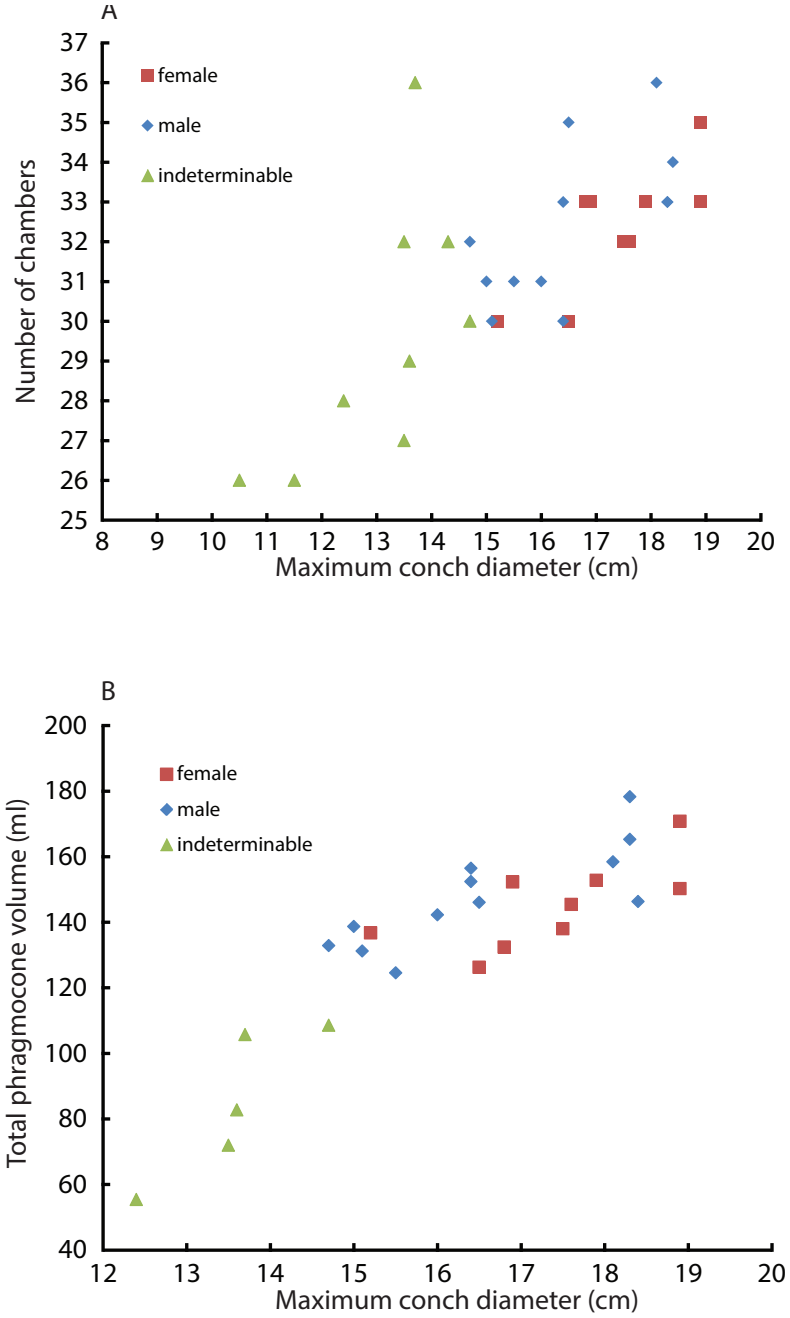

Figure 5 Comparison between males and females. Squares, diamonds, and triangles represent the female, male, and indeterminable sex, respectively. (A) Scatter plot of maximum conch diameters and chamber numbers of a specimen; (B) Scatter plot of maximum conch diameters and the phragmocone volume.

nektoplanktonic or nektonic (*Arai & Wani, 2012*). Taking this into account, the first two whorls of the conch comprise the first two growth stages, namely the embryonic and the neanic stages (*Bucher et al., 1996*; *Westermann, 1996*; *Klug, 2001*). Note that since the volumes of chambers formed before the 25th and 27th in Nm. 1 and Nm. 2 have not

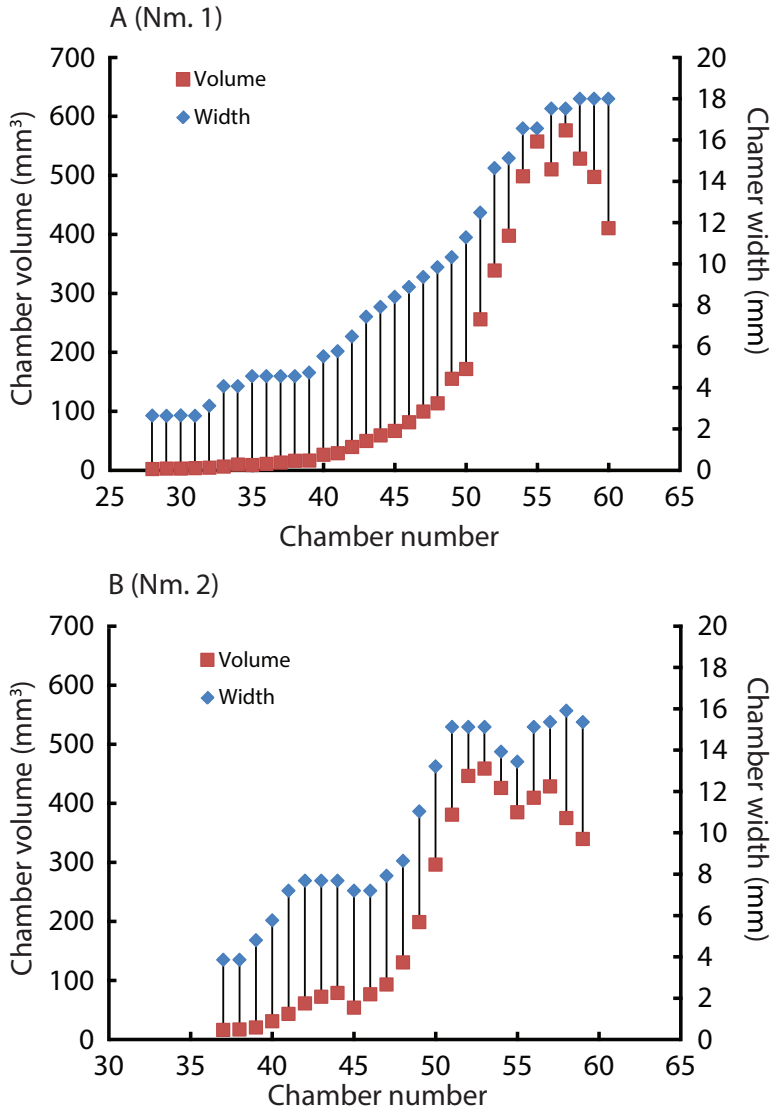

Figure 6 Volumes and widths of chambers plotted against chamber numbers in *Normannites mitis*. Squares and diamonds represent volumes and widths, respectively. (A) Nm.1; (B) Nm. 2.

been measured due to the poor resolution, the transition between the first two growth stages has not been examined. *Naglik et al. (2015)* three-dimensionally examined three different Palaeozoic ammonoid species. They documented a change in the slope of growth trajectories around the 19th–21st chamber in each specimen. The last several chambers display fluctuating growth known as terminal countdown (*Seilacher & Gunji, 1993*). In Nm. 2, an abrupt decrease of chamber volume occurred at the 45th chamber, marking another trend resulting in a lower cumulative volume than in Nm. 1. It is known that injuries can affect the septal spacing in modern *Nautilus* (*Ward, 1985*; compare *Keupp & Riedel, 1995*) as well as in ammonoids (*Kraft, Korn & Klug, 2008*). However, there are no visible injuries on the conch of Nm. 2, suggesting that this might have not been

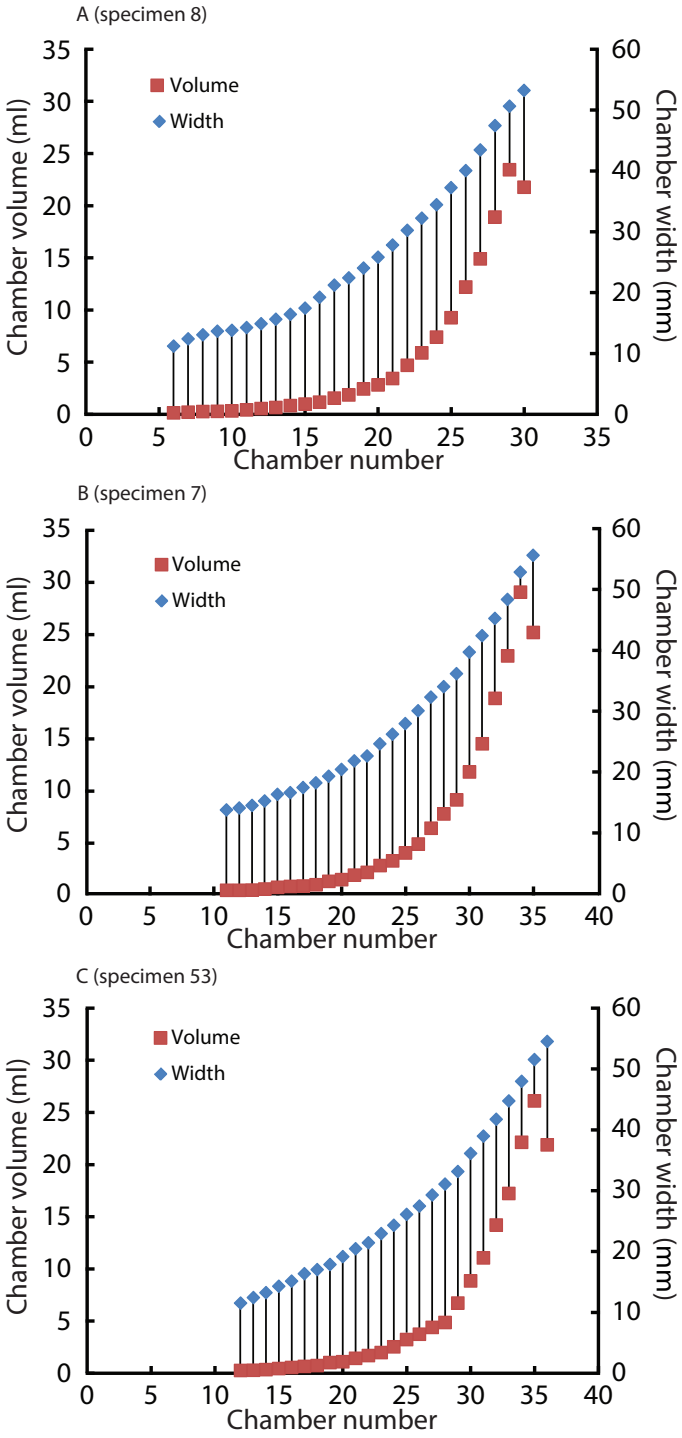

Figure 7 Volumes and widths of chambers plotted against chamber numbers in *Nautilus pompilius*. Squares and diamonds represent volumes and widths, respectively. (A) Specimen 8; (B) Specimen 7; (C) Specimen 53. Specimens with different growth trajectories were analysed.

Table 4 **Raw data of measured chamber widths of *Nautilus pompilius*.**

Nautilus pompilius

	Widths (mm)		
Chambers	**Specimen 8**	**Specimen 7**	**Specimen 53**
6	–	–	–
7	–	–	–
8	–	–	–
9	–	–	–
10	–	–	–
11	13.8	–	13.8
12	14.1	11.5	14.1
13	14.5	12.4	14.5
14	15.2	13.2	15.2
15	16.3	14.2	16.3
16	16.6	15.1	16.6
17	17.4	16.3	17.4
18	18.2	17.0	18.2
19	19.3	17.8	19.3
20	20.4	19.1	20.4
21	21.8	20.4	21.8
22	22.6	21.4	22.6
23	24.6	22.9	24.6
24	26.2	24.3	26.2
25	30.0	26.1	30.0
26	30.1	27.4	30.1
27	32.3	29.2	32.3
28	34.0	31.0	34.0
29	36.2	33.1	36.2
30	39.7	36.1	39.7
31	42.4	38.9	42.4
32	45.2	41.7	45.2
33	48.3	44.7	48.3
34	52.8	47.9	52.8
35	55.6	51.5	55.6
36	–	54.5	–

the case. Although the ammonite could have repaired a shell injury, it would be hard to recognize the presence of such a sublethal injury due to low resolution or the effects of shell replacement. Environmental changes might also have affected the conch construction. For example, in modern scleractinian corals, it is suggested that the Mg/Ca ratio in the sea water alters the skeletal growth rate (*Ries, Stanley & Hardie, 2006*). The knowledge of the sedimentary facies of the host rock from which the ammonites were extracted is insufficient to identify possible causes for the alteration of shell growth. Another possibility is the presence of parasites such as tube worms. They might have grown on the external conch, which affected the buoyancy of the ammonite. Interestingly, Nm. 1 preserves the

Table 5 **Results of statistical tests (analyses of the residual sum of squares) comparing linear regressions of males and female.**

Comparison	*N* (male)	*N* (female)	RSS (male)	RSS (female)	DF (male)	DF (female)	*t*	Significance
Chamber number vs. chamber volume (between the 1st and 5th chambers)	60	45	59.9	4,601	58	43	0.005	ns ($P > 0.5$)
Chamber number vs. chamber volume (from the 6th chamber)	332	243	108.3	104.0	330	240	16.8	s ($P < 0.05$)
Maximum diameter vs. number of chambers	12	9	46.5	14.6	10	7	1.9	s ($P < 0.1$)
Maximum diameter vs. total volume of phragmocone	12	9	927.6	721.0	10	7	2.2	s ($P < 0.1$)

Notes.
N, number of samples; RSS, residual sum of squares; DF, degree of freedom; ns, not significant; s, significant.

Table 6 **Results of a statistical test (an analysis of the residual sum of squares) comparing nonlinear regressions of males and females.**

Comparison	RSS (total)	RSS (male)	RSS (female)	DF (male)	DF (female)	F	Significance
Chamber number vs. chamber volume (from the 6th chamber)	2775.3	1670.0	1040.4	332	243	4.55	s ($P < 0.1$)

Notes.
RSS, residual sum of squares; DF, degree of freedom; ns, not significant; s, significant.

trace of a worm tube in the 41th chamber of the fifth whorl (*Tajika et al., 2015*), which had no detectable effect on chamber formation (Fig. 2A). Because of the absence of any trace of *syn vivo* epifauna on the conch, this scenario is unlikely.

The two different cumulative volumes of phragmocone chambers should result in a difference in buoyancy, given that the size of the two ammonites is more or less equal. The buoyancy of Nm. 1 was calculated by *Tajika et al. (2015)* as being positively buoyant in the (unlikely) absence of cameral liquid. Based on these calculations, they estimated the fill fraction of cameral liquid to attain neutral buoyancy as being about 27%. Unfortunately, the incompleteness of the aperture of Nm. 2 does not permit to calculate the buoyancy. It is quite reasonable, however, to speculate that Nm. 2 requires slightly less cameral liquid to reach neutral buoyancy (>27%) because of its size, its smaller phragmocone, and its most-likely similar conch mass. The fact that specimens with only minute morphological differences of the same species (*Normannites mitis*) likely expressed variation in buoyancy raises the question whether morphologically more diverse genera like *Amaltheus* (*Hammer & Bucher, 2006*) also varied more strongly in buoyancy regulation.

Ontogenetic volumetric growth of modern *Nautilus* and its intraspecific variation

Landman, Rye & Shelton (1983) reported that the first seven septa of Recent *Nautilus* are more widely spaced than the following ones; the point where septal spacing changes lies between the 7th and 8th chamber. It is considered to correspond to the time of hatching, which is also reflected in the formation of a shell-thickening and growth halt known as the nepionic constriction. This feature is also reported from fossil nautilids (*Landman, Rye & Shelton, 1983*; *Wani & Ayyasami, 2009*; *Wani & Mapes, 2010*).

In the growth trajectories of specimen 17 (Fig. 3A and Table 3), there are two abnormalities (the 5th and 6th chambers). These are supposedly artefacts caused by the low resolution of the scan combined with the small size of these structures and the resulting course surface of extracted chamber volume. This can occasionally cause some errors in calculating volumes in Matlab. But this problem occurred only in specimen 17, even though the low resolution would have caused errors in early rather than in late ontogeny.

Our results revealed a constant growth rate until the 5th or 6th chamber (Fig. 4B). Thereafter, the growth changes to another constant growth rate. Differences in the position of the nepionic constriction may be the artefact of low resolution of the scan, which might have made the very first (and possibly the second) chamber invisible. The position of the nepionic constriction, however, has some intraspecific variation (*Chirat, 2001*). *Stenzel (1964)* and *Landman et al. (1994)* showed some septal crowding between septa number 4 and 5 and between 9 and 10, respectively. Taking this into account, it is likely that our results are reflections of intraspecific variation. Nevertheless, in each examined specimen, the chamber volumes fluctuate but typically increase until the appearance of the nepionic constriction (Table 3). At the mature growth stage, most specimens show a volume reduction of the last chamber. Variability in chamber volume could be a consequence of several factors that influence the rate of chamber formation (growth rate): temperature, pH (carbon saturation degree), trace elements, food availability, sexual dimorphism, injuries, and genetic predisposition for certain metabolic features.

A relevant model for shell growth may be the 'temperature size rule' (e.g., *Atkinson, 1994*; *Irie, 2010*) which states the negative relationship between temperature and maturation size at moderate temperature, even though the growth rate slows down and the body size increases under extremely high or low temperatures. *Rosa et al. (2012)* observed a significant negative correlation between sea surface temperature and body size in coastal cephalopods. If this rule is applicable to the examined *Nautilus*, the temperature might have changed the growth rate of each individual because vertical migration of *Nautilus* is reported to range from near the sea surface to slightly below 700 m (*Dunstan, Ward & Marshall, 2011*). *Dunstan, Ward & Marshall (2011)* also suggested that the strategy for vertical migration of geographically separated *Nautilus* populations may vary depending on the slope, terrain and biological community. At this point, it is hard to conclude whether or not the temperature size rule applies because the behaviour of *Nautilus* in the Philippines can be highly different from Australian *Nautilus* as reported by *Dunstan, Ward & Marshall (2011)*. Knowledge of their behaviour or possible environmental preference during growth is necessary to examine this aspect. *Westermann et al. (2004)* described the period of chamber formation of *Nautilus pompilius* which ranges from 14 to more than 400 days. It is still likely that one individual inhabited different water depths from other individuals, producing varying trends of growth trajectories. Tracking the behaviour of modern *Nautilus* in the Philippines may provide more information on the role and applicability of the temperature size rule.

Analyses of stable isotopes have been used to estimate habitats of shelled animals (e.g., *Landman et al., 1994*; *Moriya et al., 2003*; *Auclair et al., 2004*; *Lécuyer & Bucher,*

2006; *Lukeneder et al., 2010*; *Ohno, Miyaji & Wani, 2015*). It might be worthwhile to examine the isotopic composition of the shells of a few nautilid and ammonoid shells with different volumetric changes through ontogeny, because this may shed some light on the relationships between habitat and growth trajectories.

The pH (or carbon saturation degree) influences shell secretion. A decrease of carbon saturation causes a lack of CO_3^{2-}-ions, which are required to produce aragonitic or calcitic shells (e.g., *Ries, Cohen & McCorkle, 2009*). In *Sepia officinalis*, elevated calcification rates under hypercapnic conditions have been shown by *Gutowska et al. (2010)*. This change in pH may alter the time needed to form a chamber and thereby reduce or increase the chamber volume. Similarly, trace elements like the Mg/Ca ratio in the sea water can affect the growth rate (for corals see, e.g., *Ries, Stanley & Hardie, 2006*). Food availability (e.g., lack of food) is also a possible explanation for the great variation. *Wiedmann & Boletzky (1982)* showed a link between lack of food and lower growth rates, resulting in closer septal spacing. *Strömgren & Cary (1984)* demonstrated a positive correlation between growth rate of mussels and food source. It is likely that there was at least some competition for food between *Nautilus* individuals and probably also with other animals. The individuals in a weaker position might have had access to less food or food of poorer quality.

Intraspecific variability can also originate from sexual dimorphism. In the case of *Nautilus*, males tend to be slightly larger than females with slightly broader adult body chambers (*Hayasaka et al., 2010*; *Saunders & Ward, 2010*; *Tanabe & Tsukahara, 2010*). However, in the juvenile stage, the morphological differences are not very pronounced, thus often hampering sexing. The two average slopes in the curves of chamber volumes obtained from males and females were compared using a test (analysis of the residual sum of squares: ARSS) described in *Zar (1996)*. This test was conducted independently for the embryonic stage and the other growth stages since the critical point between the 5th and the 6th chamber changes the slope of the growth curve (Fig. 4B). Moreover, an analysis of the residual sum of squares for nonlinear regressions was performed to compare the two average logistic models of males and females for the latter stage (Fig. 4C). No significant difference in the embryonic stage and a significant difference in the later stage (Tables 5 and 6) suggest that the differentiation in chamber volume between both sexes begins immediately after hatching. The results (Fig. 4) also show, however, the occurrence of conch morphologies common to both sexes. Taking this into account, their volume is not an ideal tool for sexing. The same statistical test for linear regressions was also conducted to compare the number of formed chambers (Fig. 5A) and the phragmocone volume (Fig. 5B) with maximum conch diameter between male and female individuals. The test results (Table 5) suggest that there is a significant difference between the female and male in both cases, although the significance levels are not strict (the number of chambers vs. maximum diameter: $P < 0.05$: the entire phragmocone volume vs. maximum diameter: $P < 0.1$). A greater sample, however, may yield a clearer separation. The results of a series of statistical tests (Table 5; analyses of the residual sum of squares) suggest that the males tend to produce more chambers than females with nearly the same conch diameter. Bearing

in mind that mature males are generally larger than mature females in maximum conch diameter (*Hayasaka et al., 2010*), this may potentially indicate a prolonged life span or less energetic investment in reproduction. By contrast, the addition of another chamber to males could be associated with their sexual maturity; the weight of the large spadix and a large mass of spermatophores in males might necessitate more space and buoyancy. *Ward et al. (1977)* reported that the total weight of males of *Nautilus pompilius* from Fiji exceeds that of females by as much as 20%. What remains unclear is the reason why females tend to have larger phragmocone volumes than males while they are immature. It is true, however, that even within each sex, the variability of the total phragmocone volumes is quite high (standard deviation for males: 15.4; for females: 13.4; for both males and females: 14.3). Of course one should also bear in mind the possibility that these high variabilities may have partially originated from the errors discussed in the method section.

Injuries are visible in several of the examined specimens, yet there is no link to a temporal or spatial change in chamber volume in the growth curves. *Yomogida & Wani (2013)* examined injuries of *Nautilus pompilius* from the same locality in the Philippines, reporting traces of frequent sublethal attacks rather early in ontogeny than in later stages. The frequency of sublethal attacks early in ontogeny may be one of the factors determining the steepness of the growth trajectory curves. This aspect can be tested in further studies. Additionally, morphological variability may also root in genetic variability but the causal link is difficult to test.

Covariation of chamber volumes and widths in ammonoids and nautiloids

The relationship between chamber volumes of *Nautilus pompilius* (Fig. 7) revealed that their chamber widths expanded at a constant pace irrespective of the change in chamber volume. For the construction of the *Nautilus* conch and its ontogeny, a rather constant conch morphology might have been advantageous with the buoyancy regulation depending largely on septal spacing only. Likewise, *Hoffmann, Reinhoff & Lemanis (2015)* reported on *Spirula* that has a sudden decrease of chamber volume which is not correlated with changes in whorl height or whorl width but with changes in septal spacing. By contrast, the chamber widths and volumes of the ammonites appear to covary (Fig. 6). This distinct covariation may have partially contributed to the high morphological variability with some constraints in response to fluctuating environmental conditions or predatory attacks (for details, see the discussion for *Nautilus* above). This aspect, however, needs to be examined further using an image stack of an ammonite with a higher resolution and better preservation to rule out artefacts.

CONCLUSIONS

We virtually reconstructed the conchs of two Middle Jurassic ammonites (*Normannites mitis*) and 30 specimens of Recent nautilids (*Nautilus pompilius*) using grinding tomography and computed tomography (CT), respectively, to analyse the intraspecific variability in volumetric change of their chambers throughout ontogeny. The data obtained from the constructed 3D models led to the following conclusions:

1. Chamber volumes of *Normannites mitis* and *Nautilus pompilius* were measured to compare the ontogenetic change. The growth trajectories of *Normannites mitis* and *Nautilus pompilius* follow logistic curves throughout most of their ontogeny. The last several chambers of *Normanites mitis* show fluctuating chamber volumes, while most specimens of *Nautilus pompilius* demonstrate a volume reduction of only the last chamber.
2. Growth trajectories of the two *Normannites mitis* specimens were compared. The two specimens appear to have a transition point between the 28th and 29th chamber from which the slopes of their growth curves change, which has been documented previously. However, their entire phragmocone volumes differ markedly in late ontogeny although the two shells have similar morphology and size. Intraspecific variation of buoyancy was not testable in this study due to the low sample number. This aspect needs to be addressed in future research because buoyancy analyses could provide information on the habitat of ammonoids.
3. Growth trajectories of thirty *Nautilus pompilius* conchs show a high variability, even though the high variabilitiy may have partially originated from the errors discussed in the method section.
4. Results of statistical tests for *Nautilus pompilius* corroborate that the variability is increased by the morphological difference between the two sexes: adult males have larger volumes than females with the same diameter. This may be ascribed to the formation of voluminous reproductive organs in the male (spadix). Individual chamber volumes of the female tend to be larger than those of males. The results also show that intraspecific variability within one sex is moderately strong. Examinations of their injuries, isotopic analyses of the examined conchs or tracking the behaviour of *Nautilus* could yield more information on the relationship between their variability in chamber volumes and ecology. Such data could help to reconstruct the palaeoecology of fossil nautiloids and possibly also of extinct ammonoids.
5. Covariation between the chamber widths and volumes in ammonites and *Nautilus pompilius* were examined. The results illustrate that conch construction of *Nautilus pompilius* is robust, maintaining a certain shape, whereas the conch development of the examined ammonites was more plastic, changing shape during growth under some fabricational constraints. Further investigations need to be carried out to verify the covariation between widths and volumes of ammonites with other variables such as conch thickness, conch width, and perhaps buoyancy using a reconstruction method with a higher resolution and perfectly-preserved materials.

ACKNOWLEDGEMENTS

We would like to thank Dominik Hennhöfer and Enric Pascual Cebrian (Universität Heidelberg) for carrying out the grinding tomography. Beat Imhof (Trimbach) kindly donated the two specimens of *Normannites*. We are also thankful to Torsten Scheyer (Universität Zürich) for the introduction to the use of Avizo® 8.1. Kathleen Ritterbush (University of Chicago) proofread the manuscript and corrected the English. The fruitful discussion with Kozue Nishida (The Geological Survey of Japan) is greatly appreciated.

ADDITIONAL INFORMATION AND DECLARATIONS

Funding

This study is supported by the Swiss National Science Foundation SNF (project numbers 200020_132870, 200020_149120, and 200021_149119). The funders had no role in study design, data collection and analysis, decision to publish, or preparation of the manuscript.

Grant Disclosures

The following grant information was disclosed by the authors:
Swiss National Science Foundation SNF: 200020_132870, 200020_149120, 200021_149119.

Competing Interests

The authors declare there are no competing interests.

Author Contributions

- Amane Tajika conceived and designed the experiments, performed the experiments, analyzed the data, wrote the paper, prepared figures and/or tables, reviewed drafts of the paper.
- Naoki Morimoto performed the experiments, contributed reagents/materials/analysis tools, reviewed drafts of the paper.
- Ryoji Wani and Carole Naglik contributed reagents/materials/analysis tools, reviewed drafts of the paper.
- Christian Klug wrote the paper, reviewed drafts of the paper.

Supplemental Information

Supplemental information for this article can be found online at http://dx.doi.org/10.7717/peerj.1306#supplemental-information.

REFERENCES

Akamine T. 2004. Statistical test and model selection of fish growth formula. *Bulletin of the Japanese Society of Fisheries Oceanography* **68(1)**:44–51.

Arai K, Wani R. 2012. Variable growth modes in late cretaceous ammonoids: implications for diverse early life histories. *Journal of Paleontology* **86**:258–267 DOI 10.1666/11-068.1.

Arnold JM. 1984. Cephalopod reproduction. In: Biggelar, ed. *The mollusca*, vol. 7. New York: Academic Press, 419–454.

Atkinson D. 1994. Temperature and organism size—a biological law for ectotherms? *Advances in Ecological Research* **25**:1–58 DOI 10.1016/S0065-2504(08)60212-3.

Auclair AC, Lécuyer C, Bucher H, Sheppard SMF. 2004. Carbon and oxygen isotope composition of *Nautilus macromphalus*: a record of thermocline waters off New Caledonia. *Chemical Geology* **207**:91–100 DOI 10.1016/j.chemgeo.2004.02.006.

Bucher H, Landman NH, Klofak SM, Guex J. 1996. Mode and rate of growth in ammonoids. In: Landman NH, Tanabe K, Davis RA, eds. *Ammonoid paleobiology*. New York: Plenum, 407–461.

Chirat R. 2001. Anomalies of embryonic shell growth in post-Triassic Nautilida. *Paleobiology* **27**:485–499 DOI 10.1666/0094-8373(2001)027<0485:AOESGI>2.0.CO;2.

Collins D, Ward PD, Westermann GEG. 1980. Function of cameral water in *Nautilus*. *Paleobiology* **6**:168–172.

Dunstan AJ, Ward PD, Marshall NJ. 2011. Vertical distribution and migration patterns of *Nautilus pompilius*. *PLoS ONE* **6(2)**:e16311 DOI 10.1371/journal.pone.0016311.

Garwood RJ, Rahman IA, Sutton MD. 2010. From clergymen to computers—the advent of virtual palaeontology. *Geology Today* **26**:96–100 DOI 10.1111/j.1365-2451.2010.00753.x.

Götz S. 2003. Larval settlement and ontogenetic development of *Hippuritella vasseuri* (Douvillé) (Hippuritoidea, Bivalvia). *Geologia Croatica* **56(2)**:123–131 DOI 10.4154/GC.2003.07.

Götz S. 2007. Inside rudist ecosystems: growth, reproduction and population dynamics. In: Scott RW, ed. *Cretaceous rudists and carbonate platforms: environmental feedback*, *SEPM Special Publication,* vol. 87. Tulsa: Society for Sedimentary Geology, 97–113.

Götz S, Stinnesbeck W. 2003. Reproductive cycles, larval mortality and population dynamics of a Late Cretaceous hippuritid association: a new approach to the biology of rudists based on quantitative three dimensional analysis. *Terra Nova* **15**:392–397 DOI 10.1046/j.1365-3121.2003.00515.x.

Gutowska MA, Melzner F, Langenbuch M, Bock C, Claireaux G, Pörtner HO. 2010. Acid–base regulatory ability of the cephalopod (*Sepia officinalis*) in response to environmental hypercapnia. *Journal of Comparative Physiology B* **180**:323–335 DOI 10.1007/s00360-009-0412-y.

Hammer Ø, Bucher H. 2006. Generalized ammonoid hydrostatics modelling, with application to *Intornites* and intraspecific variation in *Amaltheus*. *Palaeontological Research* **10**:91–96 DOI 10.2517/prpsj.10.91.

Haven N. 1977. The reproductive biology of *Nautilus pompilius* in the Philippines. *Marine Biology* **42(2)**:177–184 DOI 10.1007/BF00391570.

Hayasaka S, Ōki K, Tanabe K, Saisho T, Shinomiya A. 2010. On the habitat of *Nautilus pompilius* in Tanon Strait (Philippines) and the Fiji Islands. In: Saunders WB, Landman NH, eds. *Nautilus. The biology and paleobiology of a living fossil*. Dordrecht: Springer, 179–200.

Hennhöfer DK, Götz S, Mitchell SF. 2012. Palaeobiology of a *Biradiolites mooretownensis* rudist lithosome: seasonality, reproductive cyclicity and population dynamics. *Lethaia* **45**:450–461 DOI 10.1111/j.1502-3931.2012.00307.x.

Hoffmann R, Reinhoff D, Lemanis R. 2015. Non-invasive imaging techniques combined with morphometry: a case study from *Spirula*. *Swiss Journal of Palaeontology* DOI 10.1007/s13358-015-0083-0.

Hoffmann R, Schultz JA, Schellhorn R, Rybacki E, Keupp H, Gerden SR, Lemanis R, Zachow S. 2014. Non-invasive imaging methods applied to neo- and paleontological cephalopod research. *Biogeosciences Discussions* **10**:18803–18851 DOI 10.5194/bgd-10-18803-2013.

Hoffmann R, Zachow S. 2011. Non-invasive approach to shed new light on the buoyancy business of chambered cephalopods (Mollusca). In: *Extended abstract published in the abstract volume, IAMG 2011 (Mathematical Geosciences at the Crossroads of Theory and Practice), Salzburg, Austria, 1–11*. DOI 10.5242/iamg.2011.0163.

Irie T. 2010. Adaptive significance of the temperature–size rule. *Japanese Journal of Ecology* **60**:169–181.

Jacobs DK, Landman NH. 1993. *Nautilus*—a poor model for the function and behavior of ammonoids? *Lethaia* **26**:101–111 DOI 10.1111/j.1502-3931.1993.tb01799.x.

Keupp H, Riedel F. 1995. *Nautilus pompilius* in captivity: a case study of abnormal shell growth. *Berliner geowissenschaftliche Abhandlungen* **E16**:663–681.

Klug C. 2001. Life-cycles of Emsian and Eifelian ammonoids (Devonian). *Lethaia* **34**:215–233 DOI 10.1080/002411601316981179.

Klug C. 2004. Mature modifications, the black band, the black aperture, the black stripe, and the periostracum in cephalopods from the Upper Muschelkalk (Middle Triassic, Germany). *Mitteilungen aus dem Geologisch-Paläontologischen Institut der Universität Hamburg* **88**:63–78.

Klug C, Zatoń M, Parent H, Hostettler B, Tajika A. 2015. Mature modifications and sexual dimorphism. In: Klug C, Korn D, De Baets K, Kruta I, Mapes RH, eds. *Ammonoid paleobiology, volume I: from anatomy to ecology*. *Topics in geobiology,* vol. 43. Dordrecht: Springer, 252–320.

Korn D, Bockwinkel J, Ebbighausen V. 2010. The ammonoids from the Argiles de Teguentour of Oued Temertasset (early Late Tournaisian; Mouydir, Algeria). *Fossil Record* **13**:35–152 DOI 10.5194/fr-13-35-2010.

Kraft S, Korn D, Klug C. 2008. Ontogenetic patterns of septal spacing in Carboniferous ammonoids. *Neues Jahrbuch für Geologie und Mineralogie, Abhandlungen* **250**:31–44 DOI 10.1127/0077-7749/2008/0250-0031.

Kruta I, Landman N, Rouget I, Cecca F, Tafforeau P. 2011. The role of ammonites in the Mesozoic marine food web revealed by jaw preservation. *Science* **331**:70–72 DOI 10.1126/science.1198793.

Landman NH, Cochran JK, Rye DM, Tanabe K, Arnold JM. 1994. Early life history of *Nautilus*: evidence from isotopic analyses of aquarium-reared specimens. *Paleobiology* **20**:40–51.

Landman NH, Rye DM, Shelton KL. 1983. Early ontogeny of *Eutrephoceras* compared to Recent Nautilus and Mesozoic ammonites: evidence from shell morphology and light stable isotopes. *Paleobiology* **9**:269–279.

Lécuyer C, Bucher H. 2006. Stable isotope compositions of a late Jurassic ammonite shell: a record of seasonal surface water temperatures in the southern hemisphere? *eEarth Discuss* **1**:1–19 DOI 10.5194/eed-1-1-2006.

Lemanis R, Zachow S, Fusseis F, Hoffmann R. 2015. A new approach using high-resolution computed tomography to test the buoyant properties of chambered cephalopod shells. *Paleobiology* **41**:313–329 DOI 10.1017/pab.2014.17.

Lukeneder A, Harzhauser M, Müllegger S, Piller WE. 2010. Ontogeny and habitat change in Mesozoic cephalopods revealed by stable isotopes (δ^{18}O, δ^{13}C). *Earth and Planetary Science Letters* **296**:103–114 DOI 10.1016/j.epsl.2010.04.053.

Moriya K, Nishi H, Kawahata H, Tanabe K, Takayanagi Y. 2003. Demersal habitat of Late Cretaceous ammonoids: evidence from oxygen isotopes for the Campanian (Late Cretaceous) northwestern Pacific thermal structure. *Geology* **31**:167–170 DOI 10.1130/0091-7613(2003)031<0167:DHOLCA>2.0.CO;2.

Naglik C, Monnet C, Götz S, Kolb C, De Baets K, Tajika A, Klug C. 2015. Growth trajectories of some major ammonoid sub-clades revealed by serial grinding tomography data. *Lethaia* **48**:29–46 DOI 10.1111/let.12085.

Naglik C, Rikhtegar F, Klug C. 2015. Buoyancy of some Palaeozoic ammonoids and their hydrostatic properties based on empirical 3D-models. *Lethaia* DOI 10.1111/let.12125.

Ohno A, Miyaji T, Wani R. 2015. Inconsistent oxygen isotopic values between on temporary secreted septa and outer shell walls in modern *Nautilus*. *Lethaia* **48**:332–340 DOI 10.1111/let.12109.

Pascual-Cebrian E, Hennhöfer DK, Götz S. 2013. 3D morphometry of polyconitid rudist bivalves based on grinding tomography. *Facies* **59**:347–358 DOI 10.1007/s10347-012-0310-8.

Reyment RA. 1958. Some factors in the distribution of fossil Cephalopods. *Acta Universitatis Stockholmiensis—Stockholm Contributions in Geology* **1**:97–184.

Ries JB, Cohen AL, McCorkle DC. 2009. Marine calcifiers exhibit mixed responses to CO_2-induced ocean acidification. *Geology* **37**:1131–1134 DOI 10.1130/G30210A.1.

Ries JB, Stanley SM, Hardie LA. 2006. Scleractinian corals produce calcite, and grow more slowly, in artificial Cretaceous seawater. *Geology* **34**:525–528 DOI 10.1130/G22600.1.

Rosa R, Gonzalez L, Dierssen HM, Seibel BA. 2012. Environmental determinants of latitudinal size-trends in cephalopods. *Marine Ecology Progress Series* **464**:153–165 DOI 10.3354/meps09822.

Saunders WB, Landman NH. 1987. *Nautilus: the biology and paleobiology of a living fossil*. New York: Plenum.

Saunders WB, Spinosa C. 1978. Sexual dimorphism in *Nautilus* from Palau. *Paleobiology* **4**:349–358.

Saunders WB, Ward PD. 2010. Ecology, distribution, and population characteristics of *Nautilus*. In: Saunders WB, Landman NH, eds. *Nautilus. The biology and paleobiology of a living fossil*. Dordrecht: Springer, 137–162.

Seilacher A, Gunji YP. 1993. Morphogenetic countdown: another view on heteromorph shells in gastropods and ammonites. *Neues Jahrbuch für Geologie und Paläontologie Abhandlungen* **190**:237–265.

Stenzel HB. 1964. Living *Nautilus*. In: Moore RC, ed. *Treatise on invertebrate paleontology. Part K (Mollusca 3)*. Lawrence: Geological Society of America and University of Kansas Press, K59–K93.

Stevens K, Mutterlose J, Wiedenroth K. 2015. Stable isotope data (δ18O, δ13C) of the ammonite genus *Simbirskites*—implications for habitat reconstructions of extinct cephalopods. *Palaeogeography, Palaeoclimatology, Palaeoecology* **417**:164–175 DOI 10.1016/j.palaeo.2014.10.031.

Strömgren T, Cary C. 1984. Growth in length of *Mytilus edulis* L. fed on different algal diets. *Journal of Experimental Marine Biology and Ecology* **76**:23–34 DOI 10.1016/0022-0981(84)90014-5.

Sutton M, Rahman I, Garwood R. 2014. *Techniques for virtual palaeontology*. Chichester: Wiley-Blackwell.

Tajika A, Naglik C, Morimoto N, Pascual-Cebrian E, Hennhöfer D, Klug C. 2015. Empirical 3D model of the conch of the Middle Jurassic ammonite microconch *Normannites*: its buoyancy, the physical effects of its mature modifications and speculations on their function. *Historical Biology* **27**:181–191 DOI 10.1080/08912963.2013.872097.

Tanabe K, Hayasaka S, Saisho T, Shinomiya A, Aoki K. 1983. Morphologic variation of *Nautilus pompilius* from the Philippines and Fiji islands. Studies of *Nautilus pompilius* and its associated fauna from Tanon Strait, the Philippines. *Kagoshima University Research Center for the Pacific Islands, Occasional Paper* **1**:9–21.

Tanabe K, Tsukahara J. 2010. Biometric analysis of *Nautilus pompilius* from the Philippines and the Fiji Islands. In: Saunders WB, Landmann NH, eds. *Nautilus: the biology and paleobiology of a living fossil*. Dordrecht: Springer, 105–113.

Wani R. 2004. Experimental fragmentation patterns of modern *Nautilus* shells and the implications for fossil cephalopod taphonomy. *Lethaia* **37**:113–123 DOI 10.1080/00241160410006420.

Wani R, Ayyasami K. 2009. Ontogenetic change and intra-specific variation of shell morphology in the Cretaceous nautiloid (Cephalopoda, Mollusca) *Eutrephoceras clementinum* (d'Orbigny, 1840) from the Ariyalur area, southern India. *Journal of Paleontology* **83**:365–378 DOI 10.1666/08-119.1.

Wani R, Mapes RH. 2010. Conservative evolution in nautiloid shell morphology; evidence from the Pennsylvanian nautiloid *Metacoceras mcchesneyi* from Ohio, USA. *Journal of Paleontology* **84**:477–492 DOI 10.1666/09-158.1.

Ward PD. 1979. Cameral liquid in *Nautilus* and ammonites. *Paleobiology* **5**:40–49.

Ward PD. 1980. Comparative shell shape distributions in Jurassic-Cretaceous ammonites and Jurassic-Tertiary nautilids. *Paleobiology* **6**:32–43.

Ward PD. 1985. Periodicity of chamber formation in chambered cephalopods: evidence from *Nautilus macromphalus* and *Nautilus pompilius*. *Paleobiology* **11**:438–450.

Ward PD. 1987. *The natural history of Nautilus*. Boston: Allen and Unwin.

Ward PD. 1988. *In search of Nautilus*. New York: Simon & Schuster.

Ward P, Martin AW. 1978. On the buoyancy of the pearly *Nautilus*. *Journal of Experimental Zoology* **205**:5–12 DOI 10.1002/jez.1402050103.

Ward P, Stone R, Westermann G, Martin A. 1977. Notes on animal weight, cameral fluids, swimming speed, and colour polymorphism of the cephalopod *Nautilus pompilius* in the Fiji Islands. *Paleobiology* **3**:377–388.

Warnke K, Keupp H. 2005. *Spirula*—a window to the embryonic development of ammonoids? Morphological and molecular indications for a palaeontological hypothesis. *Facies* **51**:60–65 DOI 10.1007/s10347-005-0054-9.

Westermann GEG. 1996. Ammonoid life and habitat. In: Landman NH, Tanabe K, Davis RA, eds. *Ammonoid paleobiology*. New York: Plenum, 607–707.

Westermann B, Beck–Schildwächter I, Beuerlein K, Kaleta EF, Schipp R. 2004. Shell growth and chamber formation of aquarium–reared *Nautilus pompilius* (Mollusca, Cephalopoda) by Xray analysis. *Journal of Experimental Zoology Part A: Comparative Experimental Biology* **301**:930–937 DOI 10.1002/jez.a.116.

Wiedmann J, Boletzky SV. 1982. Wachstum und Differenzierung des Schulps von *Sepia officinialis* unter künstlichen Aufzuchtbedingungen–Grenzen der Anwendung im palökologischen Modell. *Neues Jahrbuch für Geologie und Paläontologie Abhandlungen* **164**:118–133.

Wormanns D, Kohl G, Klotz E, Marheine A, Beyer F, Heindel W, Diederich S. 2004. Volumetric measurements of pulmonary nodules at multi-row detector CT: *in vivo* reproducibility. *European Radiology* **14**:86–92 DOI 10.1007/s00330-003-2132-0.

Yomogida S, Wani R. 2013. Higher risk of fatality by predatory attacks in earlier ontogenetic stages of modern *Nautilus pompilius* in the Philippines: evidence from the ontogenetic analyses of shell repairs. *Lethaia* **46**:317–330 DOI 10.1111/let.12010.

Zar JH. 1996. *Biostatistical analysis*. Third edition. Upper Saddle River: Prentice Hall.

Chapter IV

What is the pattern of ontogenetic variation in cephalopods? Perspectives from 3D morphometry on Recent *Nautilus pompilius*

Tajika, A. Morimoto, N.
Wani, R. Klug, C.

Submitted to
Paleobiology

What is the pattern of ontogenetic intraspecific variation in cephalopods? Perspectives from 3D morphometry on Recent *Nautilus pompilius*

Amane Tajika, Naoki Morimoto, Ryoji Wani, and Christian Klug

Amane Tajika, and Christian Klug. Paläontologisches Institut und Museum, Universität Zürich, Karl-Schmid-Strasse 4, 8006 Zürich, Switzerland. Email: amane.tajika@pim.uzh.ch, chklug@pim.uzh.ch
Naoki Morimoto. Laboratory of Physical Anthropology, Faculty of Science, Kyoto University Kitashirakawa Oiwake-cho, Sakyo-ku, 606-8502 Kyoto, Japan. Email: morimoto@anthro.zool.kyoto-u.ac.jp
Ryoji Wani. Faculty of Environment and Information Sciences, Yokohama National University, Yokohama 240-8501, Japan. Email: wani@ynu.ac.jp

Abstract. –Intraspecific variation of organisms is of great importance to correctly carry out taxonomic work, which is a base for important disciplines in palaeontology such as biodiversity, biostratigraphy and biogeography. However, intraspecific variation is often overlooked especially in ectocochleate cephalopods (ammonoids and nautiloids), in which an excessive number of taxa was established during the past centuries. Since intraspecific variation of fossilized organisms suffers from various biases (time averaging, taphonomy, and preservation), insight of an extant example is needed. We applied 3D morphometry to 93 specimens of *Nautilus pompilius* from three different geographic populations. This dataset was used to examine the intraspecific variation throughout ontogeny in detail. Although there are slight differences between the populations, a common pattern of intraspecific variation appears to be present. High variation appears at early ontogeny, which then decreases gradually after the following ontogenetic stages. Subsequently, the variation shows an increase again before maturity until a sharp increase or decrease occurs towards the end of ontogeny. Comparison with intraspecific variation of ammonoids and belemnites illustrated that some groups have ontogenetic patterns of intraspecific variation, which are similar to that of N. pompilius. This implies that the above-mentioned ontogenetic pattern of intraspecific variation might be common in some major cephalopod clades.

Introduction

Intraspecific variation of organisms is one of the most important parameters, which is a basis for a wide range of fields of research from biodiversity to ecology, biogeography and biostratigraphy. In extinct animals, phenotypic traits, which would at least partially reflect aspects of the genotype, have been utilized to examine the intraspecific variation. The phenotypic variation, however, is frequently overlooked or underestimated when a new taxon is introduced, which often results in oversplitting (De Baets et al. 2013, 2015). This may cause a strong bias when assessing biodiversity, biostratigraphy and biogeography (Kennedy and Cobban 1976; Dzik 1985; 1990; Hughes and Labandeira 1995; Nardin et al. 2005; Korn and Klug 2007; Monnet et al. 2010; De Baets et al. 2013). For example, studies using the Paleobiology Database (PBDB; e.g., Bush and Bambach 2015) as well as classical biodiversity curves through geologic times (e.g.,Sepkoski et al. 1981) can contain biased estimation of taxonomic richness.

Ectocochleate cephalopods are an ideal group to study intraspecific variation through ontogeny because of their accretionary growth, which implies the preservation of their life history as in other shelled mollusks. Ammonoids are a well-known and well-studied extinct cephalopod group, which is regarded as being of great importance for biostratigraphy and also diversity studies (Kennedy 1977; House 1981; 1985;Kennedy and Wright 1985; House and Kerr 1989; Kennedy 1989; Korn et al. 2015). Although recently efforts have been made to understand intraspecific variation (e.g., Tanabe and Shigeta 1987; Korn and Klug 2007; Monnet et al. 2010; Bert 2014; Jattiot et al. 2015), their taxonomy has still been suffering from overestimation of their taxonomic richness (e.g., Hohenegger and Tatzreiter 1992; Dagys and Wetschat 1993; De Baets et al. 2013; De Baets et al. 2015). As far as fossil nautiloids, which are also ectocochleate cephalopods are concerned, only a very limited degree of attention has been paid to the intraspecific variation (e.g., Wani and Ayyasami 2009), which possibly results in an overestimation of their diversity (Tajika et al.

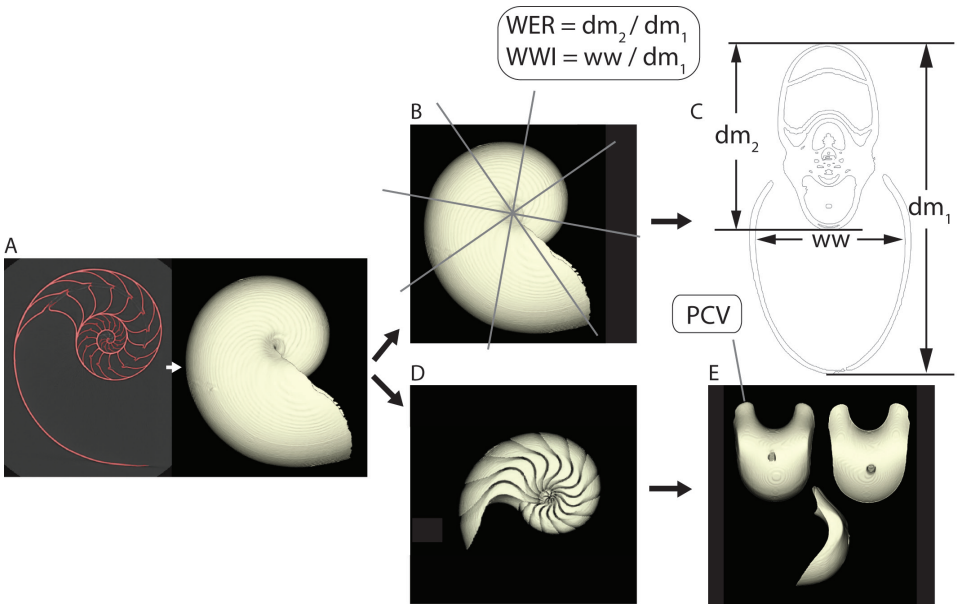

Fig. 1. 3D morphometry of *Nautilus pompilius*. A, CT-scanning, segmentation and export of 3D files. B, Producing cross sections. C, Measurements of diameter (dm) and ww (whorl width). D, Extraction of phragmocone. E, Extraction of individual phragmocone chambers volume (PCV).

2017).

Nautilus is an extant genus of ectocochleate cephalopods, which has been used most commonly as an analogy to extinct ammonoids. Although some researches on taxonomy and morphological variation of *Nautilus* (Tanabe et al. 1983; Tanabe et al. 1985; Swan and Saunders 1987) have been carried out intensively by paleontologists during the 1980's, we still lack an overview over the patterns of intraspecific variation of their main conch parameters. In fact, some biologists suggested that some of the established morphospecies of *Nautilus* need to be synonymized based on their genetic similarities (Wray et al. 1995; Bonnaud et al. 2004; Sinclair et al. 2007; Vandepas et al. 2016). Also, studies on intraspecific variation of fossilized animals suffer from time averaging (Kidwell 2002) and possible equalization of some geographic populations due to postmortem transportation. Thus, an in-depth knowledge of an extant representative is key to better understand intraspecific variation of extinct relatives. Increased knowledge of conch morphology of *Nautilus* may serve as a reference to fossil nautiloids and probably ammonoids as well. In this study, we aim to answer the following questions: 1) What is the phenotypic intraspecific variation of Recent *Nautilus*? 2) How does intraspecific variation change through ontogeny? 3) Does intraspecific variation differ between populations? 4) Is the pattern of intraspecific variation of *Nautilus* similar to or different from other cephalopods?

Materials and Methods

Conchs of 93 specimens of Recent *Nautilus pompilius* were scanned at the Laboratory of Physical Anthropology of Kyoto University using a 16-detector-array CT device (Toshiba Alexion TSX-032A) with the following data acquisition and image reconstruction parameters: beam collimation: 1.0 mm; pitch: 0.688; image reconstruction kernel: sharp (FC30); slice increment: 0.2 mm; tube voltage and current: 120 kV 100 mA. This resulted in volume data sets with isotropic spatial resolution of 0.331 mm. The specimens consist of populations from three different geographic regions with different average conch diameter:

1) *Nautilus pompilius* from the Tagnan area of the Philippines [N = 35 (adult males: N = 12, adult females: N = 9; juveniles: N = 14)] 30 specimens of them were previously examined by Tajika et al. (2015). Data of additional 5 specimens were produced for this study. The average conch diameter of adult specimens is 169 mm.
2) *N. pompilius* from Semporna, Malaysia [N = 38 (adult males: N = 26, adult females: N = 12)] The average conch diameter is 198 mm, which is much larger than commonly known from *N. pompilius*. The adult size is rather similar to that of the controversial morphospecies of *N. balauensis* (Saunders 1987; Vandepas et al. 2016). In this study, we regard this population as representatives of *N. pompilius* with a large conch diameter.

3) *N. pompilius* from Borneo, Indonesia [N = 20 (adult males: N = 11, adult females: N = 8; probably male juvenile: N = 1)] The average conch diameter is 167 mm.

Males and females were differentiated based on the aperture shape: mature males have larger shells and a broader, rounder aperture than females (e.g., Saunders and Spinosa 1978). All the examined shells were bought from a fisherman or a shell dealer between 2010 and 2013.

The obtained datasets were segmented on Avizo® 8.1 (FEI Visualization Sciences Group). The segmented data were then exported as STL files in order to perform 3D morphometry on Matlab 8.5 (MathWorks). The STL files were used to produce cross sections every 45°, which allows for morphometry at more or less 16 ontogenetic stages per specimen. On the produced cross section, the three parameters, conch diameter (dm1), the diameter of the preceding whorl (dm2) and the whorl width (ww) were measured (Fig. 1). Individual phragmocone chamber volumes (PCV) were also extracted with the method applied in Tajika et al. (2015; Fig. 1). As discussed and demonstrated by Hoffmann et al. (2014) and Tajika et al. (2015), scans of specimens do not retain their original volumes mainly due to the partial volume effect (PVE). The effect of PVE was controlled by using the same scanner, standardizing the spatial resolution (0.331*0.331*0.200 mm) and keeping the same orientation and positions of conchs and umbilicus for every specimen. This procedure contributed to equalizing the contrast difference of the innermost thin septa and outer thick septa between scans. Although the artifacts remained, the PVE affects the scans more or less uniformly. Subsequently, we calculated the following parameters which have been classically used for ammonoid and nautiloid conch morphometry (Fig. 1; Klug et al. 2015): whorl expansion rate (WER) = (dm1/dm2)2; whorl width index = ww/dm1 (WWI). WER and WWI were plotted against conch diameter and PCV against chamber number.

It should be noted that measurements for the ear-

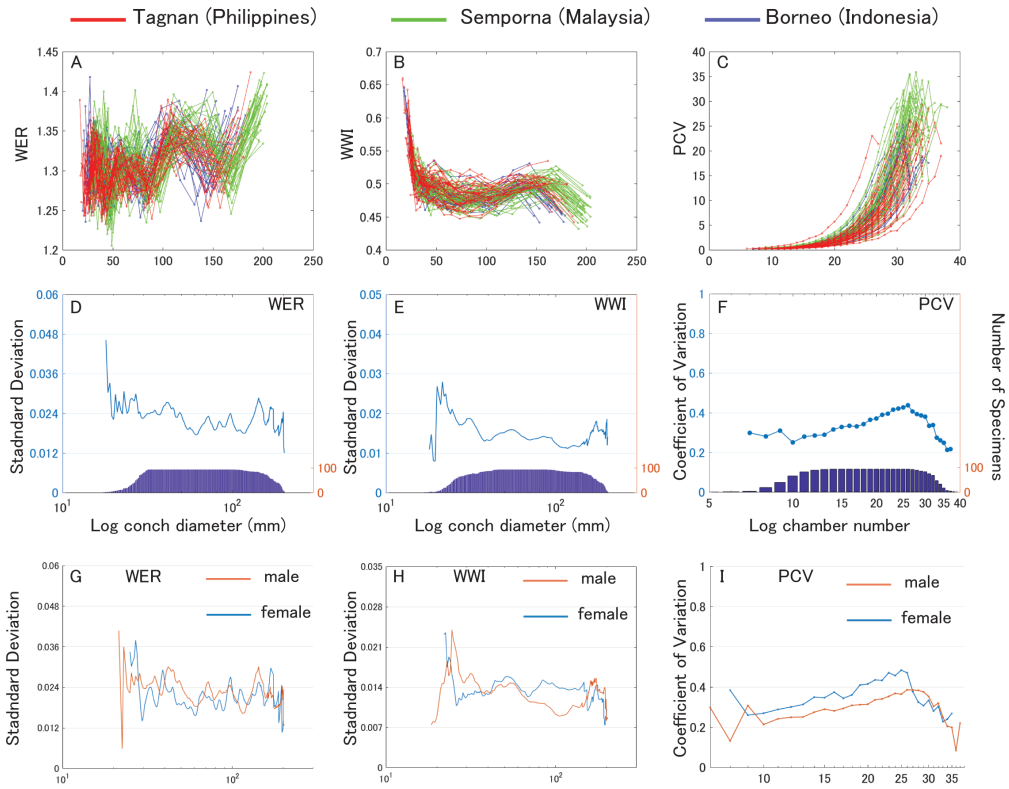

Fig. 2. Scatter plots of WER, WWI, and PCV and their intraspecific variation of *N. pompilius* through ontogeny from Philippines, Malaysia and Indonesia. Blue bar graphs represent the numbers of examined specimens (right y axis). A, Scatter plots of WER. B, Scatter plots of WWI. C, Scatter plots of PCV. D, Intraspecific variation (standard deviation) of WER. E, Intraspecific variation (standard deviation) of WWI. F, Intraspecific variation (coefficient of variation) of PCV. G, Intraspecific variation (standard deviation) of WER of males and females from all the examined populations. H, Intraspecific variation (standard deviation) of WWI of males and females from all the examined populations. I, Intraspecific variation (coefficient of variation) of PCV of males and females from all the examined populations.

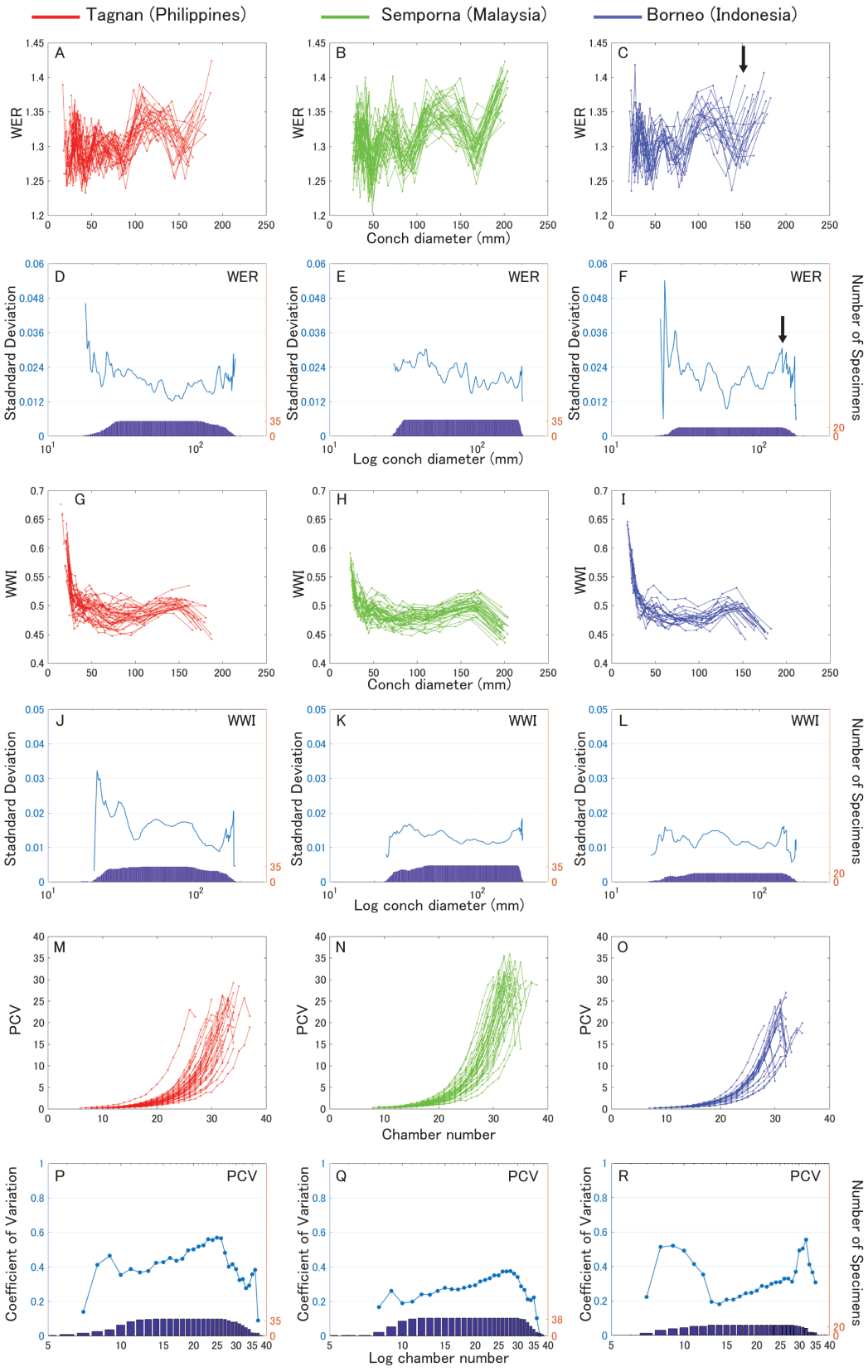
Tagnan (Philippines)
Semporna (Malaysia)
Borneo (Indonesia)
A
B
C
WER
Conch diameter (mm)
D
E
F
WER
Stadndard Deviation
Number of Specimens
Log conch diameter (mm)
G
H
I
WWI
J
K
L
M
N
O
PCV
Chamber number
P
Q
R
Coefficient of Variation
Log chamber number

← Fig. 3. Scatter plots of WER, WWI, and PCV and their intraspecific variation of *N. pompilius* through ontogeny with different populations plotted in different graphs. Blue bar graphs represent the numbers of examined specimens (right y axis). A, Scatter plots of WER in the population of the Philippines. B, Scatter plots of WER in the Malaysian population. C, Scatter plots of WER in the Indonesian population. Arrow indicates a growth change. D, Intraspecific variation (standard deviation) of WER in the population of the Philippines. E, Intraspecific variation (standard deviation) of WER in the Malaysian population. F, Intraspecific variation (standard deviation) of WER in the Indonesian population. Arrow indicates a spike, which corresponds with the growth change indicated in the Fig. 3C. G, Scatter plots of WWI in the population of the Philippines. H, Scatter plots of WWI in the Malaysian population. I, Scatter plots of WWI in the Indonesian population. J, Intraspecific variation (standard deviation) of WWI in the population of the Philippines. K, Intraspecific variation (standard deviation) of WWI in the Malaysian population. L, Intraspecific variation (standard deviation) of WWI in the Indonesian population. M, Scatter plots of PCV in the population of the Philippines. N, Scatter plots of PCV in the Malaysian population. O, Scatter plots of PCV in the Indonesian population. P, Intraspecific variation (coefficient of variation) of PCV in the population of the Philippines. Q, Intraspecific variation (coefficient of variation) of PCV in the Malaysian population. R, Intraspecific variation (coefficient of variation) of PCV in the Indonesian population.

liest ontogenetic stages are often missing (<20-30 mm in conch diameter; volumes until 10th chambers) because the scan resolution is not high enough to trace such small parts of the conch. In order to evaluate these data of WER and WWI, a series of calculations was performed. Each data point of one parameter of one species was used to create a series of equidistant data points. We produced these equidistant data in a distance of 0.5 mm using linear interpolation between two succeeding data points which allow us to compare the specimens at small increment size classes. In this study, standard deviation of WER and WWI and coefficient of variation of PCV are used as indices of intraspecific variation based on the level of measurement of our data (Stevens 1946). Standard deviation and coefficient of variation were computed at each size class and then plotted against diameter with a log scale to take the logarithmic growth of *Nautilus* into account.

As mentioned, ontogenetic data with a sufficient number of specimens is still rare in fossil cephalopods. In order to compare our results of *Nautilus* with ammonoids, we measured conch parameters of 24 specimens of the late Emsian (Devonian) ammonoid, Sellanarcestes tenuior through ontogenety. The specimens were collected from the same stratigraphic interval in Anti-Atlas of Morocco. Cross sections were produced to calculate WER and WWI. Also, intraspecific variation of septal spacing in a Jurassic belemnite Passaloteuthis laevigata, which was examined in Wani et al. (submitted) was compared as an example of phragmocone-bearing coleoids.

Results

WER, WWI, and PCV and the corresponding intraspecific variation of all the examined specimens through ontogeny are shown in Fig. 2 and Supplementary Table. Differences in intraspecific variation between the two sexes are shown in Fig. 2G, H, and I. WER, WWI, and PCV and the respective intraspecific variation were compared between the three populations from the Philippines, Malaysia, and Indonesia in Fig. 3. Overall, WER and WWI fluctuate with the same pattern in all populations (Fig. 3A, B, C). The difference occurs mainly in the timing of growth changes. On the one hand, the Malaysian population shows a rapid increase in WER at the conch diameter of around 170 mm (Fig. 3B), while on the other hand, the growth change before maturity (morphologic countdown) takes place at a smaller diameter (around 140-150 mm; Fig. 3A, C) in the populations with smaller conch diameter from the Philippines and Indonesia. As far as the intraspecific variation is concerned, it changes throughout ontogeny to different degrees, depending on the parameter and population. As mentioned in the method section, the number of specimens that yield reliable measurements from early ontogenetic stages is not sufficient, which created artifacts such as a surge or sharp decline of variation in WWR and WWI at around 20 mm in conch diameter (Fig. 2D, E). A similar sharp increase or decrease occurs also at the last growth stage, which probably roots in various adult sizes of our specimens. Also, the degree of variation in WWI of the Malaysian and Indonesian populations (Fig. 3K, L)

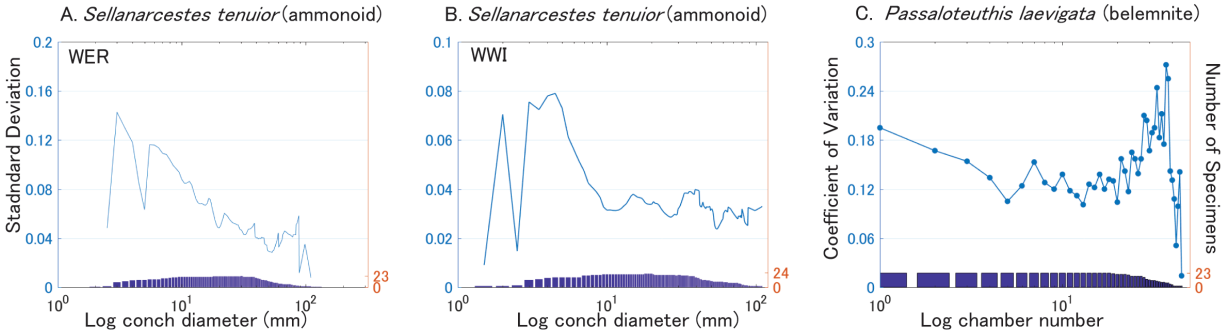

Fig. 4. Intraspecific variation of (A) WER and (B) WWI of the Devonian ammonoid *Sellanarcestes tenuior* and (C) septal spacing of the Jurassic belemnite *Passaloteuthis laevigata* (reproduced from the data in Wani et al. (submitted). Bar graphs represent the numbers of examined specimens (right y axis).

is less considerable than that of the WER (Fig. 3E, F). Although we could not examine the difference between males and females within a population due to the insufficient numbers of specimens to calculate standard deviation, males and females from all populations were compared. They demonstrate more or less the same pattern of variation.

Intraspecific variations of WER and WWI in the examined ammonoid and septal spacing in belemnites are shown in Fig. 4A, B and C. All graphs agree that intraspecific variation changes throughout ontogeny.

Discussion

Pattern of Intraspecific variation in Nautilus pompilius

Although, as discussed above, there are some errors and biases affecting our output, an overall pattern (or commonality) of variation in all the examined parameters through ontogeny between the three populations became evident: Our data show that the intraspecific variation starts with a relatively high degree during the earliest ontogeny, followed by a gradual decrease of variation until the middle to late ontogenetic stages. The hatching of *Nautilus* is known to coincide with the formation of the nepionic constriction which is a shell-thickening and a groove surrounding the (former) aperture from the umbilicus to the venter at around 26 mm in specimens with an average conch diameter (Arnold et al. 1987). The high variation at this stage is caused by the rather diverse size of hatchlings. Also, it is known that whorl section of *Nautilus* changes from a depressed to a more compressed form through ontogeny (Arnold et al. 1987). This shift toward the same conch morphology may reduce variation. There are also several spikes in variation through ontogeny. When variation is compared with the original scatter plots of each conch parameter, some of these spikes correspond with the timing of the growth changes, namely increasing and decreasing trends of the respective parameter (e.g., Fig. 3C, F). Delays, acceleration or differences in growth rates may affect the diameter at which the growth changes occur, depending on the individual, which resulted in these conspicuous spikes. Although it is not remarkable, it appears that *Nautilus* like ammonoids has several growth stages (Fig. 1 and 2) with varying conch parameters through ontogeny in addition to the well-documented embryonic and mature modification (Ward 1987; Klug 2004). By contrast, there are no striking differences between males and females (Fig. 2).

Intraspecific variation of ammonoids

As mentioned, there is not a sufficient number of studies with a great number of specimens on the intraspecific variation in ammonoids. Here, we show the example of intraspecific variation of WER and WWI of the late Emsian (Devonian) ammonoid, Sellanarcestes tenuior (Fig. 4A, B). In the graphs, the variation of WER and WWI starts with a very high value. It is likely that the variation is overestimated at the earliest ontogenetic stages due to the low sample numbers. Similarly, the low sample number probably blurred the real intraspecific variation at latest ontogenetic stages. The overall variation of WER, however, is rather similar to that of *Nautilus*. Around hatching, variation of the conchs of S. tenuior is relatively high. This is followed by a gradual decrease in variation until it starts increasing rapidly probably shortly before maturity (adult size of Sellanarcestes: about 100 mm; Klug 2001). The intraspecific variation of WWI (Fig. 4B) shows a similar trend. Variation is the highest before hatching, which decreases afterwards. Then, it fluctuates but more or less stays with the same values

until the end of ontogeny. Nevertheless, it should be noted that there are some biases in the results. First, although the specimens were collected from the same region (Anti-Atlas, Morocco) and the same stratigraphic interval, the results might still suffer from effects of time averaging (Kidwell 2002), i.e., there is a certain degree of mixing of specimens from different times, which equalizes a possible evolutionary or ecologically driven change of variation. In addition, we cannot exclude the effects of artifacts such as measurement errors, taphonomic biases, and the low sample number, which particularly affect the results obtained from small conch diameters.

As for other studies on intraspecifc variation of ammonoids, Jattiot et al. (2015) examined the Triassic ammonoid genus Anasibirites from Timor. In this study, measurements on a large number of specimens were taken in order to revise its species. Although ontogenetic data within a single specimen are missing in their study, intraspecific variation of some species was demonstrated. It appears that high variation appears at an early ontogenetic stage, followed by lower variation at later ontogenetic stages. In addition, De Baets et al. (2013) addressed intraspecific variation with ontogenetic data of a relatively large sample size. They showed intraspecific variation of the two loosely coiled Early Emsian ammonoid genera Anetoceras and Erbenoceras. They demonstrated various patterns of intrageneric variation in their figure 2. For instance, the variation of the whorl height index (WHI) and umbilical width index (UWI) in Erbenoceras appears to be slightly higher in the middle ontogenetic stages (at the diameter from 50 to 90 mm) than in early and late ontogenetic stages. By contrast, intrageneric variation of Anetoceras seems high at early ontogenetic stages with some decrease in the later ontogenetic stages as in *N. pompilius*. Korn and Klug (2007) examined the Devonian ammonoid Manticoceras. Their results also do not exactly agree with our results probably because many of the examined specimens were not measured through ontogeny within a single specimen. It is also highly likely that different ammonoids have different patterns of intraspecific variation because ontogenetic trajectories also differ quite significantly (e.g., Klug 2001).

Given the results demonstrated above and those of earlier studies, there appear to be commonalities in the pattern of intraspecific variation through ontogeny at least in some groups of ammonoids and nautiloids. Nevertheless, since the ammonoids are both morphologically and stratigraphically diverse, further studies are needed.

Intraspecific variation of belemnites

The hard parts of belemnites also grew by accretion; phragmocone and proostracum grew at the anterior edge and by the addition of septa, while the rostrum grew by the addition of calcium carbonate to its complete outer surface. The structure which contains the most easily readable information on belemnite ontogeny is the phragmocone, even though we know only few on its intraspecific variation. However, new data from Wani et al. (submitted) give us some insight into the intraspecific variation. They measured septal spacing of 23 specimens of the Jurassic belemnite Passaloteuthis laevigata from Buttenheim, Germany. We reproduced the coefficient variation of the septal spacing calculated in Wani et al. (submitted) through ontogeny here (Fig. 4C). Although the graph shows a slight fluctuation throughout ontogeny, the general pattern is quite similar to those of *N. pompilius* and some ammonoids. The intraspecific variation begins with a relatively high value at the first chamber, which declines until the 6th chamber. It then stays more or less at around 12 until the 18th chamber at which a rapid increase starts. In this study, only low numbers of specimens are available at the latest ontogeny of the preserved phragmocone, which might have caused excessive increase and decrease at the latest ontogenetic stages. It is likely that at least some groups of belemnites share a similar pattern of intraspecific variation of those in nautiloids and ammonoids. As mentioned before, however, further investigation is necessary since there are only limited data on intraspecific variation of belemnites.

Summary

With the new data from 3D morphometry of the Recent nautilid *Nautilus pompilius* of the three different geographic populations, we can now answer the questions listed in the introduction section.

1) Phenotypic intraspecific variation of Recent *Nautilus*:–Intraspecific variation of *N. pompilius* changes throughout ontogeny in males and females from three different geographic populations. The degree of intraspecific variation can be considerably high in some ontogenetic stages.

2) Changes in intraspecific variation through ontogeny:–Although there are slight differences, there is a commonality in the pattern of intraspecific variation. Intraspecific variation in all examined parameters tends to start with high values, which is followed by a decreasing phase of variation. Then, it increases again to reach high variation before maturity. There is sometimes a sharp increase or de-

cline at the latest ontogenetic stage, which may have resulted from low sample sizes. The increase or decrease may have happened around growth changes due to the fact that in different individuals growth change occurred at slightly differing sizes (conch diameters).

3) Does the intraspecific variation vary, depending on some populations?¬–The degree of variation differs between three geographic populations from the Philippines, Malaysia, and Indonesia. There is also a difference in the timing of increase or decrease of variation during ontogeny, which probably resulted from different conch sizes and timing when growth changes occurred in the individuals of these populations.

4) Is the pattern of the intraspecific variation of *Nautilus* similar to or different from those of other cephalopods?–Some ammonoid groups and a belemnite taxon show patterns of intraspecific variation resembling those of *N. pompilius*. Although different taxa have different details of intraspecific variation through ontogeny, there may be at least some groups of cephalopods which share a similar pattern of intraspecific variation. Further investigation is needed to better understand intraspecific variations of various cephalopod groups through ontogeny.

Acknowledgements

This study was kindly supported by the Swiss National Science Foundation (project numbers: 200020_169847 and 200021_149119). We thank Yusuke Takamatsu and Marc Scherrer (both Zurich) for their help with CT-scanning. René Hoffmann (Bochum) kindly lent us a silica sphere for CT-scanning. The stimulating discussions with Christoph Zollikofer (Zurich) are greatly appreciated. Also, we appreciate the reviews of XXX and XXX.

References

Arnold, J. M., N. H. Landman, and H. Mutvei. 1987. Development of the embryonic shell of *Nautilus*. Pp. 373-400. *Nautilus* The Biology and Paleobiology of a Living Fossil. Springer.

Bert, D. 2014. Factors of intraspecific variability in ammonites, the example of Gassendiceras alpinum (d'Orbigny, 1850)(Hemihoplitidae, Upper Barremian). Pp. 217-236. Annales de Paléontologie. Elsevier.

Bonnaud, L., C. Ozouf-Costaz, and R. Boucher-Rodoni. 2004. A molecular and karyological approach to the taxonomy of *Nautilus*. Comptes Rendus Biologies 327(2):133-138.

Bush, A. M., and R. K. Bambach. 2015. Sustained Mesozoic–Cenozoic diversification of marine Metazoa: A consistent signal from the fossil record. Geology 43(11):979-982.

Dagys, A., and W. Wetschat. 1993. Extensive intraspecific variation in a Triassic ammonoid from Siberia. Lethaia 26(2):113-121.

De Baets, K., D. Bert, R. Hoffmann, C. Monnet, M. M. Yacobucci, and C. Klug. 2015. Ammonoid intraspecific variability. Pp. 359-426. In C. Klug, D. Korn, K. De Baets, I. Kruta, and R. H. Mapes, eds. Ammonoid Paleobiology: from anatomy to ecology. Springer.

De Baets, K., C. Klug, and C. Monnet. 2013. Intraspecific variability through ontogeny in early ammonoids. Paleobiology 39(1):75-94.

Dzik, J. 1985. Typologic versus population concepts of chronospecies: implications for ammonite biostratigraphy. Acta Palaeontologica Polonica 30(1-2).

Dzik, J. 1990. The concept of chronospecies in ammonites. Pp. 25-30. In F. Cecca, S. Cresta, G. Pallini, and M. Santantonio, eds. Atti del Secondo Convegno Internazionale Fossili, Evoluzione, Ambiente, Pergola.

Hoffmann, R., J. A. Schultz, R. Schellhorn, E. Rybacki, H. Keupp, S. R. Gerden, R. Lemanis, and S. Zachow. 2014. Non-invasive imaging methods applied to neo- and paleo-ontological cephalopod research. Biogeosciences 11(10):2721-2739.

Hohenegger, J., and F. Tatzreiter. 1992. Morphometric methods in determination of ammonite species, exemplified through Balatonites shells (Middle Triassic). Journal of Paleontology 66(05):801-816.

House, M. 1981. Early ammonoids in space and time. Pp. 359-367. In M. House, and J. Senior, eds. The Ammonoidea: the Evolution, Classification, Mode of Life and Geological Usefulness of a Major Fossil Group. Systematics Association Special. Academic Press.

House, M. 1985. The ammonoid time-scale and ammonoid evolution. Geological Society, London, Memoirs 10(1):273-283.

House, M., and W. Kerr. 1989. Ammonoid Extinction Events [and Discussion]. Philosophical Transactions of the Royal Society of London B: Biological Sciences 325(1228):307-326.

Hughes, N. C., and C. C. Labandeira. 1995. The stability of species in taxonomy. Paleobiology 21(04):401-403.

Jattiot, R., H. Bucher, A. Brayard, C. Monnet, J. F.

Jenks, and M. Hautmann. 2015. Revision of the genus Anasibirites Mojsisovics (Ammonoidea): an iconic and cosmopolitan taxon of the late Smithian (Early Triassic) extinction. Papers in Palaeontology.

Kennedy, W. 1989. Thoughts on the evolution and extinction of Cretaceous ammonites. Proceedings of the Geologists' Association 100(3):251-279.

Kennedy, W., and C. Wright. 1985. Evolutionary patterns in Late Cretaceous ammonites. Spe. Pap. Palaeont. 33:131-143.

Kennedy, W. J. 1977. Ammonite evolution. Pp. 251-304. In A. Hallam, ed. Patterns of Evolution. Elsevier, Amsterdam.

Kennedy, W. J., and W. Cobban. 1976. Aspects of ammonite biology, biogeography, and biostratigraphy. Special Papers in Palaeontoly 17:1-94.

Kidwell, S. M. 2002. Time-averaged molluscan death assemblages: palimpsests of richness, snapshots of abundance. Geology 30(9):803-806.

Klug, C. 2001. Life-cycle of Emsian and Eifelian ammonoids (Devonian). . Lethaia 34:18.

Klug, C. 2004. Mature modifications, the black band, the black aperture, the black stripe, and the periostracum in cephalopods from the Upper Muschelkalk (Middle Triassic, Germany). Mitteilungen aus dem Geologisch-Paläontologischen Institut der Universität Hamburg 88:63-78.

Klug, C., D. Korn, N. H. Landman, K. Tanabe, K. De Baets, and C. Naglik. 2015. Describing ammonoid conchs. Pp. 3-24. In C. Klug, D. Korn, K. De Baets, I. Kruta, and R. H. Mapes, eds. Ammonoid Paleobiology: From anatomy to ecology. Springer.

Korn, D., and C. Klug. 2007. Conch form analysis, variability, morphological disparity, and mode of life of the Frasnian (Late Devonian) ammonoid Manticoceras from Coumiac (Montagne Noire, France). Pp. 57-85. In N. H. Landman, R. A. Davis, and R. H. Mapes, eds. Cephalopods present and past: new insights and fresh perspectives. Springer, Dordrecht.

Korn, D., C. Klug, and S. A. Walton. 2015. Taxonomic Diversity and Morphological Disparity of Paleozoic Ammonoids. Pp. 431-464. In C. Klug, D. Korn, K. De Baets, I. Kruta, and R. H. Mapes, eds. Ammonoid Paleobiology: From macroevolution to paleogeography. Springer, Dordrecht.

Monnet, C., H. Bucher, M. Wasmer, and J. Guex. 2010. Revision of the genus Acrochordiceras Hyatt, 1877 (Ammonoidea, Middle Triassic): morphology, biometry, biostratigraphy and intra-specific variability. Palaeontology 53(5):961-996.

Nardin, E., I. Rouget, and P. Neige. 2005. Tendencies in paleontological practice when defining species, and consequences on biodiversity studies. Geology 33(12):969-972.

Saunders, W. B. 1987. The species of *Nautilus*. Pp. 35-52. *Nautilus* The Biology and Paleobiology of a Living Fossil. Springer.

Saunders, W. B., Spinosa, C. 1978. Sexual dimorphism in *Nautilus* from Palau. Paleobiology 4:349-358.

Sepkoski, J. J., R. K. Bambach, D. M. Raup, and J. W. Valentine. 1981. Phanerozoic marine diversity and the fossil record. Nature 293(5832):435-437.

Sinclair, B., L. Briskey, W. Aspden, and G. Pegg. 2007. Genetic diversity of isolated populations of *Nautilus pompilius* (Mollusca, Cephalopoda) in the Great Barrier Reef and Coral Sea. Reviews in Fish Biology and Fisheries 17(2-3):223-235.

Stevens, S. S. 1946. On the theory of scales of measurement. Science 103 (2684):677-680.

Swan, A. R., and W. B. Saunders. 1987. Morphological variation in *Nautilus* from Papua New Guinea. *Nautilus*:85-103.

Tajika, A., P. Kürsteiner, A. Pictet, J. Lehmann, K. Tschanz, R. Jattiot, and C. Klug. 2017. Cephalopod associations and palaeoecology of the Cretaceous (Barremian–Cenomanian) succession of the Alpstein, northeastern Switzerland. Cretaceous Research 70:15-54.

Tajika, A., N. Morimoto, R. Wani, C. Naglik, and C. Klug. 2015. Intraspecific variation of phragmocone chamber volumes throughout ontogeny in the modern nautilid *Nautilus* and the Jurassic ammonite *Normannites.* PeerJ 3:e1306.

Tanabe, K., S. Hayasaka, T. Saisho, A. Shinomiya, and K. Aoki. 1983. Morphologic variation of *Nautilus pompilius* from the Philippines and Fiji islands. Studies of *Nautilus pompilius* and its associated fauna from Tanon Strait, the Philippines. Occas. Pap (1):9-21.

Tanabe, K., S. Hayasaka, and J. Tsukahara. 1985. Morphological analysis of *Nautilus pompilius*. Kagoshima University Research Center for the South Pacific, Occasional Papers 4:38-49.

Tanabe, K., and Y. Shigeta. 1987. Ontogenetic shell variation and streamlining of some Cretaceous ammonites. Pp. 165-179. Transactions and proceedings of the Paleontological Society of Japan. New series. Palaeontological Society of Japan.

Vandepas, L. E., F. D. Dooley, G. J. Barord, B. J. Swalla, and P. D. Ward. 2016. A revisited phylogeography of *Nautilus pompilius.* Ecology and Evolution 6(14):4924-4935.

Wani, R., and K. Ayyasami. 2009. Ontogenetic change and intra-specific variation of shell morphology in the Cretaceous nautiloid (Cephalopoda, Mollusca) Eutrephoceras clementinum (d'Orbigny, 1840) from the Ariyalur area, southern India. Journal of Paleontology 83(3):365-378.

Wani R. A. Tajika, K. Ikuno, T. Iwasaki. (submitted). Ontogenetic change of septal distance of early Jurassic belemnites from Germany and France. Paleontology.

Ward, P. 1987. The natural history of. *Nautilus*:1-267.

Wray, C. G., N. H. Landman, W. B. Saunders, and J. Bonacum. 1995. Genetic divergence and geographic diversification in *Nautilus.* Paleobiology 21(02):220-228.

Measurements (DM, WW, WER and WWI) of *Nautilus pompilius* from the Philippines

7

DM	WW	WER	WWI
26.724	14.858	NaN	0.5559796
30.931	16.072	1.3396304	0.5196082
34.796	17.515	1.265525	0.5033625
38.75	19.583	1.2401801	0.5053677
44.143	21.861	1.2977178	0.4952314
50.278	23.722	1.2972757	0.4718167
57.043	26.864	1.287208	0.470943
63.89	30.147	1.2544723	0.4718579
73.432	34.286	1.3210064	0.4669082
82.186	39.016	1.2526362	0.4747281
92.781	44.379	1.2744489	0.4783199
105.977	50.972	1.3046834	0.4809723
122.574	59.286	1.3377454	0.4836752
140.548	69.29	1.3147786	0.4929988
158.58	79.408	1.2730559	0.5007441
186.117	83.889	1.3774482	0.4507326

8

DM	WW	WER	WWI
21.432	13.772	NaN	0.6425905
24.966	14.135	1.3569771	0.56617
28.738	14.483	1.3249978	0.5039669
32.134	16.533	1.2503065	0.5145018
37.276	18.831	1.3456404	0.5051776
42.614	22.074	1.306911	0.5179988
48.859	24.828	1.3145725	0.5081561
55.749	28.4	1.3019221	0.5094262
63.897	31.948	1.3136715	0.4999922
73.086	35.63	1.3083003	0.4875079
82.652	40.69	1.2789052	0.4923051
94.967	47.515	1.3201969	0.5003317
111.169	54.286	1.3703199	0.4883196
128.923	65.363	1.3449106	0.5069925
147.415	74.598	1.3074423	0.5060408
171.742	81.467	1.3572807	0.4743569

10

DM	WW	WER	WWI
24.109	13.526	NaN	0.5610353
27.492	14.188	1.3003321	0.5160774
31.666	16.54	1.3267031	0.5223268
35.939	18.369	1.2880881	0.5111161
40.668	20.397	1.2804825	0.5015491
45.913	23.054	1.2745759	0.5021236
52.447	25.777	1.3048782	0.4914866
59.546	29.796	1.2890325	0.5003863
66.891	32.715	1.2619153	0.4890792
76.749	37.34	1.3164673	0.486521
86.297	42.905	1.2642878	0.4971783
99.705	49.524	1.3348808	0.4967053
113.378	56.954	1.293075	0.5023373
132.02	66.601	1.3558819	0.5044766
149.723	75.233	1.2861677	0.5024812
174.999	80.137	1.3661365	0.4579283

11

DM	WW	WER	WWI
21.515	13.388	NaN	0.6222635
24.968	13.395	1.3467433	0.5364867
28.311	14.973	1.2857097	0.5288757
32.766	17.282	1.3394806	0.527437
36.892	19.339	1.2677031	0.5242058
41.763	21.376	1.2815011	0.5118406
47.214	24.372	1.2780805	0.5162028
54.355	28.214	1.3253708	0.5190691
61.997	30.81	1.3009552	0.4969595
70.285	35.321	1.2852392	0.5025397
79.344	40	1.2743916	0.5041339
91.683	45.46	1.3352096	0.4958389
106.777	53.015	1.3563688	0.4965021
122.937	62.936	1.3255917	0.511937
140.547	72.241	1.3070071	0.5139989
163.302	76.952	1.3500189	0.4712251

12

DM	WW	WER	WWI
23.485	12.817	NaN	0.5457526
26.572	13.715	1.2801692	0.5161448
30.255	15.688	1.2964203	0.5185259
34.736	17.779	1.3181514	0.5118321
39.228	19.64	1.2753598	0.5006628
44.191	22.007	1.26904	0.4979973
50.421	25.006	1.3018329	0.4959442
56.961	28.148	1.2762398	0.4941627

15

DM	WW	WER	WWI
24.086	13.729	NaN	0.5699992
27.651	14.392	1.3179299	0.5204875
31.529	16.307	1.3001657	0.5172064
36.36	19.029	1.3299256	0.5233498
41.142	20.44	1.2803333	0.4968159
46.498	23.077	1.2773142	0.4963009
53.248	26.589	1.3114087	0.4993427
61.126	30.249	1.3177874	0.4948631

Measurements (DM, WW, WER and WWI) of *Nautilus pompilius* from the Philippines (continued)

64.777	31.097	1.2932618	0.4800624
74.191	34.952	1.3117793	0.4711084
83.81	39.552	1.2761133	0.4719246
94.823	46.091	1.2800758	0.4860741
110.326	52.258	1.3537185	0.4736689
127.619	62.095	1.338058	0.4865655
143.979	70.028	1.2728219	0.4863765
165.517	75.72	1.3215601	0.4574757

69.584	33.384	1.2958861	0.4797655
79.06	37.501	1.2909067	0.4743359
89.022	43.213	1.2678885	0.4854193
104.939	50.14	1.3895659	0.4778014
120.705	58.765	1.3230513	0.4868481
140.419	69.329	1.3533223	0.4937295
157.173	78.288	1.2528646	0.4981008
187.555	82.802	1.4239719	0.4414812

16

DM	WW	WER	WWI
25.464	13.728	NaN	0.539114
29.332	14.88	1.3268753	0.5072958
32.905	16.888	1.258463	0.5132351
37.476	18.526	1.2971275	0.494343
42.968	21.296	1.3145703	0.4956247
48.625	24.045	1.2806456	0.4944987
53.702	27.156	1.2197243	0.5056795
61.687	30.748	1.3194908	0.4984519
70.283	34.499	1.2981153	0.4908584
80.001	38.867	1.2956576	0.4858314
89.052	43.114	1.2390719	0.4841441
102.737	50.279	1.3309643	0.4893953
118.897	58.985	1.3393313	0.4961017
138.551	70.658	1.3579305	0.5099783
157.431	80.258	1.2911039	0.5097979
180.632	90.257	1.3164637	0.4996734

17

DM	WW	WER	WWI
24.568	13.156	NaN	0.5354933
28.367	14.395	1.3331752	0.5074558
32.053	16.638	1.2767638	0.5190778
36.772	18.669	1.316125	0.5076961
41.563	20.747	1.277554	0.4991699
47.527	23.386	1.3075763	0.4920571
53.46	27.281	1.2652522	0.5103068
60.773	30.457	1.2923003	0.5011601
69.053	34.074	1.291052	0.4934471
78.73	38.852	1.2999163	0.4934841
88.808	44.775	1.2724	0.5041776
101.053	50.621	1.2947748	0.5009352
117.446	57.537	1.3507595	0.4899017
135.9	68.069	1.3389441	0.5008756
157.064	78.566	1.3357168	0.5002165
180.246	89.976	1.3169763	0.4991844

20

DM	WW	WER	WWI
14.556	9.846	NaN	0.6764221
17.156	NaN	0.9178103	NaN
19.593	11.158	1.3592433	0.5694891
21.497	12.128	1.378436	0.5641717
25.044	12.846	1.1340331	0.5129372
28.441	13.945	1.1831258	0.4903133
32.514	16.258	1.2891646	0.5000308
36.046	19.088	1.3152172	0.5295456
41.382	20.327	2.0660443	0.4912039
46.973	22.11	0.5974062	0.4706959
53.855	25.104	1.2720962	0.4661406
61.173	28.79	1.3743703	0.4706325
69.566	31.985	2.7056874	0.4597792
78.716	36.075	1.2803596	0.4582931
89.274	42.292	1.2862458	0.4737326
104.04	NaN	1.3581593	NaN

23

DM	WW	WER	WWI
15.754	NaN	NaN	NaN
17.918	NaN	1.2935922	NaN
20.593	12.621	1.3208703	0.6128782
23.209	13.02	1.2702044	0.5609893
26.3	13.665	1.2840994	0.5195817
29.377	15.169	1.2476805	0.5163563
34.058	17.723	1.3440747	0.520377
38.469	19.701	1.2758027	0.5121266
43.52	22.598	1.2798409	0.5192555
48.833	25.417	1.2590676	0.5204882
56.197	29.153	1.3243399	0.5187643
64.485	33.61	1.3167131	0.5212065
73.553	37.937	1.3010182	0.5157777
83.668	42.591	1.2939515	0.5090477
95.481	49.154	1.3023123	0.514804
111.163	NaN	1.3554597	NaN

Measurements (DM, WW, WER and WWI) of *Nautilus pompilius* from the Philippines (continued)

24

DM	WW	WER	WWI
17.385	NaN	NaN	NaN
19.877	12.105	1.3072308	0.6089953
22.164	NaN	1.2433535	NaN
24.942	13.622	1.2663865	0.5461471
28.554	14.593	1.3106036	0.5110668
32.575	16.316	1.3014723	0.5008749
36.647	18.209	1.2656336	0.4968756
41.101	20.229	1.2578473	0.4921778
46.808	23.895	1.2969863	0.5104897
53.238	26.513	1.2936098	0.4980089
59.93	30.075	1.2671998	0.5018355
68.488	33.709	1.3059917	0.4921884
77.908	37.5	1.2940026	0.481337
88.035	42.566	1.2768698	0.4835122
99.929	49.179	1.2884642	0.4921394
115.964	NaN	1.3466765	NaN

25

DM	WW	WER	WWI
16.552	10.881	NaN	0.6573828
18.581	11.358	1.2601934	0.6112696
20.851	NaN	1.2592606	NaN
23.944	13.363	1.3186806	0.5580939
27.59	13.722	1.3277307	0.4973541
31.054	15.056	1.266869	0.4848329
35.16	17.387	1.2819251	0.4945108
39.773	19.387	1.279614	0.4874412
45.595	21.84	1.3141887	0.4789999
51.595	23.914	1.2805036	0.4634945
59.013	27.654	1.3082181	0.4686086
66.894	31.121	1.2849285	0.4652286
76.936	35.249	1.3227716	0.45816
86.325	39.57	1.2589659	0.458384
99.161	46.914	1.3194977	0.4731094
114.156	NaN	1.3253046	NaN

26

DM	WW	WER	WWI
18.966	NaN	NaN	NaN
21.316	11.569	1.2631646	0.5427378
24.139	12.578	1.2824107	0.5210655
27.425	NaN	1.2907874	NaN
31.393	15.087	1.3103049	0.4805848
35.512	17.11	1.2796306	0.481809
40.242	19.284	1.2841296	0.4792008
45.376	21.612	1.2714325	0.476287
51.018	23.851	1.2641379	0.4675017
57.925	26.228	1.2890959	0.4527924
65.258	29.572	1.2692157	0.4531552
73.629	32.914	1.2730055	0.4470249
83.148	37.516	1.2752808	0.4511955
95.819	43.404	1.3280048	0.4529791
110.637	51.507	1.3332068	0.4655495
126.894	NaN	1.3154713	NaN

27

DM	WW	WER	WWI
18.224	11.068	NaN	0.607331
20.814	NaN	1.3044387	NaN
23.844	13.542	1.3123423	0.5679416
27.28	14.176	1.3089724	0.5196481
30.961	15.687	1.2880752	0.5066697
35.455	17.681	1.3113693	0.4986885
39.566	20.175	1.2453439	0.5099075
45.365	23.065	1.3146118	0.5084316
52.263	26.149	1.327232	0.5003348
58.974	29.596	1.2733052	0.5018483
66.992	33.013	1.2904011	0.4927902
76.935	38.239	1.3188701	0.49703
87.549	43.838	1.2949544	0.5007253
101.364	50.432	1.3404947	0.4975336
117.033	NaN	1.3330585	NaN

28

DM	WW	WER	WWI
17.617	11.401	NaN	0.647159
20.378	NaN	1.3380095	NaN
22.753	13.359	1.2466778	0.5871314
25.841	14.235	1.2898562	0.5508688
29.143	13.98	1.271891	0.4797035
33.401	15.861	1.3135615	0.474866
37.894	18.941	1.2871287	0.4998417
42.416	21.01	1.2529061	0.495332
48.121	23.839	1.2870928	0.495397

30

DM	WW	WER	WWI
20.285	11.534	NaN	0.5685975
22.964	12.62	1.281578	0.5495558
25.882	13.137	1.2702833	0.5075728
30	13.786	1.3435284	0.4595333
34.022	15.805	1.2861072	0.4645523
38.191	18.366	1.2600924	0.4808986
43.041	20.398	1.2701138	0.4739202
49.831	23.623	1.3404002	0.4740623
56.162	25.928	1.2702404	0.4616645

Measurements (DM, WW, WER and WWI) of *Nautilus pompilius* from the Philippines (continued)

54.891	26.81	1.3011669	0.4884225
62.603	30.262	1.3007325	0.4833954
71.04	34.486	1.2877027	0.4854448
81.051	39.539	1.3016998	0.4878287
92.314	45.241	1.2972342	0.4900773
106.206	52.586	1.3236189	0.4951321
122.691	NaN	1.3345268	NaN

64.049	29.631	1.3005875	0.4626302
72.519	33.333	1.2819731	0.4596451
83.22	37.522	1.316897	0.4508772
95.311	42.753	1.3116883	0.4485631
110.294	51.362	1.3391145	0.4656826
126.099	60.49	1.3071322	0.4797025
145.091	72.542	1.3239076	0.4999759

31

DM	WW	WER	WWI
20.285	11.534	NaN	0.5685975
22.964	12.62	1.281578	0.5495558
25.882	13.137	1.2702833	0.5075728
30	13.786	1.3435284	0.4595333
34.022	15.805	1.2861072	0.4645523
38.191	18.366	1.2600924	0.4808986
43.041	20.398	1.2701138	0.4739202
49.831	23.623	1.3404002	0.4740623
56.162	25.928	1.2702404	0.4616645
64.049	29.631	1.3005875	0.4626302
72.519	33.333	1.2819731	0.4596451
83.22	37.522	1.316897	0.4508772
95.311	42.753	1.3116883	0.4485631
110.294	51.362	1.3391145	0.4656826
126.099	60.49	1.3071322	0.4797025
145.091	72.542	1.3239076	0.4999759

32

DM	WW	WER	WWI
20.285	11.534	NaN	0.5685975
22.964	12.62	1.281578	0.5495558
25.882	13.137	1.2702833	0.5075728
30	13.786	1.3435284	0.4595333
34.022	15.805	1.2861072	0.4645523
38.191	18.366	1.2600924	0.4808986
43.041	20.398	1.2701138	0.4739202
49.831	23.623	1.3404002	0.4740623
56.162	25.928	1.2702404	0.4616645
64.049	29.631	1.3005875	0.4626302
72.519	33.333	1.2819731	0.4596451
83.22	37.522	1.316897	0.4508772
95.311	42.753	1.3116883	0.4485631
110.294	51.362	1.3391145	0.4656826
126.099	60.49	1.3071322	0.4797025
145.091	72.542	1.3239076	0.4999759

33

DM	WW	WER	WWI
NaN	NaN	NaN	NaN
20.833	12.476	NaN	0.5988576
23.696	13.694	1.2937384	0.5779034
26.5	14.403	1.2506669	0.5435094
30.98	14.542	1.3666933	0.4693996
34.949	17.233	1.2726433	0.4930899
40.275	19.64	1.3280108	0.4876474
45.403	22.527	1.2708609	0.4961566
52.11	25.647	1.3172647	0.4921704
58.832	28.709	1.2746328	0.4879827
66.941	32.523	1.2946643	0.4858457
76.9	37.101	1.3196789	0.4824577
87.48	42.661	1.2940912	0.4876658
100.34	48.733	1.3156205	0.4856787
115.773	58.784	1.3312707	0.5077522
134.005	NaN	1.3397613	NaN

34

DM	WW	WER	WWI
18.926	NaN	NaN	NaN
21.759	12.195	1.3217831	0.5604577
24.388	13.048	1.2562455	0.5350172
27.605	13.563	1.2812183	0.491324
32.043	15.197	1.3473823	0.474269
37.055	17.505	1.3372952	0.4724059
41.531	19.525	1.2561779	0.4701307
47.109	22.564	1.2866576	0.4789743
54.301	25.701	1.3286417	0.4733062
61.638	28.639	1.2884911	0.4646322
70.491	32.286	1.3078871	0.4580159
80.17	36.53	1.2934702	0.4556567
92.043	42.796	1.3181285	0.4649566
105.281	49.652	1.3083335	0.4716141
122.482	58.952	1.3534572	0.4813115
141.984	NaN	1.3437989	NaN

Measurements (DM, WW, WER and WWI) of *Nautilus pompilius* from the Philippines (continued)

35

DM	WW	WER	WWI
16.674	11.002	NaN	0.6598297
19.078	NaN	1.30914	NaN
21.27	13.007	1.2429947	0.6115186
24.582	13.334	1.3356709	0.5424294
28.219	14.136	1.3177979	0.5009391
32.27	16.031	1.3077198	0.4967772
36.246	18.49	1.2616016	0.5101253
41.159	20.956	1.2894647	0.5091475
46.613	23.52	1.2825801	0.5045803
53.546	26.598	1.3195929	0.4967318
60.661	29.776	1.2834089	0.490859
69.573	34.4	1.3154136	0.4944447
79.267	38.611	1.2980858	0.4871006
91.067	44.326	1.3198884	0.4867405
105.049	51.79	1.3306437	0.493008
122.574	NaN	1.361485	NaN

36

DM	WW	WER	WWI
21.667	NaN	NaN	NaN
24.401	NaN	1.2682874	NaN
27.771	14.478	1.2952923	0.5213352
31.737	15.785	1.3060166	0.497369
36.351	18.098	1.3119008	0.497868
40.636	20.227	1.2496523	0.4977606
46.068	22.79	1.285218	0.4947035
52.135	25.288	1.2807372	0.4850484
60	27.937	1.3244749	0.4656167
67.487	31.383	1.2651375	0.4650229
77.27	36.717	1.3109363	0.4751779
87.6	41.533	1.2852464	0.474121
102.147	47.619	1.3596998	0.4661811
116.649	56.327	1.3040997	0.482876
134.683	65.662	1.3331024	0.48753
154.189	77.855	1.3106334	0.5049323

38

DM	WW	WER	WWI
20.651	NaN	NaN	NaN
23.612	14.224	1.3073244	0.6024056
27.237	14.705	1.3306168	0.5398906
31.327	16.311	1.3228758	0.5206691
35.942	18.091	1.3163363	0.5033387
40.899	20.05	1.2948543	0.490232
46.726	23.711	1.3052444	0.5074477
53.852	27.055	1.3282703	0.5023955
61.551	30.842	1.3063711	0.5010804
70.736	34.92	1.32072	0.4936666
81.032	39.43	1.312297	0.4865979
92.626	44.919	1.3066302	0.4849502
109.054	53.503	1.3861728	0.4906102
127.24	64.79	1.3613322	0.5091952
146.701	75.214	1.3292872	0.5127027
166.232	84.144	1.2839943	0.5061841

39

DM	WW	WER	WWI
23.361	13.335	NaN	0.5708232
26.52	13.438	1.2887367	0.5067119
30.81	NaN	1.3496972	NaN
34.952	17.557	1.286947	0.5023175
39.727	19.071	1.2918958	0.4800514
44.297	20.938	1.2433033	0.4726731
50.172	23.816	1.282845	0.4746871
57.349	27.185	1.3065585	0.4740274
65.35	29.792	1.2984926	0.4558837
73.54	34.272	1.2663567	0.4660321
83.502	39.643	1.2892778	0.4747551
96.061	45.503	1.3234284	0.4736886
110.746	52.011	1.329113	0.4696422
127.12	62.321	1.3175638	0.4902533
143.468	71.301	1.2737445	0.4969819
166.344	79.482	1.3443247	0.4778171

40

DM	WW	WER	WWI
23.291	13.555	NaN	0.5819845
26.263	14.15	1.2714884	0.5387808
30.06	14.802	1.3100543	0.4924152
34.86	16.898	1.3448592	0.484739
39.605	19.083	1.2907593	0.4818331
44.245	21.721	1.2480396	0.4909255
50.339	24.533	1.2944366	0.4873557
58.226	27.591	1.3379034	0.4738605
66.185	31.447	1.2920676	0.4751379
74.648	35.051	1.2720881	0.4695504

41

DM	WW	WER	WWI
25.292	NaN	NaN	NaN
28.483	NaN	1.2682507	NaN
32.002	17.093	1.2623587	0.5341229
36.211	18.808	1.2803444	0.5194002
41.941	19.862	1.3415181	0.47357
47.576	22.722	1.2867622	0.4775937
53.581	25.946	1.2683695	0.4842388
60.358	29.053	1.2689603	0.4813446
69.309	32.644	1.3185894	0.4709922
79.47	37.333	1.3147015	0.4697748

Measurements (DM, WW, WER and WWI) of *Nautilus pompilius* from the Philippines (continued)

84.576	39.775	1.2836834	0.4702871
97.235	46.601	1.321755	0.4792616
112.768	54.605	1.3450131	0.4842242
129.9	64.596	1.3269255	0.4972748
145.425	73.051	1.2533139	0.5023277
169.901	78.218	1.3649405	0.460374

89.213	43.152	1.2602301	0.4836963
101.825	48.715	1.3027244	0.4784189
118.269	57.474	1.3490654	0.48596
137.496	68.16	1.3515692	0.4957235
156.243	79.758	1.2912817	0.5104741
180.773	86.526	1.3386468	0.4786445

42

DM	WW	WER	WWI
22.972	13.333	NaN	0.5804022
26.924	14.135	1.3736673	0.5249963
30.592	15.575	1.2910307	0.50912
35.212	17.739	1.3248468	0.5037771
39.143	19.527	1.2357392	0.4988631
45.097	22.813	1.327355	0.5058651
50.925	26.331	1.2751661	0.5170545
58.124	28.875	1.3027135	0.4967827
65.597	33.14	1.2736701	0.505206
75.096	37.243	1.3105864	0.4959385
84.203	41.457	1.2572496	0.4923459
97.031	47.642	1.3279016	0.4909977
110.801	54.194	1.3039662	0.4891111
128.75	64.904	1.350228	0.5041087
144.314	72.381	1.2563842	0.5015522
166.741	80.388	1.3349588	0.482113

43

DM	WW	WER	WWI
20.157	NaN	NaN	NaN
22.832	13.242	1.283028	0.5799755
26.039	NaN	1.3006507	NaN
30.357	15.357	1.3591553	0.50588
34.354	17.18	1.2806691	0.5000873
39.134	20.47	1.2976389	0.5230746
44.83	22.899	1.3122875	0.5107963
51.429	25.357	1.3160691	0.4930487
58.754	28.827	1.3051449	0.4906389
67.405	32.616	1.316162	0.483881
77.063	36.644	1.3070963	0.4755071
86.966	42.321	1.2735241	0.4866385
101.129	48.047	1.3522358	0.4751061
117.354	57.717	1.3466179	0.4918196
135.226	67.822	1.3277754	0.5015456
153.041	78.393	1.2808409	0.5122353

44

DM	WW	WER	WWI
23.039	NaN	NaN	NaN
25.903	13.817	1.2640751	0.5334131
29.89	16	1.3315323	0.5352961
34.097	17.112	1.3013092	0.5018623
38.65	19.241	1.2848921	0.4978266
42.902	21.063	1.2321287	0.4909561
48.668	24.445	1.2868618	0.5022808
55.545	27.47	1.3025756	0.494554
63.641	30.633	1.3127561	0.4813406
72.194	34.879	1.2868509	0.4831288
82.009	39.333	1.2903895	0.4796181
92.771	44.94	1.2796802	0.4844186
108.708	51.393	1.3730885	0.4727619
124.366	60.87	1.3088212	0.4894425
143.175	70.556	1.3253514	0.4927955
161.447	80.602	1.271527	0.4992474

46

DM	WW	WER	WWI
21.35	13.089	NaN	0.6130679
24.213	14.095	1.2861791	0.5821253
27.44	15.208	1.2843134	0.5542274
31.402	17.328	1.3096233	0.551812
36.319	18.16	1.3376828	0.5000138
41.327	20.998	1.294792	0.508094
46.447	23.804	1.2631286	0.5124981
53.089	26.792	1.3064529	0.504662
61.187	29.284	1.3283399	0.4785984
69.882	33.529	1.3044046	0.4797945
79.837	38.185	1.3052021	0.478287
91.092	43.739	1.3018233	0.4801629
105.195	51.125	1.3336127	0.4860022
121.513	59.669	1.3343055	0.4910503
141.99	71.075	1.3654319	0.5005634
160.498	NaN	1.2776848	NaN

48

DM	WW	WER	WWI
22.91	12.689	NaN	0.5538629

51

DM	WW	WER	WWI
24.301	13.563	NaN	0.5581252

Measurements (DM, WW, WER and WWI) of *Nautilus pompilius* from the Philippines (continued)

25.975	13.051	1.285467	0.5024447
28.961	14.833	1.2431284	0.5121715
33.626	17.401	1.3481037	0.5174865
38.498	19.141	1.3107683	0.4971947
43.063	21.306	1.2512158	0.4947635
48.21	23.816	1.2533308	0.4940054
55.532	26.925	1.3268211	0.4848556
63.548	30.238	1.3095351	0.4758293
71.604	33.516	1.2696113	0.4680744
80.86	38.25	1.2752429	0.4730398
92.196	44.444	1.3000399	0.48206
108.172	50.538	1.376593	0.4672004
124.352	60.145	1.3215264	0.4836673
143.459	70.734	1.3309142	0.4930607
163.429	82.287	1.2977847	0.5035031
27.463	14.109	1.2771669	0.5137458
31.311	NaN	1.299864	NaN
35.383	17.126	1.2770133	0.4840177
40.689	19.866	1.3224057	0.4882401
45.758	22.793	1.2646782	0.4981205
52.215	24.869	1.3021365	0.4762808
58.566	28.414	1.2580577	0.485162
67.133	31.826	1.3139565	0.4740739
76.447	35.349	1.2967277	0.4623988
86.447	41.049	1.2787303	0.4748459
98.737	46.885	1.3045478	0.4748473
115.172	55.973	1.360611	0.4859949
133.501	67.287	1.3436162	0.5040187
150.787	76.704	1.27573	0.5086911
175.425	83.66	1.3534904	0.476899

53

DM	WW	WER	WWI
24.422	11.794	NaN	0.4829252
28.353	13.709	1.3478314	0.4835114
32.549	15.855	1.3178842	0.4871117
37.225	18.075	1.3079589	0.4855608
41.694	20.274	1.2545204	0.486257
46.93	22.371	1.266934	0.4766887
53.686	25.103	1.3086424	0.4675893
60.566	28.056	1.2727283	0.4632302
68.771	31.658	1.2892968	0.4603394
77.954	36.593	1.2848905	0.4694179
89.361	42.635	1.3140722	0.4771097
102.648	48.75	1.3194865	0.474924
117.397	56.713	1.3080159	0.4830873
135.124	66.301	1.324802	0.4906678
154.571	76.326	1.3085522	0.4937925
179.168	84.306	1.3435841	0.4705416

54

DM	WW	WER	WWI
22.506	NaN	NaN	NaN
25.122	14.348	1.2459821	0.5711329
28.46	15.21	1.283398	0.5344343
33.032	17.752	1.3471003	0.5374183
37.876	NaN	1.3147963	NaN
42.319	22.319	1.2483679	0.527399
47.638	25.508	1.267174	0.5354549
54.938	28.496	1.3299602	0.5186938
62.765	31.504	1.305237	0.5019358
71.256	35.469	1.2888661	0.4977686
80.215	40.737	1.2672675	0.5078477
91.776	46.878	1.3090224	0.5107871
107.032	52.875	1.3600943	0.4940111
124.253	63.855	1.3476791	0.5139111
141.688	74.752	1.3003264	0.5275817
161.414	86.286	1.2978254	0.5345633

56

DM	WW	WER	WWI
22.5	14.081	NaN	0.6258222
26.019	14.371	1.337261	0.5523271
29.495	15.518	1.2850369	0.5261231
34.286	18.095	1.3512535	0.5277664
38.69	20.27	1.273397	0.523908
43.951	23.051	1.2904467	0.5244704
49.835	26.382	1.2856756	0.529387
57.551	29.66	1.3336345	0.515369
65.53	33.687	1.2965062	0.5140699
74.049	37.932	1.2769034	0.5122554
83.622	43.633	1.2752716	0.5217885
98.3	50.034	1.381866	0.5089929
112.896	56.316	1.319016	0.4988308
130.039	66.797	1.3267532	0.513669
149.4	75.517	1.3199393	0.5054685
175.239	80.204	1.3758159	0.4576835

Measurements (DM, WW, WER and WWI) of *Nautilus pompilius* from Malaysia

1

DM	WW	WER	WWI
26.477	14.65	NaN	0.5533104
30.881	15.922	1.3603328	0.5155921
35.235	18.043	1.3018647	0.5120761
40.505	20.216	1.3215047	0.4990989
45.055	22.626	1.2372821	0.5021862
51.469	25.982	1.3049849	0.5048087
58.385	29.621	1.2868002	0.5073392
67.233	33.601	1.3260577	0.4997695
76.163	37.251	1.283285	0.4890958
86.673	42.34	1.2950292	0.4885028
97.806	47.744	1.2733956	0.48815
112.833	53.31	1.3308873	0.4724682
130.707	63.85	1.3419163	0.4884972
150.53	74.62	1.3263203	0.4957151
172.241	86.552	1.3092632	0.5025052
201.91	94.201	1.3741767	0.4665495

2

DM	WW	WER	WWI
24.234	14.015	NaN	0.5783197
27.695	14.891	1.3060281	0.5376783
31.832	15.459	1.3210678	0.4856434
36.073	17.434	1.2842118	0.4832978
41.316	20.294	1.3118133	0.4911899
47.914	22.408	1.3448948	0.4676712
54.751	25.512	1.3057477	0.4659641
62.104	29.364	1.286634	0.4728198
71.245	32.706	1.3160417	0.4590638
82.609	37.176	1.344454	0.4500236
93.723	41.934	1.2871751	0.4474249
108.879	50.161	1.3495715	0.4607041
126.035	57.226	1.3399669	0.4540485
146.307	71.087	1.3475593	0.4858756
166.589	82.728	1.2964699	0.4965994
197.937	91.437	1.4117615	0.46195

3

DM	WW	WER	WWI
28.196	13.906	NaN	0.4931905
31.912	15.846	1.2809526	0.496553
36.602	18.301	1.3155325	0.5
41.593	20.687	1.291311	0.4973673
46.668	23.048	1.2589193	0.4938716
52.134	26.128	1.2479688	0.5011701
59.87	29.323	1.3187924	0.4897779
66.743	32.727	1.2427762	0.4903436
75.24	36.965	1.2708261	0.4912945
83.594	42.471	1.2343907	0.5080628
97.582	48.111	1.3626654	0.4930315
111.221	54.545	1.2990748	0.49042
127.496	63.844	1.3140731	0.500753
144.94	73.376	1.2923597	0.5062509
169.15	83.922	1.3619698	0.4961395
195.683	88.806	1.3383269	0.4538258

4

DM	WW	WER	WWI
26.617	13.998	NaN	0.5259045
30.114	15.126	1.2800257	0.5022913
34.681	17.883	1.3263139	0.5156426
40.097	19.855	1.3367203	0.4951742
44.517	22.257	1.2326166	0.4999663
49.667	24.703	1.2447556	0.4973725
57.542	27.325	1.342252	0.4748705
66.476	31.359	1.3346268	0.4717342
75.14	35.717	1.2776521	0.4753394
84.556	40.706	1.2663288	0.4814088
96.426	46.768	1.3004673	0.4850144
112.357	54.523	1.3577255	0.4852657
129.273	64.362	1.3237787	0.4978766
149.111	76.111	1.3304658	0.5104318
169.46	87.102	1.2915613	0.5139974
200.448	96.445	1.3991654	0.4811472

5

DM	WW	WER	WWI
26.372	14.735	NaN	0.5587365
29.928	15.488	1.2878618	0.5175087
33.705	17.213	1.2683329	0.5106957
38.807	18.899	1.3256579	0.4869998
43.967	21.655	1.2836113	0.4925285
48.917	24.222	1.2378441	0.4951653
55.609	27.203	1.2923214	0.4891834
64	31.425	1.3245543	0.4910156

6

DM	WW	WER	WWI
25.951	14.257	NaN	0.5493815
29.291	15.598	1.2739729	0.5325185
33.79	16.588	1.3307853	0.4909145
38.082	18.524	1.2701737	0.486424
44.644	20.189	1.3743163	0.452222
49.01	23.316	1.2051558	0.4757396
56.317	25.911	1.3204125	0.460092
63.536	30.188	1.2728016	0.4751322

Measurements (DM, WW, WER and WWI) of *Nautilus pompilius* from Malaysia (continued)

73.548	35.392	1.3206319	0.4812096
83.62	39.874	1.292643	0.4768476
95.073	46.884	1.292689	0.4931369
111.212	54.748	1.3683239	0.492285
129.44	63.193	1.3546706	0.488203
149.885	74.069	1.3408473	0.4941722
171.868	86.401	1.3148424	0.5027172
203.939	91.823	1.4080255	0.4502474

73.232	34.735	1.3285015	0.4743145
82.524	39.053	1.2698685	0.473232
93.786	44.55	1.2915627	0.4750176
109.027	50.992	1.3514255	0.4677007
126.489	61.132	1.3459762	0.4832989
146.413	72.136	1.3398425	0.4926885
167.249	83.628	1.3048716	0.5000209
197.511	92.966	1.3946188	0.4706877

7

DM	WW	WER	WWI
24.387	13.869	NaN	0.5687046
28.256	14.407	1.3424701	0.509874
32.844	15.819	1.35111	0.4816405
36.957	NaN	1.2661388	NaN
43.118	20.73	1.3612058	0.4807737
48.11	23.347	1.2449546	0.4852837
55.982	26.406	1.3540232	0.4716873
63.407	29.474	1.2828551	0.4648383
72.508	33.305	1.3076678	0.4593286
82.368	38.405	1.2904619	0.4662612
95.033	44.439	1.3311648	0.4676165
109.532	51.174	1.3284131	0.4672059
125.405	59.926	1.3108339	0.4778597
145.936	72.225	1.3542385	0.4949087
168.824	83.143	1.3382692	0.4924833
196.774	91.36	1.3585232	0.464289

8

DM	WW	WER	WWI
26.737	13.886	NaN	0.5193552
30.719	15.472	1.3200452	0.5036622
35.557	16.867	1.339788	0.4743651
39.552	20.37	1.2373332	0.5150182
45.052	21.757	1.2974519	0.4829308
51.234	24.899	1.2932675	0.4859859
58.301	27.064	1.2948978	0.4642116
65.428	31.309	1.2594336	0.478526
74.901	35.05	1.3105329	0.467951
85.599	39.779	1.3060571	0.4647134
96.405	45.107	1.2684161	0.4678907
110.566	52.454	1.3153583	0.4744135
127.72	60.156	1.3343649	0.4709991
148.398	71.576	1.350014	0.4823246
168.236	80.523	1.2852327	0.4786312
196.28	86.629	1.3611758	0.4413542

9

DM	WW	WER	WWI
25.779	14.013	NaN	0.543582
29.78	15.24	1.3344959	0.5117529
33.5	17.154	1.2654361	0.5120597
38.821	19.335	1.3429005	0.4980552
43.852	21.114	1.2759844	0.4814832
49.964	24.155	1.298182	0.4834481
56.625	26.885	1.2844051	0.4747903
64.655	30.816	1.3037304	0.4766221
73.239	34.445	1.2831593	0.4703095
84.597	38.938	1.3342128	0.4602764
95.626	43.886	1.2777387	0.4589338
109.979	51.663	1.3227189	0.4697533
126.67	59.062	1.3265634	0.4662667
147.908	71.914	1.3634392	0.4862076
167.504	82.633	1.2825285	0.4933196
194.489	86.103	1.3481547	0.442714

10

DM	WW	WER	WWI
25.052	13.646	NaN	0.544707
28.186	14.096	1.2658495	0.5001064
32.435	15.582	1.3242223	0.480407
37.543	18.066	1.3397697	0.4812082
43.12	19.813	1.3191663	0.4594852
48.174	22.219	1.2481533	0.4612239
54.859	25.357	1.2967921	0.4622213
63.186	29.227	1.3266182	0.462555
72.43	33.013	1.3139996	0.4557918
81.786	37.726	1.2750317	0.461277
93.316	42.837	1.3018301	0.4590531
108.604	49.141	1.3545013	0.4524787
124.954	58.32	1.3237583	0.4667318
143.175	68.76	1.3129073	0.4802514
163.049	77.276	1.2968863	0.4739434
192.134	82.952	1.388584	0.4317403

Measurements (DM, WW, WER and WWI) of *Nautilus pompilius* from Malaysia (continued)

11

DM	WW	WER	WWI
24.083	NaN	NaN	NaN
27.401	15.242	1.2945286	0.5562571
31.624	15.585	1.3319894	0.4928219
35.813	17.892	1.2824717	0.4995951
42.141	19.815	1.3846126	0.4702072
47.035	22.765	1.245755	0.4840013
53.911	25.911	1.3137492	0.4806255
61.201	29.476	1.288731	0.4816261
72.45	34.368	1.4013924	0.4743685
82.067	39.163	1.2830995	0.4772076
93.122	44.823	1.28756	0.4813363
107.323	50.916	1.3282537	0.4744183
126.08	60.952	1.380088	0.4834391
145.978	72.03	1.3405482	0.4934305
166.698	82.986	1.3040251	0.4978224
196	90.344	1.3824561	0.4609388

12

DM	WW	WER	WWI
26.768	14.243	NaN	0.5320906
30.914	15.346	1.3337627	0.4964094
35.017	18.329	1.2830615	0.5234315
39.303	20.448	1.2597766	0.5202656
44.848	21.972	1.3020713	0.4899215
51.092	25.487	1.2978355	0.4988452
57.913	28.69	1.2848319	0.4953983
65.274	32.388	1.2703644	0.4961853
75	36.818	1.3202071	0.4909067
85.841	40.014	1.3099871	0.4661409
97.441	47.496	1.2885282	0.4874334
111.791	53.731	1.3162252	0.480638
129.848	64.249	1.3491395	0.4948016
151.976	75.402	1.3698704	0.4961441
173.199	87.475	1.2987954	0.5050549
200.05	93.471	1.3340938	0.4672382

13

DM	WW	WER	WWI
23.459	NaN	NaN	NaN
28.738	14.596	1.5007007	0.5078989
33.056	16.173	1.3230843	0.4892606
38.228	18.043	1.3374038	0.4719839
43.152	20.553	1.2742032	0.4762931
48.035	23.87	1.239121	0.4969293
54.722	26.359	1.2978017	0.4816893
62.844	29.79	1.3188752	0.4740309
71.697	33.091	1.3015904	0.4615395
80.456	38.042	1.2592585	0.4728299
91.019	43.704	1.2798151	0.4801635
105.734	50.198	1.3494761	0.4747574
121.727	58.909	1.3253925	0.4839436
140.947	70.316	1.3407192	0.4988826
158.981	80.494	1.2722685	0.5063121
187.273	86.34	1.3875859	0.4610382

14

DM	WW	WER	WWI
24.977	14.403	NaN	0.5766505
28.753	NaN	1.3252133	NaN
33.284	NaN	1.3399997	NaN
38.344	18.307	1.3271616	0.4774411
43.818	21.609	1.305901	0.4931535
48.519	24.757	1.2260794	0.5102537
55.854	28.311	1.3252105	0.5068751
64.399	31.601	1.3293817	0.4907064
74.74	35.677	1.346939	0.4773481
83.936	40.462	1.2612186	0.4820578
95.781	46.469	1.3021535	0.4851589
109.389	52.007	1.3043333	0.4754317
128.53	63.152	1.3805804	0.4913405
148.667	74.972	1.3378892	0.5042948
169.97	86.47	1.3071198	0.5087368
197.535	92.168	1.3506523	0.4665907

15

DM	WW	WER	WWI
26.565	NaN	NaN	NaN
30	16.316	1.2753309	0.5438667
34.209	18.452	1.3002841	0.5393902
38.664	20.193	1.2774173	0.5222688
45.395	22.291	1.3784864	0.4910453
50.179	25.363	1.2218783	0.5054505
56.97	27.744	1.2889867	0.4869932
64.881	31.782	1.2970079	0.4898506
75.878	36.642	1.3677184	0.4829068

16

DM	WW	WER	WWI
26.833	13.768	NaN	0.5130995
30.789	NaN	1.3165965	NaN
35.341	18.125	1.3175482	0.5128604
40.201	20.678	1.2939457	0.5143653
45.583	22.045	1.2856777	0.4836233
51.397	24.844	1.2713635	0.4833745
57.994	28.49	1.2731823	0.4912577
66.11	31.916	1.2994758	0.4827711
75.639	36.415	1.309053	0.4814315

Measurements (DM, WW, WER and WWI) of *Nautilus pompilius* from Malaysia (continued)

85.714	42.665	1.276062	0.49776
96.232	48.35	1.2604787	0.5024316
111.743	55.871	1.3483469	0.4999955
130.993	64.886	1.3742177	0.4953394
153.036	77.679	1.3648692	0.5075865
172.598	90.102	1.2719918	0.5220339
203.798	97.977	1.3942104	0.4807555

84.844	41.145	1.258203	0.4849488
96.117	47.3	1.2833885	0.4921086
110.793	53.726	1.3286917	0.4849223
128.378	62.401	1.3426307	0.4860724
146.439	71.694	1.3011648	0.4895827
166.473	82.204	1.292332	0.4937978
195.368	88.452	1.3772705	0.4527456

17

DM	WW	WER	WWI
26.967	13.645	NaN	0.5059888
30.884	NaN	1.3116012	NaN
35.728	NaN	1.3382903	NaN
39.887	20.154	1.2463653	0.5052774
45.378	22.389	1.2942792	0.4933889
50.943	25.422	1.2603128	0.4990283
57.441	28.336	1.2713788	0.4933062
65.341	31.973	1.29398	0.4893252
75.823	36.126	1.3465745	0.4764517
84.677	40.711	1.2471796	0.4807799
95.392	46.929	1.2690916	0.4919595
110.682	53.198	1.3462636	0.4806382
128.01	62.212	1.3376232	0.4859933
146.553	72.143	1.310695	0.4922656
165.069	81.925	1.2686494	0.4963076
194.773	88.192	1.3922796	0.4527938

18

DM	WW	WER	WWI
25.695	NaN	NaN	NaN
29.405	14.591	1.3096195	0.4962081
33.599	17.051	1.3056006	0.5074853
37.741	19.281	1.2617523	0.5108768
43.628	21.375	1.3362995	0.4899377
48.951	24.124	1.2589038	0.4928193
55.905	26.55	1.304302	0.4749128
63.643	30.455	1.295985	0.4785287
73.04	33.726	1.3171045	0.461747
83.314	39.319	1.3011113	0.4719375
93.975	45.644	1.2722976	0.4857036
109.395	51.97	1.3550967	0.4750674
126.178	61.963	1.3303697	0.4910761
146.681	72.251	1.3513892	0.4925723
165.129	82.821	1.267357	0.5015533
194.849	90.487	1.392354	0.4643955

19

DM	WW	WER	WWI
25.226	13.509	NaN	0.5355189
28.411	14.226	1.2684585	0.5007216
32.292	15.819	1.2918642	0.4898737
37.388	18.23	1.340524	0.4875896
43.085	20.253	1.3279684	0.4700708
48.154	22.78	1.2491441	0.4730656
54.644	25.493	1.2877164	0.4665288
63.708	29.148	1.3592614	0.457525
73.687	33.383	1.3378081	0.4530378
83.337	38.778	1.279069	0.4653155
93.726	43.399	1.2648658	0.4630412
110.75	50	1.3962632	0.4514673
128.947	59.671	1.3556108	0.462756
148.927	70.223	1.3339035	0.4715263
168.301	80.916	1.2771047	0.4807815
200.782	87.394	1.4232335	0.4352681

20

DM	WW	WER	WWI
23.752	13.619	NaN	0.5733833
27.446	14.385	1.3352351	0.5241201
31.511	16.027	1.3181543	0.508616
36.35	NaN	1.3307132	NaN
42.048	20.514	1.3380793	0.487871
47.061	23.818	1.2526554	0.5061091
53.868	26.669	1.3102054	0.4950806
60.917	30.045	1.2788373	0.4932121
71.281	34.097	1.3692115	0.4783463
80.998	39.34	1.2912223	0.485691
91.448	44.034	1.2746761	0.4815196
104.33	50.949	1.3015774	0.4883447
122.408	59.905	1.3765792	0.4893879
142.039	69.992	1.3464667	0.4927661
161.889	80.126	1.2990309	0.4949441
190.858	87.026	1.389908	0.4559725

Measurements (DM, WW, WER and WWI) of *Nautilus pompilius* from Malaysia (continued)

21

DM	WW	WER	WWI
23.735	13.433	NaN	0.5659574
26.851	NaN	1.279801	NaN
31.626	NaN	1.3872911	NaN
36.688	NaN	1.345735	NaN
42.269	20.6	1.3273818	0.4873548
46.85	23.153	1.2285002	0.4941942
53.876	26.008	1.3224264	0.4827381
61.834	29.743	1.3172372	0.4810137
71.868	34.031	1.350879	0.4735209
81.414	38.705	1.2832967	0.4754096
93.003	44.5	1.3049556	0.4784792
107.989	51.185	1.3482335	0.4739835
126.079	59.809	1.3630961	0.4743772
145.58	70.654	1.3332694	0.4853277
167.127	82	1.3179223	0.4906448
198.324	90.838	1.4081772	0.4580283

22

DM	WW	WER	WWI
27.689	NaN	NaN	NaN
31.117	NaN	1.2629347	NaN
35.733	17.173	1.3186924	0.4805922
41.555	20.165	1.3524076	0.4852605
46.725	21.884	1.2643056	0.4683574
52.285	25.501	1.2521478	0.4877307
59.431	27.863	1.2920278	0.4688294
68.062	32.559	1.3115454	0.4783727
76.947	36.543	1.2781269	0.4749113
87.376	41.404	1.2894394	0.4738601
98.118	47.194	1.2609941	0.4809923
113.185	54.419	1.3307007	0.4807969
130.687	62.494	1.3331746	0.478196
150.528	73.45	1.3266911	0.4879491
168.889	82.642	1.2588331	0.4893273
199.23	88.217	1.3915754	0.4427897

23

DM	WW	WER	WWI
26.667	13.732	NaN	0.5149436
30.198	15.497	1.2823543	0.5131797
34.233	17.822	1.28509	0.5206088
39.596	20.389	1.3378663	0.5149258
45.111	22.141	1.2979629	0.4908116
50.523	25.087	1.2543345	0.4965461
56.41	28.336	1.2466196	0.5023223
64.884	31.649	1.3230097	0.4877782
74.57	35.359	1.3208486	0.4741719
83.892	40.759	1.2656476	0.4858509
94.296	46.927	1.2634133	0.4976563
109.492	54.198	1.3482742	0.4949951
126.916	63.812	1.3435937	0.5027892
144.757	73.622	1.3009074	0.5085903
164.744	83.462	1.2952096	0.5066163
193.642	90.187	1.3815923	0.4657409

24

DM	WW	WER	WWI
26.081	NaN	NaN	NaN
30	15.179	1.3231041	0.5059667
34.534	17.516	1.325108	0.5072103
39.15	19.795	1.2851972	0.5056194
44.64	21.755	1.3001242	0.4873432
50.345	25.287	1.2719332	0.5022743
57.764	28.075	1.3164423	0.4860294
66.132	31.672	1.3107166	0.4789209
75.308	35.917	1.2967579	0.4769347
84.837	41.521	1.2690782	0.4894209
96.278	47.337	1.2879041	0.49167
112.317	54.692	1.3609334	0.4869432
128.931	65.167	1.3177217	0.5054409
147.94	77.02	1.3166081	0.5206165
166.591	86.832	1.2680368	0.5212286
196.481	91.789	1.391035	0.4671648

25

DM	WW	WER	WWI
26.971	14.45	NaN	0.5357606
31.465	16.141	1.3610102	0.5129827
35.896	18.648	1.3014774	0.5195008
40.68	NaN	1.2843097	NaN
45.658	23.438	1.2597138	0.5133383
52.281	26.114	1.3111549	0.4994931
58.922	29.03	1.2701856	0.4926852
66.604	32.275	1.2777493	0.4845805
76.011	36.207	1.3024236	0.476339
87.076	41.178	1.312333	0.4728972

26

DM	WW	WER	WWI
24.747	14.127	NaN	0.5708571
28.066	15.033	1.286222	0.5356303
31.292	16.902	1.2430987	0.5401381
36.533	19.184	1.3630257	0.5251143
42.106	21.432	1.3283646	0.5090011
48.035	24.688	1.3014504	0.5139586
53.731	27.998	1.2512217	0.5210772
62.253	31.963	1.3423653	0.5134371
71.748	35.663	1.3283087	0.4970592
83.495	40.641	1.3542578	0.4867477

Measurements (DM, WW, WER and WWI) of *Nautilus pompilius* from Malaysia (continued)

97.255	47.162	1.2474609	0.4849314
111.985	54.079	1.3258544	0.4829129
129.924	63.838	1.3460434	0.4913488
150.585	75.324	1.343336	0.5002092
168.04	84.906	1.2452654	0.5052726
197.45	92.241	1.380667	0.4671613

94.522	46.733	1.2815775	0.494414
108.371	53.461	1.3144993	0.4933146
126.573	62.152	1.3641307	0.4910368
149.694	76.157	1.3987066	0.5087512
169.638	89.374	1.2842143	0.5268513
196.119	97.565	1.3365741	0.4974786

27

DM	WW	WER	WWI
24.993	14.203	NaN	0.5682791
27.981	15.179	1.2534	0.5424753
32.671	16.68	1.3633218	0.5105445
37.446	19.928	1.3136692	0.5321797
42.197	21.838	1.2698496	0.5175249
48.091	25.526	1.2988663	0.5307854
55.067	28.815	1.3111586	0.5232717
63.828	33.031	1.3435061	0.5175002
72.732	36.622	1.29846	0.5035198
83.822	41.646	1.3282046	0.4968385
95.267	47.343	1.2917217	0.4969507
111.857	55.483	1.3786098	0.4960172
129.602	65.241	1.3424468	0.503395
150.343	77.528	1.3456838	0.5156742
171.603	89.2	1.3028167	0.5198044
203.713	97.472	1.409249	0.4784771

28

DM	WW	WER	WWI
23.569	13.248	NaN	0.5620943
26.672	NaN	1.2806453	NaN
30.918	NaN	1.3437288	NaN
35.619	17.269	1.3272131	0.4848255
40.283	19.536	1.2790283	0.4849688
45.3	22.078	1.2645989	0.4873731
52.249	24.98	1.3303305	0.4780953
59.625	28.435	1.3022693	0.4768973
68.545	32.303	1.321584	0.4712671
79.066	37.466	1.3305401	0.4738573
90.061	42.789	1.29746	0.4751113
103.43	49.789	1.3189232	0.4813787
120.563	57.572	1.3587359	0.4775263
141.82	69.981	1.3837157	0.4934494
162.182	80.97	1.3077669	0.4992539
189.602	86.617	1.3667231	0.4568359

29

DM	WW	WER	WWI
24.234	14.115	NaN	0.5824462
26.951	15.424	1.2368002	0.5722979
31.276	16.139	1.3467055	0.5160187
36.708	18.497	1.3775236	0.5038956
41.851	20.352	1.299841	0.4862966
46.782	22.882	1.2495277	0.4891197
53.171	26.667	1.2917905	0.5015328
61.563	29.344	1.3405712	0.4766499
70.853	33.807	1.3245762	0.4771428
80.678	37.637	1.2965634	0.4665088
91.934	43.318	1.2985003	0.4711859
106.946	50.588	1.3532461	0.4730238
125.16	60.551	1.3696261	0.4837888
144.915	72.562	1.3405888	0.5007211
165.186	85.268	1.299331	0.5161939
193.933	92.352	1.3783419	0.4762057

30

DM	WW	WER	WWI
26.957	14.122	NaN	0.5238714
31.111	NaN	1.3319405	NaN
35.443	17.848	1.2978754	0.5035691
40.419	19.919	1.3004995	0.4928128
44.641	22.226	1.2198227	0.4978831
50.889	24.79	1.2995111	0.4871387
58.481	28.102	1.3206318	0.4805321
66.168	33.011	1.2801664	0.4988967
74.979	36.043	1.284054	0.4807079
85.63	40.161	1.3042853	0.4690062
97.597	46.553	1.2990356	0.4769921
111.679	53.446	1.3093932	0.478568
129.375	62.448	1.342016	0.4826899
148.743	72.335	1.3218201	0.4863086
169.747	84.177	1.3023603	0.4958968
200.599	89.222	1.3965398	0.4447779

Measurements (DM, WW, WER and WWI) of *Nautilus pompilius* from Malaysia (continued)

31

DM	WW	WER	WWI
24.286	NaN	NaN	NaN
27.679	14.685	1.2989392	0.5305466
31.47	17.442	1.292685	0.5542421
35.877	18.993	1.2996869	0.5293921
41.81	20.573	1.3580886	0.4920593
47.171	23.651	1.2728869	0.5013886
53.081	27.52	1.266275	0.5184529
60.837	31.543	1.3135826	0.5184838
70.578	35.144	1.34587	0.4979455
80.449	40.352	1.2992796	0.5015849
90.616	44.739	1.2687279	0.4937208
104.935	51.625	1.3410067	0.4919712
122.762	60.193	1.3686335	0.4903227
143.978	71.821	1.3755119	0.4988332
162.654	83.044	1.2762543	0.5105561
192.153	90.732	1.3956125	0.4721862

32

DM	WW	WER	WWI
25.334	NaN	NaN	NaN
28.487	NaN	1.2644041	NaN
33.078	NaN	1.3482954	NaN
37.556	18.685	1.2890809	0.4975237
43.115	21.039	1.3179475	0.487974
48.313	23.729	1.2556576	0.4911514
55.513	27.182	1.3202658	0.4896511
63.677	30.945	1.3157573	0.4859682
73.2	35.136	1.321469	0.48
82.212	40.173	1.2613868	0.4886513
94.231	45.519	1.3137634	0.4830576
109.641	52.317	1.3538121	0.4771664
126.818	63.556	1.3378759	0.5011591
144.92	74.583	1.3058547	0.5146495
164.872	86.283	1.2943066	0.5233333
192.377	92.69	1.3614838	0.4818144

33

DM	WW	WER	WWI
25.244	13.639	NaN	0.5402868
29.288	14.644	1.3460559	0.5
33.403	16.566	1.3007431	0.4959435
38.414	NaN	1.3225379	NaN
43.36	21.182	1.2740882	0.4885148
49.643	24.653	1.3108032	0.4966058
56.7	27.744	1.304518	0.4893122
65.398	31.752	1.3303405	0.4855194
74.506	34.857	1.2979368	0.4678415
85.714	40.185	1.3234911	0.4688266
97.378	46.239	1.2906788	0.4748403
113.494	53.98	1.3583888	0.4756199
130.892	63.716	1.3300881	0.486783
153.214	76.964	1.3701581	0.5023301
173.337	87.949	1.2799283	0.5073873
203.97	94.762	1.384682	0.4645879

34

DM	WW	WER	WWI
24.819	13.876	NaN	0.5590878
28.015	14.454	1.2741269	0.5159379
32.19	NaN	1.3202638	NaN
36.77	18.096	1.3048041	0.4921403
42.629	19.576	1.3440735	0.4592179
47.843	22.857	1.2595822	0.4777501
54.86	26.095	1.3148457	0.4756653
62.48	29.744	1.297091	0.4760563
72.562	33.293	1.3487655	0.4588214
81.963	37.311	1.2759017	0.4552176
92.953	42.878	1.2861485	0.4612869
107.525	49.205	1.3381108	0.4576145
125.114	57.956	1.3539197	0.4632255
144.091	66.779	1.3263615	0.4634502
163.333	78.095	1.2849143	0.4781336
191.431	84.381	1.3736518	0.4407907

35

DM	WW	WER	WWI
23.436	13.857	NaN	0.5912698
26.563	14.286	1.2846572	0.5378158
30.694	15.724	1.3352197	0.5122825
34.66	17.761	1.2751173	0.5124351
41.006	19.727	1.3997088	0.4810759
45.397	22.012	1.2256303	0.4848779
52.454	25.595	1.3350666	0.4879513
59.802	28.415	1.299793	0.4751513
70.288	33.286	1.3814366	0.4735659
79.153	37.673	1.2681551	0.4759516
89.937	43.242	1.2910469	0.4808032

36

DM	WW	WER	WWI
22.861	NaN	NaN	NaN
26.11	14.23	1.3044376	0.5450019
29.874	15.133	1.3091006	0.5065609
34.942	16.967	1.3680714	0.4855761
39.286	18.714	1.2640961	0.4763529
44.818	22.32	1.3014555	0.4980142
52.18	25.781	1.3555115	0.4940782
59.936	29.322	1.3193723	0.4892218
68.001	32.862	1.2872268	0.4832576
79.272	37.765	1.3589674	0.4763977
91.155	42.716	1.3222737	0.4686084

Measurements (DM, WW, WER and WWI) of *Nautilus pompilius* from Malaysia (continued)

103.977	49.878	1.3365887	0.4797022
122.431	59.723	1.3864628	0.4878095
141.905	70.053	1.3434225	0.4936613
161.761	83.025	1.2994281	0.5132572
190.483	88.642	1.3866434	0.4653539

104.248	50.644	1.3078998	0.4858031
122.286	58.732	1.3759987	0.4802839
144.09	70.702	1.3883987	0.4906794
164.872	83.59	1.3092607	0.5069994
191.52	89.885	1.3493806	0.4693244

37

DM	WW	WER	WWI
25.192	14.256	NaN	0.5658939
28.376	14.703	1.2687529	0.5181491
32.699	16.795	1.3279037	0.5136243
37.651	19.089	1.3258185	0.5069985
42.864	21.734	1.2960816	0.5070455
48.434	24.514	1.2767777	0.5061321
55.13	27.187	1.295613	0.4931435
63.87	30.616	1.3422019	0.4793487
73.334	35.24	1.3183081	0.4805411
83.191	38.863	1.2868915	0.4671539
93.59	43.865	1.2656284	0.4686932
109.279	50.555	1.3633725	0.4626232
126.915	60.643	1.3488153	0.4778237
146.669	70.997	1.3355211	0.4840628
165.064	79.872	1.2665667	0.483885
196.292	87.603	1.4141663	0.4462892

38

DM	WW	WER	WWI
27.803	NaN	NaN	NaN
31.58	16.085	1.2901522	0.5093414
34.974	17.296	1.2264966	0.4945388
40.432	20.525	1.3364719	0.5076425
46.212	22.224	1.3063486	0.480914
52.164	25.383	1.2741843	0.4866
58.421	28.256	1.2542849	0.4836617
66.975	31.637	1.3142787	0.4723703
76.288	36.25	1.2974392	0.475173
86.55	41.297	1.2871278	0.4771462
97.624	46.745	1.2722693	0.4788269
112.963	53.858	1.3389342	0.4767756
129.924	63.636	1.322837	0.489794
150.409	73.801	1.3401977	0.4906688
169.835	83.434	1.2749899	0.4912651
198.613	90.595	1.3676059	0.4561383

Measurements (DM, WW, WER and WWI) of *Nautilus pompilius* from Indonesia

1

DM	WW	WER	WWI
22.282	NaN	NaN	NaN
25.844	NaN	1.3452752	NaN
29.148	15.461	1.2720321	0.5304309
33.68	16.909	1.3351395	0.5020487
38.034	18.345	1.2752632	0.4823316
44.271	21.054	1.3548607	0.4755709
50.036	23.604	1.2773988	0.4717403
57.457	27.366	1.3186232	0.4762866
65.599	30.808	1.3034925	0.4696413
76.2	35.439	1.3493217	0.4650787
85.665	40.64	1.263854	0.4744061
98.971	46.122	1.3347781	0.4660153
115.171	54.139	1.3541612	0.4700749
134.167	65.521	1.357079	0.4883541
151.624	74.336	1.2771576	0.4902654
177.182	78.351	1.3655365	0.4422063

2

DM	WW	WER	WWI
24.031	NaN	NaN	NaN
27.012	NaN	1.2634841	NaN
30.909	NaN	1.309352	NaN
35.728	17.727	1.3361263	0.4961655
40.974	19.167	1.3152228	0.4677844
46.087	22.166	1.2651446	0.4809599
52.369	24.97	1.2911945	0.4768088
59.878	28.363	1.3073324	0.4736798
68.615	32.083	1.3131174	0.46758
78.145	36.523	1.2970725	0.4673748
88.729	41.976	1.2892252	0.473081
102.963	48.991	1.346577	0.4758117
119.167	58.056	1.3395213	0.4871819
138.146	68.247	1.3438928	0.4940208
155.879	77.333	1.2732058	0.4961092
182.45	83.866	1.3699746	0.4596657

3

DM	WW	WER	WWI
23.93	13.759	NaN	0.5749687
26.732	14.149	1.2478935	0.5292907
30.622	16.103	1.3122126	0.5258638
35.195	17.939	1.3209757	0.5097031
39.916	19.748	1.2862698	0.494739
44.781	22.146	1.2586169	0.4945401
51.185	25.822	1.3064652	0.5044837
58.708	28.767	1.3155554	0.4900014
66.404	32.065	1.2793634	0.4828775
75.227	35.95	1.283391	0.4778869
85.667	41.248	1.2968198	0.4814923
98.319	47.035	1.3171881	0.4783918
113.554	54.24	1.3339206	0.4776582
130.638	65.372	1.3235312	0.5004057
149.723	75.314	1.3135239	0.5030222
173.856	79.87	1.348349	0.4594032

4

DM	WW	WER	WWI
23.361	13.938	NaN	0.5966354
26.511	14.151	1.2878621	0.5337784
30.426	NaN	1.3171569	NaN
34.733	16.79	1.3031514	0.483402
39.019	17.951	1.2620242	0.4600579
44.434	21.133	1.2968166	0.4756043
50.107	23.732	1.2716453	0.4736264
57.614	26.833	1.3220846	0.4657375
65.187	29.918	1.280165	0.4589565
73.966	35.241	1.2874853	0.4764486
83.087	39.369	1.261833	0.4738286
96.049	44.646	1.3363479	0.4648252
109.839	51.977	1.3077582	0.4732108
126.321	61.887	1.3226288	0.4899185
142.518	70.426	1.2728825	0.4941551
165.063	76.709	1.3414053	0.4647256

5

DM	WW	WER	WWI
22.688	13.125	NaN	0.5784996
25.493	13.431	1.2625526	0.5268505
29.116	15.223	1.3044323	0.5228397
33.21	17.037	1.3009911	0.5130081
38.067	18.822	1.3138917	0.494444
42.943	21.275	1.2725869	0.4954242
47.779	23.891	1.2379108	0.5000314
54.447	26.296	1.2985952	0.4829651

6

DM	WW	WER	WWI
24.641	13.519	NaN	0.5486384
27.998	NaN	1.2910331	NaN
32.069	16.342	1.3119486	0.5095887
36.389	18.22	1.2875657	0.5007008
41.591	19.818	1.3063468	0.4764973
46.617	22.241	1.25629	0.4771006
53.104	24.713	1.2976747	0.4653698
60.698	28.064	1.3064545	0.4623546

Measurements (DM, WW, WER and WWI) of *Nautilus pompilius* from Indonesia (continued)

62.769	30.109	1.3290536	0.4796795
72.356	34.328	1.3287971	0.474432
80.89	38.558	1.2498001	0.476672
92.964	44.943	1.3208087	0.4834452
107.688	51.714	1.3418532	0.4802206
126.081	62.059	1.3707702	0.4922153
142.945	70.556	1.285401	0.4935884
165.185	76.667	1.3353751	0.4641281

69.651	32.508	1.316758	0.466727
77.583	37.199	1.2407333	0.4794736
88.635	41.571	1.3052009	0.4690134
102.794	47.427	1.3450085	0.4613791
118.711	56.302	1.3336639	0.4742779
135.388	66.979	1.3007038	0.4947189
153.914	75.524	1.2923969	0.4906896
178.614	80.694	1.346712	0.4517787

7

DM	WW	WER	WWI
161.887	75.603	1.3753327	0.4670109
138.041	68.144	1.2361972	0.4936504
124.155	60.483	1.3219335	0.4871572
107.984	50.806	1.3612792	0.4704956
92.552	43.648	1.3281379	0.4716052
80.309	38.351	1.2582739	0.477543
71.594	34.11	1.3087012	0.4764366
62.583	29.758	1.3036513	0.4754965
54.812	26.333	1.3073488	0.480424
47.938	22.99	1.2657768	0.4795778
42.609	20.678	1.3249523	0.4852965
37.017	18.145	1.2786486	0.4901802
32.736	15.598	1.3332588	0.4764785
28.351	14.641	1.2639081	0.5164192
25.218	14.408	1.3311904	0.5713379
21.857	12.905	NaN	0.5904287

8

DM	WW	WER	WWI
164.295	75.706	1.3478187	0.4607931
141.517	70.37	1.279479	0.4972547
125.11	61.119	1.3315492	0.4885221
108.421	50.742	1.3272013	0.468009
94.112	44.54	1.3145695	0.4732659
82.083	39.259	1.2954813	0.4782842
72.117	34.461	1.2774345	0.4778485
63.807	30.877	1.3061751	0.4839124
55.83	27.733	1.2928692	0.4967401
49.101	24.347	1.2955093	0.4958555
43.139	21.26	1.2525109	0.4928255
38.546	19.12	1.3436026	0.4960307
33.254	17.18	1.2682075	0.5166296
29.529	15.142	1.3059076	0.512784
25.84	14.601	1.2856847	0.5650542
22.789	13.605	NaN	0.5969986

9

DM	WW	WER	WWI
163.303	78.229	1.2864593	0.479042
143.978	72.941	1.2844932	0.5066121
127.037	63.012	1.3058258	0.496013
111.17	52.857	1.3165164	0.475461
96.889	46.603	1.3187815	0.4809937
84.37	41.008	1.258418	0.4860495
75.21	36.247	1.2738941	0.4819439
66.636	32.597	1.2735249	0.48918
59.048	29.627	1.3068306	0.5017443
51.653	25.771	1.2537882	0.4989255
46.13	22.631	1.303586	0.4905918
40.403	20.002	1.3004973	0.4950622
35.429	17.785	1.3314592	0.5019899
30.704	16.246	1.1981858	0.5291167
28.05	14.026	1.3630217	0.5000357
24.026	13.776	NaN	0.5733788

10

DM	WW	WER	WWI
167.977	79.346	1.3785057	0.4723623
143.069	75.966	1.2727496	0.5309746
126.816	66.014	1.3139972	0.5205495
110.631	53.686	1.3626216	0.4852709
94.774	46.93	1.3393543	0.495178
81.892	40.84	1.2954881	0.4987056
71.949	35.525	1.2809881	0.4937525
63.57	30.753	1.2850023	0.4837659
56.079	27.732	1.3314596	0.4945167
48.6	24.37	1.2987821	0.5014403
42.645	21.177	1.2809657	0.4965881
37.679	18.917	1.2877096	0.5020568
33.204	16.993	1.3401763	0.5117757
28.682	15.134	1.3478735	0.527648
24.705	13.95	1.2781662	0.564663
21.852	NaN	NaN	NaN

Measurements (DM, WW, WER and WWI) of *Nautilus pompilius* from Indonesia (continued)

11

DM	WW	WER	WWI
156.823	74.129	1.3512561	0.4726921
134.909	69.291	1.2678466	0.5136129
119.814	60.233	1.3337181	0.5027209
103.747	49.509	1.37192	0.477209
88.575	42.814	1.3393399	0.4833644
76.536	38.32	1.2592127	0.5006794
68.205	32.727	1.2921575	0.4798329
60.001	29.354	1.3256885	0.4892252
52.112	26.79	1.308015	0.514085
45.565	23.412	1.2504034	0.5138154
40.748	20.513	1.3057928	0.5034112
35.659	18.403	1.3488026	0.5160829
30.704	16.026	1.2939568	0.5219515
26.992	14.908	1.2577378	0.5523118
24.068	13.52	1.2900843	0.5617417
21.19	12.508	NaN	0.5902784

12

DM	WW	WER	WWI
147.473	66.552	1.3084714	0.4512826
128.923	62.356	1.3131352	0.4836685
112.506	54.035	1.34186	0.4802855
97.123	44.394	1.3252221	0.4570905
84.368	38.506	1.2724972	0.4564053
74.791	34.999	1.2768894	0.4679574
66.187	31.053	1.3042582	0.4691707
57.955	27.424	1.2954034	0.4731947
50.92	24.828	1.2676531	0.4875884
45.226	22.156	1.3298586	0.4898952
39.218	19.474	1.2444343	0.4965577
35.156	16.97	1.3319321	0.4827057
30.462	14.598	1.2473471	0.47922
27.275	14.236	1.4181	0.5219432
22.904	13.333	1.2353588	0.5821254
20.607	NaN	NaN	NaN

13

DM	WW	WER	WWI
153.03	70.743	1.38774	0.4622819
129.904	65.34	1.295433	0.5029868
114.134	55.733	1.3346277	0.488312
98.795	47.331	1.3462355	0.4790829
85.148	40.229	1.3351191	0.4724597
73.691	35.243	1.2756976	0.4782538
65.244	31.467	1.2629088	0.4822972
58.057	27.946	1.3386976	0.4813545
50.178	24.686	1.330602	0.4919686
43.5	21.845	1.2714494	0.5021839
38.578	18.933	1.295107	0.4907719
33.899	16.827	1.2915059	0.4963863
29.829	15.314	1.3538697	0.513393
25.636	13.495	1.2791234	0.5264082
22.667	13.425	1.3812069	0.5922707
19.287	12.203	NaN	0.632706

14

DM	WW	WER	WWI
163.177	74.54	1.3686551	0.4568046
139.48	69.306	1.2987693	0.4968884
122.39	60.87	1.3390843	0.4973446
105.765	51.523	1.3231492	0.487146
91.947	44.191	1.3301722	0.4806138
79.723	37.779	1.2966856	0.4738783
70.011	33.714	1.2793204	0.4815529
61.898	30.206	1.3214857	0.4879964
53.845	25.906	1.311594	0.4811217
47.016	22.778	1.3057415	0.4844734
41.145	20.478	1.2449346	0.4977032
36.876	17.952	1.3272215	0.4868207
32.009	16.389	1.3535313	0.5120122
27.513	NaN	1.2830885	NaN
24.289	NaN	1.3392978	NaN
20.988	12.593	NaN	0.6000095

15

DM	WW	WER	WWI
153.036	67.543	1.3550862	0.4413537
131.465	64.821	1.2569573	0.4930666
117.26	57.671	1.2880199	0.4918216
103.321	48.958	1.3531498	0.4738437
88.821	42.514	1.2964751	0.4786481
78.007	36.923	1.2814901	0.4733293
68.909	32.329	1.2599186	0.469155
61.391	28.268	1.3170409	0.4604584
53.494	25.829	1.2996311	0.4828392

16

DM	WW	WER	WWI
143.866	67.227	1.4017048	0.467289
121.515	61.561	1.2896623	0.5066124
107.002	52.5	1.3419926	0.490645
92.367	44.194	1.361514	0.4784609
79.16	38.319	1.3294741	0.4840702
68.654	33.191	1.2841501	0.4834533
60.584	29.253	1.3060239	0.4828503
53.013	25.699	1.3155994	0.4847679
46.219	23.529	1.341487	0.5090764

Measurements (DM, WW, WER and WWI) of *Nautilus pompilius* from Indonesia (continued)

46.924	22.873	1.2529299	0.4874478
41.921	20.286	1.2631906	0.4839102
37.299	18.224	1.3205379	0.4885922
32.458	16.457	1.3431061	0.5070245
28.007	14.57	1.2758657	0.5202271
24.795	NaN	1.2693082	NaN
22.008	12.896	NaN	0.5859687

39.905	20.058	1.287609	0.5026438
35.167	17.667	1.2715207	0.5023744
31.187	15.699	1.3283842	0.5033828
27.059	NaN	1.3639828	NaN
23.169	12.491	1.3308042	0.5391256
20.084	12.167	1.2492593	0.6058056
17.969	11.506	NaN	0.640325

17

DM	WW	WER	WWI
174.831	79.524	1.4065638	0.4548621
147.414	73.448	1.2683661	0.498243
130.893	63.514	1.3526585	0.485236
112.544	51.184	1.3235912	0.454791
97.824	45.986	1.3741956	0.4700891
83.449	39.655	1.2751614	0.4752004
73.899	34.519	1.3137354	0.4671105
64.474	30.266	1.3038911	0.4694295
56.463	26.667	1.3389349	0.4722916
48.796	23.793	1.2962974	0.4876014
42.858	20.56	1.2879079	0.4797237
37.765	18.553	1.2937504	0.491275
33.202	16.054	1.3616715	0.4835251
28.453	NaN	1.2896365	NaN
25.055	13.944	1.315361	0.5565356
21.846	12.632	NaN	0.5782294

18

DM	WW	WER	WWI
174.968	79.728	1.3796416	0.4556719
148.962	75.014	1.279379	0.5035781
131.697	65.538	1.3310437	0.4976423
114.151	55.204	1.3807611	0.483605
97.145	46.395	1.319715	0.4775851
84.563	40.348	1.2879431	0.4771354
74.513	35.179	1.3004069	0.472119
65.342	31.467	1.313429	0.4815739
57.015	26.667	1.3078587	0.467719
49.855	24	1.3020078	0.481396
43.692	20.923	1.267539	0.4788749
38.808	18.667	1.3120661	0.4810091
33.88	16.599	1.3235663	0.4899351
29.449	14.613	1.3189773	0.4962138
25.642	13.54	1.2796093	0.5280399
22.668	12.403	NaN	0.547159

19

DM	WW	WER	WWI
175.298	79.477	1.3340454	0.4533822
151.772	74.926	1.3312746	0.4936747
131.54	66.615	1.3345041	0.5064239
113.867	54.133	1.3633811	0.4754055
97.519	47.451	1.3138444	0.4865821
85.078	41.888	1.3381858	0.4923482
73.546	35.692	1.2951008	0.4853017
64.626	31.289	1.3280962	0.484155
56.078	27.717	1.2984504	0.494258
49.213	24.1	1.3237316	0.489708
42.774	20.923	1.2875651	0.4891523
37.696	18.933	1.3092961	0.5022549
32.944	16.601	1.3409687	0.5039157
28.449	15.223	1.3179422	0.5350979
24.781	12.923	1.3053247	0.5214882
21.69	12.978	NaN	0.5983402

20

DM	WW	WER	WWI
155.637	76.242	1.3708589	0.4898707
132.928	68.478	1.3027377	0.5151511
116.463	59.456	1.3882744	0.5105141
98.844	49.249	1.3785448	0.4982498
84.186	43.152	1.3305657	0.5125793
72.983	37.267	1.2807332	0.5106258
64.49	32.925	1.3283805	0.5105443
55.954	29.249	1.3450538	0.522733
48.246	25.818	1.3341163	0.5351324
41.77	22.055	1.2643912	0.5280105
37.147	18.912	1.3263355	0.5091124
32.255	16.763	1.3621104	0.5197024
27.637	14.545	1.3185658	0.5262872
24.068	13.513	1.2854697	0.5614509
21.228	12.789	1.350614	0.602459
18.266	11.792	NaN	0.645571

Measurements (PCV) of *Nautilus pompilius* from the Philippines

	7	8	10	11	12	15	16	17
1	NaN	NaN	NaN	NaN	NaN	NaN	NaN	NaN
2	NaN	NaN	NaN	NaN	NaN	NaN	NaN	NaN
3	NaN	NaN	NaN	NaN	NaN	NaN	NaN	NaN
4	NaN	NaN	NaN	NaN	NaN	NaN	NaN	NaN
5	NaN	NaN	NaN	NaN	NaN	NaN	NaN	NaN
6	NaN	0.25	NaN	NaN	NaN	NaN	NaN	NaN
7	NaN	0.28	NaN	NaN	NaN	NaN	NaN	NaN
8	NaN	0.38	NaN	NaN	NaN	NaN	NaN	NaN
9	0.16	0.51	NaN	NaN	NaN	NaN	NaN	NaN
10	0.2	0.59	NaN	0.33	NaN	NaN	0.28	0.22
11	0.24	0.78	NaN	0.37	NaN	NaN	0.36	0.25
12	0.28	0.92	0.32	0.46	0.31	NaN	0.41	0.31
13	0.3	1.09	0.39	0.55	0.37	NaN	0.5	0.4
14	0.32	1.47	0.45	0.65	0.43	0.42	0.58	0.43
15	0.4	1.76	0.59	0.86	0.51	0.51	0.66	0.53
16	0.55	2.34	0.7	1.05	0.66	0.56	0.79	0.67
17	0.65	2.7	0.85	1.23	0.82	0.66	1.06	0.84
18	0.68	3.31	0.91	1.51	0.94	0.8	1.26	1.03
19	0.8	4.56	1.2	1.96	1.07	1.03	1.57	1.33
20	1.11	5.69	1.54	2.29	1.41	1.36	1.8	1.68
21	1.28	7.19	1.59	3	1.75	1.64	2.3	2.12
22	1.69	9	2.11	3.68	2.13	2.23	2.97	2.62
23	1.97	11.9	2.31	5.04	2.77	2.62	3.69	2.89
24	2.59	14.6	3.54	6.33	3.32	2.94	4.76	4.17
25	3.04	18.56	3.86	6.14	3.95	3.93	6.31	5.63
26	3.79	23.02	5.8	10.64	4.73	5.13	7.58	6.42
27	4.63	21.36	7.05	12.77	5.96	6.9	10.02	8.14
28	6.1	NaN	8.93	NaN	6.91	6.87	11.76	9.56
29	7.44	NaN	11.39	14.67	9.15	9.8	15.24	12.44
30	8.78	NaN	14.08	17.66	11.15	12.93	18.13	15.14
31	11.41	NaN	18.29	15.81	13.44	15.77	21.18	17.54
32	14.06	NaN	22.06	NaN	17	21.05	26.32	22.26
33	18.37	NaN	25.26	NaN	19.42	25.68	21.24	25.16
34	22.38	NaN	NaN	NaN	18.91	23.61	NaN	29.24
35	28.45	NaN	NaN	NaN	NaN	NaN	NaN	NaN
36	NaN	NaN	NaN	NaN	NaN	NaN	NaN	NaN
37	NaN	NaN	NaN	NaN	NaN	NaN	NaN	NaN
38	NaN	NaN	NaN	NaN	NaN	NaN	NaN	NaN

Measurements (PCV) of *Nautilus pompilius* from the Philippines

20	23	24	25	26	27	28	30	31
NaN	NaN	NaN	NaN	NaN	NaN	NaN	NaN	NaN
NaN	NaN	NaN	NaN	NaN	NaN	NaN	NaN	NaN
NaN	NaN	NaN	NaN	NaN	NaN	NaN	NaN	NaN
NaN	NaN	NaN	NaN	NaN	NaN	NaN	NaN	NaN
NaN	NaN	NaN	NaN	NaN	NaN	NaN	NaN	NaN
NaN	NaN	NaN	NaN	NaN	NaN	NaN	NaN	NaN
NaN	NaN	NaN	NaN	NaN	NaN	NaN	NaN	NaN
NaN	0.14	NaN	NaN	0.14	0.19	NaN	NaN	NaN
NaN	0.18	NaN	0.19	0.15	0.21	0.16	NaN	NaN
0.26	0.2	NaN	0.29	0.19	0.24	0.19	NaN	NaN
0.35	0.28	0.19	0.29	0.2	0.29	0.23	0.29	NaN
0.33	0.3	0.24	0.39	0.23	0.35	0.24	0.35	0.31
0.45	0.36	0.27	0.42	0.27	0.4	0.29	0.44	0.41
0.52	0.49	0.3	0.54	0.31	0.55	0.33	0.53	0.46
0.66	0.53	0.32	0.66	0.33	0.64	0.39	0.62	0.5
0.88	0.63	0.42	0.77	0.45	0.74	0.49	0.8	0.53
1.07	0.81	0.53	0.94	0.49	0.86	0.59	0.94	0.59
1.4	0.95	0.69	1.15	0.66	0.98	0.71	1.14	0.89
1.68	1.09	0.78	1.37	0.78	1.14	0.86	1.47	1.15
2.09	1.41	0.87	1.58	0.87	1.33	1.05	1.69	1.37
2.65	1.87	1.07	2.18	1.08	1.8	1.24	1.96	1.71
3.19	2.01	1.27	2.61	1.27	2.24	1.53	2.79	1.9
4.09	2.7	1.52	3.15	1.52	3.04	1.98	3.27	2.53
5.26	3.19	2.01	4.09	1.92	3.88	2.4	3.51	2.97
6.23	4.2	2.39	5.17	2.14	4.42	3.28	5.45	4.01
7.96	5.35	2.88	6.39	2.61	6.19	3.45	6.47	4.74
NaN	7.02	3.5	7.87	3.32	7.92	4.56	8.23	6.49
NaN	8.71	4.4	10.21	3.76	9.92	5.59	10.74	8.08
NaN	NaN	5.16	NaN	4.76	NaN	6.99	13.74	10.48
NaN	NaN	6.86	NaN	5.96	NaN	8.12	17.64	13.46
NaN	NaN	8.65	NaN	6.75	NaN	11.24	NaN	NaN
NaN	NaN	NaN	NaN	8.67	NaN	NaN	NaN	NaN
NaN	NaN	NaN	NaN	10.73	NaN	NaN	NaN	NaN
NaN	NaN	NaN	NaN	13.95	NaN	NaN	NaN	NaN
NaN	NaN	NaN	NaN	NaN	NaN	NaN	NaN	NaN
NaN	NaN	NaN	NaN	NaN	NaN	NaN	NaN	NaN
NaN	NaN	NaN	NaN	NaN	NaN	NaN	NaN	NaN
NaN	NaN	NaN	NaN	NaN	NaN	NaN	NaN	NaN

Measurements (PCV) of *Nautilus pompilius* from the Philippines (continued)

32	33	34	35	36	38	39	40	41
NaN	NaN	NaN	NaN	NaN	NaN	NaN	NaN	NaN
NaN	NaN	NaN	NaN	NaN	NaN	NaN	NaN	NaN
NaN	NaN	NaN	NaN	NaN	NaN	NaN	NaN	NaN
NaN	NaN	NaN	NaN	NaN	NaN	NaN	NaN	NaN
NaN	NaN	NaN	NaN	NaN	NaN	NaN	NaN	NaN
NaN	NaN	NaN	NaN	NaN	NaN	NaN	NaN	NaN
NaN	NaN	NaN	NaN	NaN	NaN	NaN	0.23	NaN
NaN	NaN	NaN	NaN	NaN	0.21	NaN	0.25	NaN
NaN	0.25	NaN	NaN	NaN	0.21	NaN	0.29	NaN
NaN	0.3	0.19	NaN	NaN	0.32	0.33	0.31	NaN
0.25	0.36	0.26	0.3	0.15	0.32	0.32	0.43	NaN
0.27	0.46	0.27	0.38	0.18	0.4	0.41	0.49	NaN
0.32	0.55	0.33	0.42	0.19	0.49	0.48	0.62	0.35
0.4	0.63	0.41	0.46	0.25	0.61	0.5	0.74	0.34
0.46	0.72	0.49	0.61	0.32	0.81	0.68	0.93	0.45
0.52	0.92	0.63	0.75	0.37	1	0.82	1.1	0.66
0.64	1.08	0.75	0.92	0.43	1.18	1.06	1.41	0.77
0.77	1.52	0.89	1.14	0.52	1.45	1.25	1.78	0.9
0.9	1.69	1.14	1.33	0.68	1.77	1.59	2.24	1.13
1.07	2.17	1.36	1.74	0.81	2.2	2.02	2.72	1.37
1.4	2.96	1.65	2.17	0.9	2.88	2.44	3.36	1.68
1.44	3.45	1.98	2.63	1.08	3.7	3.01	4.04	2.09
1.98	4.39	2.53	3.44	1.31	4.86	4.17	5.04	2.6
2.48	5.69	2.95	4.12	1.4	5.79	4.92	6.77	3.21
2.87	7.66	3.67	5.44	1.82	7.27	6.21	8.92	3.85
3.62	9.84	4.48	6.86	2.04	9.25	7.76	11.14	5.04
4.1	12.06	5.61	8.5	2.31	12.05	9.67	14.49	6.21
5.81	NaN	6.51	11.03	3.02	15.08	11.81	18.31	7.14
6.72	NaN	8.74	NaN	3.77	19.08	16.52	20.84	9.33
8.52	NaN	10.03	NaN	3.87	21.85	18.8	20.36	11.66
10.82	NaN	13.41	NaN	5.36	21.21	22.38	NaN	14.12
13.22	NaN	15.78	NaN	6.21	NaN	10.55	NaN	18.25
NaN	NaN	NaN	NaN	8.14	NaN	NaN	NaN	22.95
NaN	NaN	NaN	NaN	9.47	NaN	NaN	NaN	26.87
NaN	NaN	NaN	NaN	13.37	NaN	NaN	NaN	NaN
NaN	NaN	NaN	NaN	14.76	NaN	NaN	NaN	NaN
NaN	NaN	NaN	NaN	18.95	NaN	NaN	NaN	NaN
NaN	NaN	NaN	NaN	NaN	NaN	NaN	NaN	NaN

Measurements (PCV) of *Nautilus pompilius* from the Philippines (continued)

42	43	44	46	48	51	53	54	56
NaN	NaN	NaN	NaN	NaN	NaN	NaN	NaN	NaN
NaN	NaN	NaN	NaN	NaN	NaN	NaN	NaN	NaN
NaN	NaN	NaN	NaN	NaN	NaN	NaN	NaN	NaN
NaN	NaN	NaN	NaN	NaN	NaN	NaN	NaN	NaN
NaN	NaN	NaN	NaN	NaN	NaN	NaN	NaN	NaN
NaN	NaN	NaN	NaN	NaN	NaN	NaN	NaN	NaN
NaN	NaN	NaN	NaN	NaN	NaN	NaN	NaN	NaN
NaN	NaN	NaN	NaN	NaN	NaN	NaN	NaN	NaN
NaN	NaN	NaN	NaN	NaN	NaN	NaN	NaN	NaN
NaN	0.27	0.18	NaN	NaN	0.21	0.15	0.29	NaN
0.29	0.31	0.27	NaN	0.18	0.2	0.17	0.37	0.33
0.32	0.36	0.3	0.32	0.23	0.31	0.21	0.43	0.37
0.33	0.45	0.37	0.39	0.27	0.31	0.24	0.53	0.44
0.45	0.55	0.42	0.45	0.34	0.39	0.26	0.65	0.49
0.55	0.69	0.49	0.6	0.44	0.43	0.31	0.8	0.68
0.67	0.81	0.64	0.67	0.54	0.6	0.4	1.09	0.87
0.87	0.97	0.76	0.86	0.67	0.73	0.5	1.31	1.01
1.01	1.28	0.91	1.06	0.72	0.87	0.61	1.62	1.29
1.26	1.47	1.17	1.36	0.93	1.12	0.68	2.09	1.4
1.47	1.88	1.48	1.43	1.19	1.32	0.96	2.42	1.77
1.89	2.09	1.9	2.02	1.44	1.57	1.03	3.02	2.24
2.4	2.84	2.53	2.36	1.88	2.01	1.36	4.07	2.71
2.97	3.42	2.61	3.15	2.14	2.48	1.61	5.06	3.37
3.54	4.52	4.07	3.65	2.61	3.31	1.9	6.56	4.32
4.5	5.47	4.7	4.54	3.24	3.65	2.43	8.19	5.13
5.59	7.04	6.24	6.11	4.03	5.16	3.11	9.6	6.45
7.27	8.62	7.72	7.51	5.1	6.66	3.61	13.82	8.23
8.92	10.61	10.18	9.36	6.2	8.15	4.25	16.67	10.2
10.15	13.05	12.87	12.19	7.35	9.97	4.72	20	12.84
13.44	16.03	17.07	15.89	9.22	12.97	6.55	25.38	15.29
17.84	17.71	20.44	19.11	12.18	16.66	8.63	NaN	20
22.31	19.81	26.09	24.23	14.79	19.86	10.8	NaN	22.17
24.14	NaN	24.89	NaN	18.09	24.93	13.92	NaN	19.28
15.27	NaN	NaN	NaN	22.26	20.58	16.92	NaN	NaN
NaN	NaN	NaN	NaN	NaN	NaN	21.8	NaN	NaN
NaN	NaN	NaN	NaN	NaN	NaN	25.69	NaN	NaN
NaN	NaN	NaN	NaN	NaN	NaN	21.48	NaN	NaN
NaN	NaN	NaN	NaN	NaN	NaN	NaN	NaN	NaN

Measurements (PCV) of *Nautilus pompilius* from Malaysia

	1	2	3	4	5	6	7	8
1	NaN	NaN	NaN	NaN	NaN	NaN	NaN	NaN
2	NaN	NaN	NaN	NaN	NaN	NaN	NaN	NaN
3	NaN	NaN	NaN	NaN	NaN	NaN	NaN	NaN
4	NaN	NaN	NaN	NaN	NaN	NaN	NaN	NaN
5	NaN	NaN	NaN	NaN	NaN	NaN	NaN	NaN
6	NaN	NaN	NaN	NaN	NaN	NaN	NaN	NaN
7	NaN	NaN	NaN	NaN	NaN	NaN	NaN	NaN
8	0.25	NaN	NaN	NaN	NaN	NaN	NaN	NaN
9	0.33	0.55	0.32	0.27	0.34	NaN	0.24	NaN
10	0.35	0.39	0.36	0.36	0.39	0.36	0.29	0.25
11	0.43	0.49	0.43	0.37	0.42	0.43	0.41	0.31
12	0.51	0.61	0.46	0.51	0.53	0.5	0.47	0.3
13	0.66	0.59	0.62	0.64	0.65	0.54	0.53	0.4
14	0.7	0.89	0.73	0.69	0.77	0.68	0.69	0.51
15	0.89	1.13	1	0.85	0.89	0.76	0.53	0.54
16	0.99	1.46	1.15	1.02	0.82	1.03	0.9	0.76
17	1.26	1.78	1.31	1.39	1.29	1.19	1.13	0.9
18	1.57	1.96	1.65	1.64	1.52	1.48	1.42	1.1
19	1.87	2.63	2.11	2.07	1.8	1.58	1.52	1.32
20	2.44	3.01	2.34	2.58	2.05	2.03	2.07	1.59
21	2.98	4.06	3.14	3.28	2.66	2.69	2.7	1.87
22	3.72	5.15	3.82	4.07	2.96	3.28	3.32	2.42
23	4.72	6.29	4.67	5.13	3.97	3.83	4.49	2.72
24	6.2	8	5.14	6.36	4.89	4.93	4.91	3.42
25	6.72	9.13	6.97	8.72	6.37	6.37	6.64	4.55
26	9.29	12.98	8.44	10.57	7.69	7.7	8.77	5.49
27	11.42	13.86	10.92	13.74	9.5	9.75	10.59	6.44
28	14.99	18.46	13.71	16.95	12.58	12.76	12.79	8.1
29	18.8	21.36	16.52	22.06	14.94	15.85	17.6	11.03
30	20.41	28.67	22.61	24.63	20.07	19.82	21.93	13.41
31	26.85	29.11	28.12	30.23	23.98	23.4	23.56	17.4
32	28.71	15.65	35.23	29.64	29.07	28.04	30.65	22.68
33	25.88	NaN	27.53	NaN	34.14	28.8	30.57	27.94
34	NaN	NaN	NaN	NaN	14.73	NaN	NaN	34.25
35	NaN	NaN	NaN	NaN	NaN	NaN	NaN	24.14
36	NaN	NaN	NaN	NaN	NaN	NaN	NaN	NaN
37	NaN	NaN	NaN	NaN	NaN	NaN	NaN	NaN
38	NaN	NaN	NaN	NaN	NaN	NaN	NaN	NaN

Measurements (PCV) of *Nautilus pompilius* from Malaysia (continued)

9	10	11	12	13	14	15	16	17
NaN	NaN	NaN	NaN	NaN	NaN	NaN	NaN	NaN
NaN	NaN	NaN	NaN	NaN	NaN	NaN	NaN	NaN
NaN	NaN	NaN	NaN	NaN	NaN	NaN	NaN	NaN
NaN	NaN	NaN	NaN	NaN	NaN	NaN	NaN	NaN
NaN	NaN	NaN	NaN	NaN	NaN	NaN	NaN	NaN
NaN	NaN	NaN	NaN	NaN	NaN	NaN	NaN	NaN
NaN	NaN	NaN	NaN	NaN	NaN	NaN	NaN	NaN
NaN	NaN	NaN	0.18	NaN	NaN	NaN	NaN	0.27
0.3	0.31	0.38	0.22	NaN	NaN	NaN	0.31	0.26
0.39	0.37	0.44	0.3	NaN	0.34	0.3	0.33	0.3
0.45	0.41	0.54	0.29	0.36	0.41	0.36	0.44	0.31
0.45	0.51	0.62	0.42	0.39	0.47	0.37	0.49	0.37
0.49	0.56	0.78	0.45	0.46	0.57	0.54	0.56	0.45
0.59	0.74	0.95	0.47	0.6	0.64	0.63	0.6	0.53
0.73	0.98	1.23	0.57	0.72	0.83	0.77	0.67	0.67
0.88	1.22	1.42	0.68	0.91	1.15	0.86	0.81	0.73
1.11	1.44	1.9	0.94	1.11	1.36	1.09	1.03	0.9
1.3	1.82	2.38	1.08	1.44	1.81	1.18	1.39	1.2
1.49	2.16	2.9	1.24	1.8	2.05	1.5	1.42	1.44
1.88	2.84	3.63	1.62	2.15	2.63	1.92	2.06	1.74
2.35	3.63	4.57	1.97	2.77	3.37	2.23	1.93	2.09
2.86	4.15	5.75	2.34	3.32	4.29	2.95	3.02	2.62
3.35	5.97	7.48	2.87	4.18	5.65	3.28	3.12	3.2
4.25	7.17	9.39	3.3	5.17	6.91	4.4	3.98	4.02
5.17	9.57	11.93	3.98	6.56	8.42	6.25	5.42	5.23
6.15	11.59	15.44	5.25	8.22	10.85	6.85	6.56	6.56
7.32	15.29	17.64	5.7	10.88	12.62	9.16	8.68	7.12
8.91	19.71	21.89	8.08	13.89	17.01	10.81	10.21	8.17
11.58	24.01	25.35	8.1	16.96	21.22	14.25	13.01	12.28
13.29	27.72	29.54	10.21	21.88	21.63	17.52	15.86	14.93
18.28	29.13	NaN	14.52	25.95	31.41	22.1	20.6	19.83
21.31	NaN	NaN	17.57	24.7	35.5	27.5	26.51	22.86
25.01	NaN	NaN	22.04	NaN	NaN	33.01	31.39	26.31
30.33	NaN	NaN	27.28	NaN	NaN	27.65	32.42	20.66
27.94	NaN	NaN	34.02	NaN	NaN	NaN	NaN	NaN
NaN	NaN	NaN	24.65	NaN	NaN	NaN	NaN	NaN
NaN	NaN	NaN	NaN	NaN	NaN	NaN	NaN	NaN
NaN	NaN	NaN	NaN	NaN	NaN	NaN	NaN	NaN

Measurements (PCV) of *Nautilus pompilius* from Malaysia (continued)

18	19	20	21	22	23	24	25	26
NaN	NaN	NaN	NaN	NaN	NaN	NaN	NaN	NaN
NaN	NaN	NaN	NaN	NaN	NaN	NaN	NaN	NaN
NaN	NaN	NaN	NaN	NaN	NaN	NaN	NaN	NaN
NaN	NaN	NaN	NaN	NaN	NaN	NaN	NaN	NaN
NaN	NaN	NaN	NaN	NaN	NaN	NaN	NaN	NaN
NaN	NaN	NaN	NaN	NaN	NaN	NaN	NaN	NaN
NaN	NaN	NaN	NaN	NaN	NaN	NaN	NaN	NaN
NaN	NaN	NaN	NaN	NaN	NaN	NaN	NaN	NaN
NaN	NaN	0.2	NaN	0.29	0.25	NaN	NaN	NaN
NaN	0.26	0.25	NaN	0.26	0.34	0.35	NaN	NaN
0.24	0.36	0.29	NaN	0.4	0.38	0.42	0.21	0.34
0.29	0.41	0.35	0.23	0.42	0.44	0.53	0.23	0.43
0.35	0.54	0.4	0.37	0.53	0.55	0.61	0.26	0.51
0.44	0.61	0.37	0.32	0.58	0.72	0.73	0.33	0.63
0.51	0.75	0.55	0.4	0.83	0.89	0.95	0.4	0.74
0.66	0.92	0.75	0.49	0.94	0.99	1.23	0.5	0.87
0.8	1.11	0.84	0.59	1.24	1.26	1.52	0.6	1.04
0.86	1.28	1.06	0.76	1.49	1.36	1.91	0.7	1.43
1.2	1.61	1.2	1.01	1.8	1.79	2.21	0.86	1.65
1.44	1.92	1.5	1.19	2.34	2.17	2.62	1.12	2.29
1.68	2.44	1.86	1.6	2.9	2.68	3.24	1.14	2.77
2.12	2.92	2.06	1.96	3.54	3.33	4.3	1.42	3.19
2.73	3.6	2.84	2.34	4.39	4.1	5.12	1.96	4.08
3.17	4.52	3.36	2.54	5.09	5.26	6.41	2.14	5.52
4.1	5.32	4.41	3.52	6.7	6.68	8.76	2.87	6.53
5.37	6.76	4.82	4.33	8.85	8.12	10.8	3.51	8.47
6.24	8.87	5.62	5.38	10.64	10.36	13.67	4.32	9.94
8.51	11.05	7.53	6.61	14.29	14.05	16.43	5.56	12.54
10.52	13.98	9.75	7.32	16.89	16.85	23.72	6.71	15.13
12.43	16	11.29	9.94	21.83	20.32	27.75	8.35	19.19
16.19	20.49	14.97	12.42	26.21	26.61	32.19	9.37	23.78
19.29	23.21	18.85	15.92	30.9	31.74	15.61	11.4	29.93
23.94	26.82	21.51	19.95	21.7	28.54	NaN	14.55	35.87
29.04	26.01	24.17	24.2	NaN	NaN	NaN	20.15	29.42
23.96	NaN	24.85	28.66	NaN	NaN	NaN	23.08	NaN
NaN	NaN	NaN	29.68	NaN	NaN	NaN	27.75	NaN
NaN	NaN	NaN	NaN	NaN	NaN	NaN	29.43	NaN
NaN	NaN	NaN	NaN	NaN	NaN	NaN	NaN	NaN

Measurements (PCV) of *Nautilus pompilius* from Malaysia (continued)

27	28	30	31	32	33	34	35	36
NaN	NaN	NaN	NaN	NaN	NaN	NaN	NaN	NaN
NaN	NaN	NaN	NaN	NaN	NaN	NaN	NaN	NaN
NaN	NaN	NaN	NaN	NaN	NaN	NaN	NaN	NaN
NaN	NaN	NaN	NaN	NaN	NaN	NaN	NaN	NaN
NaN	NaN	NaN	NaN	NaN	NaN	NaN	NaN	NaN
NaN	NaN	NaN	NaN	NaN	NaN	NaN	NaN	NaN
NaN	NaN	NaN	NaN	NaN	NaN	NaN	NaN	NaN
NaN	NaN	NaN	NaN	NaN	NaN	NaN	0.23	NaN
NaN	NaN	NaN	NaN	NaN	NaN	0.27	0.28	NaN
0.28	0.27	NaN	0.31	0.3	NaN	0.22	0.36	0.17
0.36	0.34	0.28	0.34	0.32	NaN	0.3	0.36	0.23
0.4	0.35	0.2	0.37	0.36	0.35	0.36	0.5	0.3
0.49	0.47	0.23	0.5	0.47	0.43	0.38	0.61	0.28
0.7	0.55	0.33	0.56	0.5	0.55	0.44	0.8	0.36
0.8	0.7	0.42	0.71	0.65	0.6	0.55	0.98	0.47
1.01	0.86	0.46	0.97	0.83	0.76	0.57	1.24	0.6
1.1	1.04	0.63	1.14	1	0.98	0.84	1.58	0.69
1.5	1.25	0.77	1.42	1.17	1.19	0.99	2.07	0.82
1.82	1.72	0.88	1.88	1.47	1.37	1.18	2.58	1.1
2.2	1.93	0.91	2.36	1.8	1.78	1.49	3.48	1.23
2.27	2.33	1.09	2.85	2.31	2.19	1.84	4.13	1.52
2.94	2.96	1.26	3.58	2.95	2.51	2.28	5.49	1.93
3.87	4	1.61	4.77	3.63	3.38	2.85	6.96	2.69
4.72	4.95	1.97	6.13	4.68	4.17	3.28	9.03	3.18
6.41	5.63	1.92	7.79	5.57	5.22	4.3	11.46	3.97
7.56	8.01	2.57	9.57	7.71	6.8	5.28	15.17	4.36
10.74	9.37	2.99	12.55	8.07	8.32	6.55	19.77	6.08
12.06	12.3	3.74	15.91	11.12	10.58	7.69	24.76	7.5
15.48	15.21	5.12	18.8	13.49	12.59	10.28	28.65	9.15
20.58	17.44	6.15	21.81	18.11	16.51	11.46	30.52	10.68
24.67	22.41	7.11	27.11	19.79	20.73	16.54	NaN	15.61
31.47	26.76	9.85	27.29	27.18	24.82	19.8	NaN	19.51
29.65	23.84	12.46	NaN	28.24	30.52	24.71	NaN	21.15
NaN	NaN	15.42	NaN	NaN	26.16	27.07	NaN	23.35
NaN	NaN	19.89	NaN	NaN	NaN	13.9	NaN	22.57
NaN	NaN	23.93	NaN	NaN	NaN	NaN	NaN	NaN
NaN	NaN	29.22	NaN	NaN	NaN	NaN	NaN	NaN
NaN	NaN	28.77	NaN	NaN	NaN	NaN	NaN	NaN

Measurements (PCV) of *Nautilus pompilius* from Malaysia (continued)

37	38
NaN	NaN
NaN	NaN
NaN	NaN
NaN	NaN
NaN	NaN
NaN	NaN
NaN	NaN
NaN	NaN
NaN	NaN
0.29	0.25
0.36	0.35
0.46	0.34
0.51	0.36
0.64	0.41
0.8	0.47
0.94	0.68
1.14	0.97
1.45	1.1
1.75	1.16
2.11	1.6
2.66	1.81
3.37	2.3
4.14	2.93
5.28	3.69
6.97	4.5
8.42	5.16
10.8	7.11
15.21	8.44
19.37	10.88
23.46	12.42
29.01	16.27
27.8	19.57
NaN	22.01
NaN	29.01
NaN	31.57
NaN	NaN
NaN	NaN
NaN	NaN

Measurements (PCV) of *Nautilus pompilius* from Indonesia

	1	2	3	4	5	6	7	8
1	NaN	NaN	NaN	NaN	NaN	NaN	NaN	NaN
2	NaN	NaN	NaN	NaN	NaN	NaN	NaN	NaN
3	NaN	NaN	NaN	NaN	NaN	NaN	NaN	NaN
4	NaN	NaN	NaN	NaN	NaN	NaN	NaN	NaN
5	NaN	NaN	NaN	NaN	NaN	NaN	NaN	NaN
6	NaN	NaN	NaN	NaN	NaN	NaN	NaN	NaN
7	NaN	NaN	NaN	NaN	NaN	NaN	NaN	NaN
8	NaN	NaN	NaN	0.18	NaN	NaN	NaN	0.21
9	NaN	0.29	0.24	0.22	NaN	NaN	0.24	0.29
10	NaN	0.26	0.34	0.25	NaN	NaN	0.26	0.33
11	0.35	0.21	0.4	0.29	NaN	NaN	0.27	0.43
12	0.42	NaN	0.41	0.36	NaN	0.38	0.31	0.44
13	0.49	0.47	0.51	0.41	0.25	0.49	0.38	0.54
14	0.58	0.5	0.6	0.55	0.39	0.6	0.42	0.65
15	0.76	0.65	0.76	0.66	0.37	0.71	0.42	0.73
16	0.9	0.77	0.86	0.77	0.47	0.94	0.56	0.96
17	1.15	1.03	1.21	0.9	0.6	1.05	0.6	1.17
18	1.48	1.2	1.48	1.19	0.58	1.28	0.66	1.46
19	1.81	1.56	1.72	1.32	0.78	1.55	0.81	1.7
20	2.16	1.92	2.09	1.58	0.93	2.09	0.94	2.12
21	2.79	2.51	2.63	1.97	1.21	2.49	1.09	2.45
22	3.46	3.04	3.15	2.46	1.52	3.19	1.39	3.08
23	4.15	3.72	4.1	2.69	1.78	4.12	1.88	3.49
24	5.4	4.86	4.89	3.66	2.17	5.23	2.19	4.65
25	6.63	5.96	6.34	4.4	2.94	6.41	2.63	5.55
26	8.4	7.47	8.02	5.38	3.56	8.4	3.41	7.23
27	10.6	9.06	9.43	6.62	4.2	10.42	4.17	8.76
28	14.02	12.52	13.23	7.47	5.29	12.91	4.8	11.54
29	18.12	14.55	15.9	9.79	6.55	16.55	6.44	14.71
30	22.05	19.07	19.7	12.29	7.91	22.16	8.53	18.3
31	25.32	23.25	22.77	15.78	9.91	24.57	10.35	19.71
32	14.37	26.96	9.8	19.19	12.23	25.82	12.15	14.92
33	NaN	NaN	NaN	13.1	15.12	NaN	16.59	NaN
34	NaN	NaN	NaN	NaN	17.62	NaN	18.16	NaN
35	NaN	NaN	NaN	NaN	19.91	NaN	NaN	NaN
36	NaN	NaN	NaN	NaN	NaN	NaN	NaN	NaN
37	NaN	NaN	NaN	NaN	NaN	NaN	NaN	NaN
38	NaN	NaN	NaN	NaN	NaN	NaN	NaN	NaN

Measurements (PCV) of *Nautilus pompilius* from Indonesia (continued)

9	10	11	12	13	14	15	16	17
NaN	NaN	NaN	NaN	NaN	NaN	NaN	NaN	NaN
NaN	NaN	NaN	NaN	NaN	NaN	NaN	NaN	NaN
NaN	NaN	NaN	NaN	NaN	NaN	NaN	NaN	NaN
NaN	NaN	NaN	NaN	NaN	NaN	NaN	NaN	NaN
NaN	NaN	NaN	NaN	NaN	NaN	NaN	NaN	NaN
NaN	NaN	NaN	NaN	NaN	NaN	NaN	NaN	NaN
NaN	NaN	NaN	NaN	NaN	0.15	NaN	NaN	NaN
NaN	NaN	0.2	0.12	NaN	0.23	NaN	0.2	0.21
NaN	NaN	0.26	0.25	NaN	0.26	NaN	0.18	0.34
NaN	NaN	0.34	0.34	0.23	0.27	NaN	0.22	0.34
0.28	0.42	0.41	0.37	0.26	0.29	NaN	0.26	0.44
0.31	0.46	0.53	0.44	0.32	0.38	0.36	0.33	0.5
0.39	0.6	0.61	0.53	0.35	0.5	0.45	0.4	0.56
0.42	0.77	0.73	0.63	0.54	0.58	0.55	0.55	0.73
0.55	0.79	0.93	0.77	0.62	0.72	0.54	0.7	0.84
0.65	0.96	1.17	0.96	0.72	0.94	0.76	0.87	1.04
0.76	1.24	1.53	1.18	0.96	1.03	0.93	1.04	1.33
0.86	1.54	1.76	1.5	1.24	1.4	1.06	1.31	1.63
1.12	1.73	2.35	1.77	1.52	1.95	1.23	1.69	1.96
1.39	2.17	3.09	2.15	1.81	2.19	1.56	2.16	2.46
1.56	2.61	3.95	2.88	2.14	2.73	1.77	2.65	3.12
1.88	3.2	5	3.3	2.84	3.3	2.21	3.24	3.73
2.44	4.1	6.59	4.16	3.56	3.93	2.98	4.24	5.21
2.83	5.24	8.45	5.68	4.82	4.89	3.59	5.27	6.11
3.82	6.13	10.75	6.85	6.04	6.3	4.75	6.67	7.72
4.17	7.51	13.84	8.47	7.22	7.06	5.44	8.12	9.84
5.45	9.83	17.08	11.13	10.15	9.79	6.45	10.73	12.6
6.44	12.2	19.26	12.89	11.58	11.21	8.72	12.14	15.78
8.21	14.88	NaN	16.12	15.54	14.23	10.19	7.43	19.96
9.59	17.78	NaN	6.45	9.74	18.61	12.47	NaN	23.72
12.02	21.37	NaN	NaN	NaN	17.92	14.74	NaN	16.52
12.38	15.17	NaN	NaN	NaN	NaN	13.57	NaN	NaN
16.52	NaN	NaN	NaN	NaN	NaN	NaN	NaN	NaN
18.72	NaN	NaN	NaN	NaN	NaN	NaN	NaN	NaN
17.53	NaN	NaN	NaN	NaN	NaN	NaN	NaN	NaN
NaN	NaN	NaN	NaN	NaN	NaN	NaN	NaN	NaN
NaN	NaN	NaN	NaN	NaN	NaN	NaN	NaN	NaN
NaN	NaN	NaN	NaN	NaN	NaN	NaN	NaN	NaN

Measurements (PCV) of *Nautilus pompilius* from Indonesia (continued)

18	19	20
NaN	NaN	NaN
NaN	NaN	NaN
NaN	NaN	NaN
NaN	NaN	NaN
NaN	NaN	NaN
NaN	NaN	NaN
NaN	NaN	NaN
NaN	0.17	NaN
0.18	0.26	NaN
0.22	0.35	0.25
0.34	0.42	0.35
0.29	0.52	0.39
0.39	0.57	0.5
0.52	0.69	0.69
0.56	0.85	0.8
0.63	1.02	0.97
0.78	1.2	1.21
1.04	1.49	1.56
1.25	1.78	1.86
1.65	2.27	2.39
1.94	2.65	3.37
2.51	3.43	4.11
3.23	4.3	5.11
4.04	5.58	6.69
5.28	7.03	8.86
6.83	8.54	11.19
8.56	10.06	13.86
11.45	13.19	16.23
14.82	17.43	15.04
18.05	20.18	NaN
22.37	23.21	NaN
20.81	13.24	NaN
NaN	NaN	NaN
NaN	NaN	NaN
NaN	NaN	NaN
NaN	NaN	NaN
NaN	NaN	NaN
NaN	NaN	NaN

Chapter V

Cretaceous-Palaeogene incumbent replacement of associations of mollusc plankton and large filter feeders

Tajika, A. Nützel, A. Klug, C

Submitted to
Scientific Reports

Cretaceous-Palaeogene incumbent replacement of associations of mollusc plankton and large filter feeders

Amane Tajika[1], Alexander Nützel[2] & Christian Klug[1]

[1]Paläontologisches Institut und Museum, Universität Zürich, Karl Schmid-Strasse 4, CH-8006 Zürich, Switzerland.
[2]SNSB-Bayerische Staatssammlung für Paläontologie und Geologie, Department of Earth and Environmental Sciences, Palaeontology & Geobiology, GeoBio-Center LMU, Richard-Wagner-Str. 10, 80333 München, Germany

Abstract

Owing to their great diversity and abundance, ammonites and belemnites represented key elements in Mesozoic food webs. Because of their extreme ontogenetic size increase by more than two orders of magnitude, their position in the food webs likely changed during ontogeny. Here, we reconstruct reproductive rates of these cephalopods and discuss these developmental shifts in their ecologic roles. Based on similarities in conch morphology, size, habitat and abundance, we suggest that juvenile ammonites and belemnites were ecologically replaced by holoplanktonic gastropods after the Cretaceous/Palaeogene mass extinction. As primary consumers, these extinct cephalopod groups were important constituents of the plankton and a principal food source for planktivorous organisms. As victims or, respectively, profiteers of this case of ecological replacement, filter feeding chondrichthyans and cetaceans likely filled the niches formerly occupied by large pachycormid fish during the Jurassic and Cretaceous.

Introduction

The fate of individual groups of marine organisms at mass extinction intervals is often well-studied[1, 2]. By contrast, the disappearance of entire communities or ecological associations or food webs or important parts of any of these structures from the geologic past still requires a lot of palaeontological research (e.g., refs 3-5). Extinctions of entire communities or ecosystems are most conspicuous during the great mass extinctions, when usually vast new ecospace was freed and thereby, new ecological niches could form.

Although it is not the most severe of the Big Five, the end-Cretaceous mass extinction is likely the most famous among those with the greatest severity[6]. This fame roots in the facts that popular groups of organisms such as dinosaurs[7, 8] and ammonites[9-11] were erased by the consequences of an impact in Mexico and flood-basalt-eruptions in India[12-16].

Marine communities were heavily affected as reflected in the partial or total disappearance of major groups such as ammonoids and belemnites[17-21] as well as foraminifers[22, 23] and bivalves[2]. Ammonoids were both highly diverse and evolved a great disparity in the course of the Cretaceous[24, 25]; some of the most bizarre forms such as Nipponites, Diplomoceras and Didymoceras appeared. Additionally, the largest ammonoids of all times, members of the family Puzosiidae, also lived during Cretaceous times[26-28]. Puzosiids are not only gigantic but they also occurred worldwide and in great numbers.

The great abundance, wide geographical distribution, extreme diversity, middle to giant size in combination with the likely high reproductive rates of ammonites raises questions (i) for Cretaceous marine food webs that partially relied on them as planktotrophic consumers, but particularly their small offspring as food source and (ii) what groups might have replaced ammonites, belemnites and their predators or had similar ecological roles including their positions post-Cretaceous food webs.

Results

Estimating ammonoid reproductive rates. We estimated reproductive rates of large Cretaceous ammonites such as Parapuzosia seppenradensis using the following assumptions and measurements. We assume that the major part of egg-development happened in the body chamber (i)[30, 31]; we think

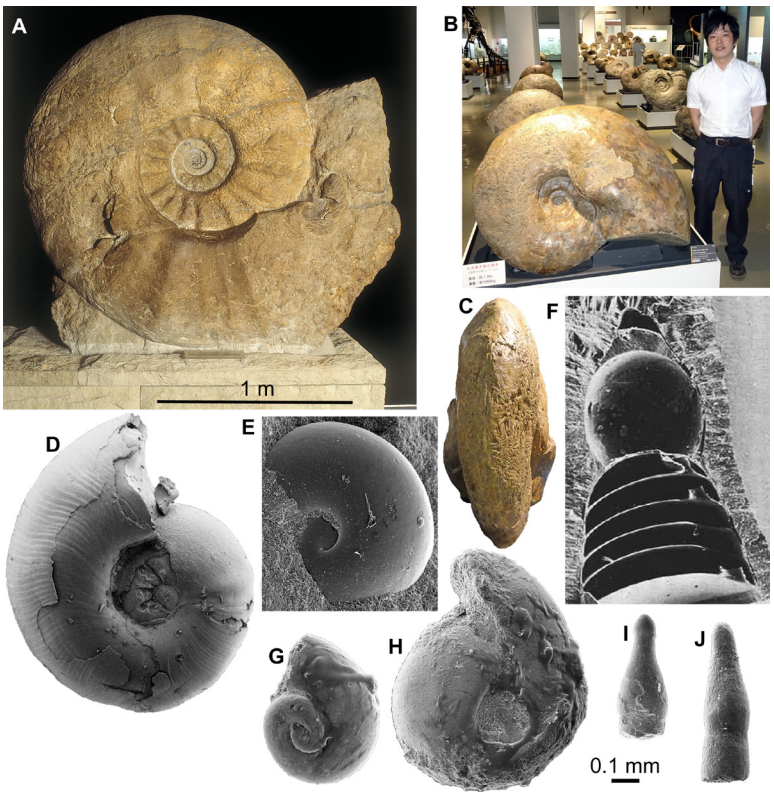

Fig. 1. Adult ammonites (A-C), juvenile ammonites (D, E), and an embryonic belemnite (F) compared to fossil conchs of Thecosomata from the Eocene of India (G-J). Photo in A courtesy A. Hendricks, Münster; D and E from Tanabe et al.[41]; F from Bandel et al.[45]; G to J from Lokho & Kumar[62]. A. *Parapuzosia seppenradensis*, Campanian, Seppenrade. B, C. *Pachydesmoceras* sp., Campanian, Hokkaido, diameter 1.3 m, D. Aiba (Mikasa) for scale. Note the symmetrical bulges in the posterior body chamber in C. D, juvenile conch of *Scaphites whitfieldi*, AMNH 44833, Turonian, U.S.A. E, embryonic conch of *Aconeceras* cf. *trautscholdi*, UMUT MM 29439–4, Aptian, Russia. F, embryonic conch of *Hibolithes* sp., GPIT Ce 1599, Callovian, Lithuania. G to J, Upper Disang Formation, Phek District, Nagaland. G, H, Limacinidae spp. I, J, Creseidae spp.

that the ammonitella represents the embryonic part of the conch (ii)[30]; we suggest that egg-size only slightly exceeded ammonitella-size (iii)[30, 31]; and (iv) we followed the proportion of 8% of the soft body volume being occupied by the gonads according to the proportions known from Recent *Nautilus*[32-34]. As far as (iv) is concerned, there is some uncertainty because the proportions of the ovaries are unknown from ammonoids due to the extremely rare and fragmentary preservation of soft parts[31, 35-38]. When regarding the specimens figured by Mironenko & Rogov[31], one tends to assume that the gonads filled an even larger portion of the body chamber. This hypothesis finds further support in symmetric bulges in the posterior body chamber in mature Pachydesmoceras (Fig. 1) and scaphitid conchs[39]. These bulges may have offered space for the growing ovaries. Owing to these assumptions, we calculated alternative egg-numbers using a body chamber volume proportion occupied by gonads of 30%.

The largest specimen of the largest ammonite species Parapuzosia seppenradensis is incomplete[26, 28]. We estimated the adult body chamber volume and the surface area of the terminal aperture assuming a body chamber length of about 180 degrees because of shell traces along the umbilical seam. Accordingly, the maximum diameter dm might have reached 2200 mm with a whorl height wh of about 800 mm and a whorl width ww of about 500 mm. The radiuses would then measure 1250 mm (r1) at the terminal aperture and 950 mm (r2) on the opposite side. Using the wh and ww values, we reconstructed a whorl cross section in CorelDraw and measured the area; accordingly, the cross section area K amounts to almost 320'000 mm2.

As demonstrated by De Baets et al.[34], derived ammonoids likely had high reproductive rates. This is corroborated by the great differences between embryo size and adult conch size. For example, in the largest specimen of Parapuzosia sep-

penradense from the Late Cretaceous of Germany, the embryonic conch measured about one millimeter in diameter at hatching, while the adult conch exceeded two meters in diameter[28, 30, 33, 34, 40, 41]. This implies a factor of at least 2000 in diameter increase between embryos and adult macroconchs.

In order to estimate gonad volume, we determined the body chamber volume VBC, which can be achieved by applying an equation introduced by Raup & Chamberlain42 and also used by De Baets et al.[34]:

$VBC = 2 / 3 * \pi * (K * Ra / lnW) * (1 - W-3\theta/2\pi)$

with K – area of the last aperture, Ra – distance coiling axis to center of mass (estimated 200 mm based on comparisons with species with similar conch shape[43, 44]), θ – angular length of the body chamber in radians (equals π here, because the body chamber is about 180° long), the whorl expansion rate for this particular body chamber length

$$W = (r1 / r2)\, 2\pi / \theta$$

with r1 – maximum conch diameter and r2 – conch diameter 180° behind the aperture.

Applying this to the lectotype of Parapuzosia seppenradense, we obtain W = 1.73 and then VBC = 137'075'470 mm^2. Depending on the proportion of the gonads, we obtain gonad volumes varying between about 10'000'000 mm^2 and 40'000'000 mm^2. Assuming an egg-volume of 1 mm^2, we obtain reproductive rates of 10'000'000 to 40'000'000 eggs per adult female Parapuzosia seppenradensis when they were semelparous. If we assume iteroparity, these numbers increase by the factor of the number of reproductive cycles. Also, if we assume that the eggs and embryos continued to grow after they were laid, the reproductive rates would increase. For an adult female of half the diameter, we would obtain egg-numbers of between 3'000'000 (8% gonad volume) and 10'000'000 eggs (30% gonad volume) at semelparity. Puzosiids and other large Cretaceaous ammonoids in the size range between 500 and 1000 mm are quite common worldwide (e.g. Pachydesmoceras).

The role of r-strategy in ammonite and belemnite ecology.

Depending on the proportional gonad size and whether or not ammonites were semelparous or iteroparous, it appears likely that adult females of the largest puzosiid ammonites such as Parapuzosia seppenradensis laid between 10'000'000 and 100'000'000 eggs. The simple calculation above itself highlights the likelihood that derived ammonites were extreme r-strategists, which produced vast amounts of offspring, likely contributing an important part of the plankton in size at the limit from micro- to macroplankton. High fecundity corresponded with high mortality and it is likely that hatchlings and juveniles of ammonites formed a major source of food in the marine realm.

As far as belemnites are concerned, their global abundance had decreased in the Late Cretaceous already, freeing ecospace for, e.g., other coleoids[19]. Nevertheless, coleoids with conical phragmocones such as belemnites, diplobelids, *Groenlandibelus* or *Naefia* share a small initial chamber and likely small embryonic conchs[45]. Accordingly, we can assume that their reproductive rates were also high, although much lower than those of the puzosiid ammonites because of the much lower size difference between adults and embryos.

Which animals ate ammonites?

Evidence for successful and unsuccessful predation on medium to large-sized ammonites is not rare but identifying the actual predator is possible only in very few cases[46, 47]. Additionally, most hard parts of ammonites (conch and lower jaw) were likely crushed by the predators and quickly dissolved in the digestive tract, making ammonites as fossilized stomach contents improbable, although a few cases have been reported where juvenile ammonoid remains are preserved in stomachs of Jurassic ammonites[37]. It is even more difficult to find evidence for predators that fed on hatchlings and neanic juveniles of ammonites (dm < 10 mm), which must have occurred in vast numbers in the world's oceans of the Mesozoic. These early post-hatching developmental stages probably lived in the water column because their conchs already had functional phragmocones and they are often found in black shales, which were deposited under hypoxic to anoxic bottom water conditions and therefore, a benthic mode of life was impossible[48, 49]. Thus, pelagic nektonic animals (including older growth stages of ammonites) are the most likely candidates as predators feeding on these young ammonites (Fig. 2). For abundant and easy prey like juvenile ammonites, a vast range of predators can be hypothesized. Like plankton today, these masses of juvenile ammonites represent perfect food sources for medium-sized to large suspension feeders (invertebrates and vertebrates). From the Cretaceous, giant planktivorous bony fishes (pachycormids[50]) have been suggested to be nektonic suspension feeders, which might have fed on plankton comprising a wealth of juvenile ammonites. In the SOM of their paper, Fried-

man et al.[50] show a fragment of the gill rakers; their filaments have a spacing of about 1 mm, which is suitable to filter out hatchlings and juvenile ammonites with conchs of a few millimeter diameter (Fig. 3). This trophic relationship is further corroborated by the extinction of this group synchronous with the demise of the Ammonoidea and Belemnitida but direct evidence is missing. Taking the direct fossil evidence from the Jurassic into account, it appears likely that ammonites also played a role as micropredators feeding on early juvenile ammonite offspring[37, 46, 51].

The extreme differences in size (three orders in magnitude) between adults and juveniles in large ammonites indicate that the range of potential predators changed significantly throughout the life history of these cephalopods. As hatchlings and small juvenile planktonic forms, moderate-sized to large suspension feeders and small predators likely used them as a food source but for adult puzosiids, only large predators such as mosasaurs, pliosaurs and large fishes can be considered, although the seeming direct evidence for such a trophic relationship as suggested by Kauffman & Kesling[52] has been falsified by Seilacher[53]. Late Cretaceous ammonites were probably not the primary food source of ichthyosaurs since the latter became extinct already in the Cenomanian whereas ammonites persisted to be diverse and abundant; in spite of a better link of their demise with the extinction of belemnites in the North Pacific near the end of the Early Cretaceous[19], belemnite decline in the Tethys at the CTB[17, 54] and direct evidence for a trophic relationsip between phragmocone-bearing coleoids and ichthyosaurs (Kear et al.[55] and references therein), Acikkol[56] suggested that a link between the severe reduction of belemnite diversity and ichthyosaur extinction is unlikely.

Which groups filled the ecospace freed by the extinction of ammonite hatchlings and planktivorous actinopterygians?

Association of the extinctions of large marine reptiles, large planktivorous fish and those of ammonites suggest trophic relationships between these groups; their extinction freed ecospace for both small zooplankton and suspension feeders. This association coincides with other major changes in the planktonic realm, especially the rise of holoplanktonic gastropods. Although a few Early Jurassic to Cretaceous heteropods are known[57-60], the major expansion of hetereopods and 'pteropods' falls into the Cenozoic (e.g., refs 61-63).

In size and their coiled form, many fossil Limacinidae (Thecosomata, planktonic opisthobranch gastropods) resemble ammonites. Similarly, the conchs of fossil Creseidae morphologically

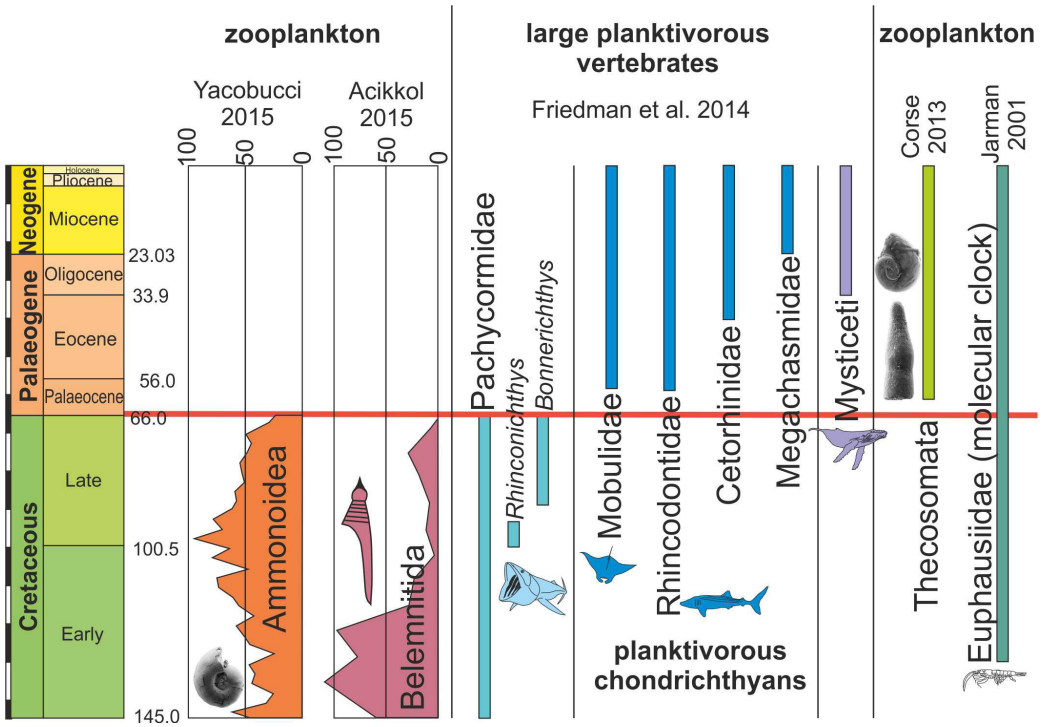

Fig. 2. Occurrences, extinctions, originations and diversity changes in plankton and large planktotrophic suspension feeders from the Cretaceous to the Palaeogene (mass extinction marked by red bar). Data from refs [50, 65, 73, 75, 76].

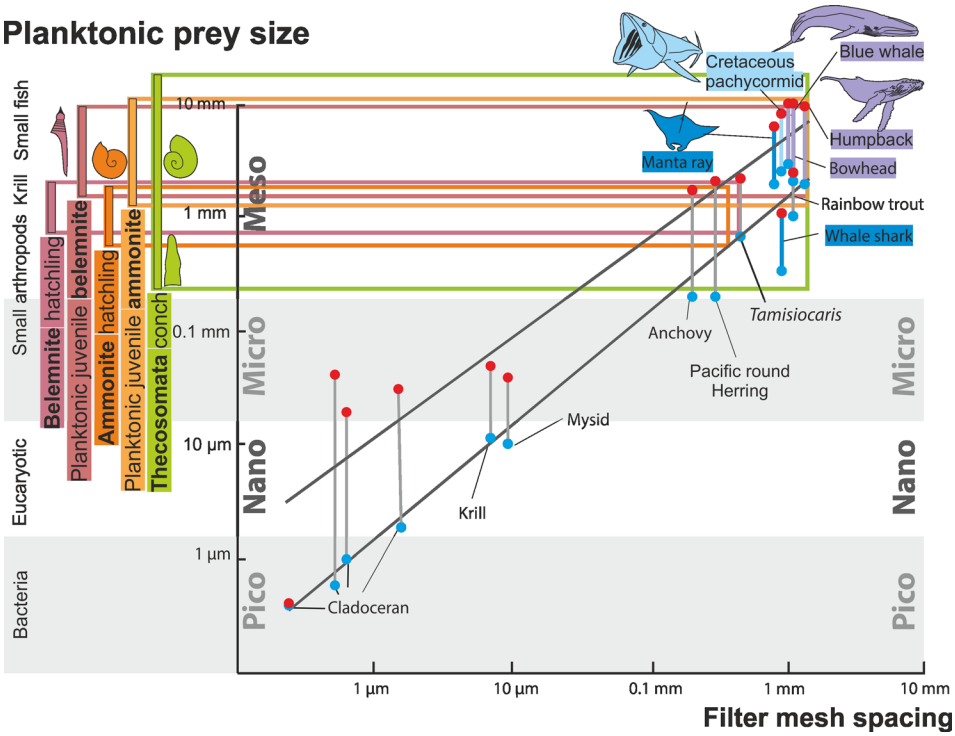

Fig. 3. Zooplankton size ranks and filter mesh spacing of planktivorous filter feeders. Modified after Vinther et al.[77], using data from Lokho & Kumar[62], Friedman et al.[50] and De Baets et al.[30].

and in size (at least roughly) correspond to hatchlings of belemnites, diplobelids and other phragmocone-bearing coleoids of the Cretaceous[45, 62]. In addition to these morphologic similarities, these groups shared the planktonic habitat. According to Janssen & King[64], 'pteropods' were already present as early as the latest Palaeocene. A number of Eocene pteropod occurrences is known worldwide[62, 65-72]. An early Palaeogene origin is supported by a combination of palaeontological and molecular clock data published by Corse et al.[73]. The latter authors even compare the uncoiling of the conch of Thecosomata with the coiling of ammonites, but they did not discuss macroecological implications. As far as abundance of these fossils is concerned, pteropods are much less frequent than subadult to adult ammonites and belemnites, while their hatchlings are similarly rare. This is probably due to the combination of their small body size as well as their thin and fragile aragonitic shells[64], which did not provide a high fossilization potential. The great majority of these thin aragonitic shells was undoubtedly rapidly dissolved during early diagenesis and as a consequence not fossilized. Nevertheless, the fact that quite a few pteropods have been reported from the Eocene implies that they were abundant and widely distributed since that period of time.

Similarities in size, overall morphology, habitat, abundance as well as the timing of their respective extinction and origination suggest that hatchlings and small individuals of ammonites as well as belemnites were ecologically replaced by planktonic opisthobranchs (Thecosomata) and other holoplanktonic gastropods. In turn, the ecological installment of the Thecosomata contributed to the dietary basis for the evolution of new groups of large planktivorous suspension feeders. As suggested by Friedman et al.[50], the Cretaceous 'giant planktivorous bony fishes' found an ecological replacement in both large suspension-feeding chondrichthyans and baleen whales. Several of these groups are known to take in important amounts of planktonic gastropods, although not exclusively. Today, thecosomes may contribute up to 50% of the zooplanktonic biomass and thus are ecologically important[74]. However, today's Manta rays (Mobulidae) are known to feed predominantly on small Crustaceans and the same holds true for several baleen whales. Nevertheless, it is somewhat unclear what these early Palaeogene suspension feeders ate, but at least the filter mesh spacing of both planktivorous, chondrichthyans and several baleen whales fits well with the size range of thecosomes.

Conclusions

Large late Cretaceous ammonites such as puzosiids reached sizes exceeding two meters in diameter. Their offspring has a conch size that is in stark contrast to the adult size; the embryonic conchs of many Cretaceous ammonites measure only about 1 mm in diameter at the time of hatching. This size relationship, conch geometry and anatomical proportions allow estimates of reproductive rates. Accordingly, the largest females might have laid between 10'000'000 and 100'000'000 eggs. Apart from this extreme example, the great abundance of ammonites, many of them of considerable size as adults, throughout the Mesozoic and the generally small size of their offspring implies that juvenile ammonites and belemnites played a fundamental role near the base of Mesozoic food webs, both as food source and as primary consumers. We assume that Mesozoic oceans were full of small hatchlings and juveniles of ammonites and belemnites in the mm to cm size range. This part of the planktonic food chain vanished with the extinction of ammonites and belemnites but may have enabled the evolutionary and ecological rise of holoplanktonic gastropod, which occupy a similar size range, conch morphologies (coiled and straight) and trophic role. This underlines the importance of ecological differentiation between different ontogenetic stages. Gill raker filament spacing in huge pachycormids correspond in size to these juvenile ammonites, suggesting a trophic link in the light of the synchronous extinction at the end of the Cretaceous.

Here, we suggest that the ecospace formerly occupied by ammonite and belemnite juveniles was filled during the post-Mesozoic rise of holoplanktonic gastropods like, e.g., the Palaeocene expansion of the Thecosomata (holoplanktonic heterobranchs). As far as the incumbent replacement of the pachycormids is concerned, it is a bit more difficult. During the early Palaeogene, three important large planktivorous lineages of chondrichthyans occur; however, modern mobulids (Manta rays), for instance, are known to feed on planktonic Crustaceans. Perhaps, stomach contents of exceptionally preserved specimens of Palaeogene planktivorous chondrichthyans will shed more light on the suspension feeders that, at least in their function as primary consumers, profited from the thecosomes that ecologically replaced juvenile ammonites. Independent of the filter feeder-side, we conclude that in r-strategists, the young offspring can play a more important ecological role than their large adults. This case of incumbent replacement underlines the significance of differences at which developmental stage the acme in ecological importance of an organism occurs.

Acknowledgements

The Swiss National Science Foundation SNF (project No. 200021_149119) kindly supported this study. Jakob Vinther (Bristol) generously provided an illustration, which was a valuable basis for one of our illustrations. We thank Kishor Kumar (Uttarakhand, India), Klaus Bandel (Hamburg) and Kazushige Tanabe (Tokyo) for providing illustrations and allowing us to use them.

References

1. Jablonski, D. Extinction and the spatial dynamics of biodiversity. Proc. Natl. Acad. Sci. USA 105, 11528-11535 (2008).
2. Jablonski, D. Raup, D. M. Selectivity of end-Cretaceous marine bivalve extinctions. Science 268, 389-391 (1994).
3. Hautmann, M. Diversification and diversity partitioning. Paleobiology 40, 162-176 (2014).
4. Hofmann, R., Hautmann, M., Brayard, A., Nützel, A. Bylund, K. G., Jenks, J. F., Vennin, E., Olivier, N. & Bucher, H. Recovery of benthic marine communities from the end-Permian mass extinction at the low-latitudes of Eastern Panthalassa. Palaeontology 57, 547-558 (2014).
5. Roopnarine, P. D. & Angielczyk, K. D. Community stability and selective extinction during the Permian-Triassic mass extinction. Science 350, 90-93 (2015)
6. McGhee, G. R. Jr., Clapham, M. E., Sheehan, P. M., Bottjer, D. J. & Droser, M. L. A new ecological-severity ranking of major Phanerozoic biodiversity crises. Palaeogeogr., Palaeoclim., Palaeoeco., 370, 260–270 (2013).
7. Sloan, R. E., Rigby, K., Van Valen, L. M. & Diane, G. Gradual dinosaur extinction and simultaneous ungulate radiation in the Hell Creek formation. Science 232, 629–633 (1986)
8. Archibald, D & Fastovsky, D. Dinosaur Extinction. In: Weishampel, D. B., Dodson, P. & Osmólska, H. (eds) The Dinosauria (2nd ed.). 672–684 (University of California Press, 2004)
9. Goolaerts, S. Late Cretaceous ammonites from Tunisia: chronology and causes of their extinction and extrapolation to other areas. Aardkundige Mededelingen 21, 1-220 (2010)
10. Kennedy, W. J. Ammonite faunas of the European Maastrichtian; diversity and extinction. In: House, M. R. (ed) The Ammonoidea: environ-

ment, ecology, and evolutionary change. System. Assoc. Spec. Vol. 47, 285-326 (1993).
11. Landman, N. H., Goolaerts, S., Jagt, J. W. M., Jagt-Yazykova, E. A., & Machalski, M. Ammonites on the brink of extinction: diversity, abundance, and ecology of the Order Ammonoidea at the Cretaceous/Paleogene (K/Pg) boundary. In: Klug, C., Korn, D., De Baets, K., Kruta, I. & Mapes, R. H. (eds), Ammonoid paleobiology: from macroevcolution to paleogeography. Topics in Geobiology 44, 497-553 (2015).
12. Keller, G., Abramovich, S., Berner, Z. & Adatte, T. Biotic effects of the Chicxulub impact, K-T catastrophe and sea level change in Texas. Palaeogeogr., Palaeoclimatol., Palaeoecol. 271,52-68 (2009).
13. Miller, K. G., Sherrell, R. M., Browning, J. V., Field, M. P., Gallagher, W., Olsson, R. K., Sugarman, P. J., Tuorto, S. & Wahyudi, H. Relationship between mass extinction and iridium across the Cretaceous-Paleogene boundary in New Jersey. Geology 38:867-870 (2010).
14. Schulte, P. et al. The Chicxulub asteroid impact and mass extinction at the Cretaceous-Paleogene Boundary. Science 327, 1214-1218 (2010).
15. Hönisch, B. et al. The geological record of ocean acidification. Science 335, 1058-1063 (2012).
16. Tobin, T. S. et al. Extinction patterns, δ18O trends, and magnetostratigraphy from a southern high-latitude Cretaceous-Paleogene section: Links with Deccan volcanism. Palaeogeogr., Palaeoclimatol., Palaeoecol. 350-352:180-188 (2012).
17. Doyle, P. A. review of the biogeography of Cretaceous belemnites: Palaeogeogr., Palaeoclimatol., Palaeoecol. 92: 207–216 (1992).
18. Marshall, C. R. & Ward, P. D. Sudden and gradual molluscan extinctions in the latest Cretaceous in western European Tethys. Science 274, 1360-1363 (1996).
19. Iba, Y., Mutterlose, J., Tanabe, K., Sano, S., Misaki, A. & Terabe, K. Belemnite extinction and the origin of modern cephalopods 35 m.y. prior to the Cretaceous–Paleogene event. Geology 39, 483–486 (2011).
20. Olivero, E. B. Sedimentary cycles, ammonite diversity and palaeoenvironmental changes in the Upper Cretaceous Marambio Group, Antarctica. Cret. Res. 34, 348-366 (2012)
21. Landman, N. H., Goolaerts, G., Jagt, J. W. M., Jagt-Yazykova, E. A., Machalski, M., Yacobucci, M. M. Ammonite extinction and nautilid survival at the end of the Cretaceous. Geology 42, 707–710 (2014)
22. Alvarez, L. W., Alvarez, W., Asaro, F. & Michel, H. V. Extraterrestrial cause for the Cretaceous-Tertiary extinction. Science 208, 1095-1108 (1980)
23. Smit, J. Extinction and evolution of planktonic formaninifera after a major impact at the Cretaceous/ Tertiary boundary. GSA Spec. Pap. 190, 329-352. (1982).
24. Ward, P. D. & Signor, P. W. III Evolutionary tempo in Jurassic and Cretaceous ammonites. Paleobiology 9, 183-198 (1983).
25. Ward, P. D. Ammonoid extinction. In: Landman, N. H., Tanabe, K. & Davis, R. A. (eds), Ammonoid Paleobiology. Plenum, New York (1996).
26. Landois, H. Die Riesenammoniten von Seppenrade, Pachydiscus Zittel seppenradensis II. Landois. Jahresbericht der Zoologischen Section des Westfälischen Provinzial-Vereins für Wissenschaft und Kunst 23: 99–108 (1895).
27. Olivero, E. B. & Zinsmeister, W. J. Large heteromorph ammonites from the Upper Cretaceous of Seymour Island, Antarctica. J. of Paleont. 63, 626-636 (1989).
28. Kennedy, W. J. & Kaplan, U. Parapuzosia (Parapuzosia) seppenradensis (Landois) und die Ammonitenfauna der Dülmener Schichten, unteres Unter-Campan, Westfalen. Geologie und Paläontologie in Westfalen 33, 1-127 (1995).
30. De Baets, K., Landman, N. H. & Tanabe, K. Ammonoid embryonic development. In: Klug, C., Korn, D., De Baets, K., Kruta, I. & Mapes, R. H. (eds), Ammonoid paleobiology: from anatomy to paleoecology. 113-205 (Springer, 2015)
31. Mironenko, A. A., & Rogov, M. A. First direct evidence of ammonoid ovoviviparity. Lethaia, DOI: 10.1111/let.12143 (2015) .
32. Tanabe, K. & Tsukahara, J. Biometric analysis of Nautilus pompilius from the Philippines and the Fiji Islands. In: Saunders, W. B. & Landman, N. H. (eds), Nautilus. 105–113 (Plenum Press, 1987)
33. Korn, D. & Klug, C. Conch form analysis, variability, and morphological disparity of a Frasnian (Late Devonian) ammonoid assemblage from Coumiac (Montagne Noire, France). In: Landman, N. H., Davis, R. A., Manger, W. & Mapes, R. H. (eds), Cephalopods – Present and Past. 57-86 (Springer, 2007).
34. De Baets, K., Klug, C., Korn, D. & Landman, N. H. Early evolutionary trends in ammonoid embryonic development. Evolution 66, 1788-1806 (2012).
35. Lehmann, U. Ammonite jaw apparatus and soft parts. In: House, M. R. & Senior, J. R. (eds), The Ammonoidea. Syst. Ass. Spec. Pap. 18, 275–287

(1981).
36. Lehmann, U. Zur Anatomie der Ammoniten: Tintenbeutel, Kiemen, Augen. Paläontol. Z. 59, 99–108 (1985).
37. Klug, C. & Lehmann, J. Soft part anatomy of ammonoids: reconstructing the animal based on exceptionally preserved specimens and actualistic comparisons. In: Klug, C., Korn, D., De Baets, K., Kruta, I. & Mapes, R. H. (eds): Ammonoid paleobiology, Volume I: from anatomy to ecology. Topics in Geobiology 43, 539-552 (Springer, 2015).
38. Klug, C., Riegraf, W. & Lehmann, J. Soft-part preservation in heteromorph ammonites from the Cenomanian-Turonian Boundary Event (OAE 2) in the Teutoburger Wald (Germany). Palaeontology 55, 1307-1331 (2012).
39. Kennedy, W. J. Thoughts on the evolution and extinction of Cretaceous ammonites. Proc. Geol. Assoc. 100, 251-279 (1989).
40. Landman, N. H., Tanabe, K. & Shigeta, Y. Ammonoid embryonic development. In: Landman, N. H., Tanabe, K. & Davis, R. A. (eds), Ammonoid Paleobiology. (Plenum, 1996)
41. Tanabe, K., Kulicki, C. & Landman, N. H. Development of the embryonic shell structure of Mesozoic ammonoids. American Museum Novitates 3621, 1–19 (2008).
42. Raup, D. M. & Chamberlain, J. A. Jr. Equations for volume and center of gravity in ammonoids shells. J. Paleontol. 41, 566–574 (1967).
43. Naglik, C., Rikhtegar, F. N. & Klug, C. Buoyancy in Palaeozoic ammonoids from empirical 3D-models and their place in a theoretical morphospace. Lethaia 49, 3–12(2016).
44. Tajika, A., Naglik, C., Morimoto, N., Pascual-Cebrian, E., Hennhöfer, D. K. & Klug, C. Empirical 3D-model of the conch of the Middle Jurassic ammonite microconch Normannites, its buoyancy, the physical effects of its mature modifications and speculations on their function. Historical Biology 27, 181-191 (2015).
45. Bandel, K., Engeser, T. & Reitner, J. Embryonic development of Hibolithes (Belemnitida, Cephalopoda). N. Jahrb. Geol. Paläont., Abh. 167, 275-303 (1984).
46. Keupp, H. Atlas zur Paläopathologie der Cephalopoden. Berliner paläobiol. Abh. 12, 1-390 (2012).
47. Hoffmann, R. & Keupp, H. Ammonoid Paleopathology. In: Klug, C., Korn, D., De Baets, K., Kruta, I. & Mapes, R. H. (eds), Ammonoid paleobiology, Volume I: from anatomy to ecology. Topics in Geobiology 43, 877-926 (Springer, 2015).
48. Nützel, A. & Mapes, R.H. Larval and juvenile gastropods from a Carboniferous black shale: palaeoecology and implications for the evolution of the Gastropoda. Lethaia 34, 143–162 (2001).
49. Mapes, R.H. & Nützel, A. Late Palaeozoic mollusc reproduction: cephalopod egg-laying behavior and gastropod larval palaeobiology. Lethaia 42, 341–356 (2008).
50. Friedman, M., Shimada, K., Martin, L.D., Everhart, M.J., Liston, J., Maltese, A. & Triebold, M. 100-million-year dynasty of giant planktivorous bony fishes in the Mesozoic seas. Science 327, 990-993 (2010).
51. Kruta, I., Landman, N. H., Rouget, I., Cecca, F. & Tafforeau, P. The role of ammonites in the marine Mesozoic food web revealed by jaw preservation. Science 311, 70-72 (2011)
52. Kauffman, E. G. & Kesling, R. V. An Upper Cretaceous ammonite bitten by a mosasaur. Contr, Michigan Univ, Mus, Paleont, 15, 193–248 (1960).
53. Seilacher, A. Mosasaurs, limpets or diagenesis: How Placenticeras shells got punctured. Mitt. Mus. Naturkde .Berlin. Geowiss. Reihe 1, 93–102(1998)
54. Christensen, W. K. Palaeobiology, phylogeny and palaeobiogeography of belemnoids and related coleoids. Berliner paläobiol. Abh. 1, 18-21 (2002).
55. Kear, A. J., Briggs, D. E. G. & Donovan, D.T. Decay and fossilization of non-mineralized tissue in coleoid cephalopods. Palaeontology 38, 105–131 (1995).
56. Acikkol, N. Testing the Cretaceous diversity of ichthyosaurs and their extinction Hypotheses using a quantitative approach. Degree project at the Department of Earth Sciences. 40 pp. (Uppsala University, 2015).
57. Bandel, K. & Hemleben, C. Observations on the ontogeny of thecosomatous pteropods (holoplanktic Gastropoda) in the southern Red Sea and from Bermuda. Marine Biology 124, 225–243 (1995).
58. Nützel, A. Larval ecology and morphology in fossil gastropods. Palaeontology 1, 1–25 (2014).
59. Teichert, S. & Nützel, A. Early Jurassic anoxia triggered the evolution of the oldest holoplanktonic gastropod Coelodiscus minutus by means of heterochrony. Acta Palaeont. Pol. 60, 269–276 (2015).
60. Nützel, A., Schneider, S., Hülse, P., Kelly, S. R. A., Tilley, L. & Veit, R. A new Early Jurassic gastropod from Ellesmere Island, Canadian Arctic – an ancient example of holoplanktonic

gastropods. Bulletin of Geosciences 91, 229–242 (2016).
61. Tracey S., Todd, J. A., & Erwin, D. H. Mollusca: Gastropoda. In: Benton, M. J. (ed), The Fossil Record. 131–167 (Chapman and Hall, 1993).
62. Lokho, K. & Kumar, K. Fossil pteropods (Thecosomata, holoplanktonic Mollusca) from the Eocene of Assam-Arakan Basin, northeastern India. Current Science 94, 647-652 (2008).
63. Janssen, A. W. & Peijnenburg, K. T. C. A. Holoplanktonic Mollusca: development in the Mediterranean Basin during the last 30 Ma and their future. In: Goffredo, S. & Dubinsky, Z. (eds), The Mediterranean Sea. Its history and present challenges. 341-362 (Springer, 2013).
64. Janssen, A. W. & King, C. Planktonic mollusks (Pteropods). In: Vinken, R. (ed), The Northwest European Tertiary Basin, Results of the International Geological Correlation Programme Project no. 124. Geol. Jahrb. 100, 356-368 (1988).
65. Bristow, C. R., Ellison, R. A., & Wood, C. J. The Claygate Beds of Essex. Proc. Geol. Assoc. 91, 261-277 (1980).
66. King, C. The stratigraphy of the London Clay. Tertiary Research Spec. Pap. 6, 1-158 (1981).
67. Curry, D. Ptéropodes éocènes de la tuilerie de Gan (Pyrénées–Atlantiques) et de quelques autres localités de SW de la France. Cahiers de Micropaléontologie 4(for 1981), 35–44 (1982).
68. Zorn, I. A systematic account of Tertiary Pteropoda (Gastropoda, Euthecosomata) from Austria. Contributions to Tertiary and Quaternary Geology 28, 95–139 (1991).
69. Hodgkinson, K. A., Garvie, C. L. & Bé, A. W. H. Eocene euthecosomatous Pteropoda (Gastropoda) of the Gulf and eastern coasts of North America. Bull. Am. Paleontol. 103, 5–62 (1992).
70. Janssen, A. W., Schnetler, K. I. & Heilmann-Clausen, C. Notes on the systematics morphology and biostratigraphy of fossil holoplanktonic Mollusca, 19. Pteropods (Gastropoda, Euthecosomata) from the Eocene Lillebaelt Clay Formation (Denmark, Jylland). Basteria 71, 157-168 (2007).
71. Ando, Y. Ujihara, A. & Ichihara, T. First occurrence of Paleogene pteropods (Gastropoda; Thecosomata) from Japan. Jour. Geol. Soc. Japan 115, 187-190 (2009).
72. Cahuzac, B. & Janssen, A. W. Eocene to Miocene holoplanktonic Mollusca (Gastropoda) of the Aquitaine Basin, southwest France. Scripta Geologica 141, 1-193 (2010).
73. Corse, E., Rampal, J., Cuoc, C., Pech, N., Perez, Y. & Gilles, A. Phylogenetic analysis of Thecosomata Blainville, 1824 (holoplanktonic Opisthobranchia) using morphological and molecular data. PLOS ONE 8, e59439, 1-20 (2013).
74. Mackas, D. L. & Galbraith, M. D. Pteropod time-series from the NE Pacific. ICES Journal of Marine Science 69, 448–459 (2012).
75. Yacobucci, M. M. Macroevolution and paleobiogeography of Jurassic-Cretaceous ammonoids. In: Klug, C., Korn, D., De Baets, K., Kruta, I. & Mapes, R. H. (eds): Ammonoid paleobiology, Volume I: from anatomy to ecology. Topics in Geobiology 43, 539-552 (Springer, 2015).
76. Jarman, S. N. The evolutionary history of krill inferred from nuclear large subunit rDNA sequence analysis. Biological Journal of the Linnean Society 73, 199-212 (2001).
77. Vinther, J., Stein, M., Longrich, N. R. & Harper, D. A. T. A suspension-feeding anomalocarid from the Early Cambrian. Nature 507, 496–497 (2014).

Conclusions and perspectives

Palaeoecology of the Alpstein

Knowledge of the fauna in the Alpstein was much increased through the documentation of cephalopod fossils (Chapter I), which occur in a relatively long geologic timespan (Barremian-Cenomanian). In total, more than 100 species of ammonoids, 6 species of nautiloids and 4 species of coleoids were documented. These cephalopod fossils as well as other macro fossils were further used to examine the regional palaeoecology. The results of Chapter II show that environmental changes, especially sea level rises accompanied by increasing temperature, which occurred from the early Barremian to the early Cenomanian, had a great impact on the palaeocommunities through time. The results also imply that ecospace utilization of a fauna (ecological disparity) is more easily affected by environmental changes than taxonomic richness (number of families). This point needs further examination with higher stratigraphic and taxonomic resolution.

Intraspecific variation of cephalopods

A detailed examination of intraspecific variation of Recent *Nautilus* was carried out. Superficially, intraspecific variation of *Nautilus* appeared negligible but it was proven to have a certain pattern of change through ontogeny regardless of geographically separated populations. Comparisons with some parameters in ammonoids and belemnites implied that at least some ammonoids and belemnites have a similar pattern of ontogenetic intraspecific variation to that of *Nautilus*: The intraspecific variation has a decreasing trend from the earliest to late ontogeny (probably just before maturity), followed by some increase near maturity. Such knowledge is essential when a new species is introduced or species assignments are carried out. Regarding ammonoid intraspefic variation, further investigation with careful sampling to avoid various biases is needed, which will bring about primary information on how intraspecific variation differs between ammonoid groups and through their evolution.

When ontogenetic changes in chamber volumes of ammonoids and *Nautilus* were compared, it turned out that there is a clear difference in the pattern of volume increase: ammonoids showed a rather fluctuating increasing trend, while *Nautilus* chamber volumes followed a much more harmonic trend. The mechanism, which caused such differences, will be further studied in my post-doctoral project.

This work (Chapter III and IV) also involved the attempt to develop a method to measure 2D and 3D parameters quantitatively using computed tomography. This is especially important in the light of conservation of *Nautilus* because *Nautilus* has been reported to be at risk of extinction and registered in the CITES since 2017. The application of computed tomography enables us to examine shells without destruction, which will allow analyses of museum collections without capturing more *Nautilus*. It is expected that a comprehensive 3D database of nautiluses will be established, which is accessible to all researchers in order to prevent unnecessary *Nautilus* fishing.

Incumbent replacement of ammonoid and belemnite hatchlings by holoplanktonic gastropods and the filter feeders living on them

Reconstruction of reproductive rates demonstrated that Cretaceous large puzosiids could produce between 33'000'000 and 10'000'000 eggs, which implies that ammonoids (as well as belemnites to a lesser degree) had a high fecundity. Such high fecundity likely made them a major source of planktonic food especially for medium to large sized suspension feeder such as pachycormids in the Cretaceous ocean. After the end-Cretaceous extinction of ammonoids and belemnites, the ecospace previously occupied by them were probably filled by other organisms. Considering morphology, size, abundance and mode of life, it is assumed that holoplanktonic gastropods are the most likely candidates. Also, it is likely that the disappearance of pachycormids as well as ammonoids and belemnites and emergence of such holoplanktonic gastropods drove the evolution of filter feeding organisms such as chondrichtyans and cetaceans after the Palaeogene.

It appears like this case of incumbent replacement from ammonoids to holoplanktonic gastropods took place rather based on randomness, i.e., there is no clear key adaptation (sensu Rosenzweig and McCord 1991) to the new incumbents. In addition, no competition for the ecological niches between previous (ammonoids and belemnites) and new (holoplanktonic gastropods) incumbents appears to have occurred until the Cretaceous since

they did not coexist. In this context, it is likely that the new incumbents (holoplanktonic gastropods) evolved and radiated merely because there is much less competition by chance in the post-ammonoid and belemnite marine realm.

References

Ager, D. 1965. Serial grinding techniques. Pp. 212-224. In B. Kummel, and D. Raup, eds. Handbook of Paleontological Techniques. WH Freeman, New York. H. Freeman and Company, San Fransisco.

Alroy, J., M. Aberhan, D. J. Bottjer, M. Foote, F. T. Fürsich, P. J. Harries, A. J. Hendy, S. M. Holland, L. C. Ivany, and W. Kiessling. 2008. Phanerozoic trends in the global diversity of marine invertebrates. Science 321(5885):97-100.

Archibald, J. D., W. Clemens, K. Padian, T. Rowe, N. Macleod, P. M. Barrett, A. Gale, P. Holroyd, H.-D. Sues, and N. C. Arens. 2010. Cretaceous extinctions: multiple causes. Science 328(5981):973-973.

Barnosky, A. D., N. Matzke, S. Tomiya, G. O. U. Wogan, B. Swartz, T. B. Quental, C. Marshall, J. L. McGuire, E. L. Lindsey, K. C. Maguire, B. Mersey, and E. A. Ferrer. 2011. Has the Earth/'s sixth mass extinction already arrived? Nature 471(7336):51-57.

Barord, G. J. 2015. On the Biology, Behavior, and Conservation of the Chambered *Nautilus*, *Nautilus* sp. The City University of New York.

Bernard, E. L., M. Ruta, J. E. Tarver, and M. J. Benton. 2010. The fossil record of early tetrapods: Worker effort and the end-Permian mass extinction. Acta Palaeontologica Polonica 55(2):229-239.

Bonnaud, L., C. Ozouf-Costaz, and R. Boucher-Rodoni. 2004. A molecular and karyological approach to the taxonomy of *Nautilus*. Comptes Rendus Biologies 327(2):133-138.

Brusatte, S. L., R. J. Butler, P. M. Barrett, M. T. Carrano, D. C. Evans, G. T. Lloyd, P. D. Mannion, M. A. Norell, D. J. Peppe, and P. Upchurch. 2015. The extinction of the dinosaurs. Biological Reviews 90(2):628-642.

Bucher, H., N. H. Landman, S. M. Klofak, and J. Guex. 1996. Mode and rate of growth in ammonoids. Pp. 407-461. Ammonoid paleobiology. Springer.

Bush, A. M., and R. K. Bambach. 2004. Did alpha diversity increase during the Phanerozoic? Lifting the veils of taphonomic, latitudinal, and environmental biases. The Journal of geology 112(6):625-642.

Bush, A. M., and R. K. Bambach. 2015. Sustained Mesozoic–Cenozoic diversification of marine Metazoa: A consistent signal from the fossil record. Geology 43(11):979-982.

Chaimanee, Y., D. Jolly, M. Benammi, P. Tafforeau, D. Duzer, I. Moussa, and J.-J. Jaeger. 2003. A Middle Miocene hominoid from Thailand and orangutan origins. Nature 422(6927):61-65.

Chamberlain, J.A. Jr. 1976. Flow patterns and drag coefficients of cephalopod shells. Palaeontology 19:539–563.

Cleal, C. J., and B. Cascales-Miñana. 2014. Composition and dynamics of the great Phanerozoic Evolutionary Floras. Lethaia 47(4):469-484.

Crame, J. 2002. Evolution of taxonomic diversity gradients in the marine realm: a comparison of Late Jurassic and Recent bivalve faunas. Paleobiology 28(2):184-207.

De Angelis, P. 2012. Assessing the impact of international trade on chambered nautilus. Geobios 45(1):5-11.

De Baets, K., D. Bert, R. Hoffmann, C. Monnet, M. M. Yacobucci, and C. Klug. 2015a. Ammonoid intraspecific variability. Pp. 359-426. In C. Klug, D. Korn, K. De Baets, I. Kruta, and R. H. Mapes, eds. Ammonoid Paleobiology: from anatomy to ecology. Springer.

De Baets, K., C. Klug, D. Korn, C. Bartels, and M. Poschmann. 2013a. Emsian Ammonoidea and the age of the Hunsrück Slate (Rhenish Mountains, Western Germany). Palaeontogr A 299(1-6):1-113.

De Baets, K., C. Klug, D. Korn, and N. H. Landman. 2012. Early evolutionary trends in ammonoid embryonic development. Evolution 66(6):1788-1806.

De Baets, K., C. Klug, and C. Monnet. 2013b. Intraspecific variability through ontogeny in early ammonoids. Paleobiology 39(1):75-94.

De Baets, K., N. H. Landman, and K. Tanabe. 2015b. Ammonoid embryonic development. Pp. 113-205. In C. Klug, D. Korn, K. De Baets, I. Kruta, and R. H. Mapes, eds. Ammonoid Paleobiology: From anatomy to ecology. Springer.

del Norte-Campos, A. G. 2005. The Chambered *Nautilus* Fishery of Northwestern Panay Island, West Central Philippines: Fishing Practices and Yield. Phuket Marine Biology Cent Research Bulletin 66:299-305.

Dunstan, A., O. Alanis, and J. Marshall. 2010. Nautilus pompilius fishing and population decline in the Philippines: A comparison with an unexploited Australian *Nautilus* population. Fisheries Research 106(2):239-247.

Dunstan, A. J., P. D. Ward, and N. J. Marshall. 2011. Vertical distribution and migration patterns of *Nautilus pompilius*. PloS one 6(2):e16311.

Engeser, T., and H. Keupp. 2002. Phylogeny of the aptychi-possessing Neoammonoidea (Aptychophora nov., Cephalopoda). Lethaia 34:79-

96.
Font, E., T. Adatte, A. N. Sial, L. D. de Lacerda, G. Keller, and J. Punekar. 2016. Mercury anomaly, Deccan volcanism, and the end-Cretaceous mass extinction. Geology 44(2):171-174.
Forey, P. L., R. A. Fortey, P. Kenrick, and A. B. Smith. 2004. Taxonomy and fossils: a critical appraisal. Philosophical Transactions of the Royal Society of London B: Biological Sciences 359(1444):639-653.
Frey, L., C. Naglik, R. Hofmann, M. Schemm-Gregory, J. FRÝDA, B. Kroeger, P. D. Taylor, M. A. Wilson, and C. Klug. 2014. Diversity and palaeoecology of Early Devonian invertebrate associations in the Tafilalt (Anti-Atlas, Morocco). Bulletin of Geosciences 89(1):75-112.
Friis, E. M., P. R. Crane, K. R. Pedersen, S. Bengtson, P. C. Donoghue, G. W. Grimm, and M. Stampanoni. 2007. Phase-contrast X-ray microtomography links Cretaceous seeds with Gnetales and Bennettitales. Nature 450(7169):549-552.
Garwood, R. J., I. A. Rahman, and M. D. Sutton. 2010. From clergymen to computers—the advent of virtual palaeontology. Geology Today 26(3):96-100.
Goswami, A., N. Milne, and S. Wroe. 2011. Biting through constraints: cranial morphology, disparity and convergence across living and fossil carnivorous mammals. Proceedings of the Royal Society of London B: Biological Sciences 278(1713):1831-1839.
Hagadorn, J. W., S. Xiao, P. C. Donoghue, S. Bengtson, N. J. Gostling, M. Pawlowska, E. C. Raff, R. A. Raff, F. R. Turner, and Y. Chongyu. 2006. Cellular and subcellular structure of Neoproterozoic animal embryos. Science 314(5797):291-294.
Hallam, A., J. Grose, and A. Ruffell. 1991. Palaeoclimatic significance of changes in clay mineralogy across the Jurassic-Cretaceous boundary in England and France. Palaeogeography, Palaeoclimatology, Palaeoecology 81(3-4):173-187.
Haq, B. U. 2014. Cretaceous eustasy revisited. Global and Planetary Change 113:44-58.
Heptonstall, W. B. 1970. Buoyancy control in ammonoids. Lethaia 3(4):317-328.
Hoffmann, R., R. Lemanis, C. Naglik, and C. Klug. 2015. Ammonoid buoyancy. Pp. 613-648. Ammonoid Paleobiology: From anatomy to ecology. Springer.
Hoffmann, R., J. A. Schultz, R. Schellhorn, E. Rybacki, H. Keupp, S. R. Gerden, R. Lemanis, and S. Zachow. 2014. Non-invasive imaging methods applied to neo- and paleo-ontological cephalopod research. Biogeosciences 11(10):2721-2739.
Hoffmann, R., and S. Zachow. 2011. Non-invasive approach to shed new light on the buoyancy business of chambered cephalopods (Mollusca). Pp. 507-517. Proceedings IAMG.
Hofmann, R., M. Hautmann, and H. Bucher. 2013. A new paleoecological look at the Dinwoody Formation (Lower Triassic western USA): intrinsic versus extrinsic controls on ecosystem revcovery after the end-Permian mass extinction. Journal of Palaeontology 87:854-880.
Hofmann, R., M. Hautmann, M. Wasmer, and H. Bucher. 2013. Palaeoecology of the Spathian Virgin Formation (Utah, USA) and its implications for the Early Triassic recovery. Acta Palaeontologica Polonica 58(1):149-173.
House M. R. 1989. Ammonoid extinction events. Philosophical Transactions of the Royal Society B 325(1228):307-326.
Hutchinson, J. R., V. Ng-Thow-Hing, and F. C. Anderson. 2007. A 3D interactive method for estimating body segmental parameters in animals: application to the turning and running performance of *Tyrannosaurus rex*. Journal of Theoretical Biology 246(4):660-680.
Jäger, M., and R. Fraaye. 1997. The diet of the Early Toarcian ammonite *Harpoceras falciferum*. Palaeontology 40(2):557-574.
Jacobs, D. K., and J. A. J. Chamberlain. 1996. Buoyancy and hydrodynamics in ammonoids. Pp. 169-224. Ammonoid paleobiology. Springer.
Jacobs, D. K., and N. H. Landman. 1993. *Nautilus*—a poor model for the function and behavior of ammonoids? Lethaia 26(2):101-111.
Kennedy, W. J. 1977. Ammonite evolution. Pp. 251-304. In A. Hallam, ed. Patterns of Evolution. Elsevier, Amsterdam.
Kermack, D. M. 1970. True serial-sectioning of fossil material. Biological journal of the Linnean Society 2(1):47-53.
Keupp, H. 2000. Ammoniten. Paläobiologische Erfolgsspiralen. Thorbecke, Sigmaringen.
Keupp, H. 2012. Atlas zur Paläopathologie der Cephalopoden. Berliner paläobiologische Abhandlungen, Band 12. Berlin. pp. 390.
Kidwell, S. M. 2002. Time-averaged molluscan death assemblages: palimpsests of richness, snapshots of abundance. Geology 30(9):803-806.
Kidwell, S. M. 2005. Shell composition has no net impact on large-scale evolutionary patterns in mollusks. Science 307(5711):914-917.
Kielan-Jaworowska, Z., R. Presley, and C. Poplin. 1986. The cranial vascular system in taeniolabidoid multituberculate mammals. Philosophical Transactions of the Royal Society B: Biological

Sciences 313(1164):525-602.
Klug, C. 2007. Sublethal injuries in Early Devonian cephalopod shells from Morocco. Acta Palaeontologica Polonica 52(4).
Klug, C., and W. Etter. 2012. Cefalópodos fósiles de Venezuela. Pp. 79-96. In M. Sanchez-Villagra, ed. Fósiles de Venezuela. Universität Zürich.
Klug, C., B. Kröger, J. Vinther, D. Fuchs, and K. De Baets. 2015. Ancestry, origin and early evolution of ammonoids. Pp. 3-24. Ammonoid Paleobiology: From macroevolution to paleogeography. Springer.
Klug, C., and J. Lehmann. 2015. Soft part anatomy of ammonoids: reconstructing the animal based on exceptionally preserved specimens and actualistic comparisons. Pp. 507-529. Ammonoid Paleobiology: from anatomy to ecology. Springer.
Korn, D., and K. De Baets. 2015. Biogeography of Paleozoic ammonoids. Ammonoid Paleobiology: From macroevolution to paleogeography 44:145.
Korn, D., A. L. Titus, V. Ebbighausen, R. H. Mapes, and M. N. Sudar. 2012. Early Carboniferous (Mississippian) ammonoid biogeography. Geobios 45(1):67-77.
Kröger, B. 2002. On the efficiency of the buoyancy apparatus in ammonoids: evidences from sublethal shell injuries. Lethaia 35(1):61-70.
Kröger, B., J. Vinther, and D. Fuchs. 2011. Cephalopod origin and evolution: a congruent picture emerging from fossils, development and molecules. Bioessays 33(8):602-613.
Kruta, I., N. Landman, I. Rouget, F. Cecca, and P. Tafforeau. 2011. The role of ammonites in the Mesozoic marine food web revealed by jaw preservation. Science 331(6013):70-72.
Landman, N. H., S. Goolaerts, J. W. Jagt, E. A. Jagt-Yazykova, and M. Machalski. 2015. Ammonites on the brink of extinction: Diversity, abundance, and ecology of the order Ammonoidea at the Cretaceous/Paleogene (K/Pg) boundary. Pp. 497-553. Ammonoid Paleobiology: From macroevolution to paleogeography. Springer.
Landman, N. H., S. Goolaerts, J. W. Jagt, E. A. Jagt-Yazykova, M. Machalski, and M. M. Yacobucci. 2014. Ammonite extinction and nautilid survival at the end of the Cretaceous. Geology 42(8):707-710.
Lane, A., and M. J. Benton. 2003. Taxonomic level as a determinant of the shape of the Phanerozoic marine biodiversity curve. The American Naturalist 162(3):265-276.
Lehmann, U. 1971. New aspects in ammonite biology. Proceedings of the North American Paleontological Convention 1:1251–1269.
Lehmann, J., C. Ifrim, L. Bulot, and C. Frau. 2015. Paleobiogeography of Early Cretaceous Ammonoids. Pp. 229-257. Ammonoid Paleobiology: From macroevolution to paleogeography. Springer.
Lemanis, R., D. Korn, S. Zachow, E. Rybacki, and R. Hoffmann. 2016a. The evolution and development of cephalopod chambers and their shape. PloS one 11(3):e0151404.
Lemanis, R., S. Zachow, F. Fusseis, and R. Hoffmann. 2015. A new approach using high-resolution computed tomography to test the buoyant properties of chambered cephalopod shells. Paleobiology 41(2):313-329.
Lemanis, R., S. Zachow, and R. Hoffmann. 2016b. Comparative cephalopod shell strength and the role of septum morphology on stress distribution. PeerJ 4:e2434.
McGhee, G. R. Jr., M. E. Clapham, P. M. Sheehan, D. J. Bottjer and M. L. Droser. 2013. A new ecological-severity ranking of major Phanerozoic biodiversity crises. Palaeogeogr., Palaeoclim., Palaeoeco., 370, 260–270.
Muir-Wood, H. M. 1934. On the internal structure of some Mesozoic Brachiopoda. Philosophical Transactions of the Royal Society of London. Series B, Containing Papers of a Biological Character 223:511-567.
Naglik, C., C. Monnet, S. Goetz, C. Kolb, K. De Baets, A. Tajika, and C. Klug. 2015a. Growth trajectories of some major ammonoid subclades revealed by serial grinding tomography data. Lethaia 48(1):29-46.
Naglik, C., F. Rikhtegar, and C. Klug. 2016. Buoyancy of some Palaeozoic ammonoids and their hydrostatic properties based on empirical 3D-models. Lethaia 49(1):3-12.
Naglik, C., A. Tajika, J. Chamberlain, and C. Klug. 2015b. Ammonoid locomotion. Pp. 649-688. Ammonoid Paleobiology: From anatomy to ecology. Springer.
Niklas, K. J., B. H. Tiffney, and A. H. Knoll. 1983. Patterns in vascular land plant diversification. Nature 303:614-616.
Mapes, R. H., and A. Nuützel. 2009. Late Palaeozoic mollusc reproduction: cephalopod egg-laying behavior and gastropod larval palaeobiology. Lethaia 42:341-356.
Powell, M. G., and M. Kowalewski. 2002. Increase in evenness and sampled alpha diversity through the Phanerozoic: comparison of early Paleozoic and Cenozoic marine fossil assemblages. Geology 30(4):331-334.
Pucéat, E., C. Lécuyer, S. M. Sheppard, G. Dromart,

S. Reboulet, and P. Grandjean. 2003. Thermal evolution of Cretaceous Tethyan marine waters inferred from oxygen isotope composition of fish tooth enamels. Paleoceanography 18(2).

Raup, D. M. 1972. Taxonomic diversity during the Phanerozoic. Science 177(4054):1065-1071.

Raup, D. M. 1975. Taxonomic diversity estimation using rarefaction. Paleobiology:333-342.

Raup, D. M. 1977. Systematists follow the fossils. Paleobiology 3(03):328-329.

Rayfield, E. J., D. B. Norman, C. C. Horner, J. R. Horner, P. M. Smith, J. J. Thomason, and P. Upchurch. 2001. Cranial design and function in a large theropod dinosaur. Nature 409(6823):1033-1037.

Rosenzweig, M. L., and R. D. McCord. 1991. Incumbunt Replacement: Evidence for Long-Term Evolutionary Progress. Paleobiology 17:202-213.

Sanders, H. L. 1968. Marine benthic diversity: a comparative study. The American Naturalist 102(925):243-282.

Saunders, W. B., and N. Landman. 2009. *Nautilus*: The Biology and Paleobiology of a Living Fossil, Reprint with Additions. Springer Science & Business Media.

Saunders, W. B., and E. A. Shapiro. 1986. Calculation and simulation of ammonoid hydrostatics. Paleobiology 12(01):64-79.

Schulte, P., L. Alegret, I. Arenillas, J. A. Arz, P. J. Barton, P. R. Bown, T. J. Bralower, G. L. Christeson, P. Claeys, and C. S. Cockell. 2010. The Chicxulub asteroid impact and mass extinction at the Cretaceous-Paleogene boundary. Science 327(5970):1214-1218.

Sepkoski, J. J. J. 1984. A kinetic model of Phanerozoic taxonomic diversity. III. Post-Paleozoic families and mass extinctions. Paleobiology 10(02):246-267.

Sepkoski, J. J. J. 1988. Alpha, beta, or gamma: where does all the diversity go? Paleobiology 14(03):221-234.

Sepkoski, J. J. J., R. K. Bambach, D. M. Raup, and J. W. Valentine. 1981. Phanerozoic marine diversity and the fossil record. Nature 293(5832):435-437.

Sinclair, B., L. Briskey, W. Aspden, and G. Pegg. 2007. Genetic diversity of isolated populations of *Nautilus pompilius* (Mollusca, Cephalopoda) in the Great Barrier Reef and Coral Sea. Reviews in Fish Biology and Fisheries 17(2-3):223-235.

Sollas, I. B., and W. J. Sollas. 1914. A study of the skull of a Dicynodon by means of serial sections. Philosophical Transactions of the Royal Society of London. Series B, Containing Papers of a Biological Character:201-225.

Sollas, W. 1904. A method for the investigation of fossils by serial sections. Philosophical Transactions of the Royal Society of London. Series B, Containing Papers of a Biological Character 196:259-265.

Sutton, M., I. Rahman, and R. Garwood. 2014. Techniques for virtual palaeontology. John Wiley & Sons.

Sutton, M. D. 2008. Tomographic techniques for the study of exceptionally preserved fossils. Proceedings of the Royal Society of London B: Biological Sciences 275(1643):1587-1593.

Sutton, M. D., D. E. Briggs, D. J. Siveter, and D. J. Siveter. 2001. Methodologies for the visualization and reconstruction of three-dimensional fossils from the Silurian Herefordshire Lagerstätte. Palaeontologia Electronica 4(1):1-17.

Sutton, M. D., D. E. Briggs, D. J. Siveter, D. J. Siveter, and J. D. Sigwart. 2012. A Silurian armoured aplacophoran and implications for molluscan phylogeny. Nature 490(7418):94-97.

Swan, A. R., and W. B. Saunders. 1987. Morphological variation in *Nautilus* from Papua New Guinea. Nautilus:85-103.

Tajika, A., and R. Wani. 2011. Intraspecific variation of hatching size in Late Cretaceous ammonoids from Hokkaido, Japan: implication for planktic duration at early ontogenetic stage. Lethaia 44(11):287.

Takeda, Y., K. Tanabe, T. Sasaki, K. Uesugi, and M. Hoshino. 2016. Non-destructive analysis of in situ ammonoid jaws by synchrotron radiation X-ray micro-computed tomography. Palaeontologia Electronica 19(3):1-13.

Tanabe, K., S. Hayasaka, T. Saisho, A. Shinomiya, and K. Aoki. 1983. Morphologic variation of Nautilus pompilius from the Philippines and Fiji islands. Studies of *Nautilus pompilius* and its associated fauna from Tanon Strait, the Philippines. Occas. Pap (1):9-21.

Tanabe, K., S. Hayasaka, and J. Tsukahara. 1985. Morphological analysis of *Nautilus pompilius*. Kagoshima University Research Center for the South Pacific, Occasional Papers 4:38-49.

Tanabe, K., and J. Tsukahara. 1987. Biometric analzsis of *Nautilus pompilius* from the Philippines and the Fiji Islands. In W. B. Saunders, and N. H. Landman, eds. Nautilus: THe Biology and Paleobiology of a Living Fossil. Plenum, New York.

Ungar, P. S., R. S. Scott, F. E. Grine, and M. F. Teaford. 2010. Molar microwear textures and the diets of Australopithecus anamensis and Australopithecus afarensis. Philosophical Transac-

tions of the Royal Society B: Biological Sciences 365(1556):3345-3354.
Vandepas, L. E., F. D. Dooley, G. J. Barord, B. J. Swalla, and P. D. Ward. 2016. A revisited phylogeography of *Nautilus pompilius*. Ecology and Evolution 6(14):4924-4935.
Ward, P. 1981. Shell sculpture as a defensive adaptation in ammonoids. Paleobiology 7(01):96-100.
Ward, P. 1996. Ammonoid Extinction. Pp. 815-824. Ammonoid Paleobiology. Plenum.
Ward, P., F. Dooley, and G. J. Barord. 2016. *Nautilus*: biology, systematics, and paleobiology as viewed from 2015. Swiss Journal of Palaeontology 135(1):169-185.
Ward, P. D. 1987. The Natural History of *Nautilus*. Allen and Unwin, Boston.
Williams, R. C., B. C. Jackson, L. Duvaux, D. A. Dawson, T. Burke, and W. Sinclair. 2015. The genetic structure of *Nautilus pompilius* populations surrounding Australia and the Philippines. Molecular ecology 24(13):3316-3328.
Wray, C. G., N. H. Landman, W. B. Saunders, and J. Bonacum. 1995. Genetic divergence and geographic diversification in *Nautilus*. Paleobiology 21(02):220-228.
Yacobucci, M. M. 2015. Macroevolution and paleobiogeography of Jurassic-Cretaceous ammonoids. Pp. 189-228. Ammonoid Paleobiology: From macroevolution to paleogeography. Springer.
Zatoń, M. 2010. Sublethal injuries in Middle Jurassic ammonite shells from Poland. Geobios 43(3):365-375.

Appendix 1-1

Additional publications linked to this dissertation

Fossilien im Alpstein
Kapitel 6.08 Perlboote (Nautiloidea)

Tajika, A. Pictet, A. Klug, C

Book chapter (in press)
Publisher: Appenzeller Verlag

6.8 Perlboote (Nautiloidea)

Amane Tajika, Antoine Pictet und Christian Klug

6.8.1 Einführung

Der wohlklingende Gattungsname *Nautilus* ist den meisten Menschen ein Begriff, nicht zuletzt durch Jules Vernes Buch “1000 Meilen unter dem Meer”. In jüngster Zeit erlangte *Nautilus* eine eher traurige Berühmtheit durch die Diskussion, ob die Gattung durch den CITES unter Schutz gestellt werden soll. Dies ist erwägenswert, weil sie regional bedroht ist durch ihre Überfischung, obwohl das Tier nur selten gegessen wird. Die Befischung zielt primär auf die schön gefärbten Schalen, die zudem eine dicke Perlmuttschicht (aus Aragonit) aufweisen.

Nautilus (ca. fünf Arten) und *Allonautilus* (ein bis zwei Arten) sind die letzten lebenden Gattungen der Familie Nautilidae (populär “Nautiliden”), die heute auf den tropischen und subtropischen Bereich des Indopazifiks begrenzt sind (Abbildung 1A, B). Die Nautiliden wiederum gehören zu den Cephalopoden (Kopffüsser). Während der Ursprung der Kopffüsser wohl im Späten Kambrium liegt, gingen die Nautiliden wohl erst im Devon oder sogar noch später aus den Orthocerida oder Oncocerida hervor.

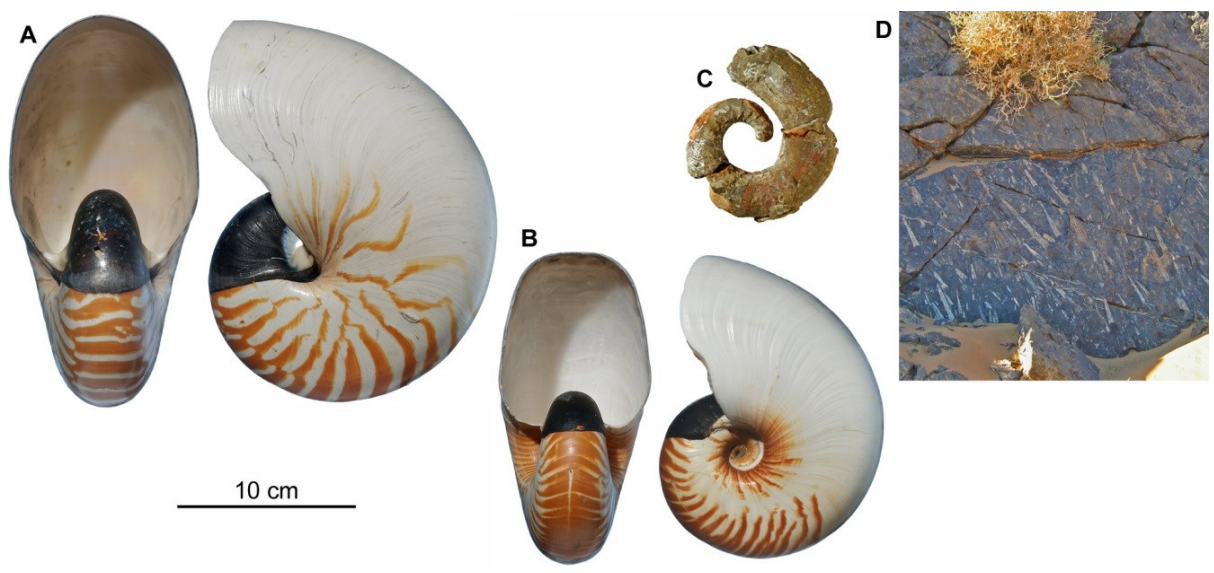

Abb. 1 Beispiele moderner und ausgestorbener Nautiliden. Massstab gilt für A bis C. A, *Nautilus belauensis* Saunders 1981. Rezent. Palau. PIMUZ 7824. Foto Heinz Lanz. B, *Allonautilus belauensis* Lighfoot 1786. Rezent. Papua Neuguinea. Sammlung Christian Klug. Foto Heinz Lanz. C, *Aphyctoceras* sp. Mitteldevon. Tafilalt, Marokko. PIMUZ 31920. Foto Mischa Haas. D, Massenvorkommen der gestreckt kegelförmigen Gehäuse von *Temperoceras ludense* (Sowerby, in Murchison 1839). Silur. Tafilalt, Marokko. Foto Christian Klug.

Die Gesteine des Alpsteins enthalten auch fossile Reste anderer Cephalopoden-Gruppen, nämlich der Ammonoideen ("Ammonshörner") und der Coleoideen (Tintenfische im weiteren Sinne). Gemeinsam mit den Muscheln, Schnecken, Kahnfüssern und Käferschnecken gehören die Kopffüsser zu den Mollusken (Weichtiere). Wie die meisten anderen Weichtiere auch verfügen die Nautiliden über kein echtes Innenskelett sondern über ein äusseres Gehäuse.

6.8.2 Anatomie

Gehäuse

Das Gehäuse der Weichtiere wird vom Mantel ausgeschieden (Abbildung 2). Der Mantel ist ein Organ, welches ausserdem mehrere Schichten Muskelfasern enthält und fast alle Weichteile umfasst. Ausserdem bildet er die Aussenwand der Mantelhöhle, welche der Ausscheidung, Atmung und Fortbewegung dient. Bei den Kopffüssern mit einem gekammerten Gehäuse bildet der Mantel die Kammerscheidewände (Septen).

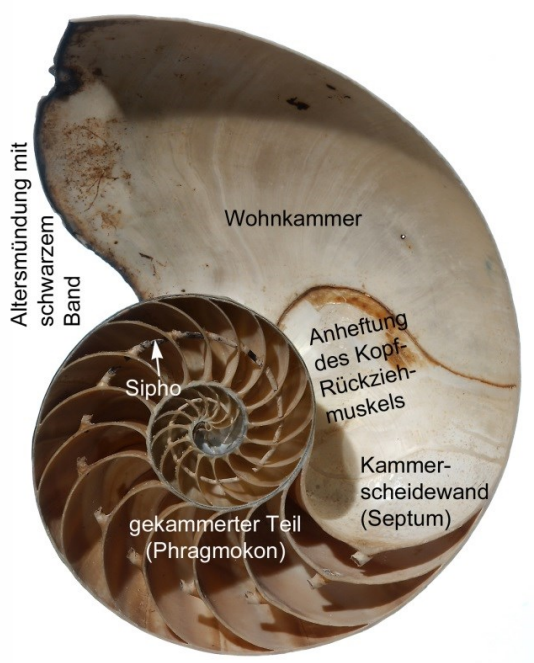

Abb. 2 Gehäuse der Nautiliden. *Nautilus pompilius* Linnaeus 1758. Rezent. Pazifik. Durchmesser 18 cm. PIMUZ 7806. Foto: Heinz Lanz, verändert nach Ernst & Klug (2011).

Das Gehäuse der Nautiliden, Ammonoideen und Belemniten besteht aus Kalk. Bei den ersten beiden Gruppen überwiegt der aragonitische Schalenanteil stark. Allen drei Gruppen ist gemein, dass ihre Gehäuse einen gekammerten Teil besitzen und eine letzte, offene Kammer. Diese letzte Kammer enthält die Weichteile und wird deshalb Wohnkammer genannt. Die Gehäuse der Nautiliden sind meist mehr oder weniger vollständig aufgerollt, mit den ältesten Teilen (dem

Embryonalgehäuse) im Zentrum. Manche Forme weisen eine Öffnung in der Mitte auf, die Nabellücke. Unter den rezenten (heute noch lebenden) Formen findet sich nur noch bei der altertümlichsten Art *Allonautilus scrobiculatus* eine kleine Nabellücke.

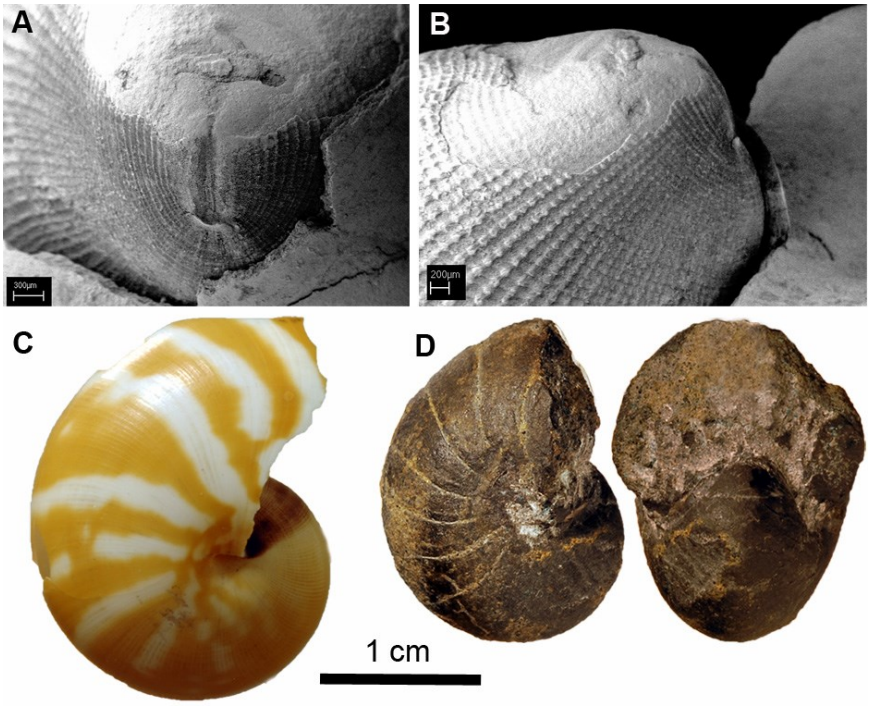

Abb. 3 Embryonalgehäuse von Nautiliden. A, B, Apikale und seitliche Ansicht der Initialschale mit Cicatrix von *Cenoceras*. Oxfordien. Jura. Ryazan, Russland. PIMUZ 31921. C, Embryonalgehäuse von *Nautilus pompilius* Linnaeus 1758. Rezent. Pazifik. PIMUZ 19129. D, Embryonalgehäuse von *Eutrephoceras* sp. Garschella-Formation. Albien. Minsterschlucht SZ. PIMUZ 4997. Fotos Christian Klug.

Das Embryonalgehäuse der Nautiliden ist recht gross mit einem Durchmesser von 5 bis etwa 30 mm zum Zeitpunkt des Schlüpfens (Abbildung 3). Zu Beginn legt der Embryo eine längsovale Platte an mit einer länglichen Narbe in der Mitte (Cicatrix). Von dort aus bildet sich eine stumpf kegelförmige Schale, an die sich rasch die spiralige Schale anschliesst. Zum Zeitpunkt des Schlüpfens sieht die Schale schon mehr oder weniger aus wie die Schale erwachsener Tiere. Rund um das Schlüpfen wird das Schalenwachstum kurz unterbrochen. Dies lässt sich manchmal auch an fossilen Gehäusen nachvollziehen, weil diese Wachstumsunterbrechung mit der Bildung einer Schalenverdickung (Einschnürung im Steinkern) einhergeht.

Gegen Ende des Wachstums ändert sich oft die Gehäusemorphologie. In der Regel wird der Nabel ein bisschen weiter, die Mündungshöhe nimmt langsamer zu und die Altersmündung ist mehr oder weniger eingeschnürt. Weiterhin ist die Schale an der Altersmündung oft verdickt und trägt manchmal ein schwarzes Band aus Chitin mit Melanin-Einlagerungen. Die gleiche Mischung aus Materialien wird auch dorsal (auf der Oberseite des Weichkörpers) auf der vorhergehenden Windung abgelagert. Bei Individuen, die in Aquarien gehalten werden, kommt es oft zu

Wachstums-Unregelmässigkeiten, die mit einer vermehrten Ausscheidung dieses Materials einhergeht.

Die Kammerscheidewände (Septen) sind mehr oder weniger radial angeordnet und mehr oder weniger Uhrglasförmig gewölbt. Sie sind fest mit der äusseren Gehäuseröhre verbunden. Die Verbindungslinie (Lobenlinie, Sutur) ist meist, im Gegensatz zu der der Ammoniten, einfach geschwungen. Sie ist dann gut zu sehen, wenn das Gehäuse mit Sediment oder Mineralien ausgefüllt wurde und die Schale aufgelöst oder abgeschliffen wurde.

Die Kammern der Kopffüsser mit gekammertem Gehäuse sind über den Sipho miteinander verbunden. Der Sipho besteht aus einer porösen und dennoch festen Röhre aus Chitin und Kalk. Er enthält einen lebenden Gewebestrang mit einer Arterie und bewerkstelligt den Austausch von Kammerflüssigkeit gegen Gas. Letzteres ähnelt in der Zusammensetzung der Luft, allerdings ist es arm an Sauerstoff und reich an Stickstoff, da es sich um ein Stoffwechselprodukt handelt.

Kieferapparat

Nautiliden besitzen zusätzlich zum Gehäuse noch weitere mineralisierte Hartteile, nämlich die Kiefer (Abbildung 4). Sowohl Ober- als auch Unterkiefer bestehen teilweise aus massivem Kalzit. Dadurch sind diese Körperteile auch gut fossil überlieferbar. Bemerkenswerter Weise sind die Kiefer nicht unbedingt dort auch häufig, wo die Gehäuse häufig sind, wahrscheinlich weil sich die verschiedenen Teile in der Strömung sehr unterschiedlich verhalten.

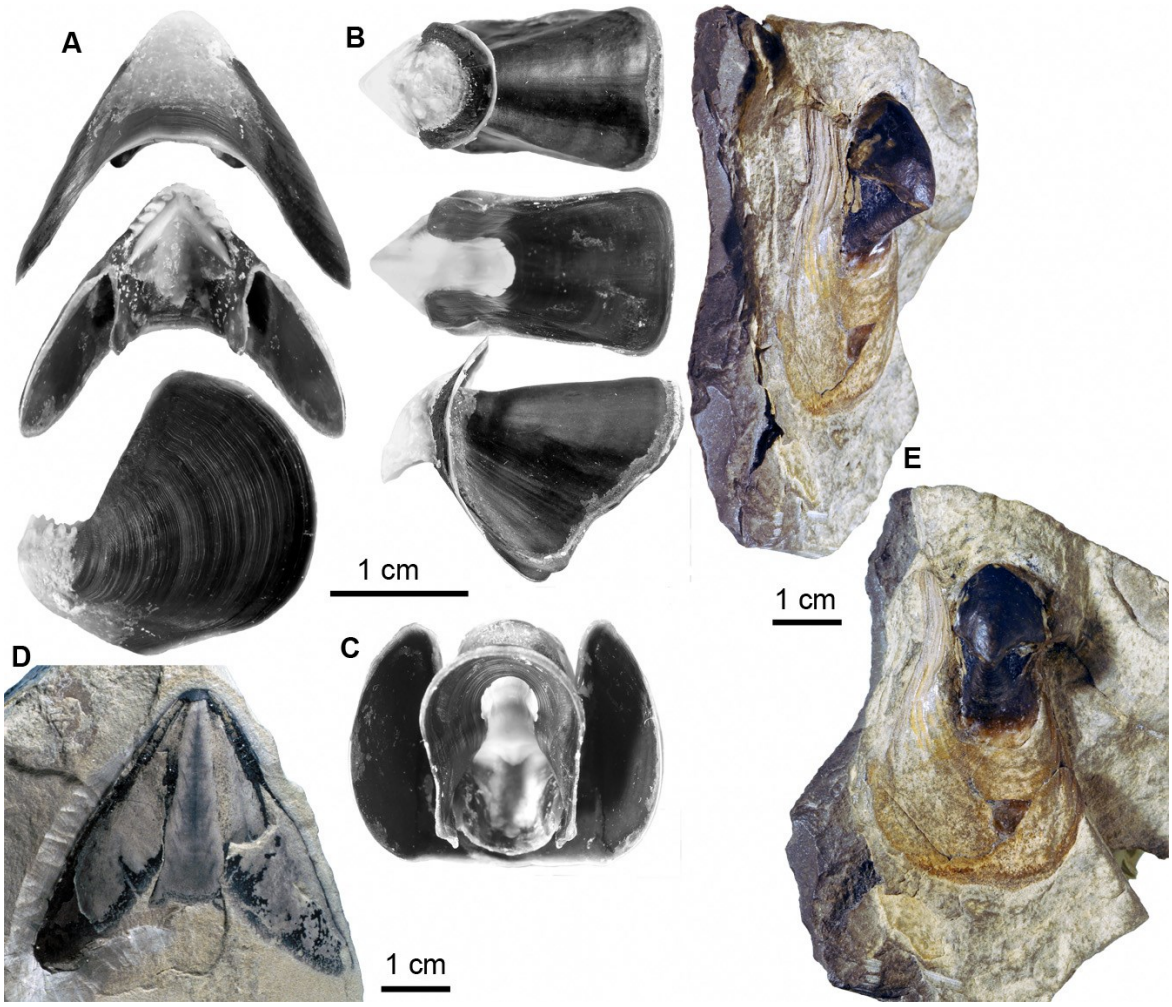

Abb. 4 Kiefer von Nautiliden. A-C, Kiefer von *Nautilus pompilius* Linnaeus 1758. Rezent. Pazifik. Staatliches Museum für Naturkunde Stuttgart, SMNS Zla. 30494. A, Unterkiefer, von unten, oben und links. B, Oberkiefer von oben, unten und links. C, beide Kiefer von hinten in Artikulation. D, E, Kiefer von *Germanonautilus*. Oberer Muschelkalk, Trias. Deutschland. D, Unterkiefer, *Conchorhynchus avirostris* (von Schlotheim 1820). Crailsheim. Muschelkalk-Museum Hagdorn, Ingelfingen, MHI 1516. E, Oberkiefer, *Rhyncholithes hirundo* (Biguet 1819, schräg seitlich und von oben. PIMUZ 17791. Fotos Christian Klug, verändert nach Klug (2001, 2009).

Zusätzlich zu den kalzitischen Bestandteilen weisen beide Kieferelemente auch chitinige Anteile auf, die allerdings deutlich seltener fossil überliefert sind. Der Unterkiefer (Conchorhynch) besteht aus zwei dreieckigen Platten, die entlang einer Kante verbunden sind. Zur Spitze hin nimmt die Dicke des Kalzits zu. Die Kaufläche weist schräg angeordnete Rippen auf. Nach hinten schliessen sich symmetrisch auf beiden Seiten breite chitinige Flügel von ovalem Umriss an. Der Oberkiefer (Rhyncholith) besteht aus einem dicken Stück Kalzit, welches im Umriss an eine steinzeitliche Pfeilspitze erinnert. Er besteht aus zwei gerundeten Tetraedern, die eine Seite teilen und eine gemeinsame, vorne geriefte Unterseite haben. Der grössere Tetraeder (Rostrum) bildet die Basis paariger, nach unten weisender chitiniger Flügel sowie einer mittigen, runden Verlängerung. Dem hinteren Tetraeder hängt eine zweilappige chitinige Verlängerung an.

Beide Kiefer artikulieren über ein kleines Gelenk, welches sich auf den chitinigen inneren Lamellen befindet. Sie sind eingebettet in ein kugeliges muskulöses Gebilde, welches als Buccal-Masse bezeichnet wird. Zwischen den Kiefern befindet sich die Raspelzunge, welche aus zahlreichen winzigen, chitinigen Zähnchen besteht. Die meisten Kopffüsser besitzen eine Raspelzunge, aber sie ist nur extrem selten fossil überliefert.

Weichkörper

Äusserlich ist nicht viel vom Weichkörper der Nautiliden zu sehen (Abbildung 5). Im Wesentlichen schaut der Kopffuss aus der Schale. Beim heutigen *Nautilus* gehören dazu die Tentakeln (bei den rezenten Tieren sind es 90), die Kopfkappe und die Lochkamera-Augen. Weiterhin sind der Trichter (Hyponom) und der Mantelrand zu sehen. Bei *Allonautilus* ist ein grosser Teil der Schale aussen vom zotteligen Periostrakum bedeckt.

Innerlich schliesst sich der Schlund (Oesophagus) an die Buccal-Masse an. Der Schlund wird umfasst vom Gehirn. An den Schlund schliesst sich der grosse Kropf mit den Verdauungsdrüsen und schliesslich der eigentliche Magen mit einem Blindsack. Der Verdauungsapparat endet mit Darm und After am Hinterende der Mantelhöhle. Hinter der Mantelhöhle befinden sich die Geschlechtsorgane. In der Mantelhöhle sind vier fiedrige Kiemen angebracht.

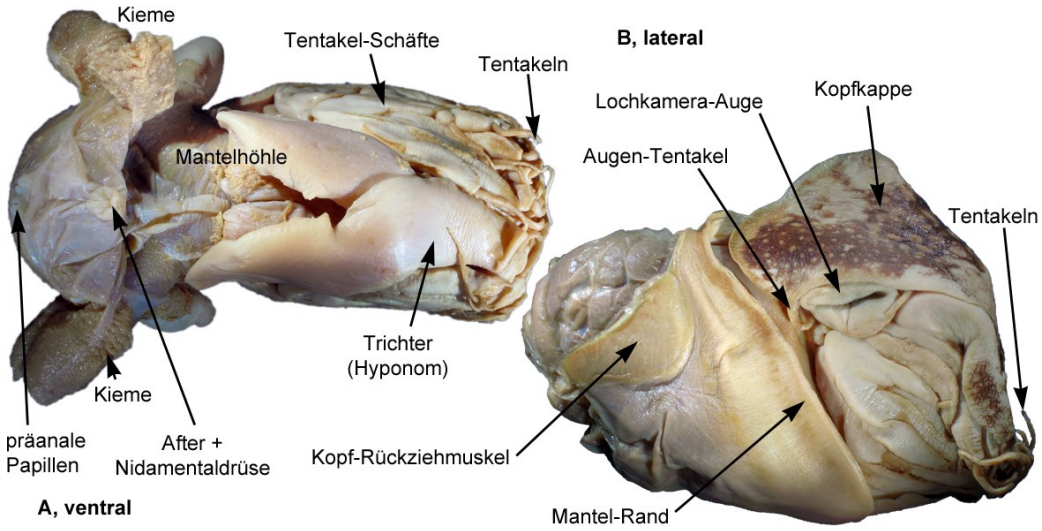

Abb. 5 Weichkörper der Nautiliden. *Nautilus pompilius* Linnaeus, 1758, Rezent. Pazifik. Staatliches Museum für Naturkunde Stuttgart, SMNS Zla. 30494. Das Tier lebte und starb im Zoo Wilhelma in Stuttgart. Fotos Christian Klug.

6.8.3 Ursprung und Evolution

Wie bereits zu Beginn des Kapitels angedeutet ist der Ursprung der Nautiliden etwas umstritten. Dies liegt weniger am Mangel an Fossilien als vielmehr an der Unklarheit, welche Bedeutung den

einzelnen Merkmalen zukommt. Während manche hauptsächlich mit dem Aufbau des Siphos argumentieren, suchen andere nach Hinweisen in der Form des Embryonalgehäuses oder des gesamten Gehäuses. Ein möglicher Stammbaum ist in Abbildung 6 dargestellt.

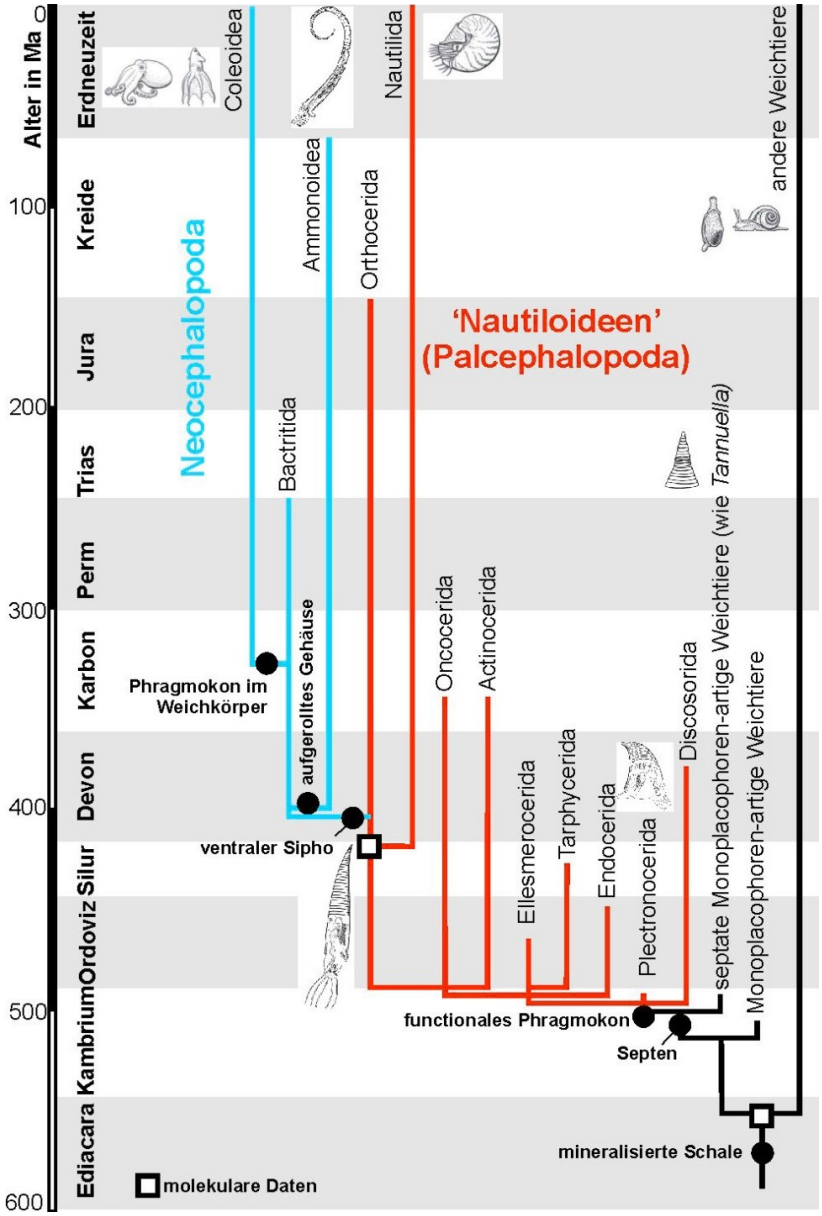

Abb. 6 Stammesgeschichte der Cephalopoden. Verändert nach Kröger et al. (2011).

6.8.4 Geschlechtsunterschiede und Reproduktion

Bei den rezenten Perlbooten unterscheiden sich die Gehäuse ausgewachsener Weibchen und Männchen nur sehr wenig. Im Durchmesser sind sich die Gehäuse sehr ähnlich, allerdings bilden die Männchen ein etwas breiteres Gehäuse. Dies hängt wohl damit zusammen, dass das Männchen

über ein relativ breites Geschlechtsorgan verfügt, den Spadix. Das bereits erwähnte schwarze Band an der Altersmündung kommt normalerweise nur bei den Weibchen vor.

Entsprechend der Grösse der Embryonen produzieren die Nautiliden-Weibchen nur wenige, recht grosse Eier (5 bis 10 pro Gelege), welche an einen harten Untergrund angeheftet werden. Die Embryonen reifen in den Eiern anschliessend noch mehrere Monate, in denen sie das grosse Dotter verbrauchen. Bereits Tage vor dem Schlüpfen schauen Teile der Schale aus der faltigen Eihülle heraus. Dies war sicherlich bei vielen Formen des Erdmittelalters ähnlich, denn Verletzungsmuster an den fossilen Embryonalschalen entsprechen dem Ort der ersten Öffnung der Eihülle.

Bedingt durch ihre langsame Fortbewegung, die Ortstreue und die niedrigen Fortpflanzungs-Raten werden leer gefischte Regionen nur sehr langsam neu besiedelt. Dies ist einer der Gründe für die heutige Gefährdung dieser interessanten Tiergruppe.

6.8.5 Lebensweise

Durch den Gas-gefüllten Teil ihres Gehäuses (Phragmokon) können Nautiliden nahezu neutralen Auftrieb erreichen. Dies erlaubt ihnen, mit wenig Energie-Aufwand zu schwimmen. Bedingt durch die räumliche Anordnung von Masse steht die Mündung auf etwa 40° von der Senkrechten. Somit befindet sich der Trichter in der Regel deutlich unter dem Schwerpunkt. Kontrahiert nun die Muskulatur (Kopfrückziehmuskel) um Wasser aus der Mantelhöhle durch den Trichter auszupressen, so bewirkt dies nicht nur eine Rückwärtsbewegung sondern auch ein Schaukeln. Das bedeutet, dass Nautiliden weder sehr schnelle noch sehr ausdauernde Schwimmer sind. Die grosse morphologische Übereinstimmung fossiler Gehäuse mit der Form heutiger Arten weist daraufhin, dass dies auch auf fossile Arten übertragbar ist.

Die Nahrung der modernen Nautiliden beschränkt sich weitgehend auf Häutungshemden von Krebsen und Aas und ist somit nicht sehr Energie-reich. Ausdauerndes Schwimmen ist folglich nicht möglich.

Insgesamt führen Nautiliden ein eher beschauliches Leben mit eher gemächlichen Bewegungen, viel davon in der Vertikalen, oft auf und ab wandernd entlang der Hänge hinter Korallenriffen. Sie erreichen Tauchtiefen bis über 700 m, wobei in etwa 800 m Tiefe die Gehäuse implodieren.

6.8.6 Diversität

Im Gegensatz zu Ammoniten waren Nautiliden nie sehr divers. In den meisten Kopffüsser-Assoziationen finden sich nur ein bis zwei Arten. Die Formenvielfalt ist auch eher beschränkt und die Evolutionsraten lagen wohl deutlich unter denen der Ammonoideen. Dies wurzelt teilweise in den niedrigen Reproduktionsraten und in der langen Dauer reproduktiver Zyklen sowie möglicherweise in der geringeren Grösse der Populationen. In diesem Zusammenhang mag es erstaunlich erscheinen, dass die Ammonoideen ausstarben, während die Nautiliden das grosse Massenaussterben am Ende der Kreide überlebten. Dafür gibt es eine Reihe möglicher Erklärungen.

Wie bereits erwähnt sind die Embryonen der Nautiliden um ein vielfaches grösser als die der Kreide-Ammoniten. Dies impliziert, dass die grossen Schlüpflinge der Nautiliden eine längere Zeitspanne ohne oder mit weniger Nahrung überdauern konnten als die Ammonoideen. Weiterhin ist es denkbar, dass ein niedrigerer Stoffwechsel es den Nautiliden erlaubte, Phasen schlechter Umweltbedingungen länger zu überstehen als ähnlich grosse Ammonoideen. Möglicherweise ist es die Kombination dieser beiden Eigenschaften, die den Nautiliden das Überleben des grossen Massenaussterbens sicherte.

6.8.7 Klassifikation

Zur Bestimmung der Nautiliden werden Merkmale der Gehäuseform, der Skulptur sowie der Form der Septen bzw. der Lobenlinie benötigt. Bei der Gehäuseform spielen die Nabelweite, die relative Gehäusebreite sowie der Windungsquerschnitt eine grosse Rolle. Die Skulptur ist zwar bei den Nautiliden nicht sehr vielfältig, dennoch spielt sie bei der Bestimmung durchaus eine Rolle. So gibt es neben den zahlreichen Formen mit glattem Gehäuse auch Arten mit Knoten, Rippen, Furchen, kräftigen Lirae oder sogar richtigen Stacheln. Die Form der Septen und somit auch die Lobenlinie sind zwar einfach, gewisse Details wie die Dimensionen der Loben (zur Mündung konkav) und Sättel (konvex), deren Anzahl und Form können unter Umständen für die Klassifikation bedeutsam sein. Fachausdrücke und Abkürzungen werden in Kapitel 6.9 erläutert.

6.8.8 Nautiliden des Alpsteins

Klasse **Cephalopoda** CUVIER 1797

Unterklasse **Nautiloidea** AGASSIZ 1847

Ordnung **Nautilida** GRAY 1821

Familie **Cymatoceratidae** SPATH 1927
Die Cymatoceraten sind in den Gesteinen des Altmann-Members durchaus häufig. Durch die auffällige Zickzack-Skulptur sind sie leicht zu erkennen.

Gattung ***Cymatoceras*** HYATT 1884
Cymatoceras neocomiense (D'ORBIGNY 1840)
Das Gehäuse dieser Art erreicht im Alpstein 20 cm, ist engnabelig (uw/dm = 0.11) und dick scheibenförmig (ww/dm = 0.30). Der Windungsquerschnitt ist deutliche höher als breit (ww/wh = 0.61). Das Gehäuse trägt ungefähr 35 kräftige, einfache sichelförmige Rippen pro halben Umgang.
Vorkommen: Altmann-Member (Spätestes Hauterivien-Frühes Barrémien), Drusberg-Member (Spätes Barrémien), Garschella-Formation (Frühes Aptien-Albien). Diese Art ist eher selten

Abb. 7 *Cymatoceras neocomiense*. Garschella-Formation. Oberrieter Chienberg. Durchmesser 20 cm. Slg. PK 7B.06.01. Fotos: Amane Tajika.

Cymatoceras subradiatum (D'ORBIGNY1850)

Das grösste uns vorliegende Exemplar misst etwa 16 cm. Das Gehäuse ist dick scheibenförmig (ww/dm = 0.57) und engnabelig (uw/dm = 0.12). Der Gehäusequerschnitt ist nur wenig breiter als hoch (ww/wh = 1.07). Im Bereich des Phragmokons befinden sich 4 bis 5 schwach ausgeprägte Rippen zwischen je zwei Lobenlinien auf der Bauchseite. Die Kammerscheidewände sind nur wenig gekrümmt.

Vorkommen: Altmann-Member (Spätestes Hauterivien-Frühes Barrémien). Hauptfundgebiet Altmann.

Abb. 8 *Cymatoceras subradiatum*. Altmann-Member. Altmann-Sattel. Durchmesser 16 cm. Die Berippung ist im Bereich des Phragmokons nur schwach ausgeprägt und hier kaum zu sehen. Slg. PK 5A.05.02. Foto Amane Tajika.

Gattung ***Eucymatoceras*** SPATH 1927

Eucymatoceras plicatum (FITTON 1835)

Bei einem Durchmesser von 15 bis 20 cm hat das globose Gehäuse (ww/dm = 0.89) einen runden, sehr breiten Windungsquerschnitt (ww/wh = 2.0) und der Nabel ist sehr eng (uw/dm = 0.07). Etwa 30 kräftige Rippen lassen sich pro halbem Umgang zählen. Diese bilden einen tiefe, dreieckige Trichterbucht auf der Bauchseite, einen dreieckigen Vorsprung am Übergang zu den Flanken und ebenso dreieckige Buchten auf den Flanken.

Vorkommen: Altmann-Member (Spätestes Hauterivien-Frühes Barrémien), Drusberg-Member (Spätes Barrémien).

Abb. 9 *Eucymatoceras plicatum*. Altmann-Member. Kohlbett unterhalb Seealp. Durchmesser 18 cm. Bei der Skulptur wurde vom Präparator offenbar etwas nachgeholfen. ETHZ 10434. Foto Amane Tajika, Illustration Christian Klug.

Gattung ***Eutrephoceras*** HYATT 1894
Diese weltweit verbreitete Gattung hat im Gegensatz zu den Cymatoceraten deutlich kleinere Gehäuse ohne Skulptur. Besonders in der Kamm-Bank findet man häufig Phragmokone dieser Gattung.

Eutrephoceras montmollini (PICTET & CAMPICHE 1859)
Das vorliegende Exemplar misst knapp 4 cm im Durchmesser. Bei dieser Grösse ist es involut (uw/dm = 0.03) und mässig dick scheibenförmig (ww/dm = 0.68). Der Windungsquerschnitt ist niedrig halbkreisförmig (ww/wh = 1.13; wh/dm = 0.64). Die Lobenlinie ist nur leicht gebogen.
Vorkommen: Garschella-Formation inkl. Kamm-Bank (Frühes Aptien-Frühes Cénomanien).

Abb. 10 *Eutrephoceras montmollini*. 1859. Kamm-Bank. Stütze 2 Säntisbahn. Durchmesser 4.3 cm. Slg. PK 7C.02.11. Foto Amane Tajika.

Eutrephoceras perlatum (MORTON 1834)

Diese Art wird nicht sehr gross. Bei einem Durchmesser von 5 cm ist das Gehäuse engnabelig (uw/dm = 0.10) und dick scheibenförmig (ww/dm = 0.73) mit breit gerundetem Windungsquerschnitt (ww/wh = 1.39; wh/dm = 0.53). Die Umgänge überlappen einander stark. Die dezent sichelförmigen Lobenlinien sind nur leicht geschwungen und auf einem halben Umgang finden sich neun Linien.

Vorkommen: Garschella-Formation inkl. Kamm-Bank (Frühes Aptien-Frühes Cénomanien). Diese Art ist im gesamten Alpstein relativ häufig.

Abb. 11 *Eutrephoceras perlatum*. Kamm-Bank. Mutteli. Durchmesser 5 cm. Slg. PK 7C.18.01. Foto Amane Tajika.

Eutrephoceras sublaevigatum (D'ORBIGNY 1850)
Die eher kleine Art ist relativ häufig im Alpstein-Gebiet. Bei einem Durchmesser von etwa 3 cm ist das Gehäuse engnabelig (uw/dm = 0.06), dick scheibenförmig (ww/dm = 0.78; wh/dm = 0.64) und hat einen breit gerundeten Windungsquerschnitt. Die Windungen überlappen einander mässig weit. Die Lobenlinie ist leicht gebogen (9 Suturen pro halben Umgang).
Vorkommen: Garschella-Formation inkl. Kamm-Bank (Frühes Aptien-Frühes Cénomanien).

Abb. 12 *Eutrephoceras sublaevigatum*. Kamm-Bank. Hinterwinden-Hornwald (Hinter Gräppelen). Durchmesser 3.6 cm. Slg. KT HW-A-0039-1. Foto Amane Tajika, Illustration Christian Klug.

Literatur

Auclair, A. C., Lécuyer, C., Bucher, H. & Sheppard, S. M. F. (2004): Carbon and oxygen isotope composition of *Nautilus macromphalus*: a record of thermocline waters of New Caledonia. Chemical Geology 207, 91–100.

Chirat, R. (2001): Anomalies of embryonic shell growth in post-Triassic Nautilida. Paleobiology 27, 485–499.

Collins, D., Ward, P. D. & Westermann, G.E.G. (1980): Function of cameral water in Nautilus. Paleobiology 6, 168–172.

Dunstan, A. J., Ward, P. D. & Marshall, N. J. (2011): Vertical distribution and migration patterns of *Nautilus pompilius*. PLoS ONE 6(2):e16311 DOI 10.1371/journal.pone.0016311.

Haven, N. (1977): The reproductive biology of *Nautilus pompilius* in the Philippines. Marine Biology 42/2, 177–184.

Klug, C. (2001): Constructional morphology and taphonomy of nautiloid beaks from the Middle Triassic of Southwest Germany. Acta Palaeontologica Polonica 46/2, 43-68. Warszawa.

Klug, C. (2009): Kompletter Nautilus-Oberkiefer aus dem Muschelkalk. Fossilien 26/9, 328-329. Goldschneck-Verlag, Korb.

Kröger, B., Vinther, J. & Fuchs, D. (2011): Cephalopod origin and evolution: a congruent picture emerging from fossils, development and molecules. Bioessays 33, 602–613.

Landman, N. H., Cochran, J. K., Rye, D. M., Tanabe, K. & Arnold, J. M. (1994): Early life history of Nautilus: evidence from isotopic analyses of aquarium-reared specimens. Paleobiology 20, 40–51.

Landman, N. H., Rye, D. M. & Shelton, K. L. (1983): Early ontogeny of *Eutrephoceras* compared to Recent *Nautilus* and Mesozoic ammonites: evidence from shell morphology and light stable isotopes. Paleobiology 9, 269–279.

Saunders, W. B. & Landman, N. H. (2010): Nautilus. The biology and paleobiology of a living fossil. Springer, Dordrecht.

Saunders, W. B. & Spinosa, C. (1978): Sexual dimorphism in Nautilus from Palau. Paleobiology 4, 349–358.

Ward, P. D. (1985): Periodicity of chamber formation in chambered cephalopods: evidence from *Nautilus macromphalus* and *Nautilus pompilius*. Paleobiology 11, 438–450.

Ward, P. D. (1987): The natural history of Nautilus. Allen and Unwin, Boston.

Ward, P. D. & Martin, A. W. (1978): On the buoyancy of the pearly *Nautilus*. Journal of Experimental Zoology 205, 5–12. DOI 10.1002/jez.1402050103.

Ward, P. D., Stone, R., Westermann, G. E. G. & Martin, A. (1977): Notes on animal weight, cameral fluids, swimming speed, and colour polymorphism of the cephalopod *Nautilus pompilius* in the Fiji Islands. Paleobiology 3, 377–388.

Appendix 1-2

Additional publications linked to this dissertation

Fossilien im Alpstein
Kapitel 6.09 Ammoniten (Ammonoidea)

Tajika, A. Kürsteiner, P. Pictet, A.
Jattiot, R. Lehmann, J. Klug, C

Book chapter (in press)
Publisher: Appenzeller Verlag

6.09 Ammoniten (Ammonoidea)

Amane Tajika, Peter Kürsteiner, Antoine Pictet, Romain Jattiot, Jens Lehmann und Christian Klug

6.9.1 Einführung

Ammoniten, Nautiliden und Belemniten gehören zu den Kopffüssern und somit zu den Weichtieren (Mollusca). Diese drei Gruppen zeichnen sich durch ein Phragmokon (gekammertes Gehäuse), eine zumindest teilweise aragonitische Schale und durch eine grosse stratigraphische und geographische Verbreitung aus. Vor allem die Ammonoideen finden Anwendung in der relativen Altersbestimmung (Biostratigraphie).

Der Begriff "Ammonoideen" leitet sich von der Unterklasse Ammonoidea ab und umfasst alle Formen ab dem Frühen Devon, während der Begriff "Ammoniten" auf Ammonitina zurückzuführen ist und nur Formen vom Jura bis zur Kreide umfasst.

6. 9.2 Anatomie

Normalerweise werden nur die mineralisierten Teile der Kopffüsser überliefert. Zu diesen gehören vor allem das Gehäuse mit dem Phragmokon und der Wohnkammer (Abb. 1) sowie, bei den mesozoischen Formen, die Unterkiefer (Aptychen). Äusserst selten können die winzigen Zähnchen der Raspelzunge (Radula) gefunden werden. Diese bestehen primär aus Chitin, welches im Lauf der Fossilisierung entweder in Phosphat umgewandelt wird oder inkohlt. Nur unter aussergewöhnlichen Bedingungen werden weitere Körperteile in der gleichen Weise umgewandelt. Bisher wurden so Reste der Kiemen, des Verdauungstraktes, des Gehirns mit Augenkapseln und fragliche Ovarien bekannt. Fossilisierte Weichteile lassen in der Regel Details vermissen, weswegen deren stammesgeschichtliche und ökologische Aussagekraft sich sehr in Grenzen hält. Entsprechend sind nur wenige anatomische Details des Weichkörpers bekannt geworden.

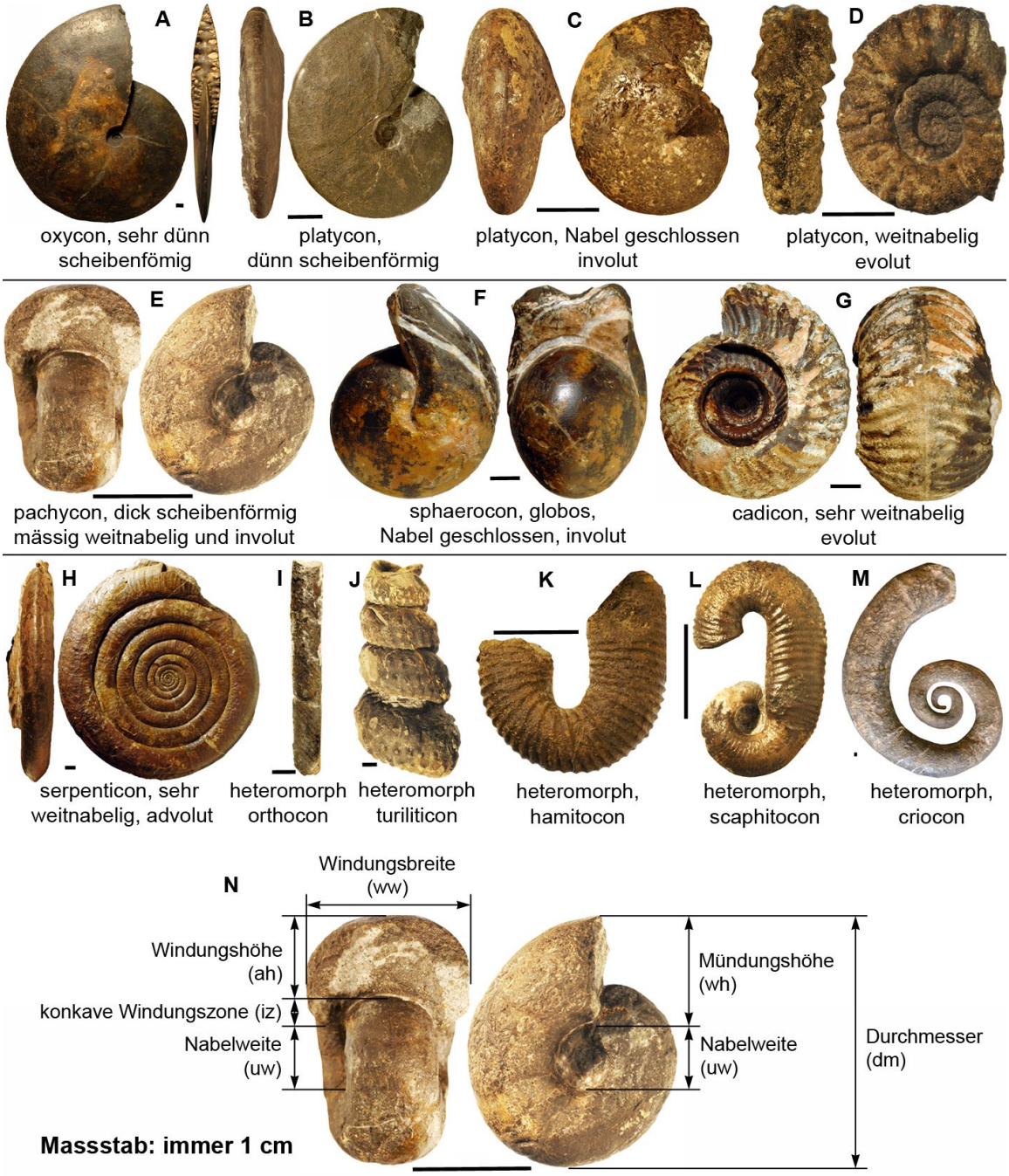

Abb. 1 Aufbau des Ammoniten-Gehäuses und Terminologie. A, *Pinacoceras*, Späte Trias, Timor, Sammlung R. Veit. B, *Beudanticeras*, Albien, Alpstein, Sammlung P. Kürsteiner. C, *Gorethophylloceras*, Albien, Alpstein, Sammlung P. Kürsteiner. D, *Cantabrigites*, Albien, Alpstein, Sammlung P. Kürsteiner. E, *Tetragonites*, Albien, Alpstein, Sammlung P. Kürsteiner. F, *Arcestes*, Späte Trias, Österreich, Sammlung R. Veit. G, *Tropites*, Späte Trias, Österreich, Sammlung R. Veit. H, *Alsatites*, Früher Jura, Österreich, Sammlung R. Veit. I, *Sciponoceras*, Cénomanien, Alpstein, Sammlung U. Oberli. J, *Mariella*, Albien, Alpstein, Sammlung U. Oberli. K, *Hamites*, Albien, Alpstein, Sammlung P. Kürsteiner. L, *Eoscaphites*, Albien, Alpstein, Sammlung P. Kürsteiner. M, Emericiceras, Barrémien, Alpstein, Naturmuseum St. Gallen. N, *Tetragonites* sp. Albien, Alpstein, Sammlung P. Kürsteiner. Illustration Christian Klug.

Gehäuse

Bei allen Ammonoideen sind zumindest Teile des Gehäuses spiralig aufgerollt. Bei den allerersten Ammonoideen ist diese Aufrollung noch unvollständig, die Umgänge berühren sich also nicht. Noch im Frühen Devon nimmt die Aufrollung des Gehäuses rasch zu und bereits im Mittleren Devon gibt es keine Ammonoideen mehr, deren Windungen sich nicht berühren. Im Mesozoikum (Späte Trias, Mittlerer Jura, Kreide) entwickelten sich mehrfach Formen, deren Gehäuse entweder lose aufgewunden oder sogar gestreckt sind („Heteromorphe"). All diesen Formen ist jedoch gemeinsam, dass zumindest das embryonale Gehäuse vollkommen aufgerollt ist. Diese Tatsache belegt, dass die Heteromorphen von Monomorphen, also Ammonoideen mit normal aufgerolltem Gehäuse, abstammen. Im Alpstein finden sich sowohl monomorphe als auch heteromorphe Formen in grosser Vielfalt.

Durch die Aufrollung des Gehäuses ist der Gebrauch der Wörter Venter bzw. ventral (bauchseitig) und Dorsum bzw. dorsal (auf dem Rücken) etwas ungewöhnlich. Weil die Aussenseite der Windungen einst Bauchseite war, bezeichnet man diese als ventral, während die gegenüberliegende Seite, wo sich die vorhergehende Windung abprägt, als Dorsum bezeichnet wird.

Wie bei den Nautiliden weist das Ammonoideen-Gehäuse einen gekammerten Teil (Phragmokon) und einen Septen-freien Teil (Wohnkammer) auf. Die Länge der Wohnkammer hängt unter anderem von der Windungszunahme ab und bestimmt auch die Orientierung des Gehäuses im Wasser zu Lebzeiten. Letzteres wurde zunächst an mathematischen und Später an empirischen Modellen nachvollzogen.

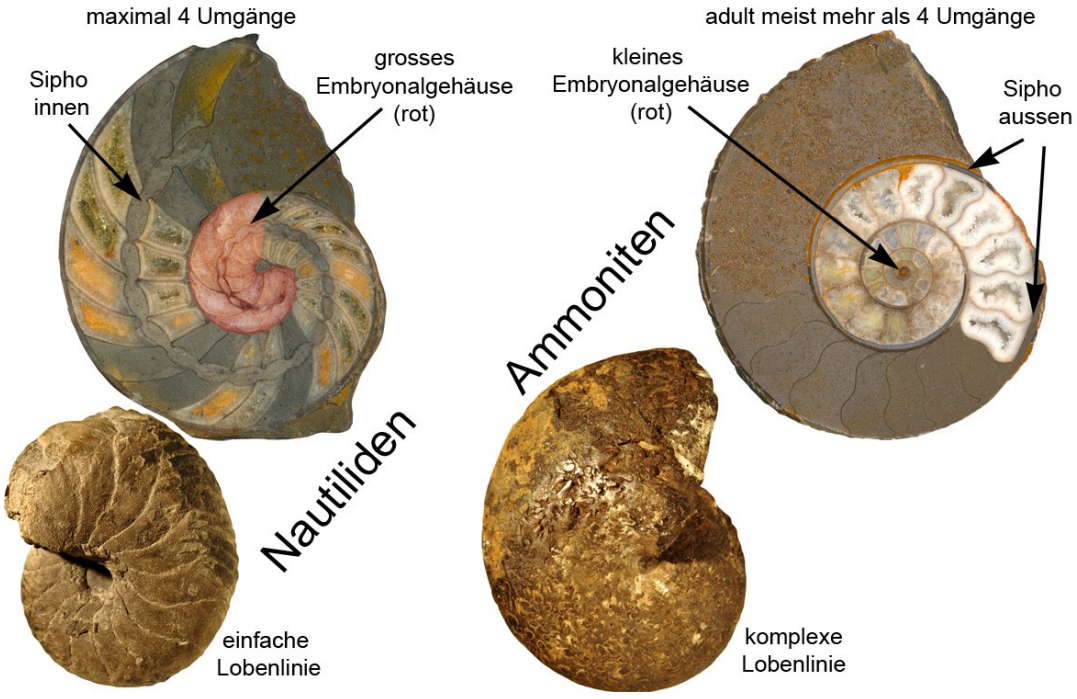

Abb. 2 Unterscheidung von Nautiliden und Ammoniten. Links oben: Nautilide *Cenoceras*, Durchmesser 6 cm, Mittlerer Jura, Böttstein AG, PIMUZ. Links unten: Nautilide *Eutrephoceras*, Durchmesser 10 cm, Barrémien, Alpstein, Sammlung P. Kürsteiner. Rechts oben: Ammonit *Ludwigia*, Mittlerer Jura, Passwang SO, PIMUZ. Rechts unten: Ammonit *Gorethophylloceras*, Durchmesser 3.2 cm, Albien, Alpstein, Sammlung P. Kürsteiner. Illustration Christian Klug.

Die wichtigsten Unterschiede im Gehäuse-Aufbau zu den Gehäusen der Perlboote (Nautiliden) liegen im Phragmokon (Abb. 2): Vor allem bei Ammonoideen des Erdmittelalters sind die Kammerscheidewände (Septen) stark verfaltet (devonische Ammonoideen haben häufig Lobenlinien, die denen der Perlboote ähneln). Die Komplexität der Lobenlinie (Anheftungslinie der Septen an der Gehäusewand) wurzelt wahrscheinlich in folgenden Eigenheiten der Ammonoideen: Zum einen ist der Sipho ventral angeheftet und bewirkt die Bildung des sogenannten Externlobus. Die seitliche Abflachung der Gehäuseröhre verursachte die Entstehung des Flankenlobus und durch die zunehmende Überlappung der Umgänge entstand der Internlobus. Nabel- und Adventivloben lassen sich einerseits durch die Verengung des Raumes durch enge Windungsabschnitte und andererseits durch die starke Querschnittsveränderung vom Embryo zum erwachsenen Tier erklären; während die Nautiliden-Embryos meist einige Millimeter bis mehrere Zentimeter messen, sind jene der Ammonoideen zwischen etwa 0.5 und 2 mm klein.
Die Kammern des Phragmokons sind durch den Sipho miteinander verbunden. Bei Ammoniten hatte dieses Organ vermutlich dieselbe Funktion wie bei den Nautiliden: Neugebildete Phragmokon-Kammern waren zunächst mit Wasser gefüllt, welches durch Osmose in den Sipho und somit den Weichkörper des Kopffüssers gelangte. Im Gegenzug wurde ein Luft-ähnliches Gasgemisch in die Kammern gepumpt, wodurch die Tiere wohl neutralen Auftrieb erhielten. So konnten die Ammoniten mit geringem Energie-Aufwand schwimmen.
Der schmale Sipho der Ammonoideen liegt auf der Aussenseite (= ventral; einzige Ausnahme sind die devonischen Clymenien). Ausserdem ist der Sipho der Perlboote wesentlich dicker, was aber wenigstens teilweise mit der Lage zusammenhängt: Durch die ventrale Lage des Ammonoideen-Siphos ist er länger, hat aber bei geringem Durchmesser trotzdem eine ähnlich grosse funktionale Oberfläche um den Austausch von Gas und Kammer-Flüssigkeit zu bewerkstelligen.

Kieferapparat
Der Kieferapparat vieler Ammonoideen ist recht gut bekannt, vor allem die Unterkiefer (Abb. 3). Oberflächlich ähneln die Kieferapparate Papageienschnäbeln. Während die Unterkiefer bei manchen Formen (vor allem in Jura und Kreide) eine mehr oder weniger dicke calcitische Auflage aufweisen, sind die Oberkiefer immer chitinig und entsprechend seltener fossilisiert. Selbst in jenen Fällen, in welchen beide Kiefer chitinig sind, fehlt oft der Oberkiefer. Dies spricht dafür, dass das Chitin dünner oder weniger stabil und daher schwerer erhaltbar war.

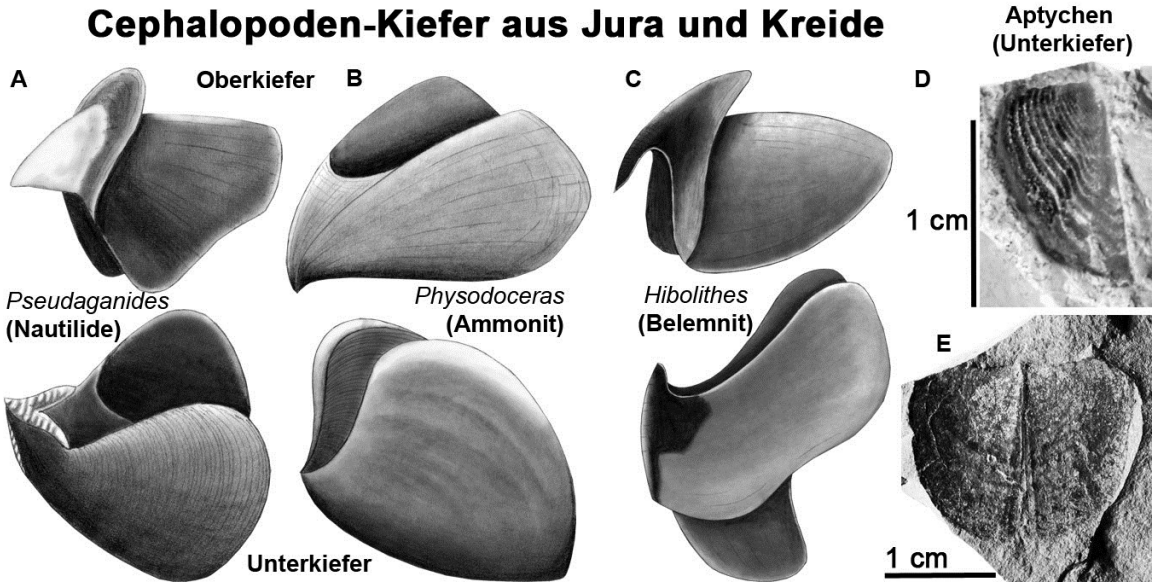

Abb. 3 Kieferapparat der Ammoniten im Vergleich mit Belemniten und Nautiliden. A-C, Cephalopoden des Kimmeridgien von Nusplingen D; verändert nach Klug et al. (2011). D, Aptychus, calcitische Erhaltung. Späte Kreide. Breggia-Schlucht TI. PIMUZ 17607. E, Aptychus, organische Erhaltung. Barrémien. Breggia-Schlucht TI. PIMUZ 23257. Alle Abbildungen Christian Klug.

Weichkörper

Manche anatomischen Aspekte können mittels aktualistischer Vergleiche rekonstruiert werden. Viel diskutiert sind Anzahl und Form der Arme, welche fossil bislang nicht bekannt sind. Die nächsten lebenden Verwandten sind einerseits die Tintenfische, deren ursprünglichste Vertreter zehn Arme hatten (z.B. die Belemniten); andererseits haben die Nautiliden heute zwar 90 Arme, Frühe embryonale Stadien haben allerdings zehn Arm-Anlagen, welche sich noch vor dem Schlüpfen mehrfach aufspalten.

Alle lebenden Kopffüsser haben gut ausgebildete Augen. Im Gegensatz zu den Tintenfischen mit ihren Linsenaugen haben die Perlboote jedoch Lochkamera-Augen. Weil die Tintenfische wie die Ammoniten von den Bactriten (eine ausgestorbene Gruppe von Kopffüssern, die meist gerade, kegelförmige Gehäuse besassen) abstammen (siehe Abb. 6 im Nautiliden-Kapitel), erscheint es wahrscheinlicher, dass die Ammoniten ebenfalls über Linsenaugen verfügten. Indizien dafür liefern Fossilien von Baculiten (Ammoniten mit gestreckten Gehäusen) aus der Kreide Norddeutschlands, welche Weichteilreste aufweisen, sowie die oft stark ausgeprägte sogenannte Augenbucht in der Mündung, in welcher wohl die Augen sassen. Weiterhin sind gelegentlich Details des Verdauungstraktes überliefert. Im Wesentlichen zeigen solche Fossilien den Schlund, den Kropf und den Magen. Schliesslich gibt es noch zwei Belege für die Kiemen.

6.9.3 Ursprung und Evolution

Genau wie die Tintenfische auch stammen die Ammonoideen von den Bactriten ab. Die Bactriten wiederum leiten sich von den Orthocerida ab. Die Orthoceriden haben gestreckte kegelförmige Gehäuse, wobei der Sipho in der Mitte durch die einfach Uhrglas-förmig gewölbten Septen läuft. Bei den Bactriten hat sich der Sipho an den bauchseitigen (ventralen) Rand verlagert. Dies bewirkte eine Einbuchtung der Septen und somit die Entstehung der ersten Verfaltung der Lobenlinie. Eine

evolutive Linie innerhalb der Bactriten brachte weitere Neuerungen hervor wie die seitliche Abflachung der Gehäuseröhre (Entstehung weiterer Loben) sowie eine beginnende Krümmung. Die etwas willkürliche Definition des Ursprungs der Ammonoideen besagt, dass die Ammonoideen mindestens einen Umgang bilden müssen. Dies war offenbar der essentielle evolutive Schritt, denn ab diesem Punkt schritt die Evolution der Ammonoideen rasend schnell voran. Die Aufrollung nahm immer mehr zu, bis schon bald sehr eng aufgewundene Gehäuse entstanden.
Zu Beginn der Evolution der Ammonoideen belegt die gerade bis wenig gekrümmte Form der Embryonalgehäuse noch eindrücklich die Abstammung von gestreckten Formen. Jedoch auch die Aufrollung des Embryonalgehäuses schritt evolutiv sehr schnell voran. Bereits im Mitteldevon waren die Embryonalgehäuse aller Ammonoideen spiralig aufgewickelt. Dies ging einher mit einer Grössenreduktion von ca. 7 mm Gehäusedurchmesser zu etwa 0.5 mm bei den Ammoniten des Erdmittelalters. Entsprechend explodierten auch die Reproduktionsraten von weniger als 100 bei den ersten Ammonoideen zu geschätzten 100 Millionen bei den Riesenformen (Puzosien) der Späten Kreide, wie sie auch im Alpstein häufig gefunden werden.

6.9.4 Dimorphismus

Bereits in den sechziger Jahren entdeckten der Pole Henryk Makowski und der Engländer John Callomon, dass viele Ammoniten-Arten in Paaren auftreten. Diese Paare kommen in den gleichen Schichten und den gleichen Regionen vor. Ausserdem haben sie identische Jugendwindungen und Lobenlinien. Unterschiede liegen vor allem in der maximalen Grösse und der Skulptur. Die kleineren Formen (Mikrokonche) haben eine kräftige Skulptur und oft eigenartige Schalenfortsätze an der Altersmündung. Die grossen Formen dagegen (Makrokonche) haben oft ein Vielfaches des Durchmessers der Mikrokonche, haben eine deutlich schwächere Skulptur und eine einfachere Mündung. Vergleiche mit heutigen Kopffüssern legen nahe, dass es sich bei den Makrokonchen um die Gehäuse der Weibchen handelt und bei den Mikrokonchen um jene der Männchen. Diese Unterschiede sind unterschiedlich stark ausgeprägt und nur von einem Bruchteil aller Ammonoideen-Arten gut dokumentiert.

6.9.5 Lebensweise

Weil die Ammonoideen ausgestorben sind, müssen indirekte Indizien verwendet werden, um die Lebensweise der Ammonoideen zu bestimmen. Die Gehäuseform liefert einige solche Indizien: Manche Gehäuse sind scheibenförmig, andere kugelig oder haben eine andere Form. Für die Dünnscheibenförmigen wird angenommen, dass sie kurze Strecken recht schnell schwimmen konnten, während die dickeren Formen eher gemächliche, dafür aber ausdauernde Schwimmer waren.

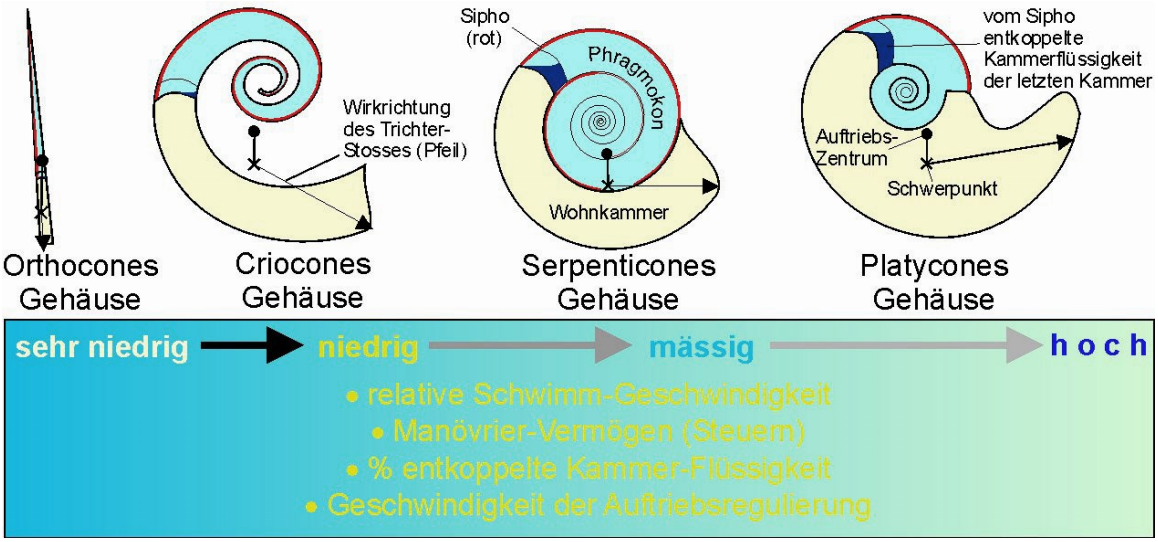

Abb. 4 Schwerpunkt und Auftriebsmittelpunkt bei verschiedenen Ammonoideen. Im Wesentlichen sind es Wohnkammerlänge und Aufrollung, welche die Gehäuse-Orientierung physikalisch bestimmen. Illustration Christian Klug, verändert nach De Baets et al. (2016).

Aus der räumlichen Massenverteilung des Gehäuses können Schwerpunkt und Auftriebsmittelpunkt rekonstruiert werden (Abb. 4). Diese beiden Punkte sollten im Ruhezustand übereinander liegen. Daraus lässt sich die Gehäuseorientierung ermitteln. Bei den meisten Formen aus Jura und Kreide war die Mündung mehr oder weniger horizontal, was wohl vorteilhaft für das horizontale Schwimmen war, da der Wasserausstoss aus dem Trichter auf ähnlicher Höhe wie der Schwerpunkt lag.

In einer Reihe von Studien wurden die stabilen Isotope von Ammoniten-Schalen aus Jura und Kreide untersucht. Aus dem Verhältnis verschiedener Isotope lässt sich annähernd die Temperatur des Wassers, in dem das Tier lebte, ermitteln. Dies erlaubt Rückschlüsse auf die Wassertiefe. Die Ergebnisse dieser Studien sind allerdings recht widersprüchlich: Manche Autoren meinen, dass die Ammoniten eher bodenbezogen lebten während andere herausfanden, dass es rechte Unterschiede in der bevorzugten Wassertiefe der verschiedenen Formen gab. Weitere Untersuchungen werden vielleicht helfen, diese Wissenslücke zu schliessen.

6.9.6 Aussterben

Die Geschichte des Lebens ist gekennzeichnet von einer generellen Zunahme der Artenvielfalt, die immer wieder durch zahlreiche kleine und wenige grosse Aussterbeereignisse reduziert wurde. Auch die Diversität der Ammoniten wurde wiederholt extrem reduziert, vor allem am Ende des Devons, am Ende des Perms (damals starben rund 80% aller im Meer lebenden Arten aus), am Ende der Trias und schliesslich am Ende der Kreide. Dabei überlebten jeweils nur sehr wenige Arten, wobei die anschliessende Diversifizierung oft sehr rasch vonstatten ging, abgesehen vom Ende der Kreide, als unter anderem die Ammoniten ausstarben.

Neben dem Aussterben der Ammonoideen verschwanden auch die Belemniten und die Dinosaurier am Ende der Kreide. Erstaunlich ist, dass die Nautiliden und die Tintenfische dieses Massenaussterben überlebten. Es ist noch nicht ganz klar, warum manche Kopffüsser ausstarben und andere überlebten. Sicher ist, dass die ausgestorbenen Gruppen kleinere Embryonen hatten.

Vielleicht waren diese auf ein kontinuierliches Nahrungsangebot angewiesen, welches durch die Naturkatastrophen am Ende der Kreide (Meteorit, Vulkanismus) wohl nicht mehr gegeben war.

6.9.7 Klassifikation

Aus dem Alpstein liegen über 100 Ammoniten-Arten vor, die hier auch abgebildet sind. 26 Arten stammen aus dem Altmann-Member der Tierwies-Formation, 7 Arten kommen aus dem Drusberg-Member der Tierwies-Formation, 33 Arten wurden in der Garschella-Formation (ohne Kamm-Bank) gefunden und die Kamm-Bank selber (Abb. 5) lieferte 42 Arten. Die Seewen-Formation lieferte wenige gut bestimmbare Arten (Abb. 6). Diese Liste ist sicherlich unvollständig, die häufigsten Arten sollten hier aber enthalten sein. Zur Bestimmung der Arten werden hauptsächlich äussere Gehäusemerkmale wie die Gehäuseform und Skulptur herangezogen. Auch die Lobenlinie liefert manchmal wichtige Indizien, wobei die Kammerscheidewände manchmal nicht zu sehen sind (aufgelöst oder durch Schale bedeckt). Mit ein bisschen Erfahrung ist die Bestimmung gut erhaltener Ammoniten einfach, vor allem auf Gattungs-Ebene.

Abb. 5 Ammoniten im Gelände: Kamm-Bank mit zahlreichen Fragmenten von *Mariella bergeri*. Foto Karl Tschanz.

Abb. 6 Ammonit im Gelände: Basis der Seewen-Formation mit grosser *Puzosia* sp. Foto Christian Klug.

Abb. 7 In den Ablagerungen der Kreide finden sich zuweilen sehr grosse Ammoniten. Nicht alle sind so schön erhalten wie diese *Puzosia* sp. aus der Garschella-Formation beim Bergli, Sennwald. Durchmesser 48 cm. Slg. PK 7B.43.12. Foto Peter Kürsteiner.

Weil das Gehäuse meist das einzige ist, was überliefert wird (als Steinkern, mit Original- oder Ersatzschale), müssen sich PaläontologInnen und SammlerInnen mit den Gehäusemerkmalen für die Bestimmung begnügen. Glücklicherweise beschränken sich diese Merkmale nicht nur auf die Unterscheidung monomorph oder heteromorph. Die Gehäuse können glatt sein oder verschiedenste Skulpturelemente tragen wie Knoten, Dornen, Rippen, Kiele und Anwachsstreifen. Der Grad der Überlappung der Windungen ist ebenfalls von Bedeutung. So spricht man bei Formen, wo sich die Umgänge berühren von ‚advolut', bei leichter Überlappung von ‚evolut' und bei starker oder völliger Überlappung von ‚involut' (Abb. 2). Dies korreliert zu einem gewissen Grad mit der Nabelweite. Der Nabel (Umbilikus) ist der Gehäuseteil, wo der letzte Umgang die vorhergehenden Umgänge nicht bedeckt. Auch hier wird unterschieden zwischen weitnabelig, engnabelig und geschlossenem Nabel. Die Nabelweite steht oft auch im Zusammenhang mit der Windungs- oder Gehäusebreite. Sowohl Nabelweite als auch Gehäusebreite wird oft in ein einfaches mathematisches Verhältnis zum Gehäusedurchmesser gesetzt. Die Gehäusebreite lässt sich einerseits beschreiben mit den naheliegenden Adjektiven breit und schmal. Für das Erscheinungsbild von Bedeutung ist auch die Windungszunahme, welche beschreibt, um wieviel ein Umgang an Höhe gewinnt. Weiterhin gibt es eine Reihe von Fachausdrücken, die eine Kombination von Aspekten der Gehäuseformen zusammenfassen:

Gehäuseform	Breite	Nabelweite	Überlappung	Windungszunahme	Skulptur
globos	sehr breit	sehr gering	sehr gross	niedrig - mässig	glatt - mittel
cadicon	sehr breit	gross	gering	niedrig - mässig	glatt - kräftig
platycon	mässig - gering	mässig - gering	mässig - gross	mässig - hoch	glatt - mittel
oxycon	gering	gering	gross	hoch	glatt
criocon	gering	sehr gross	keine	niedrig	Rippen

Tab. 1

Bei der Bestimmung von Ammoniten-Gehäusen empfiehlt es sich, eine Reihe von Aspekten zu bedenken. Eine scheinbar nur zweitrangige Frage ist diejenige nach der Erhaltung. Liegt das Stück als Steinkern oder in Schalenerhaltung vor? Je nach dem können Dornen oder andere Skulpturelemente erhalten sein oder fehlen, auch kann sich die Gehäuseform leicht unterscheiden. Innenseite und Aussenseite der Schale unterscheiden sich meist. Weiterhin ist zu bedenken, dass das Gehäuse verschiedener Lebensabschnitte recht unterschiedlich aussehen kann. Oft ändern sich Geometrie und auch die Skulptur im Laufe der Ontogenie, während des Wachstums des Individuums. Wird also die Grösse des Stückes gänzlich ignoriert, dann kann es zu Fehlbestimmungen kommen. Ein anschauliches Beispiel hierfür sind die Scaphitiden, deren Jugendwindungen normal aufgerollt sind, bei denen sich aber im Alter ein Haken-förmiger, allerdings recht charakteristischer Umgang bildet.

Abkürzungen: In den Beschreibungen werden häufig Verhältnisse angegeben, um die Gehäuseform zu beschreiben. Zur Vereinfachung werden diejenigen Abkürzungen verwendet, welche auch im Englischen gebräuchlich sind: dm - Durchmesser, ww - Windungsbreite, wh - Windungshöhe, uw - Nabelweite (umbilikale Weite). Meistens werden ww, wh und uw in ein Verhältnis zum jeweiligen Durchmesser gestellt.
Weiterhin sind folgende Begriffe gebräuchlich, um die Lage auf der Windung zu beschreiben: Ventral: bauchseitig, bei Ammoniten i.d.R. aussen. Lateral: auf den Seiten/ Flanken. Dorsal: auf dem Rücken, i.d.R. dem Nabel bzw. der nächstkleineren Windung zugewandt. Ventrolateral: am Übergang von Bauchseite zur Flanke. Dorsolateral: am Übergang vom Rücken zur Flanke. Apikal: bei turriliticonen Gehäusen in Richtung Spitze (in Richtung Embryonalgehäuse).
Weitere Begriffe: Anwachsstreifen: Wachstumslinien, sehr feine Rippen, welche die kleinsten Fortschritte im Gehäusewachstum am Mundrand dokumentieren. Sie umfassen oft nicht die ganze Windung. Lirae: ähnlich wie Anwachsstreifen, nur deutlich kräftiger.

6.9.8 Die Ammoniten des Alpsteins

Die Systematik und Reihenfolge der folgenden Beschreibung orientiert sich am Kreide-Ammoniten-Treatise (Wright et al. 1996). In diesem Werk sind alle bis im Jahre 1996 in der Literatur aufgeführten Ammoniten-Gattungen abgebildet und beschrieben.

Klasse **Cephalopoda** CUVIER 1797
Unterklasse **Ammonoidea** ZITTEL 1884
Unterordnung **Phylloceratina** ARKELL 1950
Überfamilie **Phylloceratac eae** ZITTEL 1884
Die Phylloceraten lassen sich bei Steinkernerhaltung des Phragmokons leicht an den an Eichenblätter erinnernden Sätteln in den Lobenlinien erkennen, daher der Name (*phyllon* = gr. Blatt).

Familie **Phylloceratidae** ZITTEL 1884
Unterfamilie **Phylloceratinae** ZITTEL 1884
Gattung ***Phylloceras*** SUESS 1865
Untergattung ***Hypophylloceras*** SALFELD 1924
Phylloceras* (*Hypophylloceras*) *velledae velledae (MICHELIN 1834)
Das abgebildete Gehäuse misst 3.8 cm im Durchmesser. Es ist dünn scheibenförmig (ww/dm = 0.37) und sehr involut (uw/dm = 0.08). Der Windungsquerschnitt ist seitlich abgeflacht (ww/wh = 0.64) mit flachen Flanken und gerundeter Bauchseite.
Vorkommen: Kamm-Bank (Spätestes Albien-Frühes Cénomanien).

Abb. 8 *Phylloceras* (*Hypophylloceras*) *velledae velledae*. Kamm-Bank. Stütze 2 Säntisbahn. Durchmesser 3.8 cm. Slg. PK 7C.02.04. Foto Amane Tajika.

Gattung ***Gorethophylloceras*** COLLIGNON 1949
Gorethophylloceras subalpinum (D'ORBIGNY 1841)
Dies ist einer der wenigen pyritisierten Ammoniten aus dem Alpstein. Da es sich um einen Steinkern handelt, ist die schöne Lobenlinie mit den Eichenblatt-ähnlichen Sätteln gut zu erkennen. Das Gehäuse misst 3.2 cm im Durchmesser. Es ist mässig dick scheibenförmig (ww/dm = 0.47) und sehr involut (uw/dm = 0.09) mit einem seitlich abgeflachten Windungsquerschnitt (ww/wh = 0.79), breit gerundeten Flanken und einer gerundeten Bauchseite.
Vorkommen: Garschella-Formation (Spätes Aptien-Spätes Albien).

Abb. 9 *Gorethophylloceras subalpinum*. Garschella-Formation. Schlatt (oberhalb Rüthi). Durchmesser 3.2 cm. Slg. PK 7B.20.21. Foto Amane Tajika.

Unterordnung **Lytoceratina** HYATT 1889
Viele Lytoceraten haben ein mehr oder weniger glattes Gehäuse, dessen Umgänge kaum überlappen. Ihre Lobenlinien gehören zu den kompliziertesten und ähneln denen der Phylloceraten.

Überfamilie **Lytocerataceae** NEUMAYR 1875b
Familie **Gaudryceratidae** SPATH, 1927
Gattung ***Gaudryceras*** DE GROSSOUVRE 1894
***Gaudryceras* sp.**
Gaudryceras ist eine weltweit häufige Gattung, deren Gehäuse sich durch einen weiten Nabel (uw/dm = 0.51) und eine für die Familie typische, sehr geringe Windungsüberlappung auszeichnet. Die Windungsbreite variiert je nach Art zwischen ww/dm = 0.20 und 0.45. Die Gehäuse sind meist schwach skulpturiert mit einer variablen Anzahl von Einschnürungen (Megastriae) sowie, vor allem im Alter, mit manchmal kräftigen Lirae.
Vorkommen: Garschella-Formation (Frühes Albien).

Abb. 10 *Gaudryceras* sp. Garschella-Formation. Chapf, Oberriet. Durchmesser 2.9 cm. Slg. PK 7B.10.03. Foto Christian Klug.

Familie **Lytoceratidae** NEUMAYR 1875b
Unterfamilie **Lytoceratinae** NEUMAYR 1875b
Gattung ***Lytoceras*** SUESS 1865
***Lytoceras* sp.**
Das hier abgebildete Stück misst 8.6 cm im Durchmesser. Dessen Gehäuse ist mässig dick scheibenförmig (ww/dm = 0.4) und advolut mit einem weiten Nabel (uw/dm = 0.42). Dessen kreisförmiger Windungsquerschnitt ist deutlich breiter als hoch (ww/wh = 1.22). Abgesehen von feinen Lirae ist das Gehäuse glatt. Bei der Gattung kommen manchmal Megastriae vor, also alte Mundränder, die einen breiten Kragen tragen. Das abgebildete Exemplar zeigt keine derartigen Strukturen.
Vorkommen: Die Gattung ist aus Jura und Kreide bekannt. Im Alpstein wurde sie im Altmann-Member gefunden (Spätestes Hauterivien-Frühes Barrémien).

Abb. 11 *Lytoceras* sp. Altmann-Member. Altmann. Durchmesser 8.6 cm. PIMUZ 31919. Foto Christian Klug.

Überfamilie **Tetragonitaceae** HYATT 1900
Familie **Tetragonitidae** HYATT 1900
Gattung ***Tetragonites*** KOSSMAT 1895
Tetragonites jurinianus jurinianus (PICTET 1847)
Das abgebildete Exemplar misst 4.3 cm Durchmesser. Sein Gehäuse ist dick scheibenförmig (ww/dm = 0.59) und subinvolut (uw/dm = 0.22). Der gerundet rechteckiger Windungsquerschnitt ist deutlich breiter als hoch (ww/wh = 1.24).
Vorkommen: Kamm-Bank (Spätestes Albien-Frühes Cénomanien).

Abb. 12 *Tetragonites jurinianus jurinianus*. Kamm-Bank. Säntis, Gasthaus-Hang. Durchmesser 4.3 cm. Slg. PK 7C.11.03. Foto Amane Tajika.

Tetragonites timotheanus timotheanus PICTET 1847

Das vorliegende Stück ist nur 2.6 cm gross. Dessen Gehäuse ist scheibenförmig (ww/dm = 0.46) und subevolut (uw/dm = 0.35). Sein Windungsquerschnitt ist breit rechteckig bis trapezförmig (ww/wh = 1.2). Abgesehen von drei Einschnürungen pro Umgang ist das Gehäuse glatt.
Vorkommen: Garschella-Formation (Albien).

Abb. 13 *Tetragonites timotheanus timotheanus*. Garschella-Formation. In Ränken (oberhalb Plona). Durchmesser 2.6 cm. Slg. PK 7B.23.03. Foto Amane Tajika.

Familie **Gaudryceratidae** SPATH 1927
Gattung ***Kossmatella*** JACOB 1907
Kossmatella agassiziana (PICTET 1847)
Das hier abgebildete Stück misst 3.9 cm im Durchmesser. Dessen Gehäuse ist dünn scheibenförmig (ww/dm = 0.38) und subinvolut (uw/dm = 0.28). Der gerundet trapezförmige Windungsquerschnitt ist höher als breit (ww/wh = 0.81). Der letzte halbe Umgang trägt acht breite Wulstrippen mit feinen Rippen dazwischen.
Vorkommen: Kamm-Bank (Spätestes Albien).

Abb. 14 *Kossmatella agassiziana*. Kamm-Bank. Hinterwinden. Durchmesser 3.9 cm. Slg. PK 7C.14.02. Foto Amane Tajika.

Kossmatella muhlenbecki (FALLOT 1885)
Das abgebildete Exemplar misst 3.7 cm im Durchmesser. Sein Gehäuse ist dünn scheibenförmig (ww/dm = 0.33) und subevolut (uw/dm = 0.40). Der annähernd rechteckige Windungsquerschnitt weist eine flache Bauchseite sowie flache Flanken auf und ist etwas höher als breit (ww/wh = 0.91). Der letzte Umgang trägt 16 Wulstrippen mit dazwischen liegenden, sehr feinen Rippen.
Vorkommen: Garschella-Formation (Mittleres-Spätes Albien).

Abb. 15 *Kossmatella muhlenbecki*. Garschella-Formation. Chelen-Geren, Plona. Durchmesser 3.7 cm. Slg. PK 7B.37.31. Foto Amane Tajika.

Kossmatella ventrocincta (QUENSTEDT 1848)

Diese eher kleine Art zeichnet sich aus durch gerundete Windungen mit eher geringer Windungsüberlappung. Der Nabel ist weit (uw/dm = 0.47) und die Windungen mässig breit (ww/dm = 0.27). Die Skulptur wird dominiert von breiten Knoten auf der Flankenmitte und wulstigen Rippen sowie Einschnürungen, die vor allem auf der Bauchseite deutlich zu sehen sind und auch der Bauchseite ein leicht knotiges Aussehen verleihen.

Vorkommen: Garschella-Formation (Mittleres-Spätes Albien).

Abb. 16 *Kossmatella ventrocincta*. Garschella-Formation. Bergli, Sennwald. Durchmesser 2.5 cm. Slg. PK 7B.43.11. Foto Antoine Pictet.

Unterordnung **Ammonitina** HYATT 1889
Überfamilie **Perisphinctaceae** STEINMANN 1890
Diese Gruppe ist vor allem im Späten Jura sehr artenreich und in Europa häufig. Die Gehäuse sind meist mehr oder weniger flach, eher weitnabelig und tragen in der Regel zahlreiche feine, mehr oder weniger stark verzweigte Rippen.

Familie **Holcodiscidae** SPATH 1923
Gattung ***Avramidiscus*** VERMEULEN 1996
Avramidiscus seunesi (KILIAN 1888)
Von dieser Art liegt eine halbe Windung vor. Das Gehäuse ist dünn bis dick scheibenförmig (ww/wh = 0.47) und subevolut (uw/dm = 0.37). Der Windungsquerschnitt ist nur wenig breiter als hoch (ww/wh = 1.1) mit breit gerundeter Bauchseite. Vier tiefe und nur leicht geschwungene Einschnürungen finden sich auf einem halben Umgang. Zwischen je zwei Einschnürungen finden sich acht bis elf feine Rippen.
Vorkommen: Altmann-Member (Spätes Hauterivien-Frühes Barrémien).

Abb. 17 *Avramidiscus seunesi*. Altmann-Member. Altmann-Sattel. Durchmesser 3.7 cm. Slg. PK 5A.05.64. Foto Christian Klug.

Gattung ***Astieridiscus*** KILIAN 1910
Astieridiscus morleti KILIAN 1889
Mit 3.0 cm Durchmesser ist das abgebildete Exemplar eher klein. Das Gehäuse ist sehr dünn scheibenförmig (ww/dm = 0.29) und subinvolut (uw/dm = 0.28). Dessen Windungsquerschnitt ist etwas höher als breit mit flachen Flanken (ww/wh = 0.90). Die feinen Rippen spalten sich ein erstes Mal an der Nabelkante und ein zweites Mal auf der Flankenmitte.
Vorkommen: Altmann-Member (Frühes Barrémien, *Nicklesia pulchella* Zone).

Abb. 18 *Astieridiscus morleti*. Altmann-Member. Alp Wis. Durchmesser 3.0 cm. Slg. PK 5A.13.08. Foto Amane Tajika.

Gattung ***Holcodiscus*** UHLIG 1882

Holcodiscus caillaudianus (D'ORBIGNY 1850)

Die vorliegenden Stücke messen zwischen 3.0 und 4.0 cm im Durchmesser. Das Gehäuse ist dünn bis mässig dünn scheibenförmig (ww/dm = 0.47 bis 0.48) und subinvolut (uw/dm = 0.24 bis 0.26). Der Windungsquerschnitt ist ähnlich breit wie hoch mit einer abgeflachten Bauchseite (ww/wh = 0.98 bis 1.16). Die Skulptur besteht aus zahlreichen feinen und wenigen groben Rippen. Alle Rippen sind schwach gebogen. Zwischen zwei groben Rippen stehen drei bis sechs feine Rippen, dabei kommen sowohl Schalt- als auch Spaltrippen vor. Die groben Rippen tragen ventrolaterale Knoten.

Vorkommen: Altmann-Member (Frühes Barrémien, *Kotetishvilia compressissima* Zone).

Abb. 19 *Holcodiscus caillaudianus*. Altmann-Member. Altmann-Sattel. Durchmesser 3.9 cm. Slg. PK 5A.05.85. Foto Amane Tajika. Illustration Christian Klug.

Flanken und glatter, ebenso abgeflachter Bauchseite. Die Skulptur besteht aus sechs bis neun etwas kräftigeren Rippen (Megastriae) pro Umgang. Dazwischen finden sich drei bis sechs mehr oder weniger geschwungene Spalt-, Schalt- und Einfach-Rippen. Kleine Knoten finden sich auf den Megastriae an der Nabelkante und ventrolateral an den Rippenenden.
Vorkommen: Altmann-Member (Frühes Barrémien).

Abb. 20 *Holcodiscus diversecostatus*. Altmann-Member. Vorderalp, Frümsner Alp. Durchmesser 2.4 cm. Slg. PK 5A.16.01. Foto Peter Kürsteiner.

***Holcodiscus* sp.**

Die nicht auf Art-Niveau bestimmbaren Stücke messen zwischen 2.0 und 3.0 cm. Ihre Gehäuse sind dick scheibenförmig (ww/dm = 0.38 bis 0.51) und subinvolut (uw/dm = 0.24 bis 0.27). Deren Windungsquerschnitte unterscheiden sich nur wenig in Höhe und Breite (ww/wh = 0.84 bis 1.10), mit mehr oder weniger abgeflachter Bauchseite. Die mässig groben Rippen spalten gelegentlich an Flankenknoten. Die Bauchseite trägt keine Knoten beim einen Exemplar, während das andere zwei Knotenreihen aufweist (dazwischen sind die Rippen kaum auszumachen).

Vorkommen: Altmann-Member (Frühes Barrémien, *Nicklesia pulchella- Kotetishvilia compressissima* Zone).

Abb. 21 *Holcodiscus* sp. Altmann-Member. Vorderalp, Frümsner Alp. Durchmesser 2.9 cm. Slg. PK 5A.05.42. Foto Amane Tajika.

Gattung ***Parasaynoceras*** BREISTROFFER 1947

Parasaynoceras perezianum toulai TZANKOV 1935

Von dieser Unterart liegt nur ein halber Steinkern. Diese mässig grosse Form hat ein evolutes Gehäuse mit einer Nabelweite uw/dm = 0.37, dessen Windungen einen annähernd kreisförmigen Windungsquerschnitt aufweisen (ww/wh = 0.91) mit einer geringen Windungsüberlappung. Die Nabelwand ist hoch, senkrecht zur Symmetrieebene und die Nabelkante ist gerundet. Die Skulptur besteht aus geraden Rippen, die auf der Nabelkante entspringen und laufen auch gerade über die Bauchseite. Die deutlich kräftigeren Hauptrippen spalten auf der äusseren Flanke an einem Knoten auf, um ventrolateral in einem weiteren Knoten wieder zu einer Rippe zu verschmelzen. Zwischen je zwei Hauptrippen befinden sich drei bis vier gerade Schaltrippen. Manche dieser Sekundärrippen spalten sich auf der Flanke.

Vorkommen: Altmann-Member (Frühes Barrémien, *Nicklesia pulchella- Kotetishvilia compressissima* Zone).

Abb. 22 *Parasaynoceras perezianum toulai*. Altmann-Member. Alp Wis. Durchmesser 5.1 cm. Slg. PK 5A.13.09. Foto Antoine Pictet.

Parasaynoceras tzankovi (AVRAM 1995)
Das abgebildete Stück ist 3.6 cm gross. Sein Gehäuse ist scheibenförmig (ww/dm = 0.48) und subinvolut (uw/dm = 0.26). Dessen Windungsquerschnitt ist breiter als hoch (ww/wh = 1.16) mit leicht abgeflachter Bauchseite. Fünf bis sechs feine und annähernd gerade Rippen werden von dickeren Rippen abgeschnitten. Diese dickeren Rippen tragen kräftige Knoten auf den Flanken und der Bauchseite.
Vorkommen: Altmann-Member (Frühes Barrémien).

Abb. 23 *Parasaynoceras tzankovi*. Altmann-Member. Altmann-Sattel. Durchmesser 3.6 cm. Slg. PK 5A.05.86. Foto Amane Tajika.

Überfamilie **Desmoceratacеae** ZITTEL 1895
Familie **Desmoceratidae** ZITTEL 1895
Unterfamilie **Barremitinae** BRESKOVSKI 1977
Gattung ***Barremites*** KILLIAN 1913
Barremites vocontianus (SAYN in LORY & SAYN 1896)
Das vorliegende Stück ist ein schmales, kalkiges Phragmokon (ww/dm = 0.23) mit einem Durchmesser von 5.8 cm. Dessen Gehäuse ist evolut (uw/dm = 0.25) mit einer steilen, aber nur mässig hohen Nabelwand und einer mehr oder weniger gerundeten Nabelkante. Der subovale Windungsquerschnitt ist höher als breit (ww/wh = 0.51), mit der grössten Breite in der Flankenmitte. Die Bauchseite ist breit gerundet. Das Gehäuse weist acht geschwungene Einschnürungen auf, wobei sie auf dem letzten halben Umgang von Hauptrippen begleitet werden. Zwischen diesen Primärrippen finden sich zahlreiche feine, flexuose Rippen, die auf der Flankenmitte entspringen.
Vorkommen: Drusberg-Member (Frühes-Spätes Barrémien).

Abb. 24 *Barremites vocontianus*. Drusberg-Member. Grenzchopf. Durchmesser 5.8 cm. Slg. KT TW.GC.0002. Foto Antoine Pictet.

Barremites* cf. *difficilis (D'ORBIGNY 1841)

Es liegen mehrere Exemplare aus dem Altmann- und Drusberg-Member vor. Die Gehäuse dieser häufigen Form messen 2 bis über 20 cm im Durchmesser. Das Gehäuse ist dünn scheibenförmig (ww/dm = 0.20) und engnabelig (uw/dm = 0.10 bis 0.25) mit einem hohen Windungsquerschnitt und leicht abgeflachter Bauchseite (ww/wh = 0.20 bis 0.38). Die Rippen sind schwach ausgeprägt (etwa 5 pro halben Umgang), Gut erhaltene Stücke zeigen manchmal Lirae zwischen den Rippen. Die meisten Exemplare messen 5 bis 10 cm im Durchmesser.

Vorkommen: Altmann- und Drusberg-Member (Spätestes Hauterivien-Spätes Barrémien).

Abb. 25 *Barremites* cf. *difficilis*. Altmann-Member. Altmann-Sattel. Durchmesser 20.8 cm. Slg. PK 5A.06.01. Foto Amane Tajika. Illustration Christian Klug.

Gattung ***Plesiospitidiscus*** BREISTROFFER 1947

***Plesiospitidiscus* sp.**

Plesiospitidiscus ist ein typischer Desmoceratide mit ovalem Windungsquerschnitt, einem mässig engen Nabel (uw/dm = 0.23) und schmalen Windungen, wobei sie beim abgebildeten Exemplar bedingt durch Kompaktion des Sedimentes sehr flach erscheinen. Die leicht nach hinten schwingenden Rippen sind ventrolateral leicht verdickt. Auf einem halben Umgang finden sich drei bis vier solche Rippen, dazwischen ist das Gehäuse fast glatt.

Vorkommen: Altmann-Member (Spätestes Hauterivien-Frühes Barrémien).

Abb. 26 *Plesiospitidiscus* sp. Altmann-Member. Altmann-Sattel. Durchmesser 12 cm. Slg. PK 5A.02.21. Foto Antoine Pictet.

Gattung ***Torcapella*** BUSNARDO 1970

Torcapella davydovi (TRAUTSCHOLD 1886)

Das Gehäuse erreicht etwa 15.9 cm im Durchmesser, ist dünn scheibenförmig (ww/dm = 0.30) und mässig involut (uw/dm = 0.22). Der Windungsquerschnitt ist seitlich abgeflacht und oval (ww/wh = 0.72) mit der grössten Windungsbreite auf der Flanke. 36 sichelförmige Rippen können auf einem halben Umgang gezählt werden.

Vorkommen: Altmann-Member (Spätestes Hauterivien-Frühes Barrémien, *Kotetishvilia compressissima* Zone).

Abb. 27 *Torcapella davydovi*. Altmann-Member. Chobel, Frümsner Berg. Durchmesser 15.9 cm. Slg. PK 5A.17.01. Foto Amane Tajika.

Torcapella falcata BUSNARDO 1970

Das Gehäuse erreicht knapp 14 cm im Durchmesser, ist sehr dünn scheibenförmig (ww/dm = 0.28) und mässig involut (uw/dm = 0.15). Der Windungsquerschnitt ist seitlich abgeflacht und dreieckig (ww/wh = 0.57) mit der grössten Windungsbreite auf der Flanke. 36 sichelförmige Rippen können auf einem halben Umgang gezählt werden.

Vorkommen: Altmann-Member (Spätestes Hauterivien-Frühes Barrémien, *Kotetishvilia compressissima* Zone).

Abb. 28 *Torcapella falcata*. Altmann-Member. Altmann-Sattel. Durchmesser 13.9 cm. Slg. PK 5A.05.87. Foto Amane Tajika.

Torcapella* cf. *capillosa BUSNARDO 1970

Die beiden vorliegenden Kalk-Steinkerne messen 17.5 und 21.8 cm im Durchmesser. Deren oxycone Gehäuse sind sehr dünn scheibenförmig (ww/dm = 0.22) mit einem sehr hohen, lanceolaten Windungsquerschnitt (ww/wh = 0.49) und einem sehr engen Nabel (uw/dm = 0.1). Die Nabelwand ist steil mit einer gerundeten Nabelkante. Auf dem Phragmokon finden sich schwache flexuose Rippen, während die Wohnkammer der ausgewachsenen Tiere eine feine, dichte Berippung aufweist.

Vorkommen: Drusberg-Member (Frühes-Spätes Barrèmien, *Kotetishvilia compressissima-Coronites darsi* Zone).

Abb. 29 *Torcapella* cf. *capillosa*. Drusberg-Member. Grenzchopf. Durchmesser 20 cm. Slg. PK 5B.05.16. Foto Antoine Pictet.

Torcapella* cf. *fabrei (TORCAPEL 1884)

Das Gehäuse erreicht etwa 12 cm im Durchmesser, ist sehr dünn scheibenförmig (ww/dm = 0.29) und mässig involut (uw/dm = 0.33). Der Windungsquerschnitt ist seitlich abgeflacht und oval (ww/wh = 0.64) mit der grössten Windungsbreite auf der Flanke. Die geraden bis sichelförmigen Rippen sind schwach ausgeprägt und spalten nicht auf.

Vorkommen: Altmann-Member (Spätestes Hauterivien-Frühes Barrémien, *Nicklesia pulchella-Coronites darsi* Zone).

Abb. 30 *Torcapella* cf. *fabrei*. Altmann-Member. Altmann-Sattel. Durchmesser 12.0 cm. Slg. PK 5A.05.30. Foto Amane Tajika.

Torcapella* cf. *suessiformis BUSNARDO 1970

Das abgebildete Exemplar ist mittelgross (19.4 cm) und besteht überwiegend aus dem Phragmokon und höchstens einem kleinen Wohnkammer-Rest. Die Windungen sind sehr schmal (ww/dm = 0.23) und haben einen lanzeolaten Querschnitt (ww/wh = 0.45) mit gerundeter Bauchseite. Der Nabel ist sehr eng (uw/dm = 0.14) mit einer steilen Nabelwand und gerundeter bis eckiger Nabelkante. Auf dem Phragmokon finden sich schwache flexuose Rippen, während die Wohnkammer dicht stehende, feine flexuose Rippen trägt, die sich aufspalten.

Vorkommen: Drusberg-Member (Frühes-Spätes Barrémien).

Abb. 31 *Torcapella* cf. *suessiformis*. Drusberg-Member. Grenzchopf. Durchmesser 19.4 cm. Slg. PK 5B.05.02. Foto Antoine Pictet.

Torcapella* sp. aff. *suessi (SIMIONESCU 1898)
Beim abgebildeten Stück handelt es sich um einen mittelgrossen Steinkern mit einem Durchmesser von 18 cm. Das Gehäuse ist sehr involut mit gewölbten Flanken und gerundeter Bauchseite. Es trägt dich stehende feine, flexuose Rippen.
Vorkommen: Drusberg-Member (Frühes Barrémien, *Nicklesia pulchella* - *Coronites darsi* Zone).

Abb. 32 *Torcapella* sp. aff. *suessi*. Drusberg-Member. Grenzchopf. Durchmesser 18 cm. Slg. PK 5B.05.17. Foto Antoine Pictet

***Torcapella* sp.**

Das Gehäuse erreicht über 15 cm im Durchmesser, ist sehr dünn scheibenförmig (ww/dm = 0.26) und mässig involut (uw/dm = 0.21). Der Windungsquerschnitt ist seitlich stark abgeflacht und oval (ww/wh = 0.58) mit der grössten Windungsbreite auf der Flanke. Die Rippen sind sehr schwach ausgeprägt.

Vorkommen: Altmann-Member (Spätestes Hauterivien-Frühes Barrémien, *Kotetishvilia compressissima* Zone). Drusberg-Member (Frühes Barrémien, *Kotetishvilia compressissima-Coronites darsi* Zone).

Abb. 33 *Torcapella* sp. Altmann-Member. Altmann-Sattel. Durchmesser 15.3 cm. Slg. PK 5A.05.29. Foto Amane Tajika.

Familie **Desmoceratidae** ZITTEL 1895
Unterfamilie **Puzosiinae** SPATH 1922
Gattung ***Puzosia* (*Puzosia*)** BAYLE 1878
Puzosia (Puzosia) lata SEITZ 1931
Das vorliegende Material hat Durchmesser zwischen 1.9 und 7.2 cm. Deren Gehäuse sind subevolut (uw/dm = 0.33 bis 0.36) und dünn scheibenförmig (ww/dm = 0.36 bis 0.47). Die Windungen sind breiter als hoch (ww/wh = 1.08 bis 1.13), mit der gössten Breite in der Flankenmitte. Vier bis fünf leicht gebogene Einschnürungen zieren den jeweils letzten Umgang.
Vorkommen: Kamm-Bank (Spätestes Albien-Frühes Cénomanien).

Abb. 34 *Puzosia (Puzosia) lata*. Kamm-Bank. Hinterwinden-Hornwald (Hinter Gräppelen). Durchmesser 7.2 cm. Slg. PK 7C.15.13. Foto Amane Tajika. Illustration Beat Scheffold.

Puzosia (Puzosia) mayoriana (D'ORBIGNY 1841)

Das vorliegende Material misst 4.8 cm im Durchmesser, möglicherweise handelt es sich um Jugend-Gehäuse. Diese Gehäuse sind subinvolut (um/dm = 0.26 bis 33) und sehr dünn scheibenförmig discoidal (ww/dm = 0.30 bis 0.35). Der Windungsquerschnitt ist deutlich höher als breit (ww/wh = 0.70 bis 0.85). Vier bis fünf Einschnürungen pro Umgang sind charakteristisch.

Vorkommen: Kamm-Bank (Spätestes Albien-Frühes Cénomanien).

Abb. 35 *Puzosia (Puzosia) mayoriana*. Kamm-Bank. Tal-Wänneli (NE Neuenalpspitz). Durchmesser 8.5 cm. Slg. PK 7C.07.04. Foto Amane Tajika.

Puzosia (Puzosia)* cf. *provincialis (PARONA & BONARELLI 1897)

Das Material dieser Art misst 8.9 cm im Durchmesser. Bei diesen kleinen Stücken ist das Gehäsue subinvolut (uw/dm = 0.26 bis 0.36) und dünn scheibenförmig (ww/dm = 0.36 bis 0.44). Die Windungshöhe entspricht etwa der Windungsbreite (ww/wh = 0.94 bis 1.00). Fünf bis sechs annähernd gerade bis leicht geschwungene Einschnürungen sind auf dem letzten Umgang sichtbar.

Vorkommen: Garschella-Formation (Mittleres-Spätes Albien).

Abb. 36 *Puzosia (Puzosia)* cf. *provincialis*. Garschella-Formation. Stofel, Lenziwis. Durchmesser 8.9 cm. Slg. PK 7B.26.01. Foto Amane Tajika.

Puzosia (Puzosia) quenstedti quenstedti (PARONA & BONARELLI 1897)
Das abgebildete Stück ist 3.1 cm gross. Dessen Gehäuse ist subinvolut (uw/dm = 0.29) und dünn scheibenförmig (ww/dm = 0.35) mit gerundeter Bauchseite. Abgesehen von fünf leicht S-förmig geschwungenen Einschnürungen ist das Gehäuse weitgehend glatt.
Vorkommen: Kamm-Bank (Spätestes Albien-Frühes Cénomanien).

Abb. 37 *Puzosia (Puzosia) quenstedti quenstedti*. Garschella-Formation. In Ränken (oberhalb Plona). Durchmesser 3.1 cm. Slg. PK 7B.23.34. Foto Amane Tajika.

Puzosiinae gen. et sp.

Manche Arten der Puzosien waren riesenwüchsig; der immer noch grösste Ammonit der Welt, *Parapuzosia seppenradense*, hat einen Durchmesser von 1.74 m, wobei die Wohnkammer unvollständig ist.

Das hier abgebildete Exemplar erreicht mit 17.4 cm nur ein Zehntel der grössten Puzosiiden. Das Gehäuse ist subinvolut (uw/dm = 0.33) und mässig dick scheibenförmig (ww/dm = 0.43). Höhe und Breite der letzten erhaltenen Windung entsprechen einander (ww/wh = 0.95). Es sind keine Rippen erhalten, was an der mässigen Erhaltung liegen mag.
Vorkommen: Altmann-Member (Spätestes Hauterivien-Frühes Barrémien).

Abb. 38 Puzosiinae gen. et sp. Altmann-Member. Säntis. Durchmesser 17.4 cm. ETHZ 10437. Foto Amane Tajika.

Unterfamilie **Beudanticeratinae** BREISTROFFER 1953
Gattung ***Beudanticeras* (*Beudanticeras*)** HITZEL 1902
Beudanticeras* cf. *beudanti (BRONGNIART 1822)
Diese Art misst im Alpstein meist deutlich unter 10 cm. Die Gehäuse sind sehr dünn scheibenförmig (ww/dm = 0.27 bis 0.30) und involut (uw/dm = 0.13 bis 0.16). Der Windungsquerschnitt ist oval und seitlich abgeflacht (ww/wh = ca. 0.55), mit abgeflachter oder breit gerundeter Bauchseite und einer steilen Nabelwand. Acht schwache Rippen finden sich auf einem Umgang. Sie sind auf den äusseren Flanken etwas stärker ausgeprägt als auf den inneren Flanken. Auf den Innenwindungen ist die Berippung schwächer.
Vorkommen: Garschella-Formation (Spätes Albien).

Abb. 39 *Beudanticeras* cf. *beudanti*. Garschella-Formation. Schlatt (oberhalb Rüthi). Durchmesser 7.5 cm Slg. PK 7B.20.14. Foto Amane Tajika.

Abb. 40 *Beudanticeras* cf. *beudanti*. Garschella-Formation. Schlatt (oberhalb Rüthi). Durchmesser 6.6 cm. Slg. PK 7B.20.41. Foto Amane Tajika.

Unterfamilie **Desmoceratinae** ZITTEL 1895
Die Desmoceraten haben meistens mehr oder weniger glatte Gehäuse, oft mit Einschnürungen, mässig engem Nabel und breiten gerundeten Windungen.

Gattung ***Desmoceras (Desmoceras)*** ZITTEL 1885
Desmoceras (Desmoceras) latidorsatum (MICHELIN 1838)
Die vorliegenden Exemplare messen weniger als 5 cm. Deren Gehäuse sind dick scheibenförmig (ww/dm = 0.50 bis 60) und involut (uw/dm = 0.13 bis 24). Der Windungsquerschnitt ist breit und dorsoventral abgeflacht bis rechteckig (ww/wh = 0.88 bis 1.34; nimmt im Alter ab) mit breit gerundeten Flanken und Bauchseite. Normalerweise trägt diese Art eine bis sechs gerade bis leicht gebogene Einschnürungen pro Umgang.
Vorkommen: Garschella-Formation (Frühes Aptien-Frühes Cénomanien).

Abb. 41 *Desmoceras (Desmoceras) latidorsatum*. Garschella-Formation. Wildhuser Schafboden. Durchmesser 4.2 cm. Slg. PK 7B.32.04. Foto Amane Tajika.

Überfamilie **Pulchelliaceae** DOUVILLÈ 1890
Familie **Pulchellidae** DOUVILLÈ 1890
Wie der Name schon sagt, sind die Gattungen und Arten dieser Gruppe durchaus hübsch. Die meist seitlich abgeflachten Gehäuse sind engnabelig und tragen oft flache Rippen, die vor allem bauchseitig kräftig ausgebildet sein können. Dies gibt diesen oft kleinen Formen ein leicht Blüten-artiges Aussehen.

Gattung ***Gerhardtia*** Hyatt 1903
***Gerhardtia provincialis* (D'ORBIGNY 1850)**
Wie die anderen Vertreter der Pulchelliidae weist auch diese Art ein eher kleines Gehäuse (das vorliegende Stück misst weniger als 4 cm) mit breiten Rippen auf. Das abgebildete Stück ist ein fragmentarisches, limonitisiertes Phragmokon. Dessen Gehäuse ist mässig evolut (uw/dm = 0.22) mit einem Windungsquerschnitt, der höher als breit ist (ww/wh = 0.23; ww/dm = 0.09), wohl teilweise bedingt durch die Kompaktion. Die kräftigen, gebogenen Rippen entspringen an der Nabelkante und biegen nach vorne. Im äusseren Flankendrittel spalten sich manche der Rippen auf. Ventrolateral werden die Rippen breit und kräftig, so dass die Bauchseite eine Furche bildet.
Vorkommen: Drusberg-Member (Spätestes Frühes-Mittleres Spätes Barrémien, *Gerhardtia sartousiana* Zone).

Abb. 42 *Gerhardtia provincialis*. Drusberg-Member. Höris, Frümsner Alp. Durchmesser 3.8 cm. Slg. PK 5B.22.01. Foto Antoine Pictet.

Gattung ***Kotetishvilia*** VERMEULEN 1997

Kotetishvilia compressissima (D'ORBIGNY 1841)

Vertreter der Pulchellidae messen meist weniger als 5 cm im Durchmesser. Das Gehäuse von *K. compressissima* ist involut (uw/dm = 0.04) und flach scheibenförmig. Die Bauchseite ist etwas abgeflacht und die Flanken leicht gewölbt. Der letzte Umgang trägt etwa 14 wulstige Rippen, die aus etwa sieben Primärrippen in der Nähe der Flankenmitte entspringen und auf der Bauchseite am stärksten ausgeprägt sind. Die innere Flankenhälfte ist fast glatt.

Vorkommen: Altmann-Member (Spätestes Hauterivien-Frühes Barrémien, *Kotetishvilia compressissima* Zone).

Abb. 43 *Kotetishvilia compressissima*. Altmann-Member. Altmann-Sattel. Durchmesser 3.9 cm. Slg. PK 5A.05.26. Foto Amane Tajika. Illustration Christian Klug.

Gattung ***Nicklesia*** HYATT 1903

Nicklesia pulchella (D'ORBIGNY 1841)

Sehr ähnlich *Kotetishvilia*. Wie jene Gattung ist das Gehäuse auch meist weniger als 5 cm gross, dünn scheibenförmig (ww/dm = 0.39) und involut (uw/dm = 0.10). Der Windungsquerschnitt ist oval und deutlich höher als breit (ww/wh = 0.71) und hat eine gerundete Bauchseite. Die Rippen sind kräftiger als bei *Kotetishvilia*, sie spalten ebenfalls auf der Flankenmitte auf. Etwa 13 Rippen können auf dem letzten halben Umgang gezählt warden. Auf dem inneren Flankendrittel sind die Rippen abgeschwächt.

Vorkommen: Altmann-Member (Spätestes Hauterivien-Frühes Barrémien, *Nicklesia pulchella* Zone).

Abb. 44 *Nicklesia pulchella*. Altmann-Member. Altmann-Sattel. Durchmesser 3.0 cm. Slg. KT AS-W-0026. Foto Amane Tajika.

Überfamilie **Hoplitaceae** DOUVILLÉ 1890
Familie **Hoplitidae** DOUVILLÉ 1890
Diese Familie umfasst viele, stark skulpturierte Formen mit oft kräftigen Knoten. Der Name bezieht sich auf die stark bewaffneten griechischen Krieger der Antike.

Unterfamilie **Hoplitinae** DOUVILLÉ 1890
Gattung ***Callihoplites*** SPATH 1925
Callihoplites tetragonus (SEELEY 1865)
Das abgebildete Exemplar misst 4.8 cm im Durchmesser. Dessen mässig dick scheibenfömiges Gehäuse (ww/dm = 0.50) ist subinvolut (uw/dm = 0.29). Der Windungsquerschnitt ist annähernd trapezoidal mit flach gerundetem Venter. Er ist etwas breiter als hoch (ww/wh = 1.14). Die grösste Breite liegt in der Nähe der Nabelkante. Die kräftigen Nabelknoten sind Ursprung von einem oder zwei Paaren gebogener Rippen, die in ventrolateralen Knoten enden. Der letzte Umgang trägt zehn Nabelknoten und 16 ventrolaterale Knoten.
Vorkommen: Kamm-Bank (Spätestes Albien, *Mortoniceras fallax* Zone).

Abb. 45 *Callihoplites tetragonus*. Kamm-Bank. Säntis. Durchmesser 4.8 cm. Slg. UO 17. Illustration Beat Scheffold.

Gattung ***Dimorphoplites*** SPATH 1925

***Dimorphoplites* sp.**

Bisher liegt ein deformiertes Windungsfragment vor. Zu sehen sind der annähernd rechteckige bis trapezoidale Windungsquerschnitt und der mässig weite Nabel. Charakteristisch ist die Kombination aus einem für die Hoplitidae typischen Kiel und ventrolateralen Knoten. Viele der Rippen auf den Flanken spalten an einem Knoten auf der Nabelkante; manche der Rippen verschmelzen dann wieder in einem der ventrolateralen Knoten. Es kommen auch Schaltrippen vor.

Vorkommen: Garschella-Formation (Frühes Albien).

Abb. 46 *Dimorphoplites* sp. Garschella-Formation. Bergli, Sennwald. Durchmesser 7 cm. Slg. PK 7B.43.10. Foto Antoine Pictet.

Gattung ***Discohoplites*** SPATH 1925

***Discohoplites* sp.**

Es liegt nur ein kleines, schlecht erhaltenes Gehäuse dieser Art vor. Diese misst 2.1 cm im Durchmesser und ist eher dünn scheibenförmig mit flachen Flanken. Nur der ventrale Teil der Rippen ist zu sehen. Dort biegen sie stark nach vorne in Richtung Mündung. Auf einen halben Umgang kommen etwa 20 Rippen.

Vorkommen: Kamm-Bank (Spätestes Albien).

Abb. 47 *Discohoplites* sp. Kamm-Bank. Hinterwinden-Hornwald (Hinter Gräppelen). Durchmesser 2.1 cm. Slg. PK 7C.15.16. Foto Amane Tajika.

Gattung ***Hoplites*** NEUMAYR 1875

Hoplites dentatus (SOWERBY 1821)

Vertreter dieser Gattung zeichnen sich durch eine meist recht kräftige Skulptur aus. Diese setzte sich zusammen aus scharfen Spaltrippen, die in einem Spaltknoten an der Nabelkante oder der inneren Flankenhälfte bifurkieren. Weiterhin sind oft ventrolaterale Knoten an den Rippenenden ausgebildet. Kennzeichnend ist die deutliche Furche auf der Bauchseite. Die Umgänge sind mässig breit bis breit und der Nabel kann eng oder mässig weit sein.

Vorkommen: Garschella-Formation (Frühes Albien).

Abb. 48 *Hoplites dentatus*. Garschella-Formation. Bergli, Sennwald. Durchmesser 8 cm. Slg. PK 7B.44.78. Foto Antoine Pictet.

Gattung ***Hyphoplites*** SPATH 1922

Hyphoplites curvatus curvatus (MANTELL 1822)

Zwar ist das abgebildete Exemplar nur ein Fragment, dafür zeigt es deutlich alle wichtigen Aspekte der Gehäuseform und Skulptur. Es misst 4.1 cm im Durchmesser. Die Windungshöhe entspricht in etwa der Breite (ww/uw = 0.97). Die Flanken sind abgeflacht und auf der Mitte der Bauchseite liegt eine deutliche Furche. An den Nabelknoten entspringen drei bis vier stark geschwungene Rippen. Die Rippen bilden eine Bucht auf der inneren Flankenhälfte, in der Mitte tragen sie einen dreieckigen Vorsprung und auf der äusseren Flankenhälfte folgt eine zweite gerundete Ausbuchtung. Die Rippen enden in zwei Knoten-Reihen, wobei die Knoten oft versetzt stehen.

Vorkommen: Kamm-Bank (Frühes Cénomanien).

Abb. 49 *Hyphoplites curvatus curvatus*. Kamm-Bank. Blauschnee-Girenspitz. Durchmesser 4.1 cm. Slg. TB STWG-CE34. Foto Amane Tajika.

Familie **Schloenbachiidae** PARONA & BONARELLI 1897
Gattung ***Schloenbachia*** NEUMAYR 1875
Schloenbachia varians (SOWERBY 1817)
Diese Art trägt ihren Namen zu Recht, denn sie ist sehr variabel. Sie umfasst sowohl sehr breite Formen mit kräftigen Knoten als auch schlanke Formen, die nur noch schwach skulpturiert sind. Das nur mässig gut erhaltene, hier abgebildete Exemplar misst 8.1 cm im Durchmesser. Das mässig dünn bis mässig dick scheibenförmige Gehäuse ist subinvolut (uw/dm = 0.27). Dessen Windungsquerschnitt ist seitlich leicht abgeflacht mit flachen Flanken und einem deutlichen Kiel auf der Bauchseite. Dort finden sich kräftige Rippen mit Knoten am Nabel, in der Mitte der Flanke und ventrolateral. An den Nabelknoten etspringen ein bis zwei Rippen. Pro halben Umgang sind zwölf Rippen zu sehen.
Vorkommen: Kamm-Bank (Frühes Cénomanien).

Abb. 50 *Schloenbachia varians*. Kamm-Bank. Säntis. Durchmesser 8.1 cm. Slg. UO 18. Foto Amane Tajika.

Überfamilie **Acanthocerataceae** GROSSOUVRE 1894
Familie **Brancoceratidae** SPATH 1934
Unterfamilie **Brancoceratinae** SPATH 1934
Gattung ***Hysteroceras*** HYATT 1900
Diese Gattung umfasst zahlreiche kräftig skulptierte und eher kleine Arten. Wie bei vielen anderen Ammonoideen-Gruppen ist die innerartliche Variabilität bisher nur wenig untersucht und es kann gut sein, dass die Vielzahl der Arten künstlich ist.

Hysteroceras binum (SOWERBY 1815)
Das vorliegende Exemplar misst 2.7 cm. Dessen Gehäuse ist sehr dünn scheibenförmig (ww/dm = 0.29) und involut (uw/dm = 0.32). Der Windungsquerschnitt ist höher als breit (ww/wh = 0.74) und trägt einen deutlichen Kiel. Auf dem letzten halben Umgang finden sich ventrolateral und an der Nabelkante 15 Knoten. Die von dort ausgehenden Rippen schwächen sich auf der Flankenmitte deutlich ab.
Vorkommen: Garschella-Formation (Spätes Albien).

Abb. 51 *Hysteroceras binum*. Garschella-Formation. Schlatt (oberhalb Rüthi). Durchmesser 2.7 cm. Slg. PK 7B.20.36. Foto Amane Tajika.

Hysteroceras crassicostatum (JAYET 1929)
Das vorliegende Stück misst 2.3 cm. Dessen Gehäuse ist dünn scheibenförmig (ww/dm = 0.46) und subevolut (uw/dm = 0.40) mit einem rechteckigen Windungsquerschnitt, der deutlich breiter als hoch ist (ww/wh = 1.32). Etwa 23 gerade Rippen trägt der letzte Umgang, manche sind gespalten.
Vorkommen: Garschella-Formation (Spätes Albien, *Mortoniceras inflatum* Zone).

Abb. 52 *Hysteroceras crassicostatum*. Garschella-Formation. Stofel, Lenziwis. Durchmesser 2.3 cm. Slg. PK 7B.26.16. Foto Amane Tajika.

Hysteroceras orbignyi (SPATH 1922)
Das vorliegende Stück misst 2.2 cm. Dessen Gehäuse ist sehr dünn scheibenförmig (ww/dm = 0.32) und subevolut (uw/dm = 0.40). Der Windungsquerschnitt ist gerundet bis fast quadratisch und etwas höher als breit (ww/wh = 0.90). 16 Rippen finden sich auf dem letzten halben Umgang. Sie sind leicht gebogen und manche spalten sich auf.
Vorkommen: Garschella-Formation (Spätes Albien, *Mortoniceras inflatum- Hysteroceras orbignyi* Subzone).

Abb. 53 *Hysteroceras orbignyi*. Garschella-Formation. Stofel, Lenziwis. Durchmesser 2.2 cm. Slg. PK 7B.26.06. Foto Amane Tajika.

Hysteroceras varicosum (SOWERBY 1824)
Das vorliegende Stück misst 3.1 cm. Dessen Gehäuse ist dünn scheibenförmig (ww/dm = 0.35) und subevolut (uw/dm = 0.40). Windungsbreite und Windungshöhe sind annähernd identisch (ww/wh = 1.02). Der Windungsquerschnitt ist rechteckig. Auf dem Venter findet sich ein stumpfer Kiel. Die venrolateralen Rippen sind kräftig, mehr oder weniger gerade und breit. Der letzte Umgang trägt etwa 15 Rippen, die an den Nabelknoten entspringen. Gelegentlich kommen Schaltrippen vor.
Vorkommen: Garschella-Formation (Spätes Albien, *Hysteroceras varicosum* Subzone).

Abb. 54 *Hysteroceras varicosum*. Garschella-Formation. In Ränken (oberhalb Plona). Durchmesser 3.1 cm. Slg. PK 7B.23.21. Foto Amane Tajika.

Unterfamilie **Mojsisovicziinae** HYATT 1903
Gattung ***Dipoloceras*** HYATT 1900
Dipoloceras* cf. *pseudaon SPATH 1931
Das vorliegende, stark angewitterte Exemplar misst 7.9 cm im Durchmesser. Dessen Windungsquerschnitt ist annähernd rechtecking und seitlich abgeflacht (ww/wh = 0.78) mit einem eingetieften Kiel auf der Bauchseite. Leicht S-förmig gebogene, eher schmale Rippen zieren die Flanken. Sie spalten auf der inneren Flankenhälfte auf. Annähernd 30 Rippen finden sich auf der erhaltenen halben Windung.
Vorkommen: Garschella-Formation (Spätes Albien).

Abb. 55 *Dipoloceras* cf. *pseudaon*. Garschella-Formation. Schlatt (oberhalb Rüthi). Durchmesser 7.9 cm. Slg. PK 7B.20.23. Foto Amane Tajika.

Unterfamilie **Mortoniceratinae** DOUVILLÉ 1912
Diese Gruppe zeichnet sich durch oft schön skulptierte Formen auf. Manche tragen im Alter einen riesigen bauchseitigen Fortsatz.

Gattung ***Cantabrigites*** SPATH 1933
***Cantabrigites* sp.**
Zwei Stücke konnten zwar der Gattung aber keiner Art zugeordnet werden. Sie messen 2.1 cm bzw. 3.0 cm. Diese geringe Grösse ist charakteristisch für die Gattung. Das Gehäuse ist sehr dünn scheibenförmig (ww/dm = 0.32 bzw. 0.34) und subevolut (uw/dm = 0.32 bis 0.42). Der Windungsquerschnitt ist rechteckig und etwas höher als breit (ww/wh = 0.91 bis 0.93). Auf der Bauchseite findet sich ein mehr oder weniger kräftiger Kiel. Der letzte Umgang trägt etwa 30 Rippen. Die groben Rippen entspringen an Nabelknoten. Zwischen den Primärrippen finden sich oft Schaltrippen. Die grosse Ähnlichkeit zu Mortoniceras deutet darauf hin, dass es sich bei den Arten der beiden Gattungen um dimorphe Paare handeln könnte.
Vorkommen: Garschella-Formation (Albien).

Abb. 56 *Cantabrigites* sp. Kamm-Bank. Hinterwinden-Hornwald (Hinter Gräppelen). Durchmesser 2.1 cm. Slg. PK 7C.15.31. Foto Amane Tajika.

Abb. 57 *Cantabrigites* sp. Kamm-Bank. Hinterwinden-Hornwald (Hinter Gräppelen). Durchmesser 3.0 cm. Slg. PK 7C.15.21. Foto Amane Tajika.

Gattung ***Mortoniceras (Mortoniceras)*** MEEK 1876
Mortoniceras perinflatum (SPATH 1922)
Das vorliegende Material misst 5.9 cm; ausgewachsene Exemplare erreichen jedoch Durchmesser über 15 cm. Das Gehäuse ist pachykon (ww/dm = 0.61) mit niedrigen und breiten Windungen mit breit rechteckigem Querschnitt (ww/wh = 1.35). Die Rippen stehen recht dicht mit einem Winkel von etwa 18° zwischen zwei Rippen. Jede Rippe trägt vier Knoten pro Seite.
Vorkommen: Garschella-Formation (Spätes Albien, *Mortoniceras perinflatum* Zone).

Abb. 58 *Mortoniceras perinflatum*. Garschella-Formation. Hinterwinden. Durchmesser 5.9 cm. Slg. KT HW-A-0030. Foto Amane Tajika.

Mortoniceras rostratum (SOWERBY 1817)

Das uns zur Verfügung stehende, recht verwitterte Exemplar hat einen Durchmesser von 5.1 cm. Dessen Gehäuse ist subevolut (uw/dm = 0.36). Der rechteckige Windungsquerschnitt ist höher als breit (ww/wh = 0.67). 18 Rippen kommen auf der letzten erhaltenen Mündung vor, welche jeweils fünf Knoten auf einer Seite tragen.

Vorkommen: Garschella-Formation (Spätes Albien, *Mortoniceras rostratum* Zone).

Abb. 59 *Mortoniceras rostratum*. Garschella-Formation. Schlatt (oberhalb Rüthi). Durchmesser 5.1 cm. Slg. PK 7B.20.57. Foto Amane Tajika. Illustration Beat Scheffold.

Mortoniceras* cf. *inflatum (SOWERBY 1818)

Die Gehäuse dieser Arten erreichen über 20 cm im Durchmesser, das vorliegende Stück ist jedoch unvollständig und daher nur 19.3 cm gross. Das Gehäuse ist sehr dünn scheibenförmig (ww/dm = 0.34) und subevolut (uw/dm = 0.36). Der Windungsquerschnitt ist leicht seitlich abgeflacht (ww/wh=0.92) mit flachen Flanken. Die Primärrippen entspringen an Knoten auf der Nabelkante. Dazwischen finden sich Schaltrippen. Auf dem Phragmokon stehen die Rippen etwas enger als auf der Wohnkammer. Drei Knotenreihen finden sich, welche auf dem Phragmokon starker ausgeprägt sind als auf der Wohnkammer.

Vorkommen: Garschella-Formation (Spätes Albien, *Mortoniceras inflatum* Zone).

Abb. 60 *Mortoniceras* cf. *inflatum*. Garschella-Formation. Schlatt (oberhalb Rüthi). Durchmesser 19.3 cm. Slg. KT Rü-S-0021. Foto Amane Tajika.

***Mortoniceras* sp.**

Das vorliegende Material ist fragmentarisch und daher nicht eindeutig einer Art zuzuordnen. Es ähnelt jedoch *M. pricei* SPATH 1930. Unser Exemplar misst 11.3 cm. Dessen Windungsquerschnitt ist ähnlich hoch wie breit, vielleicht etwas breiter. Jede Rippe trägt zwei Knoten pro Seite.
Vorkommen: Garschella-Formation (Spätes Albien).

Abb. 61 *Mortoniceras* sp. Garschella-Formation. Schlatt (oberhalb Rüthi). Durchmesser 11.3 cm. Slg. PK 7B.20.20. Foto Amane Tajika.

Familie ***Leymeriellidae*** BREISTROFFER 1951
Gattung ***Leymeriella*** JACOB 1907
Leymeriella regularis D'ORBIGNY 1841
Auch diese Art liegt vom Alpstein bisher nur fragmentarisch vor. Ähnlich den Hopliten sind hier kräftige Rippen mit einer tiefen Furche auf der Bauchseite kombiniert. Die Rippen sind jedoch meist einfach und Spaltknoten fehlen entsprechend. Die ventrolateralen Knoten können kräftig ausgeprägt sein. Der Nabel ist mässig eng bis mässig weit, das Gehäuse platycon bis fast pachycon.
Vorkommen: Garschella Formation (Frühes Albien).

Abb. 62 *Leymeriella regularis*. Garschella-Formation. Bergli, Sennwald. Länge des Fragmentes 2.2 cm. Slg. 7B.42.69. Foto Antoine Pictet.

Familie **Lyelliceratidae** SPATH 1921
Unterfamilie **Stoliczkaiellinae** COOPER 2012
Gattung ***Stoliczkaiella*** COOPER 2012
Untergattung ***Stoliczkaiella*** COOPER 2012
Stoliczkaiella* (*Stoliczkaiella*) *clavigera NEUMAYR 1875
Das hier abgebildete Exemplar misst fast 5 cm im Durchmesser. Dessen Gehäuse ist dünn scheibenförmig (ww/dm = 0.40) und subinvolut (uw/dm = 0.23) mit einem leicht seitlich abgeflachten Windungsquerschnitt und breit gerundeter Bauchseite (ww/wh = 0.90). Der letzte Umgang trägt 32. Die geraden Rippen sind feiner und engstehender auf den inneren Umgängen. Sie entspringen an schmalen Knoten auf der Nabelkante. Zwischen den Primärrippen finden sich Schalt- und Spaltrippen.
Vorkommen: Kamm-Bank (Spätestes Albien-Frühes Cénomanien, *Mortoniceras rostratum-Arrhaphoceras briacensis* Zone).

Abb. 63 *Stoliczkaiella* (*Stoliczkaiella*) *clavigera*. Kamm-Bank. Ebenalp. Durchmesser 4.9 cm. Slg. PK 7C.12.04. Foto Amane Tajika.

Stoliczkaiella* (*Stoliczkaiella*) *notha (SEELEY 1865)

Das Material aus dem Alpstein misst etwa 2 cm im Durchmesser. Dessen Gehäuse ist dünn scheibenförmig (ww/dm = 0.40) und involut (uw/dm = 0.12). Der Windungsquerschnitt ist seitlich abgeflacht (ww/wh = 0.74) mit flachen Flanken und breit gerundeter Bauchseite. Der letzte Umgang zeigt 32 fast gerade Spaltrippen, welche an kleinen Knoten entspringen. Auch ventrolaterale Knoten sind vorhanden.

Vorkommen: Kamm-Bank (Spätestes Albien, *Mortoniceras rostratum* Zone).

Abb. 64 *Stoliczkaiella* (*Stoliczkaiella*) *notha*. Kamm-Bank. Ebenalp. Durchmesser 2.1 cm. Slg. PK 7C.12.03. Foto Amane Tajika. Illustration Beat Scheffold.

Untergattung ***Lamnayella*** WRIGHT & KENNEDY 1978

Stoliczkaiella (Lamnayella) crotaloides (STOLICZKA 1864)

Das abgebildete Exemplar misst 5.3 cm im Durchmesser. Das Gehäuse ist dünn scheibenförmig (ww/dm = 0.41) und subinvolut (uw/dm = 0.26). Sein Windungsquerschnitt ist ähnlich hoch wie breit (ww/wh = 0.96) mit flachen Flanken und breit gerundeter Bauchseite. Der letzte Umgang weist 17 gerade Rippen auf. Auf der Wohnkammer sind die Rippen weiter auseinander und gerundet, während sie auf dem Phragmokon enger stehen und kantiger sind. Schwach ausgeprägte Knoten finden sich an der Aussenseite der Flanken.

Vorkommen: Kamm-Bank (Spätestes Albien, *Mortoniceras perinflatum* Zone).

Abb. 65 *Stoliczkaiella (Lamnayella) crotaloides*. Kamm-Bank. Ebenalp. Durchmesser 5.3 cm. Slg. PK 7C.12.01. Foto Amane Tajika.

Stoliczkaiella (Lamnayella) juigneti WRIGHT & KENNEDY 1978

Das abgebildete Exemplar misst 6.3 cm. Dessen Gehäuse ist dünn scheibenförmig (ww/dm = 0.39) und subevolut (uw/dm = 0.34). Der Windungsquerschnitt ist etwas höher als breit mit flachen Flanken und gerundeter Bauchseite (ww/wh = 0.92). Der letzte halbe Umgang trägt 15 gerade Rippen. Die Primärrippen tragen kleine Knoten. Zwischen den Primärrippen finden sich feinere und kürzere Schaltrippen, die nicht beknotet sind.

Vorkommen: Dach der Kamm-Bank (Frühes Cénomanien, *Mantelliceras mantelli* Zone).

Abb. 66 *Stoliczkaiella (Lamnayella) juigneti*. Kamm-Bank. Hornwald (Hinter Gräppelen). Durchmesser 6.3 cm. Slg. PK 7C.05.04. Foto Amane Tajika.

Familie **Forbesiceratidae** WRIGHT 1952
Gattung ***Forbesiceras*** KOSSMAT 1897
Forbesiceras largilliertianum (D'ORBIGNY 1841)
Das vorliegende verwitterte Fragment misst 9.2 cm im Durchmesser. Dessen Gehäuse ist involut (uw/dm = 0.06) und seitlich abgeflacht. Die Bauchseite ist sehr schmal und abgeflacht. Obwohl die Rippen nur mässig gut erhalten sind lässt sich erkennen, dass sie recht fein sind.
Vorkommen: Kamm-Bank (Frühes Cénomanien).

Abb. 67 *Forbesiceras largilliertianum*. Kamm-Bank. Säntis, Gasthaus-Hang. Durchmesser 9.2 cm. Slg. PK 7C.13.35. Foto Amane Tajika.

Familie **Acanthoceratidae** DE GROSSOUVRE, 1894
Unterfamilie **Mantelliceratinae** HYATT 1903
Gattung ***Mantelliceras*** HYATT 1903
Mantelliceras mantelli (SOWERBY 1814)
Das vorliegende Stück misst 8.0 cm im Durchmesser. Dessen Gehäuse ist dünn scheibenförmig (ww/dm = 0.45) und subinvolut (uw/dm = 0.24). Höhe und Breite der gerundet trapezoidalen Windungen entsprechen einander weitgehend (ww/wh = 0.96). Die Flanken sind leicht gerundet, der Venter leicht abgeflacht. Der letzte Umgang trägt 35 Rippen. Ventrolateral und an der Nabelkante finden sich manchmal Knoten, während solche dazwischen fehlen. An den Nabelkanten-Knoten entspringen je zwei Rippen, wobei auch Schaltrippen vorkommen.
Vorkommen: Garschella-Formation (Frühes Cénomanien, *Mantelliceras mantelli* - *Mantelliceras dixoni* Zone).

Abb. 68 *Mantelliceras mantelli*. Kamm-Bank. Säntis, Gasthaus-Hang. Durchmesser 8.0 cm. Slg. PK 7C.13.31. Foto Amane Tajika.

Mantelliceras saxbii (SHARPE 1857)

Exemplare der Gattung *Mantelliceras* sind im Dach der Kamm-Bank lokal nicht selten. Leider sind dort die Ammoniten oft nicht sehr gut erhalten. Das hier abgebildete Exemplar misst 7.4 cm im Durchmesser. Das Gehäuse ist sehr dünn scheibenförmig (ww/dm = 0.34) und subinvolut (uw/dm = 0.27). Dessen Flanken sind annähernd flach und die grösste Windungsbreite liegt in der Flankenmitte. Die letzte Windungshälfte trägt 20 Rippen, welche deutlich gröber sind als in den Innenwindungen. Sie verlaufen annähernd radial oder sind in Richtung der Mündung leicht konkav. Knoten an der Nabelkante und am äusseren Flankenrand sind recht deutlich ausgebildet, auf der mittleren Flanke fehlen aber Knoten.

Vorkommen: Kamm-Bank (Frühes Cénomanien, *Mantelliceras mantelli* Zone, häufig in der *Mantelliceras saxbii* Subzone).

Abb. 69 *Mantelliceras saxbii*. Kamm-Bank. Säntis, Gasthaus-Hang. Durchmesser 7.4 cm. Slg. PK 7C.13.28. Foto Amane Tajika.

Unterordnung **Ancyloceratina** WIEDMANN 1966
Viele Angehörige dieser Gruppe sind heteromorph, d.h. nicht regelmässig planspiralig aufgerollt. Die namengebende Gattung *Ancyloceras* beispielsweise hat lose aufgerollte Jugendwindungen und der letzte Umgang bildet einen langgezogenen, aufgeblähten Haken.

Überfamilie **Ancyloceratacea**e GILL 1871
Familie **Bochianitidae** SPATH 1922
Unterfamilie **Bochianitinae** SPATH 1922
Bochianitinae indet.
Diese Form hat ein orthocones Gehäuse, ist also gerade. Das vorliegende Fragment ist 7.5 cm lang. Der Gehäusequerschnitt ist elliptisch (wh/ww = 0.84). Das Fragment trägt sechs kräftige, bauchseitig zur Mündung geneigte Einschnürungen.
Vorkommen: Altmann-Member (Frühes Barrémien, *Nicklesia pulchella- Kotetishvilia compressissima* Zone).

Abb. 70 Bochianitinae indet. Altmann-Member. Altmann-Sattel. Länge 7.5 cm. Slg. KT AS-W-0015. Foto Amane Tajika.

Familie **Ancyloceratidae** GILL 1871
Unterfamilie **Crioceratitinae** GILL 1871
Gattung ***Crioceratitites*** D'ORBIGNY 1842
***Crioceratitites* sp.**
Das hier abgebildete Windungsfragment ist auf eine verschönernde Weise präpariert worden, welche verschleiert, welche Skulpturelemente wie ausgebildet waren. Dies verhindert die Bestimmung auf Art-Niveau. Das Stück ist 15.7 cm lang. Die Windung ist eindeutig criocon, die Windungen berührten sich also nicht und eine Windungsüberlappung war entsprechend nicht ausgebildet. Breite und Höhe der ovalen Windung sind annähernd gleich (ww/wh = 0.95). Die schmalen und eng stehenden Rippen tragen, soweit erkennbar, gelegentlich Knoten, welche möglicherweise ursprünglich Hohlstacheln trugen. Kräftigere, Stacheln tragende Rippen sind auf dem Fragment offenbar noch nicht ausgebildet.
Vorkommen: Altmann-Member (Spätestes Hauterivien-Frühes Barrémien).

Abb. 71 *Crioceratitites* sp. Altmann-Member. Altmann. Länge 15.7 cm. ETHZ 10438. Foto Amane Tajika.

Gattung ***Emericiceras*** SARKAR 1954
Diese Gattung ist berühmt für ihre bis etwa einen Meter grossen Gehäuse, die zum Teil grosse Stacheln tragen. Im Alpstein sind Fragmente dieser Gattung mässig häufig, komplette Exemplare jedoch sehr selten.

Emericiceras koechlini (ASTIER 1851)
Es liegt der Abdruck einer Jugendwindung vor, die zudem infolge Kompaktion leicht deformiert ist. Die Umgänge sind criocon, berühren sich also nicht. Ein leicht ovaler Windungsquerschnitt ist zu erahnen. Charakteristisch sind die groben, bedornten Rippen (Megastriae). Sie verlaufen fast radial, sind nur leicht nach hinten geneigt und schwingen am Nabel sowie der Bauchseite leicht nach vorn. Die Dornen sitzen auf der Nabelkante und der äusseren Flanke. Zwischen den Megastriae findet sich eine wechselnde Anzahl feinerer, gerader Rippen (ca. drei bis fünf Stück).
Vorkommen: Altmann-Member (Spätes Hauterivien-Frühes Barrémien).

Abb. 72 *Emericiceras koechlini*. Altmann-Member. Tierwis-Grenzchopf. Durchmesser 17.5 cm. Slg. PK 5A.02.13. Foto Antoine Pictet.

***Emericiceras* sp.**

Das im Naturmuseum von St. Gallen ausgestellte Exemplare umfasst überwiegend die planspiralen, crioconen (lose aufgewundenen) Jugendwindungen, die Haken-förmige Alterswindung fehlt zur Hälfte. Der erhaltene Abschnitt umfasst leicht deformierte Windungen mit einem Durchmesser von annähernd 30 cm. In frühen Entwicklungsstadien sind die Windungen annähernd kreisförmig im Querschnitt, in mittleren Umgängen werden sie etwas oval, im Alter wieder etwa kreisförmig. Das hier abgebildete, annähernd vollständige Exemplar hatte einen rekonstruierten Enddurchmesser von über 70 cm. Wie bei *Crioceratites* wechseln sich feinere Rippen gelegentlich mit groben Rippen ab, welche in der Jugend Stacheln und im Alter Knoten tragen. Dabei finden sich zwei bis drei Knoten auf jeder Flanke und je ein ventrolateraler Stachel oder kräftigerer Knoten pro Seite.
Vorkommen: Altmann-Member (Spätes Hauterivien-Frühes Barrémien).

Abb. 73 *Emericiceras* sp. Altmann-Member. Hintere Seealp. Dieses im Naturmuseum St. Gallen ausgestellte Exemplar ist annähernd vollständig erhalten und misst etwa 50 cm im Durchmesser. Auf dem Block sind noch Spuren der fehlenden halben Windung zu erahnen. Dahinter ist ein Modell dieses Ammoniten zu sehen (angefertigt von Beat Scheffold). Die Jugendwindungen waren sicher bedornt, wie kräftig die Dornen im Alter ausgeprägt waren, ist bei den Stücken vom Alpstein unklar. NMSG F-13599. Foto Stefan Rohner. Illustration Christian Klug.

Gattung ***Pseudothurmannia*** SPATH 1923

Pseudothurmannia mortilleti (DE LORIOL & PICTET 1868)

Das vorliegende Exemplar hat einen Durchmesser von 29.6 cm. Sein Gehäuse ist subevolut (uw/ww = 0.34). Der seitlich abgeflachte Windungsquerschnitt weist flache Flanken und eine abgeflachte Bauchseite auf. Der letzte halbe Umgang trägt 45 eng stehende und leicht geschwungene Rippen, wovon manche auf der Flankenmitte sich durch Spaltung entwickeln.

Vorkommen: Altmann-Member (Spätestes Hauterivien, Späteste *Balearites balearis*-*Pseudothurmannia ohmi* Zone).

Abb. 74 *Pseudothurmannia mortilleti*. Altmann-Member. Alpstein. Durchmesser 29.6 cm. ETHZ 10436. Foto Amane Tajika.

Pseudothurmannia* sp. aff. *picteti

Bei dem abgebildeten Stück handelt es sich um ein vollständiges ausgewachsenes Exemplar. Dessen Phragmokon ist, abgesehen von einem knappen Viertel-Umgang, verdrückt. Das Fossil ist platycon und hat einen weiten Nabel (uw/dm = 0.36). Der Windungsquerschnitt ist hoch rechteckig mit der grössten Windungsbreite im dorsalen Drittel der sonst fast parallelen Flanken. Die Bauchseite ist breit, abgeflacht und mit gerundeten Kanten. Die Nabelwand ist senkrecht mit gerundeten Nabelkanten. Die Skulptur des letzten Umganges setzt sich zusammen aus kräftigen, leicht S-förmigen Hauptrippen, die an der Nabelkante an einem schwach ausgeprägten Knoten entspringen. Zwischen den Hauptrippen-Paaren liegen je zwei schwächere Schaltrippen, die auf dem dorsalen Flanken-Drittel beginnen.

Vorkommen: Altmann Member (Spätestes Hauterivien-Spätes Frühes Barrémien).

Abb. 75 *Pseudothurmannia* sp. aff. *picteti.* Altmann-Member. Tierwis-Grenzchopf. Durchmesser 21.5 cm. Slg. PK 5A.02.22. Foto Antoine Pictet.

Unterfamilie **Leptoceratoidinae** THIEULOY 1966
Gattung ***Leptoceratoides*** THIEULOY 1966
Leptoceratoides* cf. *heeri (OOSTER 1860)
Ein 4.0 cm langes Windungsfragment eines wohl crioconen Gehäuses liegt aus dem Alpstein vor. Dessen Windungsquerschnitt ist fast kreisförmig (ww/wh = 0.96). 21 einfache, schmale, aber kräftige, radiale Rippen zieren eine Viertelwindung.
Vorkommen: Altmann-Member (Frühes Barrémien).

Abb. 76 *Leptoceratoides* cf. *heeri*. Altmann-Member. Altmann-Sattel. Länge des Fragmentes 4.0 cm. Slg. PK 5A.05.24. Foto Amane Tajika. Illustration Christian Klug.

Gattung ***Hamulinites*** THIEULOY 1966

***Hamulinites* sp.**

Das vorliegende Fragment ist 4.4 cm lang. Das komplette Gehäuse dieser Gattung ist ancylocon (= ancyloceracon), d.h. die Jugendwindungen sind lose aufgerollt und die Alterswindung endet in einem langen Haken. Der Windungsquerschnitt ist leicht elliptisch und etwas höher als breit (ww/wh = 0.89). Das Fragment trägt 16 schmale und mässig kräftige Rippen. Dorsal verschwinden die Rippen, auf der Flankenmitte sind sie am kräftigsten und auf der Bauchseite mittelkräftig.

Vorkommen: Altmann-Member (Frühes Barrémien).

Abb. 77 *Hamulinites* sp. Altmann-Member. Altmann-Sattel. Länge des Fragmentes 4.4 cm. Slg. KT AS-W-0048. Foto Amane Tajika.

Überfamilie **Turrilitaceae** GILL 1871
Familie **Anisoceratidae** HYATT 1900
Gattung ***Anisoceras*** PICTET 1854
Anisoceras armatum (SOWERBY 1817)
Das hier beschriebene Exemplar ist ein gerades Schaft-Fragment mit einer Länge von 5.6 cm. Der Gehäusequerschnitt ist annährend kreisförmig (ww/wh = 0.96) mit einer Höhe von 2.4 cm. Die Rippen sind häufig dorsal und ventral paarweise verbunden und bauchwärts nach hinten gewandt. Zwischen zwei kräftigen, Knoten-tragenden Rippen befinden sich zwei bis drei feinere, stumpfe Rippen ohne Knoten.
Vorkommen: Kamm-Bank (Spätestes Albien-Frühes Cénomanien).

Abb. 78 *Anisoceras armatum*. Kamm-Bank. Neuenalpkamm. Länge des Fragmentes 5.6 cm. Slg. KT NA-K0001. Foto Amane Tajika.

Anisoceras perarmatum PICTET & CAMPICHE 1861

Das abgebildete Schaftfragment ist 7.3 cm lang. Dessen ovaler Querschnitt ist leicht seitlich abgeflacht (ww/wh = 0.85) mit einer Windungshöhe von 2.7 cm. Kräftige Rippenpaare sind in den seitlichen Knoten miteinander verbunden und klingen dorsal aus.

Vorkommen: Kamm-Bank (Spätestes Albien-Frühes Cénomanien).

Abb. 79 *Anisoceras perarmatum*. Kamm-Bank. Tal (NE Neuenalpspitz). Länge des Fragmentes 7.3 cm. Slg. PK 7C.06.03. Foto Amane Tajika.

Anisoceras pseudoelegans PICTET & CAMPICHE 1861

Das vorliegende Schaftfragment ist leicht gekrümmt und 4.1 cm lang. An der breitesten Stelle misst das Fragment 17 mm. Der ovale Windungsquerschnitt ist nur wenig schmaler als hoch (ww/wh = 0.89). Paare kräftiger, Knoten tragender Rippen sind dorsal und ventral miteinander verbunden. Zwischen diesen Rippenpaaren befinden sich je zwei bis drei feinere Rippen, die auch über den Rücken reichen, während die kräftigen Rippen dorsal verschwinden.

Vorkommen: Kamm-Bank (Spätestes Albien).

Abb. 80 *Anisoceras pseudoelegans*. Kamm-Bank. Hinterwinden-Hornwald (Hinter Gräppelen). Länge des Fragmentes 4.1 cm. Slg. PK 7C.15.11. Foto Amane Tajika.

Gattung ***Prohelicoceras*** SPATH 1925

Prohelicoceras moutonianum (D'ORBIGNY 1850)

Das über 5 cm grosse Windungsfragment ist helicospiralig gekrümmt, also Teil einer Raumspirale. Die grösste Windungshöhe beträgt etwa 2 cm. Dessen Windungsquerschnitt ist ziemlich genau kreisförmig (ww/wh = 1.0). Die Skulptur besteht aus schwachen Rippen mit zwei bis drei kräftigen Knotenreihen.

Vorkommen: Garschella-Formation (Spätes Albien).

Abb. 81 *Prohelicoceras moutonianum*. Garschella-Formation. Stofel, Lenziwis. Windungshöhe etwa 2 cm. Slg. PK 7B.26.04. Foto Amane Tajika.

Gattung ***Protanisoceras*** SPATH 1923

Protanisoceras ventrosum CASEY 1960

Das etwa 6 cm grosse Windungsfragment ist mässig stark gekrümmt, stammt also von einer Form mit einem lose aufgerollten planspiralen Gehäuse. Die grösste Windungshöhe beträgt etwa 1.1 cm mit fast kreisförmigem Windungsquerschnitt (ww/wh = 0.9). Die Skulptur besteht aus kräftigen radialen Rippen, die zur Bauchseite hin leicht nach hinten biegen.

Vorkommen: Garschella-Formation (Spätes Albien).

Abb. 82 *Protanisoceras ventrosum*. Garschella-Formation. Bergli, Sennwald. Windungshöhe 1.1 cm. Slg. PK 7B.42.46. Foto Antoine Pictet.

Protanisoceras cantianum SPATH 1939

Auch diese Art hat ein criocones Gehäuse, bei dem die Windungen sich nicht berühren. Die Umgänge sind in der Regel breiter als hoch (ww/wh = 1.2) mit abgeflachtem Rücken und Bauchseite und stark gewölbten Flanken. Die Rippen sind auf den Flanken kräftig ausgebildet und tragen ventrolateral manchmal schwach ausgeprägte Knötchen.

Vorkommen: Garschella-Formation (Spätes Albien).

Familie **Hamitidae** GILL 1871
Gattung ***Hamites*** PARKINSON 1811
Im Alpstein sind Reste der Gehäuse dieser Gattung zwar recht häufig, allerdings hält sich die Anzahl an Bestimmungsmerkmalen in Grenzen. Im Wesentlichen gilt es, auf den Grad der Krümmung und die Berippung zu achten.

Hamites compressus SOWERBY 1814
Es liegt ein recht stark gekrümmtes Windungsfragment vor. Dieses misst 7.2 cm bei einer Windungshöhe von etwa 2.2 cm. Die Flanken sind leicht abgeflacht, während Rücken und Bauchseite wohlgerundet sind. Fünf bis sieben scharfe und fast gerade Rippen finden sich auf einem Gehäuseabschnitt von der Länge der entsprechenden Windungshöhe.
Vorkommen: Kamm-Bank (Spätestes Albien, Frühe *Mortoniceras inflatum* Zone).

Abb. 83 *Hamites compressus*. Kamm-Bank. Säntis, Gasthaus-Hang. Windungshöhe etwa 2.2 cm. Slg. PK 7C.11.01. Foto Amane Tajika.

Hamites duplicatus PICTET & CAMPICHE 1861

Das abgebildete Windungsfragment ist ziemlich gerade (orthocon) und 3.1 cm lang. Dessen ovaler Windungsquerschnitt hat eine Höhe von 0.8 cm (ww/wh = 0.91). Sieben bis zehn feine, scharfe Rippen finden sich auf einem Gehäuseabschnitt von der Länge der entsprechenden Windungshöhe. In Richtung Rücken schwingen die Rippen nach vorne, verschwinden aber fast völlig, während sie ventral nach hinten schwingen und etwas kräftiger werden.

Vorkommen: Kamm-Bank (Spätestes Albien-Frühes Cénomanien).

Abb. 84 *Hamites duplicatus*. Kamm-Bank. Lochtem-Grüenböhl. Länge des Fragmentes 3.1 cm. Slg. PK 7C.19.04. Foto Amane Tajika.

Hamites simplex D'ORBIGNY 1842

Das Gehäuse dieser Art bildet ebenfalls eine sehr lose aufgerollte Spirale. Das vorliegende Windungsfragment ist leicht gebogen und 2.8 cm lang mit einem ovalen Windungsquerschnitt von 0.8 cm Höhe (ww/wh = 0.84). Die zahlreichen, eher feinen Rippen verlaufen radial oder sind bauchseitig leicht in Richtung Mündung geneigt. Dorsal verschwinden die Rippen. Sechs Rippen finden sich auf einem Gehäuseabschnitt von der Länge der entsprechenden Windungshöhe.
Vorkommen: Kamm-Bank (Frühes Cénomanien).

Abb. 85 *Hamites simplex*. Kamm-Bank. Säntis, Gasthaus-Hang. Länge des Fragmentes 2.8 cm. Slg. PK 7C.13.05. Foto Amane Tajika.

Hamites subvirgulatus SPATH 1941

Das abgebildete, 3.5 cm lange Windungsfragment stammt von einem gyroconen Gehäuse mit einer sehr weiten Spirale. Der mehr oder weniger kreisförmige Windungsquerschnitt hat eine Windungshöhe von 0.9 cm (ww/wh = 0.95). Fünf kräftige, leicht geschwungene Rippen finden sich auf einem Gehäuseabschnitt von der Länge der entsprechenden Windungshöhe.

Vorkommen: Kamm-Bank (Spätestes Albien-Frühes Cénomanien).

Abb. 86 *Hamites subvirgulatus*. Kamm-Bank. Stütze 2 Säntisbahn. Länge des Fragmentes 3.5 cm. Slg. PK 7C.02.07. Foto Amane Tajika.

Hamites virgulatus BRONGNIART 1822

Das abgebildete Windungsfragment ist 3.0 cm lang. Der ovale Windungsquerschnitt hat eine Höhe von 1.2 cm (ww/wh = 0.86). Die Rippen sind kräftig und gerade bis leicht zur Mündung gebogen in Richtung Bauchseite. Vier Rippen finden sich auf einem Gehäuseabschnitt von der Länge der entsprechenden Windungshöhe.

Vorkommen: Garschella-Formation (Spätes Albien).

Abb. 87 *Hamites virgulatus*. Garschella-Formation. Stofel, Lenziwis. Länge des Fragmentes 3.0 cm. Slg. PK 7B.26.13. Foto Amane Tajika.

Hamites* cf. *maximus SOWERBY 1814

Das hier abgebildete Fragment ist leicht deformiert. Es stammt aus einem nur wenig gekrümmten Schaftabschnitt und ist 7.0 cm lang. Der seitlich abgeflachte, fast kreisförmige Windungsquerschnitt hat eine Höhe von 0.9 cm (ww/wh = 0.88). Die Rippen sind fein und eher stumpf. Sie verlaufen annähernd gerade. Vier bis sechs dieser feinen Rippen finden sich auf einem Gehäuseabschnitt von der Länge der entsprechenden Windungshöhe.

Vorkommen: Kamm-Bank (Spätestes Albien).

Abb. 88 *Hamites* cf. *maximus*. Kamm-Bank. Hinterwinden-Hornwald (Hinter Gräppelen). Länge des Fragmentes 7.0 cm. Slg. KT HW-A-0013. Foto Amane Tajika.

Hamites* cf. *similis CASEY 1961

Das abgebildete U-förmige Fragment ist 4.1 cm lang. Bei manchen Arten befindet sich ein solcher Haken in der Nähe der Altersmündung. Im Abschnitt mit der stärksten Krümmung ist die Windungshöhe etwas reduziert. Der leicht ovale Windungsquerschnitt hat eine Höhe von 1.0 cm (ww/wh = 0.93). Die Rippen sind schmal, scharf und engstehend. Manche Rippen spalten sich auf der Flankenmitte auf. Dorsal sind sie abgeschwächt, dorsal biegen sie leicht nach hinten, von der Mündung weg. Neun Rippen finden sich auf einem Gehäuseabschnitt von der Länge der entsprechenden Windungshöhe.

Vorkommen: Garschella-Formation (Spätes Albien).

Abb. 89 *Hamites* cf. *similis*. Kamm-Bank. In Ränken (oberhalb Plona). Länge des Fragmentes 4.1 cm. Slg. PK 7B.23.28. Foto Amane Tajika.

***Hamites* sp.**

Das abgebildete Stück ist ein gerades Schaft-Fragment von 2.5 cm Länge. Dessen ovaler Windungsquerschnitt ist 2.5 cm hoch (ww/wh = 0.91). Vier stumpfe, weitständige und fast gerade Rippen finden sich auf einem Gehäuseabschnitt von der Länge der entsprechenden Windungshöhe.
Vorkommen: Kamm-Bank (Spätestes Albien).

Abb. 90 *Hamites* sp. Kamm-Bank. Oberrieter Chienberg. Länge des Fragmentes 2.5 cm. Slg. KT CH-O-0001. Foto Amane Tajika.

Gattung ***Idiohamites*** SPATH 1925

Idiohamites* cf. *dorsetensis SPATH 1929

Das abgebildete, 5.2 cm lange Windungsfragment ist leicht gekrümmt und stammt von einem gyroconen Gehäuse. Dessen Windungsquerschnitt ist seitlich abgeflacht und oval (ww/wh = 0.75). Die Rippen sind weitstehend, breit und werden dorsal deutlich schwächer. Ventrolateral finden sich je Rippe zwei Knoten. Vier Rippen finden sich auf einem Gehäuseabschnitt von der Länge der entsprechenden Windungshöhe.

Vorkommen: Kamm-Bank (Spätestes Albien, *Mortoniceras perinflatum* Zone).

Abb. 91 *Idiohamites* cf. *dorsetensis*. Kamm-Bank. Stütze 2 Säntisbahn. Länge des Fragmentes 5.2 cm. Slg. PK 7C.02.23. Foto Amane Tajika.

Familie **Turrilitidae** GILL 1871
Vertreter dieser Familie zeichnen sich durch ein heteromorphes, Schneckenhaus-artig aufgewundenes Gehäuse aus. Das heisst, es bildet eine Raumspirale mit einem meist recht hohen Gewinde.

Gattung ***Mariella*** NOWAK 1916
Mariella bergeri (BRONGNIART 1822)
Dies ist eine der häufigsten Arten, die in der Kamm-Bank des Alpsteins vorkommen. Wie bei den Hamiten werden fast nie komplette Gehäuse gefunden. Mehr als drei Umgänge findet man selten zusammenhängend. Das abgebildete, 14.7 cm hohe Stück hat vier Umgänge mit einer maximalen Windungshöhe von 3.9 cm. Die Flanken tragen vier schräge Knoten-Reihen. Die dorsal bzw. apikal (Richtung Spitze) gelegenen Knoten sind in dieser Richtung verlängert, während die Knoten der anderen beiden Reihen mehr oder weniger runde Querschnitte haben. Die vierte Reihe, die schon fast an die nächstgrössere Windung stösst, trägt die kleinsten Knoten. Der grösste Abstand zwischen den Knoten-Reihen befindet sich zwischen den langen Knoten und der kleinste Abstand zwischen den runden Knoten. Pro halben Umgang finden sich etwa 14 Knoten auf einer Reihe.
Vorkommen: Kamm-Bank (Spätestes Albien-Frühes Cénomanien).

Abb. 92 *Mariella bergeri*. Kamm-Bank. Säntis. Höhe 14.7 cm. Slg. UO 12. Foto Amane Tajika. Illustration Beat Scheffold.

Mariella gresslyi (PICTET & CAMPICHE 1861)
Das Windungsfragment hat einen Durchmesser von 3.9 cm mit einer maximalen Windungshöhe von 2.3 cm. Auch diese Art zeichnet sich durch vier Knoten-Reihen aus, deren Knoten jeweils auf annähernd radialen schrägen Linien ausgerichtet sind. Zwischen den Reihen sind die Knoten durch doppelte Rippen miteinander verbunden. Die unterste Knotenreihe ist normalerweise von der nächstgrösseren Windung überdeckt. Auf einem Viertelumgang finden sich etwa sieben Knoten pro Reihe.
Vorkommen: Kamm-Bank (Spätestes Albien).

Abb. 93 *Mariella gresslyi*. Kamm-Bank. Chelen-Geren (Plona). Durchmesser 3.9 cm. Slg. PK 7B.37.20. Foto Amane Tajika.

Mariella miliaris (PICTET & CAMPICHE 1861)
Diese Art ähnelt *M. bergeri* stark. Das abgebildete, 9.0 cm grosse Stück ist mit drei, bis zu 2.9 cm hohen Umgängen erhalten. Der Apikalwinkel beträgt 24°. Wie bei *M. bergeri* sind auch hier vier Knoten-Reihen ausgebildet, allerdings sind nur die Knoten einer Reihe gelängt, alle anderen weisen einen annähernd kreisförmigen Querschnitt auf. Die Knoten derjenigen Reihe, die der nächstgrösseren Windung am nächsten liegt, sind kleiner als die der anderen Reihen.
Vorkommen: Kamm-Bank (Frühes Cénomanien, *Mantelliceras mantelli* Zone).

Abb. 94 *Mariella miliaris*. Kamm-Bank. Säntis. Höhe 9.0 cm. Slg. UO 14. Foto Amane Tajika.

Mariella taeniata (PICTET & CAMPICHE 1862)
Diese Art zeichnet sich durch viel breitere Umgänge aus, d.h. die Windungshöhe ist deutlich niedriger im Verhältnis zum Durchmesser des Umgangs. Das abgebildete Stück hat einen Durchmesser von knapp 2 cm mit einer Windungshöhe von maximal 0.9 cm. Bei *Mariella taeniata* finden sich nur drei Knoten-Reihen auf den Flanken, also eine weniger als bei den anderen Arten der Gattung *Mariella*. Von der obersten Knoten-Reihe ziehen sich Rippen bis zum nächsten Umgang. Diese oberste Knoten-Reihe ist von der unteren durch eine flache Furche getrennt. Jede Knoten-Reihe trägt 23 Knoten pro halben Umgang.
Vorkommen: Kamm-Bank (Spätestes Albien).

Abb. 95 *Mariella taeniata*. Kamm-Bank. Tierwis. Durchmesser 2.0 cm. Slg. TB STWG-CE2. Foto Amane Tajika.

Gattung ***Ostlingoceras*** HYATT 1900
Wie bei der Gattung *Mariella* sind auch die Gehäuse der Gattung *Ostlingoceras* turriliticon, d.h. sie bilden eine Raumspirale. Auch hinsichtlich des Apikalwinkels und der Windungszunahme sind sich beide Gattungen sehr ähnlich. Die wesentlichen Unterschiede liegen in der Skulptur, die weniger Knoten-Reihen aufweist.

Ostlingoceras costulatum PERVINQUIÉRE 1910
Das abgebildete Fragment umfasst zwei Umgänge mit einer Gesamthöhe von 4.9 cm und einer maximalen Windungshöhe von 2.4 cm. Der Apikalwinkel beträgt etwa 26°. Auch bei dieser Art ist der Windungsquerschnitt fast rechtwinklig mit flachen Flanken. Die leicht schräg stehenden Rippen sind breiter und stumpfer als bei *O. puzosianum*. Jeder Umgang trägt etwa 26 Ripen, die je zwei (manchmal auch drei) Knoten am unteren Ende tragen. Die untere Knoten-Reihe liegt ebenso auf der Naht zur nächstgrösseren Windung.
Vorkommen: Kamm-Bank (Frühes Cénomanien).

Abb. 96 *Ostlingoceras costulatum*. Höhe 4.9 cm. Kamm-Bank. Tal (NE Neuenalpspitz). Slg. PK 7C.06.02. Foto Amane Tajika.

Ostlingoceras puzosianum (D'ORBIGNY 1842)

Das abgebildete Stück umfasst etwa zwei Windungen, die zusammen etwa 4 cm hoch sind mit einer maximalen Windungshöhe von 1.5 cm. Der Apikalwinkel des Gehäuses beträgt 17°. Im Gegensatz zu anderen Turrilitiden des Alpsteins hat diese Art einen fast rechtwinkligen Windungsquerschnitt mit flachen Flanken. Die Flanken werden beherrscht von schmalen Rippen, die am unteren Ende in zwei Knoten übergehen. Die untere Knoten-Reihe liegt genau auf der Naht zum nächstgrösseren Umgang. Ein Umgang trägt 26 bis 34 Rippen, wobei die Anzahl der Knoten pro Reihe noch etwas höher ist.

Vorkommen: Kamm-Bank (Spätestes Albien, *Mortoniceras rostratum* - *Mortoniceras perinflatum* Zone).

Abb. 97 *Ostlingoceras puzosianum*. Kamm-Bank. Säntis. Windungshöhe 1.5 cm. Slg. UO 15. Foto Amane Tajika.

Gattung ***Hypoturrilites*** DUBOURDIEU 1953

Hypoturrilites gravesianus (D'ORBIGNY 1842)

Das abgebildete Windungsfragment hat eine maximale Windungshöhe von 2.7 cm. Der Windungsquerschnitt ist breit gerundet. Die Flanken tragen drei Knoten-Reihen, wovon die Knoten der obersten Reihe verlängert und kräftig sind; sie bedecken die obere Flankenhälfte. Die Knoten der anderen beiden Reihen sind gerundet konisch. Pro halben Umgang finden sich sieben Knoten in der obersten und 16 Knoten in den unteren Reihen.

Vorkommen: Kamm-Bank (Frühes Cénomanien, *Mantelliceras mantelli* Zone).

Abb. 98 *Hypoturrilites gravesianus*. Kamm-Bank. Hinterwinden-Hornwald (Hinter Gräppelen). Windungshöhe 2.7 cm. Slg. PK 7C.15.19. Foto Amane Tajika.

Hypoturrilites* cf. *collignoni WRIGHT & KENNEDY 1996

Bei dem abgebildeten Exemplar sind zwei Umgänge erhalten, mit einer maximalen Windungshöhe von 1.1 cm. Der Apikalwinkel beträgt etwa 20° bis 25°. Der Windungsquerschnitt ist annähernd rechteckig. Vier Knoten-Reihen zieren die Flanken, wobei der Abstand zwischen den unteren beiden Reihen etwas kleiner ist als zwischen den anderen Reihen. Die Knoten der vier Reihen sind in schrägen Reihen angeordnet. Die Knoten der obersten Reihe sind am grössten und verlängert, die Knoten der anderen Reihen haben einen fast kreisförmigen Querschnitt. Alle Knoten sind, zumindest im Steinkern, oben abgeflacht. Pro halben Umgang finden sich sechs bis acht Knoten in der obersten und zehn Knoten in der untersten Reihe.

Vorkommen: Kamm-Bank (Frühes Cénomanien, *Mantelliceras mantelli* Zone - *Neostlingoceras carcitanense* Subzone).

Abb. 99 *Hypoturrilites* cf. *collignoni*. Kamm-Bank. Tierwis-Stütze 2 Säntisbahn. Windungshöhe 1.1 cm. Slg. PK 7C.01.14. Foto Amane Tajika.

Gattung ***Pseudhypoturrilites*** COOPER 1999

Pseudhypoturrilites* cf. *sharpei (WRIGHT & KENNEDY 1996)

Die Windungen des abgebildeten Exemplares haben eine maximale Windungshöhe von 1.6 cm. Der Windungsquerschnitt ist gerundet rechtwinklig. Vier Knoten-Reihen bedecken die Flanken, wobei je ein Knoten aller Reihen auf schrägen Linien angeordnet ist. Die Knoten sind durch zarte Rippen miteinander verbunden. Die Knoten der ersten beiden Reihen sind kräftiger als die anderen und bedecken die obersten zwei Drittel der Flanke. Pro halben Umgang finden sich 11 Knoten in der obersten und 13 Knoten in den unteren Reihen.

Vorkommen: Kamm-Bank (Frühes Cénomanien, *Mantelliceras mantelli* - *Neostlingoceras carcitanense* Subzone).

Abb. 100 *Pseudhypoturrilites* cf. *sharpei*. Kamm-Bank. Hinterwinden-Hornwald (Hinter Gräppelen). Windungshöhe 1.6 cm. Slg. PK 7C.15.34. Foto Amane Tajika.

Gattung ***Neostlingoceras*** KLINGER & KENNEDY 1978

Neostlingoceras carcitanense (MATHERON 1842)

Bei dem abgebildeten Exemplar sind etwa dreieinhalb Umgänge erhalten, wovon der grösste eine Höhe von 1.4 cm aufweist. Trotz der schlechten Erhaltung lassen sich zwei Knoten-Reihen erkennen. Eine der Reihen befindet sich über der Mitte der Flanke, während die andere Reihe leicht verlängerte Knoten trägt und direkt über der Naht liegt. Pro halben Umgang finden sich sieben Knoten in der oberen und 12 bis 13 Knoten in der unteren Reihe.

Vorkommen: Kamm-Bank (Frühes Cénomanien).

Abb. 101 *Neostlingoceras carcitanense*. Kamm-Bank. Gartenalp. Windungshöhe 1.4 cm. ETHZ 10424. Foto Amane Tajika.

Gattung ***Turrilitoides*** GILL 1871

Turrilitoides intermedius (PICTET & CAMPICHE 1861)

Das vorliegende Stück hat eine maximale Windungshöhe von 1.6 cm. Dessen gerundeter Windungsquerschnitt ist etwas höher als breit. Auf einem halben Umgang finden sich 15 Rippen, die keine Knoten tragen.

Vorkommen: Kamm-Bank (Spätestes Albien).

Abb. 102 *Turrilitoides intermedius*. Kamm-Bank. Säntis, Gasthaus-Hang. Windungshöhe 1.6 cm. Slg. KT SG-AG-0002. Foto Amane Tajika.

Familie **Baculitidae** MEEK 1876
Gattung ***Lechites*** NOWAK 1908
Lechites gaudini (PICTET & CAMPICHE 1861)
Die Gattung zeichnet sich durch gerade Gehäuse aus. Das abgebildete Fragment ist 3.8 cm lang und besitzt einen ovalen Querschnitt, der etwas schmaler als hoch ist (ww/wh = 0.87 bis 0.93). Die Skulptur besteht bauchseitig aus zur Mündung geneigten Rippen, die auf der Bauchseite und auf dem Rücken auslaufen. Auf dem Fragment finden sich zwei bis fünf Rippen auf einem Schaftstück von der Länge der entsprechenden Windungshöhe.
Vorkommen: Garschella-Formation (Spätes Albien, *Mortoniceras pricei* Zone).

Abb. 103 *Lechites gaudini*. Kamm-Bank. Stütze 2 Säntisbahn. Länge des Fragmentes 5.0 cm. Slg. PK 7C.02.09. Foto Amane Tajika.

Gattung ***Sciponoceras*** HYATT 1894

Sciponoceras baculoides (MANTELL 1822)

Auch diese Art zeichnet sich durch ein weitgehend orthocones (gerade gestrecktes) Gehäuse aus. Das abgebildete Fragment ist 2.7 cm lang. Dessen Windungsquerschnitt ist leicht seitlich abgeflacht (ww/wh = 0.94). Die schrägen Rippen sind nur schwach entwickelt und verschwinden auf dem Rücken und der Bauchseite ganz. Das Fragment trägt eine kräftige, geschwungene Einschnürung mit einer dorsalen Einbuchtung. Wahrscheinlich befand sich an einer der Bruchstellen eine weitere Einschnürung. Zwischen diesen beiden Einschnürungen befinden sich sechs schwache Rippen.
Vorkommen: Kamm-Bank (Frühes Cénomanien).

Abb. 104 *Sciponoceras baculoides*. Kamm-Bank. Säntis, Gasthaus-Hang. Länge des Fragmentes 2.7 cm. Slg. PK 7C.13.06. Foto Amane Tajika.

Sciponoceras roto CIEŚLIŃSKI 1959

Es liegt ein Fragment eines orthoconen Gehäuses von 9.3 cm Länge vor. Das Gehäuse hat einen ovalen Windungsquerschnitt (ww/wh = 0.93), der nur sehr langsam an Höhe gewinnt. Sechs schräge Rippen (45-50°) finden sich auf einem Schaftabschnitt von einer Länge, die der Windungshöhe entspricht. Auf dem Schaft-Fragment befindet sich eine flache Einschnürung.
Vorkommen: Kamm-Bank (Frühes Cénomanien).

Abb. 105 *Sciponoceras roto*. Kamm-Bank. Säntis. Länge des Fragmentes 9.3 cm. Slg UO 08 Foto Amane Tajika. Illustration Beat Scheffold.

Überfamilie **Scaphitaceae** GILL 1871
Familie **Scaphitidae** GILL 1871
Die Vertreter dieser im Alpstein selten anzutreffenden Ammoniten-Familie zeichnen sich durch ihre heteromorphen Gehäuse aus. Die Jugendwindungen sind jedoch normal planspiral aufgerollt. Erst die letzte Windung bildet den charakteristischen Haken aus. Der Geschlechtsdimorphismus ist bei dieser Familie mässig stark ausgeprägt und betrifft im Wesentlichen die Grösse, aber auch feine Unterschiede in der Stärke der Skulptur können erkennbar sein.

Unterfamilie **Scaphitinae** GILL 1871
Gattung ***Scaphites*** PARKINSON 1811
Scaphites* cf. *simplex (JUKES-BROWNE 1875)
Lediglich ein Exemplar dieser Art liegt aus dem Alpstein vor. Es fehlen ein grosser Teil der Jugendwindungen, der grösste Teil der Wohnkammer und die Mündung. Der hinterste Teil der Alterswohnkammer und der letzte halbe Umgang des Phragmokons sind jedoch nur wenig deformiert erhalten. Das Stück ist 5.0 cm lang. Der normal aufgerollte Abschnitt des Gehäuses ist globos, also fast kugelig mit recht breiten Windungen. Die Wohnkammer ist dorsoventral abgeflacht, sehr breit und hat einen flachen Venter. Die Alterswohnkammer trägt zahlreiche, sehr feine Rippen mit sieben Knoten-Paaren.
Vorkommen: Kamm-Bank (Spätestes Albien).

Abb. 106 *Scaphites* cf. *simplex*. Kamm-Bank. Säntis, Gasthaus Hang. Länge des Fragmentes 5.0 cm. Slg. KT Sä-GS-0020. Foto Amane Tajika.

Scaphites hugardianus D'ORBIGNY 1842

Das 2.3 cm grosse Gehäuse des hier abgebildeten, adulten Exemplar ist komplett und unverdrückt erhalten; die charakteristische Einschnürung am gelappten Alters-Mundsaum ist gut zu sehen. Das Phragmokon ist globos, sehr involut und der Nabel ist vollständig geschlossen. Der Windungsquerschnitt ist dorsoventral abgeflacht mit einer breit gerundeten Bauchseite. Auf den gerundeten Flanken finden sich Knoten, zwischen denen je zwei bis drei feine Rippen liegen. Die dicht stehenden Rippen überqueren die Bauchseite ohne schwächer zu werden.

Vorkommen: Garschella-Formation (Frühes Albien).

Abb. 107 *Scaphites hugardianus*. Garschella-Formation. Säntis. Durchmesser 2.3 cm. Slg. UO 16. Illustration Beat Scheffold.

Gattung ***Eoscaphites*** BREISTROFFER 1947

Eoscaphites subcircularis (SPATH 1937)

Auch von dieser Art liegt ein komplettes Gehäuse eines ausgewachsenen Tieres vor. Es hat einen maximalen Durchmesser von 2.2 cm. Das Phragmokon ist mässig dünn scheibenförmig und subinvolut (uw/dm = 0.29). Die Alterswohnkammer besteht aus einem leicht aufgeblähten geraden Schaft und einem eng aufgerollten Haken. Die ganze Schale ist von feinen Rippen bedeckt, die vor allem in Bereichen mit stärkerer Gehäusekrümmung sich aufspalten können. An den Spaltpunkten sind manchmal feine Knoten, vor allem nahe der Altersmündung.

Vorkommen: Garschella-Formation (Frühes Albien, *Mortoniceras pricei* Zone).

Abb. 108 *Eoscaphites subcircularis*. Garschella-Formation. Chelen-Geren (Plona). Durchmesser 2.2 cm. Slg. PK 7B.26.02. Foto Amane Tajika

Überfamilie **Douvilleiceratacea**e PARONA & BONARELLI 1897
Familie **Douvilleiceratidae** PARONA & BONARELLI 1897
Unterfamilie **Douvilleiceratinae** PARONA & BONARELLI 1897
Douvilleiceras ist eine weltweit verbreitete Gattung, die ein auffällig kräftig bedorntes Gehäuse trägt. Anhand der gerippten Ventrolateralknoten ist die Gattung leicht zu erkennen.

Gattung ***Douvilleiceras*** GROSSOUVRE 1894
Douvilleiceras inaequinodum (QUENSTEDT 1849)
Wie der Name besagt, ist die Bedornung ungleich. Bei den Exemplaren vom Alsptein handelt es sich bisher ausschliesslich um Steinkerne, weswegen die eigentlichen Dornen nicht zu sehen sind sondern nur deren Knoten-förmigen Steinkern-Ansätze. Das Gehäuse weist breite Widnungen (ww/dm = 0.5) auf und hat einen mässig weiten Nabel (uw/dm = 0.33). Für die Bestimmung am bedeutendsten jedoch ist die sehr variable Skulptur. Die kräftigen Rippen verlaufen gerade über die Flanken und sind unterschiedlich stark ausgeprägt; im Alter sind sie deutlich abgeschwächt und dafür zahlreicher. Manche Rippen spalten auf, die meisten sind jedoch einfach. Alle Rippen tragen Knoten, die zur Bauchseite hin in ihrer Stärke zunehmen. Je eine Reihe Knoten sitzt auf der Nabelkante, der äusseren Flanke und ventrolateral. Von Exemplaren mit Schalenerhaltung ist bekannt, dass auf der mittleren Knotenreihe Stacheln sassen, die etwa ein Drittel der Windungsbreite messen. Die ventrolateralen Knoten trugen wohl keine solchen Stacheln, dafür sind sie radial verlängert und tragen drei bis vier in Windungsrichtung verbreiterte Knötchen.
Vorkommen: Unterer Teil der Garschella-Formation (Frühes-Mittleres Albien).

Abb 109 *Douvilleiceras inaequinodum*. Garschella-Formation. Semelenberg, Oberriet. Innenwindungen, Durchmesser 2.6 cm. Slg. PK 7B.45.02. Foto Christian Klug.

Abb 110 *Douvilleiceras inaequinodum*. Garschella-Formation. Semelenberg, Oberriet. Fragment mit deutlich sichtbaren ventrolateralen Knoten (links ventral, rechts schräg von vorn). Grösse 3.5 cm. Slg. PK 7B.45.03. Foto Christian Klug.

***Douvilleiceras* sp.**

Diese Gattung ist leicht an ihren zahlreichen Knotenreihen zu erkennen. Bisher wurden im Alpstein überwiegend mässig erhaltene Exemplare gefunden, deren Bestimmung auf Art-Niveau nicht möglich ist. Die Stücke messen zwischen 2.0 und 3.0 cm im Durchmesser und sind mehr oder weniger unvollständig sowie deformiert. Der Windungsquerschnitt ist jeweils deutlich breiter als hoch (ww/wh = 1.35). Das eine Stück hat dicke Rippen mit je vier einfachen Knoten, während das andere Stück sehr kräftige Rippen mit kräftigen ventrolateralen Wülsten aufweist. Diese Wülste tragen je drei Knoten. Die Bestimmung der Arten dieser Gattung wird erschwert durch Veränderungen der Skulptur während des Wachstums. Frühe Entwicklungsstadien verschiedener Arten unterscheiden sich häufig kaum in ihrer Skulptur.

Vorkommen: Garschella-Formation (Frühes-Mittleres Albien).

Abb. 111 *Douvilleiceras* sp. Garschella-Formation. Bergli, Sennwald. Durchmesser 2.1 cm. Slg. PK 7B.42.14. Foto Amane Tajika.

Literatur

De Baets, K., Hoffmann, R., Sessa, J. & Klug, C. (2016): Fossil Focus: Ammonoids. Palaeontology online 6, article 2: 1-15, London.

Ernst, H. U. & Klug, C. (2011): Perlboote und Ammonshörner weltweit. Nautilids and Ammonites worldwide. Verlag Dr. Friedrich Pfeil, München.

Grulke, W. (2014): Heteromorph. The rarest fossil ammonites. Nature at its most bizarre. At One Communications.

Hyatt, A. (1900): Cephaolopoda. In: Zittel, K.A. v. (Ed.): Textbook of Palaeontology. Eastman, London and New York, 502-592.

Joly, B. (2000): Les Juraphyllitidae, Phylloceratidae, Neophylloceratidae (Phylloceratacеae, Phylloceratina, Ammonoidea) de France au Jurassique et au Crétacé. Geobios 33, 5.

Joly, B. & Delamette, M. (2008): Les Phylloceratoidea (Ammonoidea) aptiens et albiens du bassin vocontien (Sud-Est de la France). Carnets de Géologie / Notebooks on Geology, Mémoire 4, Brest.

Kennedy, W. J. (1994): Cenomanian ammonites from Cassis, Bouches-du-Rhone, France. Palaeopelagos Special Publication 1, 209-254.

Kennedy, W. J. & Latil, J. L. (2007): The Upper Albian ammonite succession in the Montlaux section, Hautes-Alpes, France. Acta Geologica Polonica 57(4), 453-478.

Klein, J. (2005): Fossilium Catalogus I: Animalia pars 139. Lower Cretaceous Ammonites I: Perisphinctaceae 1, Himalayitidae, Olcostephanidae, Holcodiscidae, Neocomitidae, Oosterellidae. Backhuys Publishers, Leiden.

Klein, J. & Vašíček Z. (2011): Fossilium Catalogus I: Animalia pars 148. Lower Cretaceous Ammonites V: Desmoceratoidea. Margraf Publishers, Weikersheim.

Klein, J., Hoffmann, R., Joly, B., Shigeta, Y. & Vašíček Z. (2009): Fossilium Catalogus I: Animalia pars 139. Lower Cretaceous Ammonites IV: Boreophylloceratoidea, Phylloceratoidea, Lytoceratoidea, Tetragonitoidea, Haploceratoidea including the Upper Cretaceous representatives. Backhuys Publishers, Leiden. Margraf Publishers, Weikersheim.

Klug, C., Korn, D., De Baets, K., Kruta, I. & Mapes, R. H. (2015): Ammonoid paleobiology, Volume I: from anatomy to ecology. Topics in Geobiology 43, Springer, Dordrecht.

Klug, C., Korn, D., De Baets, K., Kruta, I. & Mapes, R. H. (2015): Ammonoid paleobiology, Volume II: from macroevolution to paleogeography. Topics in Geobiology 44, Springer, Dordrecht.

Klug, C., Schweigert, G., Dietl, G. & Fuchs, D. (2010): First record of a belemnite preserved with beaks, arms and ink sac from the Nusplingen Lithographic Limestone (Kimmeridgian, SW Germany). Lethaia 43: 445-456, Oslo.

Marcinowski, R. & Wiedmann, J. (1990): The Albian ammonites of Poland. Warszawa, PWN.

Seeley, H. G. (1865): On Ammonites from the Cambridge Greensand. Annals and Magazine of Natural History (3) 16, 225-247.

Spath, L. F. (1923-1943): A monograph of the Ammonoidea of the Gault. Palaeontographical Society, London.

Spath, L. F., (1925): On Upper Albian Ammonoidea from Portuguese East Africa, with an appendix on Upper Cretaceous ammonites from Maputoland. Annals of the Transvaal Museum 11, 179-200.

Tajika, A., Kürsteiner, P., Tschanz, K., Lehmann, J., Pictet, A., Jattiot, R. & Klug, C. (2017): Cephalopod associations and palaeoecology of the Cretaceous of the Alpstein (northeastern Switzerland). Cretaceous Research 70, 15-54. Elsevier, Amsterdam.

Vašíček, Z. & Wiedmann J. (1994): The Leptoceratoidinae: small heteromorph ammonites from the Barremian. Palaeontology 37(1), 203-239.

Vermeulen, J. (2002): Etude stratigraphique et paléontologique de la famille des Pulchelliidae (Ammonoidea, Ammonitina, Endemocerataceae). Dissertation, Université Joseph-Fourier-Grenoble I.

Wiedmann, J. (1965): Origin, limits and systematic position of *Scaphites*. Palaeontology 8:397-453.

Wiedmann, J. (1966): Stammesgeschichte und System der posttriadischen Ammonoideen. Neues Jahrbuch für Geologie und Paläontologie, Abhandlungen 127, 13-81.

Wright, C. W. (1952): A classification of the Cretaceous ammonites. Journal of Paleontology 26, 213-222.

Wright, C. W. (1996): Treatise on Invertebrate Paleontology. Part L, Mollusca 4: Cretaceous Ammonoidea (with contributions by Calloman, J. H. & Howarth, M. K.). Lawrence, Kansas and Boulder. Geological Society of America and University of Kansas.

Wright, C. W. & Kennedy, W. J. (1984-1996): The Ammonoidea of the Lower Chalk. Part 1-5. Palaeontographical Society Monograph.

Appendix 1-3

Additional publications linked to this dissertation

Fossilien im Alpstein
Kapitel 6.10 Belemniten (Belemnoidea)

Klug, C. Tajika, A

Book chapter (in press)
Publisher: Appenzeller Verlag

6.10 Belemniten (Belemnoidea)

Christian Klug und Amane Tajika

6.10.1 Einführung

Die Coleoidea oder Tintenfische zeichnen sich durch eine Tintenblase aus, die sie zur Ablenkung potentieller Fressfeinde nutzen. Dieses Organ entwickelte sich wahrscheinlich im Zusammenhang mit der Verlagerung der Schale in das Innere (Internalisierung). Dieser Prozess lässt sich an Fossilien, bei denen ja die Weichteile meist nicht erhalten sind, trotzdem nachvollziehen: die ursprünglichsten Vertreter der Tintenfische hatten ein Innenskelett bestehend aus einem gekammerten Teil (Phragmokon) und einer Wohnkammer (nach unten bzw. ventral offen; Proostracum), wobei der diese Weichteile umgebende Mantel an der Spitze des Phragmokons von aussen zusätzlich Kalk ablagerte, die Hartteile also zumindest teilweise umfasste. Diese sekundäre Ablagerung (Rostrum) ist einerseits ein eindeutiger Beweis für die Internalisierung und andererseits sehr gut fossilisierbar, da sie oft aus dickem Aragonit oder Kalzit besteht (Abb. 1). Es sind genau diese Hartteile, die im Alpstein in manchen Schichten (Altmann-Member, Garschella-Formation, Seewen-Formation) durchaus häufig sind.

6.10.2 Anatomie

Innenskelett

In der Regel werden von Belemniten nur die kalzitischen Rostren (Abb. 1) gefunden, weil sie aus massivem Kalzit bestehen. Deutlich seltener ist das aragonitische Phragmokon und noch seltener das fragile, ebenfalls aragonitische Proostracum überliefert.

Das Proostracum (Abb. 2 B) ist homolog zur Wohnkammer der Ammoniten und Nautiliden und entstand durch die Zunahme der Tiefe einer ventralen Einbuchtung. Bei den Phragmoteuthiden besteht das Proostracum aus drei Feldern, wodurch der Vorderrand dreilappig ist. Bei den Belemniten dagegen wurden die Seitenfelder reduziert, sodass das Proostracum Spatel-förmig ist.

Das Phragmokon weist zahlreiche, eng stehende, einfach Uhrglas-förmige Septen (Kammerscheidewände) mit einem dünnen, ventralen Sipho auf. Diese Eigenschaften belegen die Abstammung der Tintenfische von den Bactriten, bei denen Septen und Sipho ähnliche Formen und Proportionen aufweisen. Ebenfalls ähnlich ist die kugelförmige Anfangskammer, die auch in der Grösse der der Bactriten entspricht.

Das gesamte Rostrum (Holorostrum) besteht oft aus zwei Teilen, dem spitzen Orthorostrum (das eigentliche Rostrum, hier im Text auch so verwendet) und dem auf dem Orthorostrum sitzenden, hohlen oder weniger massiv gebauten Epirostrum. Im vorderen Bereich (Rostrum cavum) befindet sich das Phragmokon, wodurch das Rostrum dort eine kegelförmige Vertiefung aufweist (Abb. 1 I).

Das Rostrum wurde vom Muskelmantel nach innen abgeschieden, weshalb auf der Oberfläche auch Abdrücke verschiedener Weichteile wie Blutgefässe und des Flossenpaares zu sehen sind.

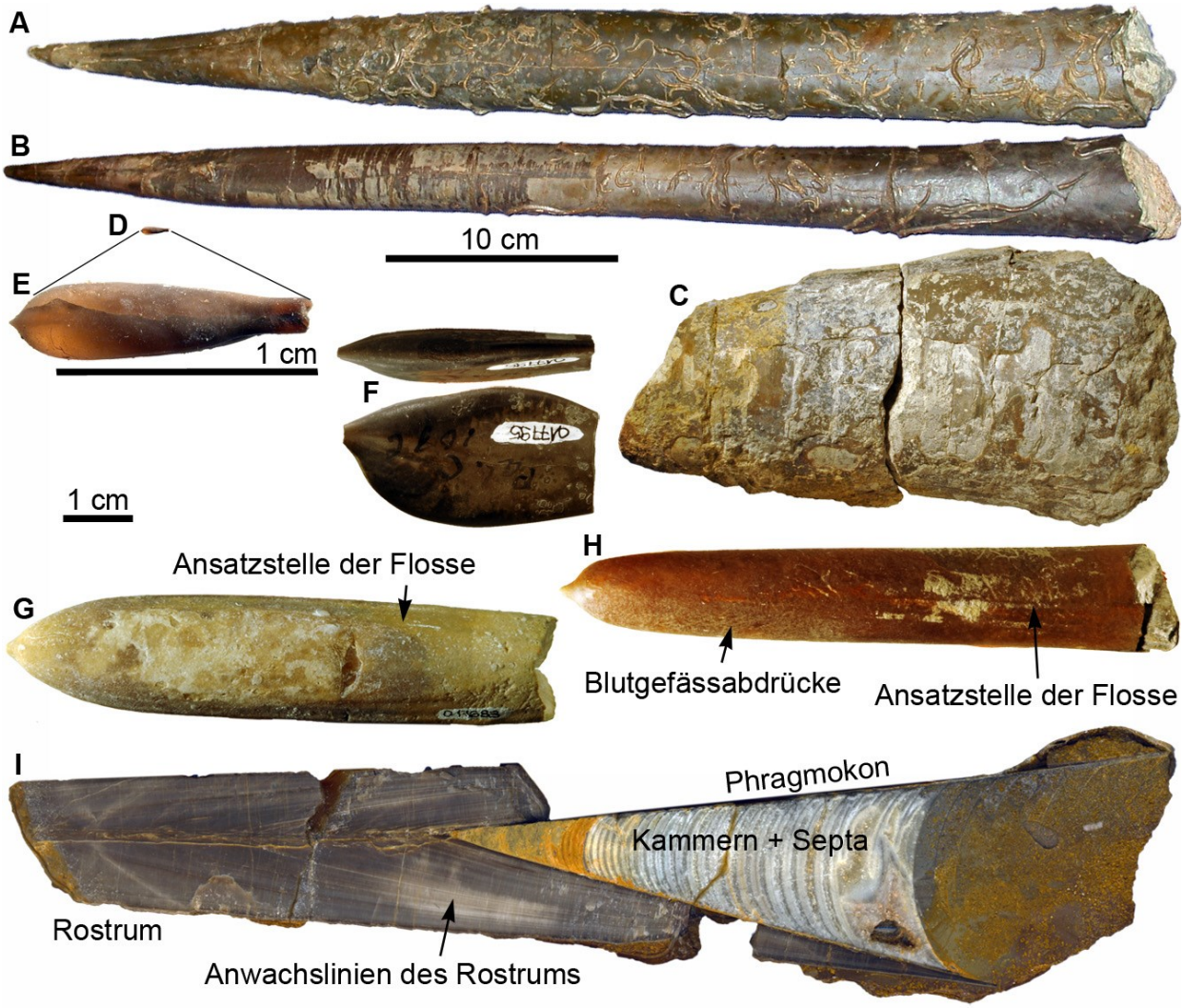

Abb. 1 Hartteile von Belemniten aus Jura und Kreide. Für A-D gilt der 10 cm-Massstab, für E der grosse 1 cm-Massstab, für alle anderen der kleine 1 cm-Massstab. A, B, zwei riesige Rostren (> 50 cm) von *Megateuthis*. Bajocien. Sengenthal D. Funde von Arno Pfeiffer und Helmut Lehmann. A, *M. gigantea* (Schlotheim, 1820). B, *M. elliptica* (Miller, 1826). C, Phragmokon eines riesigen *M. gigantea* (Schlotheim, 1820). Bajocien. Blitzberg bei Klingnau AG. PIMUZ 17125. D, E, Rostrum eines adulten Tieres der kleinsten Belemnitenart der Welt: *Suebibelus pressulus* (Quenstedt, 1857). Oxfordien. Sengenthal D. Fund von Arno Pfeiffer und Helmut Lehmann. E, vergrössert. F, eigenartige Form mit seitlich abgeflachtem Rostrum: *Duvalia dilatata* (Blainville, 1827), oben: dorsal, unten: lateral. Valanginien. Orpierres F. PIMUZ 17795. G, dorsale Ansicht von *Actinocamax mammillatus* (Nilsson, 1817). Campanien. Ignaberga-Schonen S. PIMUZ 17883. H, *Belemnitella mucronata* (Schlotheim, 1813). Campanien. Misburg D. PIMUZ 6888. I, Längsschnitt entlang der Symmetrie-Ebene von *M. gigantea* (Schlotheim, 1820). Bajocien. Balingen D. PIMUZ 19181. Fotos A, B, D, E von Andreas E. Richter. Alle anderen Fotos Christian Klug.

Kieferapparat

Im Gegensatz zu den Nautiliden und vielen Mesozoischen Ammoniten bestehen die Kiefer der Tintenfische nur aus Chitin. Äusserlich ähneln sie Papageien-Schnäbeln. Durch das Fehlen mineralischer Bestandteile sind Tintenfisch-Kiefer fossil eher selten und aus dem Alpstein bisher unbekannt. Belemniten-Kiefer wurden bislang nur ein einziges Mal beschrieben, und zwar aus dem Späten Jura. Sie ähneln den Kiefern anderer Tintenfische durchaus (siehe Kapitel 6.9 „Ammoniten“, Abb. 3). Weiterhin verfügen die Belemniten, wie viele andere Weichtiere auch, über eine Raspelzunge, welche aus zahlreichen winzigen, ebenfalls chitinigen Zähnchen bestehen. Die Raspelzunge der Belemniten wurde ebenfalls bisher nur ein einziges Mal gefunden, was an ihrer schlechten Erhaltungs-Fähigkeit liegt.

Weichkörper

Im Gegensatz zu Ammoniten und Nautiliden fanden sich an verschiedenen Fundorten (Konservat-Lagerstätten) immer wieder fossile Tintenfische mit mehr oder weniger gut erhaltenen Weichteilresten. Deswegen ist unsere Kenntnis des Weichkörpers ausgestorbener Tintenfische deutlich besser als solcher fossiler Kopffüsser, die eine äussere Schale tragen. Insgesamt unterscheidet sich die Anatomie der Tintenfische des Erdmittelalters (Mesozoikum) kaum von der Anatomie heutiger Formen.

Was die Arme betrifft, so wissen wir von den Belemniten und ähnlichen Formen, dass sie 10 Arme hatten. Die Anzahl Arme ist überliefert in der Form von zehn Doppelreihen ursprünglich chitiniger Armhäkchen, die an verschiedenen Lokalitäten gefunden wurden (Abb. 2 A). Das Vorhandensein von zehn Armen verbindet sie mit den heutigen zehnarmigen Formen (Decabrachia), zu denen u.a. Riesenkalmar, Sepien und auch die Zwergsepien gehören. Die achtarmigen Formen (Octobrachia) evoluierten durch die Reduktion eines Armpaares. Am Alpstein wurden bisher keine Reste der Octobrachia und Decabrachia im eigentlichen Sinn gefunden.

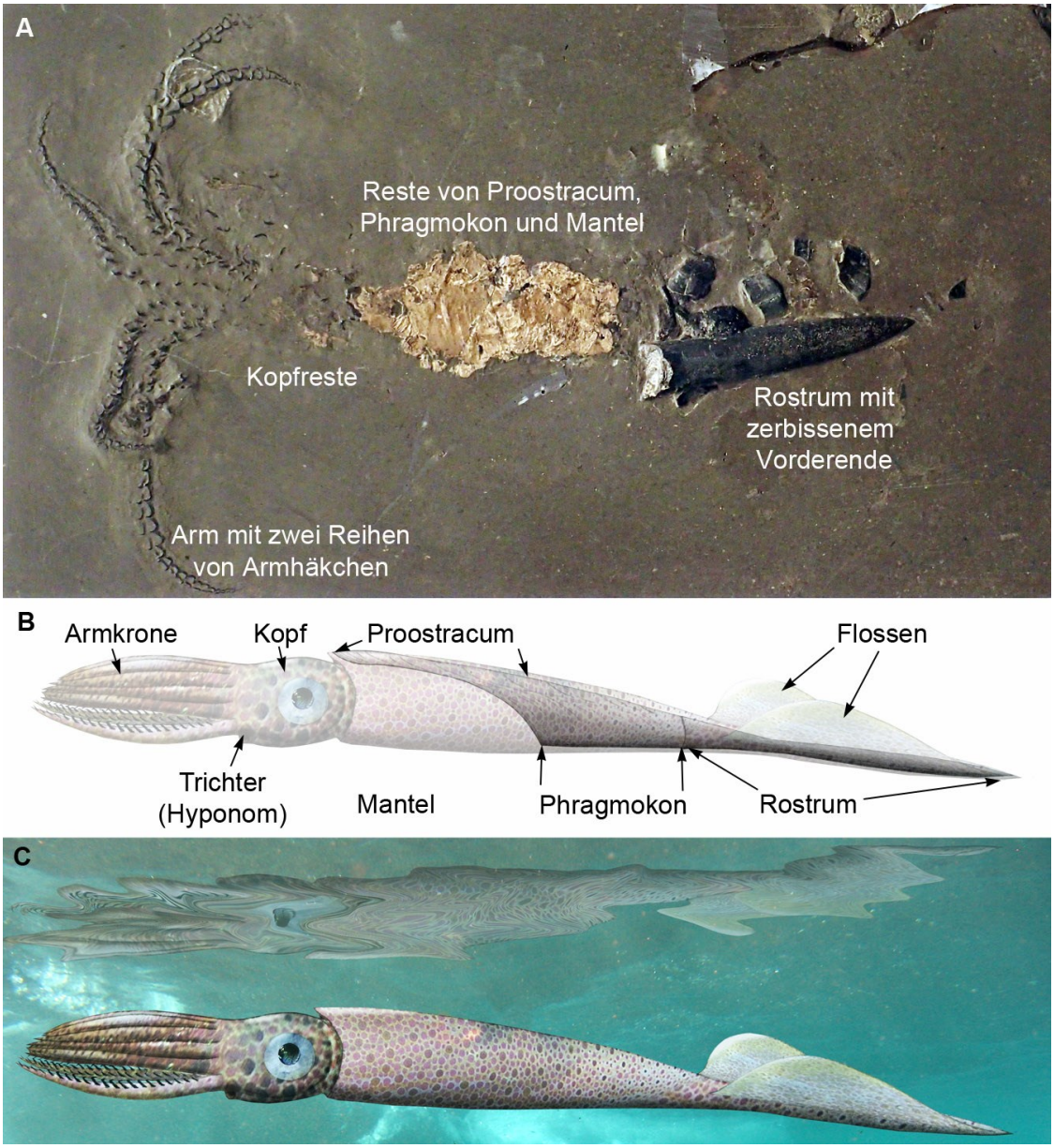

Abb. 2 Belemnitentier. A, *Passaloteuthis laevigata* (Zieten, 1831). Toarcien. Holzmaden. Museum Hauff, Holzmaden D. Länge 15 cm. B, C, Rekonstruktion von *Hibolithes semisulcatus* (Münster, 1830). Kimmeridgien. Verändert nach Klug et al. (2010). B, die Weichteile sind leicht transparent dargestellt, um das Innenskelett sichtbar zu machen. C, das lebende Tier; ob die Körperoberfläche wirklich Chromatophoren trug, wie heutige 10-armige Tintenfische, ist unbekannt. Fotos und Illustrationen Christian Klug.

Was die Augen betrifft, so gibt es heute bei den Kopffüssern zwei verschiedene Typen, das Lochkamera-Auge (eine Spezial-Entwicklung der Nautiliden) und das Linsenauge der Tintenfische. Weil alle heutigen Tintenfische über hoch entwickelte, Wirbeltier-ähnliche Linsenaugen verfügen, ist es wahrscheinlich, dass fossile Verwandte wie die Belemniten auch über diesen Augen-Typ verfügten.

Wie der Name „Kopffüsser“ impliziert, sitzen die Körperanhänge direkt am Kopf, in dem sich Sinnesorgane, Mund und Gehirn befinden. Hinter dem Kopf beginnt der Mantel, welcher bei den

Tintenfischen über drei dicke Schichten Muskulatur verfügt, die übrigens gelegentlich auch fossil überliefert ist. Der mehr oder weniger längliche Mantel enthält die Verdauungs- und Reproduktions-Organe sowie die Mantelhöhle. Die Mantelhöhle enthält After, Kiemen und die Mündung der Geschlechtsorgane. Ausserdem spielt sie eine wichtige Rolle für die Fortbewegung: Wenn sich die Mantelmuskulatur zusammenzieht, wird die Wasser-gefüllte Mantelhöhle zusammengedrückt und somit das Wasser aus dem Trichter (Hyponom) ausgestossen. Dabei entsteht ein Rückstoss, mit dem manche Tintenfische sehr schnell schwimmen oder sogar aus dem Wasser springen und kurze Strecken fliegen können. Die schwimmenden Tintenfische verfügen überdies oft über ein oder zwei Flossen-Paare, die bei den Ammoniten am Rostrum befestigt waren.

6.10.3 Ursprung und Evolution

Die Tintenfische entwickelten sich wie die Ammonoideen aus den Bactriten. Wie bereits erwähnt, wiederspiegelt sich dies in der grossen Ähnlichkeit des Phragmokons beider Gruppen. Die grundlegende Neuerung, durch die die Tintenfische entstanden, war die Internalisierung des Gehäuses. Dabei entstand das vom Muskelmantel aussen auf das Phragmokon abgelagerte Phragmokon, welches aber später in mehreren Gruppen reduziert wurde, so zum Beispiel bei den Octobrachia.

Im Alpstein sind nur die Diplobeliden und die Belemnitiden vertreten. Die Belemnoteuthiden haben ein sehr dünnes Rostrum, während dasjenige der Belemniten massiven Kalzit enthält. Möglicherweise spiegeln sich darin unterschiedliche ökologische Anpassungen wieder.

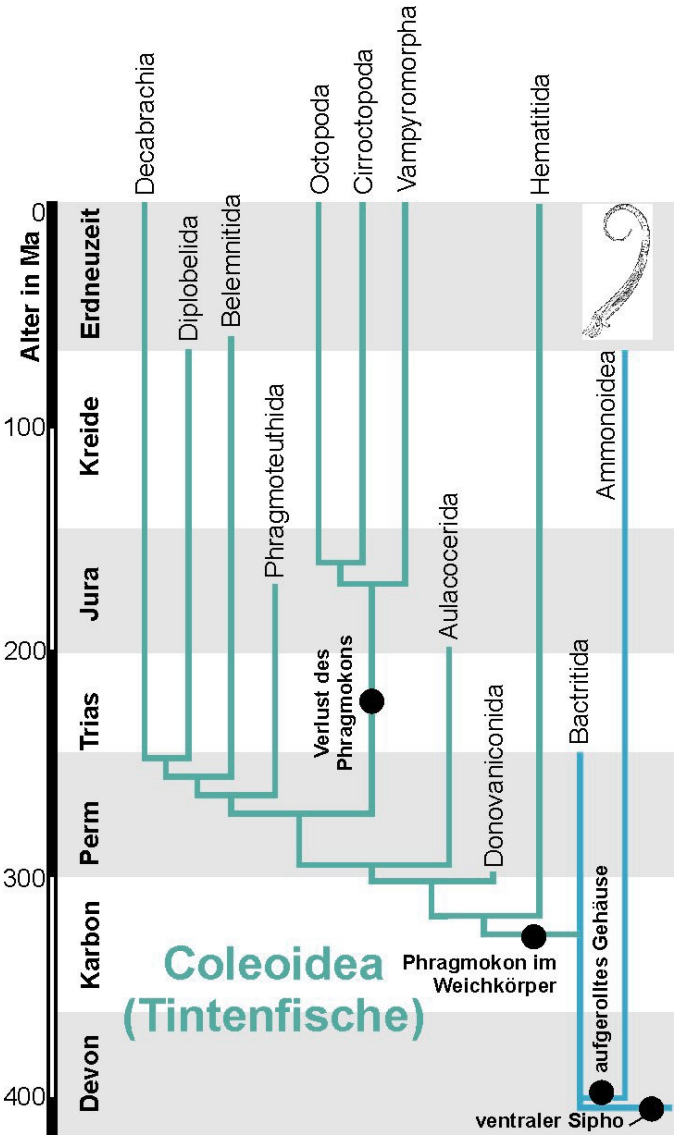

Abb 3 Ursprung und Evolution der Coleoidea (blaugrün). Wichtige evolutionäre Neuerungen (Apomorphien) sind mit einem schwarzen Kreis markiert. Verändert nach Kröger et al. (2011).

6.10.4 Geschlechtsunterschiede und Reproduktion

Bei heutigen Tintenfische sind die Unterschiede zwischen den Geschlechtern in Grösse und Form manchmal erheblich: Bei dem Papierboot *Argonauta* hat das Weibchen ein bis zu 80-faches Weichkörper-Volumen des Männchens und die 10-fache Körperlänge. Bei den Belemniten gab es wohl auch einen Dimorphismus; dieser spiegelt sich vermutlich in Paaren in der Jugend ähnlicher Formen wieder, die sich im Alter aber mehr oder weniger stark unterscheiden.

Von *Passaloteuthis* sind mehrere Exemplare bekannt geworden, bei denen die komplette Armkrone überliefert ist. Manche Exemplare tragen ein Paar grosser, gekrümmter Haken. Es wird spekuliert, dass dies die Männchen waren, die mit diesen Haken vielleicht das Weibchen bei der Paarung festhalten konnten.

Die kleinen Embryonal-Gehäuse deuten darauf hin, dass Belemniten so wie die Ammoniten r-Strategen waren, also dass jedes erwachsene Weibchen zahlreiche Eier produzierte. Die ausgedehnten Massen-Vorkommen von Belemniten-Rostren im europäischen Jura sind jedoch wohl eher durch niedrige Sedimentations-Raten und die gleichzeitige Akkumulation der gut erhaltungsfähigen Rostren zu erklären.

6.10.5 Lebensweise

Bei den heutigen Tintenfischen gibt es ein breites Spektrum an Lebensweisen. Diese reichen vom bodenlebenden (benthischen) *Octopus* über die in Bodennähe schwimmende (demersale) *Sepia*, das eher passiv driftende (planktonische) Posthörnchen (*Spirula*) oder den im offenen Meer (pelagisch) schwimmenden (nektonisch) Kalmar *Loligo* bis hin zu dem schnell schwimmenden und sogar kurze Strecken fliegenden Zehnarmer (Decabrachier) *Todarodes*.

Für die Belemniten werden verschiedene Lebensweisen diskutiert. Das Vorhandensein eines funktionalen Phragmokons deutet auf ein Leben in der Wassersäule hin. Bei Belemnoteuthinen wurden Statolithen gefunden, deren Grösse auf eine planktische bis nektoplanktische Lebensweise hindeuten, d.h. oft passiv treibend und gelegentlich aktiv schwimmend, aber nicht oder nur wenig migrierend. Für die echten Belemniten erscheint eine nektonische Lebensweise wahrscheinlich, sie waren wohl gute Schwimmer. Vereinzelte Mageninhalte und andere Hinweise auf deren Beute belegen, dass diese Tintenfische durchaus in der Lage waren, Fische zu fangen und zu fressen.

6.10.6 Aussterben

Die Belemniten und ihre nächsten Verwandten starben gemeinsam mit den Ammoniten und den Dinosauriern aus. Interessanterweise durchliefen die beiden heute bedeutendsten Gruppen, also die Decabrachia und Octobrachia, schon vor dem Aussterben der Belemniten eine Radiation. Es ist also nicht so, dass deren Aussterben plötzlich ökologische Resourcen freigegeben hätte und es dadurch zur Diversifikation kam. Vielmehr ist die fossile Überlieferung ausgestorbener Vertreter der Decabrachia und Octobrachia schlecht, aber sie waren in den Weltmeeren der Kreidezeit durchaus schon vertreten.

Eine mögliche Erklärung des selektiven Aussterbens der Ammoniten und Belemniten bei gleichzeitigem Überleben der Nautiliden liegt in der Reproduktions-Strategie. Ammoniten und Belemniten hatten winzige Schlüpflinge, welche wohl über geringe Reserven verfügten. Bei stark wechselnden Umweltbedingungen (Ende Kreide ausgelöst durch intensiven Vulkanismus und einen grossen Meteoriten) haben diese Reserven vielleicht nicht gereicht, um schwierige Phasen zu überstehen. Die viel grösseren Jungtiere der Nautiliden dagegen konnten solche Phasen eher überleben.

6.10.7 Klassifikation

Für die Bestimmung spielen bei den Belemniten Merkmale des Orthorostrums die wichtigste Rolle. Zunächst wird die generelle Form betrachtet: Sind die Rostren kurz oder lang, spitz oder stumpf, Keulen-, Finger-, Pfahl-, Nagel- oder Lanzett-förmig, mit oder ohne abgesetzter Spitze oder Papille, mit oder ohne Epirostrum usw.? Weiterhin spielt die Oberflächenstruktur eine wichtige Rolle: Sind Blutgefässabdrücke vorhanden? Wie sehen die Ansatzstellen der Flossen aus und wo liegen diese? An der Spitze befinden sich oft Furchen, die je nach Lage als Dorsal-, Ventral- oder Ventrolateralfurchen klassifiziert werden.

Weitere Informationen erschliessen sich erst, wenn man das Rostrum entlang der Symmetrieebene aufschneidet oder spaltet. Dazu gehört der Verlauf der Apikallinie (Mittellinie des Orthorostrums; sie ist gerade, dorsal oder ventral gekrümmt) und die Form der Alveole. Die Alveole ist der Hohlraum, in dem das Phragmokon lag. Je nach Form des Phragmokons variiert der Alveolen-Winkel. Zur Bauchseite durchzieht ein Spalt das Rostrum, welcher als Schlitzfeld bekannt ist. Dessen Länge, Winkel und Begrenzung werden auch zur Bestimmung herangezogen.

Die Bestimmung isolierter Belemniten-Phragmokone ist oft schwierig aufgrund der Merkmals-Armut und der geringen Unterschiede zwischen den Taxa. Es kann der Apikalwinkel und der relative Abstand zwischen den Septen gemessen werden. Manchmal unterscheidet sich auch die Neigung der Septen.

6.10.8 Coleoideen des Alpsteins

Belemniten sind im Alpstein in manchen Schichten nicht selten. Ihre Bestimmung erweist sich oft als schwierig, da die Rostren meist stark angewittert oder mit dem Umgebungsgestein verbacken sind. Rostren finden sich, genau wie andere Cephalopoden-Reste auch, vor allem im Altmann-Member, in der gesamten Garschella-Formation und in der Seewen-Formation. Die Systematik wurde Riegraf et al. (1998) entnommen.

Überordnung **Belemnophora** GRAY 1849
Ordnung **Belemnitida** MACGILLIVRAY 1840
Unterordnung **Belemnitina** MACGILLIVRAY 1840
Familie **Oxyteuthidae** STOLLEY 1911
Gattung ***Oxyteuthis*** STOLLEY 1911
?*Oxyteuthis* sp.
Nur ein einziges Exemplar kann mit Vorbehalt dieser Gattung zugeordnet werden. Die Breite und Höhe des Rostrums nimmt hinter dem Rostrum cavum nicht zu. Insgesamt ist das Rostrum Pflock- bis Kegel-förmig mit einer langen, sich gleichmässig verjüngenden Spitze. Ventrale Furchen sind nicht vorhanden.
Vorkommen: Altmann-Member (Spätestes Hauterivien-Frühes Barrémien).

Abb. 4 ?*Oxyteuthis* sp. Altmann-Member. Tierwis-Grenzchopf. Länge 5 cm. Slg. PK 5A.02.09. Foto Amane Tajika.

Unterordnung **Pachybelemnnopseina** RIEGRAF 1998
Familie **Mesohibolitidae** NERODENKO 1983
Gattung ***Neohibolites*** STOLLEY 1911
Neohibolites* cf. *minimus (MILLER 1826)

Die Gattung *Neohibolites* ist wohl die am häufigsten vorkommende Belemniten-Gattung im Alpstein. Aufgrund der meist schlechten (korrodierten) Erhaltung ist die Zuordnung auf Artniveau oft unmöglich. Diese eher kleine (daher der Artname *minimus*) bis mittelgroße Form hat schlanke, kegelförmige Rostren. Das Alveolarende ist dick und im Bereich zwischen Spitze und Alveolarende ist das Rostrum nur wenig angeschwollen. Die Ventralfurche erstreckt sich nur über das Rostrum cavum und auch der Alveolarschlitz reicht nicht hinter die Alveole. Im Material vom Alpstein sind leider nur stark korrodierte Rostren vorhanden, so dass Details der Oberfläche und der Alveole fehlen.

Vorkommen: Altmann-Member (Spätestes Hauterivien-Frühes Barrémien), Garschella-Formation inkl. Kamm-Bank (Frühes Aptien-Frühes Cenomanien), Seewen-Formation (Frühes Cénomanien).

Abb. 5A *Neohibolites* cf. *minimus* (Miller, 1826). Kamm-Bank. Tal-Wänneli (NE Neuenalpspitz). Länge 2.4 cm. Slg. PK 7C.07.08. Foto Amane Tajika. 5B *Neohibolites* cf. *minimus* (Miller, 1826). Garschella-Formation. Tierwis NE I. Länge 2.7 cm. Slg. PK 7B.05.02. Foto Amane Tajika. 5C *Neohibolites* cf. *minimus* (Miller, 1826). Garschella-Formation. Blauschnee-Girenspitz. Bildbreite 10.6 cm. Slg. PK 7B.03.02. Foto Amane Tajika.

Familie **Duvaliidae** PAVLOW 1914

Gattung **Duvalia** BAYLE 1878

Die Vertreter dieser Gattung zeichnen sich durch Orthorostren aus, die seitlich mehr oder weniger stark abgeflacht sind. Manche Arten bildeten einen deutlichen dorsalen Kiel aus. Naef (1922) vermutete, dass die Verkürzung des Rostrums auf einen Küsten-nahen Lebensraum hinweist. Dorsal ist eine tiefe Alveolarfurche ausgebildet, während ein ventrales Pendant nicht vorhanden ist. Seitenfurchen sind oft vorhanden, beim hier abgebildeten Stück jedoch nicht auszumachen.

Duvalia* cf. *lata (DE BLAINVILLE 1827)

Das Orthorostrum des abgebildeten Stückes ist 7.1 cm lang, 1.3 cm breit und 2 cm hoch. Dabei ist charakteristisch, dass das Rostrum hinter der Alveole sich leicht verbreitert, bevor es kurz vor der Spitze noch seitlich abflacht. Typisch ist auch die seitliche Abflachung. Dieser Eindruck der Abflachung wird durch einen breit gerundeten, dorsalen Kiel und die ausgebauchte Ventralseite noch verstärkt. Der Kiel liegt weiter vorne als die ventrale Wölbung. Die dorsale Alveolarfurche ist deutlich und etwas über einen Millimeter breit. Sie endet etwa 3 cm vor der Spitze.
Vorkommen: Altmann-Member (Spätestes Hauterivien-Frühes Barrémien).

Abb. 6 *Duvalia* cf. *lata*. Altmann-Member. Alp Wis. Länge 7.1 cm. Slg. KT WI-AR-0001. Fotos Christian Klug.

Ordnung **Diplobelida** JELETZKY 1965

Familie **Diploconidae** NAEF 1922

Die beiden bekannten Gattungen dieser Familie zeichnen sich durch ein kurzes und stumpfes Rostrum aus. Das Rostrum ist uns aus dem Alpstein nicht bekannt, nur Phragmocone wurden bisher gefunden. Das Proostracum soll schmal sein, jedoch ist auch dies nicht erhalten im vorliegenden Material. Einzig die Phragmokone kommen lokal im Alpstein-Gebiet vor. Der Apikalwinkel liegt bei 16 bis 18°. Die Septen stehen eng beieinander. Die kleineren Septen in Richtung Spitze stehen fast gerade, während die grösseren Septen mehr und mehr dorsal nach vorne geneigt sind.
Vorkommen: „Schörgisknorren-Bank“ (Campanien-Mittleres Maastrichtien).

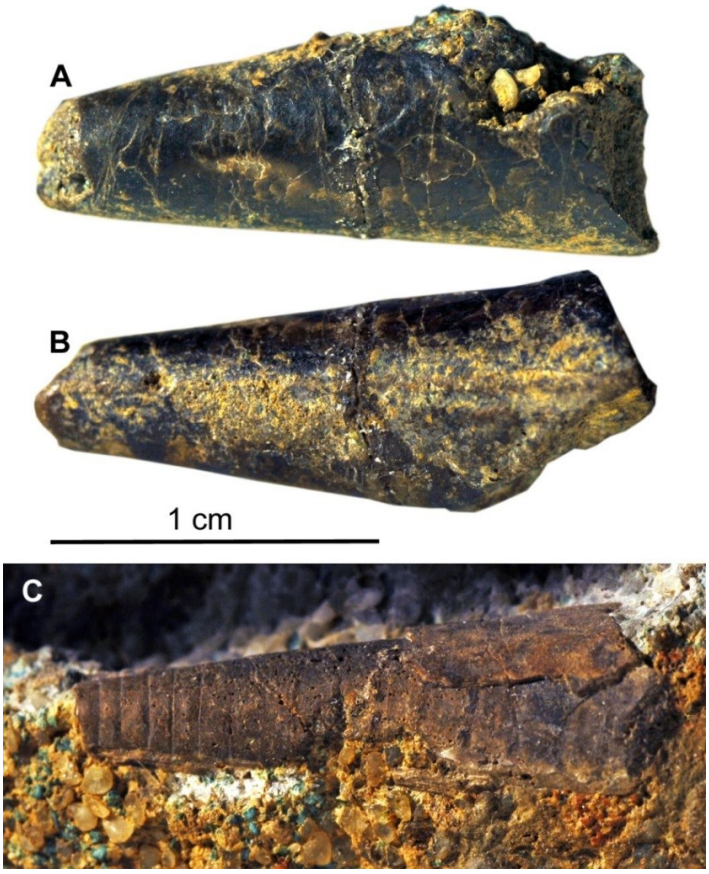

Abb. 7A, B Phragmokon eines Diploconiden. „Schörgisknorren-Bank“. Schörgisknorren, Kobelwis. Rostrum-Reste bzw. die Wand des Phragmokons sind vorhanden, denn die Septen sind nicht zu sehen. Länge 1.9 cm. Slg. PK 10B.01.21. Fotos Amane Tajika. 7C Phragmokon eines Diploconiden. „Schörgisknorren-Bank“. Schörgisknorren, Kobelwis. Steinkern mit Schalenresten, die eng stehenden, geraden Septen sind gut zu sehen. Bildbreite 2,1 cm. Slg. PK 10B.01.21. Fotos Amane Tajika.

Literatur

Doyle, P. & Macdonald, D.I.M. (1993): Belemnite battlefields. Lethaia 26, 65–80.

Fuchs, D. (2006): Fossil erhaltungsfähige Merkmalskomplexe der Coleoidea (Cephalopoda) und ihre phylogenetische Bedeutung. Berliner Paläobiologische Abhandlungen 8, 1–165.

Iba, Y., Mutterlose, J., Tanabe, K., Sano, S.-I., Misaki, A. & Terabe, K. 2011. Belemnite extinction and the origin of modern cephalopods 35 my prior to the Cretaceous−Paleogene event. Geology 39, 483-486.

Klug, C. & Fuchs, D. (2010): An earliest Hettangian (Jurassic) belemnitid from Great Britain with a preserved proostracum. In: Tanabe, K., Shigeta, Y., Sasaki, T. & Hirano, H. (eds), Cephalopods - Present and Past, 181-185. Tokai University Press, Tokyo.

Klug, C., Fuchs, D., Schweigert, G., Kruta, I. & Tischlinger, H. (2016): Adaptations to squid-style high-speed swimming in Jurassic belemnitids. Biology letters 12 (1). London. http://dx.doi.org/10.1098/rsbl.2015.0877.

Klug, C., Schweigert, G., Dietl, G. & Fuchs, D. (2010): First record of a belemnite preserved with beaks, arms and ink sac from the Nusplingen Lithographic Limestone (Kimmeridgian, SW Germany). Lethaia 43, 445-456, Oslo.

Kröger, B., Vinther, J. & Fuchs, D. (2011): Cephalopod origin and evolution: a congruent picture emerging from fossils, development and molecules. Bioessays 33, 602–613.

Muramatsu, K., Yamamoto, J., Abe, T., Sekiguchi, K., Hoshi, N. & Sakurai, Y. (2013): Oceanic squid do fly. Marine Biology 160, 1171–1175.

Naef, A. (1922): Die fossilen Tintenfische. 322 pp. Gustav Fischer, Jena.

Reitner, J. & Urlichs, M. (1983): Echte Weichteilbelemniten aus dem Untertoarcium (Posidonienschiefer) Südwestdeutschlands. Neues Jahrbuch für Geologie und Paläontologie, Abhandlungen 165, 450–465.

Riegraf, W. & Hauff, R. (1983): Belemniten mit Weichkörper, Fangarmen und Gladius aus dem Untertoarcium (Posidonienschiefer) und Unteraalenium (Opalinuston) Südwestdeutschlands. Neues Jahrbuch für Geologie und Paläontologie, Abhandlungen 165, 466–483.

Riegraf, W., Janssen, N. & Schmitt-Riegraf, C. (1998): Cephalopoda dibranchiata fossiles (Coleoidea) II. Fossilium Catalogus I: Animalia. Pars 135, 1-512. Backhuys Publ., Leiden.

Schlegelmilch, R. (1998): Die Belemniten des süddeutschen Jura. 151 pp. Gustav Fischer Verlag, Stuttgart.

Appendix 1-4

Additional publications linked to this dissertation

Ammonoid Palaeobiology
Chapter 7 Mature Modifications and Sexual Dimorphism

Klug, C. Zatoń, M. Parent,
H. Hostettler, B. Tajika, A

Book chapter (2015)
Publisher: Springer

Chapter 7
Mature Modifications and Sexual Dimorphism

Christian Klug, Michał Zatoń, Horacio Parent, Bernhard Hostettler and Amane Tajika

7.1 Introduction

Allometric growth between different parts of the shell often hampers the identification of mollusk shells, particularly in such cases where preadult shell growth varies strongly. Especially in gastropods, the terminal aperture is often less variable and yields morphological information essential for species determination (e.g. Vermeij 1993; Urdy et al. 2010a, b). In fossil mollusk shells, the adult aperture (peristome) is often missing, partially due to an early death, and partially due to destructive processes, which occurred *post mortem* (taphonomy). Therefore, the entire shell ontogeny is known only from a small fraction of all ammonoid taxa (e.g., Landman et al. 2012). Nevertheless, knowledge of the adult shell of ammonoids is very important since it can yield morphological information essential for systematics and for the reconstruction of various aspects of their paleobiology.

C. Klug (✉) · A. Tajika
Paläontologisches Institut und Museum, University of Zurich,
Karl Schmid-Strasse 6, 8006 Zurich, Switzerland
e-mail: chklug@pim.uzh.ch

A. Tajika
e-mail: amane.tajika@pim.uzh.ch

M. Zatoń
Faculty of Earth Sciences, University of Silesia,
Będzińska 60, 41-200 Sosnowiec, Poland
e-mail: mzaton@wnoz.us.edu.pl

H. Parent
Laboratorio de Paleontología, IFG−FCEIA, Universidad Nacional de Rosario,
Pellegrini 250, 2000 Rosario, Argentina
e-mail: parent@fceia.unr.edu.ar

B. Hostettler
Naturhistorisches Museum, Bernastrasse 15,
3005 Bern, Switzerland
e-mail: bernhard.hostettler@nmbe.ch

C. Klug et al. (eds.), *Ammonoid Paleobiology: From Anatomy to Ecology,*
Topics in Geobiology 43, DOI 10.1007/978-94-017-9630-9_7

In the past five decades, numerous researchers have worked on documenting mature modifications and it can be said that the maturity of an ammonoid shell can be determined with some confidence (e.g. Makowski 1962, 1971, 1991; Callomon 1963; Brochwicz-Lewiński & Różak 1976; Bucher and Guex 1990; Brooks 1991; Bucher et al. 1996; Davis et al. 1996; Schweigert and Dietze 1998; Parent 1997; Klug 2004; Parent et al. 2008a; Zatoń 2008; Landman et al. 2012). The reliable identification of mature shells is the logical prerequisite to determine sexual dimorphism. Both mature modifications and sexual dimorphism are discussed in this chapter, since these are intimately linked with each other. Much of the information contained herein comes from the original work of Davis et al. (1996).

7.2 Mature Modifications

7.2.1 Modifications in Recent Nautilida

Modern Nautilida have been studied for over a century (e.g., Griffin 1900). Much of this research was summarized in Ward (1987). Therein, he listed the mature modifications that have been seen in shells of Recent nautilids (see also Collins and Ward 1987). This list was summarized by Klug (2004) and is repeated here:

1. Shell growth band (shell thickening at the apertural edge, 25 mm wide and up to 1 mm thick).
2. Black band (evenly distributed around the aperture, 1 to 5 mm wide).
3. Deepening of the ocular sinuses.
4. Reduction of relative whorl height by a decrease in whorl expansion rate.
5. Reduction of whorl width by a decrease in whorl width expansion rate; this is accompanied by a more rounded venter.
6. Septal thickening (the terminal septum is up to 30 % thicker than the preceding ones).
7. Septal crowding.
8. Maximum shell diameter (unreliable character because of variability).
9. White ventral area.
10. Increase in body chamber length.
11. Reduction of cameral liquid (probably to compensate for the additional shell material at the aperture and the longer body chamber).

7.2.2 Modifications in Ammonoidea

Among the mature modifications known from nautilids listed above, the majority has also been documented from ammonoids, except the shell growth band, the septal thickness, the white venter, and the reduction of the cameral liquid. Some

of these mature modifications that are unknown in ammonoids potentially are unknown because they are not or only poorly preserved or expressed in a different way. For example, the shell growth band could be homologized with a (sub-)terminal shell thickening (a constriction), the white venter might be unknown because of the poor knowledge of color patterns in ammonoids (Mapes and Larson 2015), and the mature reduction of cameral liquid could be tested in the future using volume models of ammonoid shells (Hoffmann et al. 2013; Tajika et al. 2014).

Some of these structures, however, may occur in similar forms in earlier growth stages, either as consequence of an injury, adverse living conditions, and illnesses, or as a recurrent growth feature such as megastriae (growth halts; Bucher and Guex 1990; Bucher et al. 1996). These similar structures may be misinterpreted, what represents a general problem that occurs in research related to mature modifications. Therefore, to ascertain the quality of any such structure as a mature modification, it is helpful to look for other modifications supporting the hypothesis of adulthood for the material under consideration. For instance, a specimen may show septal crowding, which is insufficient as an isolated character to prove adulthood. If, however, it is additionally associated with, e.g., a crowding of growth lines and a change in shell geometry, it is more likely that the given specimen had actually reached maturity.

Another difficulty is linked with the questions of sexual maturity, semelparity, and iteroparity. Is the formation of mature modifications linked with sexual maturity in ammonoids as it is in modern nautilids? Do recurrent structures such as late ontogenetic pre-terminal growth halts coincide with phases of reproduction and would thus indicate iteroparity? These questions are currently difficult to test scientifically, because the soft-part evidence needed to do it is missing. Nevertheless, it appears likely that the ammonoids were sexually mature at the time when growth had terminated and mature modifications of the shell had formed because this is the case in Recent Nautilida.

It might appear trivial, but we still want to point out that in most cases, only a couple of the criteria for maturity listed below will be fulfilled or visible in one specimen. It is also highly unlikely that all criteria will be met in a single specimen. This is due to the fact that in some species, some of these modifications were never realized and certain modes of preservation allow the recording of some characters while others are lost (e.g., Ruzhencev 1962, 1974; Davis et al. 1996).

In the following, we will briefly discuss the most important mature modifications that have become known. Naturally, this list will be incomplete, since many taxa may have formed their own unique adult shell morphology.

7.2.2.1 Septal Crowding

Septal crowding is potentially one of the most widely recognized and published mature modifications in ammonoids, which is reflected in an overwhelming number of publications in which this prominent feature is mentioned (e.g., Westermann

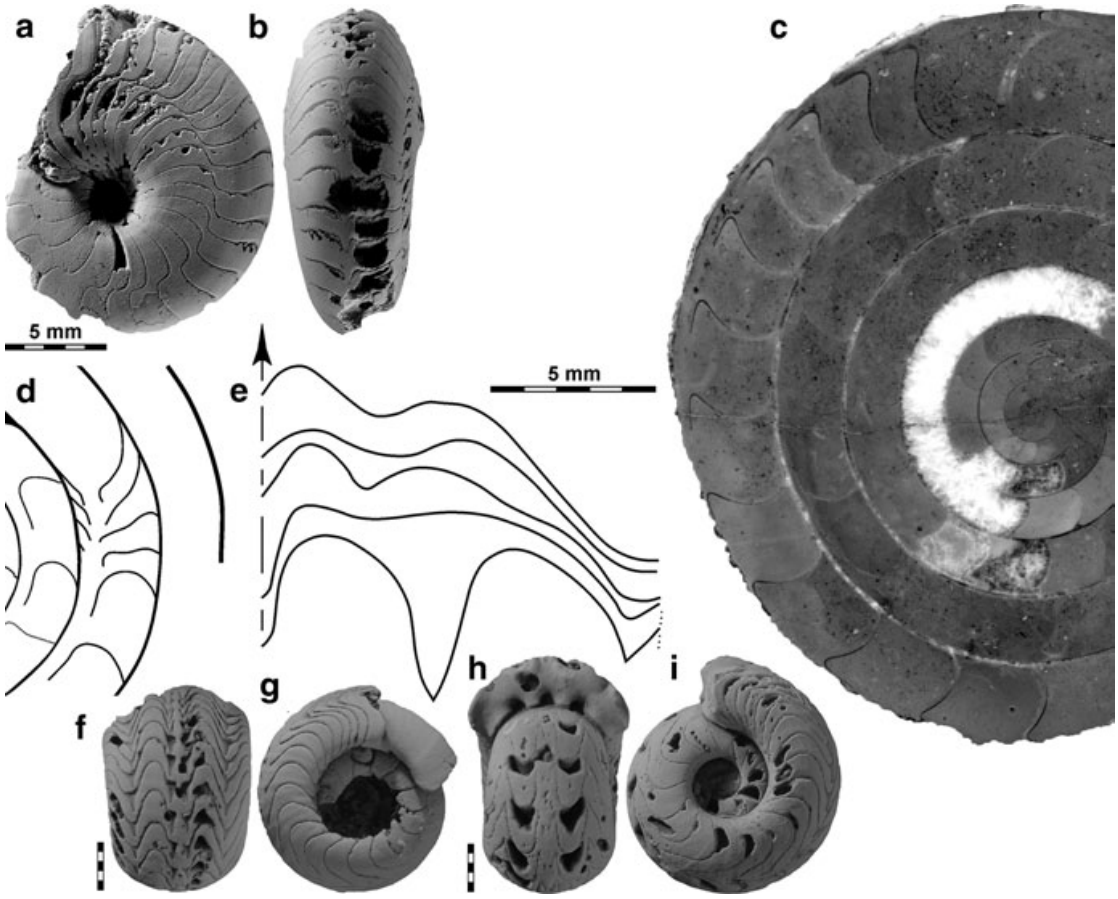

Fig. 7.1 Examples of septal crowding from the Devonian and Carboniferous. **a, b** *Pernoceras crebriseptum*, MB.C.9140.1, Milligan Canyon, Montana, US, lateral and ventral views; dm 24 mm. **c** *Sellanarcestes* sp., PIMUZ 28586, late Emsian, Oufrane, Morocco; dm 77 mm. **d**, **e** *Wocklumeria sphaeroides*, adult specimen, MB.C.9306.1, Bou Tlidat, Maïder, Morocco, from Ebbighausen and Korn (2007). **d** Septal section, note the change in septal angle and siphuncle position. **e** suture lines, note the extreme simplification (dm = 25 mm). **f–i**, *Ouaoufilalites creber*, S of Oued Temertasset, Algeria (from Korn et al. 2010). **f, g** ventral and lateral view of MB.C.18733.3. **h, i** ventral and lateral view of MB.C.18733.2

1971; Kulicki 1974; Zakharov 1977; Blind and Jordan 1979; Doguzhaeva 1982; Weitschat and Bandel 1991; Klug 2001, 2004; Ebbighausen and Korn 2007; Kraft et al. 2008). Septal crowding affects the distance of at least the last two septa (for nautilids, see, e.g., Willey 1902). This term applies to cases in which the distance between septa (best measured in angles) is reduced (Fig. 7.1). Such a reduction in septal spacing is, however, not only found in adult specimens but sometimes also in preadult ones (Korn and Titus 2006; Kraft et al. 2008 and references therein). Premature septal crowding can be caused by various factors, which can only rarely be identified. More than twenty septa might be more tightly arranged than the preceding ones (e.g., *Pernoceras crebriseptum* in Korn and Titus 2006), documenting a prolonged reduction of the growth rate near the termination of growth (Fig. 7.1). Nevertheless, septal crowding is a good indicator for adulthood when combined with other mature modifications.

7.2.2.2 Thickness of Septa and Sutural Complexity

In several ammonoids, septal thickness increases towards adulthood, mainly the last adult, crowded septa (Westermann 1971, p. 15, fig. 7.8), as in modern nautilids (Collins and Ward 1987). Furnish and Knapp (1966) reported a case of simplification of the terminal suture in Paleozoic forms. Davis et al. (1996) illustrated a *Texoceras* from the Permian of Texas, where the last sutures were not only approximated but the last suture also displays shallower lobes, which are less parabolic than the preceding ones. An impressive example has been illustrated by Ebbighausen and Korn (2007). In their fig. 7, they show the last few septa of a Late Devonian *Wocklumeria* (Fig. 7.1). In this genus, the normal septum displays some deep parabolic pointed lobes. These lobes are completely reduced in the last four septa, which are very strongly approximated and also show a strong change in inclination. This reduction (Fig. 7.1) in sutural frilling might be a consequence of the reduced space between two successive septa due to the limited forward movement of the soft body, which did not produce sufficient space to create lobes of similar length as in the preceding suture. Alternatively, the smaller chamber volume might have required a lower surface to remove the lesser amount of cameral fluid from the new chamber.

7.2.2.3 Change in Coiling and Whorl Cross Section

Many Paleozoic and Mesozoic ammonoids display a more or less strong change in coiling near the termination of growth (e.g., Trueman 1941; Parent 1997; Klug 2001; Klug and Korn 2003). In the earliest ammonoids such as *Metabactrites*, *Anetoceras* and *Erbenoceras*, the last whorl is usually more openly coiled than the preceding ones (e.g., De Baets et al. 2013a, b). One of the most common changes in coiling in planispiral ammonoids is the umbilical egression, i.e. the increase in the relative umbilical width close to adulthood. Lehmann (1981) dubbed this phenomenon "*retraction*". Conspicuous examples are found within Late Devonian Wocklumeriidae (Ebbighausen and Korn 2007), Middle Triassic Ceratitidae (e.g. Wenger 1957), Late Triassic Haloritidae (Mojsisovics 1882), Middle Jurassic Tulitidae (e.g., Hahn 1971; Zatoń 2008) and Late Cretaceous Acanthoceratidae (Kennedy and Cobban 1976).

The changes in coiling in the terminal whorl of Cretaceous heteromorphs range among the most conspicuous and thus most famous mature modifications. Many taxa formed a U-shaped terminal demi-whorl, which sometimes deviates from the coiling plane of preceding whorls. In the Late Cretaceous *Didymoceras*, the U-shaped part is separated from a helicospirally coiled preadult shell, whose coiling axis forms an angle of 60–90° to that of the terminal demi-whorl (e.g. Kennedy et al. 2000). In the Late Cretaceous *Pravitoceras*, the coiling direction changes in the opposite direction from the penultimate to the terminal demi-whorl (Matsunaga et al. 2008). In the Early Cretaceous *Hamulina* and *Heteroceras*, the U-shaped hook represents the largest part of the shell (Orbigny 1850).

Several evolutionary lineages independently produced small to medium sized forms, in which the terminal whorl is strongly elliptical or even forms a kink. For instance, the last whorl of the Late Devonian Prolobitidae is slightly elliptical and ends in a nearly straight shaft. Simultaneously, the umbilical wall closes the umbilicus (Walton et al. 2010 and references therein). The Permian *Hyattoceras* produced a similar shell form with the main difference being that the whorl forms a subtriangular cross section about 180° behind the terminal aperture (marked by a constriction), preceded and followed by a much more rounded cross section (Gemmelaro 1887; Davis 1972; Davis et al. 1969, 1996). A similar morphology evolved convergently in the Triassic families Haloritidae and Lobitidae (e.g., Mojsisovics 1882). In fully grown specimens of both groups, the last whorl is elliptical. Where the whorl height is largest, the whorl width is reduced and the whorl tapers towards the venter, while both before and after this short whorl segment, the venter is more or less broadly rounded. In the Jurassic, a couple of genera evolved comparable morphologies, but in these cases, they represent microconchs of less than 5 cm diameter and with strong apertural modifications (lappets). In the Middle Jurassic, all representatives of *Oecoptychius* display a strongly elliptical terminal whorl and some even form a distinct kink a demi-whorl posterior of the terminal aperture (Schweigert and Dietze 1998; Schweigert et al. 2003). *Cadomoceras* (Middle Jurassic; Schweigert et al. 2007), *Sutneria* (Late Jurassic; Parent et al. 2008a), and *Protophites* (Bert 2003) evolved quite similar changes in coiling in the terminal whorl.

Especially in Paleozoic forms, such a change in coiling is not always obvious. In such cases, adulthood/maturity is often reflected in more or less distinct changes in whorl expansion rate. For example, Devonian Anarcestidae commonly have a whorl expansion rate around 1.5. In the terminal whorl, the whorl expansion rate (Raup and Michelson 1965) increases to values around 2 (Klug 2001; Korn 2012). In the Devonian agoniatitids, the whorl expansion rate rises in the preadult whorls. When the specimen approached maturity, this increasing trend is inverted. At least for these Devonian ammonoids, the rule applies that forms with high whorl expansion rates show a terminal decrease while those with low whorl expansion rates display a terminal increase.

7.2.2.4 Changes in Ornament

A change in ornament near the terminal aperture is very common in ammonoids (e.g., Davis et al. 1996). Many show a decrease in ornament strength, especially as far as ribbing is concerned. This applies to such genera as Triassic *Ceratites*, Jurassic *Dactylioceras*, and Cretaceous *Acanthoceras* among many others. In some ammonoid taxa, the ornament became initially stronger and then smoothed directly behind the terminal aperture. In macroconchiate Jurassic perisphinctids, the preadult whorls sometimes carry rather closely spaced fine and sharp ribs, which more or less abruptly change into coarse and broad ribs on the last whorl (variocostation; e.g., *Crussoliceras*, *Lithacoceras, Perisphinctes*). Usually, however, the last 10–20° behind the terminal aperture are devoid of strong ribs and commonly display tightly spaced growth lines and/or lirae.

7.2.2.5 Terminal Apertural Constriction or Shell Thickening

A sudden reduction in the whorl cross section at the terminal peristome is very common in the Ammonoidea (e.g., Devonian: *Parawocklumeria*, *Wocklumeria*; Permian: *Agathiceras*, *Hyattoceras*; Triassic: *Arcestes*, *Lobites*; Jurassic: *Bullatimorphites*, *Cadoceras*; Cretaceous: *Baculites*, *Saynoceras*, *Scaphites*, *Valanginites*; e.g., Davitashvili and Khimshiashvili 1954; see Davis et al. 1996 for further examples). In some genera, this constriction is combined with a shell thickening or the terminal shell thickening may appear like a constriction in the internal mould (e.g., Devonian *Agoniatites*, *Manticoceras*; e.g., Klug 2001; De Baets et al. 2012).

7.2.2.6 Formation of Adult Apertural Modifications

Changes in the shape of the aperture (Fig. 7.2) are the most conspicuous mature modification. In some taxa, the undulation of the apertural margin with its projections and sinuses increased only slightly, while in others, this undulation became so extreme that long projections formed adjacent to the supposed ocular sinus. In microconchs of *Kosmoceras phaeinum*, these projections or lappets approached the diameter of the adult shell in length in some specimens (Arkell et al. 1957; Krimholc et al. 1958b; Makowski 1962; Callomon 1963). These extensions of the terminal peristome developed various shapes.

From the Paleozoic, only a few examples have become known. Davis (1972) and Davis et al. (1969, 1996) published Permian examples of *Adrianites* and *Hyattoceras* with strong projections at the terminal aperture. Zhao and Zheng (1977) introduced the Permian genus *Elephantoceras*, which is a small, globular form with strong ornament and long apertural lappets. Some Triassic Arcestidae carry strong ventrolateral or ventral projections (Mojsisovics 1882), while the ceratitids often lack strong lappets (e.g. Sun 1928).

Prominent lateral apertural lappets became common among Middle and Late Jurassic microconchs (Keupp and Riedel 2010). In the Haploceratoidea, several microconchs carry drop-shaped lappets, while in many Stephanoceratoidea and Perisphinctoidea, the lappets are rather straight and tongue-shaped (e.g., Zatoń 2008, 2010; Tajika et al. 2014). In *Oecoptychius*, the lateral lappets are hammer-shaped and combined with a ventral hemispherical projection (Schweigert and Dietze 1998; Schweigert et al. 2003, 2007). Another example has been discussed by Keupp and Riedel (2010): in the Middle Jurassic microconch *Ebrayiceras*, the lateral lappets are very large (half the size of the last whorl) and nearly fused with smaller ventrolateral lappets, thus forming oval ventrolateral openings.

Several groups produced more or less long ventral projections. For example, all species of the Early Jurassic Amaltheidae formed ventral projections when mature. In the Cretaceous, the genus *Mortoniceras* produced a more or less strongly curved midventral spine (Marcinowski and Wiedmann 1990; Amedro 1992).

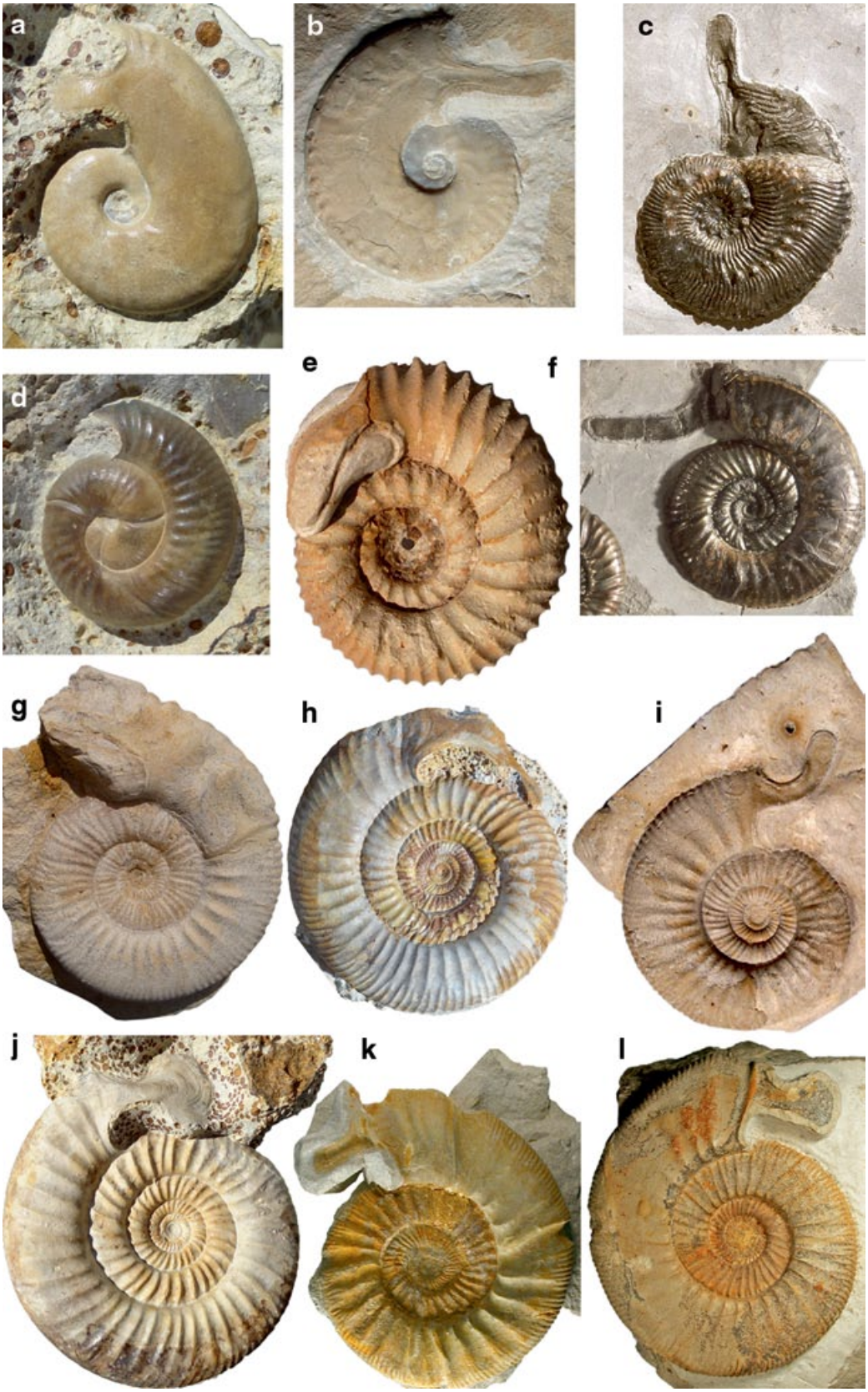

Fig. 7.2 Middle and Late Jurassic microconchs. **a** *Cadomoceras cadomense*, Bajocian. **b** *Paralingulaticeras lithographicum*, early Tithonian, Mörnsheim, Germany, dm ca. 50 mm. **c** *Kosmoceras* "*compressum*", Callovian. **d** *Neomorphoceras*, sp. Oxfordian. **e** *Normannites orbignyi*, Bajocian, Thorigné. **f** *Grossouvria* sp., Callovian. **g** *Indosphinctes* sp., Callovian, Pamproux, with three successive growth halts that all contain lappets. **h** *Cleistosphinctes* sp., Bajocian. **i** *Indosphinctes* sp.,

7.2.2.7 Muscle Scars

An increasing number of ammonoid species have become known for the preservation of muscle scars (e.g., Doguzhaeva 1981; Doguzhaeva and Kabanov 1988; Doguzhaeva and Mikhailova 1991, 2002; Doguzhaeva and Mutvei 1991, 1993, 1996; Tanabe et al. 1998; Kennedy et al. 2002; Richter 2002; Klug et al. 2008 Chap. 2.4). In most cases, the muscle scars became visible in specimens that were adult. This can be explained by the fact that in mollusks, the secretion of carbonate is commonly linked with muscle attachment, be it at the aperture or at muscle attachment sites. The longer the muscles stayed at the same place, the more carbonate was secreted, thus increasing the likelihood of its preservation. In preadult growth stages, the interim attachment sites apparently existed too briefly in one place to allow the deposition of a sufficient amount of aragonite to become visibly preserved. An additional bias might be the size of the specimen, although some small (probably adult) cheiloceratids (< 30 mm) have been reported (Richter 2002) that nicely show muscle attachment structures.

An illustrative example of sexual dimorphism in muscle scars, with connotations in soft-body organization, was described by Palframan (1969: text-fig. 11) from adult macro- and microconchs of *Hecticoceras brightii*. Besides the usual ventrolateral muscle scars in both dimorphs (Doguzhaeva and Mutvei 1991), the macroconchs have an additional ventrolateral scar behind the peristome. The microconchs also bear these additional scars but extended ventro-laterally and projected on the flanks until, at least, the umbilical shoulder.

7.2.2.8 Colour Pattern

Colour patterns are rarely preserved in ammonoids (e.g., Mapes and Davis 1996; Mapes and Larson 2015). Adult modifications of these patterns are even rarer. We are aware of only the one record already reported by Mapes and Davis (1996), namely Mapes and Sneck (1987), who described an *Owenites* in which the transverse color bands were more tightly spaced near the terminal aperture.

7.2.2.9 The Black Layer

The black layer is well-known from modern nautilids (Ward 1987). In shells of adult nautilids, a black chitinous layer less than 0.5 mm thick in the dorsal part of the shell extends beyond the apertural edge. It covers a tongue-shaped surface with an adult thickening, which is formed at the termination of growth. A similar black layer has been found in various ammonoids (Fig. 7.3), including e.g., Devo-

Callovian, Pamproux, with bent lappet. **j** *Bigotites* sp., Bajocian. **k** *Parataxioceras latifasciculatum*, middle Kimmeridgian, Gräfenberg, Germany, dm ca. 145 mm. **l** *Parataxioceras* cf. *lothari*, middle Kimmeridgian, Geisingen, Germany, dm ca. 100 mm. **a, d, h, j** Ste. Honorine Des Pertes, France, col. C. Obrist. B, K, L, col. V. Schlampp. C, F, Aichelberg, Germany, from Dietl (2013). E, G, I, col. P. Branger

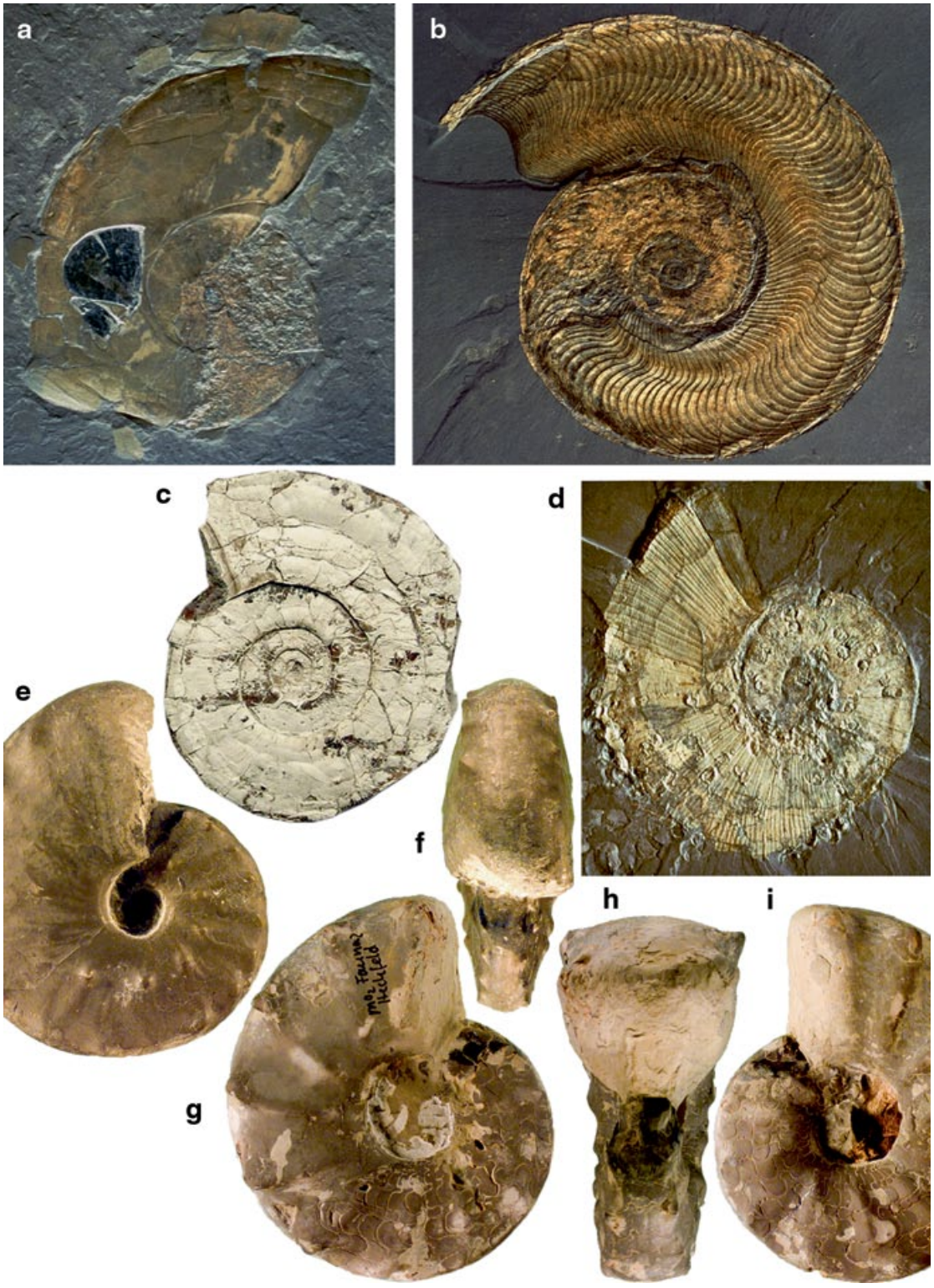

Fig. 7.3 Black layer and black band in Mesozoic ammonoids (**a–d** from Klug et al. 2007; **e–i** from Klug et al. 2004). **a** *Phylloceras heterophyllum*, SMNS 26462, tenuicostatum Zone, Ohmden, Germany; dm 87 cm. Note the jaws and the black band. **b** *Harpoceras falciferum,* falciferum-bifrons Zone, Holzmaden, dm 24 cm. **c** *Psiloceras planorbis*, PIMUZ 6519; planorbis Zone, Hettangian, Blue Anchor, Somerset, UK, dm 45 mm. Note the black band and black layer. **d** *Lytoceras ceratophagum,* SMNS 26465; falciferum Zone, Toarcian, Ohmden, Germany; dm 41 cm. **e, f** *Paraceratites atavus*, lateral and dorsal views, SMNS 24503, atavus Zone, Neckarrems, col. M. Warth; dm 61 mm. **g–i**, *Ceratites spinosus*, lateral and dorsal views, SMNS 25255–33, spinosus Zone, Heckfeld; dm 102 mm. Images: **a, b** Staatliches Museum für Naturkunde Stuttgart. **d** Urweltmuseum Hauff. **c** T. Galfetti. **e–i** W. Gerber

nian gephuroceratids (Keupp 2000), Triassic ceratitids (Klug et al. 2004), as well as Jurassic ammonites (Klug et al. 2007) and is considered as either homologous or convergent with the structure in nautilids. Of the criteria of homology, only those of position and specific structure are fulfilled, since transitional states are missing (Klug et al. 2004). Nevertheless, it is likely that the anterior edge of the black layer served for the attachment of the dorsal mantle.

7.2.2.10 The Black Band

The black band is a thin organic coating on the shell, which forms a narrow band surrounding the adult aperture in some cephalopods; it is sometimes found in modern nautilids (Ward 1987) and rarely in ammonoids (Klug 2004; Klug et al. 2007). Like the black layer, it is black due to its melanin content. So far, it has been found in *Psiloceras*, *Phylloceras*, *Lytoceras*, and *Harpoceras* from the Early Jurassic (Fig. 7.3) and two questionable specimens from the Triassic (Klug 2004; Klug et al. 2007). It is apparently linked with the adult cessation of growth and in modern nautilids, the black band has been recorded from adult females, although not all individuals appear to develop this structure. Like the black layer, the black band is probably also linked with mantle attachment at the aperture.

Davis (1972), summarized in Davis et al. (1996, p. 469), found indications for "*an actual change in the nature of shell deposition late in ontogeny*". Accordingly, the shells of adult *Adrianites* and other Permian ammonoids displayed small "*pits in the internal mold*". Davis et al. (1996) suggested that these structures are possibly homologous to the apertural attachment of the mantle at the black band in mature modern nautilids.

7.2.2.11 The Wrinkle Layer

The wrinkle layer is a structure of uncertain function that occurs in a number of ammonoids in the form of irregular shell wrinkles in the dorsal part of the shell, usually near maturity (Barrande 1877; House 1970; Walliser 1970; Senior 1971; Doguzhaeva 1981; Kulicki et al. 2001). Strength of the wrinkle layer is a character that is rarely preserved and thus of limited use. The wrinkle layer is predominantly found in nearly adult or fully mature specimens (Korn et al. 2014). Kulicki et al. (2001) already pointed out that the wrinkle layer might be comparable or even homologous to the black layer of nautilids.

7.2.3 Constructional and Functional Morphology

Some of the mature modifications of ammonoid shells are so profound that it is hard to imagine that the altered adult morphology did not affect the life style of the ammonoid and thus their evolution. Recurrent morphologies (such as convergent

evolution of apertural lappets) support this hypothesis. Several suggestions have been made with regard to functional as well as constructional interpretations of the modified adult morphology (Tajika et al. 2014): (1) change of habitat (Davis et al. 1996); (2) defense against predators (Keupp and Riedel 2010); (3) sexual display (Keupp and Riedel 2010); (4) attachment of reproductive organs (a modified arm; Landman et al. 2012); (5) change in locomotion/behavior (Klug 2001); (6) fast and metabolically economic construction of the terminal shell segment; (7) fabricational noise with a lack of function (Seilacher 1974).

(1) The change of habitat did possibly occur since the relative abundance of macroconchs or microconchs varies between localities. Especially in such cases with a large difference in adult size, it might have been important that the sexes stayed separate until the time of mating in order to reduce the time of exposure to potential "*sexual*" cannibalism (Hanlon and Forsythe 2008; Keupp and Riedel 2010). Nevertheless, this hypothesis is difficult to test.

(2) Many ammonoid species reinforced their terminal apertures by shell thickenings (e.g., *Agoniatites*, *Arcestes*, *Manticoceras*). Even constrictions without shell thickenings might have increased the resistance of the aperture against breakage by predators (Landman and Waage 1986; Keupp and Riedel 2010; Keupp 2012). It is, however, not possible at this point to test whether these modifications are effects of the terminal deceleration of growth or whether they represented antipredatory adaptations. Seilacher (1974) argued against such a function in the microconchs because in his opinion, such defensive structures would be more meaningful in the females.

(3) and (4) are nice ad hoc hypotheses and are difficult to test, especially with the lack of knowledge of the soft parts in general and the reproductive organs in particular. The extreme differences between some antidimorphs (especially *Phlycticeras* and *Oecoptychius*) suggest a comparison to the modern octobrachian *Argonauta*, in which the male measures only 2 cm in length, while the female may reach over 40 cm, when the shell is included. The male of *Argonauta* has a modified arm (hectocotylus), which is stored in a ventral sac prior to mating. This structure is somewhat reminiscent of some of the apertural modifications. Landman et al. (2012) hypothesized that ammonites with a high aperture angle had this type of arm to improve mating efficiency. Nevertheless, direct evidence for such a convergence is still missing.

(5) Klug (2001) showed that the whorl expansion rate in Middle Devonian ammonoids changed close to the cessation of growth. He argued that this change in whorl expansion rate was linked to a change in body chamber length, which, in turn, caused a change in the *syn vivo* orientation of the shell. In the main lineages of Devonian ammonoids, the adult aperture would have moved to a more horizontal position than in preceding growth stages (see also Korn and Klug 2002; Klug and Korn 2004). The latter authors concluded that this change in shell orientation improved mobility and manoeuvrability, both valuable traits to find a mating partner and good spawning grounds.

Tajika et al. (2014) empirically tested the effect of apertural lappets in the Middle Jurassic *Normannites* and found that absence or presence of these lappets would not

have altered the shell orientation significantly. Therefore, these lappets most likely did not serve the function of altering the shell orientation.

(6) Microconchs of the Haploceratoidea and Perisphinctoidea produced a pair of lateral projections or lappets in the peristome (Fig. 7.2), and most frequently their body chambers are shorter than those of macroconchs. Thus, the pair of lappets could be interpreted as the terminal shell segment for accommodating the cephalic portion of the animal. This "*shell segment*" could have been secreted rapidly and economically considering the low amount of aragonite necessary compared to a complete "*tubular*" shell segment. The muscle scars around the peristome of the haploceratoid *Hecticoceras brigthii* (see above; Palframan 1969) would indicate additional muscle development providing for support and mobility of the cephalic portion of the body.

7.3 Dimorphism

As far as the history of research on ammonoid dimorphism is concerned, we only want to mention briefly that de Blainville (1840) and d'Orbigny (1847, p. 441) were probably the first to discuss sexual dimorphism in ammonoids (see also Foord and Crick 1897; Haug 1897). In any case, broader interest in the topic grew in with the important monographs of Makowski (1962) and Callomon (1963).

Commonly, there is a smaller and a larger form in those taxa in which dimorphism is more apparent due to clear differences combined with equally visible shared juvenile characters. For these, Callomon (1955) introduced the widely used terms microconch and macroconch, respectively. These are called antidimorphs.

7.3.1 Monomorphism, Dimorphism, and Polymorphism

Adults of the two sexes of any given animal species may have similar or different shapes. If they are monomorphic, there is no significant difference in adult shape. In the case of dimorphism, two different adult morphologies can develop from morphologically similar juveniles (Davis 1972). In ammonoids, these are traditionally called microconchs (for the smaller variant) and macroconchs for the larger variant. The corresponding pairs are named antidimorphs. In the case of polymorphism, there are more than two (usually three or more) different adult morphologies. Polymorphism in modern biology refers to natural genetic variation (with phenotypic expression or not), undetectable in fossils; here, we use the term to refer to morphological differences between supposed conspecific phenotypes, which could have either a genetic or an environmental cause (compare De Baets et al. 2015a).

As did our forerunners (Davis et al. 1996), we will not repeat all details of the research on dimorphism from its beginnings in the nineteenth century (de Blainville

1840; Orbigny 1847). Instead, we recommend looking up these details in the excellent monographs by Makowski (1962) and Callomon (1963).

There are numerous articles dealing with polymorphism (McCaleb and Furnish 1964; McCaleb et al. 1964; Ivanov 1971, 1975, 1985; Kant 1973; Hirano 1978, 1979; Matyja 1986, 1994; Makowski 1991; Melendez and Fontana 1993). According to these authors, some Jurassic and Cretaceous ammonoids produced more than two forms. After Ivanov (1971, 1975, 1985) had dubbed exceptionally large forms "*megaconchs*", Matyja (1986, 1994) introduced the term "*miniconchs*" for exceptionally small specimens. He suggested that certain environmental parameters controlled the point of maturation, inducing monomorphism, dimorphism or polymorphism. In his work on modern coleoids, Mangold-Wirz (1963), Mangold-Wirz et al. (1969), as well as Mangold (1987) demonstrated how hormones produced by the optic gland can control the timing of maturation and thus size depending on the developmental state of the gonads. It was also demonstrated for Recent coleoids in captivity that environmental factors such as light intensity, temperature or food availability can have an effect on maturation and therefore adult size (e.g., Gabr et al. 1998; Moltschaniwskyj and Martínez 1998; Tafur et al. 2001; Jackson and Moltschaniwskyj 2002). Callomon (1988) criticized Matyja's ideas about polymorphism, suggesting that a larger database would be needed to test some of his hypotheses (see also De Baets et al. 2015a). Later, Dzik (1990a), analysing a rich collection of Callovian *Quenstedtoceras* ammonites from the classic locality at Łuków in eastern Poland, did not find any evidence for polymorphism.

7.3.2 Classification of Dimorphism

Bearing in mind the vast diversity and impressive variability of ammonoids, it is not surprising that dimorphism is far from uniform within this group. Consequently, various authors have attempted to meaningfully classify ammonoid dimorphism. In his pioneer monograph, Makowski (1962) introduced two kinds of dimorphs. In Type A, the microconch has five (four) to six whorls and the macroconch has seven (six) to nine whorls. Type B microconchs have seven (six) to nine whorls and the macroconchs have one additional whorl. Guex (1968) added Type O, where the microconch has three to four whorls.

Westermann (1964a) and Houša (1965) also differentiated between two types of dimorphism, where one type differs only in size, while the other differs in size and other characters, especially in the shape of the peristome. Zeiss (1969) added a third group to these two, in which dimorphism was not recognized. This leads to the question, whether dimorphism is the rule and that it only can sometimes not be identified due to taphonomic processes (loss of soft-tissues and subtle conch characters). In that case, a lot of work would await ammonoid researchers, because many more cases of dimorphism would await their detection.

7.3.3 Criteria for Dimorphism

In order to verify the hypothesis of conspecificity of two or more different adult forms, the following criteria (Makowski 1962; Callomon 1963, 1981; Westermann 1964a; Davis 1972; Davis et al. 1996) should be fulfilled:

1. The antidimorphs should differ in adult morphology;
2. They should have more or less identical early developmental stages;
3. They should occur in strata of the same stratigraphic range;
4. They should have overlapping geographic occurences;
5. They should have the same ancestors;
6. The ratio of numbers of micro- to macroconchs should be about the same through time and throughout the evolution of their clade.

Most ammonoid workers would agree on points (1) and (2). However, a few exceptions exist. McCaleb (1968) stated that in the Late Carboniferous *Syngastrioceras oblatum*, the morphological differences between macro- and microconch are larger in juvenile/preadult growth stages than in the mature stage/the last whorl. Similarly, Rein (2001, 2003) suggested that species of the Middle Triassic genus *Ceratites* show a similar morphological separation of the antidimorphs. He introduced the terms E- (referring to the smooth species *C. enodis*) and P-morph (referring to the strongly ornamented species *C. posseckeri*) for forms with smooth or strongly ornamented preadult whorls. Although further work on this issue would be welcome, we would like to point out that the coiled shells of many mollusks display the highest degree of intraspecific variability in preadult whorls (e.g., Urdy et al. 2010a, b; De Baets et al. 2015). Therefore, the question arises whether these two exceptions, where supposedly the middle whorls differ in antidimorphs instead of the adult morphology, are artifacts from normal intraspecific variability (Urlichs 2009).

Davis et al. (1996) pointed out that differences in geographical occurrences (point 4) of the antidimorphs would not be surprising since their differing morphologies might reflect differing ecological requirements. This might hold true for parts of their life but at least at some point, males and females had to meet in order to reproduce. It is still conceivable that the intersexual differences in behaviour and habitat varied between species, when the extreme differences in dimorphism throughout the ammonoid clade are taken into account.

For various reasons, the morphologic evolutionary rates among the microconch part of a lineage may seem (1) higher (Lehmann 1981; Davis et al. 1996) or (2) lower (e.g., Callomon 1969, Westermann and Riccardi 1979: p. 134) than those of the macroconchs. In the first case, this might be a primary signal, i.e. the microconchs evolved morphologically faster because the mature modifications were directly prone to sexual selection or of great importance for reproduction. Alternatively, this seeming difference in evolutionary rates might be an artifact because the microconchs might attract more attention due to their peculiar morphology, or because evolutionary change is easier to track in microconchs since they display more distinct morphological character states. In any case, these differences in mor-

phological evolution between antidimorphs may hamper evolutionary studies. In studies of dimorphism, it is important to know the phylogenetic framework of the ammonoid lineage under consideration (point 5), because this knowledge optimally contains information on the development of ancestors and other members of the clade, as well as plesiomorphies and degrees of conservativeness of traits. Finally, this phylogenetic test is needed to falsify the hypothesis that the antidimorphs under consideration indeed belong to two separate species.

In the second case, the slower morphologic evolutionary change of the microconchs with respect to the macroconchs produced the opposite pattern, like a morphological stasis of the males. This pattern is produced in lineages where the main morphologic changes developed in the subadult and/or adult ontogeny of the macroconchs. The microconchs typically stop their growth in the early ontogeny of the species, thus not reflecting the changes seen in the macroconchs.

Of course, there may be traits that are not preserved or only rarely or poorly preserved, which could potentially be used to discriminate between antidimorphs, where shell characters alone do not suffice. Till (1909, 1910) searched for dimorphic characters in the jaws, while Parent et al. (2013, p. 32) found evidence of sexual dimorphism in the aptychus (*Praestriaptychus*) of *Lithacoceras* [M]/*Silicisphinctes* [m]. Mapes and Sneck (1987) found two kinds of colour patterns in *Owenites*. Nothing is known about differences in the soft part anatomy between the antidimorphs and we can only hope that one day, exceptionally preserved soft-tissue ammonoids will be discovered, shedding more light on the internal organisation of ammonoids.

7.3.4 Sexing of Ammonoid Antidimorphs

For some, sexing of ammonoid shells seems a trivial task and it happens quite commonly that the microconch is automatically considered the male. This confidence is surprising because the ultimate evidence, namely soft-tissue preservation of reproductive organs in the antidimorphs, is still missing. The background for this slightly premature conclusion is probably the actualistic comparison with some Recent octobrachians. In *Argonauta*, which was already mentioned above, the size differences are just as striking as in *Ocythoe tuberculata*, where the female is 1 m long and so ten times as long as the male (Makowski 1962; Wells 1962, 1966; Mangold-Wirz 1963; Westermann 1969a; Mangold-Wirz et al. 1969; Roper and Sweeney 1975). By contrast, the male is slightly larger in Recent Nautilida (Willey 1895, 1902; Saunders and Spinosa 1978; Saunders and Ward 1987; Hayasaka et al. 1987), but they have a different reproductive strategy. Remarkably, aptychi have been interpreted as protecting the nidamental glands (Keferstein 1866) and Siebold (1848) even suggested that the aptychi were the micromorphic males. Nowadays, there is not much doubt that the aptychi were part of the buccal apparatus and had nothing to do with reproduction.

Numerical ratios between the antidimorphs were another line of evidence that has been explored to assign sexes to each of them. Davis et al. (1996) gave an overview

of the contradicting results of various authors who worked on ammonoids or on Recent cephalopods (Willey 1902; Coëmme 1917; Pelseneer 1926; Mangold-Wirz 1963; Makowski 1962; Mangold-Wirz et al. 1969; Westermann 1969a; Saunders and Ward 1987; Hayasaka et al. 1987). In ammonoids, the results are biased by the fact that the numerical ratios are influenced by facies and taphonomy (e.g., Callomon 1981, 1985). The most plausible line of reasoning appears to be that of Lehmann (1981), who inferred that the macroconchs were the females because the maturation of eggs takes longer than that of spermatophores, implying a longer lifespan and thus a larger adult size. Moreover, reproductive organs of females (e.g., ovaries, nidamentary glands) are often larger than the simpler reproductive organs of males.

Ammonoid eggs have been reported by several authors (Lehmann 1966; Müller 1969; Zakharov 1969; Maeda 1991; Urlichs 2009; Etches et al. 2009; Landman et al. 2010; Klug et al. 2012). In spite of these findings, there is as yet no report of a discovery of eggs within an ammonoid shell that is free of doubt (De Baets et al. 2015b). Either the preservation is insufficient to detect whether they are truly ammonoid eggs or it is unclear if such an egg mass is really *in situ* within the ammonoid.

7.3.5 Development and Dimorphism

To detect dimorphism in ammonoids, knowledge of their ontogeny is needed (see the criteria for dimorphism). Developmental heterochronies have been suggested as processes generating the differences between the antidimorphs (Gould 1977; Shea 1986). Davis et al. (1996) discussed whether microconchs were accordingly progenetic and/or hypomorphic (Landman et al. 1991; Neige 1992).

In any case, many antidimorphs display a congruent pattern of development of various shell parameters, which diverge at some point with the microconchs maturing and stopping growth at a size-wise earlier point (e.g., Makowski 1962; Guex 1973; Parent 1997; Parent et al. 2008b, 2009).

Plotting certain shell parameters throughout ontogeny (versus diameter) is an important and powerful method to demonstrate dimorphism. The graphs in Fig. 7.4 illustrate some of the patterns and features discussed above from a moderately large sample of the Early Callovian sphaeroceratid *Eurycephalites gottschei*. The growth rate measured by the relative whorl ventral height is dimorphic (Fig. 7.4a upper) with an increase in both dimorphs up to about 10 mm diameter, after which both dimorphs inverted the trend; from a diameter of about 18 mm onward, the microconch diverged by increasing the rate of growth towards the peristome (Parent 1997). The shape of the whorl cross section changed strongly during growth, but the ontogenetic trajectory is the same in micro- and macroconchs, i.e., monomorphic (Fig. 7.4a bottom). The ventral ribbing is another feature that is dimorphic with a similar trend to that found in the growth rate (Fig. 7.4b). The microconch trend diverged from a diameter of 18 mm compared to that of the macroconch, which is taken as the standard.

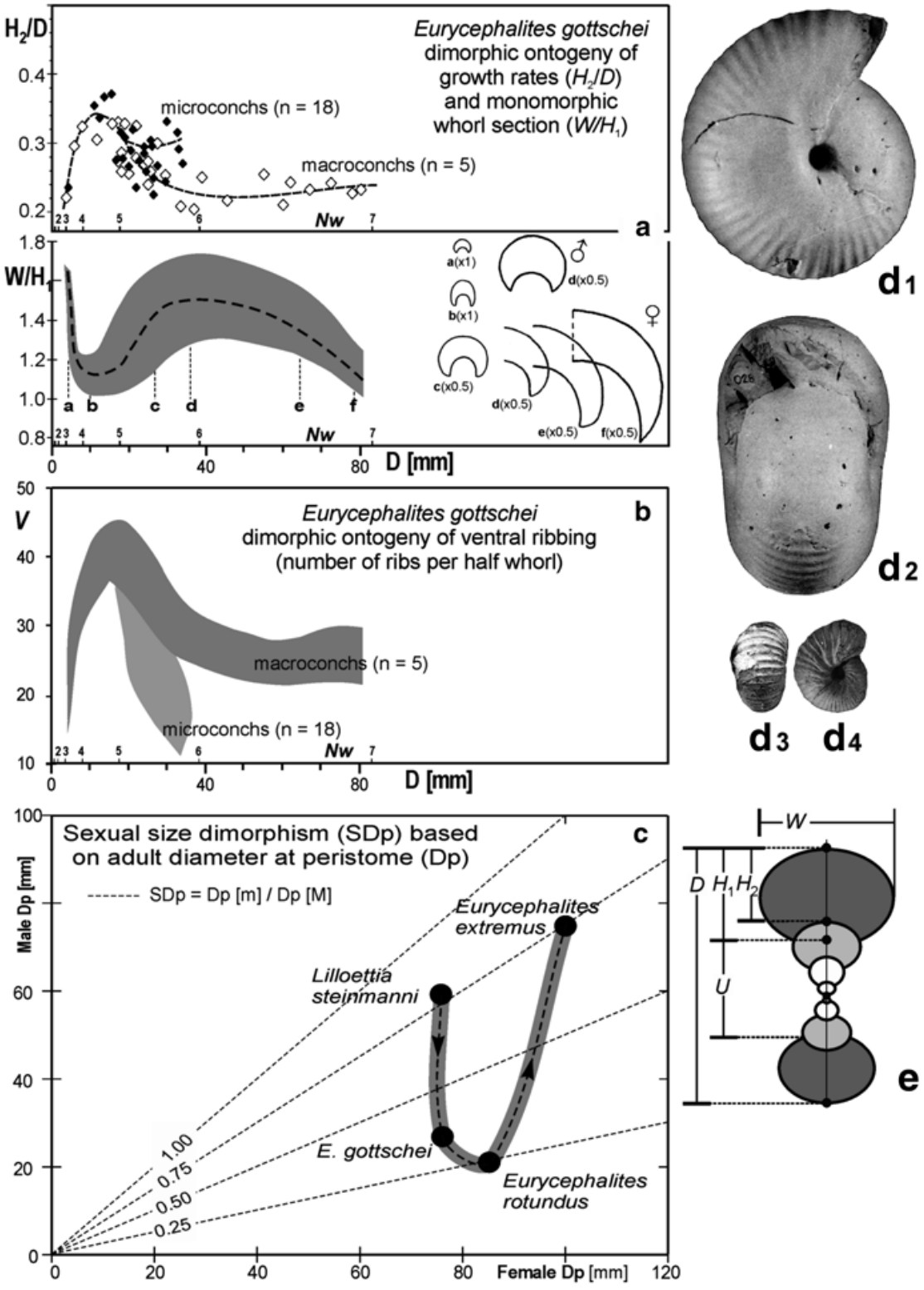

Fig. 7.4 Dimorphism of *Eurycephalites gottschei* (Tornquist 1898) [Sphaeroceratidae]. **a** (*upper*): dimorphic ontogeny of the growth rate measured as H_2/D versus diameter (*D*) and whorl number (*Nw*); **a** (*lower*), monomorphic ontogeny of the whorl section measured by W/H_1 versus *D* and *Nw* (*grey area*) and selected cross-sections (**a–f**). **b** dimorphic ontogeny of ventral rib number per half whorl (V) versus *D* and *Nw*. **c** evolution of the sexual size dimorphism in the lineage *Lilloettia* (late Bathonian)—*Eurycephalites* (Early Callovian). **d** dimorphic pair, a complete adult macroconch (**d_1–d_2**) and an adult microconch (**d_3–d_4**), both x0.4. **e** shell size dimensions. **a–b, d–e** modified from Parent (1997). **c** from data in Parent (1998)

7.3.6 Evolution of Dimorphism

Evolution of sexual dimorphism is a complex and interesting aspect in ammonoid paleobiology. However, it is also very demanding with respect to material and raw data. One of the most detailed studies is that of Schweigert and Dietze (1998) for the evolution of *Phlycticeras/Oecoptychius*. Sexual size dimorphism, the feature more readily captured by the observer, shows important changes during the evolution of many ammonoid lineages. One of them is the lineage *Lilloettia* (Late Bathonian)-*Eurycephalites* (Early Callovian), which shows important changes in the ratio of the adult micro- versus macroconch size (Fig. 7.4c), ranging from microconchs of three-quarters (*L. steinmanni* and *E. extremus*) to one third (*E. gottschei* and *E. rotundus*) the size of the macroconch.

7.3.7 Occurrences of Dimorphism

From the Hettangian onwards, Guex (1981) stated that, except for the phylloceratids, the majority of ammonites do show dimorphism. It thus appears that at least in the Jurassic and Cretaceous, whether dimorphism is detected or not largely depends on quality and quantity of the material plus the motivation of a researcher to quantitatively analyze an ammonite lineage. Presuming that the dimorphism of ammonoids really represents the different sexes, a more or less omnipresent dimorphism appears not so surprising, especially because most modern cephalopods also show more or less strong dimorphism.

In contrast to the work of Davis et al. (1996), we will not list mature modifications in great taxonomic detail in the text below, because it appears that the majority of ammonoids actually did undergo some kind of terminal growth and thus produced mature modifications. It is striking that strong apertural modifications became common only in the Jurassic, although a few Permian species (Zhao and Zheng 1977), as well as some Paleozoic nautilids (e.g., Dzik 1984) did produce strong apertural appendages.

7.3.7.1 Palaeozoic Dimorphism

Devonian: For the earliest, loosely coiled ammonoids, De Baets et al. (2013a) tested for sexual morphism in Moroccan *Erbenoceras* and *Anetoceras* and found no clear indication of it. It could be argued that dimorphism might be camouflaged in the strong intraspecific variability (Kakabadze 2004 discussed dimorphism in relation to variability) of this group, but among these two genera, the intrageneric and probably also intraspecific variability is markedly reduced toward the end of growth. Not much has been published on Devonian dimorphism after Makowski (1962) had listed several cases (Table 7.1). Walliser (1963) only shortly mentioned its existence without any detail. Later, Makowski (1991) determined the relative abundance of

Table 7.1 Sexual dimorphism in Devonian to Triassic ammonoids

Superfamily	Family	Genus	Age	Source
Tornoceratoidea	Tornoceratidae	*Tornoceras*	Famennian	Makowski 1962
Cheiloceratoidea	Cheiloceratidae	*Cheiloceras*	Famennian	Makowski 1962
	Gephuroceratidae	*Manticoceras*	Frasnian	Makowski 1962
Ceratitoidea	Acrochordiceratidae	*Acrochordiceras*	Anisian	Dzik 1990b
	Ceratitidae	*Ceratites*	Anisian, Ladinian	Müller 1969; Rein 2001, 2003; Urlichs 2009

micro- versus macrococonchs in various species of *Tornoceras*. In *T. frechi parvum,* he found 28 % macroconchs ($n = 95$), in *T. subacutum* there were 47 % macroconchs ($n = 65$), and in *T. sublentiforme*, macroconchs varied between 40 % ($n = 133$) and 45 % ($n = 95$).

Most authors have focused on descriptions of adult modifications (Table 7.2; e.g., Ruzhencev 1962; Korn 1992). Septal crowding has been mentioned commonly (e.g., Korn and Titus 2006; Ebbighausen and Korn 2007; Kraft et al. 2008), elliptical coiling is common in some clymeniids (e.g., Ebbighausen and Korn 2007), increasing umbilical width is characteristic for the earliest, loosely coiled ammonoids (e.g., De Baets et al. 2013a, b), and, of course, changes in ornament spacing have been documented (Fig. 7.5).

Carboniferous: Remarkably, we have not found an unequivocal report on ammonoid dimorphism in the Carboniferous (Nettleship and Mapes 1993). Davis et al. (1996) mentioned the work of Trewin (1970), who suggested that *Eumorphoceras* produced antidimorphs, but he used poorly preserved materials. Frest et al. (1981) examined Late Pennsylvanian *Maximites oklahomensis* and found that 40 % of the examined specimens belonged to "*form a*", which might be the macroconch according to its less strong adult modifications (Davis et al. 1996).

In some taxa, a strong wrinkle layer was secreted when the specimen approached maturity (Korn et al. 2014 and references therein). Septal crowding is also not rare (e.g. Korn et al. 2010), although we have to repeat that its value to determine maturity is limited (Kraft et al. 2008). Umbilical egression (Fig. 7.5; e.g., Frest et al. 1981) and other changes in coiling (e.g., Ruzhencev 1962) also occur in Carboniferous forms, which are visible in some of the cross sections figured in Korn et al. (2010). Ruzhencev (1962) illustrated *Dombarites*, *Homoceras*, and *Praedarelites*, which formed ventral keels near maturity.

Permian: Although many Permian ammonoids are known to have formed distinct mature modifications (Table 7.3, Fig. 7.5; Miller and Furnish 1940; Miller 1944; Ruzhencev 1962; Davis 1972; Zhao and Zheng 1977; Frest et al. 1981; Zhou 1985; Schiappa et al. 1995), not much has been published, suggesting the presence of dimorphism of the shell. Davis et al. (1969, 1996) and Davis (1972) counted the specimens of Permian *Agathiceras uralicum* and found 75 % macroconchs ($n = 110$). Table 7.3 lists mature modifications (modified from Davis et al. 1996).

Table 7.2 Mature modifications in Devonian and Carboniferous ammonoids

Taxon	Coiling	Constrictions	Ornament	Whorl section	Wrinkle layer	Septal crowding	Suture simplified	Reference
Anetoceratidae								
Anetoceras	●		●			●		De Baets et al. 2013a, b
Erbenoceras	●		●			●		De Baets et al. 2013a, b
Anarcestidae								
Sellanarcestes	●			●		●		Klug 2001
Agoniatitidae								
Agoniatites	●	●	●			●		Klug 2001
Gephuroceratidae								
Manticoceras	●	●						Korn and Klug 2007
Prolobitidae								
Prolobites	●	●	●	●		●		Bogoslovsky 1969
Wocklumerioidea								
Wocklumeria	●	●				●	●	Ebbighausen and Korn 2007
Kamptoclymenia	●	●	●					Schindewolf 1937
Pericyclidae								
Oaoufilalites	●					●		Korn and Ebbighausen 2008
Maxigoniatitidae								
Maxigoniatites	●				●			Korn et al. 1999
Girtyoceratidae								
Calygirtyoceras	●							Korn et al. 1999

Since the account of Davis et al. (1996) appeared, not a lot of new data have been published and it appears that these are still insufficient to analyze evolutionary trends in Paleozoic dimorphism. Accordingly, McCaleb's (1968, p. 29) statement that "*dimorphism is a predominant feature at the inception of an evolutionary lineage and decreases through phylogeny*" appears premature at best, if not wrong.

7.3.7.2 Triassic Dimorphism

Davis et al. (1996) listed mature modifications in Triassic ammonoids in relation to their shell shape (Table 7.4, Fig. 7.6). This information is summarized in Table 7.4. In spite of the sometimes quite conspicuous adult modifications and the incredible diversity as well as morphological disparity of Triassic ammonoids, reliably dem-

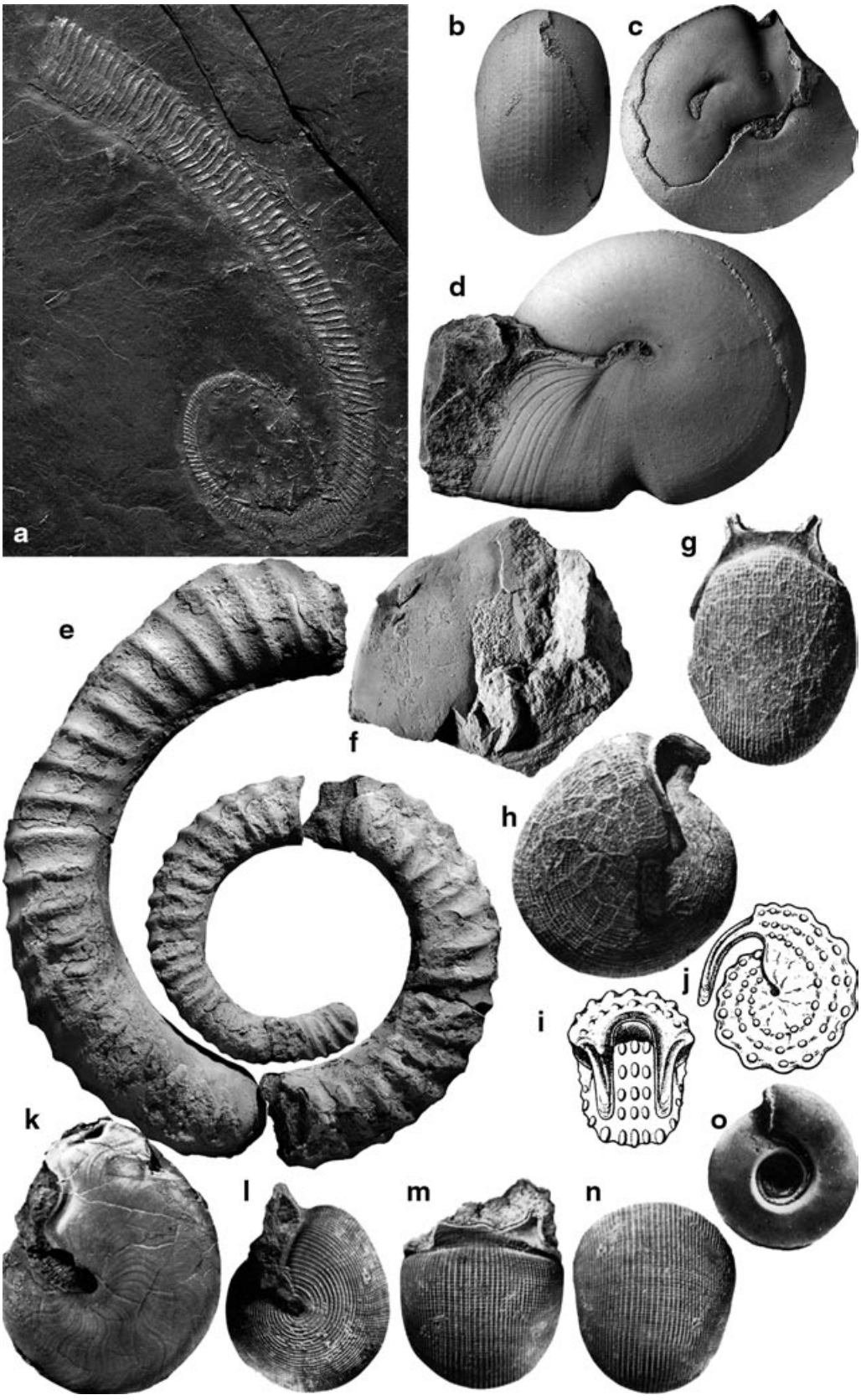

Fig. 7.5 Paleozoic mature modifications. **a** *Metabactrites fuchsi*, PWL2010/5251-LS, middle Kaub Formation, Hunsrück, Bundenbach, from De Baets et al. (2013b), dm 80 mm. Note the changes in coiling and ribbing. **b**–**d** *Prolobites aktubensis*, col. Ademmer, Kattensiepen, Germany,

Table 7.3 Mature modifications in Permian ammonoids. (modified after Davis et al. 1996)

Taxon	Coiling	Constrictions	Ornament	Lappets	Whorl section	Wrinkle layer	Thick septum	Septal crowding	Suture simplified
Adrianitidae									
Adrianites	●	●		●	●	●			
Crimites	●	●			●				
Epadrianites	●	●							
Hoffmannia	●	●	●		●				
Neocrimites	●	●	●	●					
Palermites	●	●		●	●				
Pseudagathic	●	●	●						
Sizilites	●	●	●		●				
Texoceras	●	●				●			●
Cyclolobidae									
Cyclolobus	●	●		●	●				
Mexicoceras	●	●			●		●		●
Waagenoceras	●	●			●	●		●	●
Hyattoceratidae									
Hyattoceras	●	●	●		●				
Marathonitidae									
Marathonites	●	●			●				
Pseudovidrioc		●	●		●				●
Vidrioceratidae									
Peritrochia		●		●					
Stacheoceras	●	●		●	●				
Agathiceratidae									
Agathiceras	●	●	●	●	●				
Pseudohaloritidae									
Elephanticeras		●	●	●					
Sangzhites	●	●	●	●	●				
Shangraoceras	●	●		●	●				

from Korn and Klug (2002). **b**, **c** SMF 34694. lateral and ventral view; note the elliptical constriction (internal shell projection) and the strong subterminal constriction; dm 21 mm. **d** SMF 34691; note the change in coiling, lirae spacing and the constriction; dm 28 mm. **e** *Erbenoceras advolvens*, early Esmian, Tafilalt, Morocco, from De Baets et al. (2013b); dm 156 mm; note the change in coiling. **f** *Fidelites* sp., GPIT 1862-133, *costatus* conodont Zone, Eifelian, Tafilalt, Morocco; with broad terminal constriction, from Klug (2001). **g–l** Permian ammonoids from Davis et al. (1996). **g**, **h** *Adrianites* sp., lateral and ventral views, GIUA Drawer 55, T328, Maoen Mollo, Timor, Indonesia, dm 26 mm. **i**, **j** Elephantoceras sp., Permina, from Zhao and Zheng (1977). **k** *Cyclolobus walkeri*, MNHN B 7520, Ankitohazo, Madagascar; dm 93 mm. **l-n** *Adrianites* cf. *insignis*, BMNH C37654, Sosio Limestone, Province of Palermo, Italy; dm 21 mm. **o**, *Wocklumeria sphaeroides*, nr. 572, Famennian, Kowala, Poland, from Czarnocki (1989)

Table 7.4 Mature modifications in Triassic ammonoids. (modified after Davis et al. 1996)

Taxon	Shell shape	Coiling	Elliptical coiling	Constrictions	Ornament	Apertural extensions	Whorl section	Thick shell	Septal crowding	Occluded umbilicus	Reference
Longobarditidae											
Intornites	Oxycone	●			●		●	●	●	●	Hammer and Bucher 2006
Beyrichitidae											
Eogymnotoceras	Discocone				●		●		●		Tozer 1994
Favreticeras	Discocone				●		●		●		Bucher 1992
Balatonitidae.											
Platycuccoceras	Platycone				●				●		Davis et al. 1996
Kashmiritidae											
Kashmirites	Serpenticone				●				●		Davis et al. 1996
Ussuritidae											
Palaeophyllites	Serpenticone				●				●		Davis et al. 1996
Haloritidae											
Halorites	Sphaerocone	●	●	●	●		●		●		Mojsisovics 1893
Homerites	Sphaerocone	●	●	●	●	●			●		
Arcestidae											
Amphipopanoceras	Sphaerocone	●		●			●		●		Davis et al. 1996
Arcestes	Sphaerocone	●		●		●	●	●	●		Davis et al. 1996
Tropitidae											
Tropites	Cadicone	●		●	●		●		●		Mojsisovics 1893
Ceratitidae											
Ceratites	Discocone	●			●		●		●		Wenger 1957
Discoceratites	Oxycone	●			●		●		●		Wenger 1957

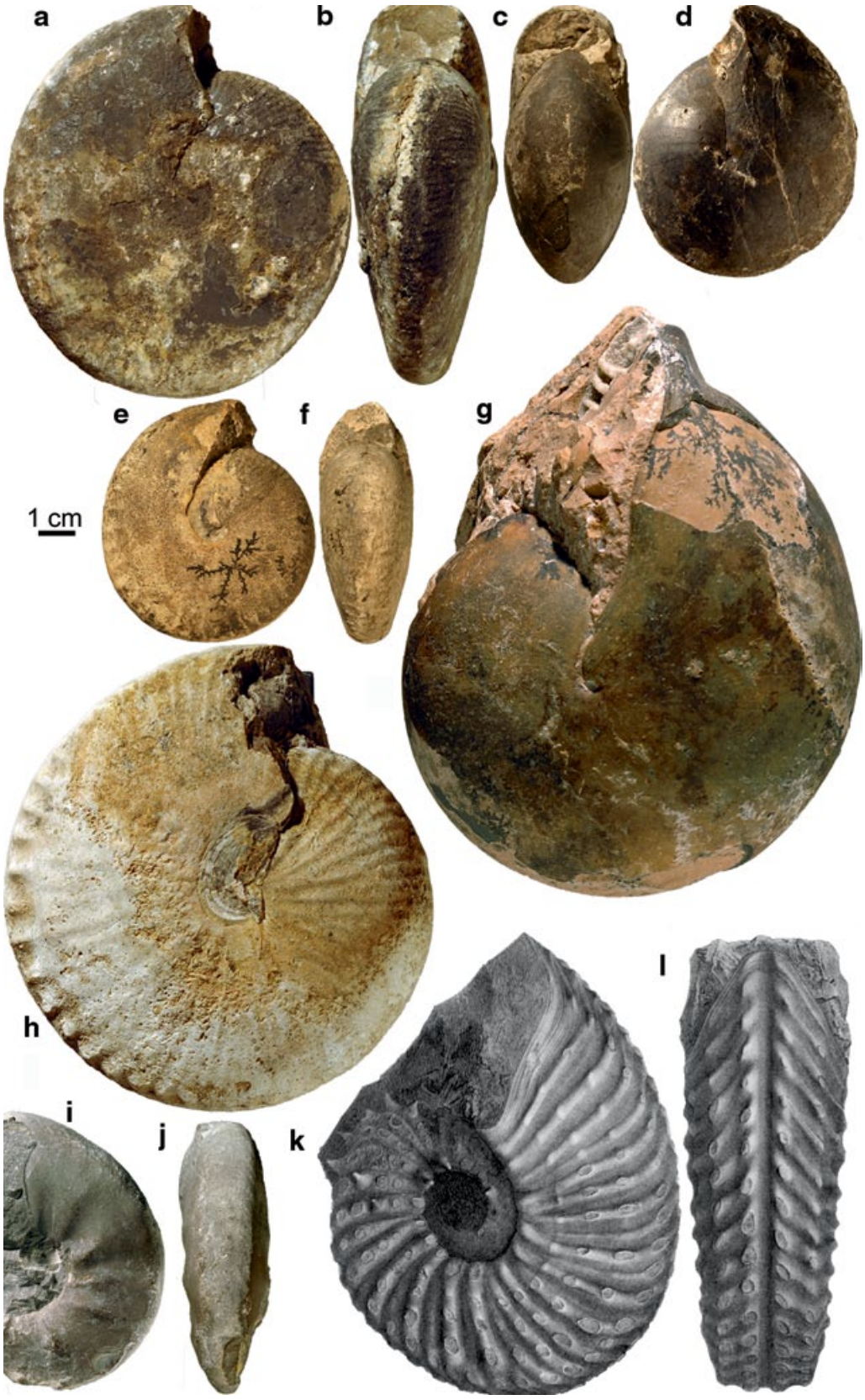

Fig. 7.6 Triassic mature modifications. **a**, **b** *Halorites macer*, PIMUZ 31068, Norian, Bihati?, Timor, Indonesia, dm 103 mm. Note the change in whorl section. **c**, **d** *Orestites* cf. *frechi*, PIMUZ 31069, Norian, Timor, Indonesia, dm 75 mm. Elliptical coiling and constricted aperture. **e**, **f** *Lobites ellipticus*, PIMUZ SQL43399, Norian, Timor, Indonesia, dm 62 mm. **g** *Arcestes* sp., PIMUZ 31067, Norian, Timor, Indonesia, dm 152 mm. **h** *Halorites* cf. *phaonis*, PIMUZ 31066, Norian, Timor, Indonesia, dm 124 mm. **i**, **j** *Ceratites* cf. *compressus*, MHI 688732, Anisian?, Garnberg, Germany, dm 75 mm. **k**, **l** *Protrachyceras archelaus*, from Mojsisovics (1882), Ladinian, Agordo, Italy, dm 132 mm

onstrated cases of dimorphism are exceedingly rare. A first report was published by Müller (1969), who found a questionable egg mass in the shell of *Ceratites*. This specimen is undoubtedly interesting, but it has neither been proven that the preserved globules are eggs nor that they are part of this ceratitid. It is also questionable because no additional soft parts are preserved in this specimen.

Similarly, the report of Dzik (1990b) of acrochordiceratid antidimorphs is doubtful, because the species of this family have been shown to be highly variable (Monnet et al. 2010). By contrast, the account of dimorphism in Middle Triassic *Ceratites* by Urlichs (2009) appears to represent one of the first profound accounts of Triassic dimorphism. He collected adult specimens and measured their sizes in populations in combination with morphometric data from juvenile to adult whorls. Thereby, he could show that the antidimorph's juvenile whorls are quite similar and they begin to diverge morphologically late in ontogeny, with clearly separated adult sizes and conch parameters. Probably, many more cases of dimorphism will be detected among Triassic ammonoids when well-preserved materials are carefully analyzed for this aspect.

7.3.7.3 Jurassic Dimorphism

Jurassic ammonoids probably contain some of the most convincing and most impressive, as well as famous, examples of sexual dimorphism (Table 7.5, Fig. 7.7). For example, Makowski's (1962) kosmoceratids became the icon of the journal *Acta Palaeontologica Polonica* and the impressive combination of extreme size difference, as well as the exotically modified aperture in the dimorphic pair *Phlycticeras* and *Oecoptychius* made them well-known among collectors (Fig. 7.8, 7.9).

Several excellent monographs on Jurassic dimorphism are readily available (Makowski 1962; Callomon 1963, 1981; Tintant 1963; Westermann 1964a, b; Elmi 1967; Davis et al. 1996). It is thus not necessary to repeat all their results. At this occasion, however, we want to summarize the categories (Fig. 7.10), which were introduced by Davis et al. (1996):

Category A: Sexual dimorphism has been shown convincingly, applying the criteria of different adult morphologies, close phylogenetic relationship reflected in their early ontogenies, shared geographic as well as stratigraphic occurrences and shared habitats.

Category B: Davis et al. (1996) grouped forms with dubious sexual dimorphism here. In many of the species included in this category, their phylogenetic relationship may be unclear, geographic ranges may differ, and preadult ontogenetic stages are either poorly known, do not match perfectly, or lack diagnostic characters (Ziegler 1974, 1987).

Category C: In this category, species are included that either appear as monomorphic (i.e., minute or no morphological differences in the shells of the sexes) or where the preservation or other factors make the assignment to an antidimorphic pair impossible. Davis et al. (1996) included several genera with strong apertural modifications such as *Gemmellaroceras* and *Cymbites*.

Table 7.5 Sexual dimorphism in Jurassic ammonoids (incomplete list)

Superfamily	Family	Genus	Age	Source
Psiloceratoidea	Psiloceratidae	*Neophyllites*	Hettangian	Guex 1981
		Psiloceras	Hettangian	Guex 1981; Hillebrandt and Krystyn 2009
		Discamphiceras	Hettangian	Guex 1981
		Badouxia	Hettangian—Sinemurian	Longridge et al. 2006
	Schlotheimiidae	*Kammerkarites*	Hettangian	Guex 1981
		Saxoceras	Hettangian	Guex 1981
		Schlotheimia	Hettangian	Guex 1981
Eoderoceratoidea	Liparoceratidae	*Liparoceras*	Pliensbachian	Callomon 1963; Callomon and Gradinaru 2005
	Dactylioceratidae	*Coeloceras*	Toarcian	Dommergues 1993
		Gabillytes/Zugodactylites	Toarcian	Guex 1973
		Mucrodactylites/Catacoeloceras	Toarcian	Guex 1973
		Collina/Porpoceras	Toarcian	Guex 1973
Hildoceratoidea	Hammatoceratidae	*Hammatoceras/Onychoceras*	Toarcian	Guex 1967
		Erycitoides	Aalenian	Howarth 2013
		Spinammatoceras	Aalenian	Howarth 2013
		Podagrosiceras	Bajocian	Howarth 2013
	Phymatoceratidae	*Haugia*	Toarcian	Keupp and Riedel 2010
	Hildoceratidae	*Tmetoceras/Tmetoites*	Aalenian	Westermann 1964b
		Leioceras	Aalenian	Makowski 1962; Keupp and Riedel 2010; Howarth 2013
		Grammoceras	Toarcian	Callomon 1963; Howarth 2013
	Graphoceratidae	*Ludwigia*	Aalenian	Howarth 2013
		Graphoceras	Aalenian	Callomon 1963; Keupp and Riedel 2010; Howarth 2013
	Sonniniidae	*Witchellia/Pelekodites*	Bajocian	Sandoval and Chandler 2000; Dietze et al. 2005

Table 7.5 (continued)

Superfamily	Family	Genus	Age	Source
		Fontannesia/Nannoceras	Bajocian	Dietze et al. 2005
Haploceratoidea	Strigoceratidae	*Strigoceras/Cadomoceras*	Bajocian	Dietze et al. 2007
		Phlycticeras/Oecoptychius	Bajocian-Callovian	Basse 1952; Arkell et al. 1957; Krimholc et al. 1958b; Makowski 1962; Schweigert and Dietze 1998; Schweigert et al. 2003
		Protophites	Oxfordian	Bert 2003
	Oppeliidae	*Oxycerites*	Bathonian	Elmi and Mangold 1966
		Ochetoceras/Glochiceras	Oxfordian	Makowski 1962; Keupp and Riedel 2010
		Neochetoceras/Lingulaticeras	Tithonian	Makowski 1962; Keupp and Riedel 2010; Schweigert 1998
		Hecticoceras	Bathonian-Callovian	Makowski 1962; Callomon 1963
		Taramelliceras/Creniceras	Oxfordian	Palframan 1966
		Trimarginites	Oxfordian	Keupp and Riedel 2010
		Cymaceras	Kimmeridgian	Keupp and Riedel 2010
		Semiformiceras/Cyrtosiceras	Tithonian	Ziegler 1974; Cecca and Rouget 2006; Keupp and Riedel 2010
		Oppelia/Oecotraustes	Bajocian	Callomon 1963
		Distichoceras/Horioceras	Callovian	Palframan 1967; Baloge and Cariou 2001
	Lissoceratidae	*Lissoceratoides*	Oxfordian	Makowski 1962
Stephanoceratoidea	Otoitidae	*Otoites/Emileia*	Bajocian	Makowski 1962; Callomon 1963; Westermann 1964a; Westermann and Riccardi 1979
		Docidoceras/Trilobiticeras	Bajocian	Keupp and Riedel 2010; Westermann 1964a
	Stephanoceratidae	*Stephanoceras/Itinsaites*	Bajocian	Dietze et al. 2013
		Cadomites/Polyplectites	Bajocian	Makowski 1962; Keupp and Riedel 2010
		Orthogarantiana/Strenoceras	Bajocian	Gauthier et al. 2002

Table 7.5 (continued)

Superfamily	Family	Genus	Age	Source
	Sphaeroceratidae	*Sphaeroceras*	Bajocian	Krimholc et al. 1958a; Makowski 1962; Callomon 1985
		Chondroceras	Bajocian	Makowski 1962; Westermann and Riccardi 1979
		Macrocephalites	Bathonian-Callovian	Krimholc et al. 1958a; Thierry 1978
		Eurycephaites	Callovian	Parent 1997
	Cardioceratidae	*Arctocephalites*	Bajocian	Callomon 1963, 1985
		Cranocephalites	Bathonian	Callomon 1963, 1985
		Longaeviceras	Callovian	Callomon 1963, 1985
		Cadoceras	Callovian	Basse 1952; Arkell et al. 1957; Callomon 1963, 1985
		Cardioceras	Oxfordian	Krimholc et al. 1958a; Makowski 1962; Callomon 1963, 1985
	Kosmoceratidae	*Kosmoceras*	Callovian	Brinkmann 1929; Raup and Crick 1981
		Sigaloceras	Callovian	Callomon 1963
Perisphinctoidea	Parkinsonidae	*Parkinsonia*	Bajocian	Makowski 1962
	Morphoceratidae	*Morphoceras/Ebrayiceras*	Bathonian	Krimholc et al. 1958b; Makowski 1962; Mangold 1970
		Asphinctites/Polysphinctites	Bathonian	Matyja and Wierzbowski 2001; Zatoń 2010
	Pachyceratidae	*Pachyceras*	Callovian	Makowski 1962; Charpy and Thierry 1976
		Tornquistes	Oxfordian	Thierry and Charpy 1982
	Tulitidae	*Morrisiceras/Holzbergia*	Bathonian	Zatoń 2008; Keupp and Riedel 2010
		Bullatimorphites	Bathonian	Krimholc et al. 1958a; Makowski 1962
		Tulites	Bathonian	Makowski 1962
	Reineckeiidae	*Rehmannia*	Callovian	Cariou 1984
		Reineckeia	Callovian	Cariou 1984; Krimholc et al. 1958b

Table 7.5 (continued)

Superfamily	Family	Genus	Age	Source
	Perisphinctidae	*Prorsisphinctes/Vermisphinctes*	Bajocian	Keupp and Riedel 2010
		Cleistosphinctes/Leptosphinctes	Bajocian	Chimšiašvili et al. 1958; Krimholc et al. 1958b; Pavia and Zunino 2012
		Procerites/Siemieradzkia	Bathonian	Keupp and Riedel 2010
		Procerozigzag/Zigzagiceras	Bathonian	Sturani 1966
		Indosphinctes/Elatmites	Callovian	Keupp and Riedel 2010; Cox 1988; Mangold 1971
		Grossouvria	Callovian	Mangold 1971
		Choffatia	Callovian	Cox 1988; Bonnot et al. 2008
		Parachoffatia/Homoeoplanulites	Callovian	Mangold 1971
		Arisphinctes/Dichotomosphinctes	Oxfordian	Callomon 1963; Enay 1966
		Perisphinctes/Dichotomoceras	Oxfordian	Enay 1966; Chimšiašvili et al. 1958; Makowski 1962; Callomon 1963
		Pseudorthosphinctes/ Orthosphinctes	Kimmeridgian	Atrops 1982; Keupp and Riedel 2010
		Proplanulites	Callovian	Chimšiašvili et al. 1958; Makowski 1962
	Ataxioceratidae	*Danubisphinctes/ Parapallasiceras*	Tithonian	Keupp and Riedel 2010
		Lithacoceras/Silicisphinctes	Tithonian	Schweigert 1998
		Choicensisphinctes	Tithonian	Parent et al. 2011, 2013
		Catutosphinctes	Tithonian	Leanza and Zeiss 1992; Parent et al. 2011
		Parataxioceras/Ataxioceras	Oxfordian	Chimšiašvili et al. 1958; Atrops 1982
	Aulacostephanidae	*Microbiplices/Ringsteadia*	Oxfordian	Wright 2010
		Aulacostephanus	Kimmeridgian	Scherzinger and Mitta 2006
	Virgatitidae	*Virgatites*	Kimmeridgian-Tithonian	Chimšiašvili et al. 1958; Makowski 1962

Table 7.5 (continued)

Superfamily	Family	Genus	Age	Source
	Aspidoceratidae	*Aspidoceras*	Kimmeridgian-Tithonian	Basse 1952; Chimšiašvili et al. 1958; Makowski 1962
		Clambites/Epipeltoceras	Oxfordian	Schweigert 1997
		Hybonoticeras/Hybonotella	Tithonian	Schweigert 1997
		Euaspidoceras/Mirosphinctes	Oxfordian	Makowski 1962; Schweigert 1997, Bonnot et al. 1994
		Peltoceras	Callovian	Chimšiašvili et al. 1958; Makowski 1962
		Peltoceratoides	Oxfordian	Arkell et al. 1957; Makowski 1962; Matyja 1994
		Physodoceras/Sutneria	Kimmeridgian-Tithonian	Geyer 1969; Schweigert 1997; Parent et al. 2008a; Keupp and Riedel 2010
		Simocosmoceras/ Pseudhimalayites	Tithonian	Schweigert 1997; Keupp and Riedel 2010
	Polyptychitidae	*Craspedites*	Tithonian	Chimšiašvili et al. 1958; Makowski 1962
		Kachpurites	Tithonian	Chimšiašvili et al. 1958; Makowski 1962; Mitta 2010

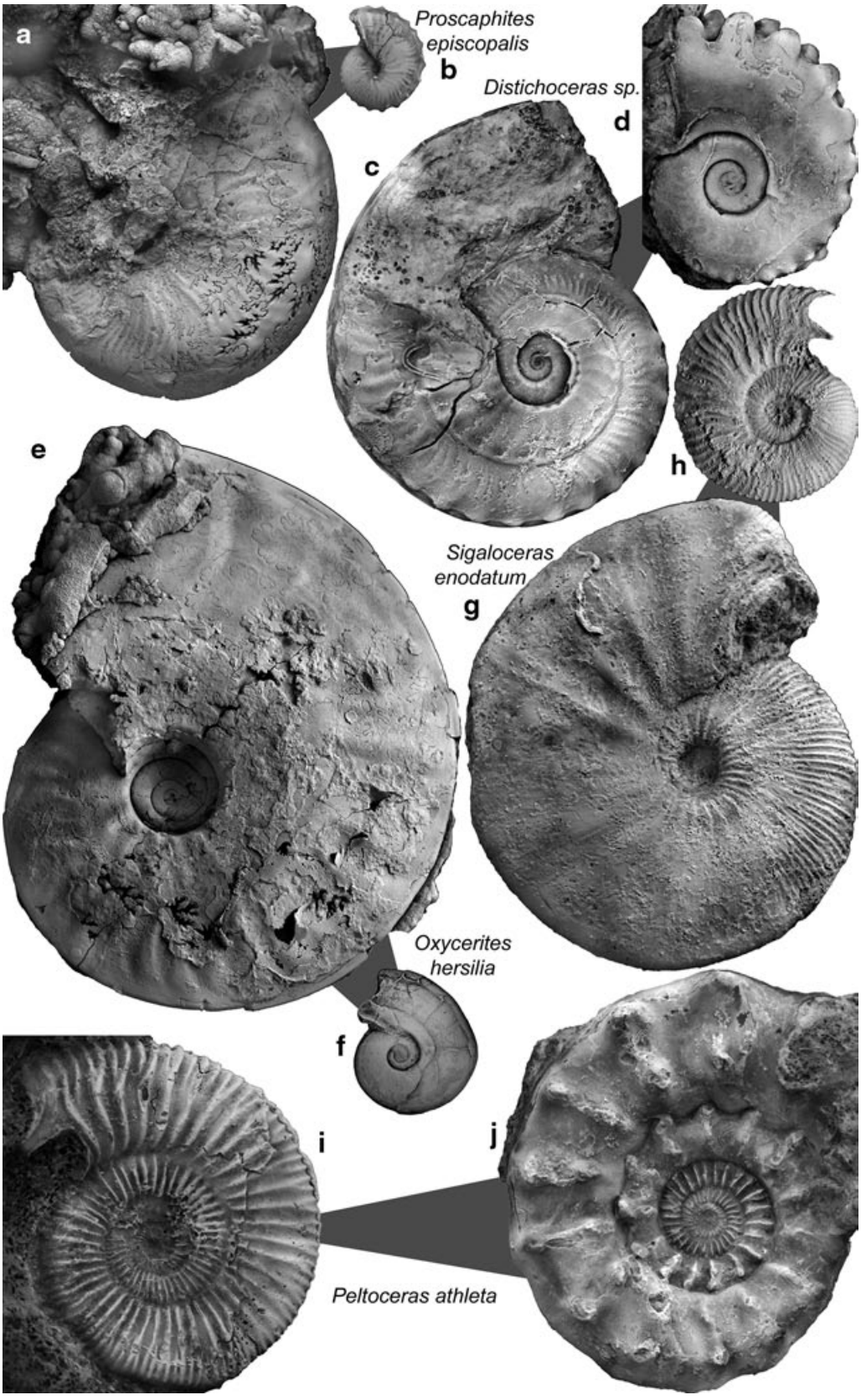

Fig. 7.7 Jurassic antidimorphs. Examples from the Jurassic of Switzerland. The *grey* triangles connect the antidimorphs, with the narrow end at the microconch. This is an example, how antidimorphic pairs could be given one species name

Fig. 7.8 Adult specimens of the antidimorphic couple *Oecoptychius refractus* (Reinecke 1818) (*top left*; microconch) and *Phlycticeras* pustulatum (Reinecke 118) (*bottom*, macroconch). Herznach-Member, Callovian, Swiss Jura Mountains. Note the morphologic and size difference

Category D: Nonsexual dimorphism and polymorphism is contained here. Such polymorphic structures have been shown by various authors (Marchand 1976; Charpy and Thierry 1976; Tintant 1976; Thierry 1978; Contini et al. 1984). According to Davis et al. (1996), this variation has nothing to do with sexual dimorphism. The problem here could be the multitude of factors controlling shape and size of antidimorphs. As discussed above, polymorphism may be caused by a variety of processes such as ecological factors (phenotypic plasticity), hormonal processes, and potentially by diseases and parasites. All these factors contribute to intraspecific variability that may have affected microconchs and macroconchs in different ways. Therefore, some of the cases included in Category D may actually represent blurred cases of sexual dimorphism.

Taking the seeming absence of dimorphism or at least its weak expression in the Triassic into account, it is remarkable how common sexual dimorphism already was in the Early Jurassic (Callomon 1963; Lehmann 1966; Guex 1967, 1968, 1973, 1981; Howarth 2013). Depending on the opinion of authors that focused on Jurassic dimorphism, i.e. which case of dimorphism to include or exclude in sexual dimorphism, the abundance of dimorphism became high to very high in the Middle to Late Jurassic (e.g. Ziegler 1974, 1987; Parent 1997; Schweigert 1997; Schweigert and Dietze 1998, Schweigert et al. 2003, 2007; Matyja and Wierzbowski 2001; Parent et al. 2008a, b, 2009; Zatoń 2008, 2010; Keupp and Riedel 2010; Bardhan et al.

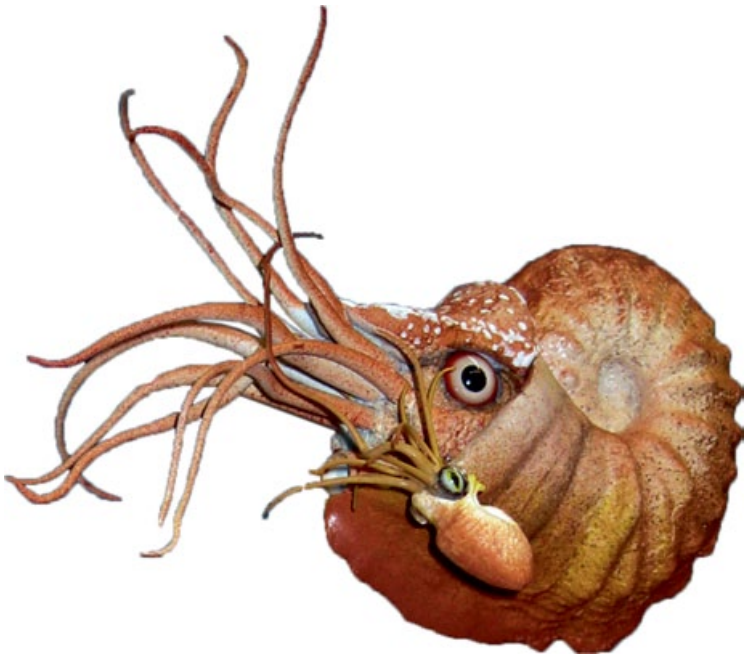

Fig. 7.9 Model of an antidimorphic pair of the Middle Jurassic *Phlycticeras*/*Oecoptychius* by B. Scheffold (Zurich). Note that *Oecoptychius* might have used a modified arm to transmit a spermatophore. Naturally, many aspects of this reconstruction are based on speculations

2012). The great success of this reproductive strategy probably originated partially in the fact that many Middle and Late Jurassic ammonoids phylogenetically root in the Hildoceratoidea (Donovan et al. 1981; Davis et al. 1996), which gave rise to many of the younger clades except for the lytoceratids and phylloceratids, which are not known to have produced clear cases of dimorphism (Fig. 7.11), except few cases such as *Juraphyllites* studied by Cope (1992). This also shows that dimorphism may well be of use as a character for phylogenetic reconstructions. Another factor for the Jurassic success of sexual dimorphism in ammonoids is certainly ecological. The energetic cost of reproduction (the energy that is available for the ovaries and thus eggs) can be significantly reduced when the size of the males, and thus their energy intake, is reduced.

The monophyletic nature of Jurassic sexual dimorphism has another important implication. Genera such as *Taramelliceras* and *Creniceras* in the Late Jurassic become more likely to have been antidimorphs (in contrast to the doubts of Davis et al. 1996) because there is a strong phylogenetic component in dimorphism; nevertheless, the situation is complicated by difficulties in taxonomic assignments, and other, similar genera such as *Proscaphites*, which also show dimorphism. It appears that in the Haploceratoidea, the majority of species produced a pronounced dimorphism. Additionally, the majority of the haploceratoidean microconchs had subcircular to ear-shaped lappets, while those in the stephanoceratids are rather elongate spatulate (*Kosmoceras*) or subovally elliptical (*Normannites*).

Interestingly, the peak in well documented sexual dimorphism in conjunction with extreme adult modifications is in the Middle Jurassic, followed by an increasing number of dubious cases in the Callovian to Kimmeridgian and decreasing abundance of mature modifications in the Tithonian (Davis et al. 1996). From the Tithonian onwards, dimorphism continued to exist.

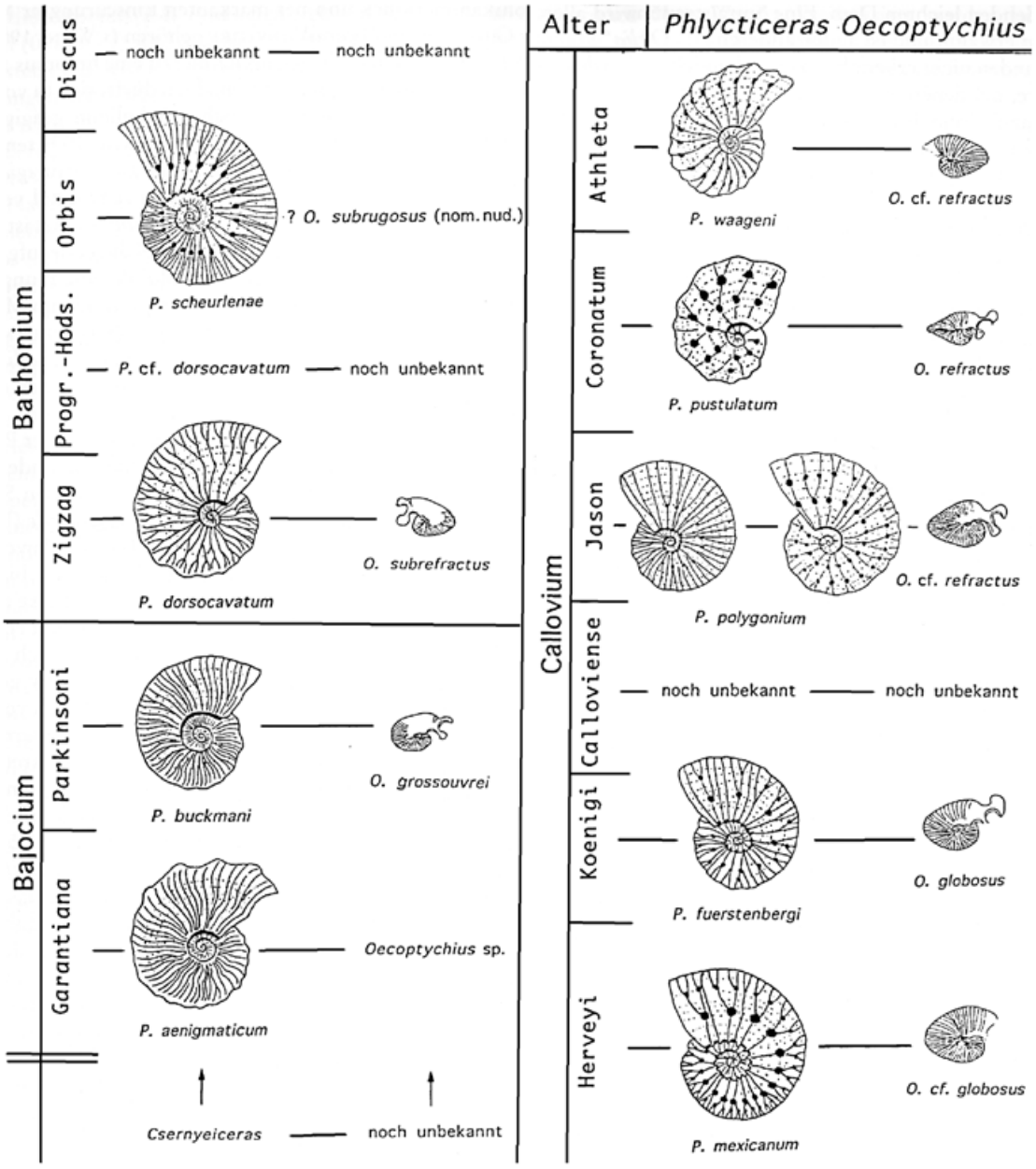

Fig. 7.10 Evolutionary change in the lineage *Phlycticeras*/*Oecoptychius*. (slightly modified from Schweigert and Dietze 1998)

7.3.7.4 Cretaceous Dimorphism

As in the Jurassic, each ammonoid clade produced different mature modifications, except for the phylloceratids. The seeming absence of dimorphism in phylloceratids might be due to the scarcity of adult specimens (Davis et al. 1996) and/or to the commonly simple ornament and more or less straight apertures.

In contrast to the phylloceratids, several Cretaceous lytoceratids do display mature modifications (Fig. 7.13). For example, some gaudryceratids changed the whorl cross section and a slight umbilical egression may occur, as well as changes in ornament (Wiedmann 1973; Cooper and Kennedy 1979; for a review of the

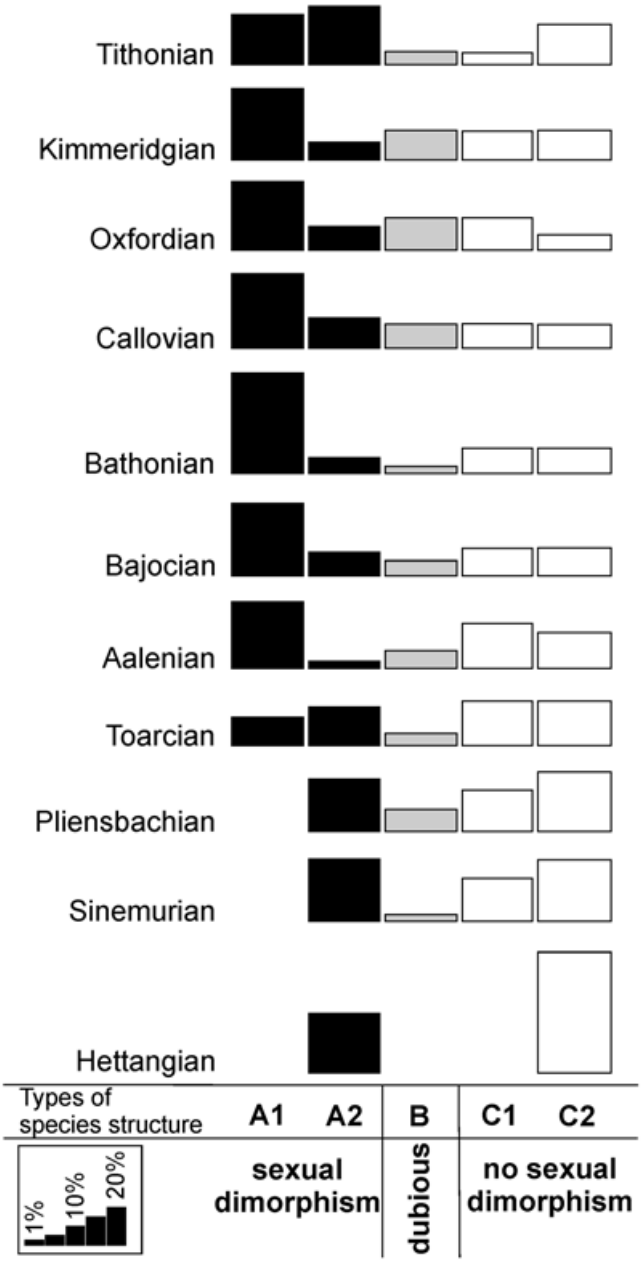

Fig. 7.11 History of dimorphism in Jurassic ammonoids, taking into account the types of species structure, i.e. the predominant type of adults depending on the amount of dimorphic forms (redrawn from Davis et al. 1996). *A1* microconchs with strong mature modifications (e.g., rostrum, lappets); *A2* microconchs with weak mature modifications; *B* groups that look like sexually dimorphic taxa but lack some features to determine dimorphism; *C1* monomorphic, small forms with adult modifications; *C2* monomorphic, moderately large to large forms without adult modifications

group see Hoffmann 2010). In haploceratoideans such as *Aconeceras*, the apertural lappets are less distinct than in the Jurassic, but also present, and combined with a short triangular ventral rostrum (Doguzhaeva and Mutvei 1991). Davis et al. (1996) mention an interesting mode of terminal countdown in *Menuites*, which is remotely reminiscent of the white venter in nautilid shells: in the microconchs of this genus, the ventral tubercles and spines vanish about a demi-whorl behind the terminal aperture (Cobban and Kennedy 1993). The venter and the ventrolateral part stay smooth until shortly behind the terminal aperture, where they re-appear. *Hauericeras*, by contrast, resembles in its terminal aperture the haploceratoideans (Obata et al. 1978). According to Klinger and Kennedy (1989), the hoplitoidean *Placenticeras kaffarium* displays a rather strong umbilical egression, which gives it a scaphitoid adult morphology. Additionally, the venter became rounded and the

ornament changed. The possibly most conspicuous adult modification in the Cretaceous among the regularly coiled ammonites is that of the Albian acanthoceratoidean *Mortoniceras*, which forms a long ventral spine, which may be directed ventrally (*M. equidistans*) or even curved posteriorly (*M. rostratum*), forming almost a complete loop (e.g., Cooper and Kennedy 1979). Additionally, the whorl cross section and ornament changed.

The most famous kinds of mature modifications are undoubtedly those of the Cretaceous heteromorphs of the superfamilies Ancyloceratoidea and Turrilitoidea. A good example is the ancyloceratoidean scaphitids (Fig. 7.13, 7.14), which have a wide geographic distribution and a rather impressive diversity. In most species of this group, a more or less straight shaft with a terminal hook follows the normally planispirally coiled phragmocone (Cobban 1951; Landman 1987). Additionally, the aperture is constricted (e.g., Landman et al. 2012). The degree of uncoiling and the length of the straight shaft in relation to the terminal diameter vary as well as the changes in ornament (e.g., in *Hoploscaphites* or *Scaphites*). The microconchs of both *Worthoceras* and *Yezoites* carry broad lappets (Fig. 7.13) with strong convex growth lines (Tanabe 1977; Kennedy 1988). In the Santonian *Scaphites (Pteroscaphites) coloradensis*, the lateral lappets occur in both antidimorphs and have a peculiar hollow spine-like morphology (Kennedy 1988; Landman 1989).

The mature modifications of some Turrilitoidea appear even more unusual. In the baculitids, the adult modifications are usually limited to changes in ornament (stronger ribs on the venter), sometimes a slight dorsal turn of the aperture and dorsal as well as ventral lappets (Kennedy 1988; Cobban and Kennedy 1991c; Klug et al. 2012). The ventral projection or rostrum can be rather long, clearly exceeding the shell diameter. Davis et al. (1996) figured a *Baculites* in which this projection is very long. They assumed that the rostrum might have attained this long size due to an injury or infection. By contrast, we have seen other specimens with similarly shaped adult apertures, thus indicating that this might be a normal adult aperture of this species (Fig. 7.13).

In many genera, such as *Nostoceras*, *Didymoceras*, *Allocrioceras* or *Emericiceras*, the terminal demi-whorl is characterized by a U-shaped part (e.g., Stephenson 1941; Kennedy 1988; Cobban and Kennedy 1994a). In most cases, the coiling direction differs more or less strongly from the preceding whorls. Sometimes, the plane of coiling stayed the same (like in the turrlilitoideans *Allocrioceras*, *Emericiceras* and *Labeceras*, and the lytoceratid *Macroscaphites*), sometimes the plane of coiling changed: in *Eubostrychoceras*, *Hyphantoceras*, *Nostoceras* and *Didymoceras*, for example, the coiling axis turned for 50–90 °. In *Didymoceras nebrascense*, this change in coiling axis is merely a continuation of a similar change in the preceding whorls; in this species, the coiling axis appears to be coiled in itself (Meek and Hayden 1856). By contrast, the Japanese *Pravitoceras* might be the only genus in which the coiling axis switches rapidly for 90 °. In all these cases, this terminal countdown of heteromorphs (Seilacher and Gunji 1993) is linked with changes in ornament.

The abundance of such a U-shaped terminal demi-whorl raises the question of the selective force behind it. Although the ultimate evidence is lost due to the ex-

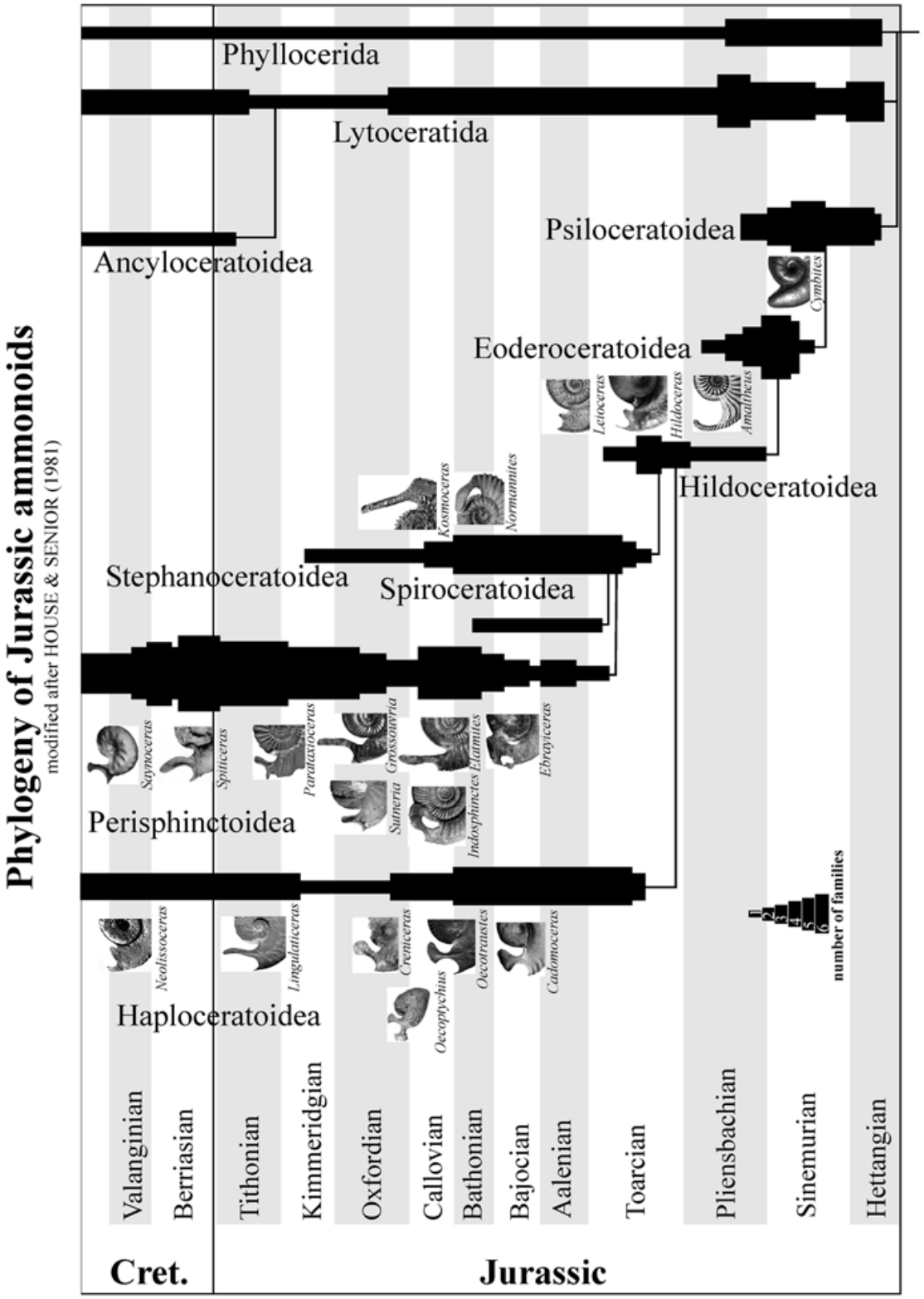

Fig. 7.12 Modified peristomes of adult microconchs of the Jurassic and Early Cretaceous. Note the rather uniform lappets in the haploceratoids, the rather straight lappets in the perisphinctoids, and the disparity in the lappets among the stephanoceratoids. Image sources: V. Schlamp (*Elatmites*, *Paralingulaticeras*, *Parataxioceras lothari*), J.-S. David (*Cadomoceras cadomense*; *Cymbites laevigatus*; *Ebrayiceras pseudoanceps*; *Hildoceras lusitanicum*; *Morrisiceras schwandorfense*; *Oecotraustes bomfordi*); D. Bert (*Kosmoceras phaeinum*); H. Chatelier (*Saynoceras*); Quenstedt (1885: *Amaltheus margaritatus*; *Leioceras opalinum*); R. Roth (*Creniceras crenatum*; *Sutneria platynota*); P. Branger (*Indosphinctes*; *Normannites orbignyi*); Dietl (2013: *Grossouvria*). Djanelidzé (1922: *Spiticeras kiliani*, modified or reduced); Atrops and Reboulet (1995: *Neolissoceras grasianum*, modified or reduced); Ernst and Klug (2011: *Oecoptychius refractus*)

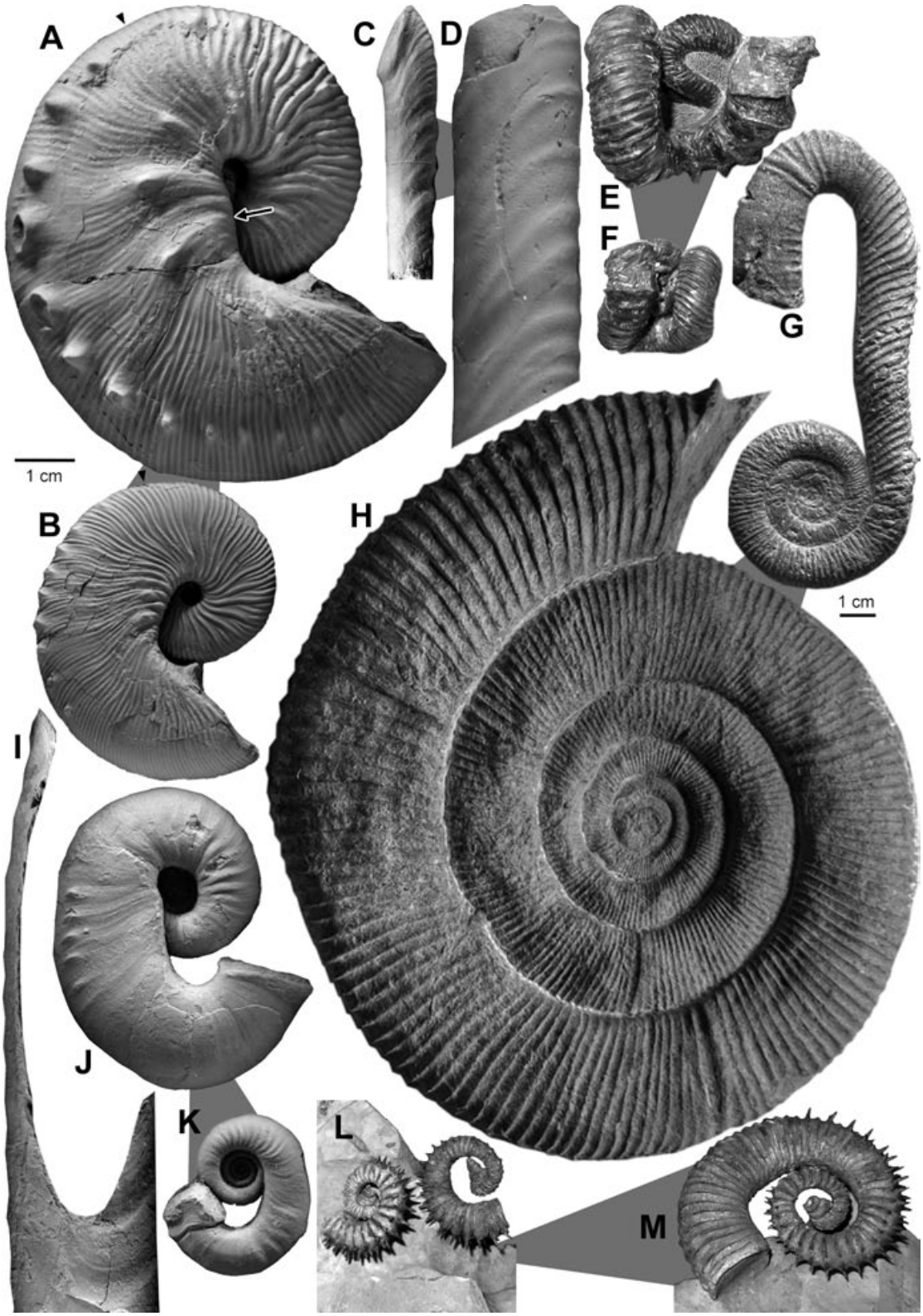

Fig. 7.13 Cretaceous antidimorphic pairs. **a**, **b** *Hoploscaphites brevis*, Pierre Shale, South Dakota. Last septum is marked by a triangle. A, Macroconch, USNM 367, lateral view, dm 90 mm. Note the bulge along the umbilical margin (*arrow*). B, Microconch, lateral view, AMNH 58514, dm 55 mm. **c**, **d** *Sciponoceras gracile*, Cenomanian, Texas. C, microconch, USNM 411539, wh 9 mm. D, Macroconch (USNM 411537, wh 17 mm. The antidimorphs differ mainly in size. **e**, **f** *Nippo-*

tinction of the Ammonoidea, one line of reasoning shall be mentioned here: it is conceivable that this upward turn of the terminal aperture enabled the heteromorphs to approach the level of the center of mass with their hyponome, thus significantly improving their swimming abilities in a horizontal direction. Such a horizontal alignment of aperture and centre of mass was achieved in most ammonoid clades and apparently there was some selection for that trait (e.g., Korn and Klug 2003; Klug and Korn 2004; Tajika et al. 2014). This might have been of particular importance at the time of mating.

Like the mature modifications, dimorphism has been reported from most Cretaceous superfamilies except for the phylloceratines (Table 7.6; Kennedy and Wright 1985a; Davis et al. 1996). Concerning members of the Desmoceratoidea, sexual dimorphism has been described for Campanian *Menuites* (Cobban and Kennedy 1993), where the antidimorphs differ strongly in size. Maeda (1993) examined the dimorphism of Campanian *Yokoyamaoceras*, where the microconch reaches only a third of the diameter of the macroconch (with two whorls less), has a stronger ornament, an aperture with lateral lappets, and a strong ventral projection. For the acanthoceratoidean *Metoicoceras* from the Cenomanian, Cobban and Kennedy (1991b) described a size difference where the macroconch is more than twice as big as its counterpart (Cobban 1953). Its microconchs are more robust and thus have a stronger ornament. Except for the ornament, which is finer in the last whorl of the microconch, the same applies to *Subprionocyclus* (Futakami 1990).

Interestingly, albeit controversial in our opinion, one view on dimorphism of the Valanginian ammonite *Valanginites nucleus* from Wąwał in central Poland was presented by Ploch (2003, 2007). Here, the size differences in identically ornamented and identically coiled specimens with purely macroconchiate modification of the terminal part of the shell (prominent lip preceded by a constriction and without lappets) have been used as the only criterion in separating micro- and macroconchs. It is all the more strange as these ammonites are associated with similarly ornamented but much smaller shells having lateral lappets, classified as *Saynoceras verrucosum* (see Dzik 1990a). Thus, it appears that *V. nucleus* might represent the macroconch and *S. verrucosum* its antidimorphic microconch (see also Bulot et al. 1990).

In scaphitids (Ancyloceratina), dimorphism is very well known. Morphological differences between the terminal whorl of scaphitid antidimorphs include adult diameter, coiling, ribbing and nodes or spines, septal crowding, and apertural modifications including lateral and/or dorsal lappets. For example, in *Hoploscaphites*, the more or less straight shaft of the terminal whorl of the macroconch carries a

nites mirabilis, Campanian, Hokkaido, Japan. The antidimorphs differ mainly in size. **g**, **h** *Macroscaphites yvani*, Barremian, Angles, France. **g** microconch with large terminal hook. **h** regularly coiled macroconch, G12/336. **i** microconch with hook, GRY/903b. **i** mature apertural margin of a microconch (?) of the Santonian *Bacu1ites thomi*, USGS 21419, Montana, with a short dorsal and a long, ventral rostrum. **j**, **k** *Yezoites puercu1us*, Turonian, Hokkaido, Japan. **j** Macroconch, AMNH 45280. **k** microconch, AMNH 45281, note the lateral lappets and the absence of nodes. **l, m** *Imerites dichotomum*, Barremian, Alpes de Haute Provence, France. **l** notice that one of the microconchs is sinistral and the other dextral; dm 45 mm. **m** macroconch, dm 75 mm. (Images: **a–d, i–k** (N. Landman). **e, f, l, m** (W. Grulke). **h, i** (D. Bert))

Table 7.6 Sexual dimorphism in Cretaceous ammonoids. (incomplete list, largely taken from Davis et al. 1996)

Superfamily	Family	Genus	Source
Haploceratoidea	Aconeceratidae	*Gyaloceras*	Kennedy and Klinger 1979
		Protaconeceras	Riccardi et al. 1987
		Sanmartino-ceras	Kennedy and Klinger 1979; Riccardi et al. 1987; Parent 1991
		Sinzovia	Riccardi et al. 1987
	Binneyitidae	*Borrisiakoceras*	Kennedy and Cobban 1976
	Haploceratidae	*Haploceras*	Bujtor 1993
Perisphinctoidea	Neocomitidae	*Berriasella*	Howarth 1992; Wright et al. 1996
		Neocomites	Fatmi 1969; Reboulet 1995
		Thurmanniceras	Bujtor 1993; Wright et al. 1996
	Olcostephanidae	*Groebericeras*	Howarth 1992
		Olcostephanus	Fatmi 1969; Bulot et al. 1990; Bujtor 1993; Wright et al. 1996
		Saynoceras	Bulot et al. 1990; Dzik 1990a
Desmoceratoidea	Desmoceratidae	*Anapuzosia*	Matsumoto 1988
		Achilleoceras	Matsumoto 1988
		Austiniceras	Matsumoto 1988
		Bhimaites	Matsumoto 1988
		Epipuzosia	Matsumoto 1988
		Grandidiericeras	Matsumoto and Saito 1987; Matsumoto 1988
		Hauericeras	Matsumoto et al. 1990b; Wright et al. 1996
		Jimboiceras	Matsumoto 1988
		Kitchinites	Matsumoto 1988; Matsumoto et al. 1990b
		Matsumotoceras	Matsumoto 1988; Matsumoto et al. 1990a
		Mesopuzosia	Matsumoto 1988; Matsumoto et al. 1990a, b

Table 7.6 (continued)

Superfamily	Family	Genus	Source
		Neopuzosia	Matsumoto 1988; Matsumoto et al. 1990b
		Pachydesmoceras	Matsumoto 1987b, 1988
		Parapuzosia	Matsumoto 1988
		Puzosia	Marcinowski 1980; Wright and Kennedy 1984; Cooper and Kennedy 1987; Matsumoto 1988; Matsumoto et al. 1990a, b; Matsumoto and Skwarko 1993
	Kossmaticeratidae	*Grossouvrites*	Olivero and Medina 1989
		Gunnarites	Kennedy and Klinger 1985
		Kossmaticeras	Matsumoto 1991b
		Maorites	Macellari 1986
		Yokoyamaoceras	Matsumoto 1991b; Maeda 1993; Keupp and Riedel 2010
	Pachydiscidae	*Anapachydiscus*	Kennedy 1986b, d, 1989; Kennedy et al. 1986; Kennedy and Henderson 1992; Kennedy and Klinger 1993
		Canadoceras	Kennedy 1986d
		Eupachydiscus	Kennedy 1986d
		Lewesiceras	Wright and Kennedy 1984; Kennedy 1986d
		Menuites	Kennedy 1986d, 1989; Kennedy and Henderson 1992; Kennedy and Klinger 1993; Cobban and Kennedy 1993
		Pachydiscoides	Kennedy 1984
		Pachydiscus	Kennedy and Summesberger 1984; Kennedy 1986d; Jagt 1989
		Teshioites	Kennedy 1986d
	Silesitidae	*Silesites*	Cecca and Landra 1994
Hoplitoidea	Hoplitidae	*Anahoplites*	Marcinowski and Wiedmann 1990
		Callihoplites	Marcinowski and Wiedmann 1990
		Euhoplites	Amedro 1992

Table 7.6 (continued)

Superfamily	Family	Genus	Source
		Hyphoplites	Wright and Kennedy 1984
	Placenticeratidae	*Hoplitoplacenticeras*	Kennedy 1986d
		Hypengonoceras	Klinger and Kennedy 1989
		Karamaites	Kennedy and Wright. 1981, 1983; Klinger and Kennedy 1989
		Placenticeras	Kennedy and Wright 1981, 1983; Kennedy 1984, 1986d, 1988; Kennedy and Cobban 1991a; Cobban et al. 1989; Klinger and Kennedy 1989; Matsumoto and Skwarko 1991; Ganguly and Bardhan 1993
Acanthoceratoidea	Acanthoceratidae	*Acanthoceras*	Moreau et al. 1983; Wright and Kennedy 1987; Kennedy and Cobban 1990; Matsumoto and Skwarko 1991
		Acompsoceras	Wright and Kennedy 1987
		Benueites	Reyment 1971, 1988
		Calycoceras	Wright and Kennedy 1987, 1990; Cobban et al. 1989; Cobban and Kennedy 1990; Matsumoto and Skwarko 1991; Kennedy and Juignet 1994
		Conlinoceras	Kennedy and Cobban 1990
		Cunningtoniceras	Wright and Kennedy 1987; Matsumoto et al. 1989; Kennedy and Cobban 1990
		Eucalycoceras	Cobban 1988a; Wright and Kennedy 1990
		Euomphaloceras	Kennedy 1988; Wright and Kennedy 1990
		Mantelliceras	Wright and Kennedy 1984; Kennedy 1989; Matsumoto and Takahashi 1992
		Metoicoceras	Kennedy et al. 1981a, 1989; Kennedy 1988, 1989; Forster et al. 1983; Cobban and Kennedy 1991b
		Mrhiliceras	Kennedy and Wright 1985b; Wright and Kennedy 1987
		Nannometoioceras	Kennedy 1988, 1989; Cobban et al. 1989
		Neocardioceras	Cobban 1988a
		Paraburoceras	Cobban et al. 1989

Table 7.6 (continued)

Superfamily	Family	Genus	Source
		Paraconlinoceras	Kennedy and Cobban 1990
		Plesiacanthoceras	Kennedy and Cobban 1990
		Plesiacanthoceratoides	Kennedy and Cobban 1990
		Protacanthoceras	Wright and Kennedy 1980, 1987; Kennedy and Wright 1985a
		Pseudaspidoceras	Matsumoto 1991a
		Pseudocalycoceras	Kennedy 1988
		Spathites	Kennedy and Cobban 1988b
		Sumitomoceras	Cobban 1988a
		Tarrantoceras	Kennedy 1988; Kennedy and Cobban 1990; Cobban 1988a
		Thomelites	Wright and Kennedy 1990
		Watinoceras	Zaborski 1987; Cobban 1988b
	Brancoceratidae	*Euhystrichoceras*	Kennedy and Wright 1981; Wright and Kennedy 1984
		Hysteroceras	Amedro 1992
		Mortoniceras	Marcinowski and Wiedmann 1990; Amedro 1992
	Coilopoceratidae	*Coilopoceras*	Kennedy and Wright 1984b; Kennedy 1988; Reyment 1988; Luger and Groschke 1989; Meister et al. 1992
		Hoplitoides	Kennedy and Cobban 1988b; Reyment 1988
	Collignoniceratidae	*Barroisiceras*	Immel 1987
		Collignoniceras	Kennedy et al. 1980, 1989
		Forresteria	Kennedy et al. 1983; Kennedy 1984; Kennedy and Cobban 1991a
		Gauthiericeras	Kennedy 1984
		Paratexanites	Kennedy 1984
		Peroniceras	Kennedy 1984
		Prionocyclus	Kennedy 1988

Table 7.6 (continued)

Superfamily	Family	Genus	Source
		Protexanites	Kennedy 1984; Kennedy and Cobban 1991a
		Submortoni-ceras	Kennedy et al. 1981b
		Subpriono-cyclus	Reyment 1982; Futakami 1990
		Yabeiceras	Kennedy et al. 1983
	Flickiidae	*Litophragmatoceras*	Kennedy and Cobban 1988a
		Salaziceras	Kennedy and Wright 1984a; Keupp and Riedel 2010
	Forbesiceratidae	*Forbesiceras*	Kennedy and Juignet 1984; Kennedy and Cobban 1990; Wright and Kennedy 1984; Matsumoto 1987a
	Lyelliceratidae	*Neophlycticeras*	Kennedy and Delamette 1994; Wright and Kennedy 1994
		Stoliczkaia	Wright and Kennedy 1984
	Sphenodiscidae	*Libycoceras*	Kassab and Hamama 1991
		Manambolites	Luger and Grosehke 1989
		Sphenodiscus	Kennedy 1986d
	Tissotiidae	*Metatissotia*	Kennedy 1984
	Vascoceratidae	*Fagesia*	Kennedy and Wright 1985a; Kennedy et al. 1987
		Hourcquia	Matsumoto and Toshimitsu 1984
		Microdiphaso-ceras	Cobban et al. 1989
		Neoptychites	Kennedy and Wright 1979; Kennedy and Cobban 1988b; Cobban and Hook 1983; Zaborski 1987
		Pseudobarroisiceras	Matsumoto and Toshimitsu 1984
		Rubroceras	Cobban et al. 1989
		Thomasites	Zaborski 1987
		Vascoceras	Cobban et al. 1989; Meister et al. 1992

Table 7.6 (continued)

Superfamily	Family	Genus	Source
Ancyloceratoidea	Ancyloceratidae	*Ancyloceras*	Klinger and Kennedy 1977; Forster and Weier 1983
		Acantholytoceras	Delanoy et al. 1995
		Acrioceras	Klinger and Kennedy 1992
		Crioceratites	Klinger and Kennedy 1992
		Emericiceras	Delanoy et al. 1995
		Hemihoplites	Delanoy et al. 1995
		Lytocrioceras	Delanoy et al. 1995
		Pseudomoutoniceras	Delanoy et al. 1995
	Heteroceratidae	*Colchidites*	Aguirre-Urreta and Klinger 1986
		Heteroceras	Aguirre-Urreta and Klinger 1986, Delanoy et al. 1995
Douvilleiceratoidea	Astiericeratidae	*Astiericeras*	Kennedy 1986a
	Douvilleiceratidae	*Douvilleiceras*	Amedro 1992
		Paraspiticeras	Aguirre-Urreta and Rawson 1993
Deshayesitoidea	Parahoplitidae	*Hypacanthoplites*	Kemper 1982
Scaphitoidea	Scaphitidae	*Acanthoscaphites*	Birkelund 1982; Kennedy 1986c; Kennedy and Summesberger 1987; Jagt and Kennedy 1989; Jagt et al. 1992
		Clioscaphites	Landman 1987
		Discoscaphites	Jeletzky and Waage 1978; Kennedy and Cobban 1993c; Landman and Waage 1993
		Hoploscaphites	Makowski 1962; Birkelund 1982; Kennedy 1986b, c, 1989, 1993; Kennedy et al. 1986; Kennedy and Summesberger 1987; Kennedy and Cobban 1993a; Landman and Waage 1993; Machalski 2005
		Jeletzkytes	Landman and Waage 1993; Kennedy and Cobban 1993a; Cobban and Kennedy 1994a; Jagt and Kennedy 1994; Kennedy and Cobban 1993c
		Rhaeboceras	Cobban 1987

Table 7.6 (continued)

Superfamily	Family	Genus	Source
		Scaphites	Cobban 1969, 1984; Cobban and Kennedy 1991a; Kennedy 1984, 1986d, 1988, 1989; Kennedy et al. 1989, 1992; Kennedy and Christensen 1991; Kennedy and Cobban 1991a, b; Marcinowski 1980, 1983; Immel 1987; Kaplan et al. 1987; Landman 1987, 1989; Jagt 1989
		Trachyscaphites	Kennedy and Summesberger 1984; Kennedy 1986d; Cobban and Kennedy 1992, 1994b
		Worthoceras	Forster et al. 1983; Kennedy 1988; Kennedy and Cobban 1988a; Kennedy et al. 1989; Cobban et al. 1989; Bujtor 1991; Keupp and Riedel 2010
		Yezoites	Tanabe 1977; Kennedy 1984, 1988; Kennedy and Christensen 1991; Kaplan et al. 1987; Keupp and Riedel 2010
Turrilitoidea	Anisoceratidae	*Allocrioceras*	Kennedy 1988
	Baculitidae	*Bacu1ites*	Kennedy 1984, 1986b, c; Jagt 1989; Cobban and Kennedy 1991b
		Boehmoceras	Kennedy and Cobban 1991b
		Eubaculites	Klinger and Kennedy 1993
		Lechites	Cooper and Kennedy 1977; Kennedy and Wright 1985a
		Sciponoceras	Marcinowski 1980; Kennedy and Juignet 1983; Kennedy 1988
	Diplomoceratidae	*Oxybeloceras*	Cobban et al. 1989
		Solenoceras	Cobban and Kennedy 1994a
	Hamitidae	*Metaptychoceras*	Cobban et al. 1989
	Labeceratidae	*Labeceras*	Klinger 1989
		Myloceras	Klinger 1989

Table 7.6 (continued)

Superfamily	Family	Genus	Source
	Nostoceratidae	*Anaklinoceras*	Davis et al. 1996
		Axonoceras	Davis et al. 1996
		Bostrychoceras	Kennedy 1986d
		Didymoceras	Cobban and Kennedy 1994a
		Eubostrychoceras	Kennedy 1986d
		Exiteloceras	Davis et al. 1996
		Hyphantoceras	Kennedy and Wright 1985a
		Nostoceras	Luger and Gröschke 1989; Kennedy and Cobban 1993a, b; Cobban and Kennedy 1994a
	Ptychoceratidae	*Lytocrioceras*	Delanoy and Poupon 1992
	Turrilitidae	*Mariella*	Kennedy and Wright 1985a
Lytoceratoidea	Macroscaphitidae	*Costidiscus*	Cecca and Landra 1994
		Macroscaphites	Cecca and Landra 1994
Tetragonitoidea	Gaudryceratidae	*Gaudryceras*	Hirano 1978, 1979

thick dorsal swelling, which gives it a pregnant appearance (e.g., Morton 1834; Kennedy and Cobban 1993a; Landman and Waage 1993; Machalski 2005). Speculatively, this bump provided extra space for the ovaries. In the corresponding microconch, the dorsal wall of the shaft is subparallel to the venter. There are also some differences in ornament (Davis et al. 1996). Landman and Waage (1993) examined the size-differences between the antidimorphs of the Maastrichtian species *Hoploscaphites (Jeletzkytes) spedeni*. Although the macroconchs are in average almost twice as large as their counterparts, the size distribution of both antidimorphs does overlap (Fig. 7.14). This size overlap varies between the species (Landman and Waage 1993), but it is not entirely clear whether the presence or absence of an overlap and its quality are predominantly controlled by (1) difference in adult diameter of the antidimorphs, (2) difference in intrasexual variability, (3) sample size or (4) ecology.

It is also remarkable that in the Maastrichtian *Hoploscaphites comprimus*, some morphological differences between the antidimorphs already occur in the normally coiled juvenile part (Landman and Waage 1993), making sexing of juvenile specimens possible.

Among the Turrilitoidea, there are also many cases of likely dimorphism, although often the main difference between the antidimorphs is size (e.g., *Didymoceras*, *Bostrychoceras*, *Nipponites*, *Oxybeloceras, Sciponoceras*; Kennedy 1988; Cobban and Kennedy 1994a). A nice example for dimorphism in the Lytoceratina is the genus *Macroscaphites*, in which the microconch develops a long straight shaft with a U-shaped hook at the end, while the macroconch consists only of a regularly coiled shell with a terminal constriction (Fig. 7.13). Most other lytoceratines display more normal kinds of dimorphism, i.e. mainly differences in size (*Gaudryceras*, *Costidiscus*, *Tetragonites*; Wiedmann 1973).

Davis et al. (1996) reported a couple of possible cases of Cretaceous trimorphism. One case was published by Hirano (1978, 1979) and concerns the lytoceratin *Gaudryceras*. A second case comprises scaphitids of the genera *Scaphites, Clioscaphites*, and *Scaphites (Pteroscaphites)*. Wiedmann (1965) thought that the species of the latter genus were the microconchs of those of the former two genera, based on the same morphology of juvenile shells, same stratigraphic occurrences and the adult size and morphological differences. This interpretation appears to be incorrect because dimorphism was demonstrated for the macroconchs as proposed by Wiedmann (1965) by both Cobban (1951) and Landman (1987), and later also in *Scaphites (Pteroscaphites)* by Landman (1989). In many cases, the mix of intraspecific variability within both sexes, evolutionary changes, phenotypic plasticity (Wilmsen and Mosavinia 2011) and dimorphism blurs the patterns of disparity in ammonoid populations to such extent that the various phenomena can hardly be distinguished (Kennedy and Wright 1979; Reyment 1988; Kassab and Hamama 1991).

The ratios of numbers of macroconchs (M) to microconchs (m) have also been determined for various species (Davis et al. 1996):

Hoploscaphites constrictus, France: 1.9 M: 1 m (Kennedy 1986b),

H. constrictus, Poland: 2.2 M: 1 m (Makowski 1962),

H. nicolletii, South Dakota: 20 M: 1 m (Landman and Waage, 1993),

H. comprimus, South Dakota: 1.5 M: 1 m (Landman and Waage 1993),
Menuites oralensis, Colorado: 2 M: 1 m (Cobban and Kennedy 1993),
M. portlocki complexus, Wyoming: 3.2 M: 1 m (Cobban and Kennedy 1993),
Scaphites hippocrepis, Wyoming: 0.5 M: 1 m (Cobban 1969),
S. hippocrepis III, Montana: 0.8 M: 1 m (Cobban 1969),
Scaphites 1eei III, New Mexico: 0.7 M: 1 m (Cobban 1969).

Another interesting aspect of dimorphism is the geographically varying ratio of the antidimorphs, for example in *Metoicoceras* (Kennedy 1988; Cobban et al. 1989) and *Hoploscaphites* (Landman and Waage 1993; Machalski 2005).

Some evolutionary trends in sexual dimorphism in Cretaceous ammonites have been described. Klinger and Kennedy (1989) examined *Placenticeras* from the Albian to the Maastrichtian and discovered that the early antidimorphs of this genus differed mainly in size, while younger, more derived forms differed also in ornament strength. Landman (1987) studied a population of Turonian *Scaphites whitfieldi* in which some of the specimens can be assigned to macroconchs or microconchs, while many forms display intermediate sizes and morphologies. In more derived scaphitids from the Maastrichtian, the assignment of antidimorphs can be done more easily because the dimorphism is more strongly expressed (Landman and Waage 1993).

7.4 Open Questions

7.4.1 Intraspecific Variability of Antidimorphs

Only a few studies are available dealing with the intraspecific variability of dimorphic species (compare De Baets et al. 2015a). This is understandable, because often it is difficult or impossible to get hold of a sufficiently large collection of mature specimens that are suitably preserved. Nevertheless, we are convinced that such populations of various ages are available in several museums worldwide, awaiting examination. Potential outcomes of such studies are a better understanding of the biological background of polymorphism, more confident separation of consecutive dimorphic species in evolutionary lineages, additional support for (or falsification of) dimorphism in cases of dubious dimorphism, an enhanced knowledge of the differences in variability between the antidimorphs, and raw data for further evolutionary studies.

7.4.2 Macroevolution of Mature Modifications and Dimorphism

Similar to the preceding topic, evolutionary aspects of dimorphism have only rarely or indirectly been addressed (one example is the work by Schweigert and Dietze 1998 on *Oecoptychius* and *Phlycticeras*; Fig. 7.9). It appears that the Haploceratoidea

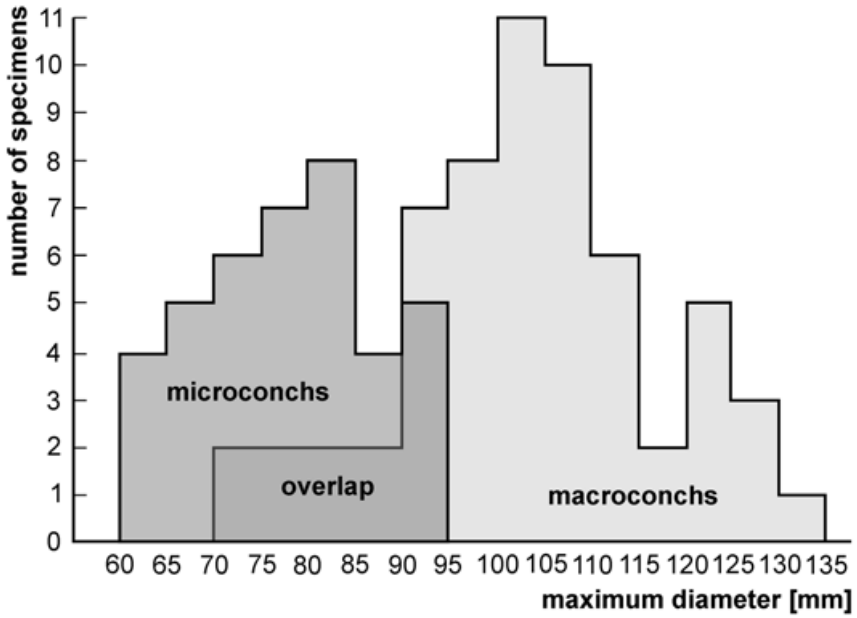

Fig. 7.14 Histogram of adult size in a collection of Maastrichtian *Hoploscaphites spedeni* from South Dakota. Macroconchs are usually larger than microconchs, but the size ranges overlap. (Redrawn from Davis et al. 1996 and Landman and Waage 1993)

could be an especially rewarding group in which to examine evolutionary changes in dimorphs (Fig. 7.11).

It has been suggested that evolutionary rates differed between antidimorphs; these rates may be difficult to quantify. By contrast, differences in variability of the antidimorphs through phylogeny could be studied in some small lineages (Fig. 7.14)

7.4.3 Taxonomic Treatment of Antidimorphs

Classically, partially because of the lack of knowledge, most antidimorphic pairs have been assigned to different taxa, occasionally reaching family level. Normally, members of one biological or morphological species should carry the same name according to the International Code of Zoological Nomenclature. As in trace fossils, the certainty of identity with respect to systematic nomenclature is often not given (for discussions see Callomon 1969; Lehmann 1981; Westermann 1969b). This is probably the reason why Demanet (1943) as well as Furnish and Knapp (1966) added various terms to the species name in order to state that they assume that two forms belong to the same species and at the same time, mark which form belongs to which sex. Although it appears reasonable to assign such antidimorphs, where it has been convincingly shown that they are conspecific, to the same species, this would imply applying different nomenclatorial rules depending on the state of knowledge (the problem could be solved by using partial names for cases that are not clear). An additional problem arises when diversity counts are carried out. If one species is knowingly subdivided into two, namely the antidimorphs, this would increase

diversity artificially. Ammonoid researchers need to agree on a unified treatment that addresses this problem.

7.4.4 Devonian to Triassic Dimorphism

Compared to Paleozoic and Triassic dimorphism (if it existed at all), identification of Jurassic and Cretaceous antidimorphic pairs appears easy. Davis et al. (1996) have already found the seeming lack or scarcity of pre-Jurassic dimorphism intriguing. Taking the roots of Jurassic dimorphism into account, some researchers considered that dimorphism was absent before the Toarcian. By contrast, Guex (1981) stated that already in the Hettangian, dimorphism was not rare. This, in combination with the work of Urlichs (2009), points to the possibility of a reasonably common but not yet detected dimorphism prior to the Jurassic. Further support for this hypothesis comes from the repeated occurrences of morphologies that resemble Jurassic microconchs in various respects, such as e.g., Devonian *Prolobites* and *Wocklumeria*, Permian *Elephantoceras* and *Adrianites*, Triassic *Coroceras* and dwarf *Arcestes* or *Lobites*.

These are just some out of many open questions. Davis et al. (1996, p. 521) actually listed many more such questions at the end of their article. We do not repeat this here but recommend it to those further interested.

Acknowledgments Some of the insights in this chapter grew in the course of research projects with the numbers 200021-113956/1, 200020-25029, and 200020-132870 funded by the Swiss National Science Foundation SNF. Images were kindly provided by Neil Landman (New York, USA), Günter Schweigert and Gerd Dietl (both Stuttgart, Germany), Jean-Stéphane David (Saint Dolay, France), Victor Schlamp (Lappersdorf, Germany), Christian Obrist (Rickenbach, Switzerland), Didier Bert (La Mure-Argens, France), Patrick Branger (Poitiers cedex, France), Wolfgang Grulke (Oborne, UK), Andreas E. Richter (Augsburg, Germany), Pierre-Yves Boursicot (Hauts-de-Seine, France). Margaret Yacobucci (Bowling Green), Izabela Ploch (Warsaw), and Kristin Polizzotto (Brooklyn) reviewed the manuscript and provided valuable constructive suggestions to improve it.

References

Aguirre-Urreta MB, Klinger HC (1986) Upper Barremian Heteroceratinae (Cephalopod, Ammonoidea) from Patagonia and Zululand, with comments on the systematics of the subfamily. Ann S Afr Mus 96(8):315–358

Aguirre-Urreta MB, Rawson PF (1993) The Lower Cretaceous ammonite *Paraspiticeras* from the Neuquen Basin, west-central Argentina. Neues Jahrb Geol Paläontol 188:187–233

Amedro F (1992) L'Albien du bassin anglo-Parisien: ammonites, zonation phylétique, séquences. Bull Cent Rech Explor Prod Elf-Aquitaine 16:187–233

Arkell WJ, Furnish WM, Kummel B, Miller AK, Moore RC, Schindewolf OH, Sylvester-Bradley PC, Wright CW (1957) Part L. Mollusca 4: Ammonoidea. In: Kaesler RL (ed) Treatise on invertebrate paleontology, Part L, Mollusca 4 (revised). GSA and University of Kansas Press, Lawrence

Atrops F (1982) La sous-famille des Ataxioceratinae dans le Kimmeridgien inférieur du Sud-Est de la France. Doc Lab Géol Lyon 83:1–371

Atrops F, Reboulet S (1995) *Neolissoceras* (*Carinites*), nouveau sous-genre d'ammonites du Valanginien du bassin vocontien (SE de la France). CR Acad Sci Paris 321(IIa):1203–1210

Baloge P-A, Cariou E (2001) Les Distichoceratinae (Ammonitina) du Centre-Ouest de la France. Palaeontogr A 261:125–159

Bardhan S, Dutta R, Chanda P, Mallick S (2012) Systematic revision and sexual dimorphism in *Choffatia* (Ammonoidea: Perisphinctoidea) from the Callovian of Kutch, India. Palaeoworld 21:29–49

Barrande J (1877) Systême Silurien du centre de la Bohème, Première Partie: Récherches paléontologiques. 2, Classes des Mollusques, Ordre des Céphalopodes. By the author, Paris

Basse, E (1952) Céphalopodes, Nautiloidea, Ammonoidea. In: Pivéteau J (ed) Traité de Paléontologie, vol 2. J. B. Baillière, Paris, pp 522–688

Bert D (2003) Etude de *Protophites vannii* sp. nov. (Ammonoidea), sous-zone a *Cardioceras vertebrale*, Oxfordien moyen, et evolution du genre *Protophites* Ebray, 1860. Riviéra Sci 87:69–84

Birkelund T (1982) Maastrichtian ammonites from Hemmoor, Niederelbe (NW-Germany). Geol J A 61:13–33

de Blainville MHD (1840) Prodrome d'une monographie des ammonites. In: Supplément du Dictionnaire des Sciences Naturelles, Bertrand. Paris, pp 1–31

Blind W, Jordan R (1979) "Septen-Gabelung" an einer *Dorsetensia romani* (Oppel) aus dem nordwestdeutschen Dogger. Paläontol Z 53(3/4):137–141

Bogoslovsky BI (1969) Devonskie ammonoidei. I. Agoniatity, vol 124 (Trudy Paleontologicheskogo Instituta Akademiya Nauk SSSR) Nauka, Moskva, pp 1–341

Bonnot A, Neige P, Tarkowski R, Marchand D (1994) *Mirosphinctes* Schindewolf et *Euaspidoceras* Spath du Niveau Vert de Zalas [Pologne] (Oxfordien Inférieur, Zone a Cordatum): Dimorphes sexuels? Bull Pol Acad Sci (Earth Sciences) 42:181–205

Bonnot A, Boursicot P-Y, Ferchaud P, Marchand D (2008) Les Pseudoperisphinctinae (Ammonitina, Perisphinctidae) de l'horizon à Leckenbyi (Callovien supérieur, zone à Athleta) de Montreuil-Bellay (Maine-et-Loire, France) et description d'une nouvelle espèce, *Choffatia isabellae*. Carnets Géol 5:1–27

Brinkmann R (1929) Monographie der Gattung *Kosmoceras*. Abh Ges Wiss Göttingen, Math-Phys KI, NF 13(4):1–123

Brochwicz-Lewiński W, Różak Z (1976) Some difficulties in recognition of sexual dimorphism in Jurassic perisphinctids (Ammonoidea). Acta Palaeontol Pol 21:115–124

Brooks MJ (1991) The ontogeny of sexual dimorphism: Quantitative models and a case study in labrisomid blennies (Teleostei: *Paraclinus*). Syst Zool 40(3):71–283

Bucher H (1992) Ammonoids of the Shoshonensis Zone (Middle Anisian, Middle Triassic) from NW Nevada. Jahrb Geol Bundesanst 135(2):423–466

Bucher H, Guex J (1990) Rythmes de croissance chez les ammonites triasiques. Bull Geol Lausanne 308:191–209

Bucher H, Landman NH, Klofak, SM, Guex J (1996) Mode and rate of shell growth. In: Landman NH, Tanabe K, Davis RA (eds) Ammonoid paleobiology. Plenum, New York

Bujtor I (1991) A new *Worthoceras* (Ammonoidea, Cretaceous) from Hungary, and remarks on the distribution of *Worthoceras* species. Geol Mag 128:537–542

Bujtor L (1993) Valanginian ammonite fauna from the Kisújbánya Basin (Mecsek Mts., South Hungary) and its palaeobiogeographical significance. Neues Jahrb Geol Paläontol Abh 188:103–131

Bulot L, Company M, Thieuloy J-P (1990) Origine, évolution et systematique du genre Valanginien *Saynoceras* (Ammonitina, Olcostephaninae). Geobios 23:399–413

Callomon JH (1955) The ammonite succession in the Lower Oxford Clay and Kellaway beds at Kidlington, Oxfordshire, and the zones of the Callovian Stage. Phil Trans R Soc Lond (Biol) 239:215–264

Callomon JH (1963) Sexual dimorphism in Jurassic ammonites. Trans Leic Lit Philos Soc 57:21–56

Callomon JH (1969) Dimorphism in Jurassic Ammonoidea. Some reflections. In: Westermann GEG (ed) Sexual dimorphism in fossil Metazoa and taxonomic implications. International union of geological sciences. A 1 Schweizerbart, Stuttgart, pp 111–125

Callomon JH (1981) Dimorphism in ammonoids. In: House MR, Senior JR (eds) The Ammonoidea, vol 18. Systematics Association by Academic Press, London pp 257–273

Callomon JH (1985) The evolution of the Jurassic ammonite family Cardioceratidae. Spec Pap Palaeontol 3349–90

Callomon JH (1988) [Review of] Matyja BA (1986) Developmental polymorphism in Oxfordian ammonites. Acta Geol Pol 36:37–68 (Cephalopod Newsl 9:14–16)

Callomon JH, Gradinaru E (2005) From the thesaurus of the museum collections. I. Liassic ammonites from Munteana (Svinita Zone, Southern Carpathians, Romania). Acta Palaeontol Rom 5:49–65

Cariou E (1984). Les Reineckeiidae (Ammonitina, Callovien) de la Tethys occidentales. Dimorphisme et evolution. Etude a partir des gisements du centre-ouest de la France. Doc Lab Géol Lyon HS 8:1–599

Cecca E, Landra G (1994) Late Barremian-early Aptian ammonites from the Maiolica formation near Cesana Brianza (Lombardy Basin, northern Italy). Riv It Paleont Strat 100(3):395–422

Cecca F, Rouget I (2006) Anagenetic evolution of the Early Tithonian ammonite genus *Semiformiceras* tested with cladistic analysis. Palaeontology 49:1069–1080

Charpy N, Thierry (1976) Dimorphisme et polymorphisme chez *Pachyceras* Bayle (Ammonitina, Stephanocerataceae) du Callovien supérieur (Jurassique moyen). Haliotis 6:185–218

Chimšiašvili NG, Kamsyeva-Elpatevskaja VG, Bodylevskij VI et al. (1958) Nadsemejstvo Perisphinctaceae. In: Orlov JA (ed) Osnovy paleontologii, molluski-golovonogie, II. Moskva, pp 85–96

Cobban WA (1951) Scaphitoid cephalopods of the Colorado Group. US Geol Surv Prof Pap 239:1–42

Cobban WA (1953) Cenomanian ammonite fauna from the Mosby Sandstone of central Montana, US Geol Surv Prof Pap 243D:45–55

Cobban WA (1969) The Late Cretaceous ammonites *Scaphites leei* Reeside and *Scaphites hippocrepis* (DeKay) in the Western Interior of the United States. US Geol Surv Prof Pap 619:1–29

Cobban WA (1984) Molluscan record from a mid-Cretaceous borehole in Weston County, Wyoming. US Geol Surv Prof Pap 1271:1–24

Cobban WA (1987) The Upper Cretaceous ammonite *Rhaeboceras* Meek in the Western Interior of the United States. US Geol Surv Prof Pap 1477:1–15

Cobban WA (1988a) *Tarrantoceras* Stephenson and related ammonoid genera from Cenomanian (Upper Cretaceous) rocks in Texas and the Western Interior of the United States. US Geol Surv Prof Pap 1473:1–30

Cobban WA (1988b) The Upper Cretaceous ammonite *Watinoceras* Warren in the Western Interior of the United States. US Geol Surv Bull 1788:1–15

Cobban WA, Hook SC (1983) Mid-Cretaceous (Turonian) ammonite fauna from Fence Lake area of west-central New Mexico, NM. Bur Mines Miner Resour Mem 41:1–50

Cobban WA, Kennedy WJ (1990) Variation and ontogeny of *Calycoceras (Proeucalycoceras) canitaurinum* (Haas, 1949) from the Upper Cretaceous (Cenomanian) of the Western Interior of the United States. US Geol Surv Bull 1881:BI–B7

Cobban WA, Kennedy WJ (1991a) A giant scaphite from the Turonian (Upper Cretaceous) of the Western Interior of the United States. US Geol Surv Bull 1934:A1–A2

Cobban WA, Kennedy WJ (1991b) Evolution and biogeography of the Cenomanian (Upper Cretaceous) ammonite *Metoicoceras* Hyatt. 1903, with a revision of *Metoicoceras praecox* Haas, 1949. US Geol Surv Bull 1934:BI–B11

Cobban WA, Kennedy WJ (1991c) *Baculites thomi* Reeside 1927, an Upper Cretaceous ammonite in the Western Interior of the United States. US Geol Surv Bull 1934:C

Cobban WA, Kennedy WJ (1992) Campanian *Trachyscaphites spiniger* ammonite fauna in northeast Texas. Palaeontology 35(1):63–93

Cobban WA, Kennedy WJ (1993) The Upper Cretaceous dimorphic pachydiscid ammonite *Menuites* in the Western Interior of the United States. US Geol Surv Prof Pap 1533:1–14

Cobban WA, Kennedy WJ (1994a) Upper Cretaceous ammonites from the Coon Creek Tongue of the Ripley Formation at its type locality in McNairy County, Tennessee. US Geol Surv Bull 2073:BI–B12

Cobban WA, Kennedy WJ (1994b) Middle Campanian (Upper Cretaceous) ammonites from the Pecan Gap Chalk of central and northeastern Texas. US Geol Surv Bull 2073:D1-D9

Cobban WA, Hook SC, Kennedy WJ (1989) Upper Cretaceous rocks and ammonite faunas of southwestern New Mexico. NM Bur Mines Miner Resour Mem 45:1–137

Coemme S (1917) Note critique sur le genre *Cadomoceras*. Bull Soc Géol Fr 417:44–54

Collins D, Ward PD (1987) Adolescent growth and maturity in Nautilus. In: Saunders WB, Landman NH (eds) Nautilus. The biology and paleobiology of a living fossil, vol 6. Plenum Press, New York 421–432 (Topics in Geobiology)

Contini D, Marchand D, Thierry J (1984) Réflexion sur la notion de genre et de sous-genre chez les ammonites: Exemples pris essentiellement dans le Jurassique moyen. Bull Soc Géol Fr 26(4):653–661

Cooper MR, Kennedy WJ (1977) A revision of the Baculitidae of the Cambridge Greensand. Neues Jahrb Geol Paläontol Mh 11:641–658

Cooper MR, Kennedy WJ (1979) Uppermost Albian (Stoliczkaia dispar zone) ammonites from the Angolan littoral. Ann S Afr Mus 77(10):175–308

Cooper MR, Kennedy WJ (1987) A revision of the Puzosiinae (Cretaceous ammonites) of the Cambridge Greensand. Neues Jahrb Geol Paläontol Abh 174(1):105–121

Cope JCW (1992) Dimorphism in a Tethyan Early Jurassic *Juraphyllites*. Lethaia 25:439–441

Cox B.M. (1988) English Callovian (Middle Jurassic) perisphinctid ammonites. Part 1. Monogr Palaeontogr Soc Lond 140:1–54

Czarnocki J (1989) Klimenie Gór Świętokrzyskich (Prace Państwowego Instytutu Geologicznego), vol 127 Wydawnictwa Geologiczne, Warszawa, pp 1–91

Davis RA (1972) Mature modification and dimorphism in selected late Paleozoic ammonoids. Bull Am Paleontol 62(272):23–130

Davis RA, Furnish WM, Glenister BF (1969) Mature modification and dimorphism in late Paleozoic ammonoids. In: Westermann GEG (ed) Sexual dimorphism in fossil Metazoa and taxonomic implications (IUGS, Series A1). Schweizerbart, Stuttgart, pp 101–110

Davis RA, Landman NH, Dommergues J-L, Marchand D, Bucher H (1996) Mature modifications and dimorphism in ammonoid cephalopods. In: Landman NH, Tanabe K, Davis RA (eds) Ammonoid paleobiology. Plenum, New York

Davitashvili LSh, Khimshiashvili NG (1954) On the question of the biological significance of the apertural formation of ammonites. Works Paleobio Sect Acad Sci Georgian Soviet Soc Re 2:44–76 [in Russian]

De Baets K Klug C Korn D Landman NH (2012) Evolutionary trends in ammonoid embryonal development. Evolution 66:1788–1806

De Baets K Klug C Monnet C (2013a) Intraspecific variability through ontogeny in early ammonoids. Paleobiology 39:75–94

De Baets K Klug C Korn D Bartels C Poschmann M (2013b) Emsian Ammonoidea and the age of the Hunsrück Slate (Rhenish Mountains, Western Germany). Palaeontogr A 299(1–6):1–113

De Baets K, Bert D, Hoffmann R, Monnet C, Monnet C, Yacobucci MM, Klug C (2015a) Ammonoid Intraspecific Variability. This volume

De Baets K, Landman NH, Tanabe K (2015) Ammonoid embryonic development. This volume

Delanoy G, Poupon A (1992) Sur le genre *Lytocrioceras* Spath, 1924 (Ammonoidea, Ancyloceratina). Geobios 25(3):367–382

Delanoy G, Ropolo P, Magnin A, Autran G, Poupon A, Gonnet R (1995) Sur le dimorphisme chez les Ancyloceratina (Ammonoidea) du Crétacé inférieur. Comptes Rendus Acad Sci Sér IIa 321:537–543

Demanet F (1943) Les horizons marins du Westphalien de la Belgique et leurs faunes. Mém Mus R Hist Nat Belg 101:1–166

Dietl G (2013) Der Braune Jura ober-ε und ζ. Fossilien. Sonderheft "Der Braunjura am Fuß der Schwäbischen Alb", pp 30–46

Dietze V, Callomon JH, Schweigert G, Chandler RB (2005) The ammonite fauna and biostratigraphy of the Lower Bajocian (Ovale and Laeviscula zones) of E Swabia (S Germany). Suttg Beitr Naturk B 353:1–82

Dietze V, Chandler RB, Callomon JH (2007) The ovale zone (Lower Bajocian, Middle Jurassic) at Little Down Wood (Dundry Hill, Somerset, SW England). Stuttg Beitr Naturk B 368:1–45

Dietze V, Bosch K, Franz M, Kutz M, Schweigert G, Wannenmacher N, Studer S (2013) Die Humphriesianum-Zone (Unter-Bajocium, Mitteljura) am Kahlenberg bei Ringsheim (Oberrheingraben, SW Deutschland). Palaeodiversity 6:29–61

Djanélidzé A (1922) Les *Spiticeras* du sud-est de la France. Mém Explic Carte Géol détaill Fr VI: 1–255

Doguzhaeva L (1982) Rhythms of ammonoid shell secretion. Lethaia 15:385–394

Doguzhaeva LA (1981) The wrinkle layer in the shell of ammonoids. Paleontol Z 1:38–48 [In Russian]

Doguzhaeva LA, Kabanov GK (1988) Muscle scars in ammonoids. Dokl Akad Nauk USSR 301:210–212

Doguzhaeva LA, Mikhailova IA (1991) New data on muscle system of heteromorphic ammonites. Dokl Akad Nauk USSR 318(4):981–984

Doguzhaeva LA, Mikhailova IA (2002) The jaw apparatus of the heteromorphic ammonite *Australiceras whitehouse*, 1926 (Mollusca: Cephalopoda) from the Aptian of the Volga Region. Dokl Akad Nauk USSR 382:38–40

Doguzhaeva LA, Mutvei H (1991) Organization of the soft body in *Aconeceras* (Ammonitina), interpreted on the basis of shell morphology and muscle scars. Palaeontogr A 218:17–33

Doguzhaeva LA, Mutvei H (1993) Shell ultrastructure, muscle scars, and buccal apparatus in ammonoids. Geobios 15:111–119

Doguzhaeva LA, Mutvei H (1996) Attachment of the body to the shell in ammonoids. In: Landman NH, Tanabe K, Davis RA (eds) Ammonoid paleobiology. Plenum, New York

Dommergues J-L (1993) The Jurassic ammonite *Coeloceras*: An atypical example of dimorphic progenesis elucidated by cladistics. Lethaia 27(2):143–152

Donovan DT, Callomon JH, Howarth MK (1981). Classification of the Jurassic Ammonitina. In: House MR, Senior JR (eds) The Ammonoidea, vol 18. Systematics Association by Academic Press, pp 101–155

Dzik J (1984) Phylogeny of the Nautiloidea. Palaeont Pol 45:1–220

Dzik J (1990a) The concept of chronospecies in ammonites. In: Pallini G, Cecca F, Cresta S, Santantonio M (eds) Atti del secondo convegno internazionale Fossili Evoluzione Ambiente. Pergola

Dzik J (1990b) The ammonite *Acrochordiceras* in the Triassic of Silesia. Acta Palaeontol Pol 35(1–2):49–65

Ebbighausen V, Korn D (2007) Conch geometry and ontogenetic trajectories in the triangularly coiled Late Devonian ammonoid *Wocklumeria* and related genera. Neues Jahrb Geol Paläontol Abh 244:9–41

Elmi S (1967) Le Lias supérieur et le Jurassique moyen de l'Ardeche. Docum Lab. Géol Lyon 19(1–3):1–845

Elmi S, Mangold C (1966) Eude de quelques *Oxycerites* du Bathonien Inférieur. Trab Lab Géol Fac Sc Lyon, NS 13:143–181

Enay R (1966) L'Oxfordien dans la moitié sud du Jura français. Nouv Arch Mus Hist Nat Lyon 8:1–624

Ernst HU, Klug C (2011) Perlboote und Ammonshörner weltweit. Nautilids and Ammonites worldwide. Pfeil Verlag, München

Etches S, Clarke J, Callomon J (2009) Ammonite eggs and ammonitellae from the Kimmeridge clay formation (Upper Jurassic) of Dorset, England. Lethaia 42:204–217

Fatmi AN (1969) Dimorphism in some Jurassic and Lower Cretaceous ammonites from West Pakistan. Geonews (Geol. Surv. Pakistan) 1(2):6–13

Foord AH, Crick GC (1897) Catalogue of the fossil Cephalopoda in the British Museum (Natural History). Part III. Containing the Bactritidae and Part of the suborder Ammonoidea. British Museum (Natural History), London

Förster R, Weier H (1983) Ammoniten und Alter der Niongala-Schichten (Unterapt, Slid-Tanzania). Mitt Bayer Staatsslg Paläontol Hist Geol 23:51–76
Förster R, Meyer R, Risch H (1983) Ammoniten und planktonische Foraminiferen aus den Eibrunner Mergeln (Regensburger Kreide, Nordostbayern). Zitteliana 10:123–141
Frest TJ, Glenister BF, Furnish WM (1981) Pennsylvanian-Permian Cheiloceratacean ammonoid families Maximitidae and Pseudohaloritidae. Paleontol Soc Mem 11 (Paleontol suppl to) 55(3):1–46
Furnish WM, Knapp WD (1966) Lower Pennsylvanian fauna from eastern Kentucky; Part 1, Ammonoids. J Paleontol 40(2):296–308
Futakami M 1990. Turonian collignoniceratid ammonites from Hokkaido, Japan. Stratigraphy and paleontology of the Cretaceous in the Ishikari province, central Hokkaido. (Part 3, l, vol 1). Kawamura Gakuen Women's University, Japan, pp 235–260
Gabr HR, Hanlon RT, Hanafy MH, El-Etreby SG (1998) Maturation, fecundity and seasonality of reproduction of two commercially valuable cuttlefish, *Sepia pharaonis* and *S. dollfusi*, in the Suez Canal. Fisch Res 36:99–115
Ganguly T, Bardhan S (1993) Dimorphism in *Placenticeras mintoi* from the Upper Cretaceous Bagh Beds, central India. Cretac Res 14:747–756
Gauthier H, Branger P, Boursicot P-Y, Trévisan M, Marchand D (2002) La faune *d'Orthogarantiana* Bentz (Garantianinae, Stephanoceratidae) de la sous-zone à Polygyralis (z. à Niortense, Bajocien sup.) nouvellement découverte au nord de Niort (Deux-Sèvres, France). Une preuve du dimorphisme *Orthogarantiana/Strenoceras*. Géol Fr 1:81–86
Gemmellaro GG (1887) La fauna dei calcari con Fusulina della valle del Fiume Sosio nella Provincia di Palermo. Fascio I-Cephalopoda, Ammonoidea. G Sci Nat Econ 19:1–106
Geyer OF (1969) The ammonite genus *Sutneria* in the Upper Jurassic of Europe. Lethaia 2:63–72
Gould SJ (1977) Ontogeny and phylogeny. Harvard University Press, Cambridge
Griffin LE (1900) The anatomy of *Nautilus pompilius*. Mem Natl Acad Sci 8:101–203
Guex J (1967) Dimorphisme sexuel d'un groupe d'*Hammatoceras* et position systématique du genre *Onychoceras*. Bull Soc Vaud Sci Nat 69:423–434
Guex J (1968) Note préliminaire sur le dimorphisme sexuel des Hildocerataceae du Toarcien moyen et supérieur de l'Aveyron (France). Soc Vaud Sci Nat Lausanne Bull 70(327):57–84
Guex J (1973) Dimorphisme des Dactylioceratidae du Toarcien. Eclogae Geol Helv 66:545–583
Guex J (1981) Quelques cas de dimorphisme chez les ammonïodés du Lias inférieur. Bull Soc Vaud Sci Nat 75:239–248
Hahn W (1971) Die Tulitidae S. Buckman, Sphaeroceratidae S. Buckman und Clydoniceratidae S. Buckman (Ammonoidea) des Bathoniums (Brauner Jura ε) im südwestdeutschen Jura. Jahresh Geol Landesamtes Baden-Württ 13:55–122
Hammer Ø, Bucher H (2006) Generalized ammonoid hydrostatics modelling, with application to *Intornites* and intraspecific variation in *Amaltheus*. Paleontol Res 10:91–96
Hanlon RT, Forsythe JW (2008) Sexual cannibalism by *Octopus cyanea* on a Pacific coral reef. Mar Freshw Behav Physiol 41:19–28
Haug E (1897) Observations a la suite d'une note de Ph. Glangeaud sur las forme de l'ouverture de quelques ammonites. Bull Soc Géol Fr Ser 325:107
Hayasaka S, Oki K, Tanabe K, Saisho T, Shinomiya A (1987) On the habitat of *Nautilus pompilius* in Tafton Strait (Philippines) and the Fiji Islands. In: Saunders WB, Landman NH (eds) *Nautilus*. The biology and paleobiology of a living fossil. Plenum, New York
Hillebrandt A, Krystyn L (2009) On the oldest Jurassic ammonites of Europe (Northern Calcareous Alps, Austria) and their global significance. Neues Jahrb Geol Paläontol Abh 253:163–195
Hirano H (1978) Phenotypic substitution of *Gaudryceras* (a Cretaceous ammonite). Trans Proc Palaeontol Soc Jpn NS 109:235–258
Hirano H (1979) Importance of transient polymorphism in systematics of Ammonoidea. The Gakujutsu Kenkyu Sch Educ Waseda Univ Ser Biol Geol 28:35–43
Hoffmann R (2010) New insights on the phylogeny of the Lytoceratoidea (Ammonitina) from the septal lobe and its functional interpretation, vol 29. Revue de Paléobiologie, Genève, pp 1–156

Hoffmann R, Schultz JA, Schellhorn R, Rybacki E, Keupp H, Gerden SR, Lemanis R, Zachow S (2013) Non-invasive imaging methods applied to neo- and paleontological research. Biogeosci Discuss 10:18803–18851. doi:10.5194/bgd-10-18803-2013

Housa V (1965) Sexual dimorphism and the system of Jurassic and Cretaceous Ammonoidea (Preliminary note). Casas Nar Muz 134:33–35

House MR (1970) The goniatite wrinkle layer. Smithson Contrib Paleontol 3:23–32

Howarth MK (1992) Tithonian and Berriasian ammonites from the Chia Gara Formation innorthern Iraq. Palaeontology 35(3):597–655

Howarth MK (2013) Part L, Revised, Volume 3B, Chapter 4: Psiloceratoidea, Eoderoceratoidea, Hildoceratoidea. Treatise 57:1–139

Immel H (1987) Die Kreideammoniten der nordlichen Kalkalpen. Zitteliana 15:3–163

Ivanov AN (1971) About some growth alterations in ammonite shells. Bull Mosc Soc Nat Hist Geol Sect 46:155 [in Russian]

Ivanov AN (1975) Late ontogeny of ammonites and, in particular, of the micro-, macro-, and megaconchs. Coll Stud Notes Sci W Yarosl St Ped Inst 142:5–57 [in Russian]

Ivanov AN (1985) Were micro- and macroconchs of ammonites sexual dimorphs? In: Taxonomy and ecology of Cephalopoda. Scientific papers. Academy of Sciences of the USSR, Zoological Institute, Scientific Council on the Problem of "Biological Bases of Utilization, Remaking, and Protection of the Animal World", Malacological Committee, Leningrad, 32–34 [in Russian]

Jackson GD, Moltschaniwskyj NA (2002) Spatial and temporal variation in growth rates and maturity in the Indo-Pacific squid *Sepioteuthis lessoniana* (Cephalopoda: Loliginidae). Mar Biol 140:747–754

Jagt JWM (1989) Ammonites from the early Campanian Vaals Formation at the CPL Quarry (Haccourt, Liege, Belgium) and their stratigraphic implications. Meded. Rijks Geol Dienst 43(1):1–18

Jagt JWM, Kennedy WJ (1989) *Acanthoscaphites varians* (Lopuski, 1911) (Ammonoidea) from the Upper Maastrichtian of Haccourt, NE Belgium. Geol Mijnb 68:237–240

Jagt JWM, Kennedy WJ (1994) *Jeletzkytes dorfi* Landman and Waage 1993, a North American ammonoid marker from the lower Upper Maastrichtian of Belgium, and the numerical age of the Lower/Upper Maastrichtian boundary. Neues Jahrb Geol Paläontol Mh 4:239–245

Jagt JWM, Kennedy WJ, Burnett J (1992) *Acanthoscaphites tridens* (Kner, 1848) (Ammonoidea) from the Vijlen Member (Lower Maastrichtian) of Gulpen, Limburg, The Netherlands. Geol Mijnb 71:15–21

Jeletzky JA, Waage KM (1978) Revision of *Ammonites conradi* Morton 1834, and the concept of *Discoscaphites* Meek 1870. J Paleontol 52:1119–1132

Kakabadze MV (2004) Intraspecific and intrageneric variabilities and their implication for the systematics of Cretaceous heteromorph ammonites; a review. Scr Geol 128:17–37

Kant R (1973) Allometrisches Wachstum paläozoischer Ammonoideen: Variabilität und Korrelation einiger Merkmale. Neues Jahrb Geol Paläontol Abh 143:153–192

Kaplan U, Kennedy WJ, Wright CW (1987) Turonian and Coniacian Scaphitidae from England and North-Western Germany. Geol J 103:5–39

Kassab AS, Hamama HH (1991) Polymorphism in the Upper Cretaceous ammonite *Libycoceras ismaeli* (Zittel). J Afr Earth Sci 12(3):437–448

Keferstein W (1866) Cephalopoden. In: Die Klassen und Ordnungen des Thierreichs wissenschaftlich dargestellt in Wort und Bild von Hans Georg Bronn. Fortgesetzt von Wilhelm Keferstein, (vol 3, part 2). Verlag Winter, Leipzig, pp 1337–1406

Kemper E (1982) Die Ammoniten des späten Apt und frühen Alb Nordwestdeutschlands. Geol Jahrb A 65:553–557

Kennedy WJ (1984) Systematic paleontology and stratigraphic distribution of the ammonite faunas of the French Coniacian. Spec Pap Palaeontol 31:1–160

Kennedy WJ (1986a) Observations on *Astiericeras astierianum* (d'Orbigny, 1842) (Cretaceous Ammonoidea). Geol Mag 123(5):507–513

Kennedy WJ (1986b) The ammonite fauna of the Calcaire a *Baculites* (Upper Maastrichtian) of the Cotentin Peninsula (Manche, France). Palaeontology 29:25–83

Kennedy WJ (1986c) The ammonite fauna of the type Maastrichtian with a revision of *Ammonites colligatus* Binkhorst 1861. Bull Inst R Sci Nat Belg (Sciences de la Terre) 56:151–267
Kennedy WJ (1986d) Campanian and Maastrichtian ammonites from northern Aquitaine, France. Spec Pap Palaeontol 36:1–145
Kennedy WJ (1988) Late Cenomanian and Turonian ammonite faunas from north-east and central Texas. Spec Pap Palaeontol 39:1–131
Kennedy WJ (1989) Thoughts on the evolution and extinction of Cretaceous ammonites. Proc Geol Assoc 100(3):251–279
Kennedy WJ (1993) Campanian and Maastrichtian ammonites from the Mons Basin and adjacent areas. vol 63. Bull lnst R Sci Nat Belg (Sciences de la Terre) 63:99–131 (Belgium)
Kennedy WJ, Christensen WK (1991) Coniacian and Santonian ammonites from Bornholm, Denmark. Bull Geol Soc Den 38:203–226
Kennedy WJ, Cobban WA (1976) Aspects of ammonite biology, biogeography, and biostratigraphy. Spec Pap Palaeontol 17:1–93
Kennedy WJ, Cobban WA (1988a) *Litophragmatoceras incomptum* gen. et sp. nov. (Cretaceous Ammonoidea), a cryptic micromorph from the Upper Cenomanian of Arizona. Geol Mag 125(5):535–539
Kennedy WJ, Cobban WA (1988b) Mid-Turonian ammonite faunas from northern Mexico. Geol Mag 125:593–612
Kennedy WJ, Cobban WA (1990) Cenomanian ammonite faunas from the Woodbine Formation and lower part of the Eagle Ford Group, Texas. Palaeontology 33:75–154
Kennedy WJ, Cobban WA (1991a) Coniacian ammonite faunas from the United States Western Interior. Spec Pap Palaeontol 45:1–96
Kennedy WJ, Cobban WA (1991b) Upper Cretaceous (upper Santonian) *Boehmoceras* fauna from the Gulf Coast region of the United States. Geol Mag 128(2):167–189
Kennedy WJ, Cobban WA (1993a) Ammonites from the Saratoga Chalk (Upper Cretaceous), Arkansas. J Paleontol 67:404–434
Kennedy WJ, Cobban WA (1993b) Campanian ammonites from the Annona Chalk near Yancy, Arkansas. J Paleontol 67:83–97
Kennedy WJ, Cobban WA (1993c) Maastrichtian ammonites from the Corsicana Formation in northeast Texas. Geol Mag 130(1):57–67
Kennedy WJ, Delamette M (1994) *Neophlycticeras* Spath, 1922 (Ammonoidea) from the Upper Albian of Ain, France. Neues Jahrb Geol Palaontol Abh 191(1):1–24
Kennedy WJ, Henderson RA (1992) Non-heteromorph ammonites from the Upper Maastrichtian of Pondicherry, South India. Palaeontology 35:381–442
Kennedy WJ, Juignet P (1983) A revision of the ammonite faunas of the type Cenomanian. 1. Introduction, Ancyloceratina. Cretac Res 4:3–83
Kennedy WJ, Juignet P (1984) A revision of the ammonite faunas of the type Cenomanian. 2. The families Binneyitidae, Desmoceratidae, Engonoceratidae, Placenticeratidae, Hoplitidae, Schloenbachiidae, Lyelliceratidae and Forbesiceratidae. Cretac Res 5:93–161
Kennedy WJ, Juignet P (1994) A revision ofthe ammonite faunas of the type Cenomanian, 5. Acanthoceratinae *Calycoceras* (*Calycoceras*), *C*. (*Gentoniceras*) and *C*. (*Newboldiceras*). Cretac Res 15:17–57
Kennedy WJ, Klinger HC (1979) Cretaceous faunas from Zululand and Natal, South Africa. The ammonite superfamily Haploceratacеae Zittel, 1884. Ann S Afr Mus 77(6):85–121
Kennedy WJ, Klinger HC (1985) Cretaceous faunas from Zululand and Natal, South Africa. The ammonite family Kossmaticeratidae Spath. 1922. Ann S Afr Mus 95(5):165–231
Kennedy WJ, Klinger HC (1993) On the affinities of *Cobbanoscaphites* Collignon, 1969 (Cretaceous Ammonoidea). Ann S Afr Mus 102(7):265–271
Kennedy WJ, Summesberger H (1984) Upper Campanian ammonites from the Gschliefgraben (Ultrahelvetic, Upper Austria). Beitr Paläontol Österr 11:149–206
Kennedy WJ, Summesberger H (1987) Lower Maastrichtian ammonites from Nagoryany (Ukrainian SSR). Beitr Paläontol Österr 13:25–78
Kennedy WJ, Wright CW (1979) Vascoceratid ammonites from the type Turonian. Palaeontology 22:665–683

Kennedy WJ, Wright CW (1981) *Euhystrichoceras* and *Algericeras*, the last mortoniceratine ammonites. Palaeontology 24:417–435
Kennedy WJ, Wright CW (1983) *Ammonites polyopsis* Dujardin, 1837, and the Cretaceous ammonite family Placenticeratidae Hyatt, 1900. Palaeontology 26:855–873
Kennedy WJ, Wright CW (1984a) The Cretaceous ammonite *Ammonites requienianus* d'Orbigny, 1841. Palaeontology 27:281–293
Kennedy WJ, Wright CW (1984b) The affinities of the Cretaceous ammonite *Neosaynoceras* Breistroffer, 1947. Palaeontology 27:159–167
Kennedy WJ, Wright CW (1985a) Evolutionary patterns in Late Cretaceous ammonites. Spec Pap Palaeontol 33:131–143
Kennedy WJ, Wright CW (1985b) *Mrhiliceras* n.g. (Cretaceous Ammonoidea), a new Cenomanian mantelliceratine. Neues Jahrb Geol Paläontol Mh 9:513–526
Kennedy WJ, Wright CW, Hancock JM (1980) Collignoniceratid ammonites from the mid-Turonian of England and northern France. Palaeontology 23:557–603
Kennedy WJ, Juignet P, Hancock JM (1981a) Upper Cenomanian ammonites from Anjou and the Vendee, western France. Palaeontology 24:25–84
Kennedy WJ, Klinger HC, Summesberger H (1981b) Cretaceous faunas from Zululand and Natal, South Africa. Additional observations on the ammonite subfamily Texanitinae Collignon, 1948. Ann S Afr Mus 86(4):115–155
Kennedy WJ, Wright CW, Klinger HC (1983) Cretaceous faunas from Zululand and Natal, South Africa. The ammonite subfamily Barroisiceratinae Basse, 1947. Ann S Afr Mus 90(6):241–324
Kennedy WJ, Bilotte M, Lepicard B, Segura F (1986) Upper Campanian and Maastrichtian ammonites from the Petites-Pyrenees, southern France. Eclogae Geol Helv 79:1001–1037
Kennedy WJ, Wright CW, Hancock JM (1987) Basal Turonian ammonites from west Texas. Palaeontology 30:27–74
Kennedy WJ, Cobban WA, Hancock JM, Hook SC (1989) Biostratigraphy of the Chispa Summit Formation at its type locality: A Cenomanian through Turonian reference section for trans-Pecos Texas. Bull Geol Inst Univ Upps NS 15:39–119
Kennedy WJ, Hansotte M, Bilotte M, Burnett J (1992) Ammonites and nannofossils from the Campanian of Nalzen (Ariege, France). Geobios 25(2):263–278
Kennedy WJ, Landman NH, Cobban WA, Scott GR (2000) Late Campanian (Cretaceous) heteromorph ammonites from the western interior of the United States. Bull Am Mus Nat Hist 251:1–88
Kennedy WJ, Cobban WA, Klinger HC (2002) Muscle attachment and mantle-related features in Upper Cretaceous *Baculites* from the United States Western Interior. Abh Geol Bund-Anst 57:89–112
Keupp H (2000) Ammoniten—paläobiologische Erfolgsspiralen. Thorbecke, Stuttgart
Keupp H (2012) Atlas zur Paläopathologie der Cephalopoden. Berl Paläobiol Abh 12:1–390
Keupp H, Riedel F (2010) Remarks on the possible function of the apophyses of the Middle Jurassic microconch ammonite *Ebrayiceras sulcatum* (Zieten 1830), with a discussion on the palaeobiology of Aptychophora in general. Neues Jahrb Geol Paläontol Abh 255:301–314
Klinger HC (1989) The ammonite subfamily Labeceratinae Spath, 1925. Systematics, phylogeny, dimorphism and distribution (with a description of a new species). Ann S Afr Mus 98(7):189–219
Klinger HC, Kennedy WJ (1977) Cretaceous faunas from Zululand, South Africa and southern Mozambique. The Aptian Ancyloceratidae (Ammonoidea). Ann S Afr Mus 73(9):215–359
Klinger HC, Kennedy WJ (1989) Cretaceous faunas from Zululand and Natal. South Africa. The ammonite family Placenticeratidae Hyatt, 1900, with comments on the systematic position of the genus *Hypengonoceras* Spath, 1924. Ann S Afr Mus 98(9):241–408
Klinger HC, Kennedy WJ (1992) Cretaceous faunas from Zululand and Natal, South Africa. Barremian representatives of the ammonite family Ancyloceratidae Gill, 1871. Ann S Afr Mus 101(5):71–138
Klinger HC, Kennedy WJ (1993) Cretaceous faunas from Zululand and Natal, South Africa. The heteromorph ammonite genus *Eubaculites* Spath, 1926. Ann S Afr Mus 102(6):185–264
Klug C (2001) Life-cycles of Emsian and Eifelian ammonoids (Devonian). Lethaia 34:215–233

Klug C (2004) Mature modifications, the black band, the black aperture, the black stripe, and the periostracum in cephalopods from the Upper Muschelkalk, vol (Middle Triassic, Germany). Mitt Geol-Paläont Inst Univ Hamburg 88:63–78

Klug C, Korn D (2003) Morphological pathways in the evolution of Early and Middle Devonian ammonoids. Paleobiology 29:329–348

Klug C, Korn D (2004) The origin of ammonoid locomotion. Acta Palaeontol Pol 49:235–242

Klug C, Korn D, Richter U, Urlichs M (2004) The black layer in cephalopods from the German Muschelkalk (Middle Triassic). Palaeontology 47:1407–1425

Klug C, Brühwiler T, Korn D, Schweigert G, Brayard A, Tilsley J (2007) Ammonoid shell structures of primary organic composition. Palaeontology 50:1463–1478

Klug C, Meyer E, Richter U, Korn D (2008) Soft-tissue imprints in fossil and Recent cephalopod septa and septum formation. Lethaia 41:477–492

Klug C, Riegraf W, Lehmann J (2012) Soft-part preservation in heteromorph ammonites from the Cenomanian-Turonian Boundary Event (OAE 2) in the Teutoburger Wald (Germany). Palaeontology 55:1307–1331

Korn D (1992) Heterochrony in the evolution of Late Devonian ammonoids. Acta Palaeontol Pol 37(1):21–36

Korn D (2012) Quantification of ontogenetic allometry in ammonoids. Evol Dev 14(6):501–514

Korn D, Ebbighausen V (2008) The Early Carboniferous (Mississippian) ammonoids from the Chebket el Hamra (Jerada Basin, Morocco). Foss Rec 11:83–156. doi:10.1002/mmng.200800004

Korn D, Klug C (2002). Ammoneae Devonicae. In: Riegraf W (ed) Fossilium Catalogus 1: Animalia, vol 138.Backhuys, Leiden, pp 1–375

Korn D, Klug C (2003) Morphological pathways in the evolution of early and middle Devonian ammonoids. Paleobiology 29:329–348

Korn D, Klug C (2007) Conch form analysis, variability, and morphological disparity of a Frasnian (Late Devonian) ammonoid assemblage from Coumiac (Montagne Noire, France). In: Landman NH, Davis RA, Manger W, Mapes RH (eds) Cephalopods—present and past. Springer, New York

Korn D, Titus A (2006) The ammonoids from the Three Forks Shale (Late Devonian) of Montana. Foss Rec 9:198–212

Korn D, Klug C, Mapes RH (1999) Viséan and Early Namurian Ammonoids from the Tafilalt (Eastern Anti-Atlas, Morocco). Abh Geol Bundesanst 54:345–375

Korn D, Bockwinkel J, Ebbighausen V (2010) The ammonoids from the Argiles de Teguentour of Oued Temertasset (early Late Tournaisian; Mouydir, Algeria). Foss Rec 13:35–152

Korn D, Mapes RH, Klug C (2014) The coarse wrinkle layer of Palaeozoic ammonoids: new evidence from the Early Carboniferous of Morocco. Palaeontology 57:771–781. doi:10.1111/pala.12087

Kraft S, Korn D, Klug C (2008) Ontogenetic patterns of septal spacing in Carboniferous ammonoids. Neues Jahrb Geol Miner Abh 250(1):31–44

Krimholc GJ, Sazonov NT, Kamsyeva-Elpatevskaja VG (1958a) Nadsemejstvo Stephanoceratataceae. In: Orlov JA (ed) Osnovy Paleontologii, Molluski-Golovonogie, II. Izdatel'stvo Akademii Nauk SSSR, Moskva, pp 75–79 [in Russian]

Krimholc GJ, Kamsyeva-Elpatevskaja VG, Kachadze IP (1958b) Nadsemejstvo Kosmoceratataceae. In: Orlov JA (ed) Osnovy Paleontologii, Molluski-Golovonogie, II. Izdatel'stvo Akademii Nauk SSSR, Moskva, pp 79–82 [in Russian]

Kulicki C (1974) Remarks on the embryogeny and postembryonal development of ammonites. Acta Palaeontol Pol 19:201–224

Kulicki C, Tanabe K, Landman NH, Mapes RH (2001) Dorsal shell wall in ammonoids. Acta Palaeontol Pol 46:23–42

Landman NH (1987) Ontogeny of Upper Cretaceous (Turonian-Santonian) scaphitid ammonites from the Western Interior of North America: Systematics, developmental patterns, and life history. Bull Am Mus Nat Hist 185(2):117–241

Landman NH (1989) Iterative progenesis in Upper Cretaceous ammonites. Paleobiology 15:95–117

Landman NH, Waage KM (1986) Shell abnormalities in scaphitid ammonites. Lethaia 19:211–224
Landman NH, Waage KM (1993) Scaphitid ammonites of the Upper Cretaceous (Maastrichtian) Fox Hills Formation in South Dakota and Wyoming. Bull Am Mus Nat Hist 215:1–257
Landman NH, Dommergues J-L, Marchand D (1991) The complex nature of progenetic species—examples from Mesozoic ammonites. Lethaia 24:409–421
Landman NH, Mapes RH, Cruz C (2010) Jaws and soft tissues in ammonoids from the Lower Carboniferous (Upper Mississippian) Bear Gulch Beds, Montana, USA. In: Tanabe K, Shigeta Y, Sasaki T, Hirano H (eds) Cephalopods—present and past. Tokai University Press, Tokyo
Landman NH, Cobban WA, Larson NL (2012) Mode of life and habitat of scaphitid ammonites. Geobios 45:87–98
Leanza H, Zeiss A (1992) On the ammonite fauna of the lithographic limestones from the Zapala region (Neuquén province, Argentina), with the description of a new genus. Zbl Geol Paläontol I 1991(6):1841–1850
Lehmann U (1966) Dimorphismus bei Ammoniten der Ahrensburger Lias-Geschiebe. Paläontol Z 40(1–2):26–55
Lehmann U (1981) The ammonites: their life and their world. Cambridge University Press, New York
Longbridge LM, Smith PL, Tipper H (2006) The Early Jurassic ammonite *Badouxia* from British Columbia, Canada. Palaeontology 49:795–816
Luger P, Groschke M (1989) Late Cretaceous ammonites from the Wadi Qena area in the Egyptian Eastern Desert. Palaeontology 32(2):355–407
Macellari CE (1986) Late Campanian-Maaastrichtian ammonite fauna from Seymour Island (Antarctic Peninsula). Paleontol Soc Mem 18:1–55
Machalski M (2005) Late Maastrichtian and earliest Danian scaphitid ammonites from central Europe: Taxonomy, evolution, and extinction. Acta Palaeontol Pol 50:653–696
Maeda H (1991) Sheltered preservation: a peculiar mode of ammonite occurrence in the Cretaceous Yezo Group, Hokkaido, north Japan. Lethaia 24:69–82
Maeda H (1993) Dimorphism of Late Cretaceous false-puzosiine ammonites, *Yokoyamaoceras* Wright and Matsumoto, 1954 and *Neopuzosia* Matsumoto, 1954. Trans Proc Palaeontol Soc Jpn NS 169:97–128
Makowski H (1962) Problem of sexual dimorphism in ammonites. Palaeontol Pol 12:1–92
Makowski H (1971) Some remarks on the ontogenetic development and sexual dimorphism in the Ammonoidea. Acta Geol Pol 21:321–340
Makowski H (1991) Dimorphism and evolution of the goniatite *Tornoceras* in the Famennian of the Holy Cross Mountains. Acta Palaeontol Pol 36:241–254
Mangold C (1970) Morphoceratidae (Ammonitina-Perisphinctoidea) Bathoniens du Jura Méridional, de la Niévre et du Portugal. Geobios 3:43–130
Mangold C (1971) Les Perisphinctidae (Ammonitina) du Jura meridional au Bathonien et au Callovien. Doc Lab Géol Fac Sci Lyon 41:1–246
Mangold K (1987) Reproduction. In: Boyle PR (ed) Cephalopod life cycles. Comparative reviews, vol 2. Academic Press, London, pp 157–200
Mangold-Wirz K (1963) Biologie des Cephalopodes benthiques et nectoniques de la Mer Catalane. Vie Milieu (Suppl) 13:1–285
Mangold-Wirz K, Lu CC, Aldrich EA (1969) A reconsideration of forms of squid of the genus *Illex* (Illicinae, Ommastrephidae). II. Sexual dimorphism. Can J Zool 47:1153–1156
Mapes RH, Davis RA (1996) Color patterns in ammonoids. In: Landman NH, Tanabe K, Davis RA (eds) Ammonoid paleobiology. Plenum, New York
Mapes RH, Larson NL (2015) Ammonoid Color Patterns. This volume
Mapes RH, Sneck DA (1987) The oldest ammonoid "colour" patterns: description, comparison with *Nautilus,* and implications. Palaeontology 30:299–309
Marchand D (1976) Quelques précisions sur le polymorphisme dans la famille des Cardioceratidae Douville (Ammonoides). Haliotis 6:119–140
Marcinowski R (1980) Cenomanian ammonites from German Democratic Republic, Poland, and the Soviet Union. Acta Geol Pol 30(3):215–325

Marcinowski R (1983) Upper Albian and Cenomanian ammonites from some sections of the Mangyshlak and Tuarkyr regions, Transcaspia, Soviet Union. Neues Jahrb Geol Paläontol Mh 3:156–180

Marcinowski R, Wiedmann J (1990) The Albian ammonites of Poland. Palaeontol Pol 50:1–94

Matsumoto T (1987a) Notes on *Forbesiceras* (Ammonoidea) from Hokkaido (Studies of Cretaceous ammonites from Hokkaido-LX). Trans Proc Palaeontol Soc Jpn NS 145:16–31

Matsumoto T (1987b) Notes on *Pachydesmoceras*, a Cretaceous ammonite genus. Proc Jpn Acad 63B:5–8

Matsumoto T (1988) A monograph of the Puzosiidae (Ammonoidea) from the Cretaceous of Hokkaido). Palaeont. Soc Jpn Spec Pap 30:1–131

Matsumoto T (1991a) On some acanthoceratid ammonites from the Turonian of Hokkaido (Studies of the Cretaceous ammonites from Hokkaido-LXIX). Trans Proc Palaeontol Soc Jpn NS 164:910–927

Matsumoto T (compiler, 1991b) The mid-Cretaceous ammonites of the family Kossmaticeratidae from Japan. Palaeontol Soc Jpn Spec Pap 33:1–143

Matsumoto T, Saito R (1987) Little known ammonite *Crandidiericeras* from Hokkaido (Studies of Cretaceous ammonites from Hokkaido-LVIII). Trans Proc Palaeontol Soc Jpn NS 145:1–9

Matsumoto T, Skwarko SK (1991) Ammonites of the Cretaceous Ieru Formation, western Papua New Guinea. BMR J Aust Geol Geophys 12(3):245–262

Matsumoto T, Skwarko SK (1993) Cretaceous ammonites from south-central Papua New Guinea. AGSO J Aust Geol Geophys 14(4):411–433

Matsumoto T, Takahashi T (1992) Ammonites of the genus *Acompsoceras* and some other acanthoceratid species from the Ikushunbetsu Valley, central Hokkaido. Trans Proc Palaeontol Soc Jpn NS 166:1144–1156

Matsumoto T, Toshimitsu S (1984) On the systematic positions of the two ammonite genera *Hourcquia* Collignon, 1965 and *Pseudobarroisiceras* Shimizu, 1932. Mem Fac Sci Kyushu Univ Ser D Geol 25(2):229–246

Matsumoto T, Suekane T, Kawashita Y (1989) Some acanthoceratid ammonites from the Yubari Mountains, Hokkaido-Part 2. Sci Rep Yokosuka City Mus 37:29–44

Matsumoto T, Nemoto M, Suzuki C (1990a) Gigantic ammonites from the Cretaceous Futaba Group of Fukushima Prefecture. Trans Proc Palaeontol Soc Jpn NS 157:366–381

Matsumoto T, Toshimitsu S, Kawashita Y (1990b) On *Hauericeras* de Grossouvre, 1894, a Cretaceous ammonite genus. Trans Proc Palaeontol Soc Jpn NS 158:439–458

Matsunaga T, Maeda H, Shigeta Y, Hasegawa K, Nomura S-I, Nishimura T, Misaki A, Tanaka (2008) First discovery of *Pravitoceras sigmoidale* Yabe from the Yezo Supergroup in Hokkaido, Japan. Paleontol Res 12:309–319. doi:10.2517/prpsj.12.309

Matyja BA (1986) Developmental polymorphism in Oxfordian ammonites. Acta Geol Pol 36(1–3):37–68

Matyja BA (1994) Developmental polymorphism in the Oxfordian ammonite subfamily Peltoceratinae. In: Palaeopelagos Special Publication 1. Proceedings of the 3rd Pergola International Symposium, Rome, pp 277–286

Matyja BA, Wierzbowski A (2001) Palaeogeographical distribution of early Bathonian ammonites of the *Asphinctites-Polysphinctites* group. Hantkeniana 3:89–103

McCaleb JA (1968) Lower Pennsylvanian ammonoids from the Bloyd Formation of Arkansas and Oklahoma. Geol Soc Am Spec Pap 96:1–123

McCaleb JA, Furnish WM (1964) The Lower Pennsylvanian ammonoid genus *Axinolobus* in the southern midcontinent. J Paleontol 38(2):249–255

McCaleb JA, Quinn JH, Furnish WM (1964) Girtyoceratidae in the southern midcontinent. Okla Geol Surv Circ 67:1–41

Meek FB, Hayden FV (1856) Descriptions of new fossil species of Mollusca collected by Dr. F. V. Hayden, in Nebraska Territory; together with a complete catalogue of all the remains of Invertebrata hitherto described and identified from the Cretaceous and Tertiary formations of that region. Proc Acad Nat Sci Phila 8:265–286

Meister C, Alzouma K, Lang J, Mathey B (1992) Les ammonites du Niger (Afrique occidentale) et la transgression transsaharienne au cours du Cénomanien-Turonien. Geobios 25(1):55–100

Melendez G, Fontana B (1993) Intraspecific variability, sexual dimorphism, and non-sexual polymorphism in the ammonite genus *Larcheria* Tintant (Perisphinctidae) from the middle Oxfordian of western Europe. In: House MR (ed) The ammonoidea: environment, ecology, and evolutionary change (Systematics Association Special), vol 47. Clarendon Press, Oxford

Miller AK (1944) Permian cephalopods. In: King RE, Dunbar CO, Cloud PE Jr, Miller AK (eds) Geology and paleontology of the Permian area northwest of Las Delicias, southwestern Coahuila, Mexico, vol 52. Geological Society of America, Washington, DC, pp 71–127 (Geologial Society of America Special Papers)

Miller AK, Furnish WM (1940) Permian ammonoids of the Guadalupe Mountain region and adjacent areas. Geol Soc Am Spec Pap 26:1–242

Mitta VV (2010) Late Volgian *Kachpurites* Spath (Craspeditinae, Ammonoidea) of the Russian Platform. Paleontol J 44:622–631

Mojsisovics von Mojsvar E (1893) Das Gebirge um Hallstatt, Theil I, Die Cephalopoden der Hallstätter Kalke. K-K Geol Reichsanst Wien Abh 6(2):1–835

Mojsisovics von Mojsvar JAE (1882) Die Cephalopoden der mediterranen Triasprovinz. Abh K-K Geol Reichsanst Wien Abh 10:1–322

Moltschaniwskyj NA, Martínez P (1998) Effect of temperature and food levels on the growth and condition of juvenile *Sepia elliptica* (Hoyle, 1885): an experimental approach. J Exp Mar Biol Ecol 229:289–302

Monnet C, Bucher H, Wasmer M, Guex J (2010) Revision of the genus *Acrochordiceras* Hyatt, 1887 (Ammonoidea, Middle Triassic): Morphology, biometry, biostratigraphy and intraspecific variability. Palaeontology 53:961–996

Moreau P, Francis IH, Kennedy WJ (1983) Cenomanian ammonites from northern Aquitaine. Cretac Res 4:317–339

Morton SG (1834) Synopsis of the organic remains of the Cretaceous groups of the United States. Illustrated by nineteen plates, to which is added an appendix containing a tabular view of the Tertiary fossils discovered in America. Key & Biddle, Philadelphia, pp. 1–88

Müller AH (1969) Ammoniten mit "Eierbeutel" und die Frage nach dem Sexualdimorphismus der Ceratiten (Cephalopoda). Monatsber Dtsch Akad Wiss Berl 11:411–420

Neige P (1992) Mise en place du dimorphisme (sexuel) chez les Ammonoides. Approche ontogénétique et interprétation hétérochronique. DEA University Bourgogne, pp 1–50

Nettleship MT, Mapes RH (1993) Morphologic variation, maturity, and sexual dimorphism in an Upper Carboniferous ammonoid from the Midcontinent. GSA, Abstracts with Program 25(2):67

Obata I, Futakami M, Kawashita Y, Takahashi T (1978) Apertural features in some Cretaceous ammonites from Hokkaido. Bull Natl Sci Mus (Tokyo) Ser C (Geol) 4(3):139–155

Olivero EB, Medina FA (1989) Dimorfismo en *Grossouvrites gemmatus* (Huppe) (Ammonoidea) del Cretacico superior de Antartica. Actas Cuarto Congreso Argentino de Paleontología y Bioestratigrafía (Mendoza), pp 65–74

Orbigny A d' (1847) Paléontologie Française. Terraines jurassiques. Part I: Céphalopodes. Masson, Paris

Orbigny A d' (1850) Prodrôme de paléontologie stratigraphique universelle des animaux mollusques & rayonnés faisant suite au cours élémentaire de paléontologie et de géologie stratigraphiques. Tom, vol 2. Masson, Paris, pp 1–427

Palframan DFB (1966) Variation and ontogeny of some Oxfordian ammonites. *Taramelliceras richei* (de Loriol) and *Creniceras renggeri* (Oppel) from Woodham Buckinghamshire. Palaeontology 9:290–311

Palframan DFB (1969) Taxonomy of sexual dimorphism in ammonites: mor-phogenetic evidence in *Hecticoceras brightii* (Pratt). In: Westermann GEG (ed) Sexual dimorphism in fossil Metazoa and taxonomic implications, vol 1. Stuttgart, Schweizerbart, pp 125–154 (IUGS A)

Parent H (1991) Ammonites Cretácicos de la Formación Rio Mayer (Patagonia austral) *Hatchericeras patagonense* Stanton (Barremiano) y *Sanmartinoceras patagonicum* Bonarelli (Albiano). Inst Fisiogr Univ Nac Rosario Notas A 15:1–8

Parent H (1997) Ontogeny and sexual dimorphism of *Eurycephalites gottschei* (Tornquist) (Ammonoidea) of the Andean Lower Callovian (Argentine-Chile). Geobios 30:407–419
Parent H (1998) Upper Bathonian and lower Callovian ammonites from Chacay Melehué (Argentina). Acta Palaeontol Pol 43:69–130
Parent H, Scherzinger H, Schweigert G (2008a) Sexual phenomena in Late Jurassic Aspidoceratidae (Ammonoidea). Dimorphic correspondence between *Physodoceras hermanni* (Berckhemer) and *Sutneria subeumela* Schneid, and first record of possible hermaphroditism. Palaeodiversity 1:181–187
Parent H, Schweigert G, Scherzinger A, Enay R (2008b) *Pasottia*, a new genus of Tithonian oppeliid ammonites (Late Jurassic, Ammonoidea: Haploceratoidea). Bol Inst Fisiogr Geol 78:23–30
Parent H, Greco AF, Bejas M (2009) Size-Shape Relationships in the Mesozoic planispiral ammonites. Acta Palaeontol Pol 55:85–98
Parent H, Garrido AC, Schweigert G, Scherzinger A (2011) The Tithonian ammontie fauna and stratigraphy of Picún Leufú, southern Neuquén Basin, Argentina. Rev Paléobiol 30:45–104
Parent H, Garrido AC, Schweigert G, Scherzinger A (2013). Andean Lower Tithonian (Picunleufuense Zone) ammonites and aptychus from Estancia Maria Juana, southern Neuquén Basin, Argentina. Boletín del Instituto de Fisiografía y Geología 83:27–34
Pavia G, Zunino M (2012) Ammonite assemblages and biostratigraphy at the Lower to Upper Bajocian boundary in the Digne area (SE France). Implications for the definition of the Lower Bajocian GSSP. Rev Paléobiol Vol Spéc 11:205–227
Pelseneer P (1926) La proportion relative des sexes chez les animaux et particulièrement chez les Mollusques. Acad R Belg Cl Sci (Mem 2ieme Ser) 8(11):1–258
Ploch I (2003) Taxonomic interpretation and sexual dimorphism in the Early Cretaceous (Valanginian) ammonite *Valanginites nucleus* (Roemer, 1841). Acta Geol Pol 53:201–208
Ploch I (2007) Intraspecific variability and problematic dimorphism in the Early Cretaceous (Valanginian) ammonite *Saynoceras verrucosum* (d'Orbigny, 1841). Acta Geol Sin 81:877–882
Quenstedt FA (1885) Die Ammoniten des Schwäbischen Jura. Schweizerbart, Stuttgart
Raup DM, Crick RE (1981) Evolution of single characters in the Jurassic ammonite *Kosmoceras*. Paleobiology 7:200–215
Raup DM, Michelson A (1965) Theoretical morphology of the coiled shell. Science 147:1294–1295
Reboulet S (1995) L'évolution des ammonites du Valanginien-Hauterivien inférieur du Bassin Vocontien et de la Plate-forme Provencale (Sud-Est de la France). Doc Lab Géol Lyon 137:1–371
Rein S (2001) Neue Erkenntnisse zur Evolutionsbiologie der germanischen Ceratiten – Ontogenese, Phylogenese und Dimorphismusverhalten. Freib Forsch C 492:99–120
Rein S (2003) Zur Biologie der Ceratiten der *spinosus*-Zone – Ergebnisse einer Populationsanalyse, Teil I: Populationsstatistik, Sexual-Dimorphismus und Artkonzept. Veröff Naturkundemus Erf 22:29–50
Reyment RA (1971) Vermuteter Dimorphismus bei der Ammonitengattung *Benueites*. Bull Geol Inst Univ Uppsl NS 3(1):1–18
Reyment RA (1982) Size and shape variation in some Japanese upper Turonian (Cretaceous) ammonites. Stock Contrib Geol 37(16):201–214
Reyment RA (1988) Does sexual dimorphism occur in Upper Cretaceous ammonites? Senckenb leth 69(1/2):109–119
Riccardi AC, Aguirre Urreta MB, Medina FA (1987) Aconeceratidae (Ammonitina) from the Hauterivian-Albian of southern Patagonia. Palaeontogr A 196:105–185
Richter U (2002) Gewebeansatz-Strukturen auf pyritisierten Steinkernen von Ammonoideen. Geol Beitr Hann 4:1–113
Roper CFE, Sweeney MJ (1975) The pelagic octopod *Ocythoe tuberculata* Rafinesque, 1814. Bull Am Malacol Union 1975:21–28
Ruzhencev VE (1962) Superorder Ammonoidea. The ammonoids—general part. In: Ruzhencev VE (ed) Molluscs Cephalopods. I. Publishing House of the Academy of Science of the USSR, Moscow [in Russian]

Ruzhencev VE (1974) Superorder Ammonoidea. General section. In: Orlov YA, Ruzhencev VE (ed) Fundamentals of paleontology. V. Mollusca: Cephalopoda I. Jerusalem

Sandoval J, Chandler RB (2000) The sonniniid ammonite *Euhoploceras* from the Middle Jurassic of South-West England and southern Spain. Palaeontology 43:495–532

Saunders WB, Spinosa C (1978) Sexual dimosphism in *Nautilus* from Palau. Paleobiology 4:349–358

Saunders WB, Ward PD (1987) Ecology, distribution and population characteristics of *Nautilus*. In: Saunders WB, Landman NH (eds) Nautilus. The biology and paleobiology of a living fossil. Plenum Press, New York

Scherzinger A., Mitta V. (2006) New data on ammonites and stratigraphy of the Upper Kimmeridgian and Lower Volgian (Upper Jurassic) of the middle Volga Region (Russia). Neues Jahrb Geol Paläontol Abh 241:225–251

Schiappa TA, Spinosa C, Snyder WS (1995) *Nevadoceras*, a new Early Permian adrianitid (Ammonoidea) from Nevada. J Paleontol 69:1073–1079

Schindewolf OH (1937) Zur Stratigraphie und Paläontologie der Wocklumer Schichten (Oberdevon). Abh Preuß Geol Landesanst, NF 178:1–132

Schweigert G (1997) Die Ammonitengattungen *Simocosmoceras* Spath und *Pseudhimalayites* Spath (Aspidoceratidae) im süddeutschen Oberjura. Stuttg Beitr Naturk B 246:1–29

Schweigert G (1998) Die Ammonitenfauna des Nusplinger Plattenkalks (Ober-Kimmeridgium, Beckeri-Zone, Ulmense-Subzone, Württemberg). Stuttg Beitr Naturk B 267:1–61

Schweigert G, Dietze V (1998) Revision der dimorphen Ammonitengattungen *Phlycticeras* Hyatt—*Oecoptychius* Neumayr (Strigoceratidae, Mitteljura). Stuttg Beitr Naturk B 269:1–59

Schweigert G, Dietl G, Dietze V (2003) Neue Nachweise von *Phlycticeras* und *Oecoptychius* (Ammonitina: Strigoceratidae: Phlycticeratinae). Stuttg Beitr Naturk B 335:1–21

Schweigert G, Dietze V, Chandler RB, Mitta V (2007) Revision of the Middle Jurassic dimorphic ammonite genera *Strigoceras*/*Cadomoceras* (Strigoceratidae) and related forms. Stuttg Beitr Naturk B 373:1–74

Seilacher A (1974) Fabricational noise in adaptive morphology. Syst Biol 22:451–465

Seilacher A, Gunji YP (1993) Morphogenetic countdown: another view on heteromorph shells in gastropods and ammonites. Neues Jahrb Geol Paläontol Abh 190:237–265

Senior JR (1971) Wrinkle-layer structures in Jurassic ammonites. Palaeontology 14:107–113

Shea BT (1986) Ontogenetic approaches to sexual dimorphism in anthropods. Hum Evol 1(2):97–110

Siebold CT (1848) Lehrbuch der vergleichenden Anatomie, vol 1. Veit, Berlin

Stephenson LW (1941) The larger invertebrates of the Navarro Group of Texas (exclusive of corals and crustaceans and exclusive of the fauna of the Escondido Formation). (University of Texas) Bulletin 4101:1–641

Sturani C (1966) Ammonites and stratigraphy of the Bathonian in the Digne- Barreme area (southeastern France, Dept. Basses- Alpes). Boll Soc Paleontol Ital 5:3–57

Sun YC (1928) Mundsaum und Wohnkammer der Ceratiten des Oberen deutschen Muschelkalks. Weg, Leipzig

Tafur R, Villegas P, Rabí M, Yamashiro C (2001) Dynamics of maturation, seasonality of reproduction and spawning grounds of the jumbo squid *Dosidiscus gigas* (Cephalopoda: Ommastrephidae) in Peruvian waters. Fish Res 54:33–50

Tajika A, Naglik C, Morimoto N, Pascual-Cebrian E, Hennhöfer DK, Klug C (2014) Empirical 3D-model of the conch of the Middle Jurassic ammonite microconch *Normannites,* its buoyancy, the physical effects of its mature modifications and speculations on their function. Historical Biology, 11 pp. doi: 10.1080/08912963.2013.872097

Tanabe K (1977) Functional evolution of *Otoscaphites puerculus* (Jimbo) and *Scaphites planus* (Yabe), Upper Cretaceous ammonites. Mem Fac Sci Kyushu Univ Ser D Geol 23(3):367–407

Tanabe K, Landman NH, Mapes RH (1998) Muscle attachment scars in a Carboniferous goniatite. Paleontol Res 2(2):130–136

Thierry J (1978) Le genre *Macrocephalites* au Callovien inférieur (Ammonites, Jurassique moyen). Mém Géol Univ Dijon 4:1–490

Thierry J, Charpy N (1982) Le genre *Tornquistes* (Ammonitina, Pachyceratidae) a l'Oxfordien inférieur et moyen en Europe occidentale. Geobios 15:619–677
Till A (1909) Die fossilen Cephalopodengebisse. K-K Geol Reichsanst Jahrb 58(4):573–608
Till A (1910) Die fossilen Cephalopodengebisse. Folge 3. K-K Geol Reichsanst Jahrb 59:407–426
Tintant H (1963) Les Kosmoceratides du Callovien inférieur et moyen d'Europe occidentale. University of Dijon, France
Tintant H (1976) Le polymorphisme intraspécifique en paléontologie. Exemple pris chez les ammonites. Haliotis 6:49–69
Tornquist A (1898) Der Dogger am Espinazito Pass. Paläontol Abh NF 3(2):3(135)–69(201)
Tozer KT (1994) Canadian Triassic ammonoid faunas. Geol Surv Can Bull 467:1–663
Trewin NH (1970) A dimorphic goniatite from the Namurian of Cheshire. Palaeontology 13:40–46
Trueman AE (1941) The ammnonite body chamber, with special reference to the buoyancy and mode of life of the living ammonite. Q J Geol Soc Lond 96:339–383
Urdy S, Goudemand N, Bucher H, Chirat R (2010a) Allometries and the morphogenesis of the molluscan shell: a quantitative and theoretical model. J Exp Zool B 314:280–302
Urdy S, Goudemand N, Bucher H, Chirat R (2010b) Growth dependent phenotypic variation of molluscan shell shape: implications for allometric data interpretation. J Exp Zool B 314:303–326
Urlichs M (2009) Weiteres über Dimorphismus bei *Ceratites* (Ammonoidea) aus dem Germanischen Oberen Muschelkalk (Mitteltrias) mit Revision einiger Arten. Neues Jahrb Geol Paläontol Abh 251:199–223
Vermeij GJ (1993) A natural history of shells. Princeton University Press, Princeton
Walliser OH (1963) Dimorphismus bei Goniatiten. Paläontol Z 37(1–2):21
Walliser OH (1970) Über die Runzelschicht bei Ammonoidea. Gött Arb Geol Paläontol 5:115–126
Walton SA, Korn D, Klug C (2010) Size distribution of the late devonian ammonoid *Prolobites*: indication for possible mass spawning events. Swiss J Geosci 103:475–494
Ward PD (1987) The natural history of *Nautilus*. Allen and Unwin, Boston
Weitschat W, Bandel K (1991) Organic components in phragmocones of boreal Triassic ammonoids; implications for ammonoid biology. Paläontol Z 65:269–303
Wells MJ (1962) Brain and behavior in cephalopods. Stanford University Press, Stanford
Wells MJ (1966) The brain and behavior of cephalopods In: Wilbur KM, Younge CM (eds) Physiology of mollusca. Academic Press, New York
Wenger R (1957) Die Germanischen Ceratiten. Paleontogr A 108:57–129
Westermann GEG (1964a) Sexual-Dimorphismus bei Ammonoideen und seine Bedeutung für Taxionomie der Otoitidae (einschliesslich Sphaeroceratinae; Ammonitina, M. Jura). Palaeontogr A 124(1–3):33–73
Westermann GEG (1964b) The ammonite fauna of the Kialagvik formation at Wide Bay, Alaska Peninsula. Part I. Lower Bajocian (Aalenian). Bull Am Palaeontol 47:327–503
Westermann GEG (1969a) Supplement: sexual dimorphism, migration, and segregation in living cephalopods. In: Westermann GEG (ed) Sexual dimorphism in fossil Metazoa and taxonomic implications (IUGS, Series A1). Schweizerbart, Stuttgart
Westermann GEG (1969b) Proposal: classification and nomenclature of dimorphs at the genus-group level [with discussion]. In: Westermann GEG (ed) Sexual dimorphism in fossil Metazoa and taxonomic implications (IUGS, Series A1). Schweizerbart, Stuttgart
Westermann GEG (1971) Form, structure, and function of shell and siphuncle in coiled Mesozoic ammonoids. Life Sci Contrib R Ont Mus 78:1–3
Westermann GEG, Riccardi AC (1979) Middle Jurassic ammonoid fauna and biochronology of the Argentine-Chilean Andes. Part II: Bajocian Stephanocerataceae. Palaeontogr A 164:85–188
Wiedmann J (1965) Origins, limits, and systematic position of *Scaphites*. Palaeontology 8:397–453
Wiedmann J (1973) The Albian and Cenomanian Tetragonitiae (Cretaceous Ammonoidea), with special reference to the Circum-Indic species. Eclogae Geol Helv 66:585–616
Willey A (1895) In the home of the *Nautilus*. Nat Sci Lond 6(40):405–414

Willey A (1902) Contribution to the natural history of the pearly nautilus. In: Zoological results based on material from New Britain, New Guinea, Loyalty Islands, and Elsewhere, collected during the years 1895, 1896, and 1897. Cambridge University Press, Cambridge

Wilmsen M, Mosavinia A (2011) Phenotypic plasticity and taxonomy of *Schloenbachia varians* (J. Sowerby, 1817) (Cretaceous Ammonoidea). Paläontol Z 85:169–184

Wright CW, Kennedy WJ (1980) Origin, evolution and systematics of the dwarf acanthoceratid *Protacanthoceras* Spath, 1923 (Cretaceous Ammonoidea). Bull Br Mus (Nat Hist) Geol 34(2):65–107

Wright CW, Kennedy WJ (1984) The Ammonoidea of the Lower Chalk. Part I. (Monograph Palaeontographical Society London 567, part of vol 137 for 1983). Palaeontographical Society, London, pp 1–126

Wright CW, Kennedy WJ (1987) The Ammonoidea of the Lower Chalk. Part 2. (Monograph Palaeontographical Society London 573, part of vol 139 for 1985). Palaeontographical Society, London, pp 127–218

Wright CW, Kennedy WJ (1990) The Ammonoidea of the Lower Chalk. Part 3. (Monograph Palaeontographical Society London 585, part of vol 144 for 1990). Palaeontographical Society, London, pp 219–294

Wright CW, Kennedy WJ (1994) Evolutionary relationships among Stoliczkaiinae (Cretaceous ammonites) with an account of some species from the English Stoliczkaia dispar Zone. Cretac Res 15:547–582

Wright CW, Callomon JH, Howarth MK (1996) Cretaceous Ammonoidea. In: Kaesler RL (ed) Treatise on invertebrate paleontology, Part L, Mollusca 4 (revised). GSA and University of Kansas Press, Lawrence

Wright JK (2010) The Aulacostephanidae (Ammonoidea) of the Oxfordian/Kimmeridgian boundary beds (Upper Jurassic) of Southern England. Palaeontology 53:11–52

Zaborski PMP (1987) Lower Turonian (Cretaceous) ammonites from south-east Nigeria. Bull Br Mus (Nat Hist) Geol 41(2):31–66

Zakharov YD (1969) Problems of sexual dimorphism in fossil cephalopods, an impotant subject in modern systematics. In Gramm N, Krassilov VA (eds) Problems of phylogeny and systematics. Acad Sci USSR, Far Eastern Geological Institute, All Union Paleontology Society of Vladivostok [in Russian]

Zakharov YD (1977) Ontogeny of ceratites of the genus *Pinacoceras* and developmental features of the suborder Pinacoceratina. Paleontol J 4:445–451

Zatoń M (2008) Taxonomy and palaeobiology of the Bathonian (Middle Jurassic) tulitid ammonite *Morrisiceras*. Geobios 41:699–717

Zatoń M (2010) Bajocian-Bathonian (Middle Jurassic) ammonites from the Polish Jura. Part 2: families Stephanoceratidae, Perisphinctidae, Parkinsoniidae, Morphoceratidae and Tulitidae. Palaeontogr A 292:115–213

Zeiss A (1969) Dimorphismus bei Ammoniten des Unter-Tithon. Mit einigen allgemeinen Bemerkungen zum Dimorphismus-Problem. In: Westermann GEG (ed) Sexual dimorphism in fossil Metazoa and taxonomic implications. International Union Geological Science, A1. Schweizerbart, Stuttgart

Zhao J, Zheng Z-G (1977) The Permian ammonoids from Zhejiang and Jiangxi. Acta Palaeontol Sin 16(2):217–254

Zhou Z (1985) Several problems on the Early Permian ammonoids from south China. Palaeontol. Cathayana 2:179–210

Ziegler B (1974) Über Dimorphismus und Verwandtschaftsbeziehungen bei 'Oppelien' des oberen Juras (Ammonoidea: Haploceratacea). Stuttg Beitr Naturk B 11:1–42

Ziegler B (1987) Der weiße Jura der Schwäbischen Alb. Stuttg Beitr Naturk C 23:1–71

Appendix 1-5

Additional publications linked to this dissertation

Ammonoid Palaeobiology
Chapter 17 Ammonoid Locomotion

Naglik, C. Tajika, A.
Chamberlain, J. Klug, C.

Book chapter (2015)
Publisher: Springer

Chapter 17
Ammonoid Locomotion

Carole Naglik, Amane Tajika, John Chamberlain and Christian Klug

17.1 Introduction

The locomotor capacity of ammonoids is still a matter of much debate. This question is intimately linked with questions concerning ammonoid habitat and buoyancy (Ritterbush et al. 2014). Aspects of buoyancy were reviewed by Hoffmann et al. (2015). Based on theoretical models of ammonoid buoyancy (e.g., Trueman 1941; Saunders and Shapiro 1986) in combination with the latest empirical studies on volume models of ammonoids (Tajika et al. 2015; Naglik et al. 2015), we can now confidently reject the hypothesis of an obligatorily benthic mode of life for most ammonoids advocated by Ebel 1983 (see also Westermann 1993, 1996; Kröger 2001 or Jacobs and Chamberlain 1996 for views contrasting Ebel's ideas). The function of the phragmocone as a buoyancy device has been corroborated by a great number of studies (see Hoffmann et al. 2015 and references therein) including the latest volume models of ammonoid shells and the linked buoyancy calculations (Tajika et al. 2015; Naglik et al. 2015), most mathematical models of buoyancy (Hoffmann et al. 2015), the convergent evolution of an upward orientation of the aperture in many

C. Naglik (✉) · A. Tajika · C. Klug
Paläontologisches Institut und Museum, University of Zurich, Karl Schmid-Strasse 6,
8006 Zurich, Switzerland
e-mail: carole.naglik@pim.uzh.ch

A. Tajika
e-mail: amane.tajika@pim.uzh.ch

C. Klug
e-mail: chklug@pim.uzh.ch

J. Chamberlain
Department of Earth and Environmental Sciences,
Brooklyn College of CUNY, Brooklyn, NY 11210, USA

Doctoral Programs in Biology and Earth and Environmental Sciences,
CUNY Graduate Center, New York, NY 10016, USA
e-mail: JohnC@brooklyn.cuny.edu

C. Klug et al. (eds.), *Ammonoid Paleobiology: From Anatomy to Ecology,*
Topics in Geobiology 43, DOI 10.1007/978-94-017-9630-9_17

major ammonoid lineages (e.g., Raup and Chamberlain 1967; Bayer and McGhee 1984; Saunders and Shapiro 1986; Klug 2001; Korn and Klug 2003; Monnet et al. 2011) and the increase of phragmocone complexity through ammonoid evolution (Saunders 1995; Saunders and Work 1996, 1997; Daniel et al. 1997; Saunders et al. 1999). This is significant because *syn vivo* shell orientation can be used as an indicator of locomotion and habitat preference, although there are great limits for the accuracy of such conclusions.

Several authors have sought information on habitat depth and swimming speed in the physical properties of ammonoid shells. For example, shell implosion depths suggest limits for maximum diving depths (e.g., Westermann 1973, 1996; Saunders and Wehman 1977; Jacobs 1992a; Hewitt 1996; Batt 2007). Inferences on diving depth and ammonoid behavior have also been drawn based on siphuncle properties (e.g., Westermann 1971, 1996; Mutvei and Reyment 1973; Mutvei 1975; Chamberlain and Moore 1982; Ward 1982; Hewitt 1996). Oxygen isotopes have also been used to approximate diving/living depths of ammonoids (Moriya et al. 2003; Lukeneder et al. 2010, Lukeneder 2015; Moriya 2015).

Similarly, streamlining and drag have been quantified for a wide range of shell shapes (Kummel and Lloyd 1955; Westermann 1971, 1996; Reyment 1973; Chamberlain 1976, 1981; Chamberlain and Westermann 1976; Jacobs 1992b, Jacobs et al. 1994; Monnet et al. 2011; Ritterbush and Bottjer 2012; Ritterbush et al. 2014), and the results related to mode of life. Mutvei and Reyment (1973) as well as Mutvei (1975) argued that muscle attachment was too small and weak to allow ammonoids to swim well. However, there is some indication suggesting that ammonoids may have powered their locomotion with a muscular mantle not firmly attached to the shell (Jacobs and Landman 1993; Jacobs and Chamberlain 1996). Muscle attachment is discussed in detail in Doguzhaeva and Mapes (2015).

Sedimentary facies in which ammonoids are preserved may provide some information about lifestyle and habitat (Wang and Westermann 1993; Westermann 1996; Tsujita and Westermann 1998; Westermann and Tsujita 1999), although post mortem transport can complicate the picture (e.g., Kennedy and Cobban 1976; Tanabe 1979: Westermann 1996 and references therein). Nevertheless, the broad range of facies types in which ammonoid remains occur in combination with the great disparity in shell morphology supports a wide variety of life habitats and habits for these animals that in principle relate to differing locomotor capabilities as exemplified by Jacobs et al (1994).

Another line of evidence comes from sublethal injuries. It was especially Keupp (review in Keupp and Hoffmann 2015), who, in a series of articles (Keupp 1984, 1985, 1992, 1996, 1997, 2000, 2006, 2008, 2012), proposed that several types of injuries commonly recorded in ammonoid shells were inflicted by benthic crustaceans. If that is correct, this would support at least a temporarily demersal habitat for ammonoids showing such injuries; other injuries related to nektic predators, however, corroborate a nektic mode of life for at least some ammonoid groups (compare Ritterbush et al. 2014; Keupp and Hoffmann 2015).

Finally, *syn vivo* epizoans also provide some information on swimming direction and orientation of the shell (Keupp et al. 1999). However, such cases of epizoans

that can be interpreted in that respect are rare (Seilacher 1960, 1982a, b; Keupp et al. 1999; Seilacher and Keupp 2000; Hauschke et al. 2011). De Baets et al. (2015b) review information obtained from epizoans attached to ammonoids as a function of orientation (e.g., Seilacher 1960). Their results support the swimming orientations discussed herein.

Because ammonoids apparently did not produce unequivocal trace fossils of their movements *syn vivo*, no evidence from this source is available to help interpret ammonoid locomotion.

17.2 Limits of Research on Ammonoid Locomotion

Because ammonoids are extinct, we cannot provide direct, observational evidence on their swimming ability from study of the living creatures. There is no direct way to measure such parameters as maximal swimming speed, maneuverability, or the efficiency of the musculature in extinct animals like ammonoids. Thus, in this paper we attempt to reconstruct ammonoid swimming ability and maneuverability using indirect evidence that can be gleaned from the fossil record; from analogy to the performance of modern relatives; and from awareness of the uncertainties inherent in such an effort.

There are only a few aspects of ammonoid locomotion, which at the outset appear highly plausible to us:

1. Ammonoids generally were able to produce neutral buoyancy by means of their buoyancy apparatus.
2. Most ammonoids were not fully benthic since they did not leave any traces in the sediment, had often upward pointing apertures and were preyed upon by nektic organisms or only from below by benthic organisms.
3. Most ammonoids were probably capable of swimming movement powered by jet propulsion, arm beating, or other mode of propulsion.
4. Locomotor capabilities were not uniform across all ammonoid taxa since they had sometimes quite large differences in shell orientation, hyponomic sinus, body size or shell shape.

17.3 Shell Orientation

17.3.1 Mathematical Models

With his pioneering work on ammonoid shell geometry and buoyancy, Trueman (1941) initiated a line of investigation that continues down to the present day, in which palaeontologists utilize mathematical modeling techniques to gain insight on ammonoid buoyancy and shell orientation. These models usually employ the parameters used by Raup and Chamberlain (1967), namely W (expansion rate), K

(area of last generating curve) and R (distance from the coiling axis). However, such models are predicated on a number of simplifications (e.g., Trueman 1941; Raup (1967); Raup and Chamberlain (1967); Ebel 1983; Saunders and Shapiro 1986; Shapiro and Saunders 1987; Okamoto 1988, 1996; Klug 2001; Korn and Klug 2003). Commonly, these models include the assumption of self-similar (gnomonic), logarithmic shell growth, uniform shell thickness independent of position on the whorl section and the presence of a stable coiling axis. None of these simplifying assumptions necessarily coincide with actual ammonoid shells, i.e., shell growth in ammonoids was not perfectly logarithmic (e.g., Okamoto 1996; Klug 2001; Korn 2012; Tajika et al. 2015; Naglik et al. 2015), shell thickness varies and the coiling axis can permanently change its position throughout ontogeny (e.g., Urdy et al. 2010a, b).

Most authors, who produced mathematical models of shell geometry (Trueman 1941; Raup 1967; Raup and Chamberlain 1967; Saunders and Shapiro 1986; Okamoto 1988, 1996), tested their models, usually with data from Recent nautilids (Packard et al. 1980; Chamberlain 1987; Ward 1987; Jacobs and Landman 1993), and found reasonably good agreement between their results and the modeled attributes of the living animal. According to these models, the orientation of the aperture largely depended on the whorl expansion rate and ranged between about 30° and 110° from the vertical direction in normally coiled ammonoids with planispiral shells (Saunders and Shapiro 1986). In straight bactritoids (Fig. 17.1) and other heteromorph ammonoids, the aperture may have faced more or less downward, for example in more or less orthoconic forms (without counterbalancing options) such as baculitids or in some early ammonoids with very loosely coiled shells such as *Metabactrites* (e.g. Klug and Korn 2004), or in subadult *Anisoceras*, turrilitids and other heteromorphs. As shown in Fig. 17.1, shell orientation may have varied quite strongly throughout ontogeny.

As shown by Westermann (1996), the majority of Mesozoic ammonoids had body chamber lengths between 200° and 300° (Fig. 17.2). According to him and the model by Saunders and Shapiro (1986), this would coincide with an apertural orientation of about 80° to 100°, i.e. with the aperture oriented more or less horizontally. Only forms with extremely high or extremely low whorl expansion rates and body chambers shorter than half a whorl or exceeding one whorl in length would have had an aperture oriented below 50° from vertical.

17.3.2 Mechanical Models

In addition to mathematical modeling, some authors have employed mechanical, i.e. physical, models to help reconstruct shell orientation in ammonoids. Among the first to use such models were Mutvei and Reyment (1973), who built metal-coated, plastic shell models, vacuum molded from real ammonoid and *Nautilus* shells, to investigate the buoyancy and floating position of the animals thus modeled. These authors were later followed in using physical models by, e.g., Elmi (1991, 1993), Seki et al. (2000), Klug and Korn (2004), Westermann (2013) as well as Parent et al. (2014).

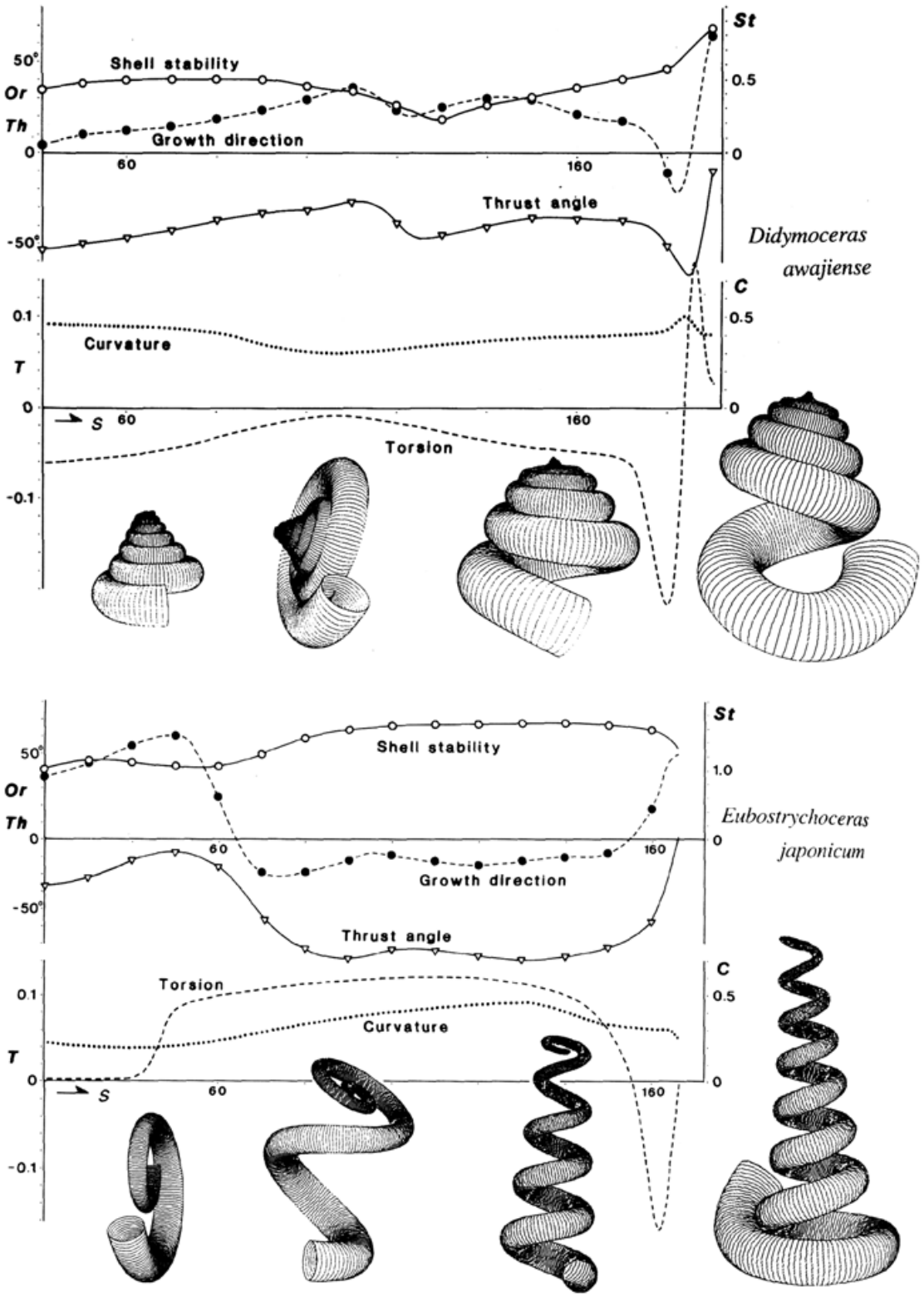

Fig. 17.1 Shell curvature, torsion, growth direction as well as hydrodynamic characters such as hydrodynamic stability, orientation of the aperture and hyponome jet thrust angle. (Source: Okamoto 1996)

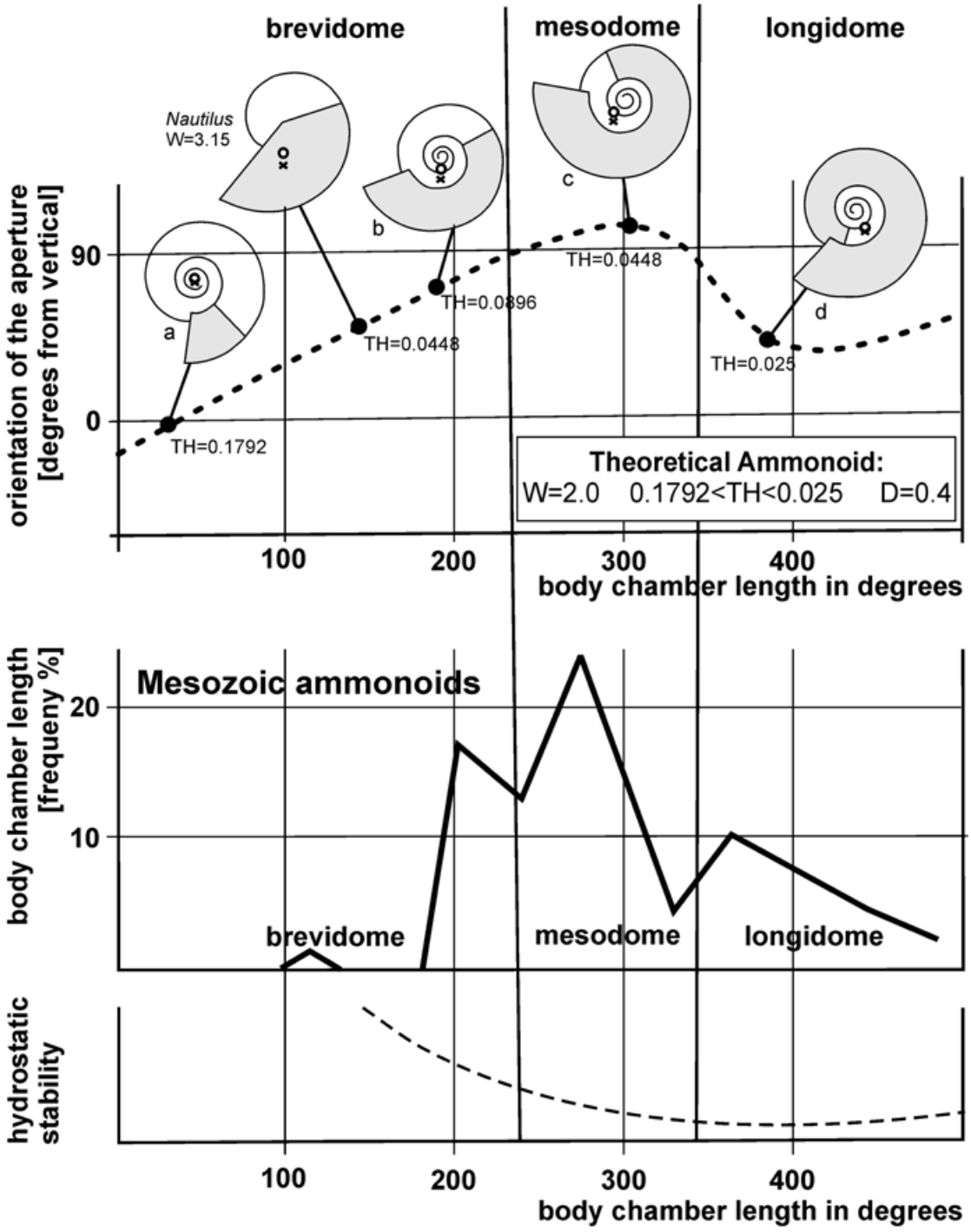

Fig. 17.2 Relationships between shell coiling, body chamber length, orientation of the aperture and hydrostatic stability of Mesozoic ammonoids. *W* whorl expansion rate, *TH* relative shell thickness, *D* relative distance between coiling axis and generating curve. Note the three peaks in body chamber length abundance and that these peaks coincide with a commonly sub-horizontal apertural margin and thus upward facing aperture. (Modified after Westermann (1996) incorporating a graph of Saunders and Shapiro (1986))

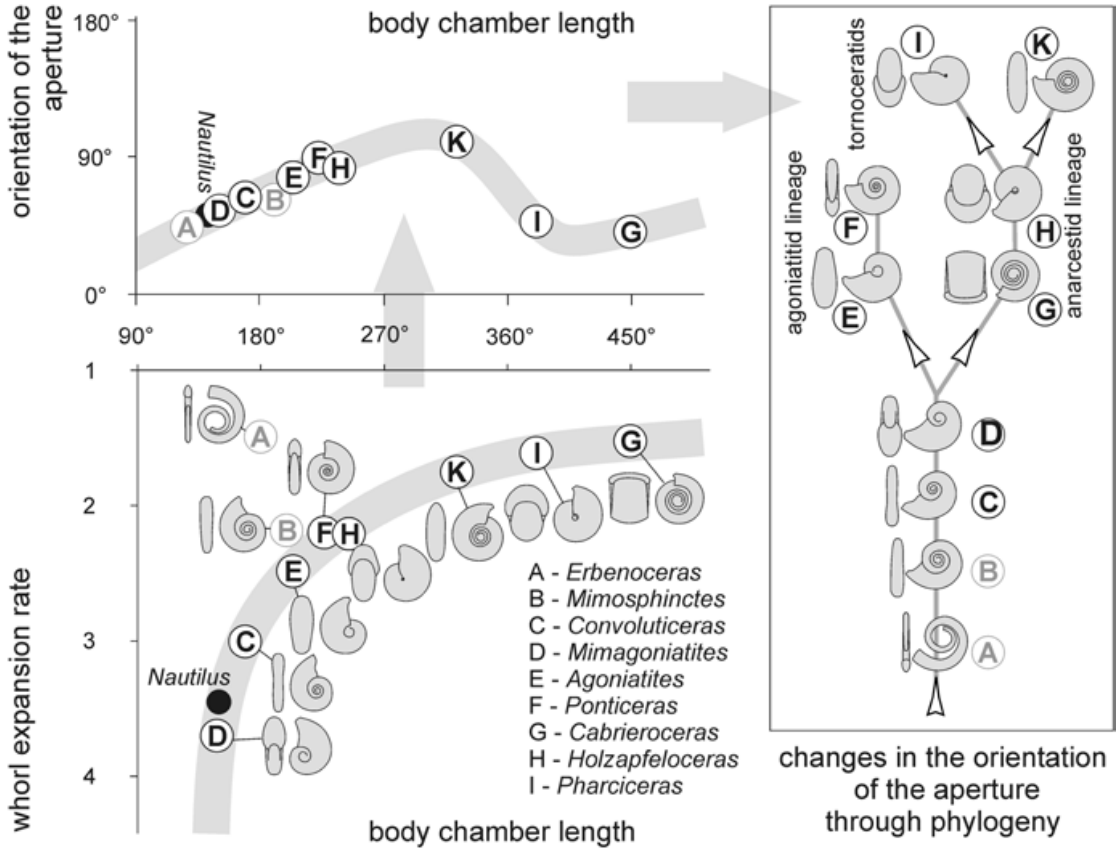

Fig. 17.3 Relationships between shell coiling, body chamber length, orientation of the aperture throughout the evolution of Devonian ammonoids. Note that three of the most important clades more or less independently evolved horizontal apertures early in the evolution of ammonoids. (Source: Klug and Korn 2004)

Klug and Korn (2004) showed, how shell orientation changed from facing downward in Orthocerida and Bactritida with orthoconic shells to oblique downward in Ammonoidea with loosely coiled shells, to oblique upward in less loosely coiled forms, to more or less horizontally upward in fully coiled shells (Fig. 17.3, 17.4). A progression of this type in aperture orientation is associated with iterative evolutionary trends (Fig. 17.3) in the major Devonian ammonoid clades (Mimosphinctoidea, Mimagoniatitoidea, Agoniatitoidea; Korn and Klug 2003) and even in parallel in two Devonian clades (Auguritidae and Pinacitidae; Monnet et al. 2011).

The question of whether ectocochleate cephalopods with orthoconic shells were capable of bringing their shell and body into a horizontal position is of long interest (e.g., Schmidt 1930; Ward 1976). Using physical models, Westermann (2013) demonstrated that a horizontal position in baculitid ammonoids could have been achieved by accumulating liquid in the most apical chambers. Such a horizontal position of cephalopods with orthoconic shells may also have been achieved with apical intracameral or intrasiphuncular deposits (e.g., Actinocerida, Endocerida) or chamber liquid (Westermann 1977, 2013; House 1981). For baculitids, Westermann (2013) suggested a vertical orientation of the shells of juveniles and a nearly horizontal orientation of subadults and adults because he assumed that juveniles had

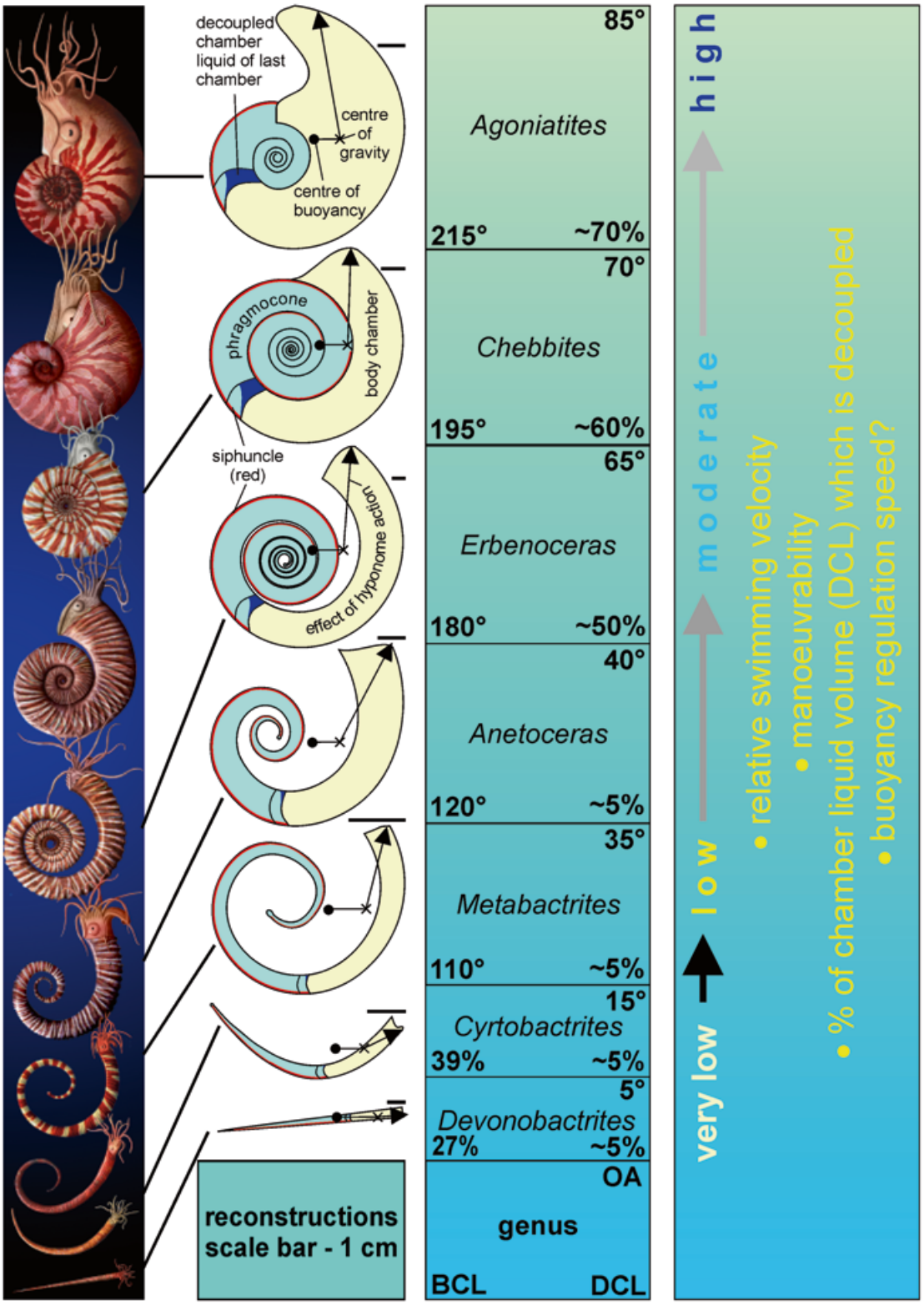

Fig. 17.4 Evolution of coiled ammonoid shells from straight bactritid shells and the consequences for body chamber length, aperture orientation, thrust angle of the hyponome jet, hydrodynamic stability and interpretations for swimming capabilities throughout evolution. (Modified after Klug and Korn 2004 as well as Klug et al. 2008). *BCL* body chamber length, *OA* orientation of the aperture, *DCL* decoupled chamber liquid.

phragmocones with more or less uniformly distributed liquid while in adults, the chamber liquid accumulated apically as a counterweight. The spatial distribution of chamber liquid might have also played a role in other ammonoids (Ward 1979, 1982; Kaplan 2002; Klug et al. 2008), although quantitative evidence on liquid distribution in ammonoid phragmocones has not yet been obtained.

Parent et al. (2014) experimented with a physical model comprised of weights and levers to assess the possible effect of the position of aptychi in aptychophoran ammonites on shell orientation. They concluded that in cases where the aptychus contains a sufficient mass and density relative to the animal's soft tissue and shell, the forward and backward movement of the buccal mass would have affected the orientation of the shell. Ammonites, such as some aspidoceratids, could have altered shell orientation in such a way that the aperture was lowered to < 25° from the vertical position.

Earlier physical models suggested capability of certain heteromorph ammonites (particularly the so-called "*shaft and hook shaped body chamber*" ammonoids; Kaplan 2002) to change their shell orientation (Kakabadzé and Sharikadzé 1993; Monks and Young 1998) by displacement of fluid and gas in the phragmocone (Kakabadzé and Sharikadzé 1993), or by moving the soft body of the animal within the living chamber, assuming that the animal was much smaller than its body chamber (Monks and Young 1998).

17.3.3 Empirical Models

We use the term "*empirical models*" to mean three-dimensional physical models of ammonoid shells constructed from stacks of cross-sections cut through a real shell. A similar approach was first employed by Chamberlain (1969), who built Plexiglas shell models from computer-produced topographic cross-sections of hypothetical ammonoid shells, which he then used for hydrodynamic experimentation (Chamberlain 1976, 1980, 1981). More recently, tomographic techniques have been developed, which greatly advance our skill to more confidently reconstruct *syn vivo* shell orientation(e.g., Longridge et al. 2009; Hoffmann and Zachow 2011; Hoffmann et al. 2013; Tajika et al. 2015; Naglik et al. 2015).These models are based on image stacks produced by different tomographic methods. Attempts to obtain image stacks by computer tomography often failed due to the lack of density contrast. This is probably the reason for the relatively late appearance of tomographic images of the interior of ammonoids in the scientific literature. Accordingly, tomographic data were sometimes obtained by serial sectioning (Tajika et al. 2015; Naglik et al. 2015). The latter method has the advantage that the images provide colour information and lack certain artifacts occurring in CT-data such as ring artifacts (see Hoffmann et al. 2013). In any case, these empirical models (Fig. 17.5) largely corroborate the results of mathematical modeling: forms with body chambers < 100° or > 360° have low apertures while the majority of shell forms with body chambers of 200° to 300° have more or less horizontally arranged apertures facing upward (Tajika et al. 2015; Naglik et al. in press).

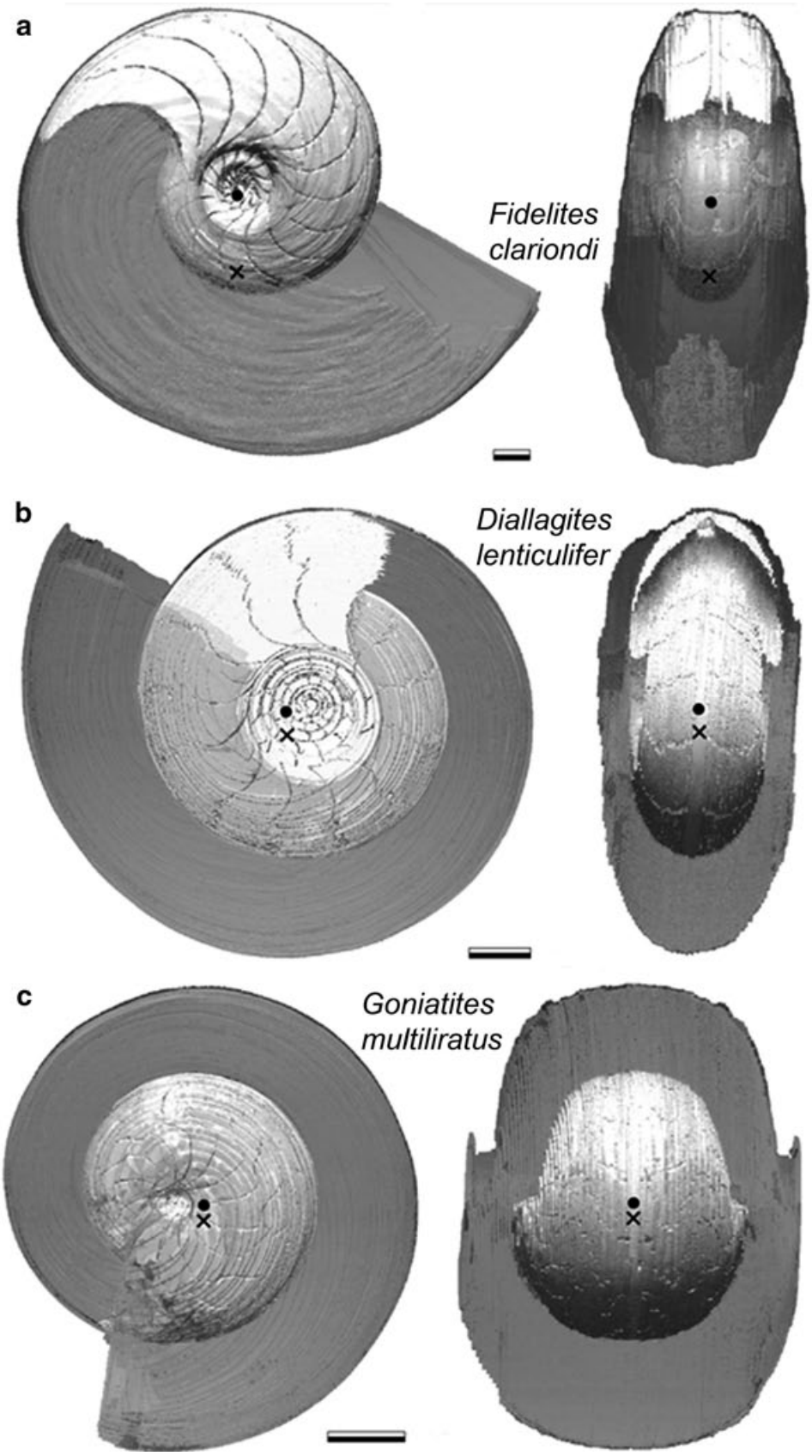

Fig. 17.5 Three Paleozoic ammonoids that have been subjected to grinding tomography in order to produce virtual 3D-reconstructions. Based on the image stacks, centers of mass (x) and buoyancy (o) were established based on these empirical models. (From Naglik et al. 2015). Scale bar: 0.5 cm

17.4 Muscles, Drag and Power

Because we cannot directly observe live ammonoids swimming, testing hypotheses on ammonoid swimming speed and swimming behavior presents obvious challenges to researchers interested in such matters. A wide variety of approaches to these issues are possible, but so far interest has centered primarily on muscles used to generate propulsion, drag, and power.

17.4.1 Muscles

Muscle attachment structures are reviewed by Doguzhaeva and Mapes (2015). According to them, jet-powered swimming could have been possible for forms with a body chamber length of one whorl or less and muscle attachments that would permit some muscles to extend straight across the body chamber and attach to the head and to the funnel.

A basic question here is the following: which of the extant cephalopods, if any, have a propulsive muscular system and mode of locomotion similar to that of ammonoids? The following kinds of muscular systems characterize modern cephalopods:

1. *Nautilus*-like: Because Recent nautilids are the only extant ectocochleate cephalopods, they have commonly been used as paradigms to understand the paleobiology of ammonoids. In modern nautilids, the large cephalic retractor muscles, which are attached to the inner shell wall of the body chamber, pull the head complex back into the body chamber, thus compressing the mantle cavity and expelling a propulsive jet of water out of the hyponome (Packard et al. 1980; Chamberlain 1981, 1987). The occurrence of apparent retractor muscle attachment scars in some ammonoids, as pointed out in Doguzhaeva and Mapes (2015), suggests that such ammonoids may have powered themselves by a "piston-pump" system not unlike what is seen in *Nautilus*.
2. Squid-like: Taking cephalopod phylogeny into account, ammonoids are more closely related to coleoids than to nautilids (Jacobs and Landman 1993; Kröger et al. 2011), and perhaps one may thus expect some similarities in coleoid and ammonoid propulsion systems. Modern squids use their muscular mantle (Bone et al. 1981) to pressurize mantle cavity water, which is then ejected through the funnel. However, the mantle in squids is not surrounded by shell as in *Nautilus*, or ammonoids, and does not function in shell secretion. It is generally considered that ammonoids also used their mantle to secrete the shell, as do ectocochleate cephalopods in general. Whether this necessarily implies that the ammonoid mantle was attached to the inner shell surface, and was secretory rather than muscular and incapable of compressing the mantle cavity is open to debate. In this regard, Jacobs and Landman (1993) as well as Jacobs and Chamberlain (1996) have suggested that the absence of large lateral muscle scars in some ammonoids

may mean that such animals used a squid-like system of propulsion involving the mantle. It has even been suggested that some ammonoids may actually have internalized shells (Doguzhaeva and Mutvei 1991, 1993), but in such cases, the mantle cavity was still located inside the body chamber of the shell. The *Nautilus* hyponome is also muscular and can direct and further compress the propulsive flow, but unlike the tubular funnel in coleoids, the *Nautilus* hyponome is a flap of tissue with folded, overlapping edges. Westermann (2013) proposed that some ammonoids may have had a powerful, coleoid-like tubular hyponome that was the main source of propulsive power. Nevertheless, the fins (probably not present in ammonoids) sometimes also play a role in squid locomotion (Packard 1972; Well 1995; Boyle and Rodhouse 2005)

3. *Argonauta*-like: Females of the octobrachian *Argonauta* produce an egg-case that is used both to shelter the eggs and to pick up air at the water surface in order to regulate buoyancy (Finn and Norman 2010). The shell differs from ammonoid shells in the absence of chambers and the fact that the *Argonauta* shell is secreted by two modified arms; other characters also differ (compare Hewitt and Westermann 2003). The mantle is not firmly attached to the shell and propulsion is carried out by means of the mantle as in other octobrachians (Young 1960; Finn and Norman 2010; Rosa and Seibel (2010).It is highly unlikely that ammonoids propelled themselves in a way analogous to that of a female *Argonauta*.
4. *Vampyroteuthis/Octopus*-like: *Vampyroteuthis* and several octobrachians can swim by contracting their arms with the velar skins, thus expelling water (Boyle and Rodhouse 2005). Since hardly anything is known about ammonoid arms (Klug and Lehmann 2015), it is currently impossible to conclude if such a mode of locomotion occurred in ammonoids.

In our view, it is likely, but not proven, that many ammonoids used longitudinal muscles to power jet propulsion. Evidence for the use of arms, velar webs, fins and mantle muscles in ammonoid locomotion is still poor or lacking. The possible efficiency, energy requirements and energy consumption associated with ammonoid propulsion are discussed in Chap. 17.4.3 below.

17.4.2 Drag

Drag is a physical term, which describes the forces that counteract the motion of an object moving through a fluid, namely seawater in the case of ammonoids. Drag is the product of the inertial and viscous forces acting on such an object, and thus depends on size, shape, and speed of the object, and on the density and viscosity of the fluid. Drag is one of the physical aspects of ammonoids that can be measured directly, even on fossil specimens (Schmidt 1930; Kummel and Lloyd 1955; Chamberlain 1976, 1980, 1981; Chamberlain and Westermann 1976; Jacobs 1992b; Jacobs et al. 1994; Jacobs and Chamberlain 1996). Drag force is usually measured directly, as was done in the studies noted immediately above. In situations where separated flow occurs, as would normally be the case for medium-sized and large

ammonoids moving relatively fast, drag can also be calculated from the following equation.

$$F_D = \tfrac{1}{2} \rho \, v^2 \, C_d A$$

F_D—drag force; ρ—density of the medium (seawater); v—velocity of the object (ammonoid); C_d—drag coefficient of the object (a dimensionless number which can be thought as representing the shape of the moving object); A—an area representative of the size of the moving object.

For objects, such as ammonoids, which have complex shapes, and thus complex flow interactions, shell volume raised to the two-thirds power ($V^{2/3}$) is generally the areal parameter of choice (Chamberlain 1976; Vogel 1981). It is important to understand that C_d is not a constant; it is a coefficient that varies widely for a given object depending on flow conditions. Flow state around an object, like an ammonoid, is described in terms of the Reynolds number.

$$Re = dm \, v / \upsilon \quad \text{with} \quad \upsilon = \gamma / \rho$$

Re—Reynolds number; dm—specimen shell diameter in the direction of motion; v—velocity of the object; υ—kinematic viscosity of seawater (viscosity [γ] divided by seawater density [ρ]). When Re is low ($Re < 1000$ approximately), flow is attached to the object (this is often referred to as Stokes Flow); drag is due entirely to surface friction; C_d is very high, often more than 100, and varies directly with velocity and Re. Spherical objects generate the least drag because they have the smallest surface area, and hence least frictional drag per unit volume. For ammonoids, these conditions would hold for small ammonoids swimming slowly. When Re exceeds approximately 10,000, flow is separated to some degree from the object (this is often referred to as separated or non-Stokes flow); drag is due to a combination of friction and an adverse pressure gradient created by the separation; and C_d is low and often constant, or nearly so, as Re and velocity change, fusiform objects generate the least drag because they have the smallest possible pressure drag component (fusiform shapes minimize the extent and magnitude of separation and the posterior low pressures that derive from separation). For many objects operating in separated flow, a large reduction in C_d occurs when the character of the fluid boundary layer lying on the surface of the object converts from laminar to turbulent conditions. For ammonoids, separated flow would hold for large ammonoids swimming quickly. At intermediate values of Re ($1000 > Re < 10{,}000$ approximately), flow is unstable and can vary from a separated to attached state depending on such factors as object shape and surface features. This would apply to ammonoids of intermediate size moving at intermediate speeds.

Several authors examined drag using ammonoid models (Schmidt 1930; Kummel and Lloyd 1955; Chamberlain 1976; Jacobs 1992b; Jacobs and Chamberlain 1996). Modeling focused on the shell only (Kummel and Lloyd 1955; Chamberlain 1976); the shell and attached prostheses imitating extruding soft parts (Chamberlain 1980); or shell and artificial surface sculpture (Chamberlain 1981). For models

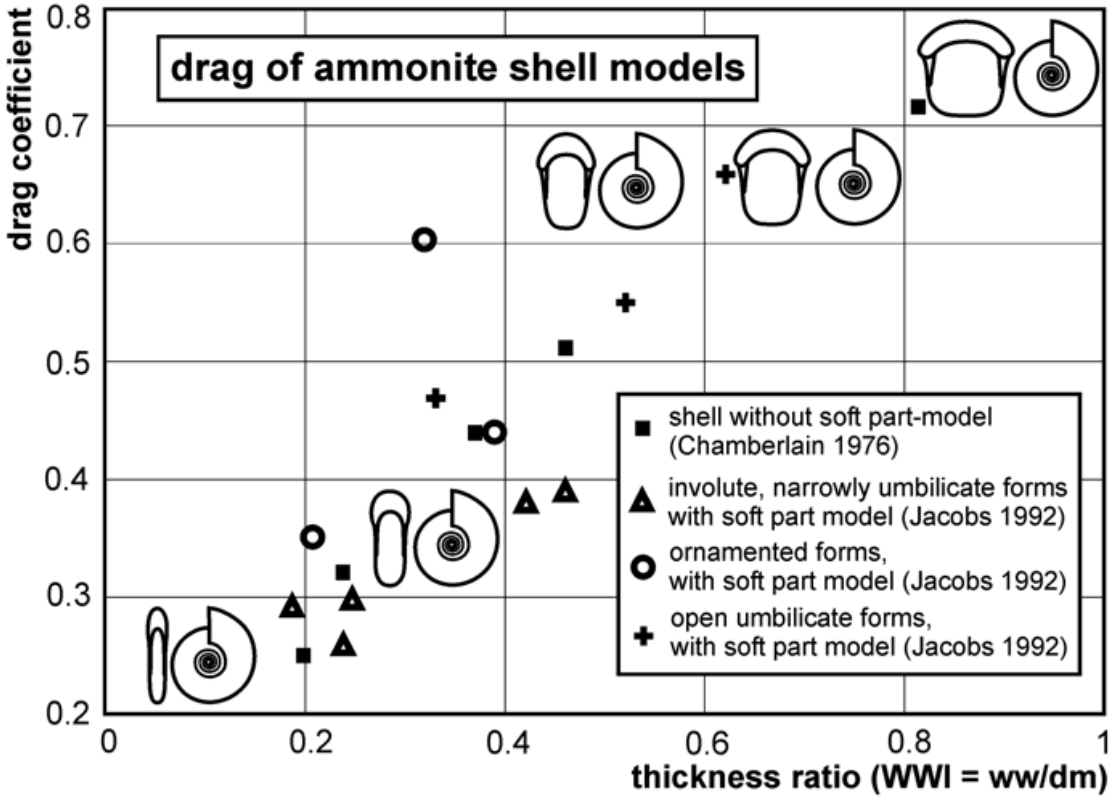

Fig. 17.6 Relationship between the thickness ratio and the drag coefficient, depending to a lesser degree on other factors such as umbilical width and ornament strength. These data (Chamberlain 1976; Jacobs 1992b) were obtained from models in a water tank (modified after Jacobs and Chamberlain 1996)

with representative values of Raup's W and D values (Raup 1966, 1967; Raup and Chamberlain 1967), Chamberlain (1976) determined drag coefficients in separated flow (i.e. for higher velocities and larger shells) where pressure drag is the key hydrodynamic factor. These experiments on models revealed that narrower shells had lower drag values. It appears to be mainly shell thickness and umbilical width, which play important role in generating drag in such flow conditions (Fig. 17.6).

In a later study, Jacobs (1992b) focused on drag for ammonoids of small size and low velocity (Re below about 25000), where frictional drag is the key hydrodynamic factor (see also Jacobs and Chamberlain 1996). Some results of Jacobs (1992b) are reproduced in Fig. 17.7. Note that in each graph in Fig. 17.7, the curves for wide and narrow forms cross at a point between Reynolds numbers of 5000 and 10,000. At Re less than the crossing value, the wider shells have lower drag coefficients (less frictional drag in Stokes flow) than the narrow shells, but at Re greater than the crossing value, the narrow shells have lower drag coefficients (less pressure drag in separated flow). This implies that different shell morphologies are more efficient at different sizes and swimming speeds (Table 17.1). Narrow forms produce less drag than wide forms at higher Reynolds numbers (faster speeds, larger size), while wide shells generate less drag at low Reynolds numbers (slower speeds, smaller size) than do narrow shells. This situation implies that the com-

Table 17.1 Possible swimming behavior of ammonoids in dependence of their shell shape. (Modified after Jacobs and Chamberlain 1996). For *Baculites*, we used the interpretation of Westermann (2013). Additional information comes from Klinger (1981) and Seki et al. (2000)

Shell shape	Slow, continuous swimming	Fast, continuous swimming	Acceleration	Vertical
Compressed involute				
Oxyconic (e.g., *Sphenodiscus*)	Poor	Good	Excellent	Moderate
Platyconic with rounded venter (e.g., *Oppelia*)	Moderate	Excellent	Good	Moderate
Platyconic with tabulate venter (e.g., *Anahoplites*)	Good?	Good	Moderate	Moderate
Moderately compressed				
Platyconic, moderately evolute (e.g., *Mesobeloceras*)	Moderate	Good	Moderate	Moderate
Involute juvenile (e.g., *Scaphites*)		Moderate	Moderate	Moderate
Evolute, rounded whorls (e.g., *Lytoceras*)	Moderate	Moderate	Poor	Moderate
Compressed evolute	Good	Moderate	Moderate	Good
Depressed				
Sphaeroconic involute (e.g., *Goniatites*)	Moderate	Poor	Poor	Moderate
Cadiconic, evolute (e.g., *Cabrieroceras*, *Gabbioceras*)	Moderate	Poor	Poor	Moderate
Heteromorphic				
Orthoconic (e.g., *Baculites*)	Moderate	Moderate	Excellent?	Moderate
Torticonic (e.g., *Turrilites*)	Poor	Poor	Poor	Good
Loosely coiled in three dimensions (e.g., *Nipponites, Didymoceras*)	Poor	Poor	Poor	Good

mon ammonoid ontogenetic change in shell morphology from depressed juvenile whorls to more compressed whorl shape near maturity could be linked with this flow state dependent change in drag coefficient (Jacobs and Chamberlain 1996). The latter authors also suggested that morphologic change related to hydrodynamic factors operating in the evolution of ammonoid clades should be linked with different host facies. This link was examined by various authors (e.g., Ziegler 1967; Batt 1989; Bayer and McGhee 1984; Marchand 1992; Courville and Thierry 1993;

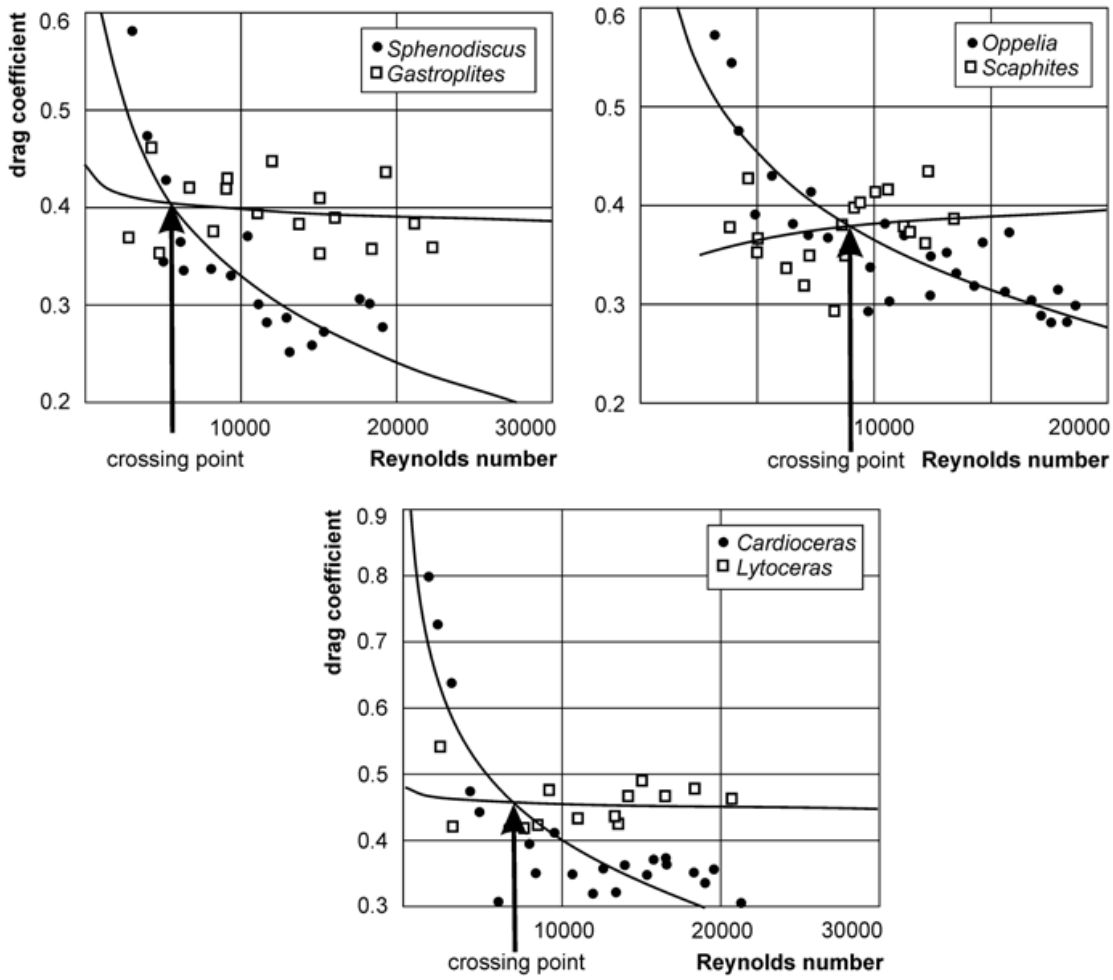

Fig. 17.7 Relationships between drag coefficients and Reynolds number (Re) of three different pairs of Jurassic and Cretaceous ammonoids. In each pair, one form has a narrow shell (*dots*), and one has a wide shell (*open squares*). Note that in each graph the curves for the two forms cross at a point between Reynolds numbers of 5000 and 10000. At Re less than the crossing value, the wider shells have lower drag coefficients (less frictional drag in Stokes flow) than the narrow shells, but at Re greater than the crossing value, the narrow shells have lower drag coefficients (less pressure drag in separated flow)

Jacobs et al. 1994; Klug 2002; Kawabe 2003). Such studies are hampered by the possibility that ammonoid shells were transported post mortem and the imperfect knowledge of habitat depth, because the sedimentary context in which ammonoids are preserved mainly informs about the energy in the water column and the volume of sediment that is delivered in combination with accommodation space. It is possible that ammonoids could have lived in more quiet waters near the sea-floor or in more agitated waters near the surface uncharacteristic of the sedimentary context of the rock itself. Additional factors, such as time-averaging might also complicate straight forward interpretations (compare De Baets et al. 2015a).

In any case, the measurable disparity of ammonoids throughout ontogeny and evolution as well as the recurrent ontogenetic change in shell shape indicate that minimizing drag played an important role in ammonoid evolution. It also indicates

that different forms were possibly specialized for different modes of life with correspondingly different swimming abilities.

17.4.3 Power

The use and availability of power for swimming in ammonoids cannot be measured directly and thus has to be addressed based on actualistic comparisons with living organisms (e.g., Trueman and Packard 1968).

The physical term, power, simply describes the ratio between the work, W, expended in a time interval, t:

$$P = \Delta W / \Delta t$$

Assuming constant velocity during the time interval in question, this can be modified to the following equation using drag force F_D and velocity v:

$$P = F_D \; v$$

Power consumption during swimming thus depends directly on drag coefficient and can be estimated from the relationship between drag coefficient and Reynolds number, and thus with respect to size and velocity (Jacobs 1992b; Jacobs and Chamberlain 1996). In order to assess the differences in power consumption as a function of shell form, size and velocity, Jacobs (1992b) produced drag data for the thick genus *Gastroplites* (ww/dm = 0.42) and the thin genus *Sphenodiscus* (ww/dm = 0.19). His results are reproduced here in Fig. 17.8. According to Fig. 17.8, *Gastroplites* would require less power at sizes below 10 cm and velocities below 50 cm/s. At a shell size of 10–100 cm and speeds below 15 cm/s, the two shell shapes would require about the same power. At higher speeds and sizes exceeding 10 cm, *Sphenodiscus* would need less power and swim more economically. Whether these ammonoids could actually produce the power necessary to swim at these speeds cannot be inferred from such data, however.

Knowledge of swimming speed in fossil ammonoids requires knowledge of the power output generated by live ammonoids. The power produced by live ammonoids is unknown. However, one can gain useful insight into this matter by applying to this question data on power output of modern swimmers, particularly modern cephalopods. Of primary interest is the power output of modern analogues in sustained swimming (powered by aerobic muscle contraction), and in burst swimming (powered by anaerobic muscle contraction). Also of interest is metabolic scope, i.e., the difference between the power requirements during inactivity and periods of maximum activity. Unsurprisingly, power output and metabolic scope differ strongly between living cephalopods such as *Nautilus* with very low metabolic rates and the active squid *Illex* with a high metabolic scope (O'Dor 1982, 1988a, b; Chamberlain 1987; O'Dor and Wells 1990; O'Dor et al. 1990, 1993; O'Dor and Webber 1991). Even among squids, metabolic rates can vary strongly depending on

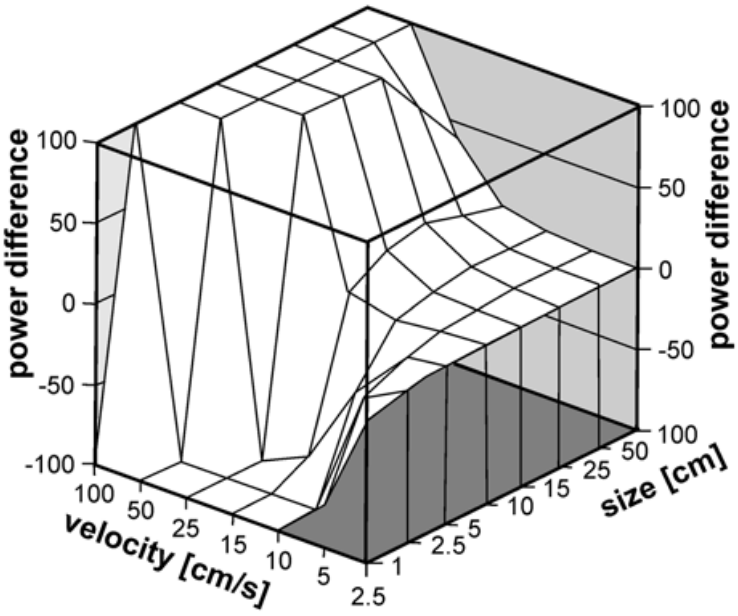

Fig. 17.8 Differences in power consumption (in ergs/s/cm^3) in a broad, depressed form (*Gastroplites*) and in a narrow, laterally compressed form (*Sphenodiscus*). Power difference was calculated by subtracting the power required per unit volume in *Sphenodiscus* from that of *Gastroplites*. Depending on this ratio, one obtains positive or negative values: when the values of power difference are negative, *Gastroplites* requires less power. The greatest power difference is seen at low sizes and high velocities. Jacobs and Chamberlain (1996) considered these differences as so profound that they appear to be biologically significant. Power differences > 100 ergs/s/cm^3 are not shown (modified after Jacobs and Chamberlain 1996)

their habitats (Seibel et al. 1997). For instance, the deep-sea squid *Vampyroteuthis infernalis* has a metabolic rate a hundred times lower than the shallow water *Gonatus onyx* (Seibel et al. 1997).

Estimates of power production in ammonoids depend on whether Recent nautilids are considered the better model organisms with their similarly constructed external shell or whether coleoids should rather be used as paradigms because they are more closely related to ammonoids. Several authors (e.g., Trueman 1941; Swan and Saunders 1987; Jacobs and Landman 1993; Kröger et al. 2011) have argued in favor of coleoids rather than nautilids on the basis of shell form and phylogeny. In order to estimate sustainable swimming speeds in ammonoids, Jacobs (1992b) argued that a metabolic rate of 200 ml of oxygen per kilogram per hour, which is close to that of *Sepia* (O'Dor and Webber 1991), probably represents a reasonable figure for most ammonoids. He also advocated that for ammonoids, sepiids represent the most meaningful model organisms among coleoids because like ammonoids, they have a large chambered phragmocone, which greatly limits the relative proportion of propulsive muscle (and soft tissue generally) to total volume of the animal (see also Chamberlain 1981, 1990, 1992, 1993). By comparison, squids like *Illex*, pack their bodies much more fully with propulsive muscle. O'Dor and Webber (1991) found that the metabolic scope of the highly active *Illex* was four times larger than in *Sepia* and additionally, the efficiency of their muscles exceeds that of sepiids. In

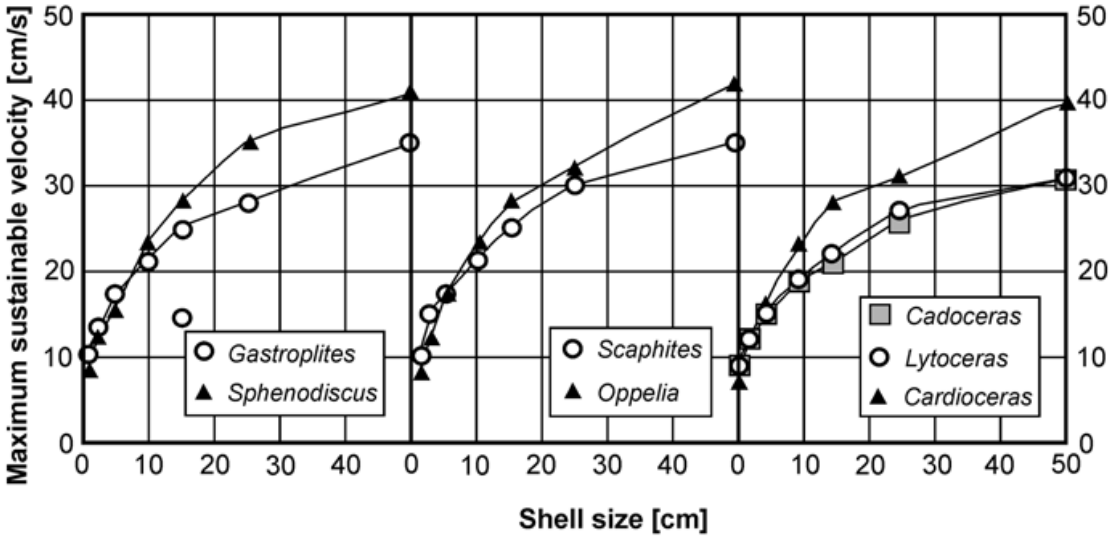

Fig. 17.9 Maximum sustainable swimming velocities in seven ammonoid genera. These are arranged in groups of two or three, always comprising a genus with a more compressed and one with a more depressed shell form. The velocity values are based on the assumption that the maximum power availability was 400 ergs/s/cm^3. Overall, the curves resemble each other and in the curve pairs, they cross each other at a size of 5 to 10 cm (modified after Jacobs (1992b) as well as Jacobs and Chamberlain (1996))

consequence, power output is ten times higher in *Illex*, thus making *Sepia* the better actualistic model organism for ammonoids (Jacobs and Chamberlain 1996).

O'Dor and Webber (1991) observed swimming speeds of maximally 65 cm/s (2.3 km/h), which required a power output of 1000 µJ/s/cm^3. Jacobs (1992b) as well as Jacobs and Chamberlain (1996) concluded that in ammonoids, this figure would probably not have exceeded 600 µJ/s/cm^3 because only about 40 % of the organism's volume is occupied by soft parts. The maximum swimming speeds of some ammonoid species, which are based on these assumptions, are depicted in Fig. 17.9. Maximum swimming speeds of large ammonoids like *Sphenodiscus* with a shell diameter of 25 cm would not have exceeded 100 cm/s (3.6 km/h). *Gastroplites* of the same size would have a speed of about 70 cm/s (2.5 km/h). The latter velocity corresponds to the maximum in *Sepia* (Jacobs and Chamberlain 1996). As a lower limit of energy availability, *Nautilus* can be used as model. Nautilus can activate up to 100 µJ/s/cm^3, i.e. a tenth of that of *Sepia*. Using this figure, a 25 cm *Gastroplites* could reach 40 cm/s (0.54 km/h) and *Sphenodiscus* would have been able to swim 55 cm/s (1.98 km/h). These results are similar to swimming velocity estimates based primarily on drag considerations made by Chamberlain (1981, Fig. 17.8).

In summary, Jacobs (1992b) as well as Jacobs and Chamberlain (1996) found that swimming speed of ammonoids likely depended on various factors including shell shape (e.g. Table 17.1), body chamber angle, size, energy availability and power consumption. For large size, ammonoids with compressed shell form (low ww/dm ratio) could swim faster than those with depressed shells (high ww/dm ratio); while at small size this relationship is reversed.

17.4.4 Acceleration

Accelerating an object in a fluid involves accelerating fluid entrained in the object's wake and also fluid in direct contact with the surface of the object, i.e. in the boundary layer. In the case of swimming organisms, this also applies and in order to estimate swimming speeds and energy requirements, this added mass has to be taken into account (Chamberlain 1987; Jacobs 1992b; Jacobs and Chamberlain 1996). The force required to accelerate this added mass can be quantified by the following equation, which was introduced by Daniel (1984):

$$G = -ar\,V\,(du/dt)$$

G—acceleration reaction force; a—added mass coefficient (a function of thickness ratio ww/dm); r—density of the fluid; V—volume of the object/ammonoid; du/dt—acceleration.

The acceleration reaction force occurs both in acceleration and deceleration (Daniel 1984; Chamberlain 1987; Jacobs 1992b; Jacobs and Chamberlain 1996). For ammonoids, the symmetry of the shell in swimming direction, shell shape, differences in acceleration and deceleration processes as well as the formation of vortices in the wake play a role.

In cephalopods, acceleration is produced by a series of water expulsions from the hyponome with interim phases of water intake into the mantle cavity. The animal accelerates when the propulsive muscles contract forcing water from the mantle cavity and decelerates during the recovery phase of the propulsive cycle when water is taken into the mantle cavity in preparation for the next mantle cavity contraction. When an organism starts swimming, energy is mainly invested in acceleration while at higher speeds when velocity is more constant, the energetic cost of drag rises. Acceleration force also depends on the width of the ammonoid shell (ww/dm ratio; Fig. 17.10) and it roughly doubles from ww/dm = 0.2 to a value of 0.4 (Jacobs and Chamberlain 1996). According to Daniel (1984, 1985), the ratio of energetic costs of drag to that of acceleration varies from 48 % in a small squid accelerating from 0 to 2000 cm/s^2 to 62 % in a medusa accelerating to 700 cm/s^2 to 92 % in a salp accelerating to 23 cm/s^2. These values show that the faster an organism accelerates to a higher velocity, the lower the relative energy investment into added mass and the higher the investment into overcoming drag.

This relationship points to a potentially multiple functions of shell shape in ammonoids. While some shell morphologies reduced drag, other shell morphologies, such as oxycones with a small umbilicus, would have reduced the energetic cost invested in added mass (Jacobs 1992b; Jacobs and Chamberlain 1996). In that respect, ammonoids with narrow oxyconic shells would resemble ambush predators among fish (e.g. pike, barracuda) whose body geometry is too elongate to be purely adapted to reduce drag. Instead, their long and narrow shape strongly reduces acceleration reaction force and enables them to accelerate strongly from a standing start. While there is no corroboratory evidence for an ambush predator strategy

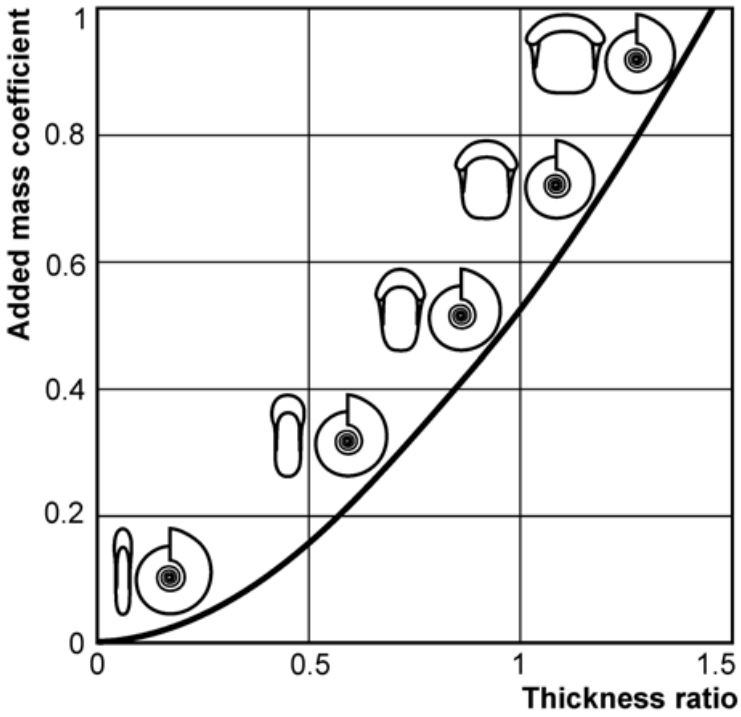

Fig. 17.10 Depending on shell shape and ornament, differing amounts of added mass of water accelerated with the ammonoid in the boundary layer and the wake can be expected. The acceleration reaction is a linear function velocity change (acceleration) and a function of the added mass coefficient, which -in turn- depends on shell shape and orientation relative to the direction of acceleration. According to these relationships, ammonoids with laterally compressed shells had substantially less added mass than ammonoids with depressed shells (modified after Jacobs (1992b) as well as Jacobs and Chamberlain (1996))

in oxyconic ammonoids, the fact that oxyconic shell form evolved many times iteratively and sometimes even in parallel (e.g., Bayer and McGhee 1984; Klug and Korn 2002; Monnet et al. 2011) shows that this shell shape may indeed have had a positive adaptive benefit for ammonoids.

17.4.5 Cost of Transportation

The cost of transportation (COT) is a metric that describes the energetic cost of locomotion. COT has been defined in a variety of ways. For example, in his comparison of the energy cost of different styles of animal locomotion Schmidt-Nielsen (1972) defined COT as (metabolic rate/(body weight and speed). O'Dor (1988a) and O'Dor and Webber (1991) in their study of squid locomotion, and Chamberlain (1990) in his study of *Nautilus* locomotion, determined COT by calculating metabolic output from oxygen consumption data for swimming animals. In all such approaches the aim has been to express COT in terms of the propulsive power produced by a swimming animal relative to some measure of its size, speed, and distance travelled. COT is thus simply stated in terms of propulsive power per unit of animal size per unit of speed or distance traveled where animal size is represented by weight or volume.

The power produced by a swimming ammonoid can be expressed as follows:

$$P = W/t = (F\ d)/t = F\ v$$

where P is the metabolic output (power) used to produce locomotion; W is the work needed for locomotion; t is the time interval over which the locomotion occurs; F is the force or thrust developed by the swimming ammonoid and is assumed to be constant over the interval t; d is the distance traveled; and v is the animal's velocity, also assumed to be constant.

Jacobs (1992b) and Jacobs and Chamberlain (1996) used the power-required data and the efficiency assumptions of Jacobs (1992b) to evaluate COT for a few representative ammonoids. Following Jacobs (1962b), they calculated COT as propulsive power per unit of total shell volume per unit of distance traveled. Their results are diagrammed in Fig. 17.11. The upper panel in this figure indicates that, assuming *Sepia* metabolic output, *Gastroplites* COT depends on size. Larger animals have lower COTs for a given velocity than smaller ones. This is largely the result of larger animals operating in separated flow where drag coefficients are smaller while small animals operate in Stokes flow where drag coefficient is much higher for objects of the same shape. The upper panel also indicates that if we assume *Gastroplites* had a lower metabolic output equivalent to that of *Nautilus*, its COT would also be lower. Perhaps the most interesting observation to be made from Fig. 17.11 is that for each curve there is a specific velocity for which COT is minimal. If energy conservation in swimming ammonoids mirrors that of flying animals, where flight speed usually reflects minimal COT, and there is no reason why it should not, this may mean that this minimal COT speed represents the usual swimming speed for the ammonoid to which the curve applies. The steepness of the curve on either side of the minimum COT speed implies that there would be considerable gain in cost to the animal in moving away from this optimum speed. The lower panel in Fig. 17.11 shows that the modern swimmers plotted here, both coleoids and fish, have COT-velocity curves much less steeply inclined as velocity increases above the minimum COT speed. This means that these modern animals are not nearly so constrained in terms of COT in varying their swimming speed than is the case for the ammonoids plotted here as well. Swimming over a range of velocities does not greatly influence their COT. It would appear that these modern swimmers have a much more flexible swimming repertoire than did fossil ammonoids.

Jacobs (1992b) as well as Jacobs and Chamberlain (1996) suggested that due to their neutral buoyancy, ammonoids, like *Nautilus*, may have had a low use of energy at rest and that the cost of transportation in ammonoids was accordingly low at low velocities. Alternatively, if ammonoids were closer to sepiids in their metabolic rates, the cost of transportation would have been lower at higher swimming speeds depending on their size (Fig. 17.11). Jacobs and Chamberlain (1996, p. 210) summarized this idea as follows: "*ammonoids may not have been pursuit predators, comparable to tuna or some squids, that spend long periods of time chasing down prey at high speed. This would deny the utility of the neutrally buoyant shell in limiting energetic expenditure. However, life styles that require only intermittent bursts*

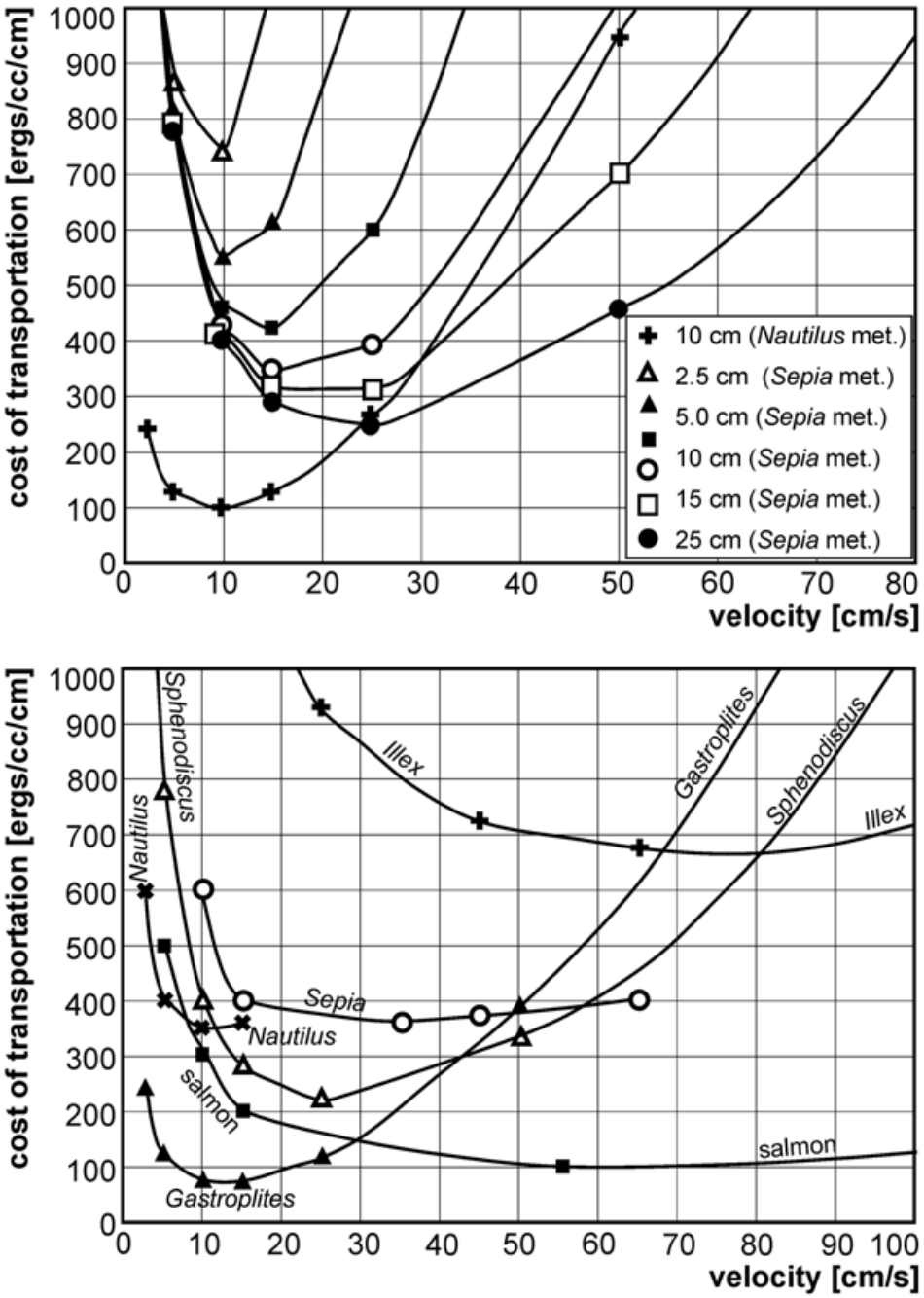

Fig. 17.11 Cost of transportation (*COT*) in relation to velocity depends on shell size and metabolic rate (upper diagram) and differs between modern animal groups (lower diagram). Modified after Jacobs (1992b) as well as Jacobs and Chamberlain (1996). The efficiency of energy conversion into propulsion force is estimated to be 10 %. The upper diagram shows the COT for various sizes of *Gastroplites*, assuming metabolic rates (O'Dor and Webber 1991) of *Sepia* (3900 ergs/s/cm^3) and in one case of *Nautilus* (1/7th of *Sepia*). With increasing size, less energy is required for locomotion. The lower diagram shows the COT of *Sphenodiscus* and *Gastroplites* in comparison to various recent cephalopods and a fish (O'Dor and Webber 1991). Resting metabolic rates were estimated for *Sphenodiscus* to resemble that of *Sepia* and for *Gastroplites* to resemble that of *Nautilus*. At higher velocities, the costs rise much faster in the shelled swimmers than in fishes and squids. However, the ammonoid curves are based on a series of estimates for the metabolic rates, added mass and other modes of locomotion (fins in *Sepia*)

of energy, such as ambush predation, seem possible, and oxyconic shell shape […] *may have been conducive to such a mode of life*." It should be remembered that high speed is not required for successful predation. A predator must only move faster than its prey. If its prey is slow, a predator can be slow also. Oxycones would not need the fast burst speed of *Illex* or *Sphyraena* (barracuda) to prey on slower moving ammonoids.

Jacobs (1992b) and Jacobs and Chamberlain (1996) also pointed out that energy used for transport is energy that cannot be used in other ways; there is a trade-off between these costs and the energetic cost of other life functions. Nautilids have a low metabolism and can fast over lengthy time spans. In such a case, slow swimming speeds (O'Dor et al. 1990) are advantageous in promoting prolonged food searches (Wells 1987; Chamberlain 1990; Jacobs and Chamberlain 1996), as is the case for *Nautilus* (Ward and Wicksten 1980). Wells and O'Dor (1991) thought that other ectocochleates such as ammonoids may have pursued a similar low energy mode of life. They supported this hypothesis by pointing out that increasing numbers of fish occupied high energy nektonic habitats (for these macroecological changes, see Signor and Brett 1984; Bambach 1999; Kröger 2005; Klug et al. 2010) and would have competitively excluded most ammonoids from these habitats. The problem with this hypothesis is twofold: (1) As Jacobs and Chamberlain (1996) pointed out, ammonoids are more closely related to coleoids (some of which use considerable energy in relation to body size and also swim at high velocities) than they are to low energy nautilids (Jacobs and Landman 1993; Kröger et al. 2011). (2) The radiation of gnathostome fish in the Silurian and Devonian, a major event in the evolution and history of diversification of fishes, was also a time in which ammonoids originated and rapidly diversified (Klug et al. 2010). The diversification of teleostean fish in the Mesozoic also appears to be largely independent of ammonoid diversity changes (Jacobs and Chamberlain 1996), although the Cretaceous diversification of deep-bodied acanthopterygians may have been a factor influencing ammonoid diversity late in their history (Chamberlain 1993). Some heteromorphs might have been slower swimmers than nautilids in horizontal direction, although this requires further research (e.g., Ward 1979; Westermann 1996).

17.4.6 The Role of Ornament

As in sharks (Reif 1982; Oefner and Lauder 2012) and golf balls, a fine regular surface ornament can reduce drag by forcing conversion of the boundary layer around an ammonoid shell from laminar to turbulent flow at lower Reynolds numbers than would normally be the case. Boundary layer conversion reduces the scale of the turbulent wake and the pressure drag that results from it. Chamberlain and Westermann (1976) and Chamberlain (1981) examined this phenomenon and concluded that it could have a positive effect for some ammonoids by bringing lower drag and more efficient swimming into the velocity range of some ammonoids. Nevertheless, the lowering of the coefficient of drag would have been significant at Reynolds numbers exceeding 40,000, a figure that could potentially only be achieved in large ammonoids moving at relatively high velocities (Chamberlain 1981).

Jacobs and Chamberlain (1996) speculated that in cadicones, the coarse ribs or nodes as in *Cabrieroceras*, *Gastrioceras* or *Teloceras* might have caused the formation of vortices covering the entire umbilicus. Similarly, they suggested that, in forms with tabulate venter (or with ventral band as in Devonian forms such as *Gyroceratites*, *Armatites* or *Kosmoclymenia*), the water might have been divided into two fields, thus maintaining flow attachment and reducing turbulence in their wake, at least at certain velocities and sizes. They also reasoned that ribs tend to be the largest near the aperture and to be oriented in swimming direction, thus stabilizing the shell orientation during backward swimming in forms, which are more or less involute and carry moderately strong ribs such as *Cardioceras*. Westermann (1966) even speculated that this might be a driving force behind Buckman's law of covariation, although this law can be conveniently explained by morphogenetic processes (Monnet et al. 2015) without an adaptive interpretation (compare Hewitt 1996 for an alternative functional explanation). In contrast, strong ornament significantly increased drag (Chamberlain 1976; Jacobs 1992b; Hewitt 1996; Jacobs and Chamberlain 1996), thus supporting indirectly its possibly defensive function shell sculpture (e.g., Ward 1981).

17.4.7 Hydrodynamics Through Ammonoid Development

As discussed in Hoffmann et al. (2015), the flow regime in which ammonoid swimming took place changed through ontogeny as ammonoids grew in body size and shell diameter. Ontogenetic size increase covered two orders of magnitude or more in most ammonoid taxa. While embryonic shells (Landman et al. 1983; De Baets et al. 2012) vary about one order in magnitude in size between the earliest forms (>5 mm) and several derived Mesozoic forms (ca. 0.5 mm), the adult shells vary from less than 1 cm to over 2 m. Because small individuals have less power in relation to drag, adult ammonoids could probably swim one to two orders of magnitude faster than hatchlings (Jacobs and Chamberlain 1996).

In hatchlings, much of the energy invested in locomotion will be absorbed by skin friction drag. Jacobs and Chamberlain (1996) guessed that a hatchling of 1 mm diameter might have attained a swimming speed of 1 cm/s, which corresponds to a Reynolds number near 10. Accordingly, shells with a high whorl width index would have been favorable. In that light, the common decrease in whorl width index, which occurs at that size, appears less surprising (Fig. 17.12). Jacobs and Chamberlain (1996) assumed that added mass and acceleration was more important for small than for large individuals. Consequently, early ontogenetic stages would have profited more from compressed shell shapes, which would have reduced the energetic cost of the acceleration reaction. Taking limited energy resources into account, it becomes clear that hatchlings and early juveniles were limited in most cases to a rather passive, probably planktonic mode of life. Residence of early ontogenetic stages in the water column is evidenced by ammonitellae and early ontogenetic stages of ammonoids in black shale deposits (e.g., Landman 1988; Mapes and Nützel 2008) and other lines of evidence (Landman et al. 1996; Ritterbush et al. 2014; De Baets et al. 2015c).

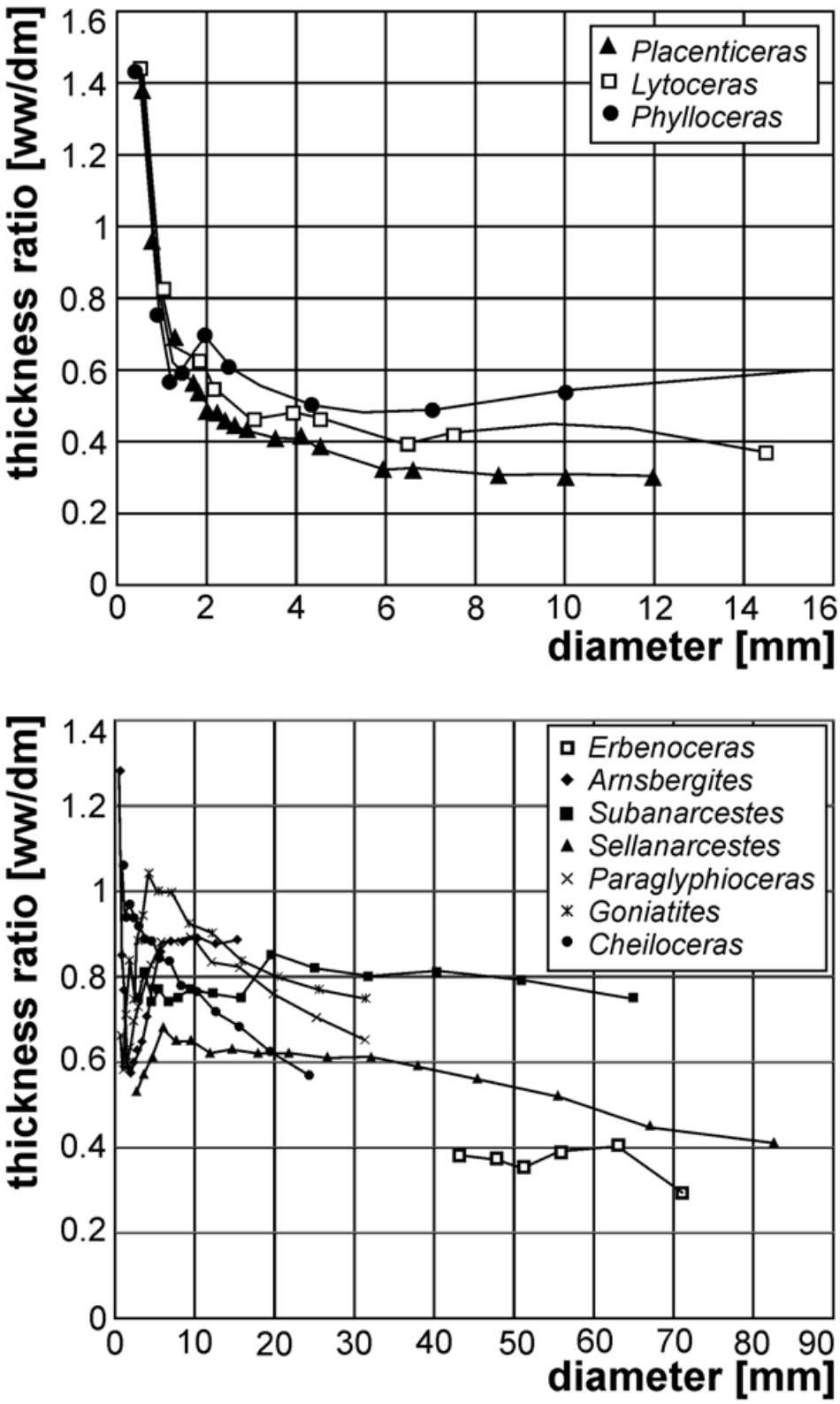

Fig. 17.12 Thickness ratio and shell size in Mesozoic (*top*) and Paleozoic ammonoids (*bottom*) through ontogeny. Modified after Jacobs (1992b) as well as Jacobs and Chamberlain (1996) with new data first reported here. Between hatching (dm < 5mm) and the end of the neanic stage (ca. 10 mm), ammonoids moved only slowly and had wide shells and thus swam at low Reynolds numbers. In all ammonoids, whorl width is reduced after the neanic stage, in Mesozoic forms to values between 0.3 and 0.6 and in Paleozoic forms to values between 0.3 and 0.8. These observations suggest that the ontogenetic late neanic change in shell shape may be an adaptation reflecting the change in hydrodynamic flow conditions

Such accumulations of early ontogenetic stages have often, although not exclusively, been found from the Devonian to the Cretaceous in strata, where benthic life was strongly limited (compare De Baets et al. 2015c). Jacobs (1992b) suggested that the serpenticonic shell shape commonly found in ammonoids (Raup 1967) permitted ammonoids to optimize shell shape for swimming as Reynolds number increased during growth. In contrast, most nautilids (except the aturiids) avoided the smallest size-range for their juveniles, which would have forced the juveniles into a passive planktonic mode of life and similarly, serpenticonic shell shapes are absent in post-Paleozoic Nautilida. Because of these poor locomotory capabilities of ammonoid hatchlings, Jacobs and Chamberlain (1996) considered the possibility of brood care in ammonoids, which finds some support in the occasionally extreme size-dimorphism among ammonoids (e.g., in scaphitids; compare De Baets et al. 2012; 2015c). Walton et al. (2010) speculated on brood care in the Late Devonian genus *Prolobites* based on the extremely low body chamber and terminal aperture, but in this case perhaps outside of the shell of the brooding adult.

Independent of the presence or absence of brood care in ammonoids, the profound morphologic changes that occur around hatching, at the end of the neanic stage, and at maturity (e.g., Westermann 1996; Klug 2001; Korn and Klug 2003) likely had effects on the physical framework for locomotion. It is also striking that commonly, morphologic changes occur at shell diameters between 1 and 2 cm, i.e., when active swimming became feasible for the young ammonoids.

17.5 Information from Epizoans

Some sessile organisms are known to attach themselves in an oriented way depending on the prevailing current direction. Ammonoid shells are well-known to have been inhabited by numerous different invertebrates *syn vivo* (Seilacher 1960; Davis et al. 1999). Some of these epizoans have accordingly been used to interpret the predominant swimming direction of ammonoids. For example, Seilacher (1960) showed bivalve overgrowth on *Buchiceras*, which supported an oblique upward orientation of the aperture of this Cretaceous ammonite.

Keupp et al. (1999) Seilacher and Keupp (2000) as well as Keupp (2012) described a Tithonian aspidocerid inhabited by numerous cirripeds. These epizoans likely attached themselves to the shell of the living ammonite because its aptychi are still in the body chamber and the cirripeds are well articulated. The feeding appendages point in the direction of the aperture, thus suggesting forward swimming, i.e. not backward, as it is usually done by modern cephalopods. This is consistent with the interpretations of Parent et al. (2014) regarding the effect of the aptychi in this genus on swimming speed and swimming direction. Forward swimming would have the advantage that the low hydrodynamic stability of many ammonoids would not have played a big role, because the ammonite shell would have followed the propellent.

Hauschke et al. (2011) described the oriented attachment of a cirripede (goose neck barnacle) on a baculitid. Their findings support forward swimming, but there is also some indication for an approximately horizontal shell orientation during

swimming of this orthoconic ammonite. Westermann (2013) contradicts this interpretation, arguing that these cirripedes might actually have colonized shells without a clear preference of orientation and because he thinks that the apical parts of the phragmocones were largely free of chamber water at such early ontogenetic stages. In addition with the rather long body chambers, it would have made young baculitids swim with their shells in a more or less vertical position.

17.6 Facies of the Host Rock and Habitats

It is one of the classical arguments in cephalopod paleobiology as to whether the host rock facies of a cephalopod fossil can be considered as an indicator of habitat in the live animal. The main reason for doubting the usefulness of studies on the rocks that contain ammonoids is the likelihood of post mortem transport (e.g., Kennedy and Cobban 1976; Tanabe 1979; Marchand 1984). Post mortem transport of nautilids over thousands of kilometers has been shown by various authors (Iredale 1944; Hamada 1964; Stenzel 1964; Toriyama et al. 1965; House 1973, 1987; Chirat 2000). In contrast, Chamberlain et al. (1981) argued that the strong pressure gradient between phragmocone chambers and ambient pressure in modern *Nautilus* leads to rapid post mortem waterlogging of the shell in animals dying within the normal depth range of the live animals (100–300 m). This would rapidly produce negative buoyancy and cause the empty shell to sink, thus precluding significant post-mortem drift (Maeda and Seilacher 1996). Animals dying at shallow depths would have a much greater chance of reaching the ocean surface and drifting significantly from their original habitat. Independent of the correctness of the preceding opinion, some recurring patterns have been found where the same taxa have been discovered in different regions in similar facies (Fig. 17.13 and 17.14; e.g., Westermann 1996). In such cases, one could argue that the same ammonoid taxa may have lived in the same part of a transgression or regression, which thus produced fossils in similar rock types. Especially when ammonoids are found in small basins with restricted connections to the oceans, the probability of extended distances of drift is lower. Naturally, even within small basins, a great range of habitats existed.

Ammonoids were probably not capable of long distance high speed swimming like some modern decabrachian squids or certain pelagic fishes such as tuna. For that reason, Jacobs and Chamberlain (1996) suggested that ammonoids either lived in conditions with slow currents or currents like ocean gyres or in a demersal habitat in regions with slow or absent bottom currents. In one way or the other, ammonoids had to be able to remain in a habitat with favorable conditions, i.e., sufficient food, oxygen, and also mating partners. In turn, it can be expected to find ammonoid remains more commonly in sediments typical for moderate to low water currents (Jacobs 1992b; Jacobs et al. 1994), although not in the deep sea as their shells would have imploded there, or dissolved if below the carbonate compensation depth.

There are several studies, which examined relationships between ammonoid shell shapes and sedimentary facies. For example, Batt (1989, 1993) used shell morpholo-

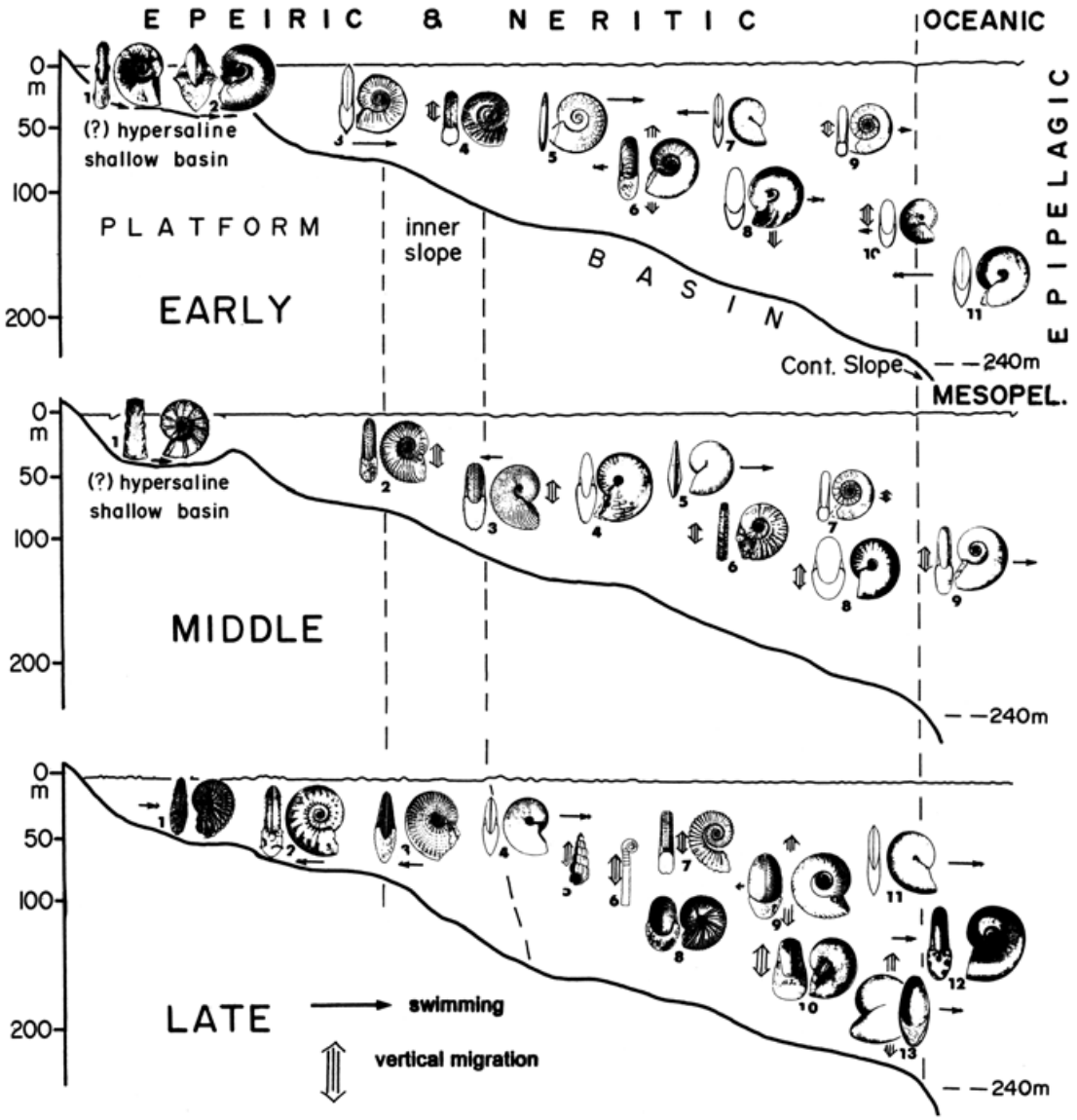

Fig. 17.13 Triassic ammonoid habitats from Wang and Westermann (1993) and Westermann (1996). Early Triassic: *1 Tirolites*, *2 Otoceras*, *3 Inyoites*, *4 Hellenites*, *5 Gyronites*, *6 Anasibirites*, *7 Hedenstroemia*, *8 Isculitoides*, *9 Leiophyllites*, *10 Paranannites*, *11 Procarnites*. Middle Triassic: *1 Ceratites*, *2 Anolcites*, *3 Trachyceras*, *4 Beyrichites*, *5 Longobardites*, *6 Balatonites*, *7 Leiophyllites*, *8 Ptychites*, *9 Monophyllites*. Late Triassic: *1 Tibetites*, *2 Distichites*, *3 Acanthinites*, *4 Discotropites*, *5 Cochloceras*, *6 Rhabdoceras*, *7 Choristoceras*, *8 Juvavites*, *9 Tropites*, *10 Cladiscites*, *11 Pinacoceras*, *12 Rhacophyllites*, *13 Arcestes*

gies to interpret oxygen availability near the sea-floor. In his opinion, heteromorphs like baculitids and loosely coiled forms lived in the water column, while the more tightly coiled heteromorphs and the normally coiled ammonoids occupied a more demersal habitat. Therefore, if the latter group is missing, this might be an indicator of hypoxic to anoxic conditions near the sea-floor (e.g., Monnet and Bucher 2007). Bayer and McGhee (1984) as well as McGhee et al. (1991) employed a more evolutionary approach. They documented how, in the parts of Middle Jurassic transgressive-regres-

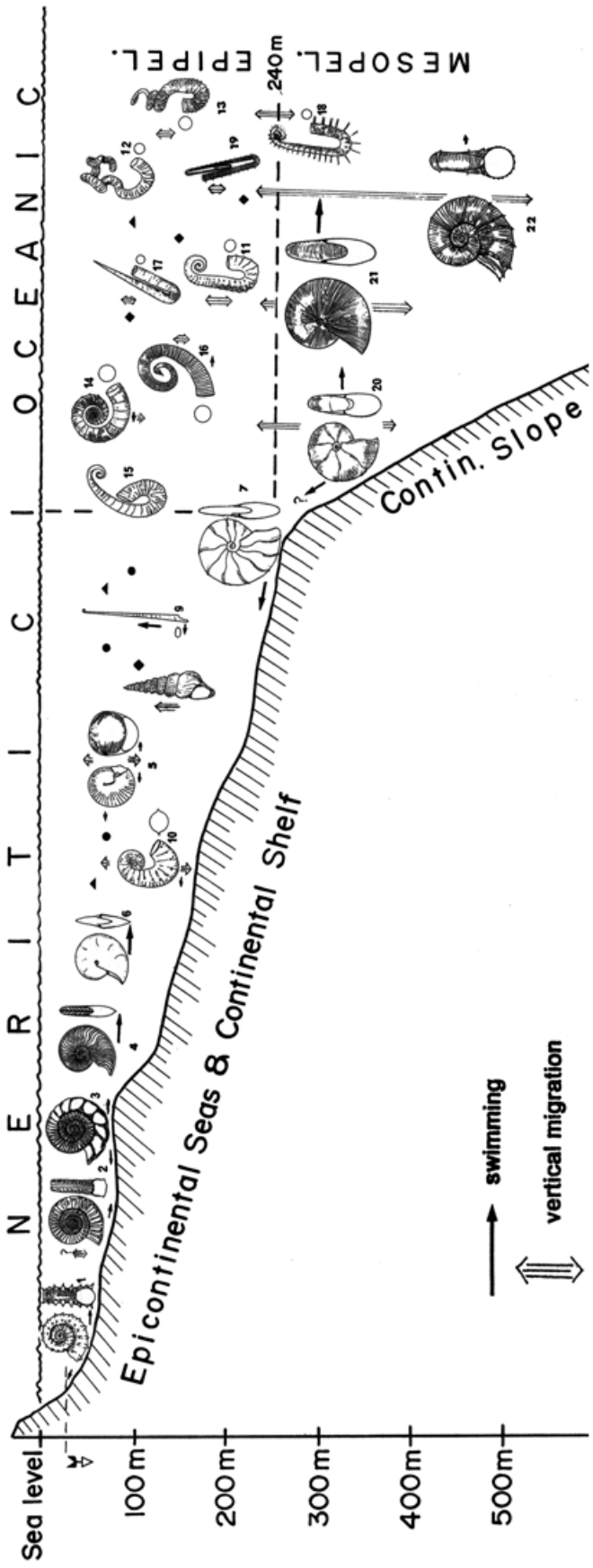

Fig. 17.14 Jurassic and Cretaceous ammonoid habitats from Westermann (1990) and Westermann (1996): *1 Peltoceras*, *2 Arietites*, *3 Perisphinctes*, *4 Harpoceras*, *5 Sphaeroceras*, *6 Oxycerites*, *7 Barremites*, *8 Turrilites*, *9 Baculites*, *10 Scaphites*, *11 Ancyloceras*, *12 Nipponites*, *13 Didymoceras*, *14 Crioceratites*, *15 Labeceras*, *16 Glyptoxoceras*, *17 Hamulina*, *18 Anisoceras 19 Pseudoxybeloceras*, *20 Holcophylloceras*, *21 Phylloceras*, *22 Lytoceras*

sive "Klüpfel cycles" with higher water energy, more involute and compressed shell forms evolved in the Leioceratinae and Graphoceratinae iteratively. Landman and Waage (1993) found that the lineages of the genera *Hoploscaphites* and *Jeletzkytes* both evolved more compressed representatives while the facies changed from the deeper water Pierre Shale to the shallower water sandy Fox Hills Formation. Jacobs et al. (1994) found that more compressed, lower drag shell morphs of *Scaphites whitfieldi* are associated with sandy facies in the Cretaceous Carlisle Shale of the American Western Interior while thicker higher drag shell morphs of the same species occur in finer grain facies. A similar pattern was reported by Courville and Thierry (1993) from *Thomasites* but inverse patterns are sometimes also found in strongly ornamented taxa such as *Schloenbachia* (Wilmsen and Mosavinia 2011), which can complicate interpretations (Ritterbush et al. 2014; De Baets et al. 2015a). Westermann (1996) listed a great number of examples for several marine basins, where he assigned certain ammonoid groups to distinct habitats (Fig. 17.13, 17.14). Klug (2002) suggested that Early and Middle Devonian anarcestids and agoniatitids, which mainly differ in whorl expansion rate and umbilical width, had different ecological preferences since he found them in more clayey or more limey facies, respectively. However, this study used low specimen numbers, thus leading to a low statistical power.

In the Early and Middle Devonian, two such lineages evolved in parallel as shown by Monnet et al. (2011). In the Auguritidae and Pinacitidae, oxyconic shell forms with closed umbilicus evolved independently, and in both lineages, the most derived forms occurred in carbonates that were probably deposited under shallower water conditions than those associated with the ancestral forms. Most of the studies listed in the preceding paragraphs appear to coincide with the interpretations of Jacobs (1992b) as well as Jacobs and Chamberlain (1996), but there are not many such studies, their statistical power tends to be low, and the causality between habit, habitat and shell morphology is difficult to establish with certainty; this can only be achieved by combining multiple lines of evidence including analysis of shell shape, facies and geographic distribution, isotope analysis, etc. (e.g., Tsujita and Westermann 1998; Ritterbush et al. 2014).

A different approach to identify habitat depth is discussed in detail in Chaps. 17.1 and 2. In these studies, stable isotopes of oxygen have been used to assess the habitat depth of various Cretaceous ammonoids (Moriya et al. 2003; Lukeneder et al. 2010). Unfortunately, the error sources of such studies are often large and the number of these studies is still too low. Examination of oxygen isotopes in ammonoid shells is still one of the most promising methods to reveal new information on ammonoid habitats.

17.7 Swimming Modes

Taking the uncertain knowledge of ammonoid soft parts into account, most interpretations of the 'ammonoid power plant' are based on actualistic comparisons. Packard et al. (1980) examined the swimming modes in Recent nautilids (see also

Crick 1898; Chamberlain 1987, 1990, 1992). In *Nautilus*, very slow movement can be produced by the water expelled through the hyponome during aeration of the gills. Normal swimming speeds are produced by mantle cavity water expelled by contraction of the cephalic retractor muscles and funnel muscles. The animal moves forward, backward, up, or down, depending on the orientation of the highly flexible hyponome (Johanson et al. 1972; Ward et al. 1977; Packard et al. 1980; Chamberlain 1981; 1987; Wells and Wells 1985; Webber and O'Dor 1986; Wells and O'Dor 1991).

Many squids including *Sepia* have lateral fins, which function in thrust production and in turning in some squid locomotor behaviors. Octobrachians and some decabrachians use their arms, sometimes connected with velar skins, to swim by expelling water entrained within their arm crowns with rhythmic beating of their arms, in the style of medusoid cnidarian bells. These two modes of locomotion appear unlikely to have been present in ammonoids, or at least, there is no evidence at all yet to support their occurrence among ammonoids.

The most likely mode of swimming is by contracting the mantle cavity, although it is not clear, which muscles were responsible for this task in ammonoids. There are several alternatives, namely the mantle musculature (as in coleoids), the cephalic retractors (as in nautilids) or potentially also other longitudinal muscles (not realized in Recent forms) in combination with the hyponome musculature. It appears also likely that the water was expelled through a hyponome, since hyponomic sinuses are present in many ammonoids. Hyponomes have not yet been found fossilized in ammonoids. Thus, another open question is the flexibility of the ammonoid hyponome. Was it long and flexible enough to point backwards and allow forward swimming?

Recently, Westermann (2013) revived a hypothesis earlier introduced by Schmidt (1930). This "*Twin nozzle-Hypothesis*" roots in the fact that many Mesozoic ammonoids have a more or less long ventral projection (e.g., in *Amaltheus*) combined with a probably more or less horizontal aperture. This would be an adverse combination of character states for straight backwards swimming, because the mentioned ventral apertural projection would have interfered with movement of the hyponome. Therefore, these authors suggested that the hyponome had evolved two openings, one on each side of the ventral projection. Both hyponome parts could be moved independently according to them. This is an interesting idea but so far, it is not supported by fossil evidence.

Monnet et al. (2011) discussed the peculiar way, in which the umbilicus was closed in some Devonian Auguritidae and Pinacitidae. The most derived representatives of both families have largely covered the umbilicus with a projection of the lateral shell over the umbilicus. This projection formed umbilical sinuses, which might have been horizontally aligned with the hyponome sinus. It would have allowed these species to take in water from the swimming direction into the mantle cavity (in *Nautilus*, water is taken in at the same place according to Packard et al. 1980), accelerating the water by compressing the mantle cavity, and expelling it out of the hyponome. This means that these forms potentially sucked water into the mantle cavity after completion of a hyponome jet.

Acknowledgements We greatly appreciate the financial support by the Swiss National Science foundation (project numbers 200021-113956/1, 200020-25029, -132870, and -149120). We greatly appreciate the effort the reviewers Kenneth De Baets (Erlangen) and Benjamin J. Linzmeier (University of Wisconsin-Madison) have put into their reviews, thereby helping us to improve our manuscript.

References

Bambach RK (1999) Energetics in the global marine fauna: a connection between terrestrial diversification and change in the marine biosphere. Geobios 32:131–144

Batt RJ (1989) Ammonite shell morphospace distribution in the Western Interior Greenhorn Sea and some paleoecological implications. Palaios 4:32–43

Batt RJ (1993) Ammonite shell morphotypes as indicators of oxygenation in a Cretaceous epicontinental sea. Lethaia 26:49–63

Batt RJ (2007) Sutural amplitude of ammonite shells as a paleoenvironmental indicator. Lethaia 24:219–225

Bayer U, McGhee GR Jr (1984) Iterative evolution of Middle Jurassic ammonite faunas. Lethaia 17:1–16

Bone Q, Pulsford A, Chubb AD (1981) Squid mantle muscle. J Mar Biol Assoc UK 61:327–342

Boyle P, Rodhouse P (2005) Cephalopods: ecology and fisheries. Wiley, Oxford

Chamberlain JA Jr (1969) Technique for scale modeling of cephalopod shells. Palaeontology 12:48–55

Chamberlain JA Jr (1976) Flow patterns and drag coefficients of cephalopod shells. Palaeontology 19:539–563

Chamberlain JA Jr (1980) The role of body extension in cephalopod locomotion. Palaeontology 23:445–461

Chamberlain JA Jr (1981) Hydromechanical design of fossil cephalopods. In: House MR, Senior JR (eds) The Ammonoidea. Syst Assoc Spec, vol 18. Academic, London

Chamberlain JA Jr (1987) Locomotion of *Nautilus*. In: Saunders WB, Landman NH (eds) *Nautilus*-The biology and paleobiology of a living fossil. Plenum, New York

Chamberlain JA Jr (1990) Jet propulsion of *Nautilus*: a surviving example of early Paleozoic locomotor design. Can J Zool 68:806–814

Chamberlain JA Jr (1992) Cephalopod locomotor design and evolution: the constraints of jet propulsion. In: Rayner MV, Wootton RJ (eds) Biomechanics and evolution. Cambridge University Press, Cambridge

Chamberlain JA Jr (1993) Locomotion in ancient seas: constraint and opportunity in cephalopod adaptive design. Geobios Spec Mem 15:49–61

Chamberlain JA Jr, Moore WA (1982) Rupture strength and flow rate of *Nautilus* siphuncular tube. Paleobiology 8:408–425

Chamberlain JA Jr, Westermann GEG (1976) Hydrodynamic properties of cephalopod shell ornament. Paleobiology 2:316–331

Chamberlain JA Jr, Ward PD, Weaver JS (1981) Post-mortem ascent of Nautilus shells: implications for cephalopod paleobiogeography. Paleobiology 7:494–509

Chirat R (2000) The so-called 'cosmopolitan palaeobiogeographic distribution' of tertiary Nautilida of the genus *Aturia* Bronn 1838: the result of post-mortem transport by oceanic palaeocurrents. Palaeogeogr Palaeoclim Palaeoecol 157:59–77

Courville P, Thierry J (1993) Nouvelles données biostratigraphiques sur les dépôts cénomanoturoniens du Nord-Est du fossé de ia Bénoué (Nigeria). Cretaceous Research 14(4–5):385–396

Crick GS (1898) On the muscular attachment of the animal to the shell in some fossil Cephalopoda (Ammonoidea). Trans Linn Soc NY 7:71–113

Daniel TL (1984) The unsteady aspects of locomotion. Am Zool 24:121–134

Daniel TL (1985) Cost of locomotion: unsteady medusan swimming. J Exp Biol 119:149–164
Daniel TL, Helmuth BS, Saunders WB, Ward PD (1997) Septal complexity in ammonoid cephalopods increased mechanical risk and limited depth. Paleobiology 23:470–481
Davis RA, Mapes RH, Klofak SM (1999) Epizoa on externally shelled cephalopods. In: Rozanov AY, Shevyrev AA (eds) Fossil cephalopods: recent advances in their study. Russian Academy of Sciences, Palaeontological Institute. Moskva
De Baets K, Klug C, Korn D, Landman NH (2012) Evolutionary trends in ammonoid embryonal development. Evolution 66:1788–1806
De Baets K, Bert D, Hofmann R, Monnet C, Yacobucci MM, Klug C (2015a) Ammonoid intraspecific variation. This volume
De Baets K, Keupp H, Klug C (2015b) Parasitism in ammonoids. This volume
De Baets K, Landman NH, Tanabe K (2015c) Ammonoid embryonic development. This volume
Doguzhaeva LA, Mapes RH (2015) Muscle scars in ammonoid shells. This volume
Doguzhaeva LA, Mutvei H (1991) Organization of the soft body in *Aconeceras*(Ammonitina), interpreted on the basis of shell morphology and muscle scars. Palaeontogr A 218:17–33
Doguzhaeva LA, Mutvei H (1993) Structural features in Cretaceous ammonoids indicative of semi-internal or internal shells. In: House MR (ed) The Ammonoidea: environment, ecology, and evolutionary change. Syst Assoc Spec, vol 47. Clarendon Press, Oxford
Ebel K (1983) Berechnungen zur Schwebefähigkeit von Ammoniten. N Jb Geol Paläont Mh 1983:614–640
Elmi S (1991) Données expérimentales sur l'architecture fonctionelle de la coquille des ammonodes Jurassiques. Géobios, Mémoire Spécial 13:155–160
Elmi S (1993) Loi des aires, couche-limite et morphologie fonctionnelle de la coquille des Céphalopodes (Ammonoides). Geobios 26(Suppl 1):121–138
Finn JK, Norman MD (2010) The argonaut shell: gas-mediated buoyancy control in a pelagic octopus. Proc Ro Soc B 277(1696):2967–2971. doi:10.1098/rspb.2010.0155
Gaillard C (1977) Cannelures d'érosion et figures d'impact dues à des coquilles d'ammonites à épines (Oxfordien supérieur du Jura français). Eclogae Geol. Helvetiae 70:701–715
Hamada T (1964) Notes on drifted *Nautilus* in Thailand. Sci Pap Coll Gen Educ Univ Tokyo 14:255–277
Hauschke N, Schöllmann L, Keupp H (2011) Oriented attachment of a stalked cirripede on an orthoconic heteromorph ammonite—implications for the swimming position of the latter. N Jahrb Geol Paläont Abh 202:199–212
Hewitt RA (1996) Architecture and strength of the ammonite shell. In: Landman NH, Tanabe K, Davis RA (eds) Ammonoid paleobiology. Plenum, New York
Hewitt RA, Westermann GEG (2003) Recurrences of hypotheses about ammonites and *Argonauta*. J Paleontol 77:792–795
Hoffmann R, Zachow S 2011 Non-invasive approach to shed new light on the buoyancy business of chambered cephalopods (Mollusca). Extended Abstract IAMG Salzburg 2011:1–9
Hoffmann R, Schultz JA, Schellhorn R, Rybacki E, Keupp H, Gerden SR, Lemanis R, Zachow S (2013) Non-invasive imaging methods applied to neo- and paleontological cephalopod research. Biogeosciences Discuss 10:18803–18851:2013. doi:10.5194/bgd-10-18803-2013
Hoffmann R, Lemanis R, Naglik C, Klug C (2015) Ammonoid buoyancy. This volume
House MR (1973) An analysis of Devonian goniatite distributions. In: Hughes NF (ed) Organisms and continents through time. Spec Pap Palaeont 12:305–317
House MR (1981) On the origin, classification and evolution of the early Ammonoidea. In: House MR, Senior JR (eds) The Ammonoidea: the evolution, classification, mode of life and geological usefulness of a major fossil group. Academic, London
House MR (1987) Geographic distribution of *Nautilus* shells. In: Saunders WB, Landman NH (eds) *Nautilus*. The biology and paleobiology of a living fossil. Plenum, New York
Iredale T (1944) Australian pearly *Nautilus*. Austr. Zool 10:294–298
Jacobs DK (1992a) The support of hydrostatic load in cephalopod shells-adaptive and ontogenetic explanations of shell form and evolution from Hooke 1695 to the present. In: Hecht MK, Wallace B, Macintyre RJ (eds) Evolutionary biology, vol 26. Plenum, New York

Jacobs DK (1992b) Shape, drag, and power in ammonoid swimming. Paleobiology 18:203–220
Jacobs DK, Chamberlain JA (1996) Buoyancy and hydrodynamics in ammonoids. In: Landman NH, Tanabe K, Davis RA (eds) Ammonoid paleobiology. Topics in geobiology13. Plenum, New York
Jacobs DK, Landman NH (1993) Is *Nautilus* a good model for the function and behavior of ammonoids? Lethaia 26:101–110
Jacobs DK, Landman NH, Chamberlain JA Jr (1994) Ammonite shell shape covaries with facies and hydrodynamics: iterative evolution as a response to changes in basinal environment. Geology 22:905–908
Johansen W, Soden PD, Trueman ER (1972) A study in jet propulsion: an analysis of the motion of the squid, *Loligo vulgaris*. J Exp Biol 56:155–156
Kakabadzé MV, Sharikadzé MZ (1993) On the mode of life of heteromorph ammonites (heterocone, ancylocone, ptychocone). Geobios 26(Suppl 1):209–215
Kaplan P (2002) Biomechanics as a test of functional plausibility: testing the adaptive value of terminal-countdown heteromorphy in Cretaceous ammonoids. Abh Geol B-A 57:181–197
Kawabe F (2003) Relationship between mid-Cretaceous (upper Albian–Cenomanian) ammonoid facies and lithofacies in the Yezo forearc basin, Hokkaido, Japan. Cret Res 24:751–763
Kennedy WJ, Cobban WA (1976) Aspects of ammonite biology, biogeography, and biostratigraphy. Spec Pap Palaeontol 17:1–94
Keupp H (1984) Pathologische Ammoniten—Kuriositäten oder paläobiologische Dokumente? (Teil 1). Fossilien 1(6):258–262, 267–275
Keupp H (1985) Pathologische Ammoniten—Kuriositäten oder paläobiologische Dokumente? (Teil 2). Fossilien 2(1):23–35
Keupp H (1992) Rippenscheitel bei Ammoniten-Gehäusen. Fossilien 5:283–290
Keupp H (1996) Paläopathologische Analyse einer Ammoniten-Vergesellschaftung aus der Mittleren Volga-Stufe des subpolaren Urals. Fossilien 1:45–54
Keupp H (1997) Paläopathologische Analyse einer "Population" von *Dactylioceras athleticum* (Simpson) aus dem Unter-Toarcium von Schlaifhausen/Oberfranken. Berliner geowiss Abh E 25:243–267
Keupp H (2000) Ammoniten—paläobiologische Erfolgsspiralen. Thorbecke, Stuttgart
Keupp H (2006) Sublethal punctures in body chambers of Mesozoic ammonites (forma aegra fenestra n.f.), a tool to interpret synecological relationships, particularly predator-prey interactions. Paläontol Z 80:112–123
Keupp H (2008) Wer hat hier zugebissen? Ammoniten-Prädation. Fossilien 2008(2):109–112
Keupp H (2012) Atlas zur Paläopathologie der Cephalopoden. Berliner geowiss Abh E 12:1–390
Keupp H, Hoffmann R (2015) Ammonoid paleopathology. This volume
Keupp H, Röper M, Seilacher A (1999) Paläobiologische Aspekte von syn vivo- besiedelten Ammonoideen im Plattenkalk des Ober-Kimmeridgiums von Brunn in Ostbayern. Berliner geowiss Abh E 30:121–145
Klinger HC (1981) Speculation on buoyancy control and ecology in some heteromorph ammonites. In: House MR, Senior JR (eds) The Ammonoidea. Syst Assoc, Spec, vol 18. Academic, London
Klug C (2001) Life-cycles of Emsian and Eifelian ammonoids (Devonian). Lethaia 34:215–233
Klug C (2002) Quantitative stratigraphy and taxonomy of late Emsian and Eifelian ammonoids of the eastern Anti-Atlas (Morocco). Cour Forschungsinst Senck 238:1–109
Klug C, Korn D (2002) Occluded umbilicus in the Pinacitinae (Devonian) and its palaeoecological implications. Palaeontology 45:917–931
Klug C, Korn D (2004) The origin of ammonoid locomotion. Acta Palaeont Pol 49:235–242
Klug C, Lehmann J (2015) Soft-part anatomy of ammonoids: reconstructing the animal based on exceptionally preserved specimens and actualistic comparisons. This volume
Klug C, Meyer E, Richter U, Korn D (2008) Soft-tissue imprints in fossil and Recent cephalopod septa and septum formation. Lethaia 41:477–492
Klug C, Kröger B, Kiessling W, Mullins GL, Servais T, Frýda J, Korn D, Turner S (2010) The Devonian nekton revolution. Lethaia 43:465–477

Korn D (2012) Quantification of ontogenetic allometry in ammonoids. Evol Dev 14:501–514. doi:10.1111/ede.12003

Korn D, Klug C (2003) Morphological pathways in the evolution of Early and Middle Devonian ammonoids. Paleobiology 29:329–348

Kröger B (2001) Comments on Ebel's benthic-crawler hypothesis for ammonoids and extinct nautiloids. Paläontol Z 75:123–125

Kröger B (2005) Adaptive evolution in Paleozoic coiled cephalopods. Paleobiology 31:253–268

Kröger B, Vinther J, Fuchs D (2011) Cephalopod origin and evolution: a congruent picture emerging from fossils, development and molecules. Bioessays 12. doi:10.1002/bies.201100001

Kummel B, Lloyd RM (1955) Experiments on the relative streamlining of coiled cephalopod shells. J Paleontol 29:159–170

Landman NH (1988) Early ontogeny of Mesozoic ammonites and nautilids. In: Wiedmann J, Kullmann J (eds) Cephalopods-present and past. Schweizerbart, Stuttgart

Landman NH, Cobban WA (2007) Ammonite touch marks in Upper Cretaceous (Cenomanian-Santonian) deposits of the Western Interior Sea. In: Landman NH, Davis RA, Mapes RH (eds) Cephalopods present and past: new insights and fresh perspectives. Springer, Dordrecht

Landman NH, Waage KM (1993) Scaphitid ammonites of the Upper Cretaceous (Maastrichtian) fox hills formation in South Dakota and Wyoming. Bull Am Mus Nat Hist 215:1–257

Landman NH, Rye DM, Shelton KL (1983) Early ontogeny of *Eutrephoceras* compared to recent *Nautilus*and Mesozoic ammonites: evidence from shell morphology and light stable isotopes. Paleobiology 9:269–279

Landman NH, Tanabe K, Shigeta Y (1996) Ammonoid Embryonic Development. In: (Eds) Landman, N.H., Tanabe, K., Davis, R.A. *Ammonoid Paleobiology. Vol. 13, Topics in Geobiology.* 343–405. Plenum Press, New York

Longridge LM, Smith PL, Rawlings G, Klaptocz V (2009) The impact of asymmetries in the elements of the phragmocone of early Jurassic ammonites. Palaeontol Electron 12(1A):1–15

Lukeneder A (2015) Ammonoid habitats and life history. This volume

Lukeneder A, Harzhauser M, Müllegger S, Piller WE (2010) Ontogeny and habitat change in Mesozoic cephalopods revealed by stable isotopes (delta^{18}O, delta^{13}C). Earth and Planetary Science Letters 296:103–111. doi:10.1016/j.epsl.2010.04.053

Maeda H, Seilacher A (1996) Ammonoid taphonomy. In: Landman NH, Tanabe K, Davis RA (eds) Ammonoid paleobiology. Plenum, New York

Mapes RH, Nützel A (2008) Late Palaeozoic mollusc reproduction: cephalopod egg-laying behavior and gastropod larval palaeobiology. Lethaia 42:341–356

Marchand D (1984) Ammonites et paléoenvironnements; une nouvelle approche. Geobios Mém. spécial 8:101–107

Marchand D (1992) Ammonites et paléoprofondeur: les faits, les interprétations. Paleovox 1:49–68

McGhee GC, Bayer U, Seilacher A (1991) Biological and evolutionary responses to transgressive-regressive cycles. In: Einsele G, Ricken W, Seilacher A (eds) Cycles and events in stratigraphy. Springer, Berlin

Monks N, Young JR (1998) Body position and the functional morphology of Cretaceous heteromorph ammonites. Palaeontol Electron 1:15

Monnet C, Bucher H (2007) European ammonoid diversity questions the spreading of anoxia as primary cause for the Cenomanian/Turonian (Late Cretaceous) mass extinction. Swiss J Geosci 100:137–144

Monnet C, Klug C, De Baets K (2011) Parallel evolution controlled by adaptation and covariation in ammonoid cephalopods. BMC Evol Bio 11(115):1–21

Monnet C, De Baets K, Yacobucci MM (2015) Buckman's rules of covariation. In Klug C, Korn D, De Baets K, Kruta I, Mapes RH (eds): Ammonoid Paleobiology, Vol.2: From macroevolution to biogeography. Springer, Dordrecht

Moriya K (2015) Isotope signature of ammonoid shells. This volume

Moriya K, Nishi H, Kawahata H, Tanabe K, Takayanagi Y (2003) Demersal habitat of Late Cretaceous ammonoids: evidence from oxygen isotopes for the Campanian (Late Cretaceous) northwestern Pacific thermal structure. Geology 31:167–170

Mutvei H (1975) The mode of life in ammonoids. Paläontol Z 49:196–206
Mutvei H, Reyment RA (1973) Buoyancy control and siphuncle function in ammonoids. Palaeontology 16:623–636
Naglik C, Monnet C, Götz S, Kolb C, De Baets K, Klug C (2015) Growth trajectories in chamber and septum volumes in major subclades of Paleozoic ammonoids. Lethaia 48(1):29–46
Naglik C, Rikhtegar F, Klug C (in press) Buoyancy of some Palaeozoic ammonoids and their hydrostatic properties based on empirical 3D-models. Lethaia 10pp. DOI 10.1111/let.12125
O'Dor RK (1982) Respiratory metabolism and swimming performance of the squid, *Loligo opalescens*. Can J Fish Aquat Sci 39:580–587
O'Dor RK (1988a) The energetic limits on squid distributions. Malacologia 29:113–119
O'Dor RK (1988b) The forces acting on swimming squid. J Exp Biol 137:421–442
O'Dor RK, Webber DM (1991) Invertebrate athletes: trade-offs between transport efficiency and power density in cephalopod evolution. J Exp Biol 160:93–112
O'Dor RK, Wells MJ (1990) Performance limits of "antique" and "state-of-the-art" cephalopods, *Nautilus* and squid. Am Malacol Union Prog Abstr. 56th Ann Meeting, 52
O'Dor RK, Wells MJ, Wells J (1990) Speed jet pressure and oxygen consumption relationships in free-swimming *Nautilus*. J Exp Biol 154:383–396
O'Dor RK, Forsythe J, Webber DM, Wells J, Wells MJ (1993) Activity levels of *Nautilus* in the wild. Nature 362:626–627
Oeffner J, Lauder GV (2012) The hydrodynamic function of shark skin and two biomimetic applications. J Exp Biol 215:785–795
Okamoto T (1988) Analysis of heteromorph ammonoids by differential geometry. Palaeontology 31:35–52
Okamoto T (1996) Theoretical modeling of ammonoid morphology. In: Landman NH, Tanabe K, Davis RA (eds) Ammonoid paleobiology. Topics in geobiology 13. Plenum, New York
Packard A (1972) Cephalopods and fish: the limits of convergence. Biol Rev 47:241–307
Packard A, Bone Q, Hignette M (1980) Breathing and swimming movements in a captive *Nautilus*. J Mar Biol Assoc UK 60:313–327
Parent H, Westermann GEG, Chamberlain JA Jr (2014) Ammonite aptychi: functions and role in propulsion. Geobios 47:45–55
Raup DM (1966) Geometric analysis of shell coiling: general problems. J Paleont 40:1178–1190
Raup DM (1967) Geometric analysis of shell coiling: coiling in ammonoids. J Paleontol 41:43–65
Raup DM, Chamberlain JA Jr (1967) Equations for volume and center of gravity in ammonoid shells. J Paleontol 41:566–574
Reif WE (1982) Morphogenesis and function of the squamation in sharks. 1. Comparative functional morphology of shark scales, and ecology of scales. N Jahrb Geol Paläont Abh 164:172–183
Reyment RA (1973) Factors in the distribution of fossil cephalopods. Part 3: experiments with exact models of certain shell types. Bull Geol lnst Univ Uppsala N S 4:7–41
Ritterbush K, Bottjer DJ (2012) Westermann Morphospace displays ammonoid shell shape and hypothetical paleoecology. Paleobiology 38:424–446. doi:10.1666/10027.1
Ritterbush K, De Baets K, Hoffmann R, Lukeneder A (2014) Pelagic Palaeoecology: the importance of recent constraints on ammonoid palaeobiology and life history. J Zool. doi:10.1111/jzo.12118
Rosa R, Seibel BA (2010) Voyage of the argonauts in the pelagic realm: physiological and behavioural ecology of the rare paper nautilus, *Argonauta nouryi*. ICES J Mar Sci J du Conseil 67:1494–1500
Rothpletz A (1909) Über die Einbettung der Ammoniten in die Solnhofener Schichten. Abh math-phys Kl der königl Bayr Akad der Wiss München 24(2):313–337
Saunders WB (1995) The ammonoid suture problem: relationship between shell and septal thickness and sutural complexity in Paleozoic ammonoids. Paleobiology 21:343–355
Saunders WB, Shapiro EA (1986) Calculation and simulation of ammonoid hydrostatics. Paleobiology 12:64–79

Saunders WB, Wehman DA (1977) Shell strength of *Nautilus* as a depth limiting factor. Paleobiology 3:83–89

Saunders WB, Work DM (1996) Shell morphology and suture complexity in Upper Carboniferous ammonoids. Paleobiology 22:189–218

Saunders WB, Work DM (1997) Evolution of shell morphology and suture complexity in Paleozoic prolecanitids, the rootstock of Mesozoic ammonoids. Paleobiology 23:301–325

Saunders WB, Work DM, Nikolaeva SV (1999) Evolution of complexity in Paleozoic ammonoids. Science 286:760–763

Schmidt H (1930) Ueber die Bewegungsweise der Schalencephalopoden. Paläontol Z 12:194–208

Schmidt-Nielsen K (1972) Locomotion: energy cost of swimming, flying and running. Science 177:222–228

Seibel BA (2007) On the depth and scale of metabolic rate variation: scaling of oxygen consumption rates and enzymatic activity in the class Cephalopoda (Mollusca). J Exp Biol 210:1–11

Seibel BA, Thuesen EV, Childress JJ, Gorodezky LA (1997) Decline in pelagic Cephalopod metabolism with habitat depth reflects differences in locomotory efficiency. Biol Bull 192:262–278

Seilacher A (1960) Epizoans as a key to ammonoid ecology. J Paleont 34:189–193

Seilacher A (1963) Umlagerung und Rolltransport von Cephalopodengehäusen. N Jahrb Geol Paläont Mh 11:593–615

Seilacher A (1982a) Ammonite shells as habitats in the Posidonia shales of Holzmaden—floats or benthic islands? N Jahrb Geol Paläont Mh 1982:98–114

Seilacher A (1982b) Ammonite shells as habitats—floats or benthic islands? In Einsele G, Seilacher A (eds) Cyclic and event in stratification. Springer, Berlin. doi:10.1007/978–3-642-75829-4_38

Seilacher A, Keupp H (2000) Wie sind Ammoniten geschwommen? Fossilien 5:310–313

Seki K, Tanabe K, Landman NH, Jacobs DK (2000) Hydrodynamic analysis of Late Cretaceous desmoceratine ammonites. Rev Paléobiol Vol spéc 8:141–155

Shapiro EA, Saunders WB (1987) *Nautilus* shell hydrostatics. In: Saunders WB, Landman NH (eds) *Nautilus*—The biology and paleobiology of a living fossil. Plenum, New York

Signor PW III, Brett CE (1984) The mid-Paleozoic precursor to the Mesozoic marine revolution. Paleobiology 10:229–245

Stenzel HB (1964) Living *Nautilu*s. In: Moore RC (ed) Treatise on invertebrate paleontology part K (Mollusca 3). Geological Society of America and University of Kansas Press, Lawrence, pp. K59–K93

Summesberger H, Jurkivsek B, Kolar-Jurkovsek T (1999) Rollmarks of soft parts and a possible crop content of Late Cretaceous ammonites from the Slovenian karst. In: Olóriz F, Rodríguez-Tovar FJ (eds) Advancing research on living and fossil Cephalopods. Kluwer Academic/Plenum, New York

Swan RTH, Saunders, WB (1987) Function and shape in late Paleozoic (mid-carboniferous) ammonoids. Paleobiology 13:297–311

Tajika A, Naglik C, Morimoto N, Pascual-Cebrian E, Hennhöfer DK, Klug C (2015) Empirical 3D-model of the conch of the Middle Jurassic ammonite microconch *Normannites*, its buoyancy, the physical effects of its mature modifications and speculations on their function. Historical Biology: An International Journal of Paleobiology, 27(2):181–191. DOI: 10.1080/08912963.2013.872097

Tanabe K (1979) Palaeoecological analysis of ammonoid assemblages in the Turonian *Scaphites* facies of Hokkaido, Japan. Palaeontology 22:609–630

Toriyama R, Sato T, Hamada T, Komalarjun P (1965) *Nautilus pompilius* drifts on the west coast of Thailand. Jpn J Geol Geog. 36:149–161

Trammer J, Niechwedowicz M (2007) Hydrodynamically controlled anagenetic evolution of Famennian goniatites from Poland. Acta Palaeont Pol 52:63–75

Trueman AE (1941) The ammonite body chamber, with special reference to the buoyancy and mode of life of the living ammonite. Q J Geol So. 96:339–383

Trueman ER, Packard A (1968) Motor performances of some cephalopods. J Exp Biol 49:495–507
Tsujita CJ, Westermann GEG (1998) Ammonoid habitats and habits in the Western Interior Seaway: a case study from the Upper Cretaceous Bearpaw Formation of southern Alberta, Canada. Palaeogeogr Palaeoclim Palaeoecol 144:135–160
Urdy S, Goudemand N, Bucher H, Chirat R (2010a) Allometries and the morphogenesis of the molluscan shell: a quantitative and theoretical model. J Exp Biol B 314:280–302
Urdy S, Goudemand N, Bucher H, Chirat R (2010b) Growth-dependent phenotypic variation of molluscan shells: implications for allometric data interpretation. J Exp Biol B 314:303–26
Vogel S (1981) Life in moving fluids: the physical biology of flow. Princeton University Press, Princeton
Walton S, Korn D, Klug C (2010) Size distribution of the Late Devonian ammonoid *Prolobites*: indication for possible mass spawning events. Swiss J of Geosci 103:475–494
Wang Y, Westermann GEG (1993) Paleoecology of triassic ammonoids. Geobios Mem Spec 15:373–392
Ward PD (1976) Stratigraphy, paleoecology and functional morphology of heteromorph ammonites of the Upper Cretaceous Nanaimo Group, British Columbia and Washington. PhD thesis McMaster University Library, Thesis QE788134 (39005047235555), Hamilton, Canada
Ward P (1979) Functional morphology of Cretaceous helically-coiled ammonite shells. Paleobiology 5:415–422
Ward PD (1981) Shell sculpture as a defensive adaptation in ammonoids. Paleobiology 7:96–100
Ward PD (1982) The relationship of siphuncle size to emptying rates in chambered cephalopods: implications for cephalopod paleobiology. Paleobiology 8:426–433
Ward PD (1987) The natural history of *Nautilus*. Allen and Unwin, Winchester
Ward PD, Wicksten MK (1980) Food sources and feeding behavior of *Nautilus macromphalus*. Veliger 23:119–124
Ward PD, Stone R, Westermann GEG, Martin A (1977) Notes on animal weight, cameral fluids, swimming speed, and colour polymorphism of the cephalopod, *Nautilus pompilius*, in the Fiji Islands. Paleobiology 3:377–388
Webber DM, O'Dor RK (1986) Monitoring the metabolic rate and activity of free-swimming squid with telemetered jet pressure. J Exp Biol 126:205–224
Wells MJ (1987) Ventilation and oxygen extraction by *Nautilus*. In: Saunders WB, Landman NH (eds) *Nautilus*-The biology and paleobiology of a living fossil. Plenum, New York
Wells MJ (1995) The evolution of a racing snail. Mar Freshw Behav Physiol 25:1–12
Wells MJ, O'Dor RK (1991) Jet propulsion and the evolution of Cephalopods. Bull Mar Sci 49:419–432
Wells MJ, Wells J (1985) Ventilation and oxygen uptake by *Nautilus*. J Exp Biol 118:297–312
Westermann GEG (1966) Covariation and taxonomy of the Jurassic ammonite *Sonninia adicra* Waagen. N Jb Geol Paläont Abh 124:289–312
Westermann GEG (1971) Form, structure and function of shell and siphuncle in coiled Mesozoic ammonoids. Life Sci Contrib R Ont Mus 78:1–39
Westermann GEG (1973) Strength of concave septa and depth limits of fossil cephalopods. Lethaia 6:383–403
Westermann GEG (1977) Form and Function of orthocone cephalopod shells with concave septa. Paleobiology 3:300–321
Westermann GEG (1990) New developments in ecology of Jurassic-Cretaceous ammonoids. In: Pallini G, Cecca F, Cresta S, Santantonio M (eds) Fossili, evoluzione, ambiente. Atti II Conv Int Pergola 1987. Tecnostampa, Ostra Vetere
Westermann GEG (1993) On alleged negative buoyancy of ammonoids. Lethaia 26:246. doi:10.1111/j.1502–3931.1993.tb01526.x
Westermann GEG (1996) Ammonoid life and habitat. In: Landman NH, Tanabe K, Davis RA (eds) Ammonoid paleobiology. Plenum, New York
Westermann GEG (2013) Hydrostatics, propulsion and life-habits of the Cretaceous ammonoid *Baculites*. Rev Paléobiol 32:249–265

Westermann GEG, Tsujita CJ (1999) Life habits of ammonoids. In: Savazzi E (ed) Functional morphology of the invertebrate skeleton. Wiley, Hoboken

Wilmsen M, Mosavinia A (2011) Phenotypic plasticity and taxonomy of *Schloenbachia varians* (J. Sowerby, 1817) (Cretaceous Ammonoidea). Paläontol Z 85:169–184

Young JZ (1960) Observations on *Argonauta* and especially its method of feeding. Proc Zool Soc London 133:471–479

Ziegler B (1967) Ammonitenökologie am Beispiel des Oberjura. Geol Rundsch 56:439–446

Appendix 2

Collaboration with other projects (abstracts)

1. Wani, R. **Tajika, A.** Ikuno, K. Iwasaki, T. (submitted to *Palaeontology*) Ontogenetic change of septal distance of early Jurassic belemnites from Germany and France.

2. Naglik, C. Monnet, C. Goetz, S. Kolb, C. De Baets, K. **Tajika, A.** Klug, C. (2015) Growth trajectories of some major ammonoid sub-clades revealed by serial grinding tomography data. Lethaia, DOI: 10.1111/let.12085.

ONTOGENETIC CHANGE OF SEPTAL DISTANCE OF EARLY JURASSIC BELEMNITES FROM GERMANY AND FRANCE

Ryoji Wani [1,*], Amane Tajika [2], Kenji Ikuno [3, 4], Tetsuro Iwasaki [3]

[1] Faculty of Environment and Information Sciences, Yokohama National University, Yokohama 240-8501, Japan; wani@ynu.ac.jp
[2] Paläontologisches Institut und Museum, Universität Zürich, Karl-Schmid-Strasse 4, 8006 Zürich
[3] Graduate School of Environment and Information Sciences, Yokohama National University, Yokohama 240-8501, Japan
[4] The Museum of Nature and Human Activities, Hyogo 669-1546, Japan
* Corresponding author.

Abstract: Ontogenetic changes of distances between succeeding septa were analysed with well-preserved specimens of belemnites. In the examined species (Passaloteuthis laevigata, Parapassaloteuthis zieteni, and Pseudohasitites longiformis) that were collected in Buttenheim, Germany and Lixhausen, France, the ontogenetic changes of septal distances demonstrated exponentially increasing trends with no sharp decreasing trend at the earliest ontogenetic stage. No decreasing trend at the earliest ontogenetic stage is a unique character in contrast with those in modern cuttlefish and modern and fossil nautiloids, in which the decreasing trends are related to the hatching events. These ontogenetic trends of septal distances suggest that the embryonic belemnites had a protoconch with no chamber. The hatchlings with no chamber and therefore small embryonic shell diameter in the examined belemnites are similar to those in ammonoids. Significant difference of a statistical test to compare the protoconch size between the two localities suggests that they were in different populations of each species.

Key words: septa, distance between succeeding septa, ontogenetic change, hatching, belemnite, Jurassic

Lethaia
AN INTERNATIONAL JOURNAL OF PALAEONTOLOGY AND STRATIGRAPHY

Growth trajectories of some major ammonoid sub-clades revealed by serial grinding tomography data

CAROLE NAGLIK, CLAUDE MONNET, STEFAN GOETZ, CHRISTIAN KOLB, KENNETH DE BAETS, AMANE TAJIKA AND CHRISTIAN KLUG

LETHAIA

Naglik, C., Monnet, C., Goetz, S., Kolb, C., De Baets, K., Tajika, A. & Klug, C. 2014: Growth trajectories of some major ammonoid sub-clades revealed by serial grinding tomography data. *Lethaia*, DOI: 10.1111/let.12085.

Molluscs such as ammonoids record their growth in their accretionary shells, making them ideal for the study of evolutionary changes in ontogeny through time. Standard methods usually focus on two-dimensional data and do not quantify empirical changes in shell and chamber volumes through ontogeny, which can possibly be important to disentangle phylogeny, interspecific variation and palaeobiology of these extinct cephalopods. Tomographic and computational methods offer the opportunity to empirically study volumetric changes in shell and chamber volumes through ontogeny of major ammonoid sub-clades in three dimensions (3-D). Here, we document (1) the growth of chamber and septal volumes through ontogeny and (2) differences in ontogenetic changes between species from each of three major sub-clades of Palaeozoic ammonoids throughout their early phylogeny. The data used are three-dimensional reconstructions of specimens that have been subjected to grinding tomography. The following species were studied: the agoniatitid *Fidelites clariondi* and anarcestid *Diallagites lenticulifer* (Middle Devonian) and the Early Carboniferous goniatitid *Goniatites multiliratus*. Chamber and septum volumes were plotted against the septum number and the shell diameter (proxies for growth) in the three species; although differences are small, the trajectories are more similar among the most derived *Diallagites* and *Goniatites* compared with the more widely umbilicate *Fidelites*. Our comparisons show a good correlation between the 3-D and the 2-D measurements. In all three species, both volumes follow exponential trends with deviations in very early ontogeny (resolution artefacts) and near maturity (mature modifications in shell growth). Additionally, we analyse the intraspecific differences in the volume data between two specimens of *Normannites* (Middle Jurassic). □ *3-D reconstruction, allometry, ammonoidea, ontogeny, palaeozoic, tomography, volumes.*

Carole Naglik [carole.naglik@pim.uzh.ch], Christian Kolb [christian.kolb@pim.uzh.ch], Amane Tajika [amane.tajika@pim.uzh.ch], Christian Klug [chklug@pim.uzh.ch], Paläontologisches Institut und Museum, Universität Zürich, Karl-Schmid-Strasse 4, Zürich 8006, Switzerland; Claude Monnet [claude.monnet@univ-lille1.fr], Géosystèmes – UMR 8217, Université de Lille 1, UFR Sciences de la Terre (SN5), Avenue Paul Langevin, Villeneuve d'Ascq 59655 cedex, France; Stefan Goetz (in memoriam); Kenneth De Baets [kenneth.debaets@fau.de], GeoZentrum Nordbayern Fachgruppe PaläoUmwelt Friedrich-Alexander-Universität Erlangen-Nürnberg, Loewenichstraße, 28 Erlangen 91054, Germany; *manuscript received on 13/08/2013; manuscript accepted on 23/04/2014.*

Acknowledgements

I would like to express my deepest gratitude to my supervisor Prof. Dr. Christian Klug (Zurich). Without his support, patience and encouragements, this dissertation would not have been completed. I appreciate the chance I received from him to carry out the project, great inspirations for research and countless things I learned from him.

I am also very grateful to the members of my PhD committee. Prof. Dr. Ryoji Wani (Yokohama) kindly put his Nautilus collection at my disposal for examination and helped during my field work in Japan. PD Dr. Dieter Korn (Berlin) accepted to be a committee member and shared his knowledge with me. Prof. Dr. Hugo Bucher (Zurich) provided working space and constructive criticism during committee meetings. Prof. Dr. Marcelo Sánchez accepted to be a committee member as well and inspired me to work hard.

This dissertation was completed with a lot of support by many colleagues during field work and in the laboratory. In particular, I would like to thank:

- Naoki Morimoto (Kyoto) for introducing me to the world of Matlab, letting me use the program he developed and sharing his knowledge on general evolutionary biology, which led to stimulating discussions and yielded interesting research questions. He also provided accommodation during CT-scanning at Kyoto University.
- Carole Naglik (Zurich) for helping with the transport of fossils and sharing her expertise on grinding tomography.
- Peter Kürsteiner (Uzwil) and Karl Tschanz (Zurich) for introducing me to the geology of the Alpstein, putting their cephalopod collection at my disposal and helping with the compilation of the Alpstein fossil data.
- Antoine Pictet (Geneva) for sharing his comprehensive knowledge on Cretaceous ammonoids and the geology of the Swiss Alps.
- Romain Jattiot (Zurich) for helping me with the field work in the Alpstein and Japan, sharing his knowledge on Cretaceous ammonoids, helping with the linguistic part of literature studies and stimulating scientific discussions.
- Christoph Zollikofer for insightful discussions about 3D morphometry of Nautilus and ammonoids.
- René Hoffmann for discussions, providing a silica sphere for CT-scanning of Nautilus and sharing his technical knowledge on tomography.
- Jens Lehmann (Bremen) for sharing his vast knowledge on Cretaceous ammonoids.
- Kenneth De Baets (Erlangen) for sharing his knowledge, help during field work in Germany and interesting discussions.
- Toni Bürgin (St. Gallen) for kindly letting me examine the collection of the Naturemuseum St. Gallen.
- Urs Oberli (St. Gallen) for providing access to his collection and preparing some of his fossils for my research.
- Thomas Bolliger (Aathal) for showing his private collection of Cretaceous ammonites.
- Bernhard Hostettler (Bern), René Kindlimann (Aathal), Heinz A. Kollmann (Vienna), Ursula Menkveld-Gfeller (Bern), Iwan Stössel (Schaffhausen) for taxonomic identifications of countless fossils from the Alpstein.
- Markus Hebeisen (Trubschachen) for teaching me how to prepare ammonoids with an airscribe and facilitating cultural interaction in our institute.
- Rosi Roth (Zurich) for giving me an introduction to ammonoid photography.
- Kenji Ikuno (Sanda) and Daisuke Aiba (Mikasa) for help during field work in Japan and interesting discussions.
- Ken'ichi Kurihara (Sapporo) for letting me examine the collection of Mikasa City Museum.
- Marc Scherrer and Yusuke Takamatsu (both Zurich) for help with test-scanning of Nautilus.
- Ashley Latimer (Zurich) for linguistic help during my field work in France.
- Heike Götzmann and Heinrich Walter (both Zurich) for helping to solve my administrative and technical problems in our institute.

I am also thankful to the Palaeontological Institute and Museum of the University of Zurich for the good

atmosphere. For that, I would like to especially thank Linda Frey and Kristof Veitschegger. A great appreciation is also given to the family of my supervisor for the pleasant time we shared, which helped keep me healthy and relaxed, especially in difficult times.

I would also like to thank my parents Jun and Mayumi for their patience and enduring encouragement. I would not have been able to start my studies in Zurich without them.

Funding

- This dissertation would not have been completed without the funding from the Swiss National Science Foundation (project No. 200020_169847 and 200021_149119).
- Some meeting participations were supported by the Swiss Palaeontological Society and Swiss Geological Society.